

REPORT DOCUMENTATION PAGE

Form Approved
OMB No. 0704-0188

The public reporting burden for this collection of information is estimated to average 1 hour per response, including the time for reviewing instructions, searching existing data sources, gathering and maintaining the data needed, and completing and reviewing the collection of information. Send comments regarding this burden estimate or any other aspect of this collection of information, including suggestions for reducing the burden, to Department of Defense, Washington Headquarters Services, Directorate for Information Operations and Reports (0704-0188), 1215 Jefferson Davis Highway, Suite 1204, Arlington, VA 22202-4302. Respondents should be aware that notwithstanding any other provision of law, no person shall be subject to any penalty for failing to comply with a collection of information if it does not display a currently valid OMB control number.

PLEASE DO NOT RETURN YOUR FORM TO THE ABOVE ADDRESS.

1. REPORT DATE (DD-MM-YYYY) 26-06-2002		2. REPORT TYPE Final		3. DATES COVERED (From - To) Sep 1999 - Jun 2002	
4. TITLE AND SUBTITLE A Multi-Disciplinary Assessment of the Hydrofoil Concept for Fast Ships				5a. CONTRACT NUMBER N00014-99-3-0010	
				5b. GRANT NUMBER	
				5c. PROGRAM ELEMENT NUMBER	
				5d. PROJECT NUMBER	
6. AUTHOR(S) Owen Berry, Bob Coopersmith, Sabine Goodwin, Burton Gray, Jeff Layton, Dean McAllister, Charlie Novak, Bob Olliffe, and Tim Takahashi				5e. TASK NUMBER	
				5f. WORK UNIT NUMBER	
7. PERFORMING ORGANIZATION NAME(S) AND ADDRESS(ES) Lockheed Martin Aeronautics Company 86 South Cobb Drive, Marietta, GA 30063				8. PERFORMING ORGANIZATION REPORT NUMBER	
9. SPONSORING/MONITORING AGENCY NAME(S) AND ADDRESS(ES) Office of Naval Research Ballston Center Tower One 800 North Quincy Street Arlington, VA 22217-5660				10. SPONSOR/MONITOR'S ACRONYM(S)	
				11. SPONSOR/MONITOR'S REPORT NUMBER(S)	

12. DISTRIBUTION/AVAILABILITY STATEMENT:

Approved for public release. Distribution is unlimited.

13. SUPPLEMENTARY NOTES

20020709 119

14. ABSTRACT

A multi-disciplinary analysis design analysis determining the feasibility and practicability of long-range high speed ships of varied design philosophy is presented. A hydrofoil ship is a dynamic lift vehicle that does not depend upon buoyancy for lift during cruise; as such, it presents an aircraft-like design problem. The small waterplane area (SWA) ship depends on static lift or buoyancy. The sizing and synthesis problem is first bounded using basic principles and linear theory. These equations are used to develop an understanding of the effect of the primary variables upon vehicle performance.

15. SUBJECT TERMS

Small waterplane area ships, hydrofoils, viscous drag reduction, Von Karman efficiency.

16. SECURITY CLASSIFICATION OF:			17. LIMITATION OF ABSTRACT UU	18. NUMBER OF PAGES 583	19a. NAME OF RESPONSIBLE PERSON Charlie Novak
a. REPORT U	b. ABSTRACT U	c. THIS PAGE U			19b. TELEPHONE NUMBER (Include area code) (770) 494-8582

***A Multi-Disciplinary Assessment of the
Hydrofoil Concept for Fast Ships
N00014-99-3-0010***

Final Report

Prepared by

***Lockheed Martin Aeronautics Company
Advanced Development Programs¹
Marietta, Georgia***

¹Owen Berry, Bob Coopersmith, Sabine Goodwin, Burton Gray, Jeff Layton, Dean McAllister, Charlie Novak,
Bob Olliffe, & Tim Takahashi

Final Report Outline and Statement-of-Work Tasks

- **Overview**
 - 1 Specification of Mission Requirements
 - 2 Identification of Technical Performance Measures
- **Hydrodynamics**
 - 3 Development of Candidate Hydrofoil Concepts
 - 8 Development of Optimum Candidate Foil Sections
 - 9 Development of Candidate Hydrofoil Components
 - 12 Detailed Multidisciplinary Assessment of Select Optimized Configurations - Design Verification & Validation
- **Stability and Control**
 - 5 Development of Candidate Control System Concepts
- **Structures**
 - 6 Development of Candidate Structural Concepts
 - 12 Detailed Multidisciplinary Assessment of Select Optimized Configurations - Design Verification & Validation
- **Propulsion**
 - 4 Development of Candidate Propulsion Concepts
- **Vehicle Design and Integration**
 - 7 Development of Candidate Hull Concepts
 - 9 Development of Candidate Hydrofoil Components
 - 11 Synthesis of Optimum Hydrofoil Configurations
- **Vehicle Performance and Sizing**
 - 10 Development of Simplified Multidisciplinary Relations for Configuration Synthesis
 - 11 Synthesis of Optimum Hydrofoil Configurations
 - 13 Sizing of Select Optimized Configurations

Overview

Abstract

A multidisciplinary design analysis determining the feasibility and practicality of a long-range high speed ships of varied design philosophy is presented. A hydrofoil ship is a dynamic lift vehicle that does not depend upon buoyancy for lift during cruise; as such, it presents an aircraft-like design problem. The small waterplane area (SWA) ship depends on static lift or buoyancy. The sizing and synthesis problem is first bounded using basic principles and linear theory. These equations are used to develop an understanding of the effect of the primary design variables upon vehicle performance.

Introduction

The Lockheed Martin Aeronautics Company of Marietta, GA, sponsored by the Office of Naval Research (ONR), has engaged in a science and technology effort to determine the feasibility of high-speed ships for military and/or commercial transport. The target mission requirements include: a cruise speed in excess of 70 knots, a range suitable for unrefueled transoceanic operation, an overall vehicle size commensurate with standard berths, a beam narrow enough to permit Suez Canal transit, a shallow draft for port entry, and "reasonable" power requirements.

Fast ships hold the promise of significantly reducing transit time as compared to conventional sealfit. They may enable the military to deliver a first-response force of personnel and materiel in a matter of days anywhere in the world. Fast ships also have far reaching implications for commercial trade; they may cost-effectively bridge the gap between low cost but very slow (several weeks) conventional ships and expensive but fast (few days) air cargo. The transportation technology targeted by this effort may help realize the benefits of the 21st century global economy.¹

1 Kennell, C., "Design Trends in High Speed Transport," Marine Technology, Vol. 35, No. 3, p. 127-134, 1998

Transportation Efficiency

The metric of transportation efficiency used here is based upon the monograph of Gabrielli and von Karman²:

$$vonK = V \cdot (L / D)$$

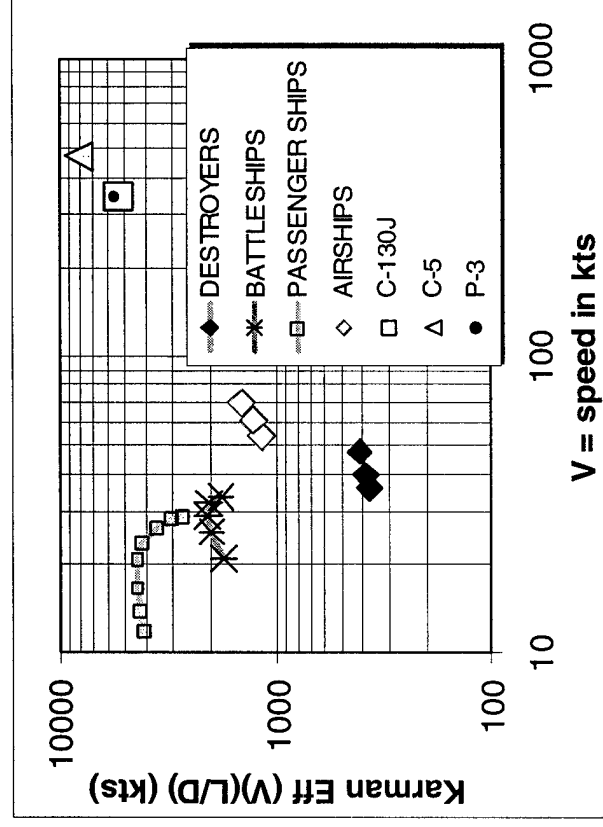
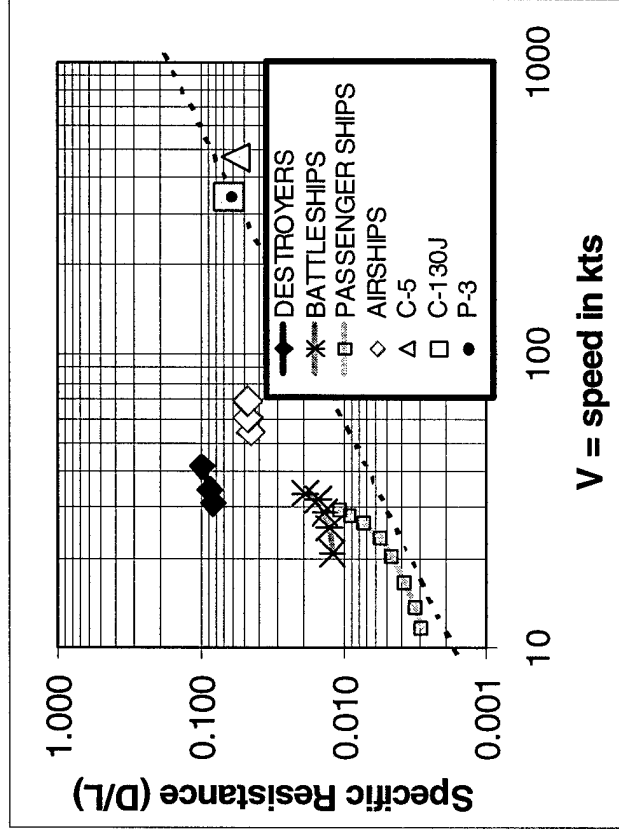
which is expressed in the dimension knots.

In the following figure, selected data from the original monograph is shown, accompanied by some data representing more recent Lockheed Martin aircraft. A line representing a "Karman Efficiency" condition of 5000-kts accompanies this data. The second plot represents the same data points specifically in terms of Karman Efficiency. Dedicated military vehicles (destroyers and battleships) do not require a high level of Karman Efficiency; but both commercial shipping and successful long-range transport aircraft tend to attain Karman Efficiency values on order of 5000-kts. The desired objective function for design must therefore serve two masters: to maximize both payload at range and to maximize Karman Efficiency.

An accurate estimation of both range and Karman Efficiency is predicated upon establishing values for the thrust specific fuel consumption, the hydrodynamic efficiency and the usable mass fraction of a candidate vehicle.

2 Gabrielli, G and Karman, Th. von , "What Price Speed?," Mechanical Engineering, Vol. 72. No. 10, p. 775-781, 1950.

Transportation Efficiency



Multi-Disciplinary Assessments

Scope and Methods

This study seeks to establish feasibility and practicality constraints for a long-range hydrofoil transport ship. A hydrofoil fast ship, like an aircraft, is a dynamic lift vehicle. Unlike a conventional ship, at cruise speed it does not depend upon hull buoyancy for lift. This key distinction results in great kinship between this nautical design exercise and the aircraft sizing and synthesis process. This effort considers the interplay between hydrodynamics, structures, propulsion and stability & control disciplines.

Due to the unique nature of this vehicle and mission (high speed, large size and long range), the prior-art hydrofoil database is insufficient to base an empirical design optimization process. First, the design space must be bounded; a limited range of potential vehicles must be identified. Secondly, the sensitivity of performance metrics to the primary design variables must be shown. To build a useful knowledge base, the technical work is organized into a multi-tiered optimization process as shown in the following slide. Essentially, four parallel yet coupled multi-disciplinary design optimizations must exist:

1. hydrofoil wing sections must be designed subject to multidisciplinary (structural, mission performance, stability and control) constraints;
2. these sections must be used to develop finite hydrofoil wings, control surfaces and support struts;
3. these studies will provide the basis for optimized vehicle configurations that uphold structural and controllability metrics; and,
4. these configurations will be integrated with available propulsion options and sized to achieve mission requirements.

This monograph focuses on the top two priorities: bounding the design space and documenting the design sensitivity to perturbations of the primary design variables.

Multi-Disciplinary Assessments

- **Design Tiers - from specific to general :**
 - 2-D Hydrofoil Section Element
 - Hydrofoil “Wing/Strut” Components
 - Underwater Hydrofoil Configuration
 - Overall Vehicle Size / Configuration
- **Multidisciplinary Analysis used to reinforce synthesis at each tier.**
 - High-fidelity tools used to substantiate design at the detailed level
 - Analysis produces empirical relations used at higher levels
 - Detailed high-fidelity analysis of final candidate design(s)
- **Design variables**
 - Chosen for optimization appropriate to each tier
 - Large number of overall design variables
 - Reduced number of design variables at any given tier

■ HYDRODYNAMICS
■ STAB. & CONTROL
■ PROPULSION
■ STRUCTURES



Requirements and Design Constraints

The requirements in the following slide became the bounds for the design space during the study. At onset to the program, the anticipated sustentation system of choice was the hydrofoil, however as the performance of hybrid static lift systems were exploited the upper limits to displacement, LOA and Beam were pushed so that the bounds of the sustentation triangle could be better understood.

Additional data was required and LM Aero subcontracted CSC-Advanced Marine for support in the area of ship mass properties and hydrodynamic expertise. Mr. Andrew Kondracki and Mr. J. Otto Scherer supported this effort.

Requirements from DARPA Study

- **Design Requirements :**
 - DARPA Fast Ship Technology Study, May 28, 1997
 - LMAS/ONR Phase I Study

Parameter	Minimum	Target	Bonus	Comment
Sustained Transit Speed	50 kts	70 kts	75 kts	Operations
Un-refueled Range at Transit Speed	5000 nM	6000 nM	10000 nM	Global Reach
Payload	1000 MT	1500 MT	2000 MT	One Fully Equipped Infantry Company
Fully Loaded Displacement	<15,000 T	12,000 T	<10,000 T	Economy
Overall Length	< 650 ft		< 500 ft	Berthing Size
Overall Width	< 213ft		115 ft	Panama Canal
Overall Draft	< 23 ft		<16 ft	Port Entry
Ride Quality	<0.1g RMS		<0.03g RMS	Personnel Fatigue
Propulsion Power @ speed	<200khp		<100khp	Economy

- **Implications**
 - Payload Fraction : 1,500T/12,000T = 12%
 - Design Feasible if
 - » Mean L/D = 20, SFC = 0.10 lb/lb-thrust-hr, Fuel Fraction = 35%
 - » Mean L/D = 25, SFC = 0.10 lb/lb-thrust-hr, Fuel Fraction = 29%
 - » Mean L/D = 30, SFC = 0.10 lb/lb-thrust-hr, Fuel Fraction = 25%

Requirements from BAA

- Design Requirements :
 - BAA 98-023

Parameter	Minimum	Target	Bonus	Comment
Sustained Transit Speed		70 kts		Operations
Un-refueled Range at Transit Speed		6000 nM		Global Reach
Payload		5000 MT		

- Implications
 - Payload Fraction : 5,000T @ 12% -> 40,000T Ship!
 - Other sizing restrictions from DARPA operations research not addressed
 - Additional information required to define design
 - » payload volume
 - » sea state capability
 - » powerplant limitations/restrictions
 - » materials limitations/restrictions
 - » 'technology factors'

Identified Specifications

- **LM Interpretation of Customer Requirements**
- **Vehicle Configuration (per DARPA Systems Analysis)**
 - Fully laden displacement : not to exceed 15,000T
 - Length: not to exceed 650 feet
 - Beam (foils retracted) : not to exceed 200 feet
 - Draft (foils retracted) : not to exceed 23 feet
- **Payload**
 - Maximize payload within 15,000T total vehicle mass limitation
 - Provisions for up to 5000T payload
 - 100 pound per square foot average payload density
 - No specific provision for internal storage of outsized payloads.
- **Range**
 - Un-refueled range : 6000nm @ >1500T payload
- **Speed**
 - Mean transit speed : not less than 70kts in calm seas
 - Operation in sea state 5, speed not specified.
- **Materials (for hull, foils and struts)**
 - Current technology engineering materials (metallic and composite)

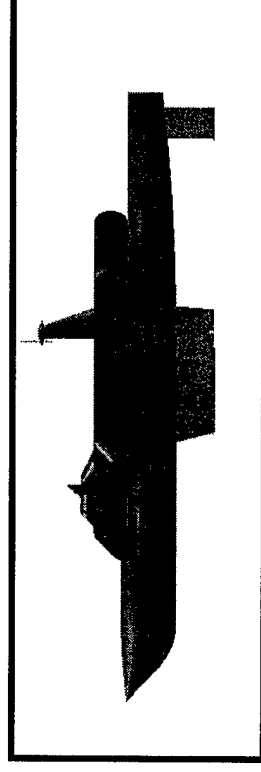
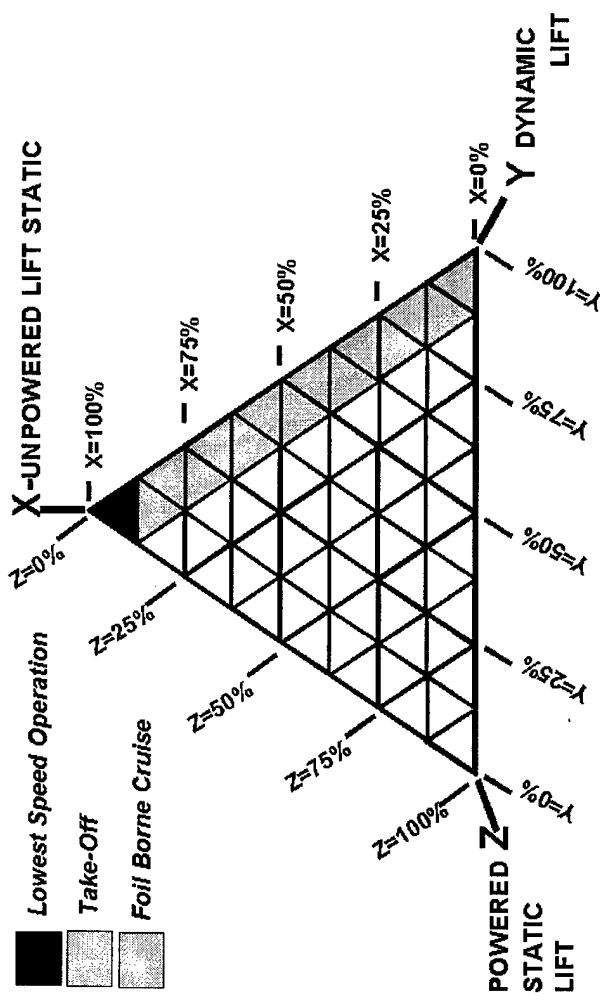
Addition Design Data Required

Additional information required for vehicle design, but outside LM Aero Databases include:

- **Hull Structural Design**
 - preferred MIL-STD guidelines?
- **Hull Mass Properties**
 - preferred references for empirical relations?
- **Subsystems Requirements**
 - preferred references
 - » subsystem identification
 - » subsystem power requirements
 - » subsystem space requirements
 - » subsystem mass properties
- **Handling Qualities**
 - preferred MIL-STD guidelines?
- **Sea State Model**
 - preferred model
 - model must address wave height, velocity distribution both at the surface at up to 20-ft depth

Hydrofoil Design Space – Sustention Triangle

- General Theory of Static Lift Payload Performance
 - Understand how to trade hydrodynamic performance for fuel fraction through the choice of submerged body sections and propulsion integration in order to maximize mission performance

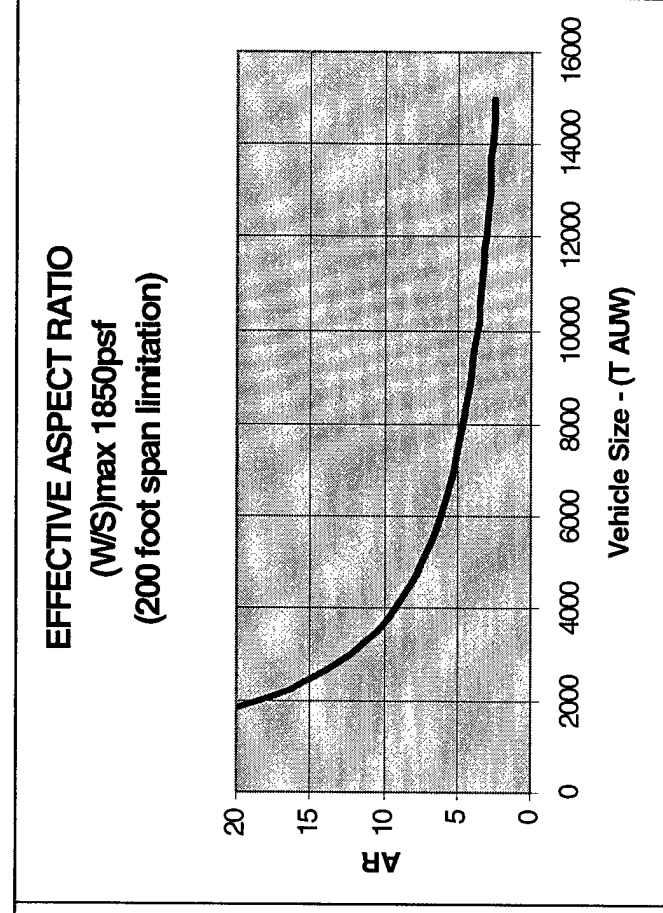
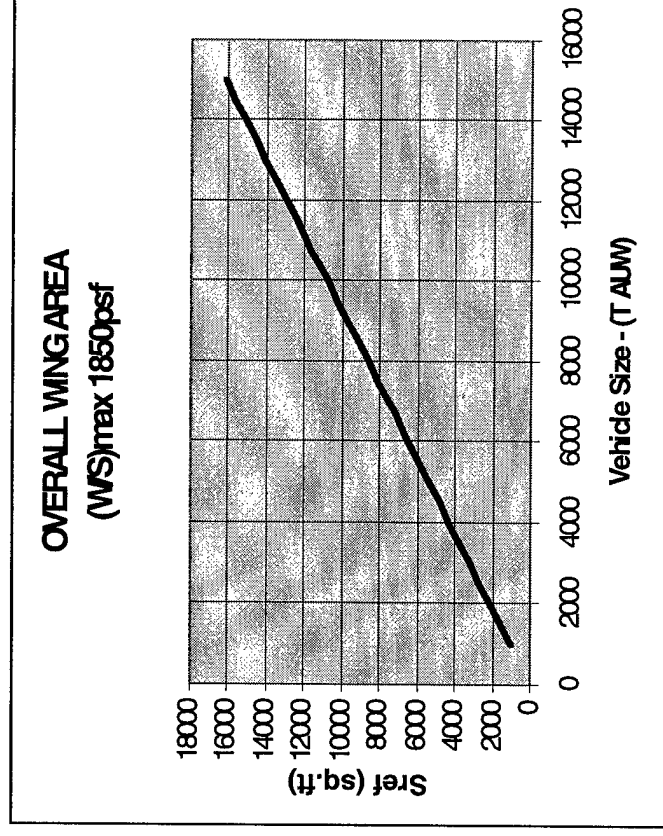


Hydrofoil Sustention System Design Space Defined

Upper and lower bounds to the problem were established using the maximum beam constraint of 200ft. As is shown in the following slide, the wing reference area and aspect ratio can be determined if the; cavitation-free lift characteristics of the wing section are chosen, and displacement of the ship is selected.

Hydrofoil Sustention System Design Space Defined

- Untrimmed 3DOF Database Used for Sizing Exercise
- Trade Study Space :
 - Overall Vehicle Size : 3000 -> 15000T AUW
 - Wing Area : appropriate for vehicle size and 200ft span limit
 - Cavitation Limitation : per P70/40/2.0A35 section
 - CD0 : 0.0050 (no drag mitigation) to 0.0010 (80% viscous reduction)

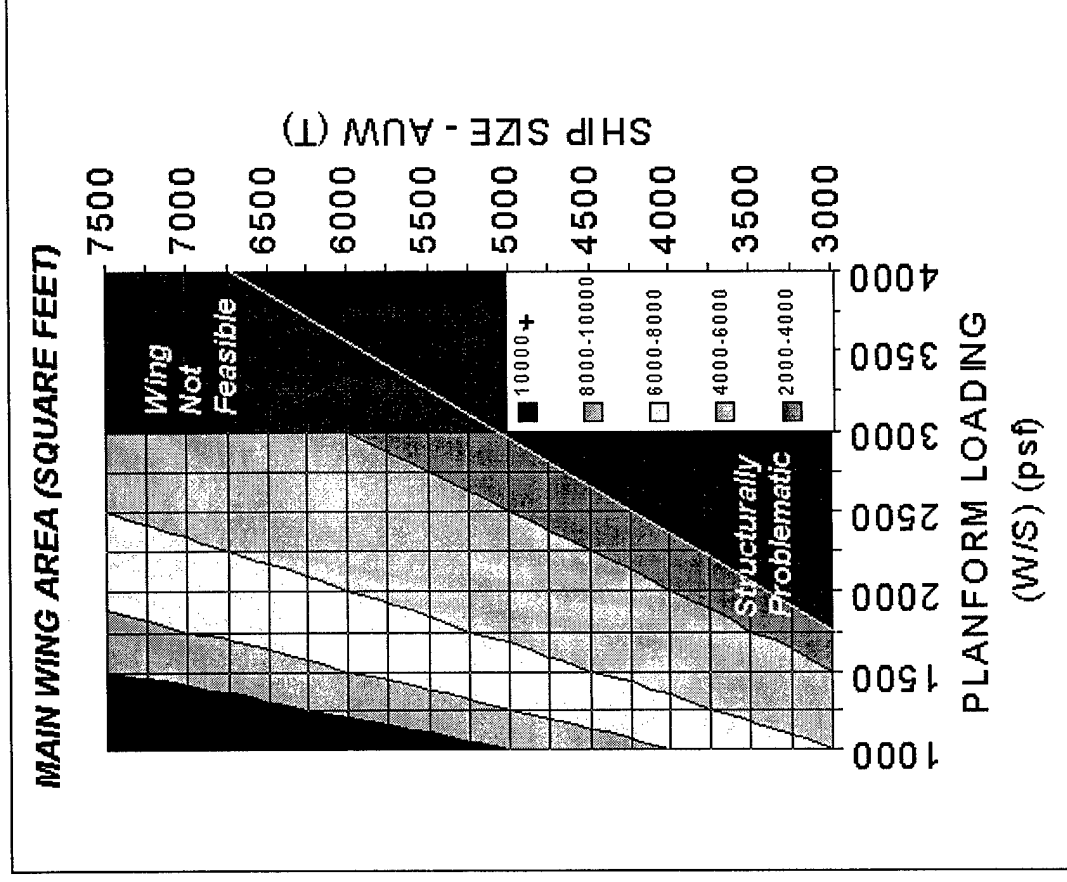
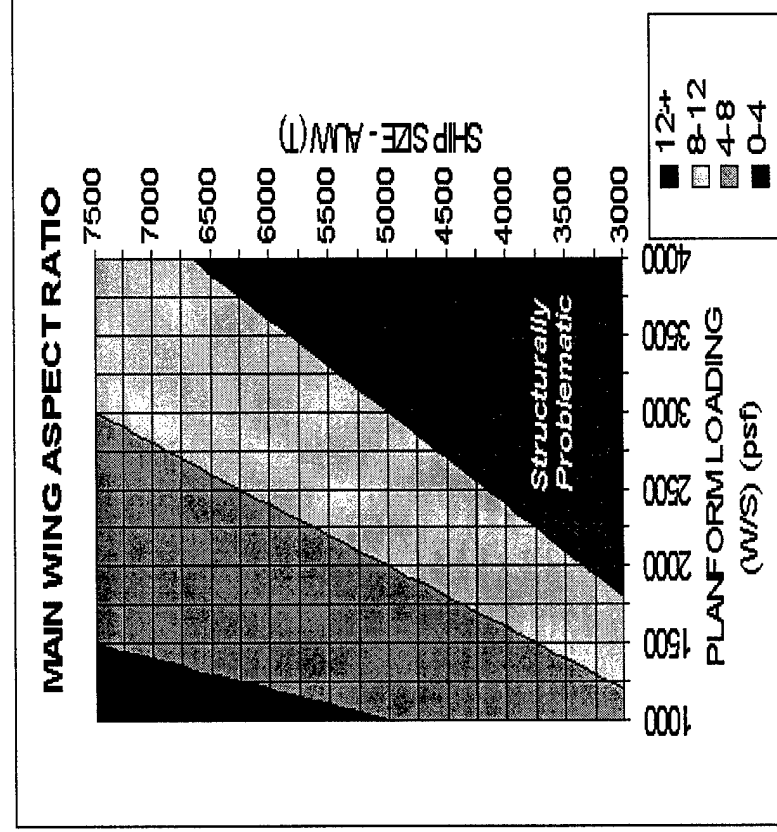


and is related to Wing Loading/Aspect Ratio...

If the combination of wing loading and aspect ratio are both high, the structural design and integration problem becomes problematic. The upper bounds for the design space was set at aspect ratio 12. At wing loading at and above 3000 pounds per square foot, the design was considered unfeasible. This made the large hydrofoils (>7500 Tons) impractical (structural solidity greater than what practical fabrication techniques would allow). As the study continued, the impact of the fixed beam with a air-coupled propulsion system set the upper bounds of the hydrofoil All-Up-Weight (AUW).

and is related to Wing Loading/Aspect Ratio...

- Wing Size and Aspect Ratio as function of W/S_{max} & AUW
 - Very High AR wings shown to have structural difficulties



L/D and von K Efficiency Estimates

Performance estimates early on suggested that without viscous drag reduction the trimmed Lift-to-Drag ratios (L/D) were less than 25 and for the range of cruise speeds in which cavitation could be precluded, the von Karman efficiency parameter (Velocity times L/D) would be on the order of 1000, or significantly below the goal value of 5000.

L/D and von K Efficiency Estimates

Trimmed L/D Estimates and
Von Karman Efficiency
Estimates.

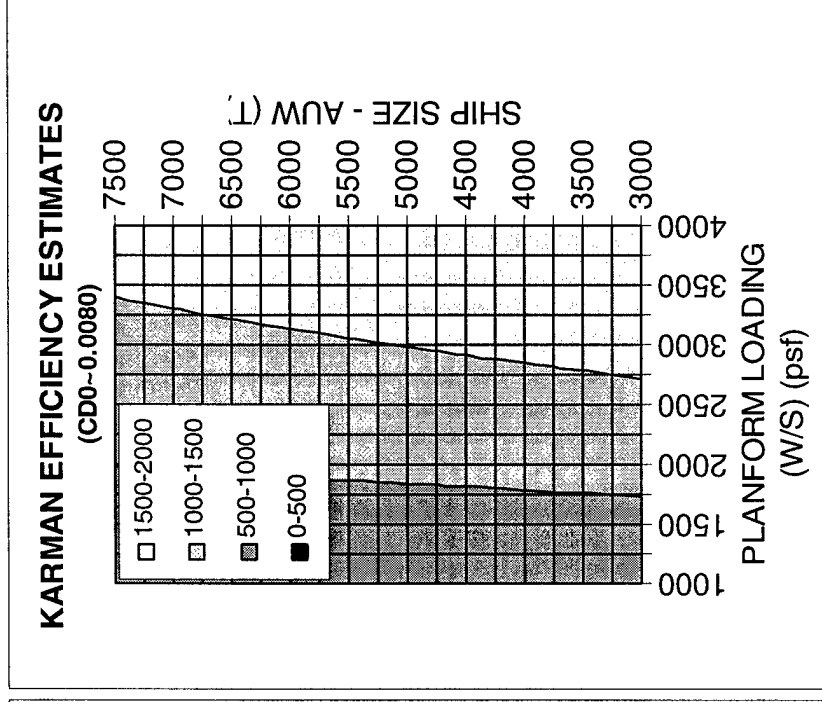
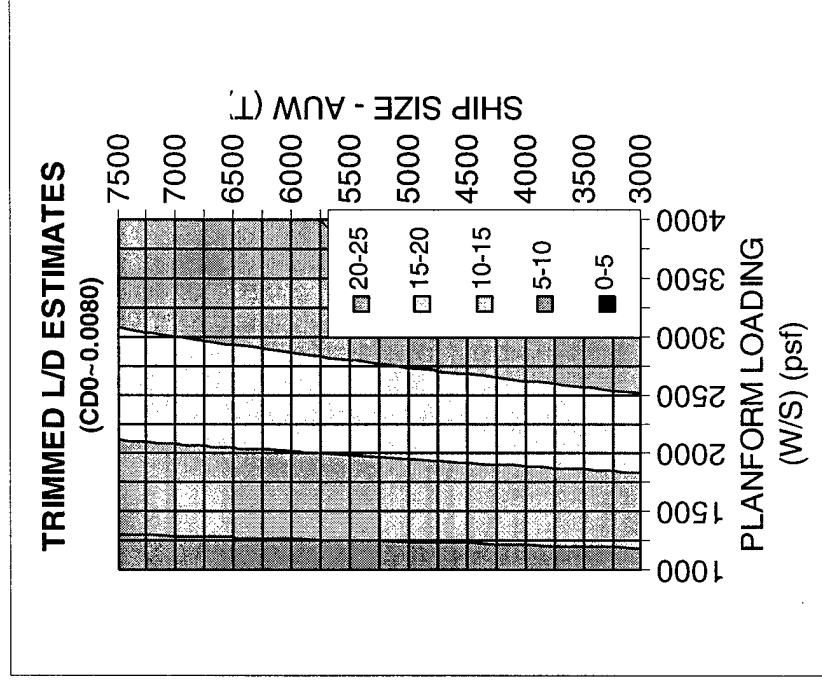
Without Viscous Drag

Mitigation

CD0 ~ 0.0080

Trimmed L/Ds < 25

vonK < 1000



L/D and von K Efficiency Estimates

If viscous drag is reduced through some type of drag reduction technology, the efficiency of the system in terms of L/D and von Karman parameter increases. Reducing the viscous drag to 50% of its original value elevates the L/D to less than 40. Note that the full elimination of the viscous drag would require an L/D of 70+ at 70 knots to meet the von Karman efficiency goal. In that case, the key is to have a very low inviscid (wave and induced) drag.

L/D and von K Efficiency Estimates

Trimmed L/D Estimates and
Von Karman Efficiency
Estimates.

With 50% Viscous Drag

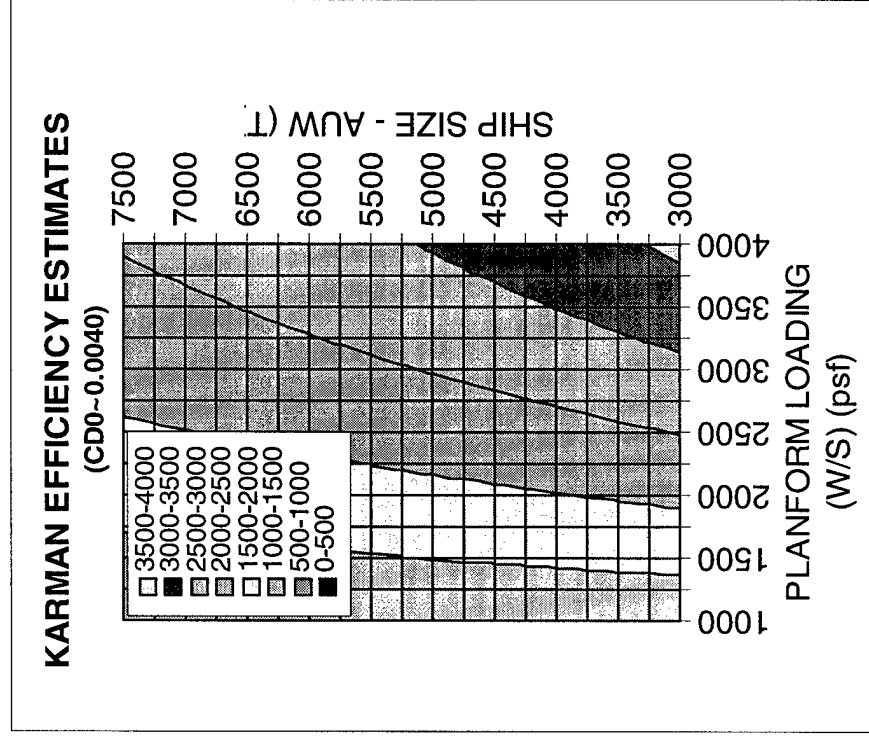
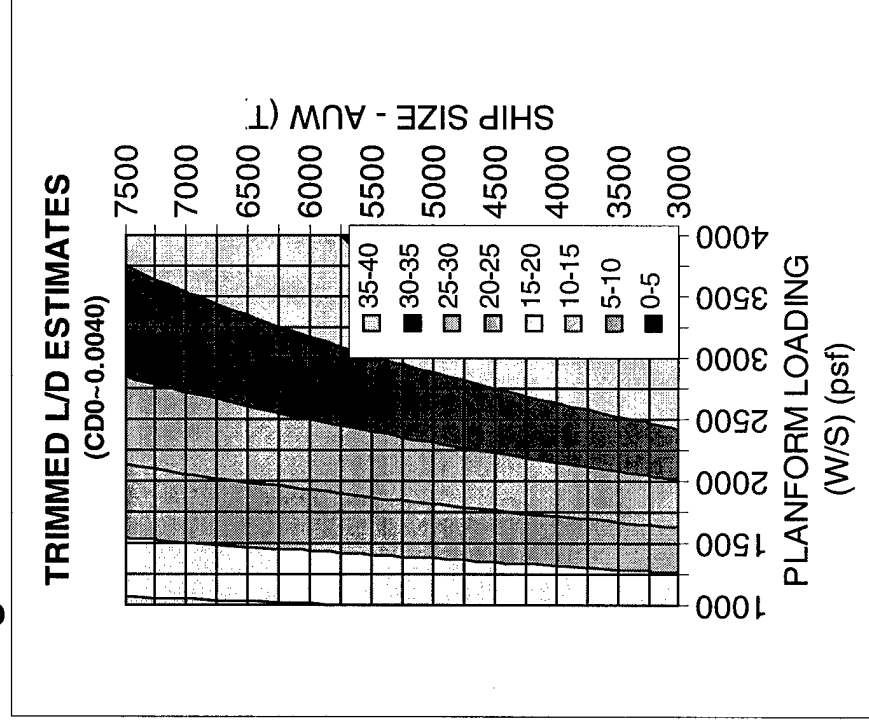
Mitigation

CD0 ~ 0.0040

Trimmed L/Ds

~25 to 40

vonK ~ 2000's



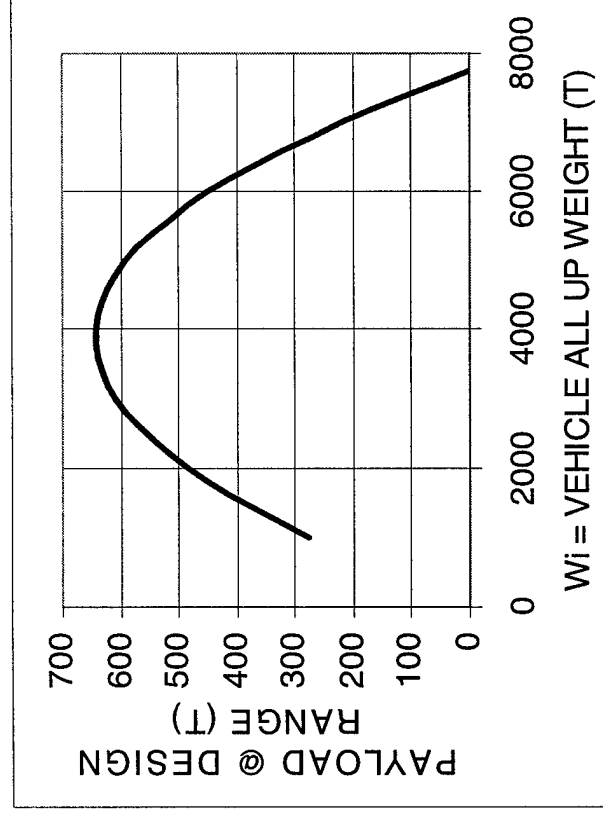
Optimum Size

The optimum sized ship was a key consideration with respect to the constraints of the study. Operationally, the hydrofoil ship behave like a transport aircraft. As fuel is burned off, the required lift decreases, and the integration of fuel burned over the mission becomes the Breugot integral.

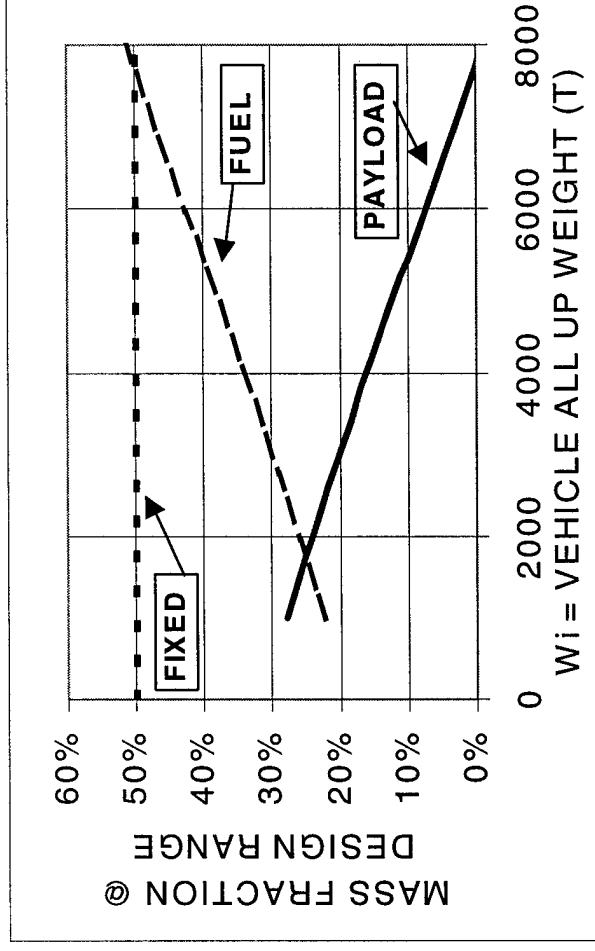
Initially, the fixed weight fraction was treated as an independent variable and the optimal ship size fell out from the combination of the type of propulsion system, and the L/D of the selected ship as constrained by the 200 foot beam and the 6000 nautical mile range goal. As the ship increases in size, the L/D decreases due to the decreasing aspect ratio of the wing. In addition, the thrust specific fuel consumption for an air coupled propulsion system decreases also due to the increase in disk loading. The results of the Breugot range study is shown in the followign slide. Note that maximum payload does not occur at the maximum payload range!

Optimum Size

- “First-Principles” Sizing Exercise shows existence of “Optimum” Ship Size
 - Fixed Weight Fraction (FWF) is an *Independent Variable*
 - Increasing ship size leads to : declining L/D and increasing TSFC (for air coupled propellers).
 - Payload fraction declines. Absolute Payload reaches peak at intermediate vehicle size.
- Higher Fidelity Solutions add realism in key areas :
 - Fixed Weight Fraction (FWF) is a *Dependent Variable*
 - Effects of wing geometry/configuration on mass fraction, wetted area, L/D
 - Propulsion system details : efficiency at cruise thrust, sizing and weights for peak thrust requirements.



Vehicle Sizing. Payload Capacity at Design Range, $R=6000\text{nM}$, as a Function of Vehicle All-Up Weight, W_i . $b=200\text{-ft}$; $h=20\text{-ft}$; $t/c=5\%$; $k_2=100\%$; $V=70\text{-kts}$; $FWF=50\%$.



Vehicle Sizing. Mass Fraction for Payload and Fuel at the Design Range, $R=6000\text{nM}$, as a Function of Vehicle All-Up Weight, W_i . $b=200\text{-ft}$; $h=20\text{-ft}$; $t/c=5\%$; $k_2=100\%$; $V=70\text{-kts}$; $FWF=50\%$.

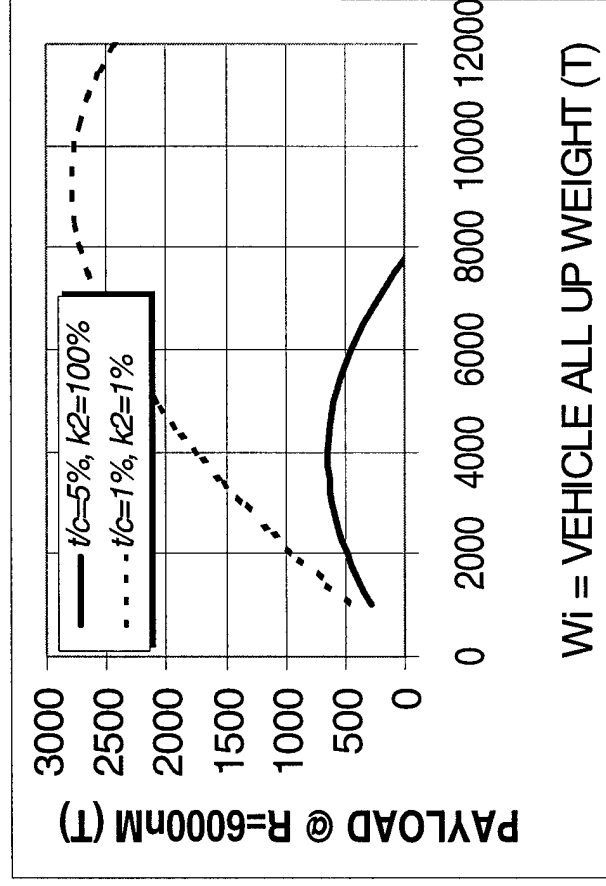
Optimum Size (cont'd)

The ingoing parameters for the optimal size study were initially chosen to be the full viscous drag and a realistic wing thickness. Goal values for viscous drag reduction (1% Schoenherr k2) and profile drag (foil thickness to chord, t/c , 1%) were examined and the results showed for a fixed propulsion system, that the maximum von Karman efficiency parameter did not occur at the maximum payload at range condition. Clearly a reduction in drag at zero lift (Cdo) favors a larger ship.

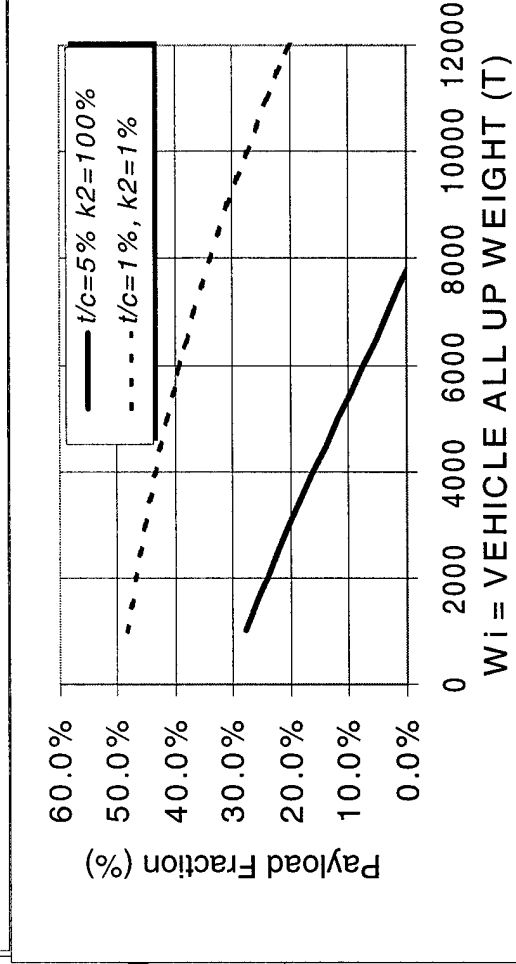
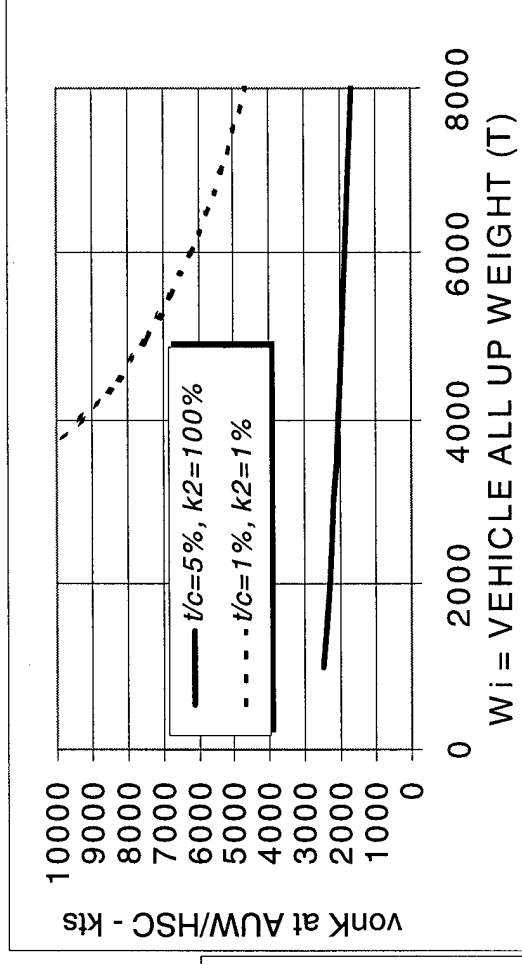
Optimum Size (cont'd)

- “First-Principles” Sizing Exercise shows existence of “Optimum” Ship Size

- Compare representative design from paper with “Theoretical Limit” design ($k_2=1\%$, $t/c=1\%$, $FWF=50\%$)
- Optimum Payload @ Range not at peak vonK



Vehicle Sizing. Payload Capacity at Design Range,
 $R=6000\text{nm}$, as a Function of Vehicle All-Up Weight, W_i .
 $b=200\text{-ft}$; $h=20\text{-ft}$; ($t/c=5\%$; $k_2=100\%$ and $t/c=1\%$;
 $k_2=1\%$); $V=70\text{-kts}$; $FWF=50\%$.



Feasible Vehicle Sizes - Effect of Viscous Drag Mitigation

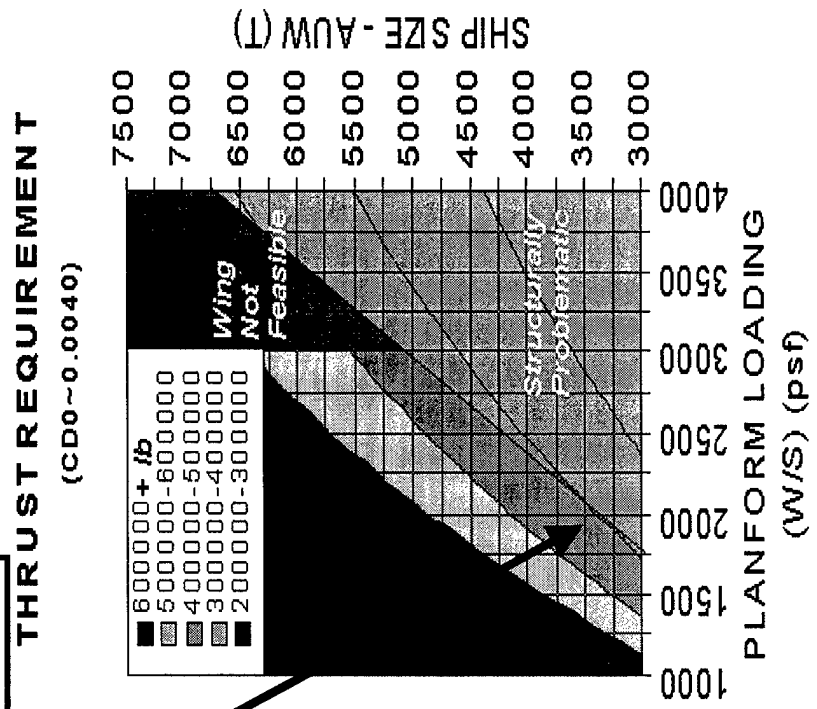
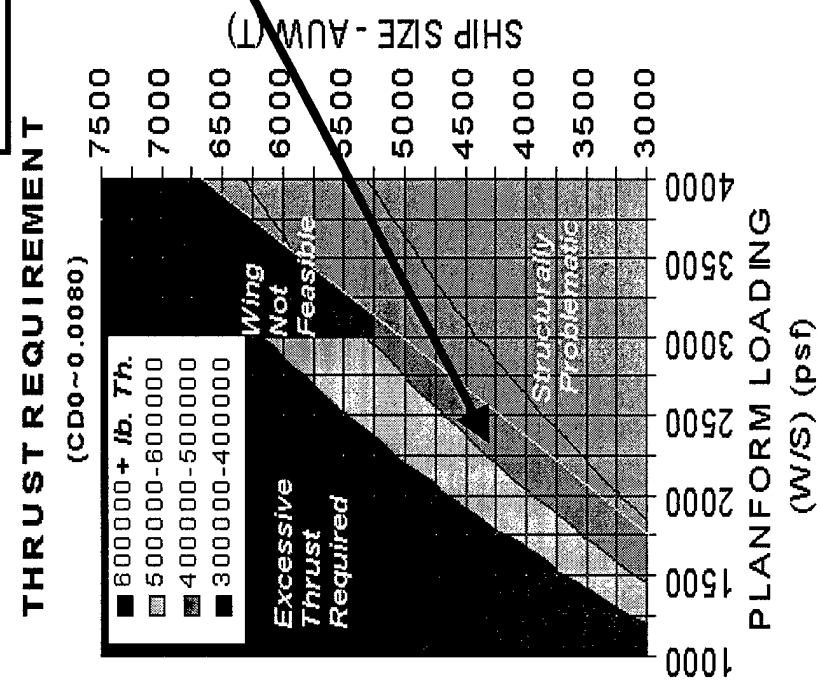
The range of feasible hydrofoil sizes is limited, largely to the combinations of the design constraints, propulsion system integration (air and water coupled propulsors) characteristics, structural material currently available and the amount of viscous drag reduction. If three water jets with total thrust near 900000 pounds were available, the largest hydrofoil that could be scaled off of the 4000T, 125 ft beam system would be in the range of 10KT to 12KT total displacement.

Feasible Vehicle Sizes - Effect of Viscous Drag Mitigation

Without Viscous Drag Mitigation, the practical vehicle size is severely constrained by low TSFC Thrust Limitations, Wing Planform Limitations and Structural Feasibility Concerns.

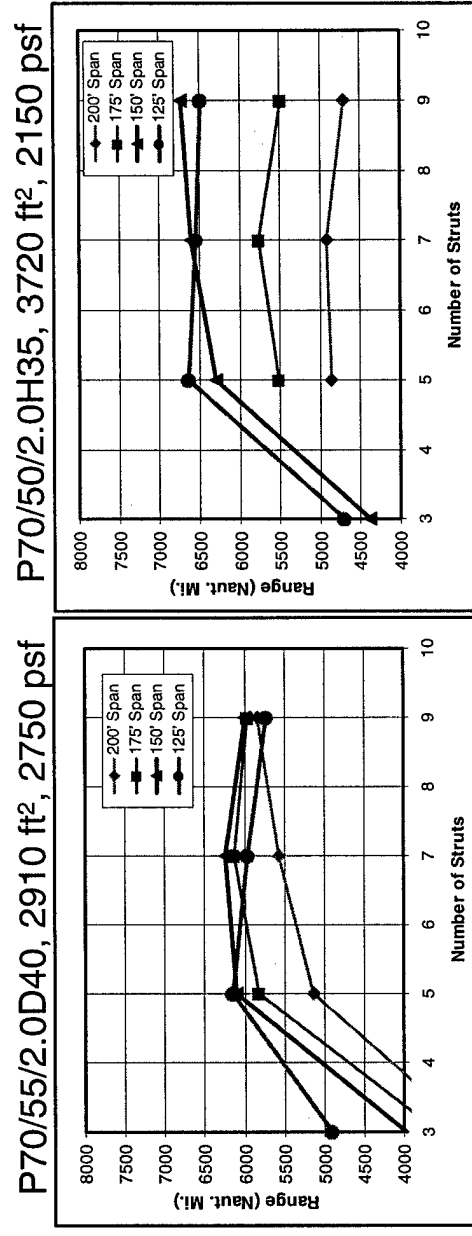
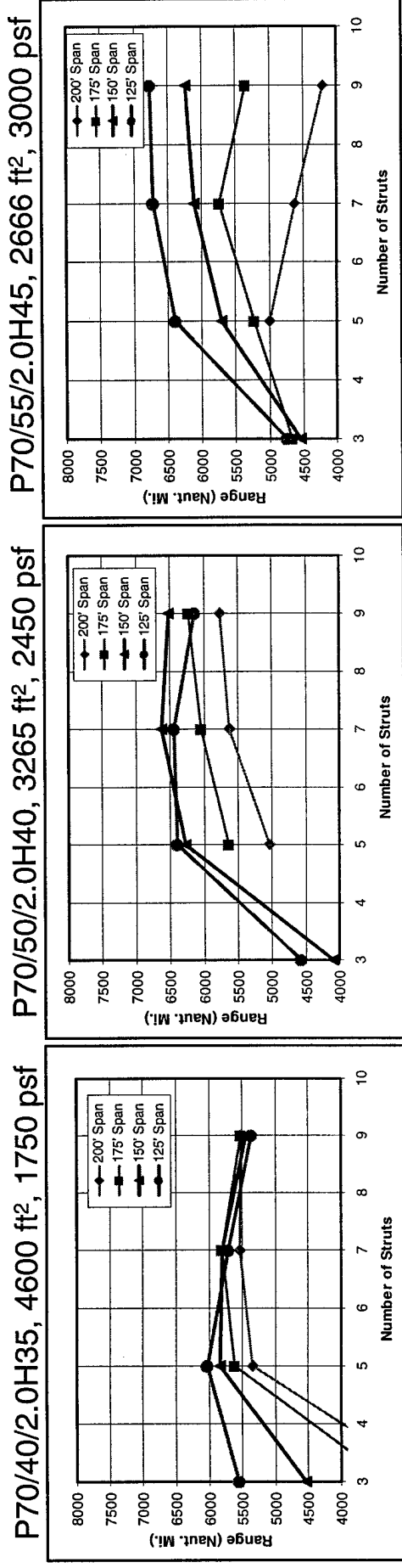
Optimum TSFC solutions are for ~400,000 lb cruise thrust, leading optimum sized ships to 4000T-6000T for W/S=2450psf; 3500T-5000T for W/S=1750psf (depending upon CD0)

Feasible Design Space



Hydrofoil Structural Sizing Results

Range Vs. Number of Struts and Wing Span



Maximum theoretical zero-payload range = 6767 nautical miles (FWF = 45%)

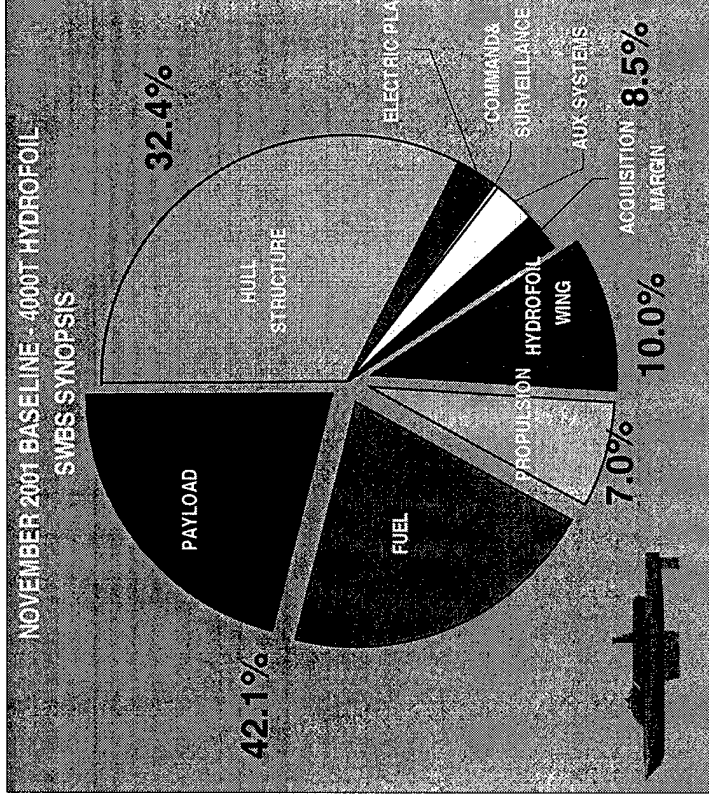
Hydrofoil SWBS – CSC-based Assessment

Bottoms-Up type payload range estimates were needed as well. It is important to realize that a high von Karman efficiency is not a guarantee to economic feasibility. The fraction of the system weight that can be used for economic purposes should be the real indicator of usefulness or practicality.

Nonetheless, the mass fraction of the ship that was used for sustentation was only as good as the estimates of the other on-board systems and their fraction of the total. Since the technical background of LM Aeronautics was largely aero-structural, CSC-Advanced Marine was brought on board to support the development of a Ship Weight Breakdown Structure (SWBS) and identify candidate hull designs and resistance estimates. The results of the that effort are shown in the following pie-chart. Sustentation weight is directly estimated and added to the SWBS. At 4000 tons the hydrofoil wing contributes to 10% of AUW. Propulsion estimates are based on a air-coupled approach and the remaining payload/fuel fraction is on the order of 42%. The Fixed Weight Fraction (FWF) is then 58%. At the onset of the study, the goal was for a FWF of no greater than 50%.

Hydrofoil SWBS – CSC-based Assessment

4000T Hydrofoil



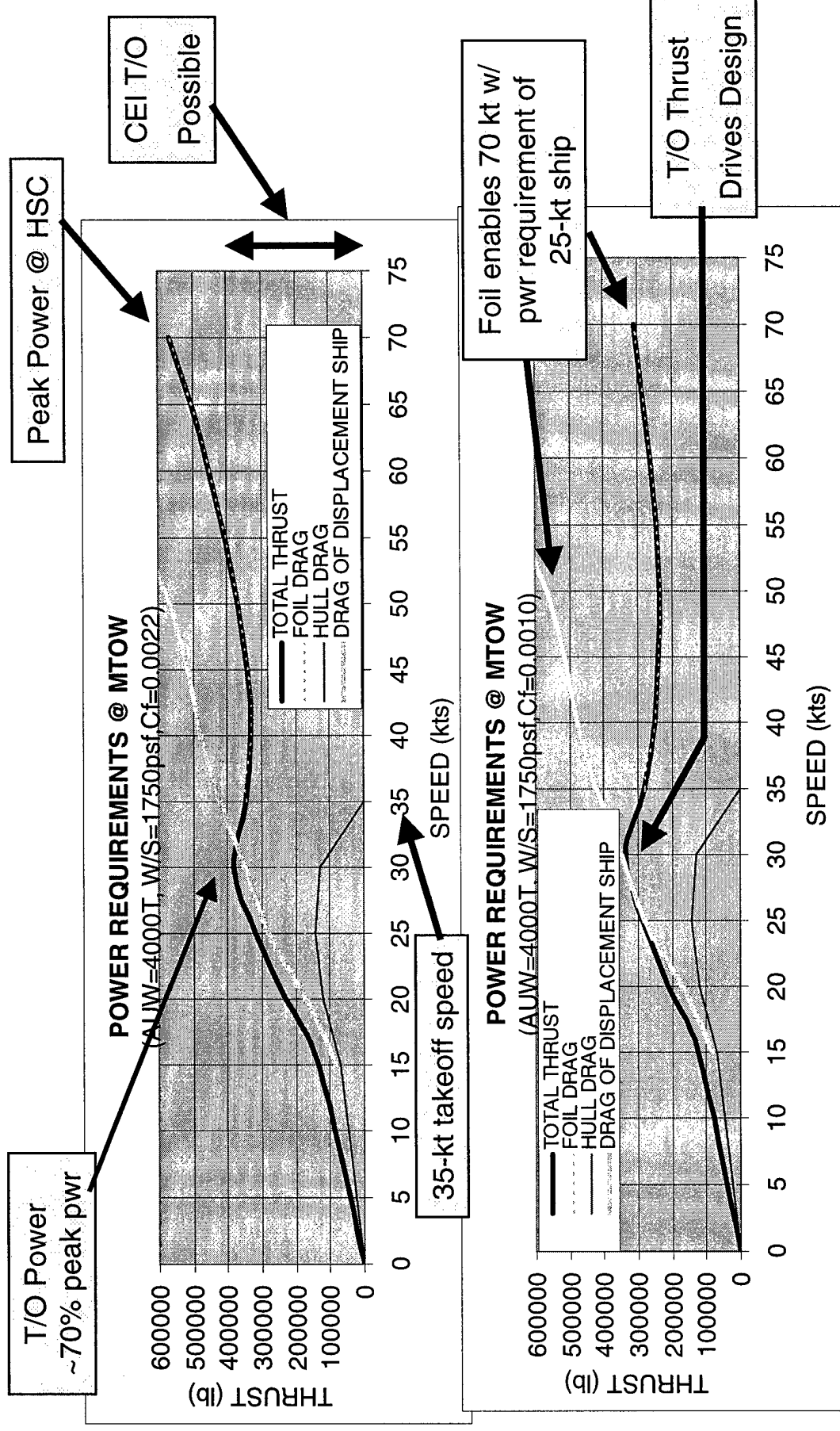
The fraction of the All Up Weight (AUW) for the Foil and Strut System is approximately 10% and the Payload/Fuel is on the order of 42%

4KT Hydrofoil Take-Off Thrust Requirement

For the 4000 Ton Hydrofoil, the ship hull resistance is combined with the foil drag and the take-off power requirement is determined. The air-coupled system restricted to 400000-500000 pounds total thrust due to the beam constraint. A water-coupled system is not beam restricted and could produce 150000 pounds thrust per LM6000 with a water jet from 5 knots through 70 knots. Reducing viscous drag will reduce overall cruise power needs, the take-off will then be the pinch point in the power speed curve.

4KT Hydrofoil Take-Off Thrust Requirement

- Recall that Dimensional Drag sizes Powerplant



4KT Hydrofoil Propulsion System Summary

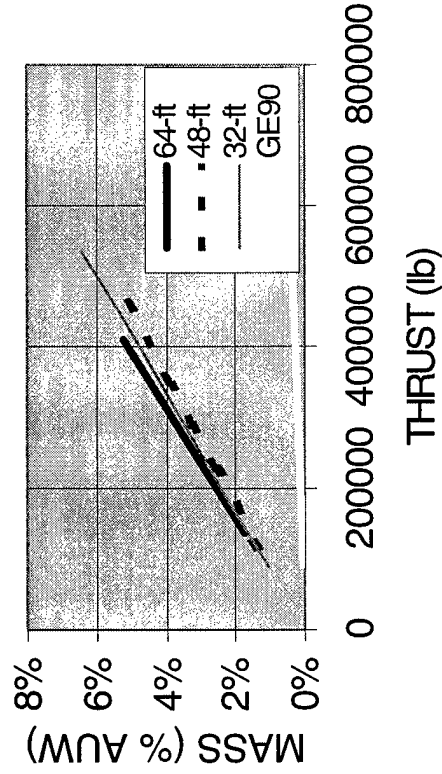
Various means of provided thrust-required were examined. The air-coupled systems resulted in large, high risk propellers with TSFC's ranging from 0.12 to 0.18. The water coupled systems, either super-cavitating propellers or water pumps, were capable of similar thrust levels at TSFC's of 0.10 to 0.12. For the 4000 Ton hydrofoil, three 50KSHP LM6000 gas generators would be needed. Auxiliary thrust could be provided with a commercial turbo-fan engine for a small FWF penalty is hump speed drag is higher than expected.

4KT Hydrofoil Propulsion System Summary

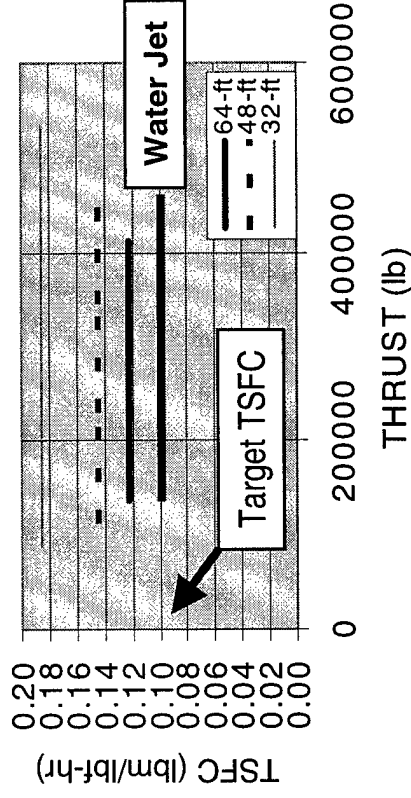
MOTOR	PROP DIA (ft)	WT (T)	THRUST @ 70-kts	TSFC @ 70-kts
LM-6000	64	70	136920 lb	0.122
LM-6000	48	52	116273 lb	0.145
LM-6000	32	43	89107 lb	0.185
LM-6000	9.0	70	150000+ lb	0.10

MOTOR	FAN DIA (ft)	WT (T)	THRUST @ 70-kts	TSFC @ 70-kts
GE-90	12	3	92000 lb	>0.3

PROPULSION SYSTEM MASS
(NORMALIZED TO 4000T AUW)

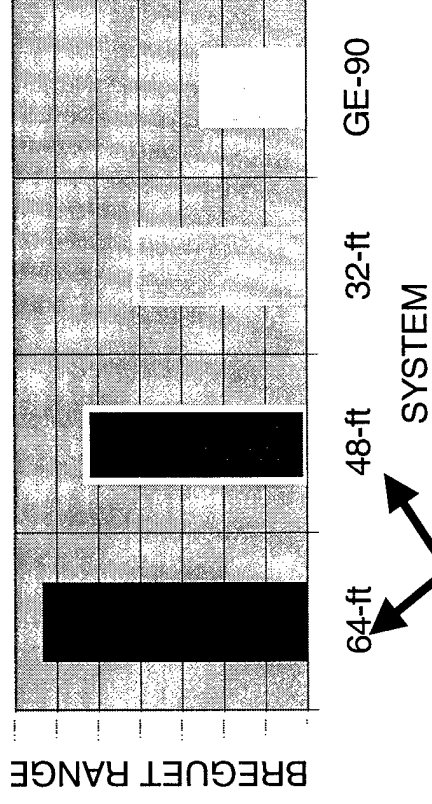


PROPULSION SYSTEM TSFC
(LM6000 Gas Generator)



PROPULSION SYSTEM TRADE STUDY

(NORMALIZED TO 4000T AUW, ~50% FWF, 400,000-lb Thrust)



Efficient Options limited to 400000-500000 lb Thrust

Hydrofoil Sizing/Synthesis Closure

- What really is the “Optimum”?
 - Meets the primary requirement
 - » Payload @ Range
 - Balance wing weight, wing buoyancy with hydrodynamic efficiency
 - “Reduced sweep” wing section options are not markedly better than the optimum performance wing sections
 - Meets the secondary requirements
 - » 65-m / 213-ft Beam & “Reasonable” Power
 - Balance induced drag at take-off, wing-section takeoff speed and hull drag
 - Water Coupled system – 900,000 lbs thrust, Air-Coupled System-450,000 lbs thrust
 - Maximizes the tertiary requirement
 - » High von Karman Efficiency
 - » $k_2=100\%$ solutions $\rightarrow L/D \sim 15$, $\text{vonK} = (70\text{-kt})(15) = 1050\text{-kt}$
 - » $k_2 = 50\%$ solutions $\rightarrow L/D \sim 30$, $\text{vonK} = (70\text{-kt})(30) = 2100\text{-kt}$

Hydrofoil Payload Range Conundrum

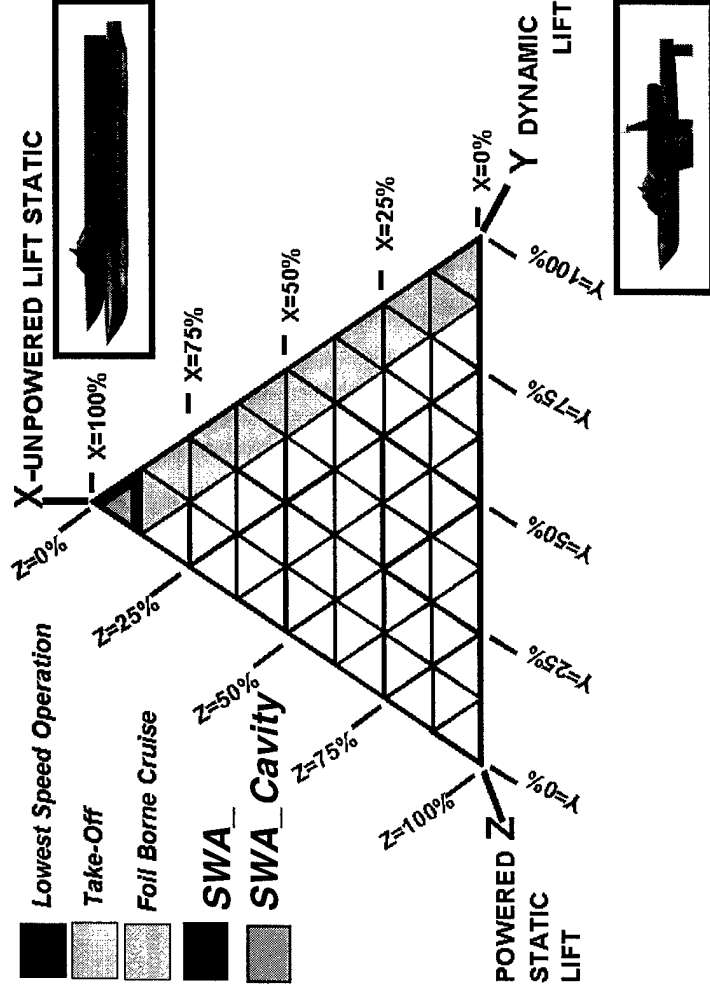
- **Design Space Broadens**
 - Many different solutions provide similar range performance!
- **“Best” and “Runners Up” Dependent upon “Goodness Criterion”**
 - Best Range @ Zero-Payload not Best Range @ 1000T Payload
 - Best Range @ Payload not necessarily Highest Karman Efficiency
- **Contributing Factors to Payload-Range Behavior**
 - Trade-off between FWF and L/D
 - Configuration insensitivity is due to :
 - » improvements in L/D occur at an expense in weight
 - » reductions in foil system weight tend to reduce L/D
- **Effect of Viscous Drag Mitigation ($k_2 < 100\%$)**
 - » CD0 less important » Buoyancy more important » Induced Drag more important
 - » $k_2 < 100\%$ drives design to high buoyancy, high wetted area designs
- **1000+T payload capacity @ 6000nM requires $k_2 < 50\%$**
- **With little payload-range difference between top candidates secondary effects become design discriminator (i.e. Take-Off Power)**
- **The Next Step is to Investigate the Mixed Buoyancy System to determine if there is a Optimum!**

Expanded Design Space – Sustention Triangle

The sustention triangle is useful in describing the trade-off between the un-powered static lift ($x=100\%$) and the dynamic lift ($y=100\%$). Small waterplane area vessels have been known to have low wave making resistance as their sustention is below the free surface. They do suffer from viscous resistance as do most conventional surface running ship. An alternative to this may be a cavity ship, which with a small amount of powered lift (pressurized air supply) act to dramatically reduce the viscous drag on the lower surface of the submerged hull. The nomenclature which will be used is a Small Waterplane Area Cavity Hull or SWACH.

Expanded Design Space – Sustention Triangle

- General Theory of Static Lift Payload Performance
 - Understand how to trade hydrodynamic performance for fuel fraction through the choice of submerged body sections and propulsion integration in order to maximize mission performance



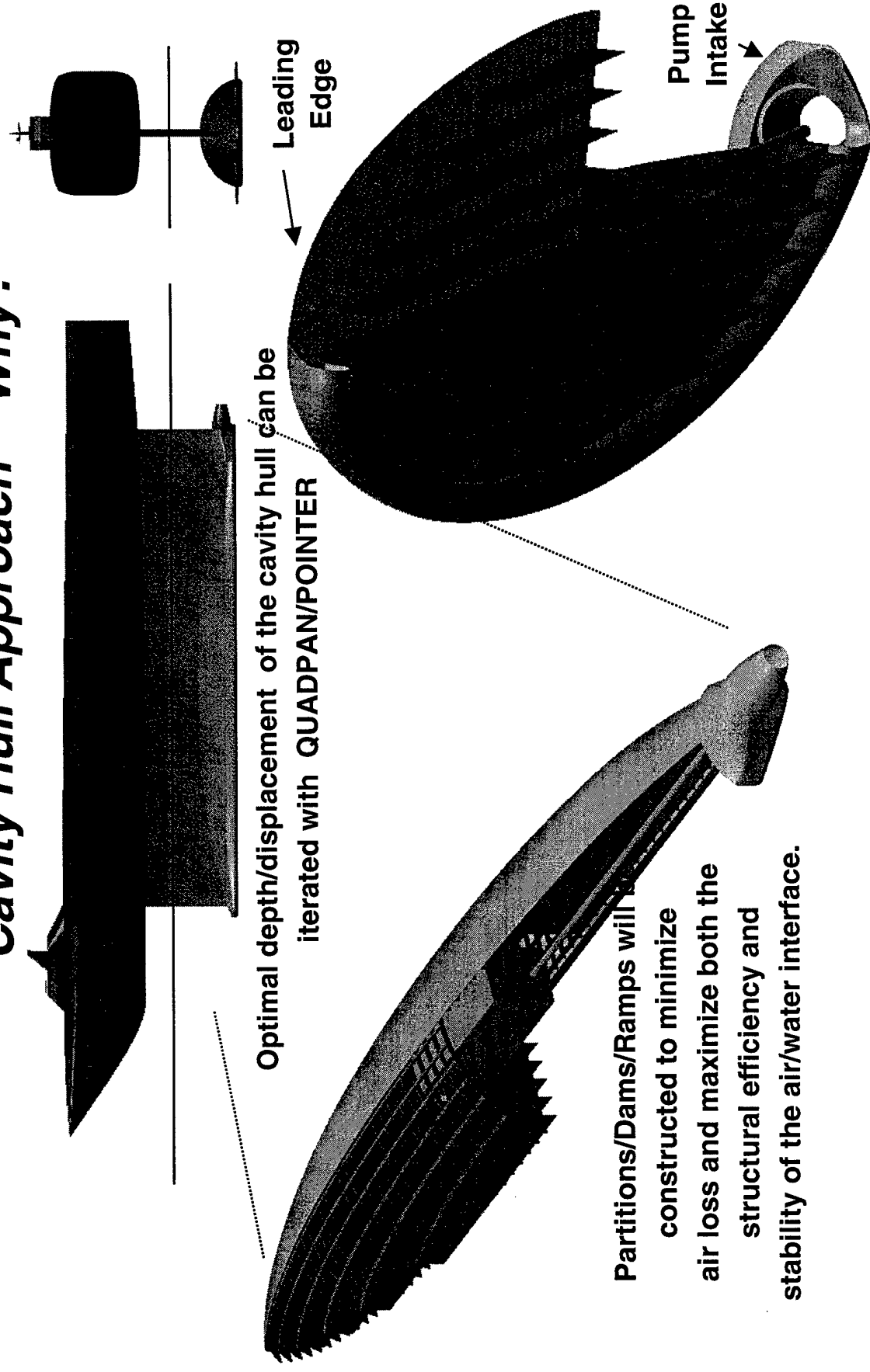
NOTE : if dramatic viscous drag reduction* is feasible, static lift may ultimately prove to be competitive with dynamic lift. (I.e. a SWA_CH ship becomes the preferred solution above 12 KT.)

***This is to specific and should be generalized to read:
dramatic viscous drag reduction and the cavity hull approach**

Cavity Hull Approach – Why?

The advantage of the cavity hull is shown in the following slide. An air-to-water interface is provided on the lower surface of the flat bottom hull. The depth and shape of the individual cavities as well as the airflow demand would have to be determined with technology trades, nonetheless the means for a much reduced viscous resistance is provided.

Cavity Hull Approach – Why?



Benefit: One-Half the Wetted Skin Friction of a Full Ellipsoid Buoyant Body

Mixed Buoyancy Trade Study

The most complex situation occurs where we have a mixed-buoyancy vehicle, in particular one where the vehicle's buoyancy exceeds its structural weight. For the general case, the vehicle would begin its flight operating as a dynamic lift vehicle - burning off fuel, and, consequently demanding less lift until, perhaps, so much fuel is burned off so that the vehicle reverts to operating as a displacement hull. Excess theoretical buoyancy resulting from further fuel consumption would be offset by taking on ballast. The total lift of the vehicle is the simply the sum of the static and the dynamic lift. The standard dynamic lift nomenclature varies somewhat to include the follow differences.

Traditional Hydrodynamic L/D

- » $L/D = \text{Lift_Dynamic} / \text{Drag}$
- » Buoyancy of wing system book-kept as a reduction in "all up weight"

System L/D

- » $L/D_{\text{system}} = (\text{Lift_Dynamic} + \text{Lift_Static}) / \text{Drag}$
- » Buoyancy of wing system book-kept as static lift

Payload over Range

- » Not a function of buoyancy book-keeping

Karman Efficiency

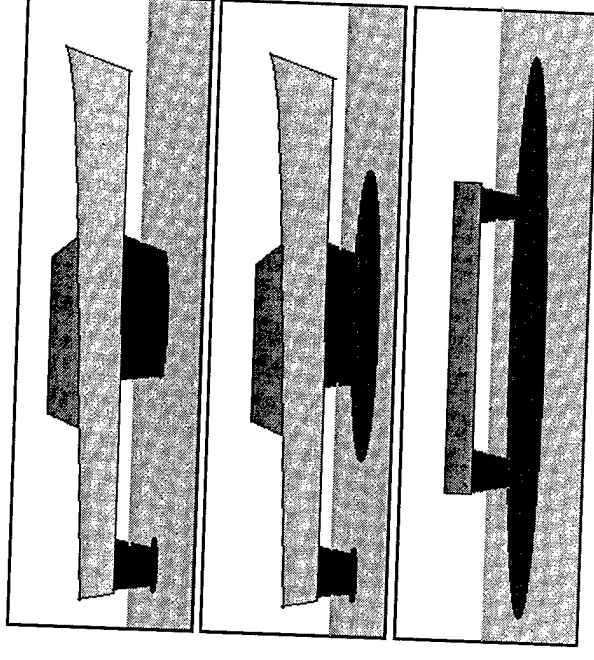
- Metric depends upon buoyancy book-keeping

Mixed Buoyancy Trade Study

- Design Trade
 - Document Effect of Buoyancy Fraction,
 $BF = \text{Lift_Static} / (\text{Lift_Static} + \text{Lift_Dynamic})$
 - » impact on underwater configuration
 - » impact on hydrodynamic efficiency
 - » impact on payload/range
 - » “optimum” buoyancy fraction
 - for a given vehicle size
 - for underwater viscous drag reduction (k_2 factor)

Examples:

- Dynamic Lift Hydrofoil
- Mixed Static/Dynamic Lift (HYSWAS)
- Static Lift (Small Waterline Area)

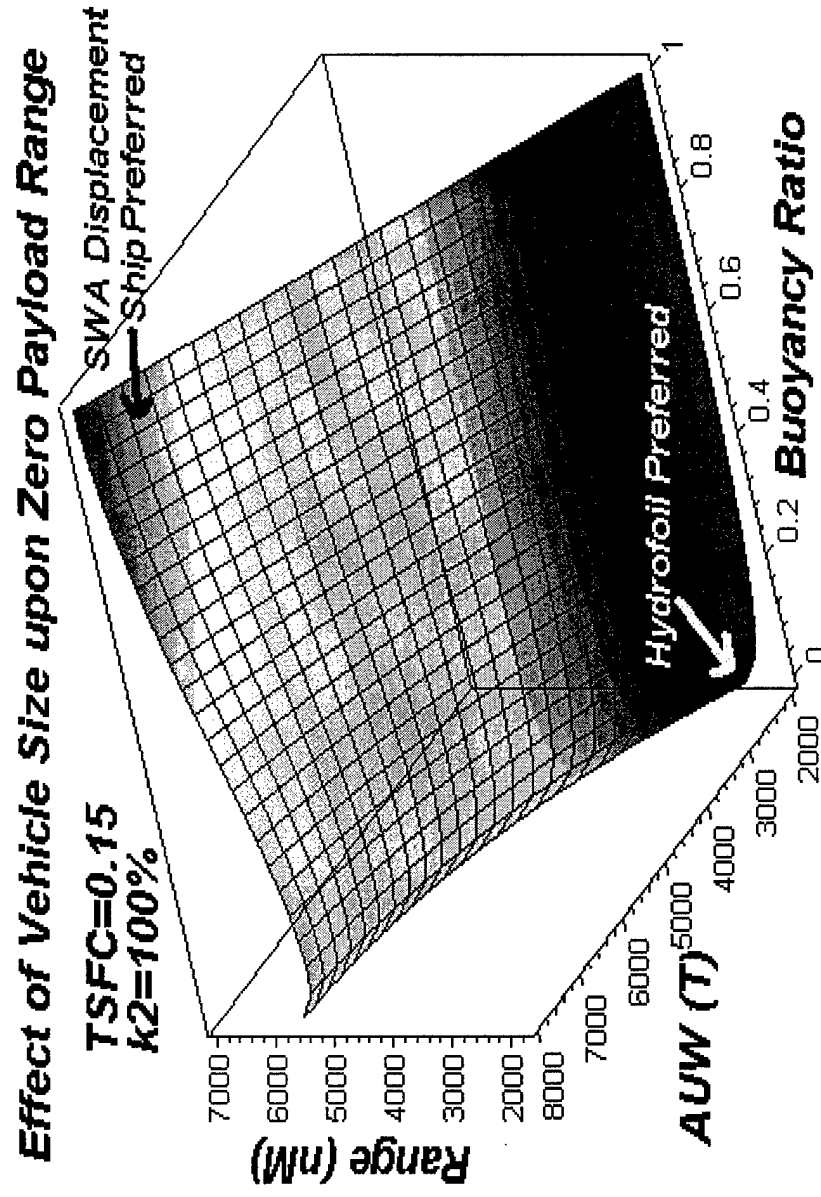


Mixed Static/Dynamic Lift Vehicles at Varied AUW

As shown indirectly with the reduced viscous drag on the pure hydrofoil, the impact of varied sustentation (which can come without either induced drag or wave drag) was determined by integrating the revised mixed static/dynamic equations. The impetus for additional investigations into SWA ship is shown in the following slide. As the size of the ship increases, the amount of buoyant lift becomes evermore effective and leads to ships with increased range.

Mixed Static/Dynamic Lift Vehicles at Varied AUW

- A small Hydrofoil Ship has greater hydrodynamic efficiency, hence greater range than a small SWA displacement ship. L/D of hydrofoils declines with increasing size. L/D of SWA ship increases with increasing size. Crossover around 5000T AUW.

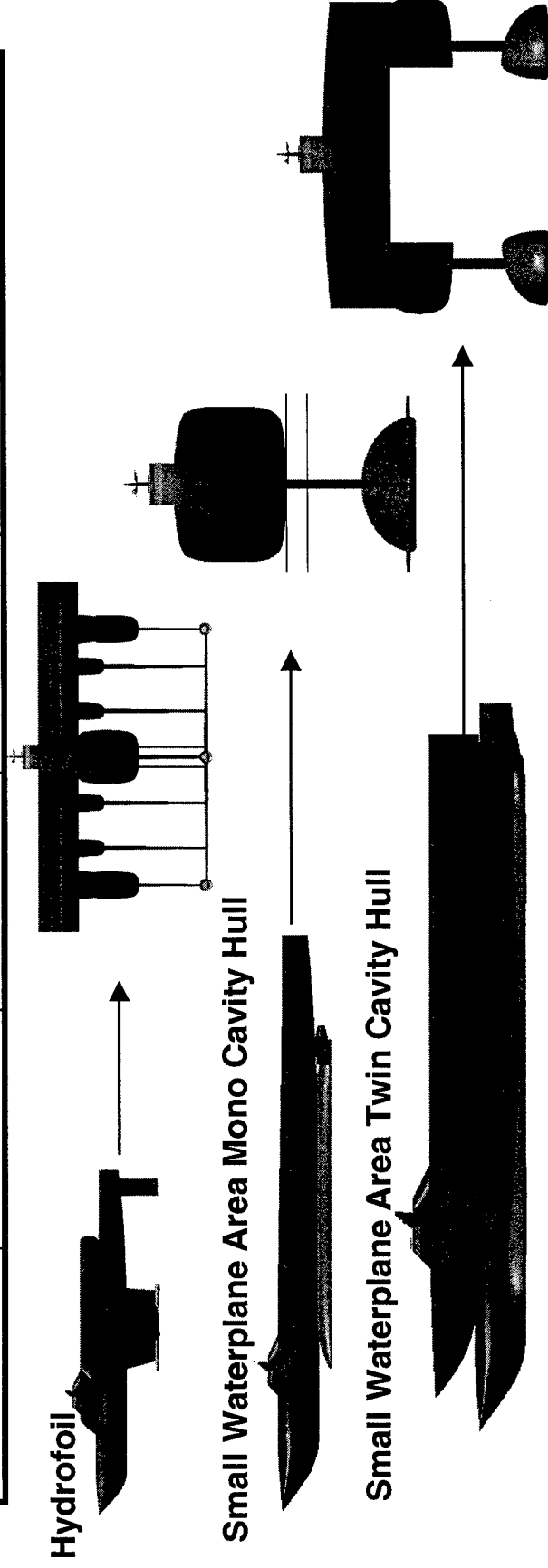


Drag Sources and Physical Dimensions for the Varied Vessel Types

The ships investigated varied with respect to the type and number of hulls, support structures, trim effectors and propulsion integration types. The goal was to examine the range of ships that would satisfy the previously laid out design constraints and determine the potential performance using a combination 1st order drag prediction methods and where possible implement higher-order methods such as free-surface potential flow codes coupled with a modern optimizer. Note that the sources of drag are similar for all of the designs under investigation. The following slides show the variations of the designs that either do, or do not satisfy the design constraints of: port depth, berthing length and the maximum beam. As shown, the largest vessel that fully satisfied the design constraints was the 31.5KT SWATCH. Above that displacement the constraints are exceeded, first in depth, and then in beam and length.

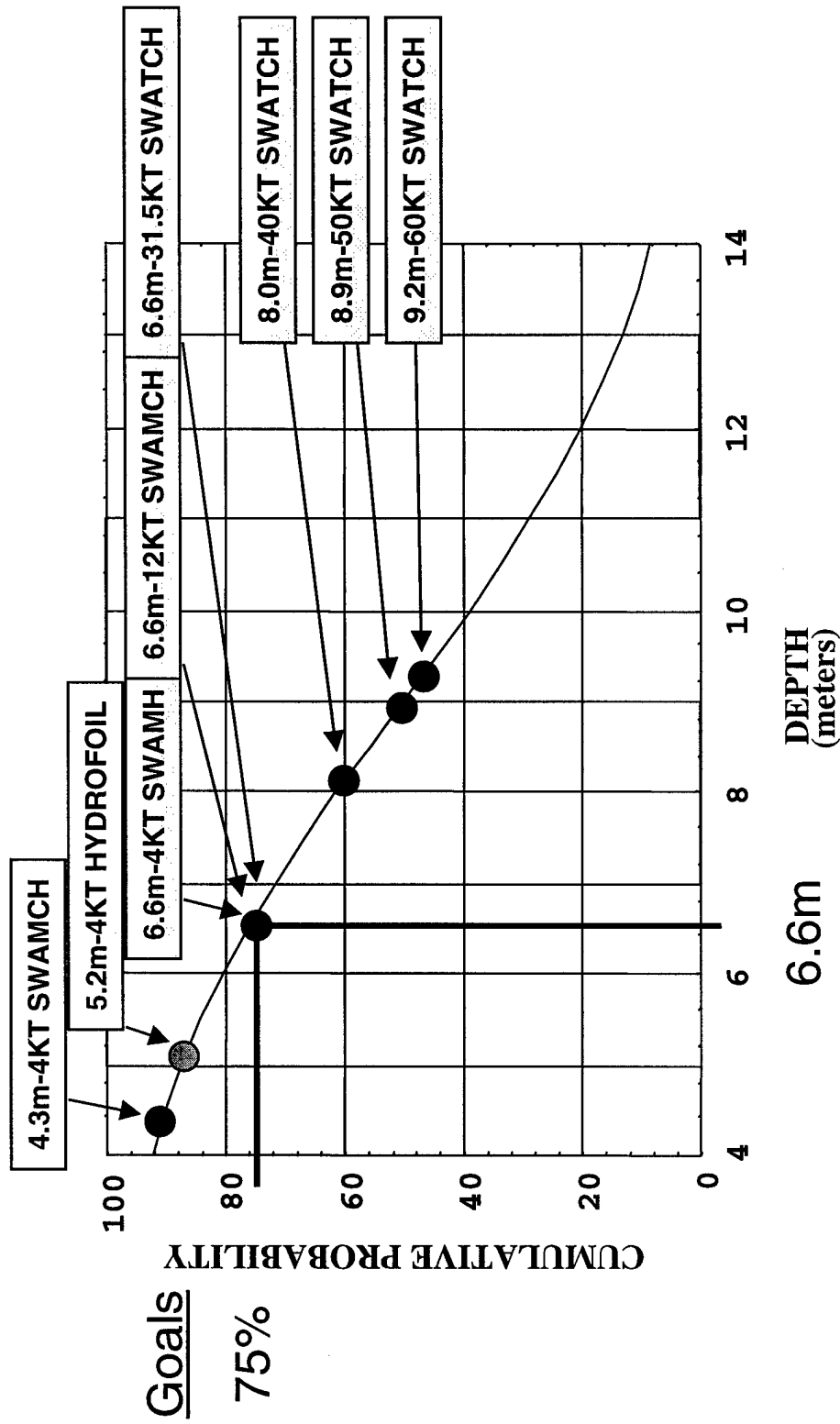
Drag Sources for the Varied Vessel Type

Vessel	Wave Drag	Induced Drag	Friction & Form	Spray Drag	Propulsion Drag
Hydrofoil	1-Foil, 9-Vert. 1-Horz.	1-Foil 1-Horz.	1-Foil, 9-Vert. 1-Horz.	9-Vert.	3-Pumps
SWAMCH	1-Body, 4-Horz. 1-Vert.		1-Body, 4-Horz. 1-Vert.	1-Vert.	1-Pump 1-Cavity
SWATCH	2-Bodies 2-Vert.		2-Bodies 2-Vert.	2-Vert.	2-Pumps 2-Cavities



***QUADPAN/POINTER Performance Roll-Up**

Port Depth* as a Design Constraint



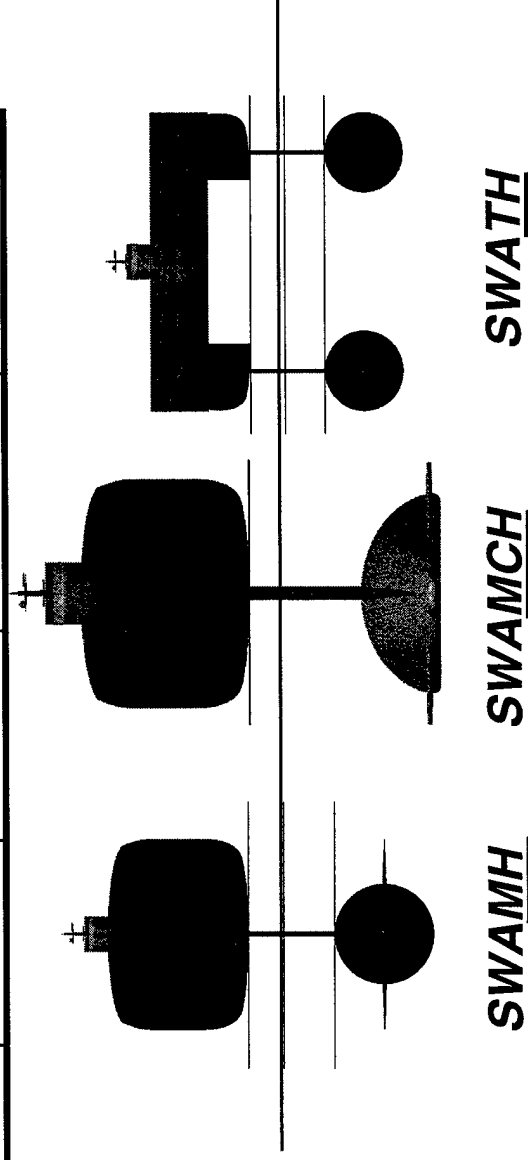
Lloyd's Ports of the World

Line(s) = Gaussian Distribution: mean = 9.0 m; $\sigma = 3.55$ m

*Statistics and compilation received from A. Ellinthorpe

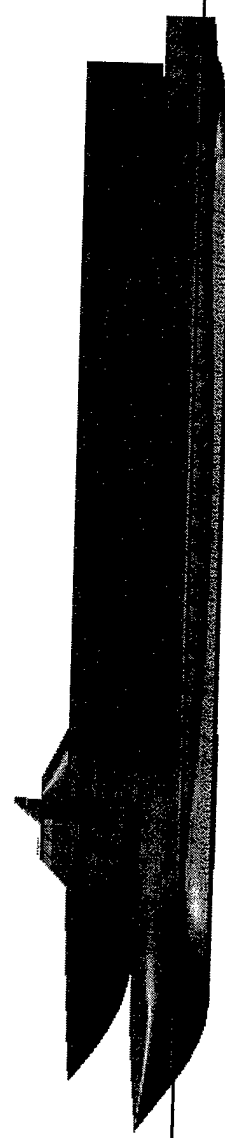
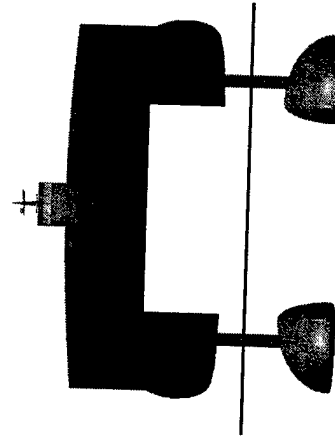
SWAMH, MCH & TH Vessels – 4000T to 12000T

Displacement	4KT MH	4KT MCH	12KT MCH	4KT TH
L.O.A.-ft.	477	477	650	315
BEAM-ft.	64.6	64.6	87.9	100
DRAFT-ft.	21	14	21	21
Body Length-ft.	231	257	392	185
Body Diameter-ft.	34.2	50/20	77/31	27.9
Body Fineness Ratio	6.75	12.8	12.6	6.75
L/B Ratio-ft.	7.4	7.4	7.4	3.1
Floor Area sq.ft.	11900	11900	22400	11200



SWATCH Vessels – 31,500T to 60,000T

Displacement	31.5KT	40KT	50KT	60KT
L.O.A.-ft.	650	650	739	785
BEAM-ft.	200	208	236	251
DRAFT-ft.	21	26	29	30
Body Length-ft.	496	523	563	600
Body Height-ft.	33	34	37	39
Body Width-ft.	50	53	57	60
L/B Ratio-ft.	3.25	3.13	3.13	3.13
Floor Area sq.ft.	60800	60800	81700	91000

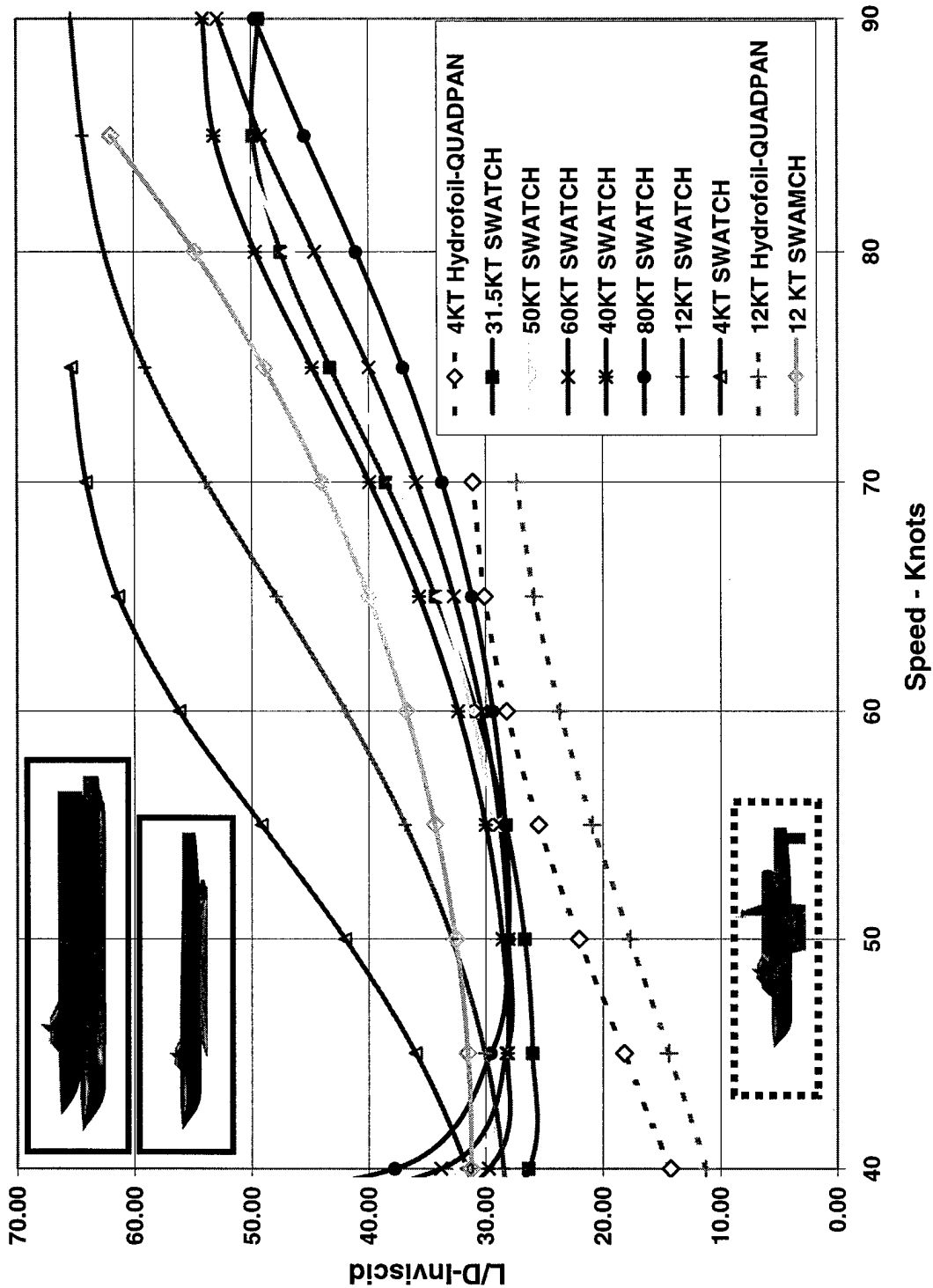


Hydrodynamic Efficiency – Varied Designs

The following two slides contrast the varied drag sources and their magnitudes for the ships shown in the previous slides. Most noteworthy is the elevated efficiency of the larger SWA ships. The hydrofoil at 4KT is more efficient than a SWA of comparable displacement. As the SWA displacement increases, the wave drag hump speed is pushed higher and higher. The difference between the 12 KT mono and catamaran cavity ships shows the benefit of a depressed hump speed. Careful examination will show that there is an optimal size ship for a common body design.

Inviscid Hydrodynamic Efficiency – Varied Designs

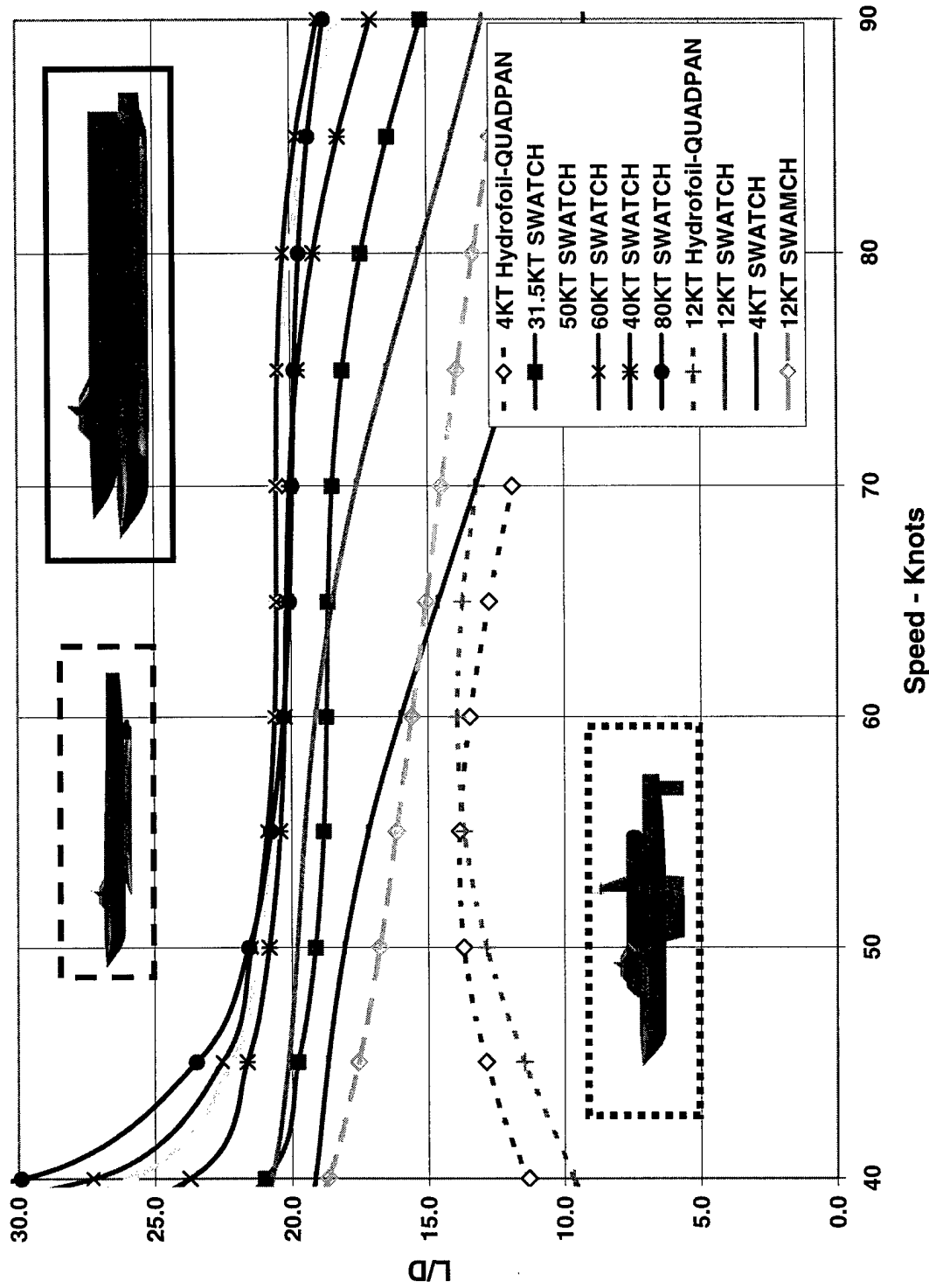
Ship Lift-to-Inviscid Drag Ratio



Hydrodynamic Efficiency – Varied Designs

Ship Lift-to-Drag Ratio

Full Skin Friction, 1.5% t/c SWATCH Struts, P29TA12 Bodies

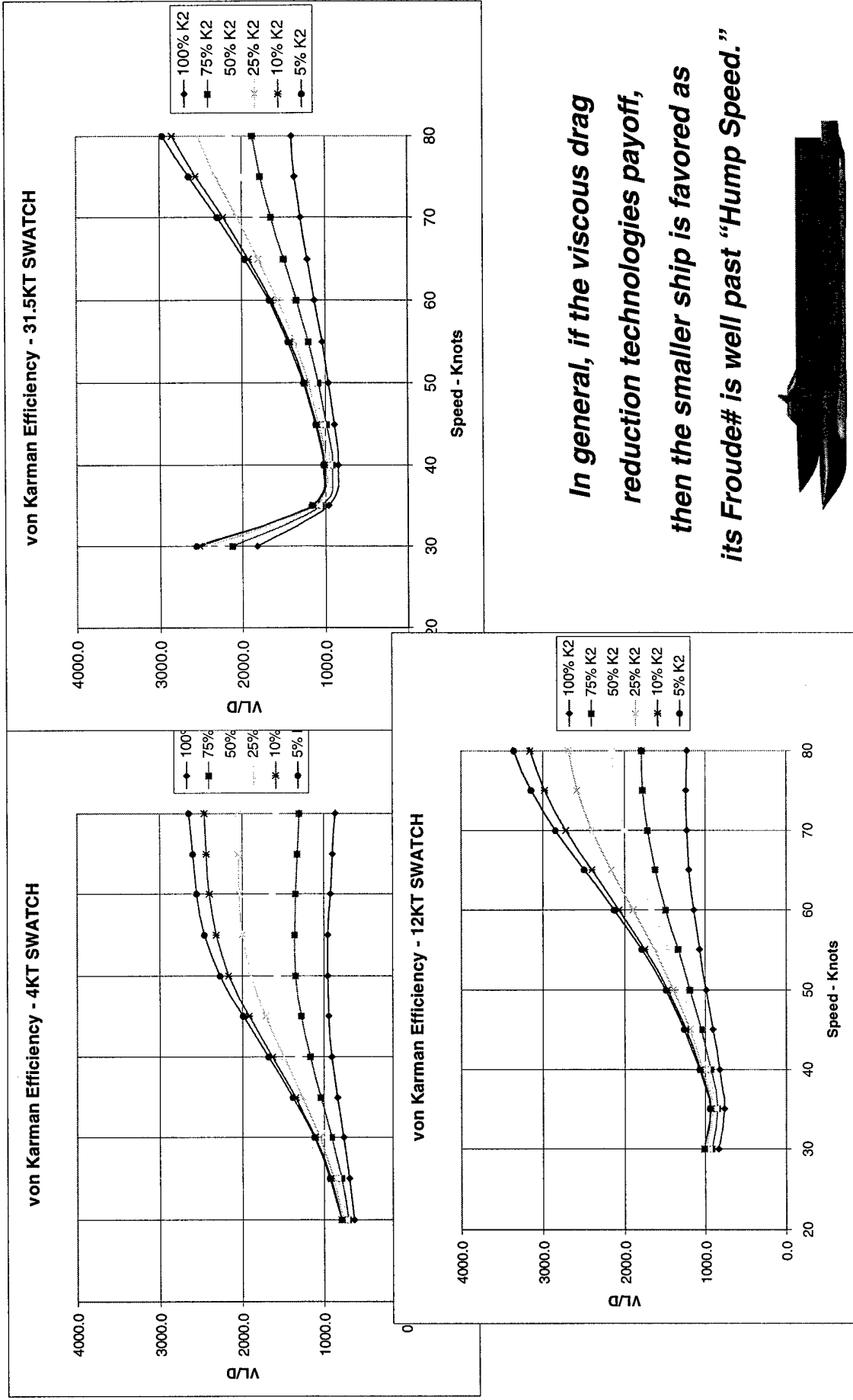


Varying amounts of viscous drag reduction had a significant impact on performance. The key measure was the von Karman efficiency parameter. The following plots are for varied designs and varied amount of viscous drag reduction. For the SWATCH ships in general, if the viscous drag reduction technologies pan-out, the smaller ship is favored as its Froude# number at cruise is well past "Hump Speed." If the drag reduction goals are not met, the larger ship is favored with its higher volumetric efficiency. Finally, if the ship size is pushed to 80KT, the wave drag becomes a limiting factor. Two modes of operation may be possible based on a "Double Hump" wave drag behavior with the larger ships.

As for the hydrofoil at a fixed wing aspect ratio, there is little advantage in growing its size. Support and control effector wave and spray drag work against it non-linearly.

In the last of the von Karman efficiency plots, the mono- and catamaran cavity hull ship are compared. Clearly, the reduced wave drag of the SWATCH favors the SWAMCH at a constant displacement.

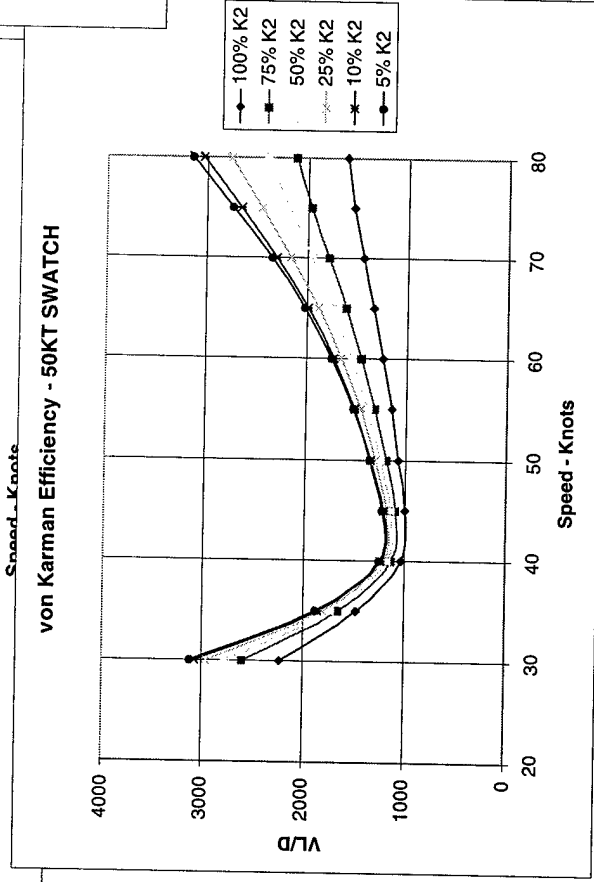
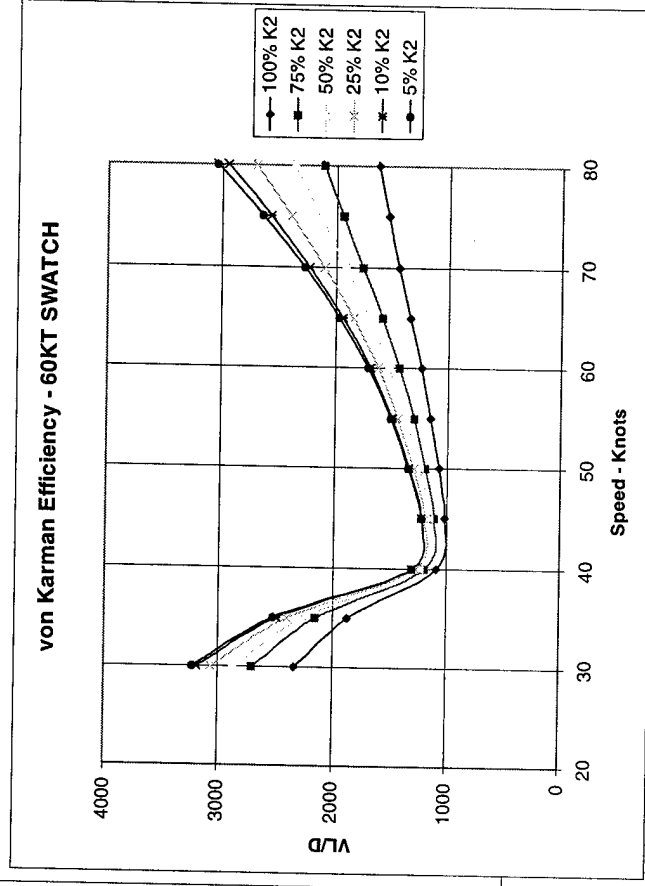
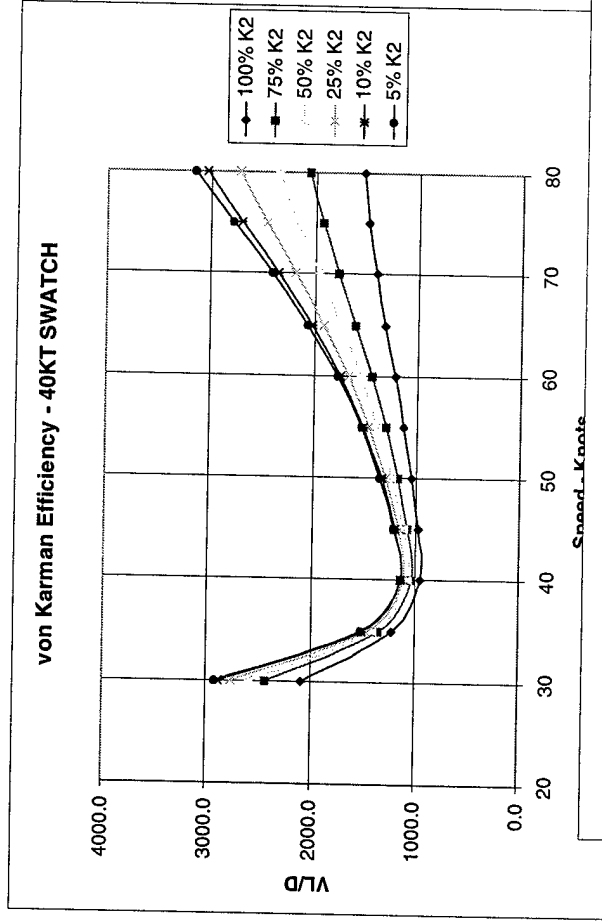
von Karman Efficiency – 4KT, 12KT & 31.5KT SWATCH



In general, if the viscous drag reduction technologies payoff, then the smaller ship is favored as its Froude# is well past "Hump Speed."

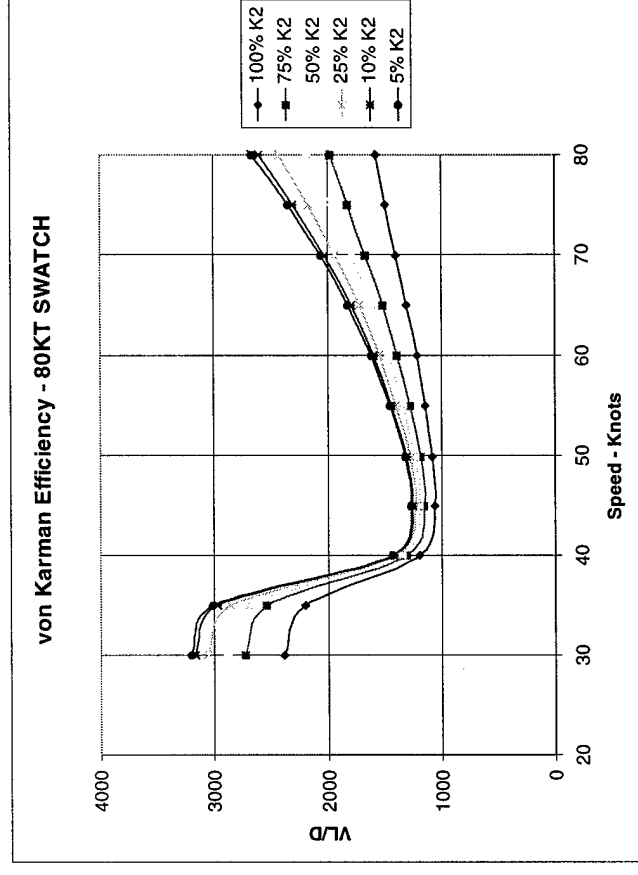
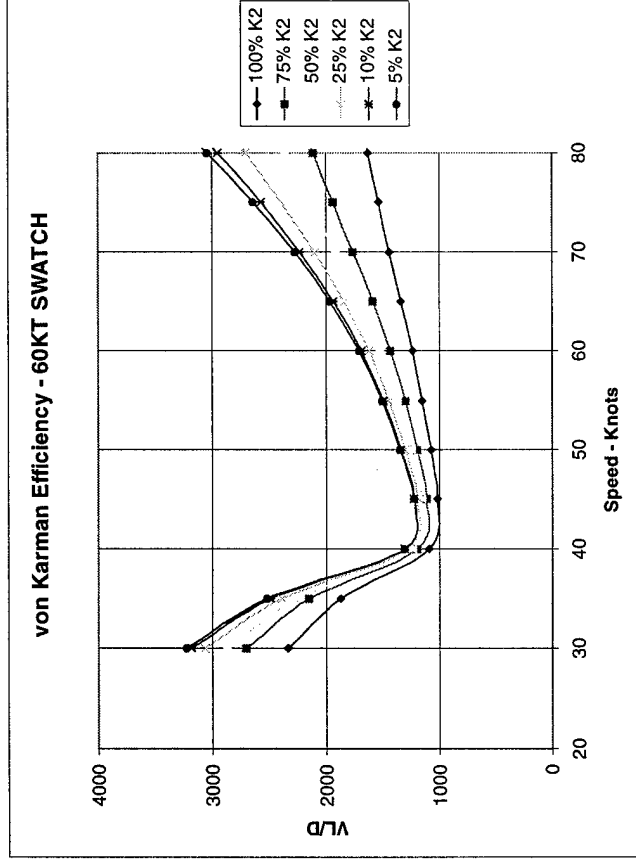


Karman Efficiency – 40KT,50KT & 60KT SWATCH



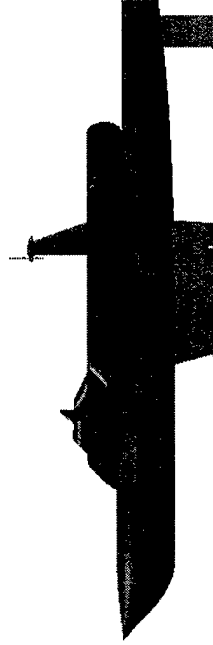
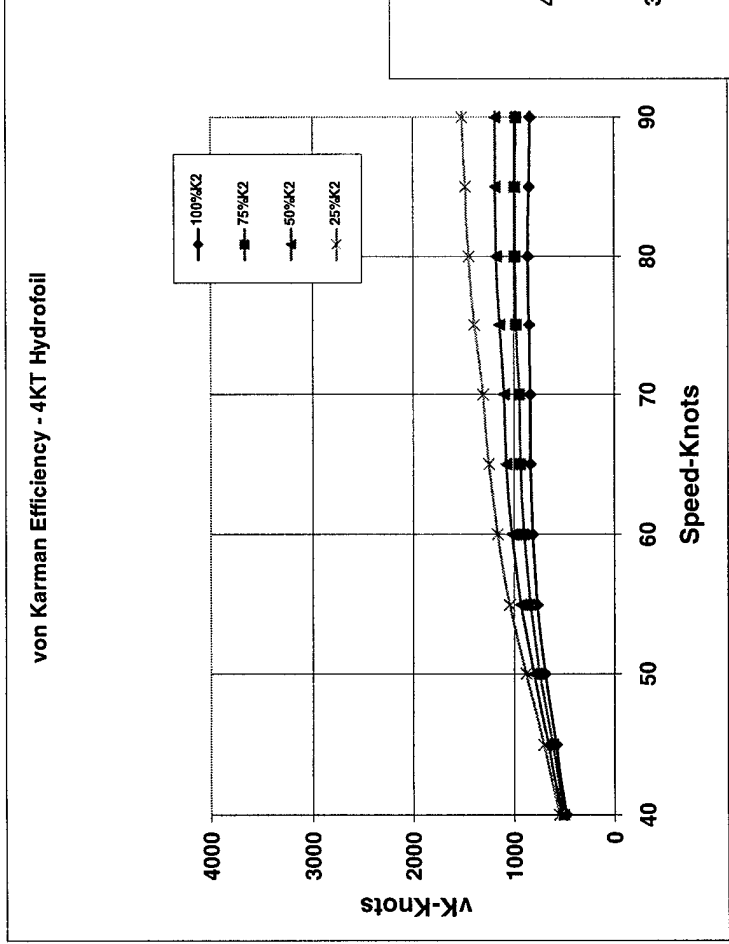
If viscous drag reduction technologies do not pan-out, the larger ship is favored as with its higher volumetric efficiency.

Karman Efficiency – 60KT & 80KT SWATCH

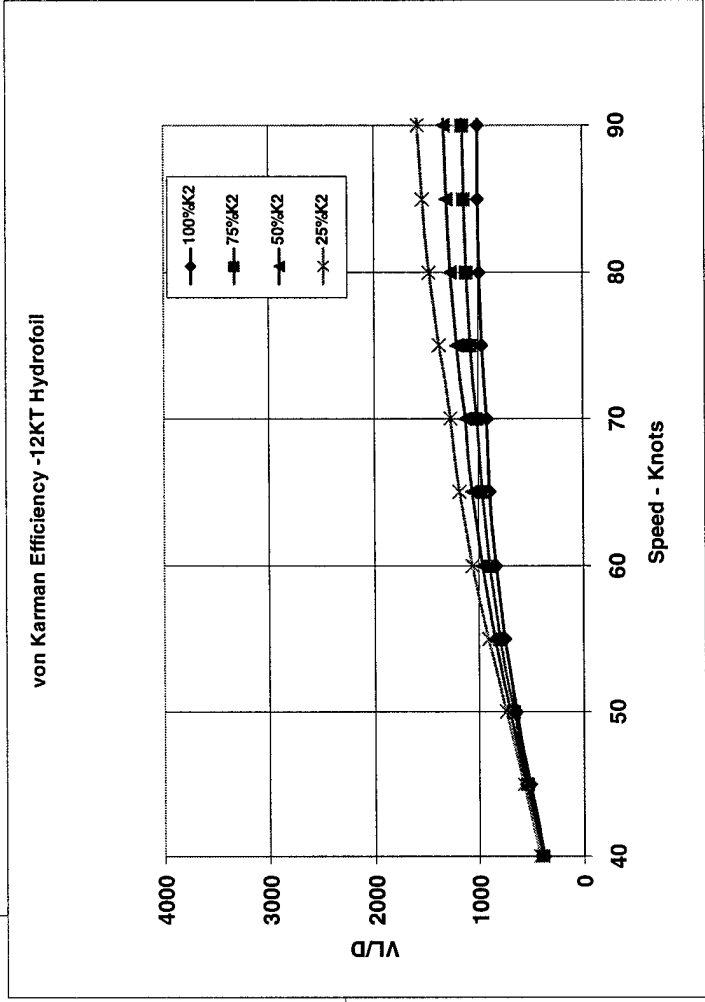


***If the ship size is pushed to 80KT, the
Wave drag becomes the limiting factor
Note that with the “Double Hump” Froude
number behavior – two efficient modes of
operation may be possible!***

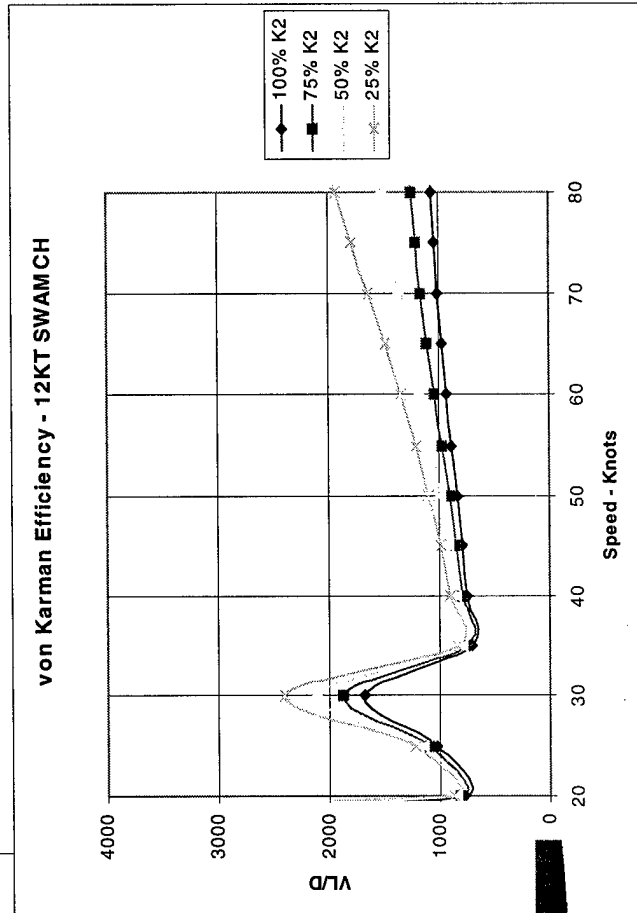
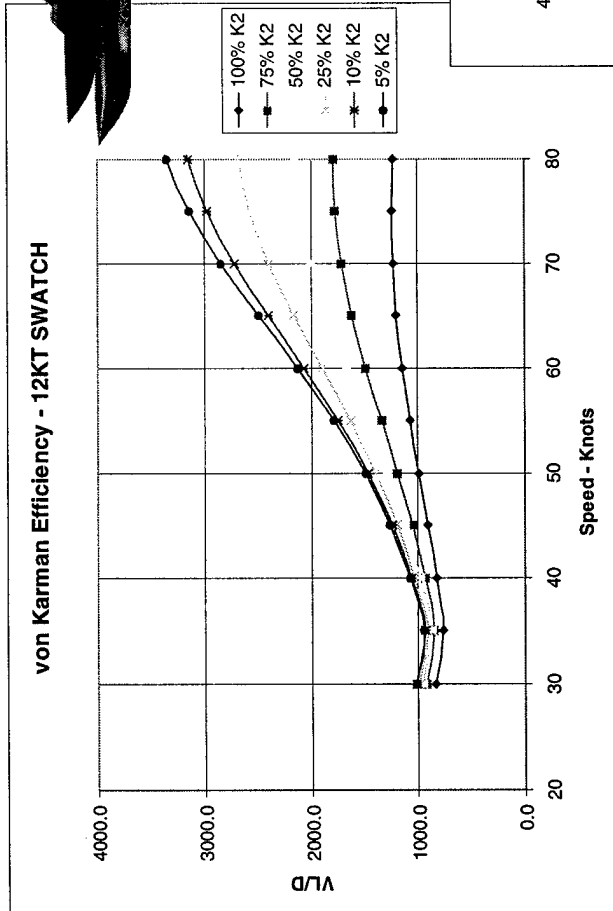
Karman Efficiency – 4KT and 12KT Hydrofoils



For the Hydrofoils at a fixed Wing Aspect Ratio, there is very little advantage of going to a larger vessel from a von Karman basis. Trim-related and spray drag are key limiters to higher performance.



Karman Efficiency -12KT Cat and Mono SWA Cavities



Design Comparison –Assessment in Tons

	4KT HYDRO	4KT SWAMCH	12KT SWAMCH	31.5KT SWATCH	40KT SWATCH	50 KT SWATCH	60KT SWATCH
HULL STRUCTURE	1297	1297	3892	10217	12974	16217	19461
OPERATIONS SYSTEMS	340	340	1020	2678	3401	4251	5102
SUSTENTION	400	495	837	2197	3428	4276	5174
PROPULSION PLANT	279	279	1256	2737	2790	3488	4185
PAYLOAD/FUEL	1684	1589	4994	13671	17406	21767	26078

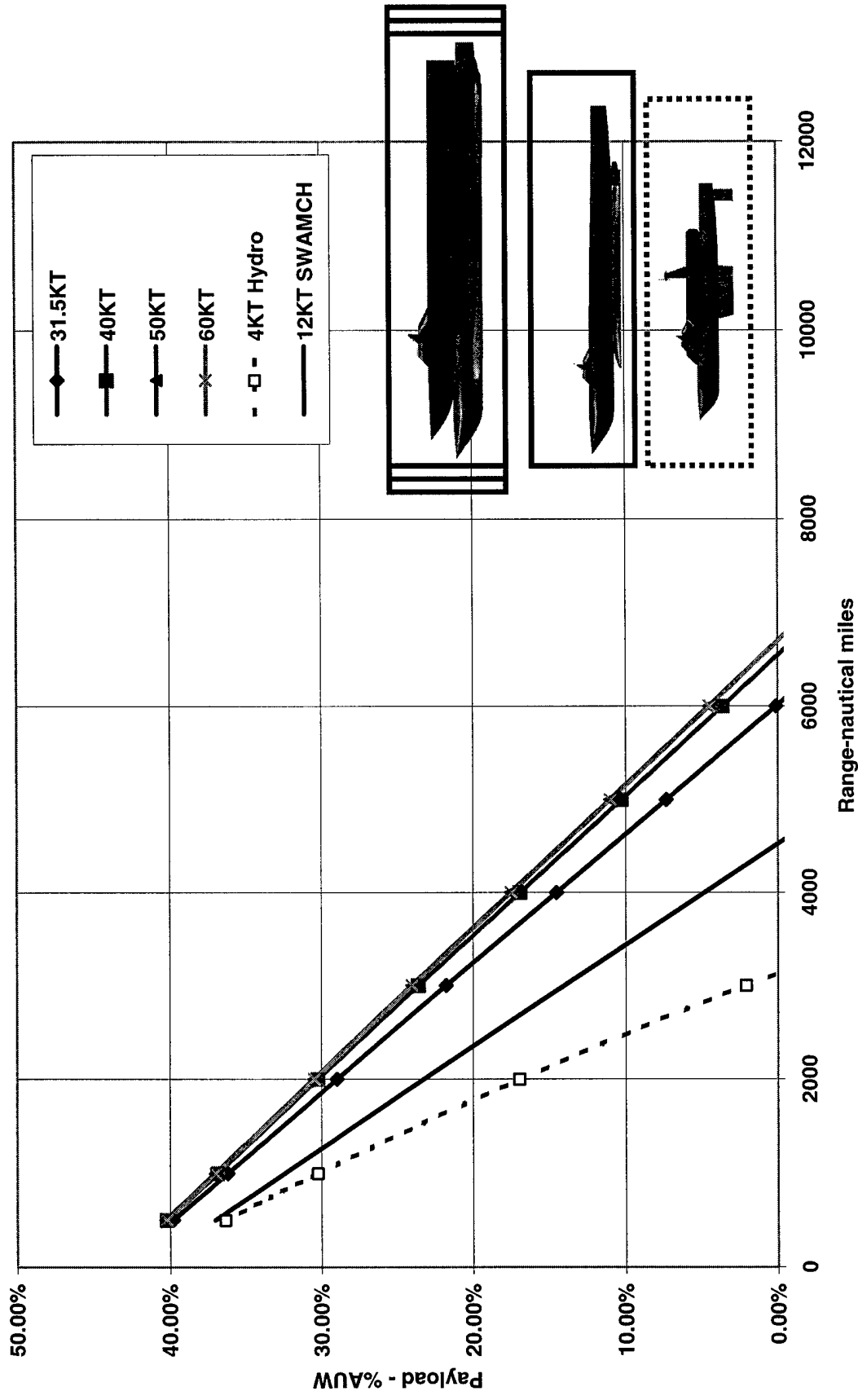
CSC-based SWBS values were used and linearly scaled for the above water structure. Payload/Fuel and the Sustention mass properties were a fallout of the design synthesis process

SWA_xCH vs. Hydrofoil Sizing Comparisons

Payload and range of each of the ship were estimated using the hydrodynamic performance calculations and the assessments of the varied amounts of fixed weight fractions. The cavity hull systems were capable of payload a global range if viscous drag reduction technologies were applied. The hydrofoil falls short in both range and payload using a propulsion system common in TSFC to the SWA ships. Note that the strut sizes used were for maximum payload range at a full viscous drag value.

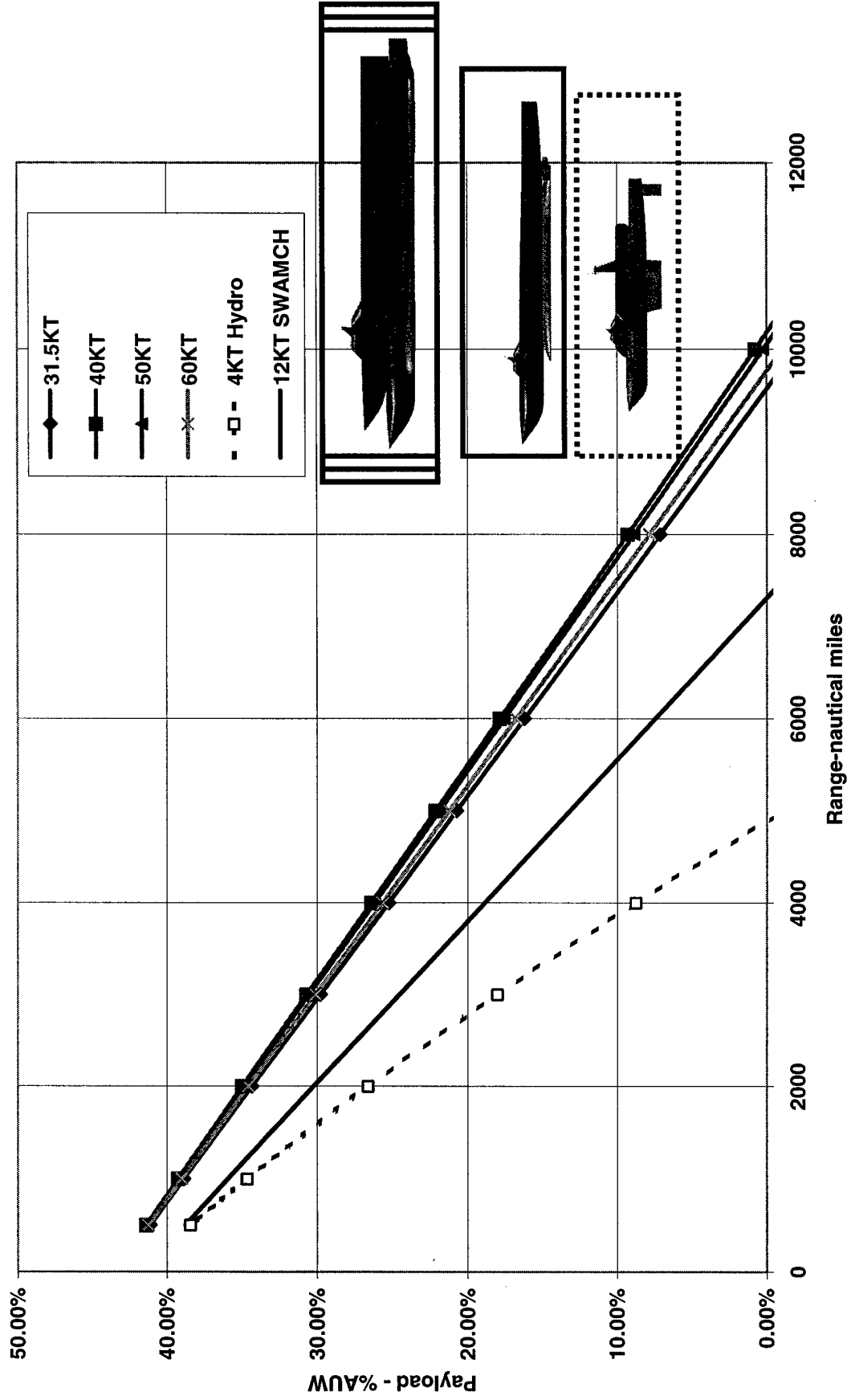
SWAxCH vs. Hydrofoil Sizing Comparisons

Payload vs. Range for SWATCH Designs - 100%K2 (Full Viscous Drag)
 P29TA12 Cavity Bodies, 1.5% t/c Struts, w/ Interference Effects, 1.4 JVR Pumps



SWAxCH vs. Hydrofoil Sizing Comparisons

Payload vs. Range for SWATCH Designs - 25%K2 (25%Viscous Drag)
 P29TA12 Cavity Bodies, 1.5% t/c Struts, w/ Interference Effects, 1.4 JVR Pumps



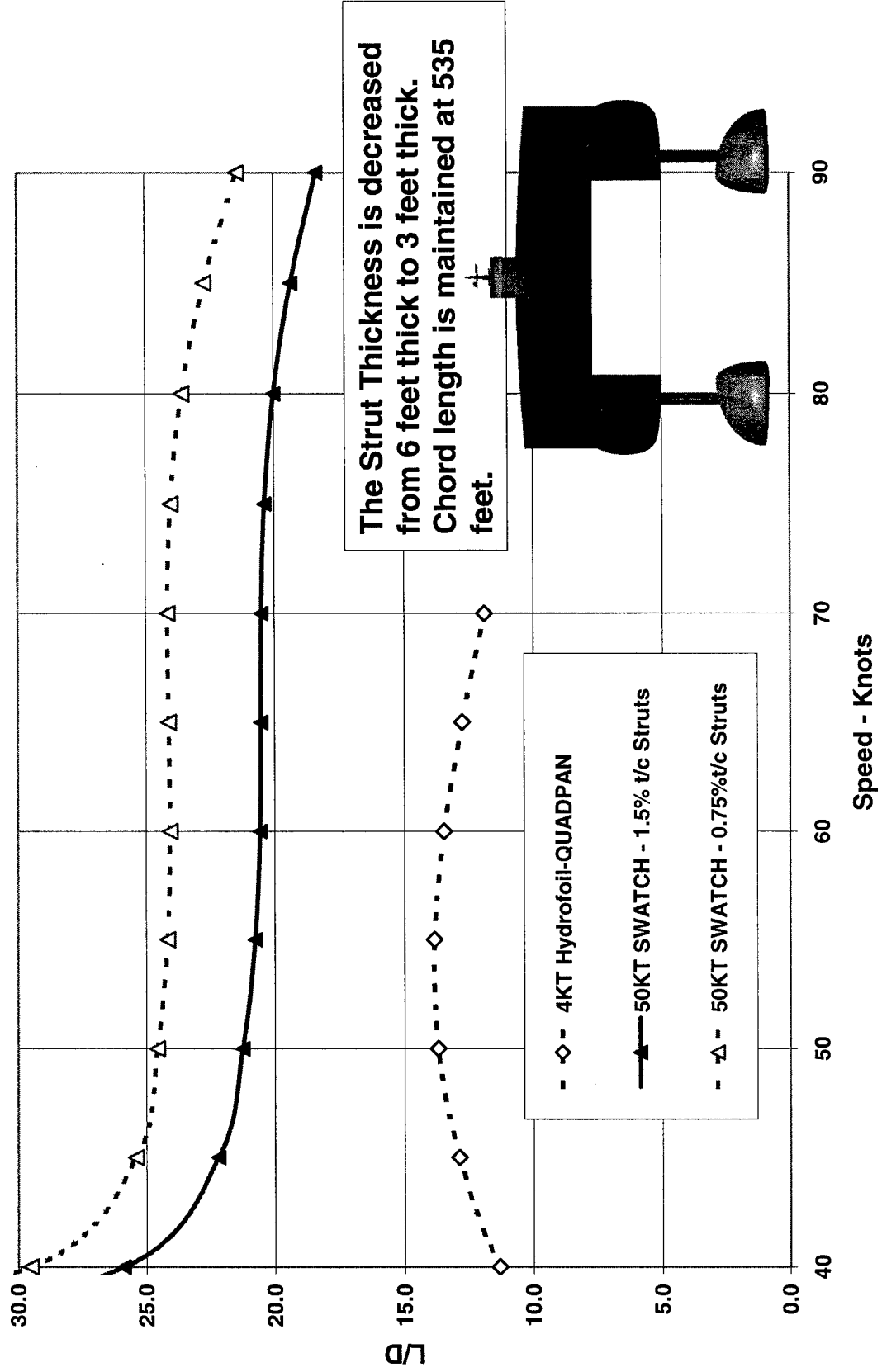
50KT SWATCH Strut Sizing Comparisons

The following sequence of slides shows that the optimal payload range strut for 6000 nautical miles must include a estimate of viscous drag reduction. There is a significant difference is von Karman efficiency and power required if viscous drag reduction is applied. Nonetheless, using a first order trade such as shown the payload range turn out to be almost equivalent between the 1.5% t/c strut at 100% K2 and the 0.75% strut at 25% K2.

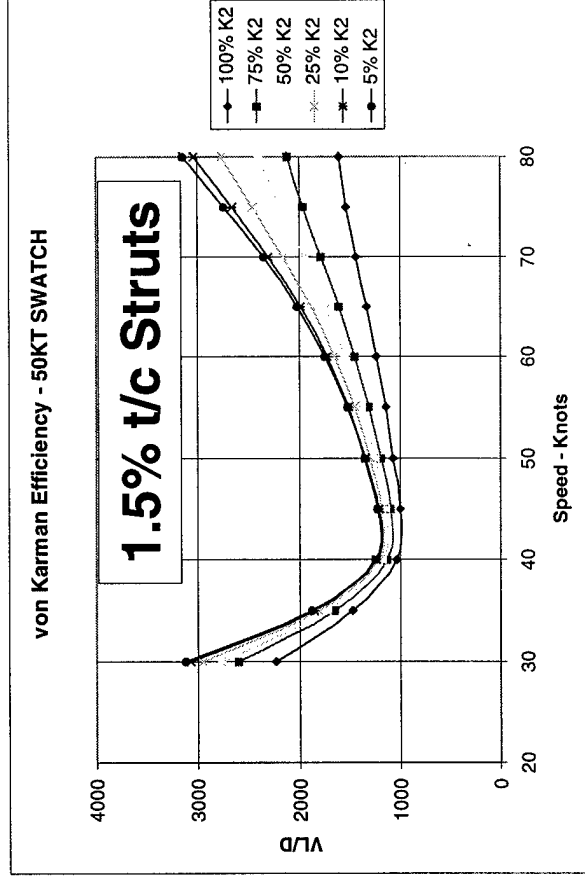
50KT SWATCH Strut Sizing Comparisons

Ship Lift-to-Drag Ratio

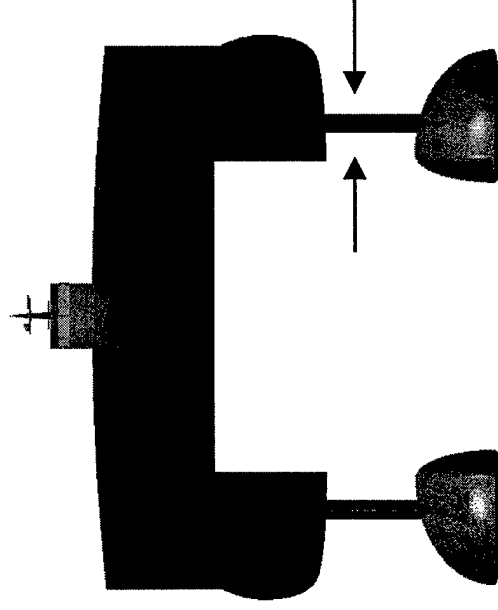
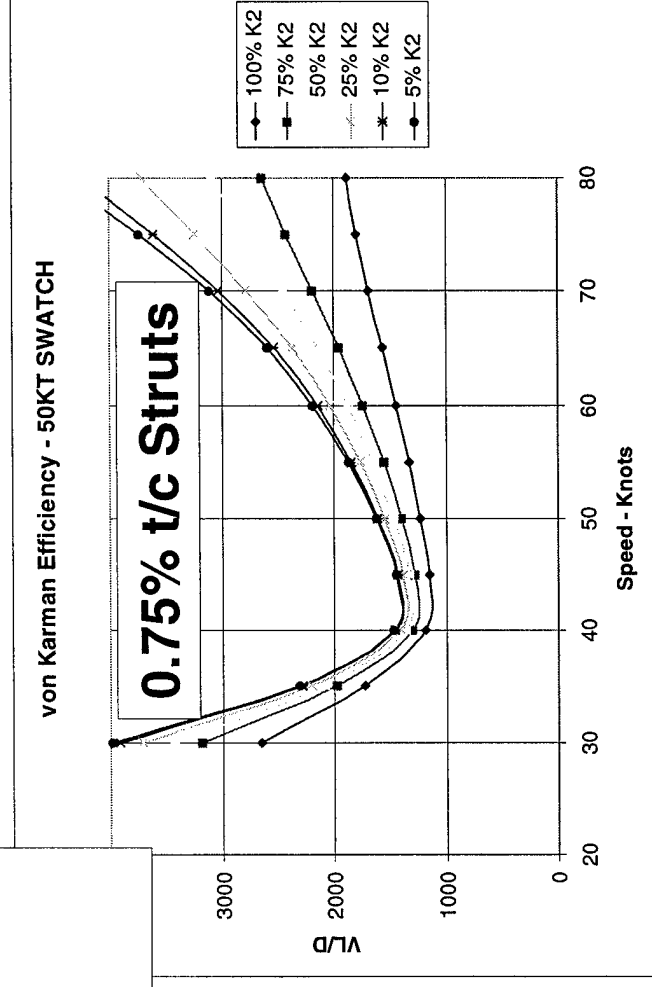
Full Skin Friction, Varied Struts, P29TA12 Bodies



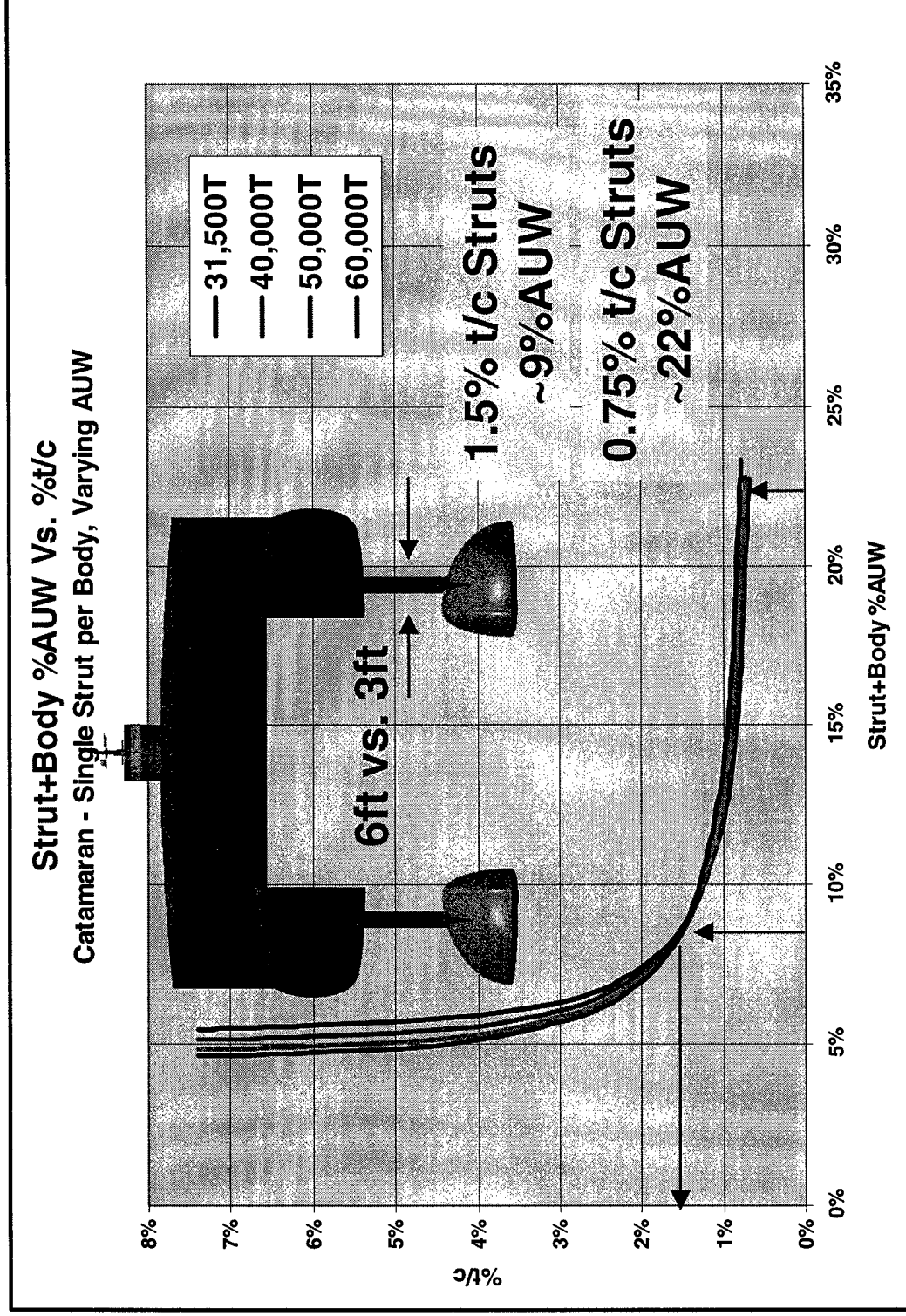
50KT SWATCH Strut Sizing Comparisons



As the Strut Thickness is decreased from 6 feet thick to 3 feet thick the von Karman Efficiency increases accordingly.

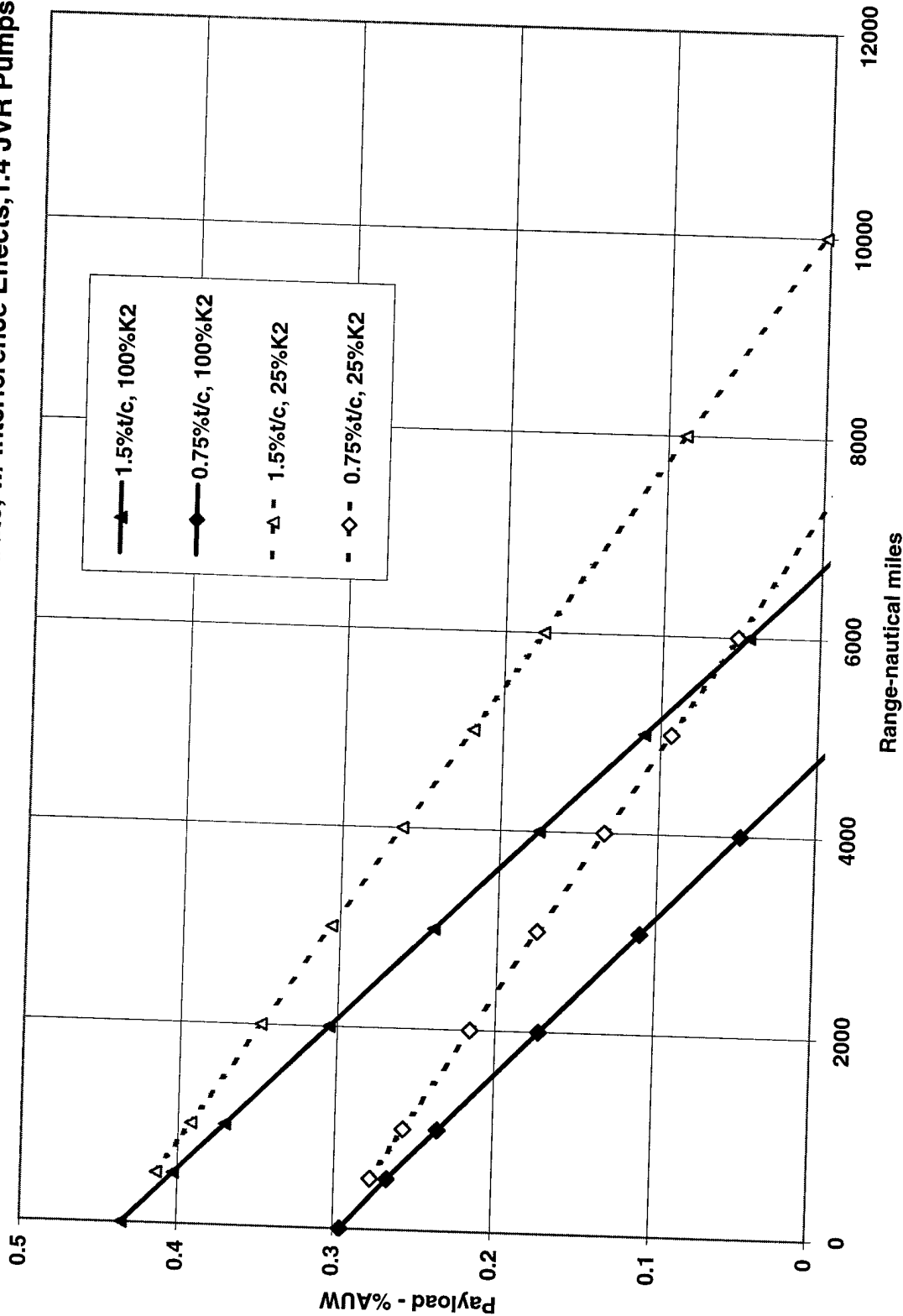


50KT SWATCH Strut Sizing Comparisons



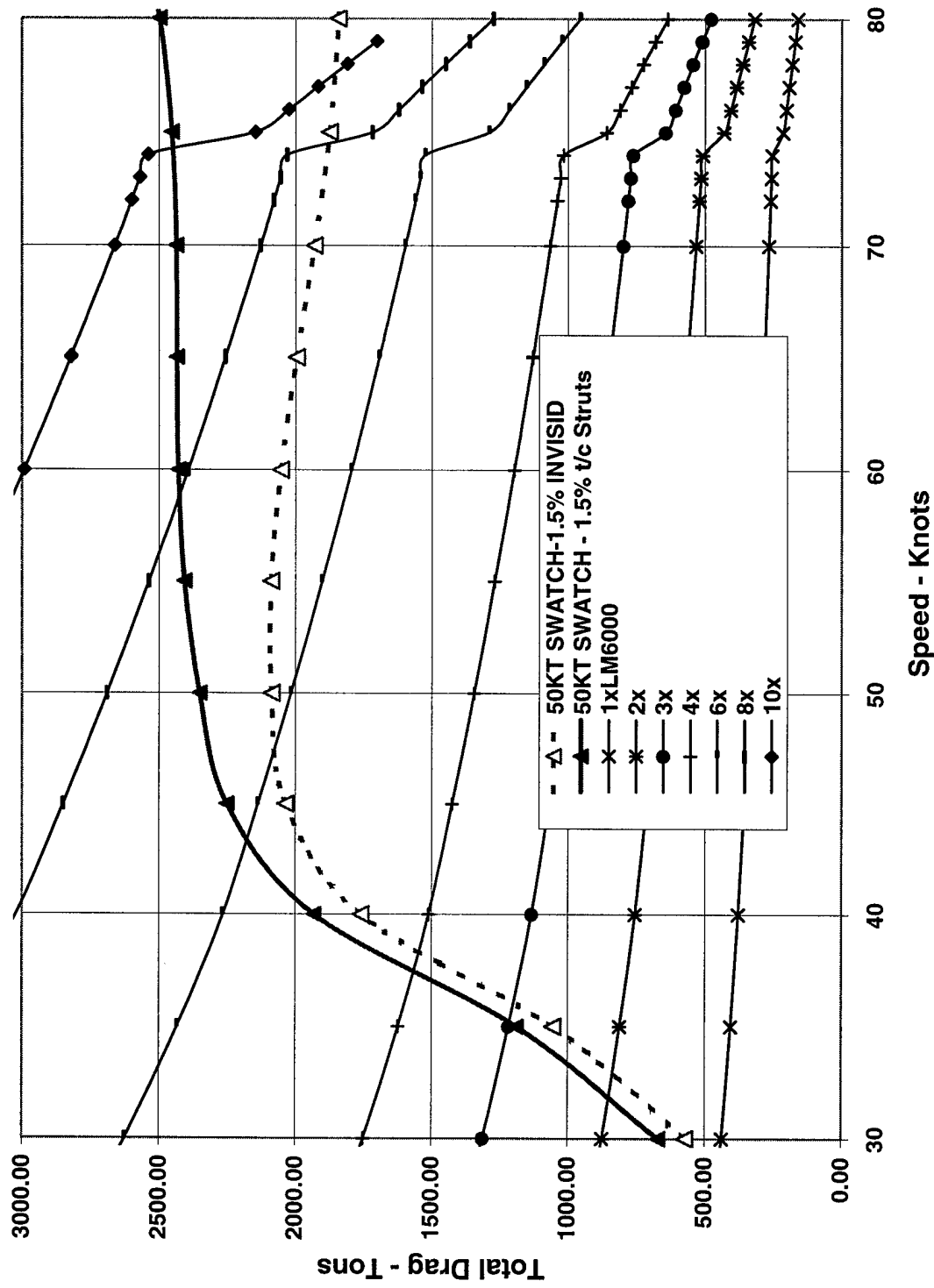
50KT SWATCCH Strut Sizing Comparisons

Payload vs. Range for 50KT SWATCCH Designs
P29TA12 Cavity Bodies, 1.5% and 0.75% t/c Struts, w/ Interference Effects, 1.4 JVR Pumps



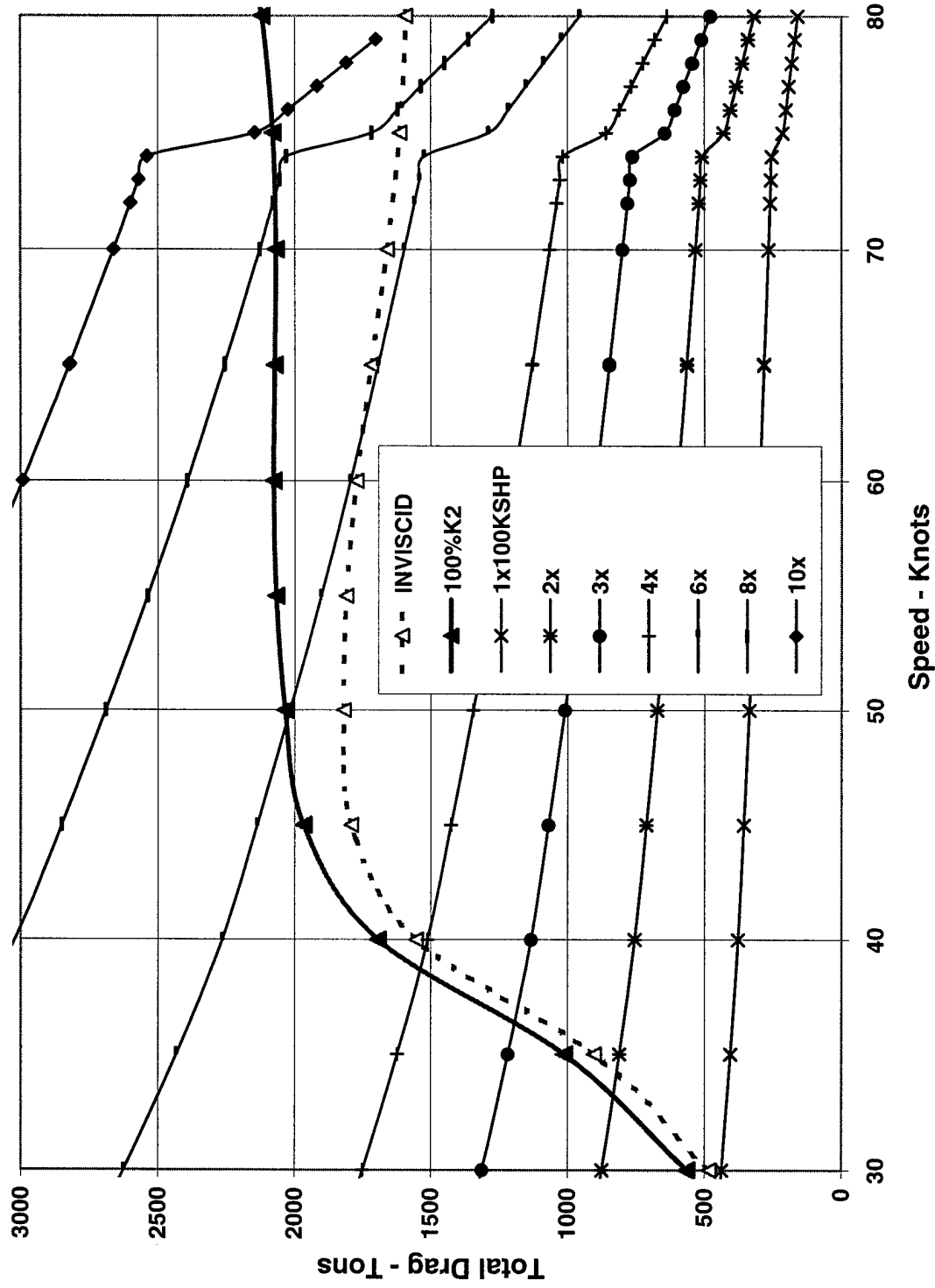
Thrust Required – 50KT SWATCH 1.5% Struts

50KT Ship Total Drag vs Available Thrust
P29TA12 Bodies, 1.5% t/c Struts



Thrust Required – 50KT SWATCH 1.5%Struts

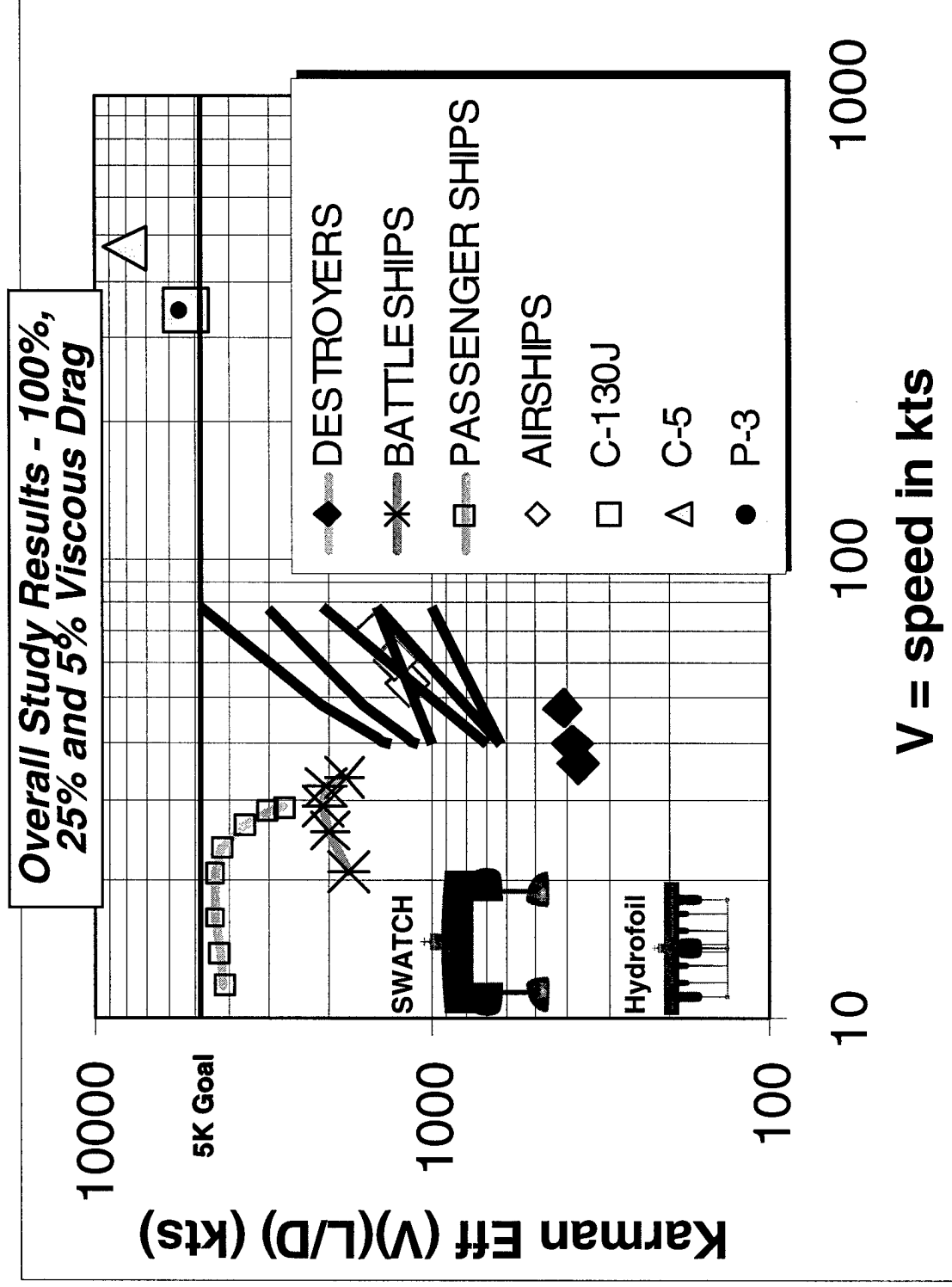
50KT Ship Total Drag vs Available Thrust
P29TA12 Bodies, 0.75% t/c Struts



Hydrodynamic Efficiency – Comparison

In the end, the maximum von Karman efficiency parameter will be of benefit. The following plot shows that with significant viscous drag reduction applied, the goal of $V(L/D)=5000$ is approachable.

Hydrodynamic Efficiency – Comparison



Hydrodynamics

Sub-Cavitating vs. Super-Cavitating foil

The hydrofoil wing section design is predicated upon the use of a foil operating without cavitation. Cavitation is the formation of gas bubbles (air or water vapor) in the seawater due to a reduced pressure. Cavitation in untreated sea water will begin at a small positive absolute pressure (approximately the vapor pressure).

Super-cavitating foil sections are sometimes considered for high-speed operation. Such a foil has a gas-filled cavity extending over much of the upper surface. A super-cavitating section eliminates upper surface skin friction at the expense of high form drag. The cavity drag coefficient becomes larger as the foil lift coefficient is increased. Therefore, a super-cavitating foil is appropriate for a lightly loaded ship. A large hydrofoil operates at a higher Reynolds number and has (proportionately) less friction drag, which favors a sub-cavitating foil. In any event, the super-cavitating foil offers little possibility for a high lift-to-drag ratio, even when superior to the sub-cavitating foil.

For a cavitation-free foil, the local absolute pressure on the foil must always remain above the vapor pressure of seawater. Therefore, the critical suction pressure near the wing occurs when the upper surface suction equals the vapor pressure of water. In dimensionless form, the critical pressure, or "cavitation number," σ , is:

$$\sigma = -C_p = -(P_V - P_s) / q_{water}$$

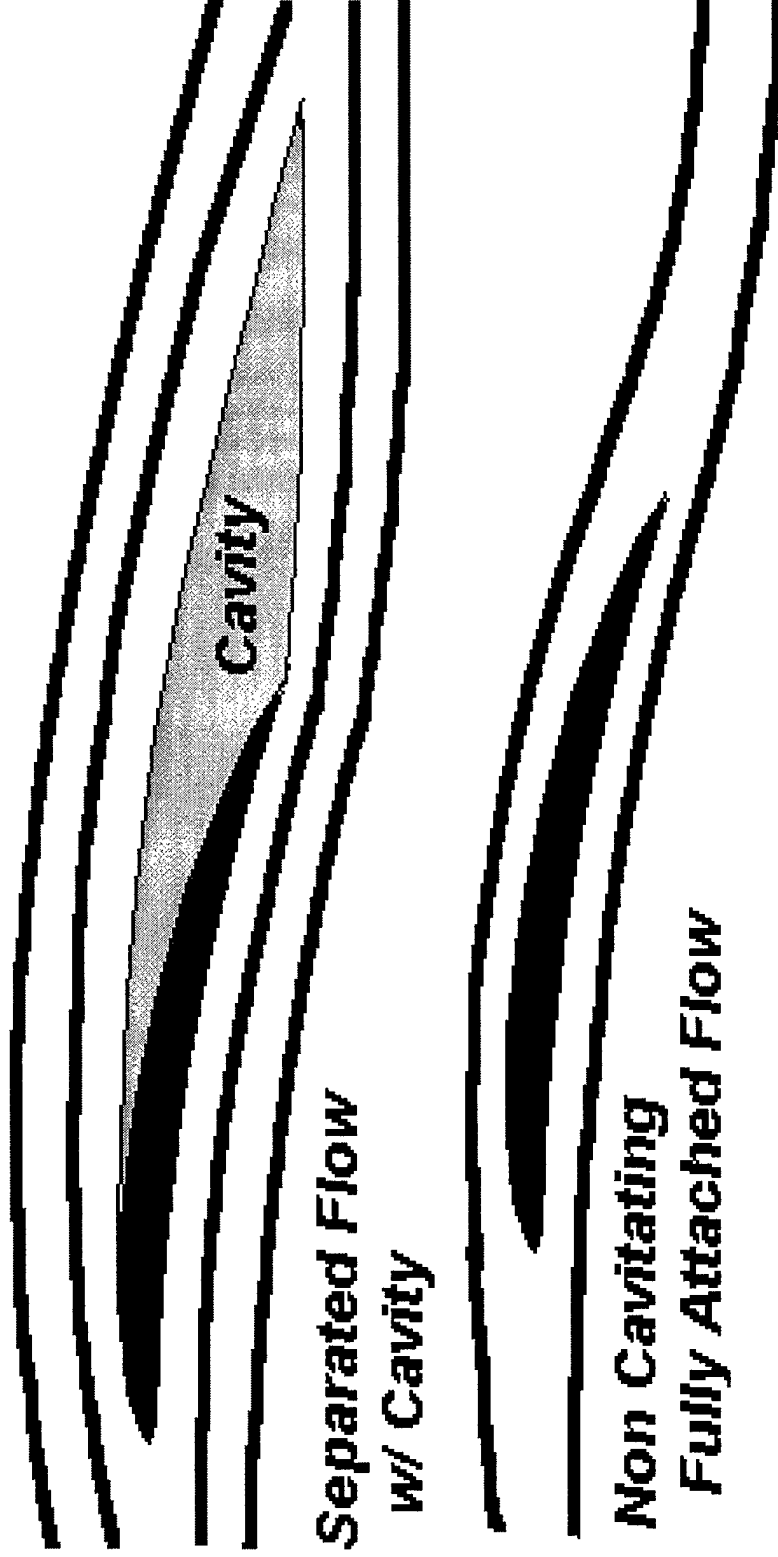
where the static pressure, P_s , is a function of the submergence depth, h :

$$P_s = P_\infty + \rho_{water} \cdot g \cdot h$$

and the vapor pressure, P_v , is 35.6 lb/ft².

For a typical design problem, a speed of 70 knots and a depth of 20 feet, the cavitation number is 0.24.

Sub-Cavitating vs. Super-Cavitating foil



Theoretical Limits to Wing Loading

Limiting values of the wing loading may be obtained through two-dimensional linear thin-foil theory. In thin-foil theory, the lift of the foil is viewed as originating from a superposition of the contributions of the pressures due to camber, incidence and thickness. Note that the cambered and inclined foils have equal lift contributions from the upper and lower surfaces. The thickness form has symmetrical pressure contributions that mutually cancel. Hence, the resultant lift of a foil (in thin-foil theory) is due only to its camber and incidence, not to its thickness.

The maximum lift, which may be generated without cavitation by a foil with vanishing thickness, occurs when the upper surface pressures of the foil are at the onset of cavitation. The upper surface is then at a uniform pressure of $C_p = -\sigma$. Theory requires the lower surface to then be at a uniform pressure of $C_p = +\sigma$. The maximum lift coefficient that can be obtained is the sum of the net pressures :

$$C_{L_{\max}} = 2\sigma$$

The maximum wing loading that can be obtained, therefore, is:

$$(W/S)_{\max} = C_L \cdot q_{\text{water}} = 2\sigma \cdot q_{\text{water}}$$

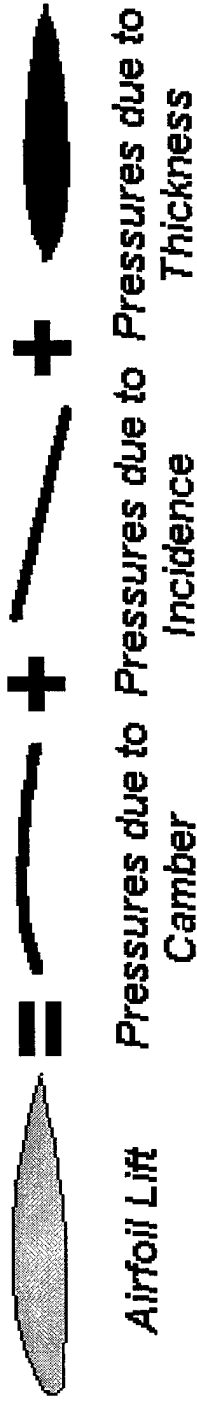
From a purely hydrodynamic point of view, the optimal wing section is an infinitely thin section cambered to obtain the ideal loading at the design point. Although an infinitely thin section is a physically implausible design, it does, however, serve the useful purpose of providing an upper bound for the design wing loading.

For unswept wings of finite thickness, the cavitation-free wing loading is diminished due to the influence of the symmetric pressure contributions of thickness. Camber is then added to decrease the upper surface pressure to the uniform cavitation incipient pressure, $C_p = -\sigma$. The required anti-symmetric pressure due to camber is the difference between the target upper surface pressure and the pressure due to thickness; the pressure due to thickness added to the pressure due to camber also yields the theoretical lower surface pressure.

The area under the "pressure due to thickness curve" is the net lift of the upper surface of the thickness form (at zero angle-of-attack). Let its magnitude, which is proportional to the thickness ratio, be k (t/c), where k is a constant whose value depends upon the thickness distribution of the foil section. The maximum lift coefficient obtainable from a thick foil without cavitation is then:

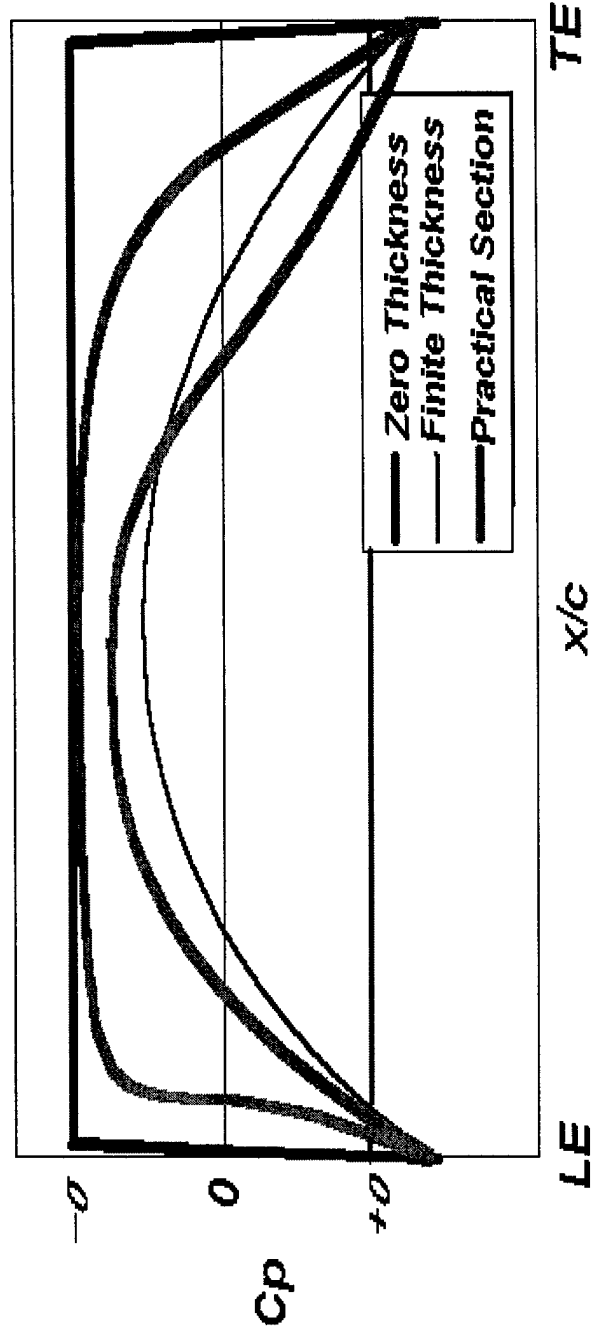
$$C_{L_{\max}} = 2[\sigma - k(t/c)]$$

Theoretical Limits to Wing Loading

$$\text{Airfoil Lift} = \text{Pressures due to Camber} + \text{Pressures due to Incidence} + \text{Pressures due to Thickness}$$


The diagram illustrates the theoretical limits to wing loading by decomposing the total lift of an airfoil into three components. On the left, a shaded airfoil is shown. To its right is an equals sign, followed by three terms separated by plus signs. Each term is represented by a simplified airfoil shape: a curved line for camber, a straight line for incidence, and a thickened airfoil for thickness. Below these terms are the labels 'Camber', 'Incidence', and 'Thickness' respectively.

IDEALIZED WING PRESSURE DISTRIBUTION



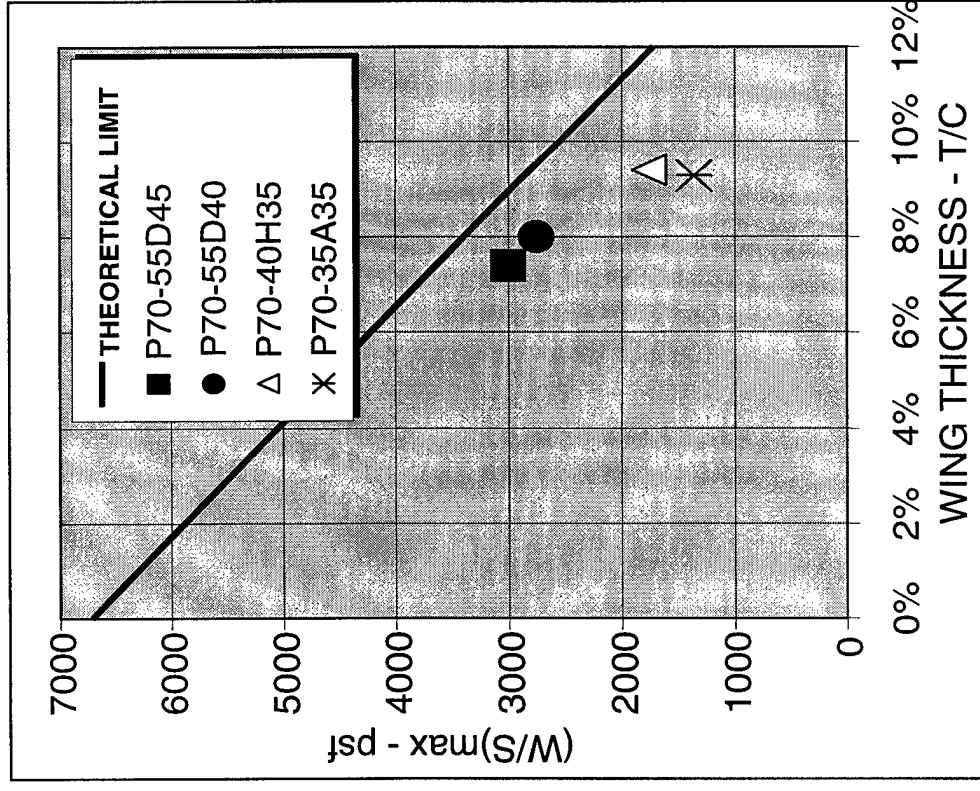
Practical Limits to Wing Loading

Two features are necessary in a well-designed foil; these tend to further diminish the potential maximum wing loading. The first design requirement is a need to promote cavitation-free operation over a range of speed and loading. This implies that the foil must function over a range of angle-of-attack; the section must be blunt enough so that the flow does not prematurely separate due to the adverse pressure gradient near the leading edge. The second design requirement is a need to provide performance at realistic Reynolds numbers. The adverse pressure gradient near the trailing edge of the foil section must not be so great as to promote premature flow separation.

Practical foils designed to satisfy these requirements are compared to the theoretical maximum wing loading that can be obtained. The absolute maximum wing loading would occur with zero wing thickness. Constraints on minimum wing thickness are determined by structural considerations and the need for the foil to operate over a range of angle-of-attack. A foil designed to operate only for the cruise condition can be thinner than one which must operate over a range of speeds and weights. The relatively thick section is the result of the multi-point design criterion.

Practical Limits to Wing Loading

Comparison of Practical Wing Performance to
Theoretical Maximums. (from thin foil theory : $V=70$ -
kts, $h=20$ -ft, $k=1.5$).



Hydrofoil Design Technical Challenge

We must design a section that operates without cavitation over the following:

1. From minimum foil-borne speed up to cruise speed at initial weight
2. At cruise speed from initial weight down to final weight
3. From cruise speed down to minimum foil-borne speed at final weight

The cavitation-free operating region of a given foil may be described by a cavitation diagram, a plot of lift coefficient C_l as a function of the peak suction pressure Cp_{min} . In the foil design and evaluation process, the values of C_L and Cp_{min} are typically determined by numerical model (either inviscid panel method or viscous CFD). For high speed sections, the cavitation limited C_{Lmax} is significantly less than the C_{Lmax} limited by stall.

Note that lines of constant (W/S) on the cavitation diagram are straight lines through the origin, since:

$$\frac{C_L}{\sigma} = \frac{(W/S) / q_{water}}{\sigma - (P_v - P_s) / q_{water}} = \frac{(W/S)}{(P_s - P_v)} = const$$

Simple sweep theory affects the cavitation diagram as follows:

$$Cp_{min@A} = Cp_{min@A=0^\circ} \cdot \cos^2 A$$

$$C_{L@A} = C_{L@A=0^\circ} \cdot \cos^2 A$$

where A is the sweep. The addition of sweep functionally moves the cavitation envelope both down and to the left, enabling performance at higher speeds. The tailoring of the section thickness distribution with sweep can result in improved performance over the required operating range. In practice, viscous considerations limit the use of highly swept thick foils (these sections often exhibit premature trailing edge separation).

The following equation applies for the maximum wing loading of swept wings:

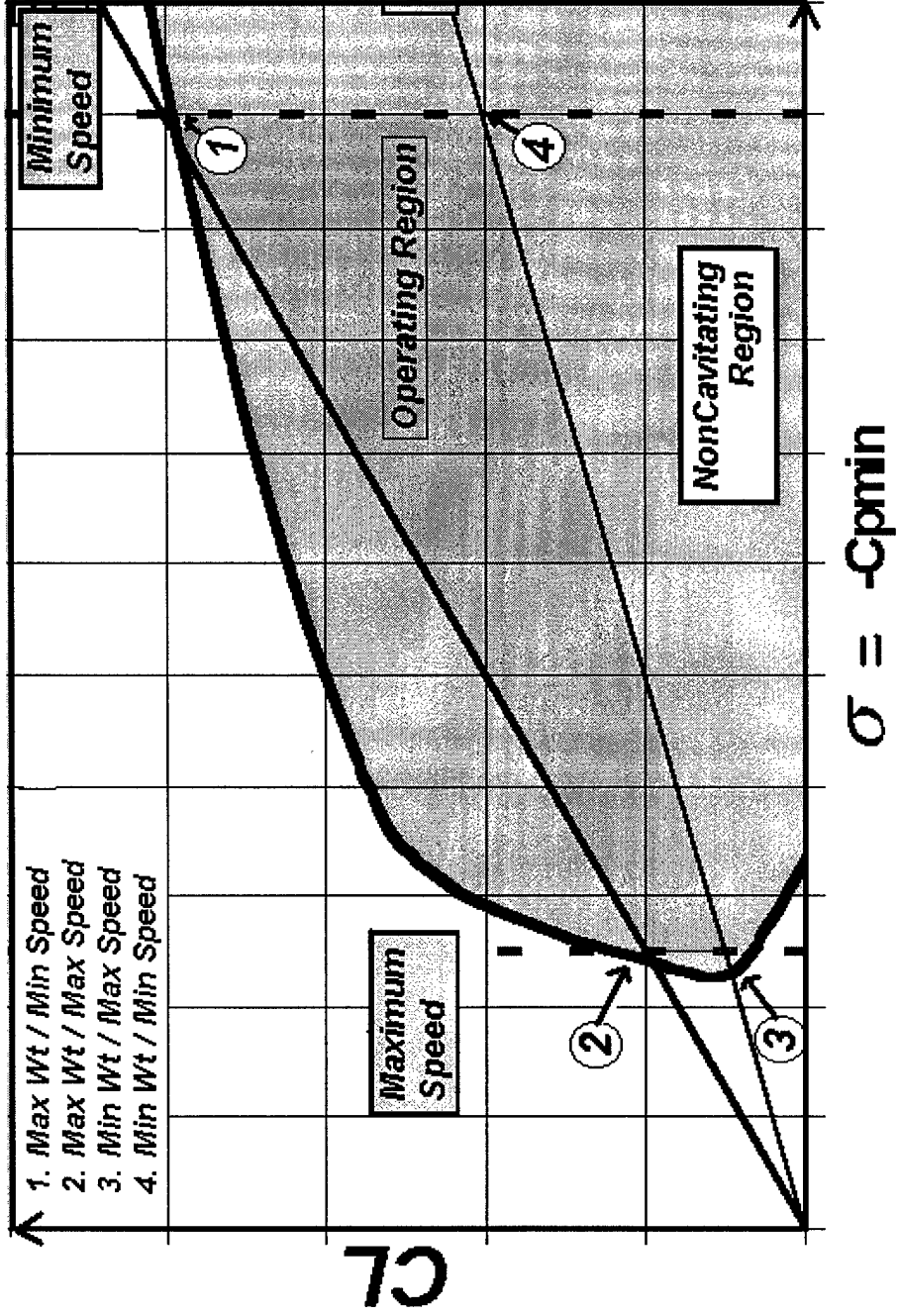
$$C_{Lmax} = 2[\sigma - k(t/c)_{streamwise} \cos A]$$

Hydrofoil Design Technical Challenge

$$\sigma = \frac{p}{q}$$

$$C_L = \frac{W}{qS}$$

$$C_L = \frac{W}{pS} \sigma$$



Basic Foil Section Design Methodology

The objective of this procedure is to find the foil section which has a given thickness form and a given target pressure distribution over the top surface. The mean camber line of the foil is defined by the Fourier coefficients A_n :

$$\frac{dy}{dx} = -\alpha_i + \sum_{n=1}^{\infty} A_n \cos n\theta$$

The thickness form is defined by the Fourier coefficients B_n :

$$\begin{aligned} \frac{dy}{dx} = & -\frac{1}{2}\lambda \tan \frac{1}{2}\theta + \frac{1}{2}\tau \cot \frac{1}{2}\theta \\ & + \sum_{n=1}^{\infty} B_n \sin n\theta + \mu \operatorname{sgn} \theta \cos \theta \end{aligned}$$

The leading edge radius is $\lambda^2/2c$, the trailing edge radius is $\tau^2/2c$, the trailing edge closure angle is $2\arctan\mu$, and the design angle of attack is α_i . To ensure a closed foil, the following identity must be satisfied:

$$B_1 = \lambda - \tau$$

We can decompose the pressure as the sum of a term due to camber, Cp_C , and a term due to thickness, Cp_T . The upper surface pressures due to camber are:

$$Cp_C = -2(\alpha - \alpha_i) \tan \frac{1}{2}\theta - 2 \sum_{n=1}^{\infty} A_n \sin n\theta$$

The upper surface pressures due to thickness are:

$$\begin{aligned} Cp_T = & -(\lambda + \tau) + 2 \sum_{n=1}^{\infty} B_n \cos n\theta - \frac{4\mu}{\pi} \\ & + 2\mu \cos \theta \cdot \log_e \frac{1 + \cos \theta}{1 - \cos \theta} \end{aligned}$$

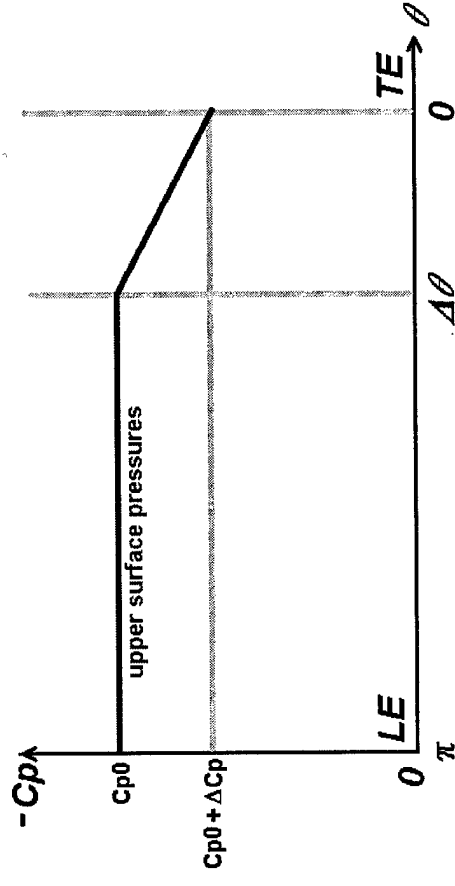
We can then solve for the camber distribution that produces the target pressures.

Basic Foil Section Design Methodology

$$\frac{x}{c} = \frac{1 - \cos \theta}{2}$$

$$Cp = Cp_0; \quad \Delta\theta \leq \theta \leq \pi$$

$$Cp = Cp_0 + \frac{\Delta Cp}{\Delta\theta} (\Delta\theta - \theta); \quad 0 < \theta \leq \Delta\theta$$



$$A_n = \left\{ \begin{array}{l} \frac{2}{\pi} \left(\sum_{m \text{ even}} \frac{2n}{n^2 - m^2} \left(B_m + \frac{4\mu m}{\pi(m^2 - 1)} \right) \right. \\ \left. - \frac{Cp_0 + \lambda + \tau}{n} - \frac{\Delta Cp - \frac{\Delta Cp \sin n \Delta\theta}{\Delta\theta} \frac{n}{2n}}{2n} \right), n \text{ odd} \\ \\ \frac{2}{\pi} \sum_{m \text{ odd}} B_m \frac{2n}{n^2 - m^2} - \frac{\Delta Cp - \frac{\Delta Cp \sin n \Delta\theta}{\Delta\theta} \frac{n}{2n}}{2n}, n \text{ even} \end{array} \right. \quad (25)$$

Foil Optimization Methodology

The wing section design methodology is summarized as follows:

1. Inverse thin foil theory is employed to design foil sections possessing a uniform pressure over the upper surface at one angle of attack.
2. An exact potential flow analysis is performed to obtain foil cavitation characteristics (C_L vs. Cp_{min}) over the entire flight envelope.
3. The mission performance characteristics of the candidate foil are computed.
4. A numerical optimizer is used to seek out those design variables which optimize the performance.
5. This process is repeated for varying design speed, sweep, thickness, etc.

It is essential that the foil analysis procedure be fast; the optimizer may have to evaluate thousands of foils before converging to an optimum.

Once an optimum foil is determined, it is analyzed "off-line" using a 2-D CFD methodology to ensure that the predicted cavitation characteristics are maintained.

Foil Optimization Methodology

Design Optimization Strategy

- **Foil Design Variables**
 - A_n , B_n , λ , τ , σ , Λ
- **Generate Foil Geometry (LINFOIL)**
 - from previous effort
- **Exact Potential Flow Analysis (QUADPAN)**
 - generates cavitation envelope Cp_{min} vs. CL
 - multiply both Cp_{min} and CL by $\cos^2 \Lambda$
- **Compute Technical Performance Measures**
 - minimum and maximum planform loading (W/S)
 - mean cruise speed (V)
 - mean hydrodynamic efficiency (L/D)
 - Karman efficiency (V L/D)
- **Verify Viscous Performance Using MSEs**
 - separation points
 - form drag

Use "Pointer"
to
Maximize (W/S)
or (V (L/D))

Wing/Strut - Design Rules

The problem of selecting the optimum foil section for a hydrofoil wing or strut is now described.

Maximize the wing loading W/S for a given depth and sweep angle subject to the following constraints:

1. Cavitation free operation over entire weight and speed range.
2. Minimum foil loading of half the maximum loading.
3. Operation at specified minimum speed (for example, 45 kt).
4. Operation at specified maximum speed (for example, 70 kt).
5. Minimum thickness ratio (for example, 5%).
6. Minimum leading edge radius.

The limitations of the foil design procedure are:

1. 2-D analysis (corrected for sweep).
2. Inviscid analysis.
3. No free surface effects.
4. No strut interference.

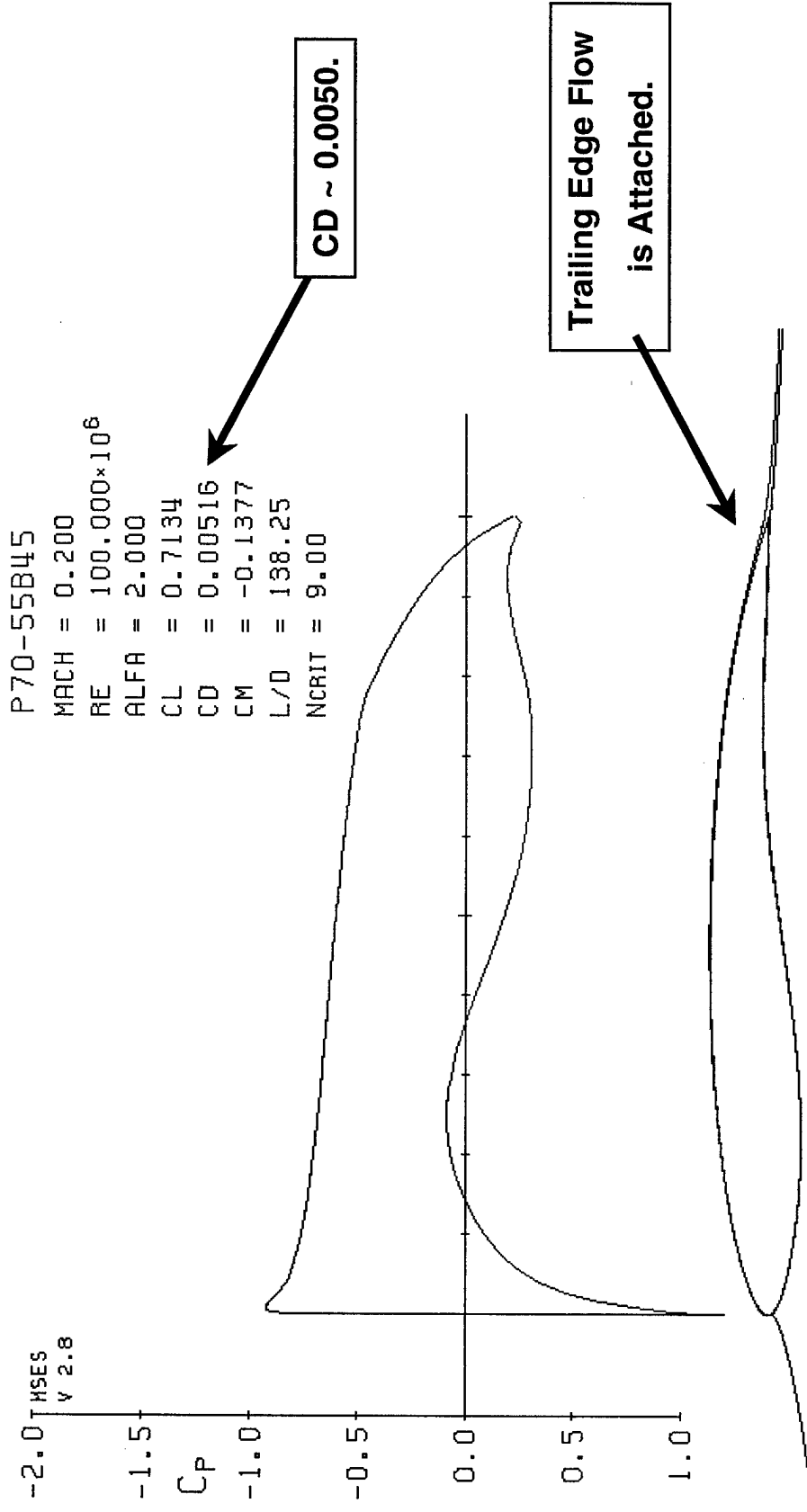
Each of these limitations, however, are later addressed by higher fidelity analysis.

Strut foil sections are designed with a similar procedure, except that the foil is symmetric, and there are no minimum loading or speed constraints.

- **Foil Nomenclature :**

- DESIGNER / MAX-SPEED / MIN-SPEED / LOADING RATIO / TYPE / VERSION / SWEEP
- designer = "P" (PONTER)
- loading ratio = max wing loading / min wing loading
- type = "W" (wing), "S" (strut), etc.
- version = "A", "B", "C",
- max-speed and min-speed are in knots, sweep is in degrees
- (min-speed, loading ratio and type are sometimes omitted with the defaults being 40 knots, 2.0, and wing, respectively)

Wing/Strut - Design Rules



P70/55/2.0B45 is an acceptable foil. Flow is attached. Drag is typical.

Viscous Performance Limits Design Sweep

In theory, the hydrodynamic performance of a hydrofoil will increase with additional wing sweep. In practice, viscous considerations limit the use of highly swept foils.

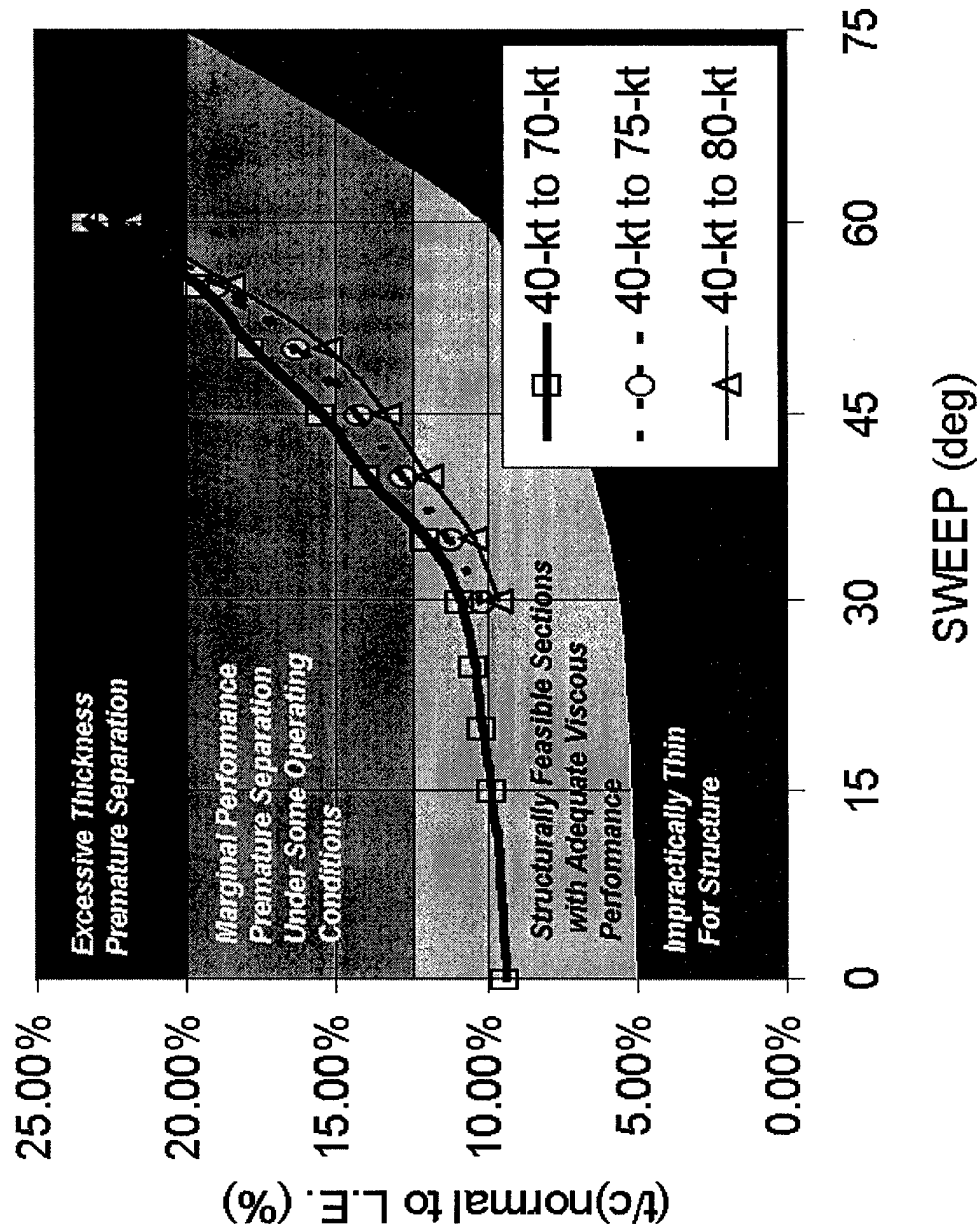
Foil sections of higher thickness-to-chord ratio are required to take advantage of increased sweep. Here we are talking about thickness ratio measured in a direction normal to the leading edge, which determines the hydrodynamic characteristics. The thickness ratio measured stream-wise is less by a factor of $\cos \Lambda$, because the stream-wise chord is longer.

Flow separation is invited as the thickness ratio of foils increase. This will quickly increase drag and reduce lift beyond a certain thickness ratio. It is seen from the plot that, practically speaking, sweep is probably limited to a maximum of 45 degrees.

Viscous Performance Limits Design Sweep

Foils Designed Using POINTER

$$(W/S_{max})/(W/S_{min})=2$$



Optimum Sweep Trade Study

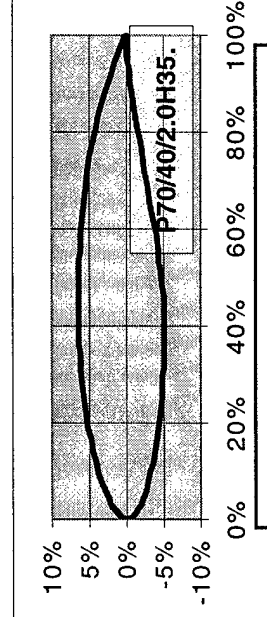
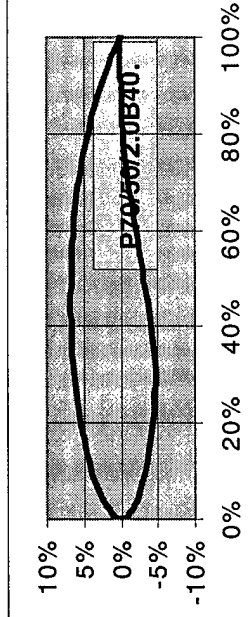
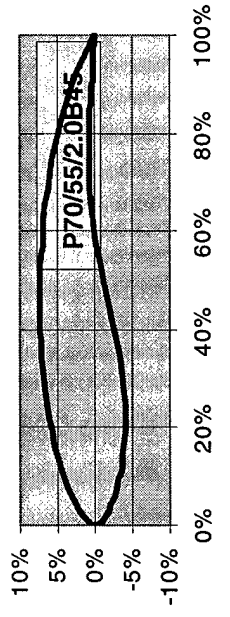
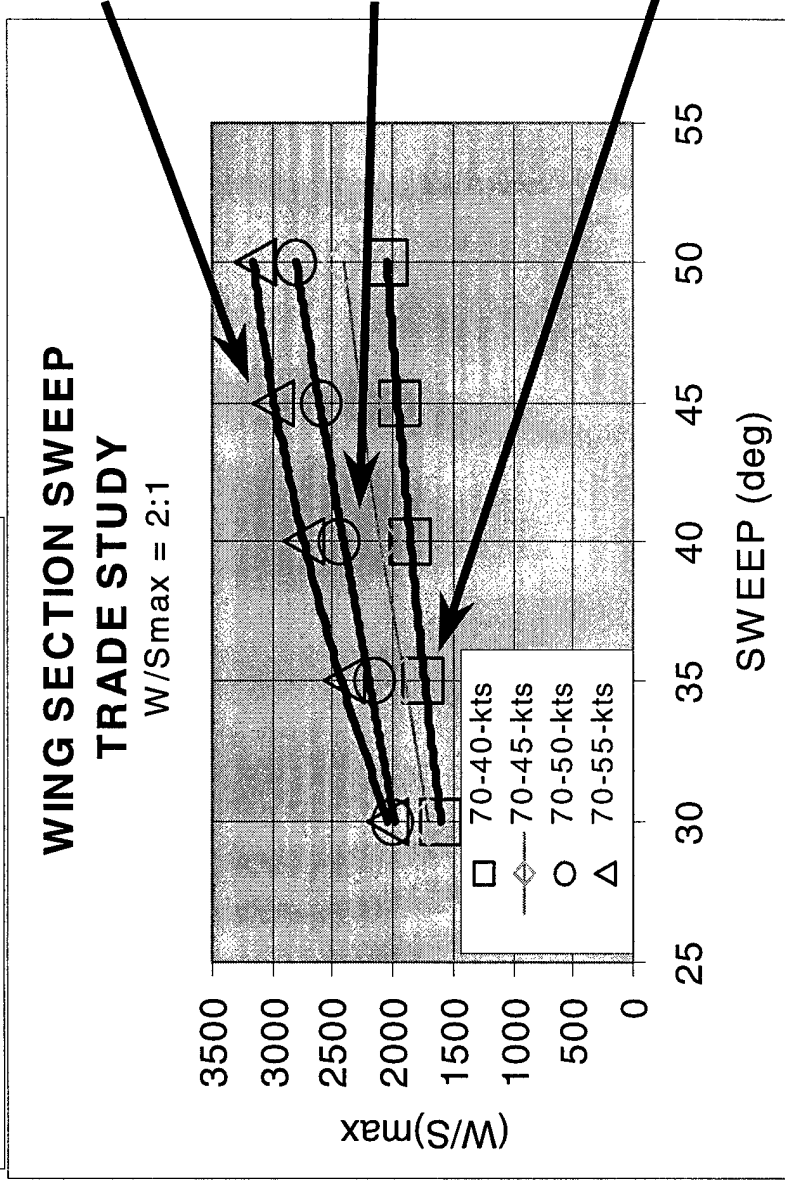
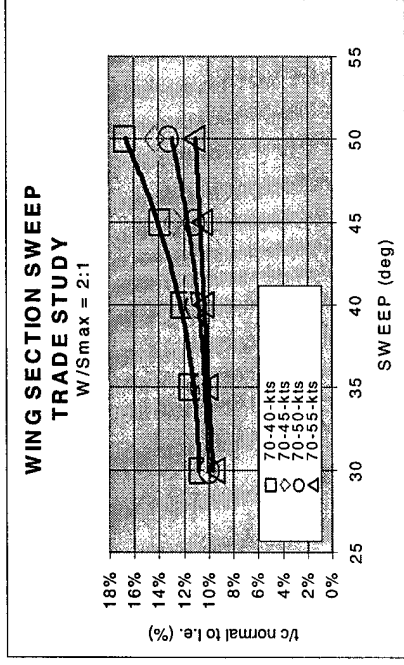
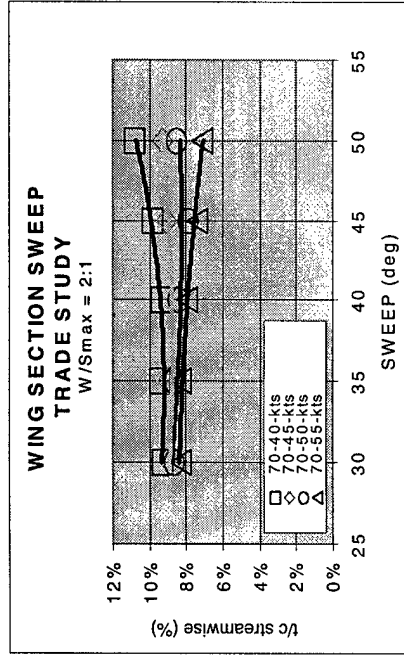
As the wing sweep is increased, foils can be developed which sustain greater loading, and thus, better hydrodynamic performance. The graph shows the maximum wing loading attained as a function of wing sweep and operating speed range. For a given operating speed range, wing loading increases with increasing sweep angle. Also, narrowing the range of operating speeds enables increased wing loading.

The practical limit of wing sweep is determined by the onset of flow separation. As wing sweep is increased, thicker foil sections are needed to attain the higher wing loading promised. Thicker sections are prone to flow separation and the resultant form drag and decreased lift.

It was previously noted that the maximum usable wing sweep is about 45 degrees. Higher sweep will result in foil sections thick enough to have appreciable flow separation. At 45 degrees sweep, the maximum attainable wing loading for an operating range of 55-70 knots is 3000 pounds per square foot.

A requirement for lower minimum speed will decrease the achievable wing loading. However, leading and/or trailing edge flaps can be used to enable lower speeds than can be attained by a wing of fixed section.

Optimum Sweep Trade Study



All Sections Shown Normal to L.E.

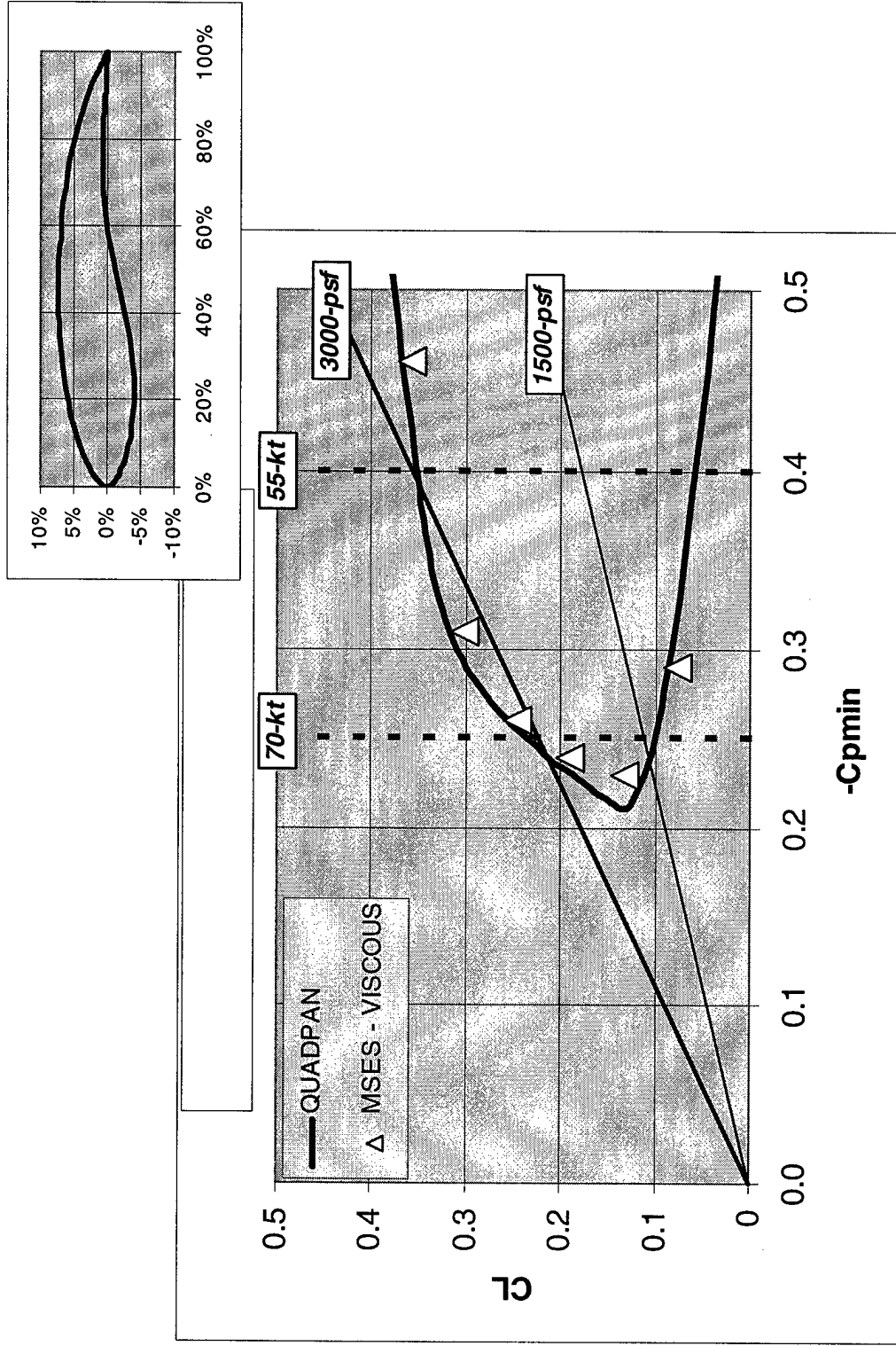
Cavitation Diagram of Foil P70/55/2.0/B45

Foil p70/55/2.0/b45 is a section designed for a wing of 45 degrees sweep. It attains a maximum wing loading of 3000 pounds per square foot, with a non-cavitating operating range from 55 to 70 knots. It is also operational at speeds up to 70 knots at half the maximum wing loading to allow for fuel burn-off.

The thickness-to-chord ratio normal to the leading edge is 10.5%. The stream-wise thickness ratio is 7.4%.

The foil was designed from potential flow calculations using QUADPAN. The cavitation envelope was verified with 2-D viscous computations using MSES (Euler equations + interactive boundary layer).

Cavitation Diagram of Foil P70/55/2.0/B45



Main Wing Design - P70/55B45 – 90%*c* Drooped TE

To achieve a high maximum wing loading, it is necessary to restrict the range of non-cavitating operating speeds. Thus, by increasing the minimum speed to 55 knots, foil p70-55b45 attains a wing loading of 3000 pounds per square foot. For foil-borne operation at lower speed, it is necessary to employ variable wing geometry using leading and/or trailing edge flaps.

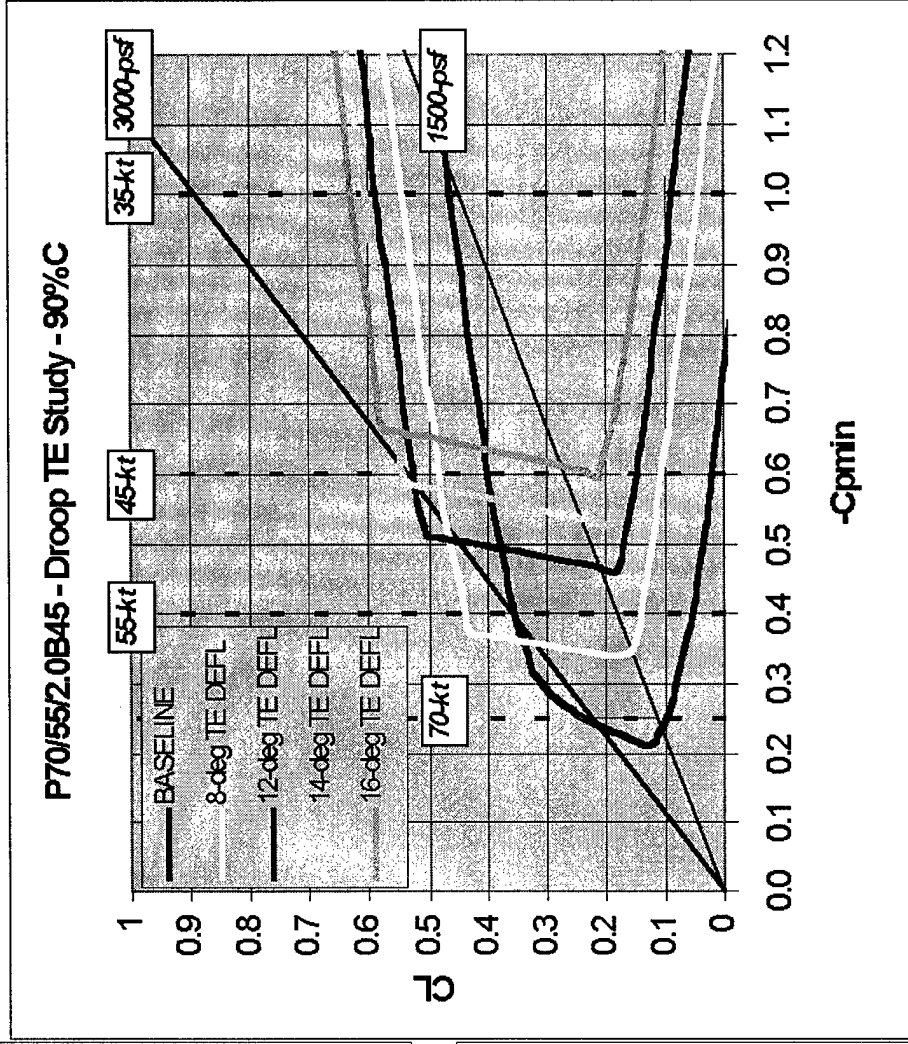
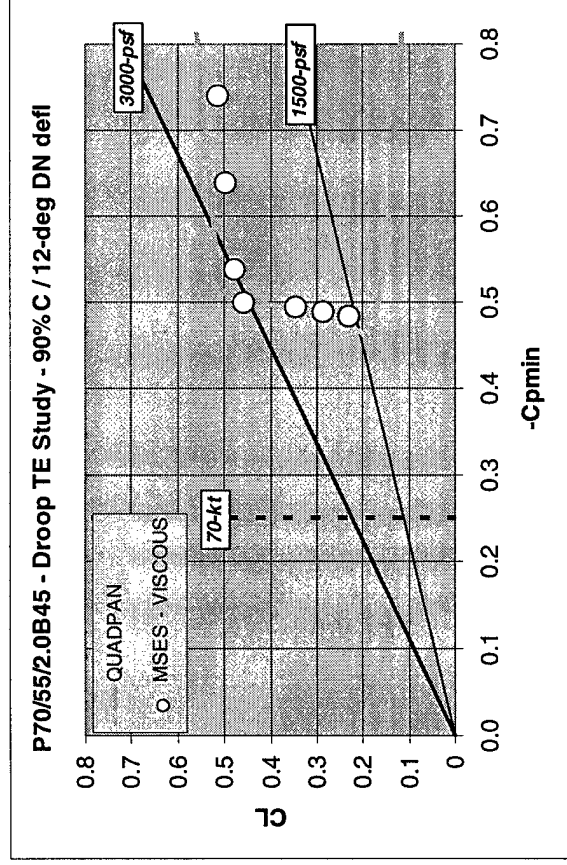
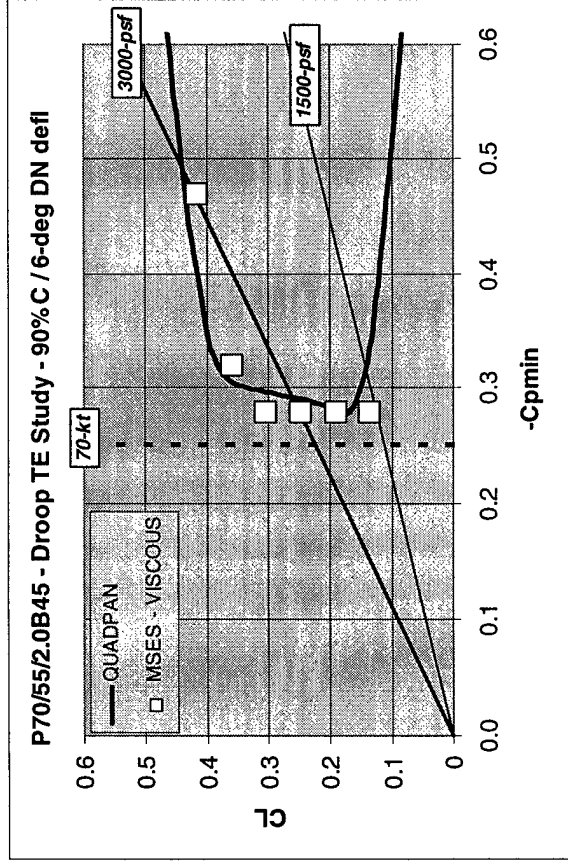
A drooped trailing edge is created by hinging the foil at 90% chord on the lower surface. The upper surface will then roll out in a circular arc.

Additional cavitation envelopes are shown for deflections ranging from 8 to 16 degrees. The droop allows non-cavitating operation at lower speeds and higher lift coefficients. The cavitation envelope shows that the minimum operating speed can be reduced to 44 knots by drooping the trailing edge 14 degrees. Further deflection of the trailing edge, however, will not enable operation at lower speeds (at a wing loading of 3000 pounds per square foot).

The cavitation diagrams for the trailing edge droop were constructed using QUADPAN. Verification at two droop angles with viscous computation at a Reynolds number of 100,000,000 were done using MSES. Good agreement is shown between QUADPAN and MSES for both 6° and 12° droop.

Recent computation shows the addition of a leading edge flap hinged at 12% chord and drooped 6 degrees will reduce the minimum speed down to 40 knots (with a trailing edge droop of 15 degrees).

Main Wing Design - P70/55B45 - 90%*c* Drooped TE

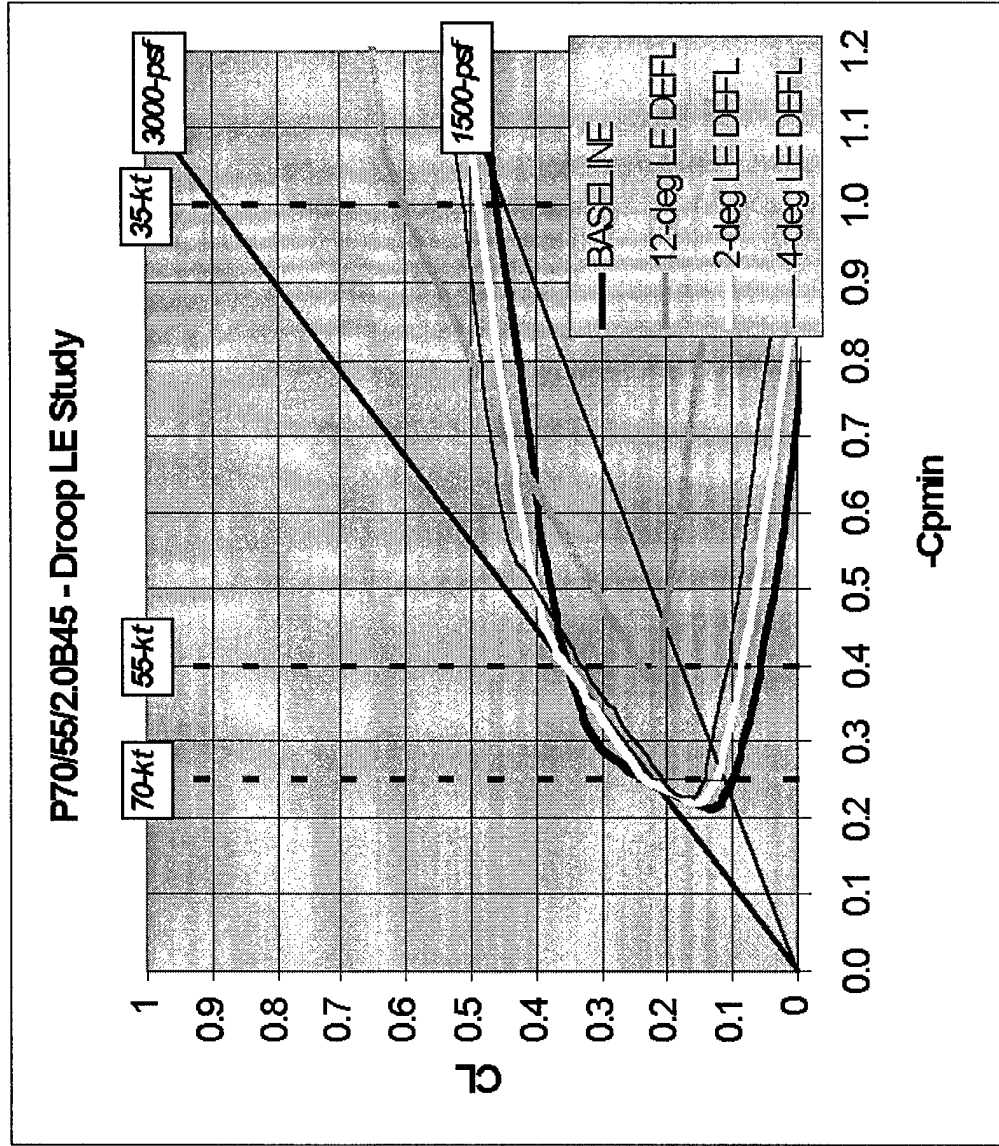


Main Wing Design - P70/55B45 – Drooped LE

The effect of a drooped leading edge on foil p70-55b45 is shown. The foil is hinged at 12% chord on the lower surface. The upper surface will then roll out in a circular arc.

The cavitation envelope shows that the drooped leading edge is ineffective in reducing the minimum operating speed. Smaller leading edge flaps were equally unsuccessful when used without trailing edge droop.

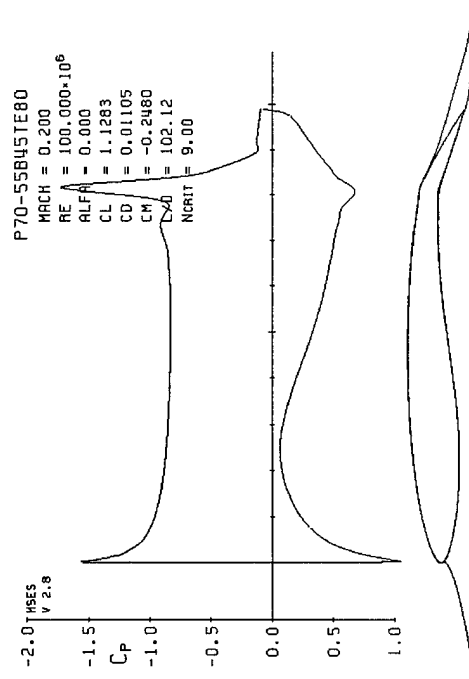
Main Wing Design - P70/55B45 - Drooped LE



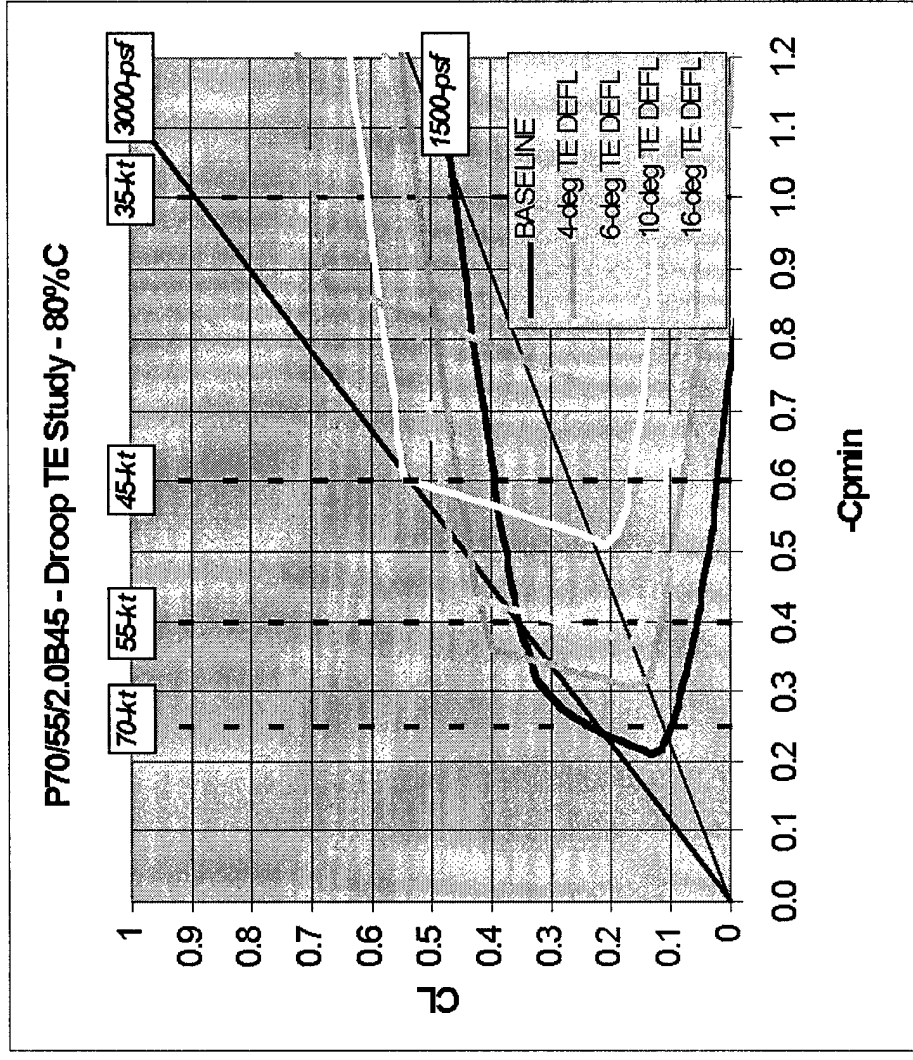
Main Wing Design - P70/55B45 – 80%c Drooped TE

The effect of a trailing edge flap hinged at 80% chord is shown. It seems that the minimum speed is reduced to 45 knots at a deflection of 10 degrees. Viscous analysis shows, however, that the trailing edge flow is separated under these conditions.

Main Wing Design - P70/55B45 – 80%*c* Drooped TE



Trailing Edge Flow
is Separated.

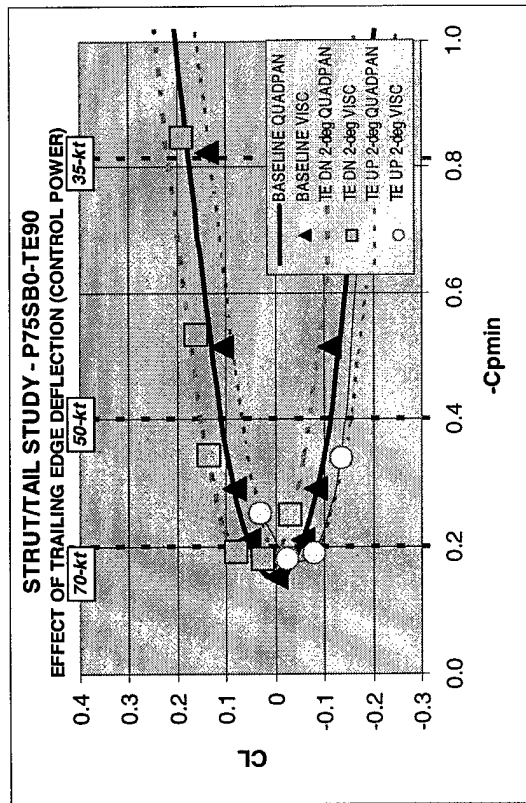


Strut Section Design

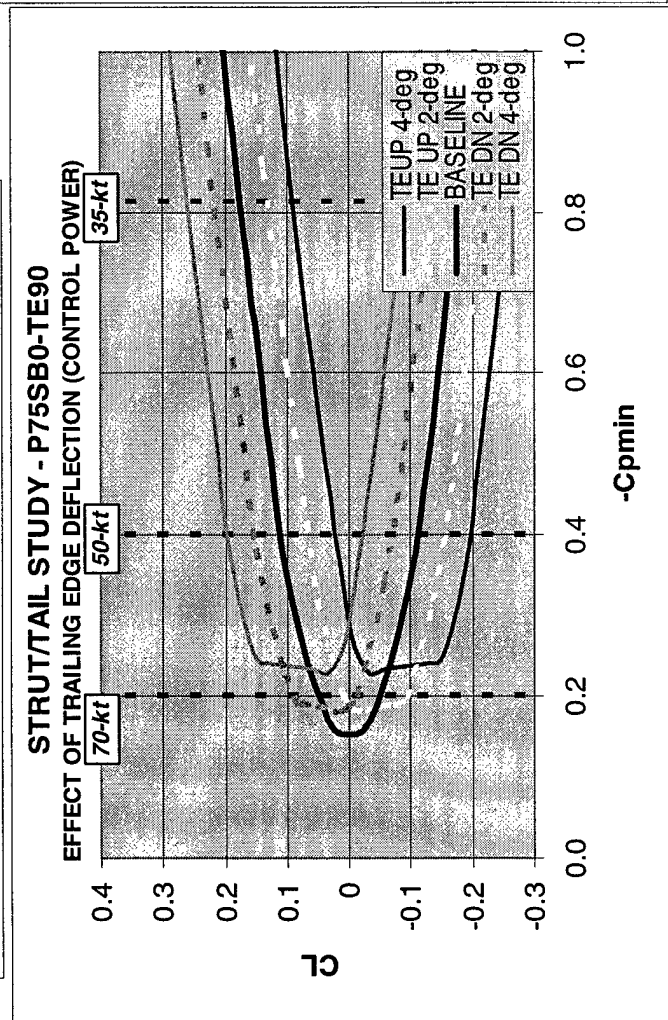
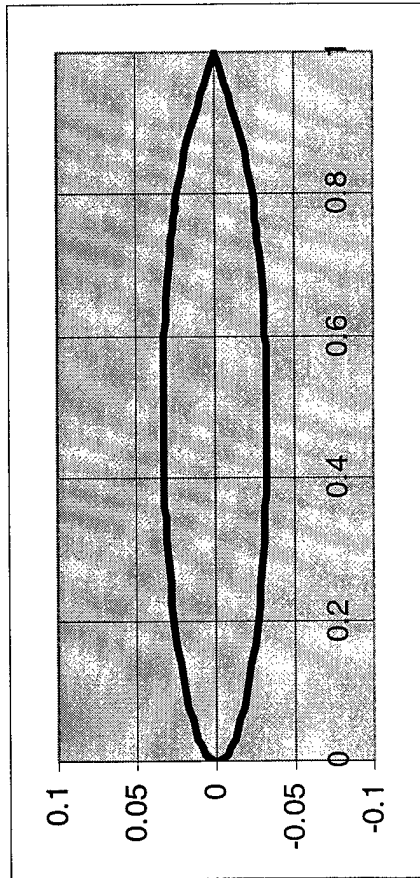
The cavitation diagrams for two symmetrical foil sections suitable for use as struts are compared. The foil p75sb0 has a higher top speed than p70sa0. At a speed of 70 knots, the higher speed foil yields slightly reduced CL range. This is offset by the ability of the higher speed foil to provide control power. With a trailing edge flap hinged at 90% chord, p75sb0 allows a 2 degree deflection at 70 knots without cavitating. This results in a maximum lift coefficient of 0.08.

The potential flow results are verified by viscous computation.

Strut Section Design

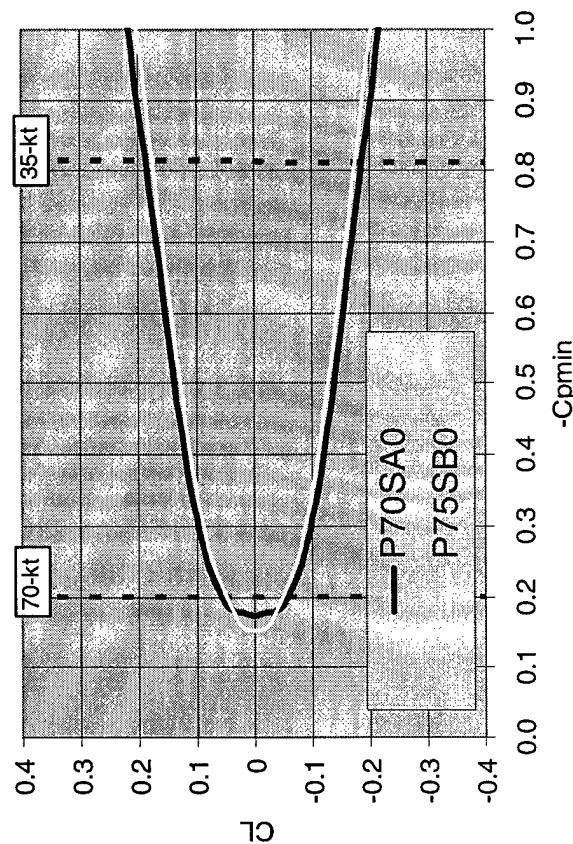


P75SB0 Normal to LE

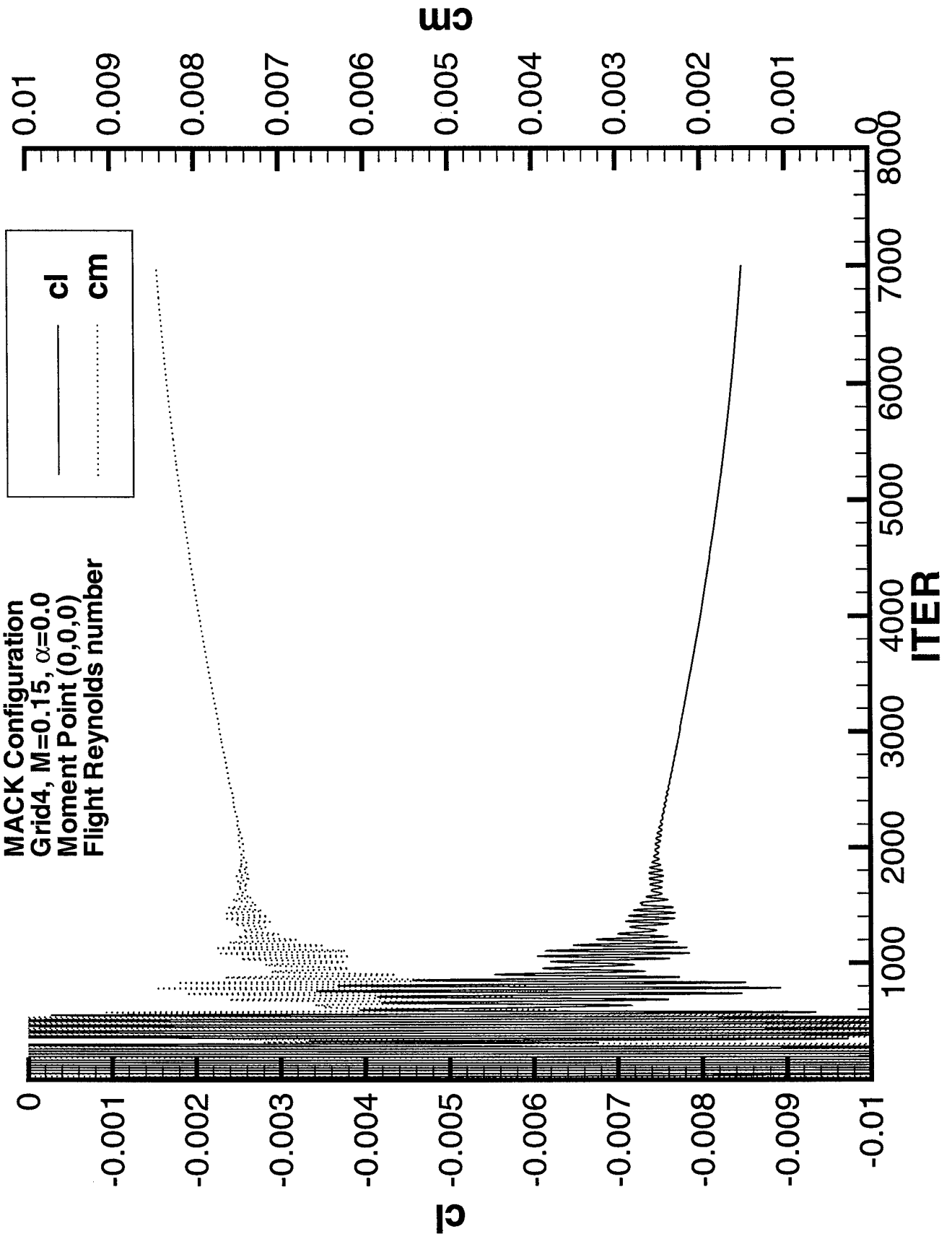


TAIL / STRUT STUDY

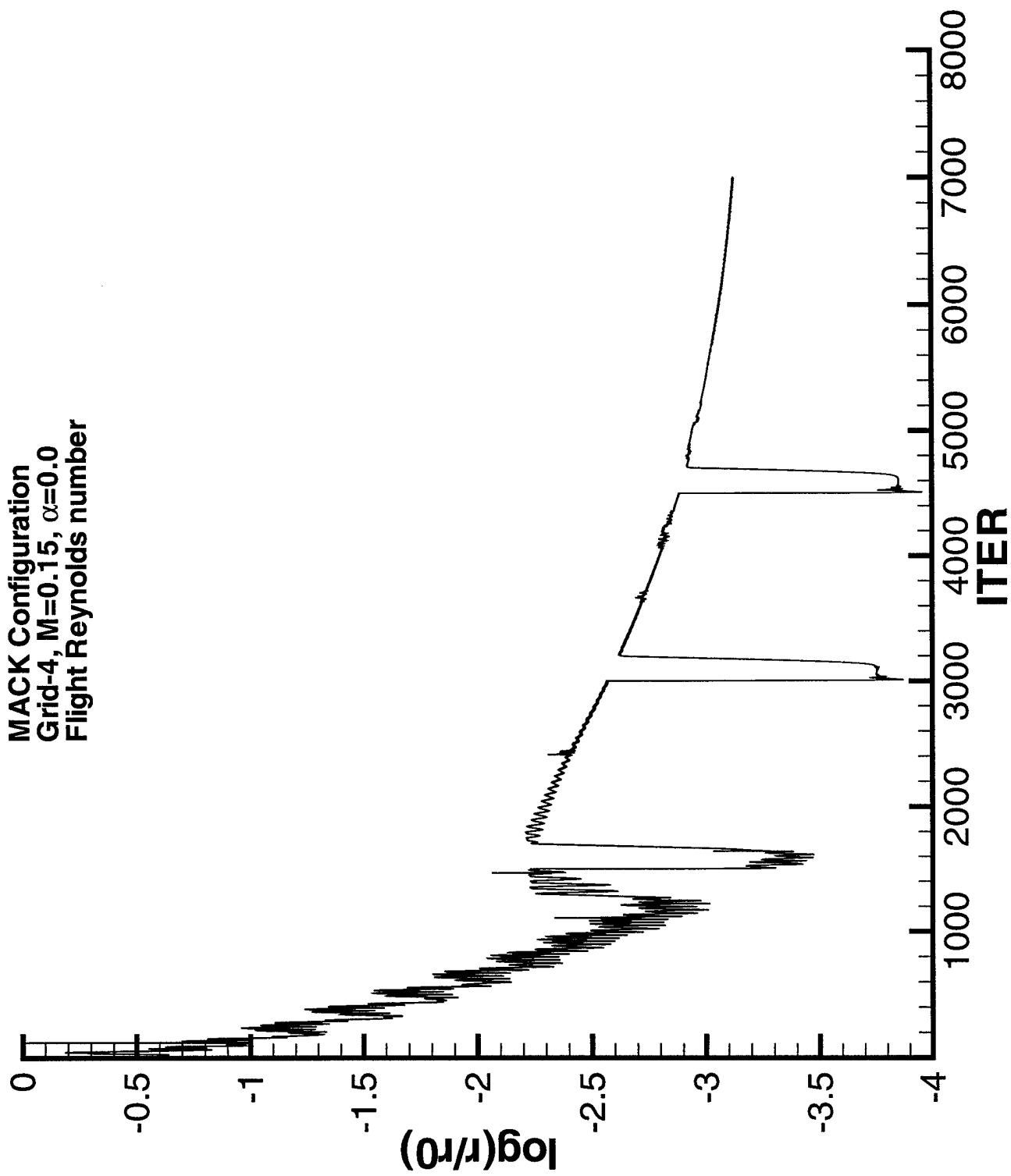
EFFECT OF DESIGN SPEED RANGE



MACK Configuration
Grid4, $M=0.15$, $\alpha=0.0$
Moment Point (0,0,0)
Flight Reynolds number



MACK Configuration
Grid-4, $M=0.15$, $\alpha=0.0$
Flight Reynolds number



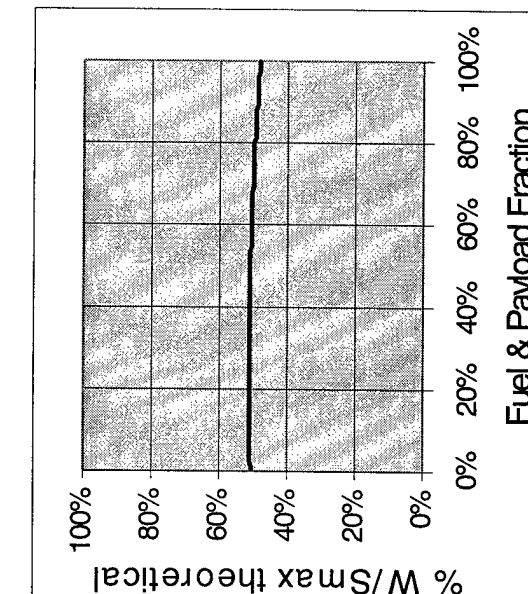
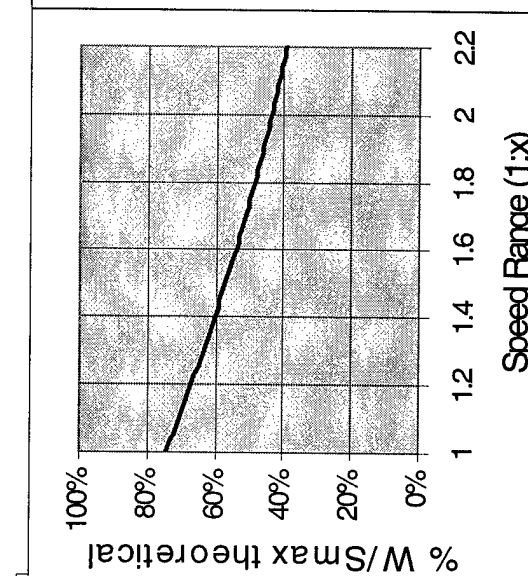
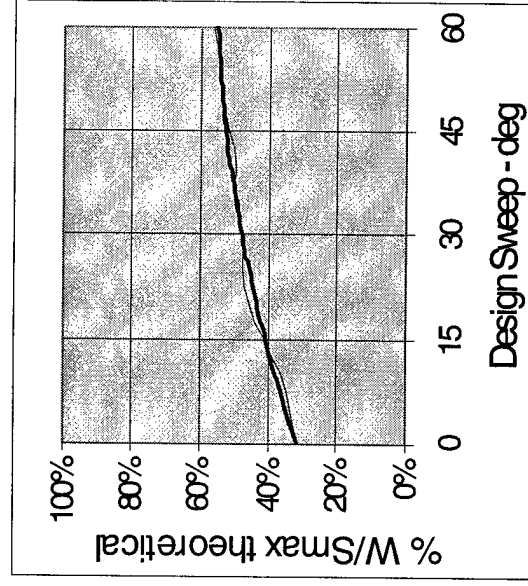
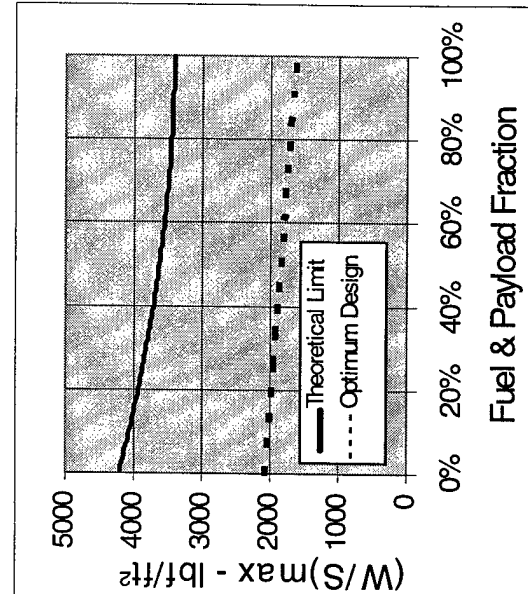
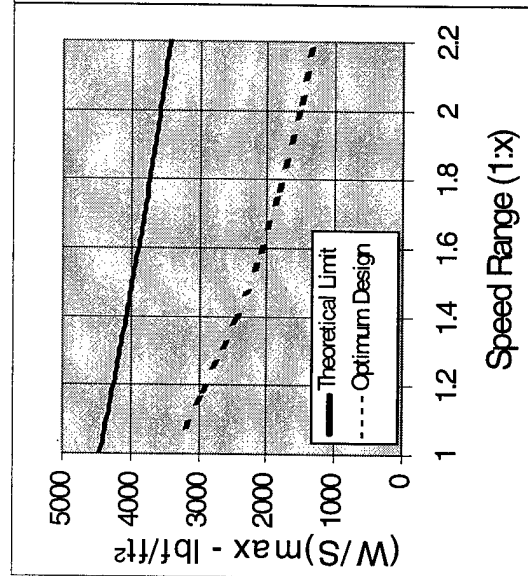
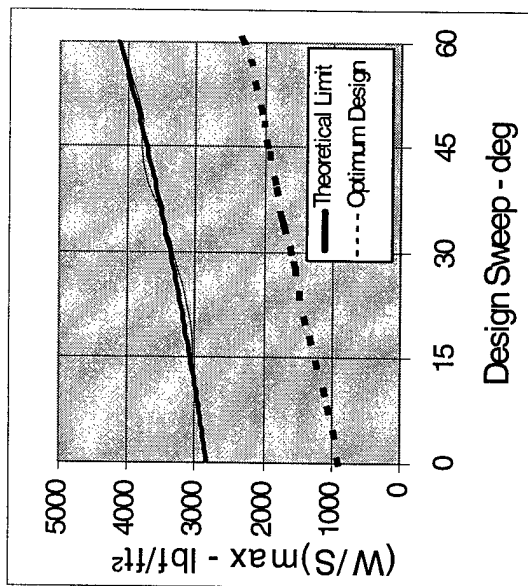
Sensitivity of Maximum Wing Loading to Design Variables

The sensitivity of $(W/S)_{max}$ to design sweep is shown for a family of foils designed for cavitation-free operation from $V_{min} = 40$ knots to $V_{max} = 70$ knots, $(W/S)_{max}/(W/S)_{min} = 2$ (corresponding to a Fuel&Payload Fraction of 50%) and an operating depth, $h=20$ feet. As the design sweep is increased, foils can be developed which not only sustain greater loading, but proportionately greater loading (in this case, reaching a maximum loading of 56% of theory at a sweep of $\Lambda=60^\circ$. It should be noted that this procedure has proved useful to develop foils with a leading edge sweep, Λ , of less than 60° . When a greater design sweep is specified, the "optimized" foils become prone to premature trailing edge separation; the cavitation diagram of the "optimized" foil sections as assessed using the inviscid QUADPAN no longer correlate well with those assessed using the viscous MSES code.

The sensitivity of $(W/S)_{max}$ to design speed range is shown for a family of foils designed for cavitation-free operation at a top-speed, V_{max} , of 70 knots. As before, $(W/S)_{max}/(W/S)_{min} = 2$ (corresponding to a Fuel&Payload Fraction of 50%) and the operating depth is fixed at $h = 20$ feet. As the design speed range is reduced, thinner foils can be developed which sustain both greater wing loading and proportionately greater wing loading. An example narrow speed range foil ($V_{min}=V_{max}=70$ knots) achieves a practical loading of maximum loading of 72% of theory.

The sensitivity of $(W/S)_{max}$ to design loading range is shown for a family of foils designed for cavitation-free operation from $V_{min}=40$ knots to $V_{max}=70$ knots for a fixed wing sweep, $\Lambda=40^\circ$ and a fixed operating depth of, $h = 20$ feet. As the Fuel&Payload Fraction is reduced, thinner foils can be developed which sustain greater loading; but this design variable tends to have little influence on the practical percentage of theoretical performance which may be attained.

Sensitivity of Maximum Wing Loading to Design Variables



Wave-Making Resistance

The wave-making resistance of wings, struts, and bodies is calculated from a potential flow analysis using the panel method QUADPAN. In this approach, Rankine singularities are used in combination with a flat free-surface which extends sufficiently far in all directions to capture the wave-making activity. The linearized boundary condition of constant pressure on the free-surface is applied, together with a suitable radiation condition to preclude upstream waves. The free-surface effects on hydrodynamic lift, moment, and induced drag, as well as wave drag, are determined.

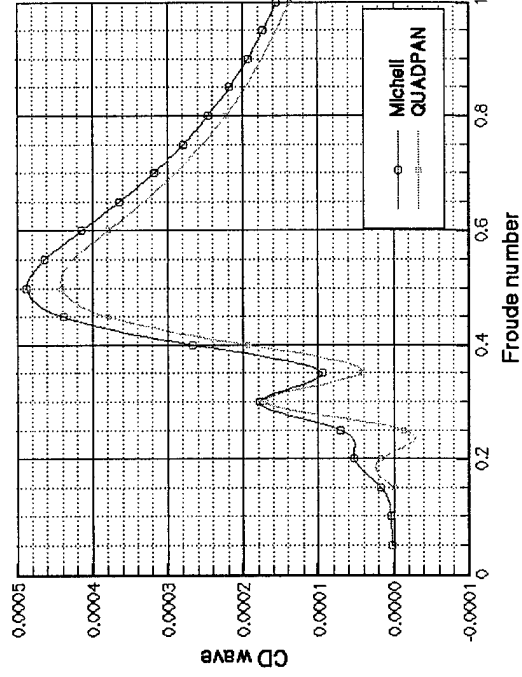
The method is equally applicable for vehicles traveling on the water surface and for those traveling below it. If the vehicle intersects the free-surface, only the wetted portion is paneled. Therefore, there are gaps in the free-surface where it intersects the configuration.

Calculations of the wave-making resistance and wave elevation contours for a Wigley hull (a hull shape defined by parabolic contours) are presented. In the free-surface contour pictures, red represents high elevation, and blue represents low elevation. The waves are confined to a wedge whose half-angle is approximately twenty degrees (as in the Kelvin point source solution). The picture of the lower Froude number shows a dominance of the transverse waves, while that of the higher Froude number shows predominantly diverging waves. The increase of wave-length with increasing Froude number is also clearly shown.

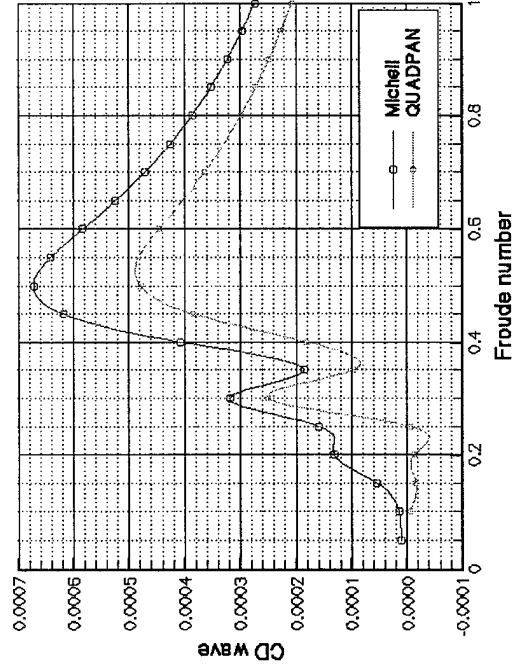
The plots of wave resistance coefficient versus Froude number compares the computed QUADPAN results with those obtained from Michell's thin ship theory. The agreement is closer for the thinner of the two hulls, as expected. The QUADPAN results for the thicker hull, however, should be more accurate than Michell's theory. The slightly negative drag at low Froude number computed by QUADPAN is an artifact of the coarse grid that was used; the drag becomes positive as the grid is refined to a higher density.

Wave-Making Resistance

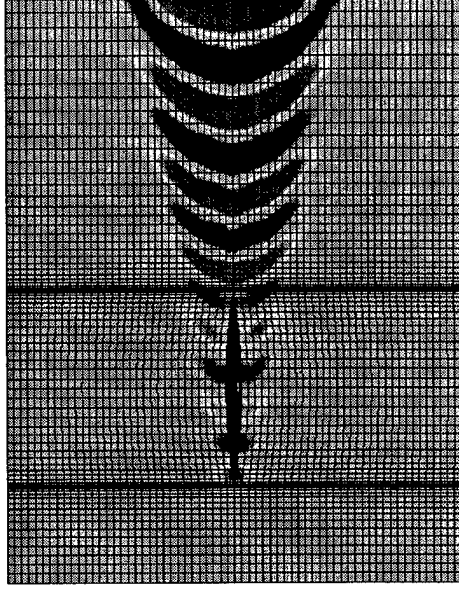
length/beam = 20 length/draft = 8



length/beam = 10 length/draft = 16

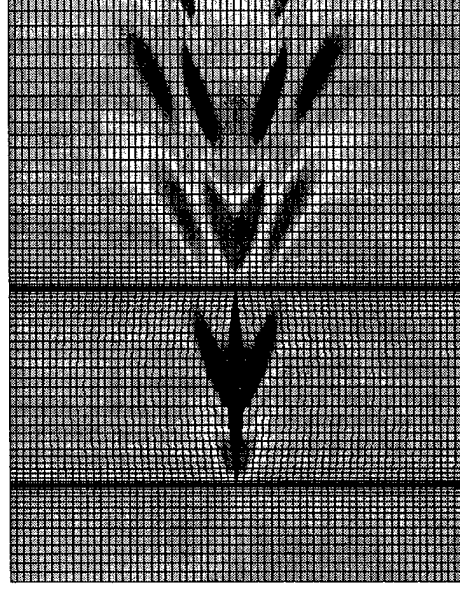


Wigley hull free surface elevation Froude 0.228



length/beam = 10 length/draft = 16

Wigley hull free surface elevation Froude 0.452



High Fidelity Analysis Tools and QUADPAN Grid For Integrated Hydrofoil Geometry

High Fidelity Analysis Tools Used On Integrated Hydrofoil Geometry :

QUADPAN is an in-house 3-D low-order panel method which solves the Prandtl-Glauert equation of linear potential flow for arbitrary configurations. It employs a distribution of constant strength source and doublet singularities on quadrilateral elements over the surface of the body. The boundary condition of zero normal velocity for each element leads to a linear system of equations. Pressures are integrated over the surface of the body to compute forces and moments.

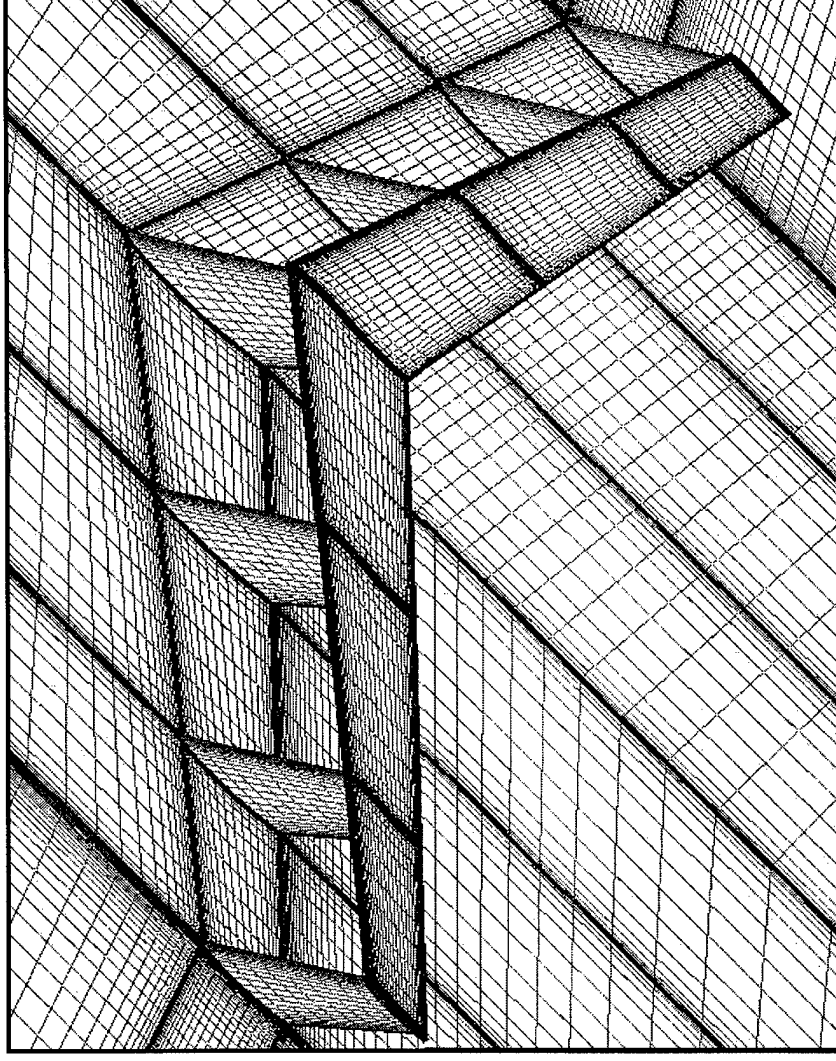
QUADPAN has a free-surface boundary condition for the computation of the hydrodynamics of vehicles moving in the neighborhood of an air-water interface. This can be used for the motion of seaplanes through the water, as well as conventional ships and hydrofoils. The boundary condition at the free surface is one of constant pressure, linearized for small disturbances. A body experiences changes in lift due to the presence of the free boundary, and a component of resistance caused by wave-making.

GRIDGEN is an interactive, graphically oriented system used for the generation of 3-D grids. It is commercial software under development by Pointwise, Inc.

QUADPAN Grid On Integrated Hydrofoil Geometry :

The figure shows the surface grid of quadrilateral elements on the detailed, integrated hydrofoil/strut geometry. The hydrofoil cross-section used for this analysis is P70-55/B45 and the strut cross-section is P75-40/SA0. The blue part of the grid in the figure shows the area to which the free surface boundary condition was applied (water surface). The hydrofoil wing and the seven struts are shown in red and pink respectively. The total number of elements for this grid is 47,682 among which 19,300 are solid surface elements, 19,142 are water surface elements and 9,240 are wake elements (not shown).

High Fidelity Analysis Tools and QUADPAN Grid For Integrated Hydrofoil Geometry



QUADPAN Grid On Hydrofoil Geometry

QUADPAN Solution For 4,000 T Ship And Elimination Of Side Load On The Struts

QUADPAN Solution (4,000 T ship at 70 Knots, Froude 4.4) :

The solution at Froude 4.4 (4,000T ship at 70 knots) was computed using a parallel version of the QUADPAN code on a dual processor SGI Octane. These calculations required approximately 5 Gigabytes of memory and were performed using approximately 8 hours of CPU time (distributed over two processors).

The picture on the left displays contours of constant pressure coefficient (C_p) obtained from the QUADPAN solution. The color red indicates a high pressure region, and the color blue indicates low pressure on the surface. The cavitation number for this speed is 0.24 at the depth of the upper wing surface. Any dark blue color in the figure (where C_p is more negative than -0.24) indicates an area where the predicted pressure is below the vapor pressure of water. In such regions, cavity formation prevents the occurrence of negative absolute pressure.

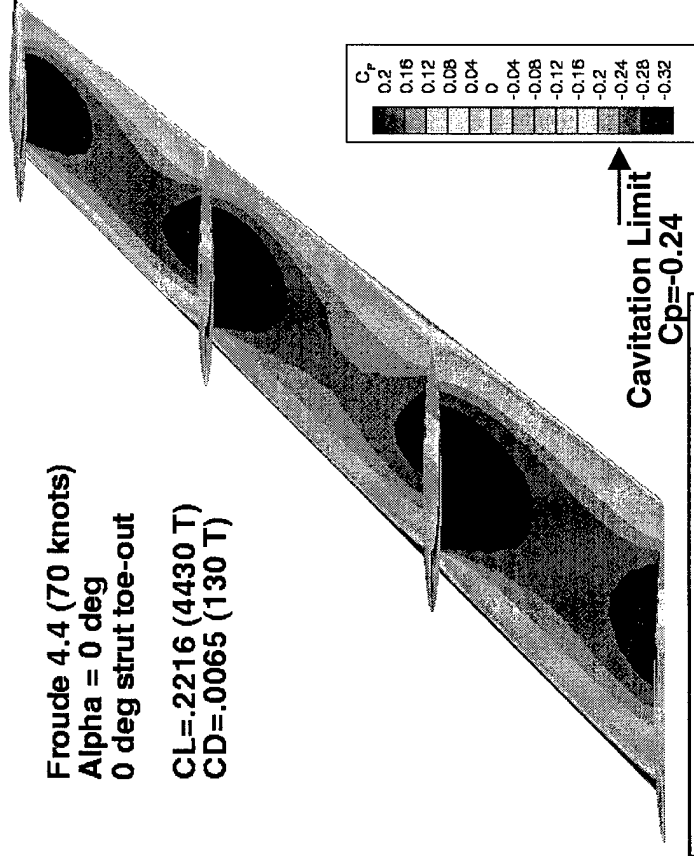
The interference between the foil and the struts create cavitation regions around their juncture. In addition, a considerable side load is observed on the three most outboard struts. This is as a result of the swept wing which causes a span-wise inboard flow, inducing an angle of attack on the three outboard struts.

Elimination of side load on struts :

In order to eliminate the side load on the three outboard struts, the effect of introducing a toe-out angle to the struts (leading edge of the strut rotated outboard) was studied. This aligns the struts with the incoming free-stream flow and eliminates the side load. In order to determine the proper toe angle, struts were rotated through a range of angles varying between one and six degrees.

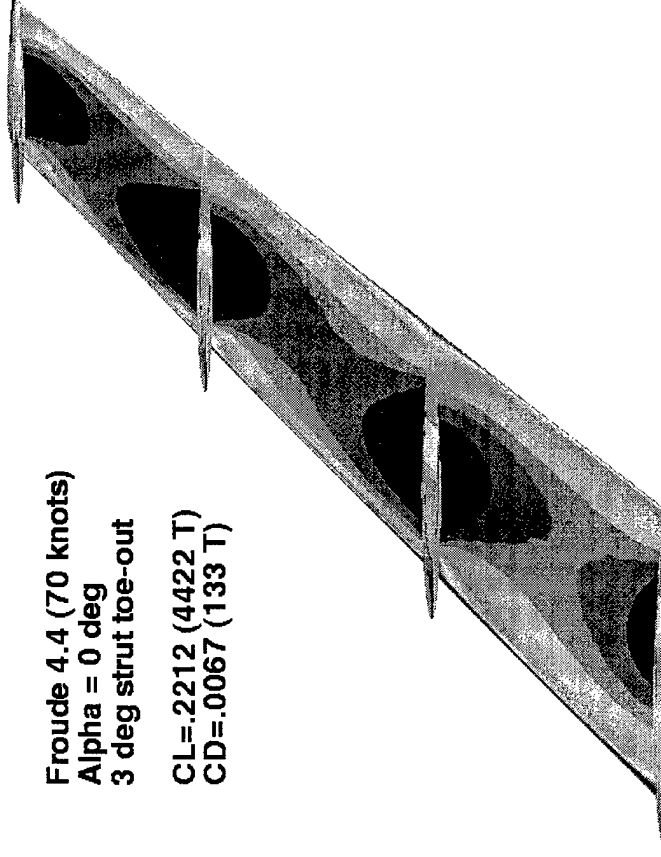
The solutions indicate that introducing a three to four degree toe angle eliminates the side force on the three outboard struts. Contours of C_p with the three degree toe angle imposed on all struts (except for the centerline strut) are shown in the right figure. The pressures inboard and outboard of the struts are now of comparable magnitude. However, strut toe-out does not eliminate the interference effects of the struts and the wing, and the resultant cavitation. The issue of cavitation suppression will now be addressed.

QUADPAN Solution For 4,000 T Ship And Elimination Of Side Load On The Struts



Froude 4.4 (70 knots)
Alpha = 0 deg
0 deg strut toe-out
CL=-.2216 (4430 T)
CD=.0065 (130 T)

QUADPAN solution for 4,000 T Ship
(no toe-out)



Froude 4.4 (70 knots)
Alpha = 0 deg
3 deg strut toe-out
CL=-.2212 (4422 T)
CD=.0067 (133 T)

QUADPAN solution for 4,000 T Ship
(3 degree toe-out on 3 outboard struts)

Wing/Strut Cavitation Suppression

In order to reduce the suction pressure at the intersection of the struts and the hydrofoil, two possible approaches for re-design were considered. The goal was to design a modified hydrofoil/strut intersection which would not have any cavitation, but could carry close to 4,000T (3,811T, accounting for wing and strut buoyancy) all-up weight. It is important to remember that the original clean hydrofoil (without struts) was designed for 4,000T of lift. The challenge is not only to reduce the strut interference, but also to retain as much lift as possible to meet our design requirements.

The figure shows design concepts that were considered for cavitation suppression :

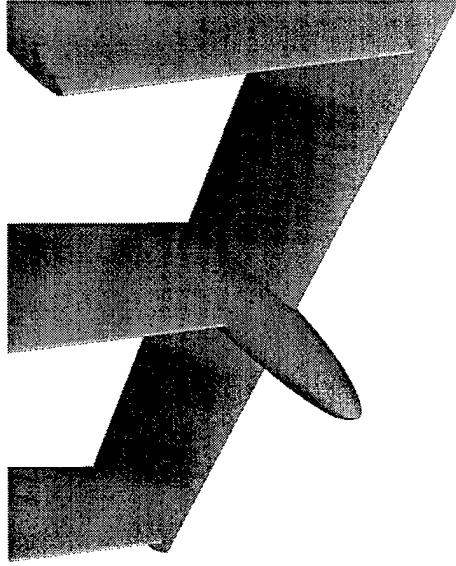
Approach 1 : Nosecone Strut Fairing Concept

Design a body fairing (nosecone) for the wing/strut intersection which is long and slender in order to govern the strut/foil juncture flow.

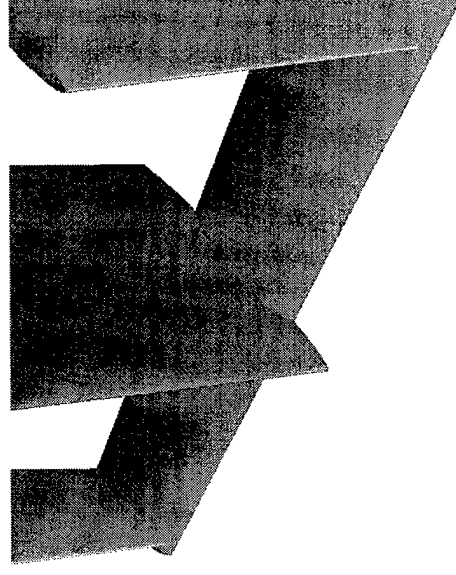
Approach 2 : Streamlined Strut Design Concept

Re-design the strut in such a way that it follows a streamline over the hydrofoil wing. This should create a path of minimum flow disturbance and, as a result, reduce interference effects. Design such a strut section by introducing camber and a varying thickness distribution to the original strut section.

Wing/Strut Cavitation Suppression



Nosecone Design



Streamlined Strut Design

Wing/Strut Cavitation Suppression Nosecone Design

Concept and design

The design of a nosecone was the first concept considered to eliminate the cavitation regions on the integrated hydrofoil geometry. The idea behind this concept is that a long and slender body fairing at the wing/strut intersection will govern the flow. It was anticipated that such a fairing would reduce and possibly eliminate the region of cavitation observed in the earlier computations.

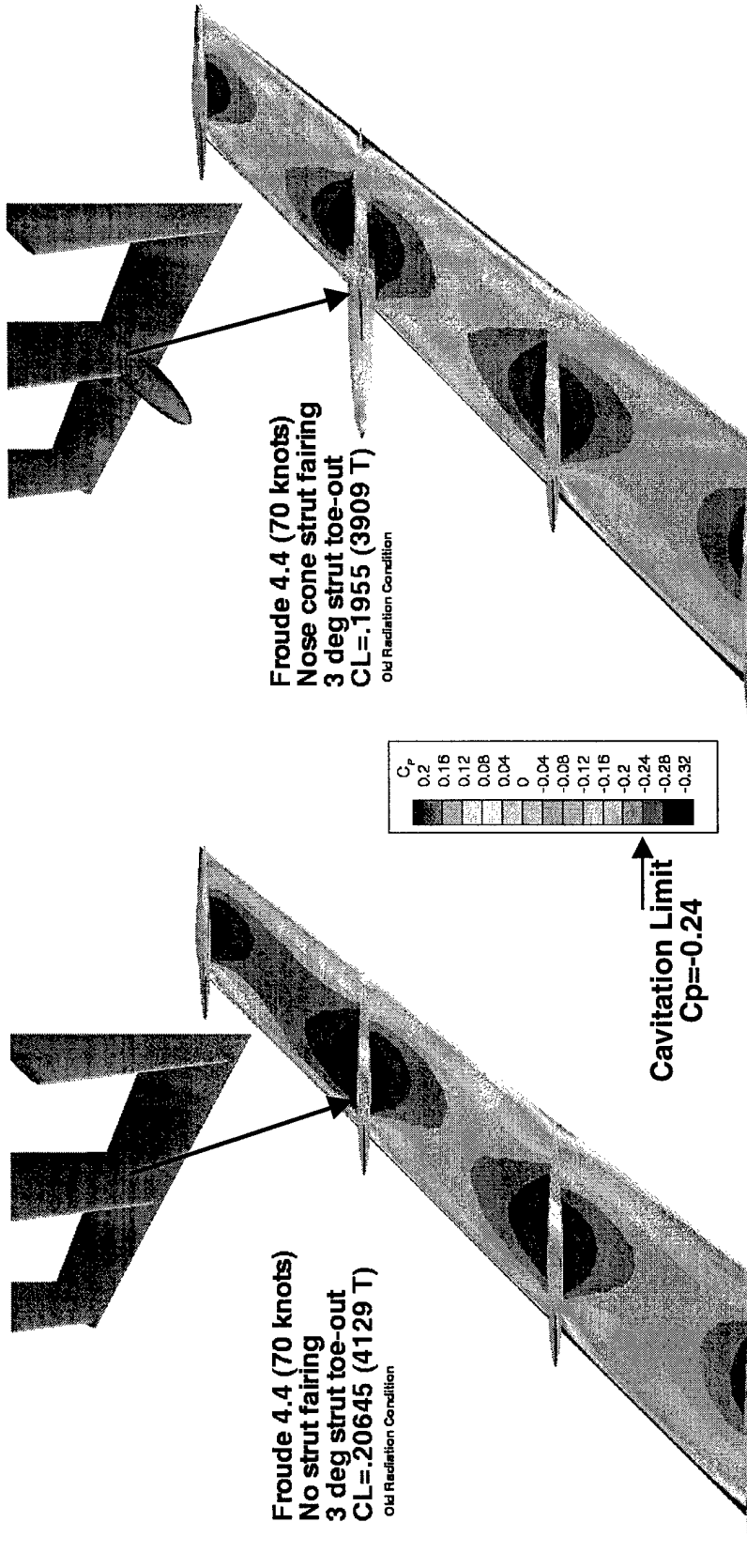
It was not obvious what the fairing diameter and aspect ratio (cone length/diameter) needed to be in order to produce the required effect. Nose cones have been successfully designed and used in the past to eliminate propeller burn and blowout on high speed powerboats. For a boat going 80 miles per hour, an aspect ratio of 3.5 is typical. Based on this information, two nosecones with different diameters and aspect ratio of 3.5 were designed and analyzed.

QUADPAN results

The larger diameter nosecone performed better than the one of smaller diameter. Only results for the bigger nosecone are shown here. In an effort to reduce the labor needed to verify the effect of the fairing, it was modeled on only one of the strut/foil intersections (second from outboard).

Comparing the region around the fairing before and after the re-design, we observe that there is less cavitation without too much loss of lift. However, this design has only reduced, not eliminated the cavitation region. Clearly, an even bigger nosecone is required in order to sufficiently govern the flow. Because the dimensions of the nosecone are required to be large in order for it to be effective, this concept is not considered an efficient approach for cavitation suppression.

Wing/Strut Cavitation Suppression Nosecone Design



QUADPAN solution for 4,000 T Ship (no re-design)

QUADPAN solution for 4,000 T Ship (nosecone fairing)

Wing/Strut Cavitation Suppression Streamlined Strut Design

Concept and Design

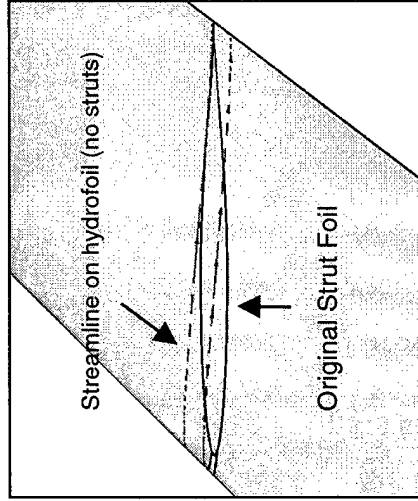
This concept requires the re-design of the strut cross section in order for its shape to follow the path of an undisturbed streamline over the hydrofoil. If a strut is designed to follow the streamline over the isolated hydrofoil (no struts present), the path of minimum flow disturbance has been found, and interference effects are eliminated as much as possible.

In order to design such a strut, the first step was to obtain the streamlines over the upper surface of the isolated hydrofoil. The picture (top/left) shows two typical streamlines in red and the original strut/foil intersection in black. The next picture (top/middle) shows a 2 dimensional plot of such a streamline (the scales on the chord-wise and span-wise axis are not the same). Over the wing, the streamlines are parallel to each other and at an angle (leading edge out) of 4 degrees (we had already found this when working towards eliminating the side load on the struts). In addition, an s-type curvature is also observed at the leading and trailing edges of the hydrofoil.

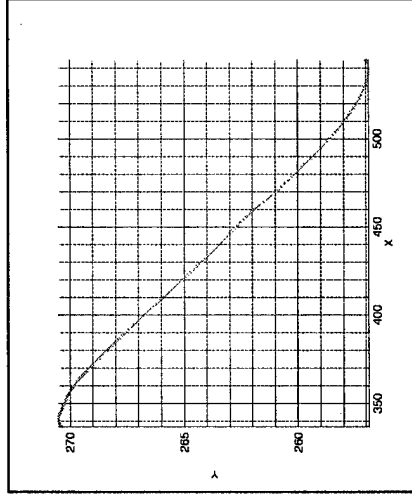
Based on these observations, a new streamlined strut shown in the next figure (top/right) was designed. A constant thickness distribution (equal to the maximum thickness of the original strut design) was used over the hydrofoil. In order to further control the flow, the leading edge of the strut was moved forward of the hydrofoil and the trailing edge of the strut was moved behind it. The simulated deflection boundary condition available in QUADPAN was next employed to determine the necessary strut design. This option allows the user to impose a deflection of (part of) the strut without actually having to construct a new grid. For small deflections, the simulated boundary condition accuracy approaches that of an actual re-gridding.

The strut was divided into four inboard and four outboard sections (top/right picture), separately rotated using the simulated deflection boundary condition. Three kinds of deflections were employed in order to suppress cavitation. First, a toe-out simulated deflection rotated each panel by the same amount (see bottom/left picture). This is equivalent to rotating the complete strut. Second, the front sections were deflected inboard and the back sections were deflected outboard to create an s-shape. This is equivalent to introducing camber to the strut (see bottom/middle picture). Finally, as an added benefit, a concave thickness deflection was also defined (see bottom/right picture). This type of concave strut section ("peanut" shape) will further slow down the flow above the hydrofoil, and increase the pressure to help suppress cavitation. A combination of these boundary conditions was needed in order to obtain the best results.

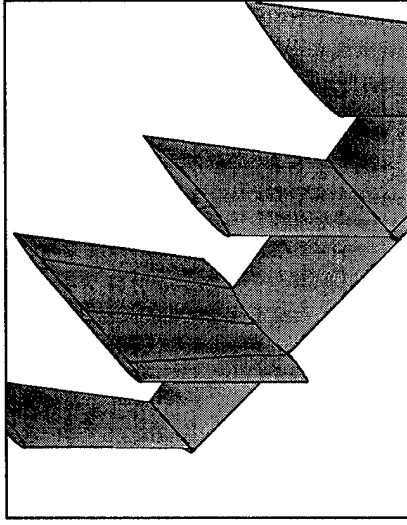
Wing/Strut Cavitation Suppression Streamlined Strut Design



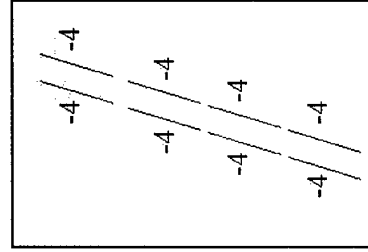
Typical undisturbed streamlines on hydrofoil. No struts present



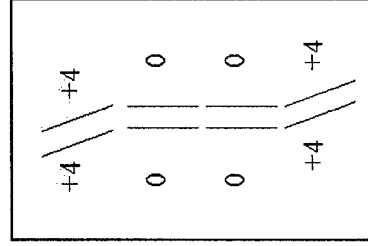
Details of undisturbed streamline on hydrofoil. No struts present



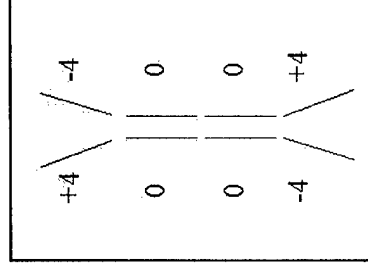
Implementation model for streamlined strut design (8 panels)



Toe-out



Camber



Concave Thickness

Wing/Strut Cavitation Suppression Streamlined Strut Design

QUADPAN Solutions For Streamlined Strut Design Using Simulated Deflections

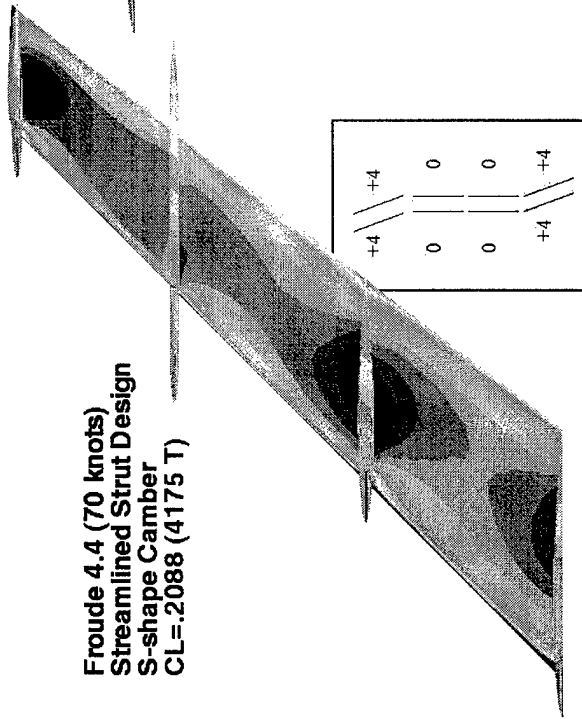
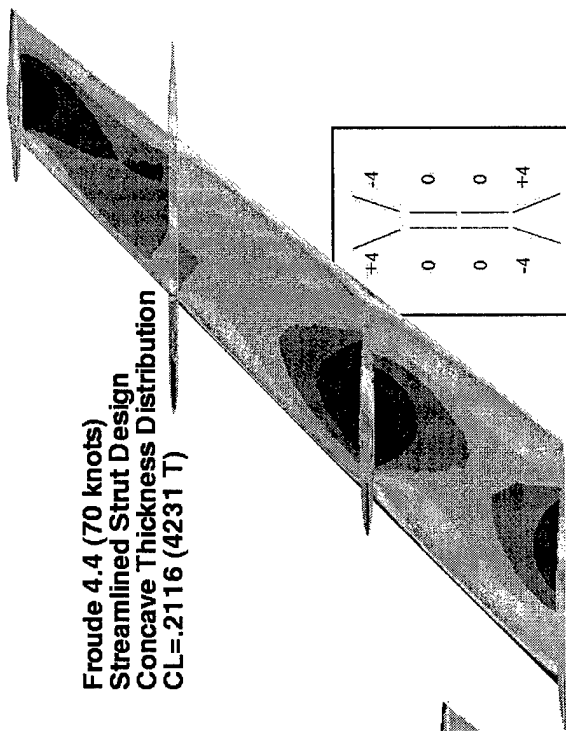
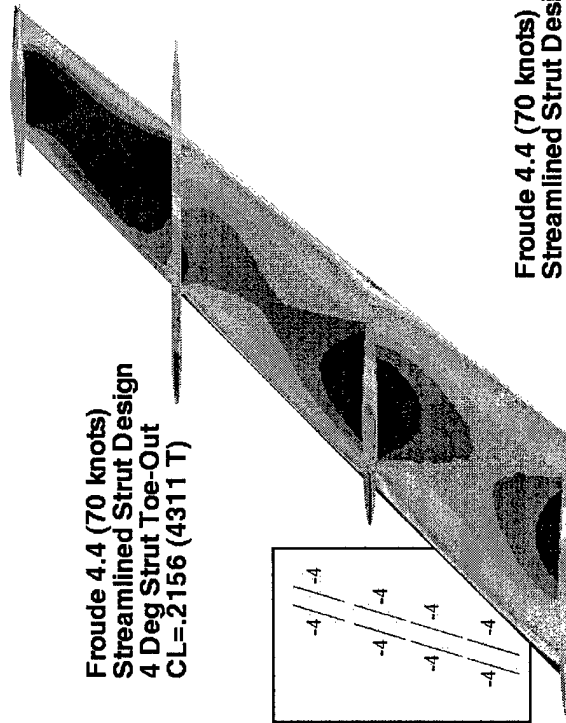
First, each of the deflections was applied separately to observe the effects on the flow. The left picture shows the effect of introducing a 4 degree toe-out to the strut. The middle picture shows the effect of adding camber to the strut and the right picture shows the effect of introducing a concave thickness distribution to the strut. Each of these contributes to reducing the interference effects. However, cavitation has not been completely eliminated with any of the separate deflections.

Next, a solution was computed using a linear combination of these deflections. The left picture on the next page shows the result of applying a linear combination of toe-out, s-shape camber and concave thickness distribution. The pictures on the right show the QUADPAN solution on the original integrated geometry and the isolated hydrofoil geometry. The streamlined strut design does an excellent job at suppressing the cavitation while conserving most of the lift (lift was only reduced from 4422 T to 4059 T). The pressures in the neighborhood of the affected strut are now similar to the isolated hydrofoil.

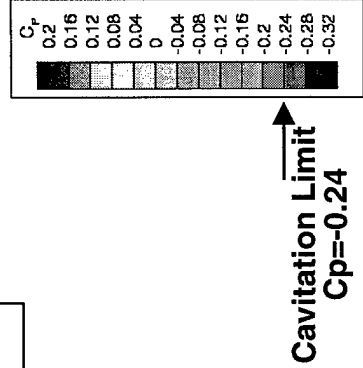
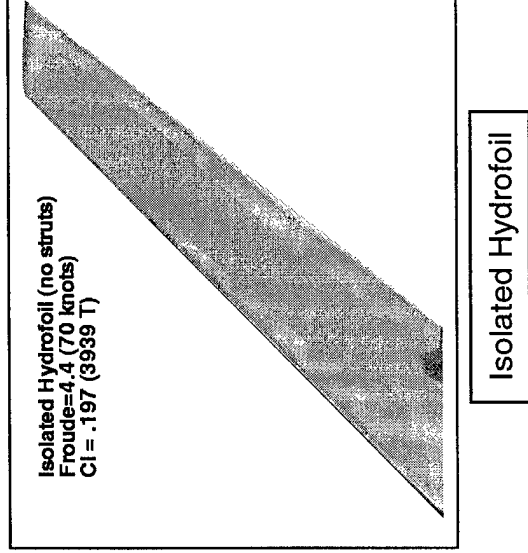
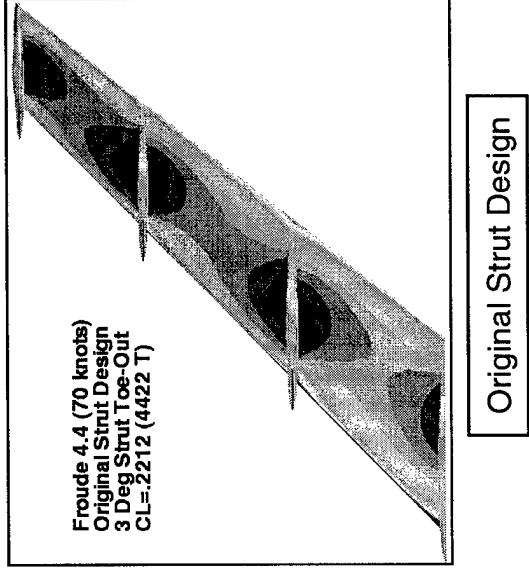
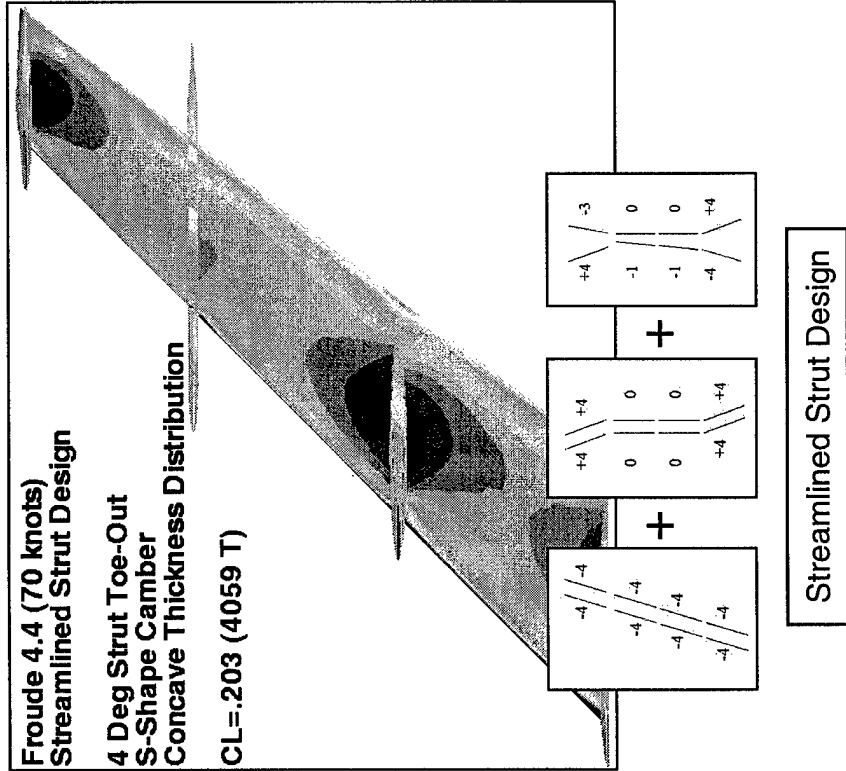
QUADPAN Solutions For Streamlined Strut Design

Finally, an actual strut was designed based on the simulated deflections. The left picture on the next page shows the streamlined strut design. The QUADPAN solution for this geometry is shown on the right. It is clear that this new strut design is very efficient at suppressing the cavitation. However the lift for this design is 3,663 T, substantially below the design requirement of 4,000T. When the other struts are also replaced with the streamlined design, the lift will be further reduced. The loss of lift can be overcome by increasing the wing area of the hydrofoil.

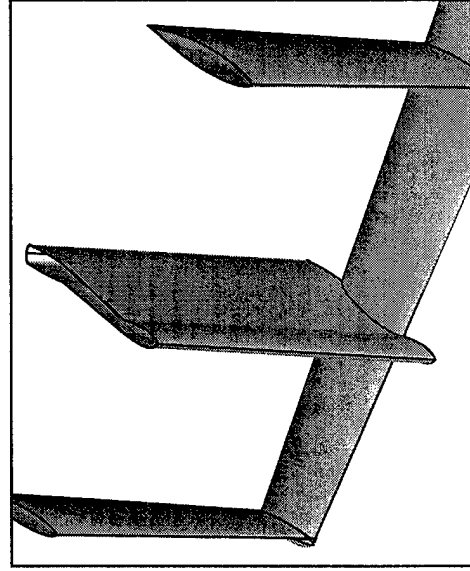
Wing/Strut Cavitation Suppression Streamlined Strut Design



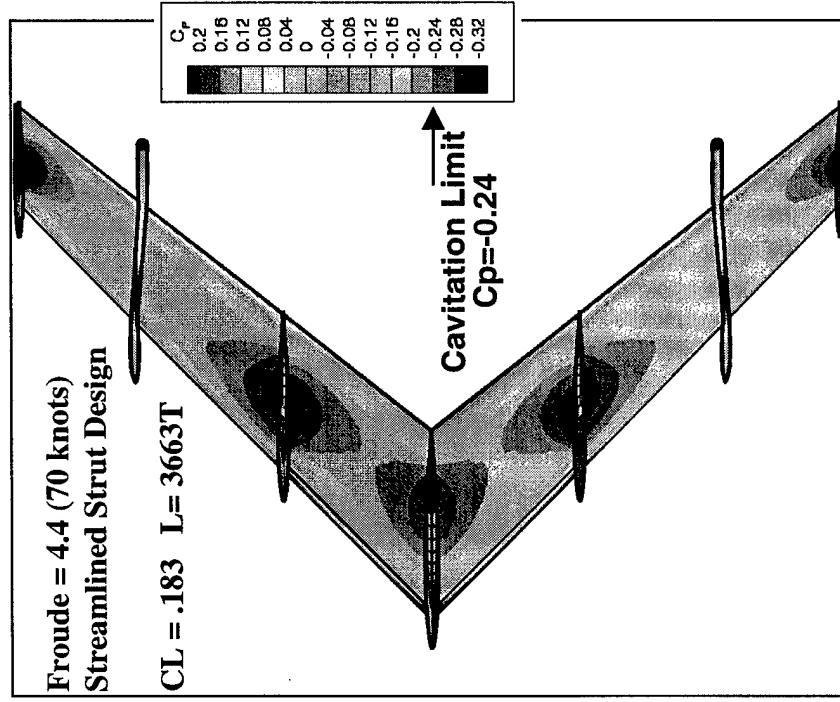
Wing/Strut Cavitation Suppression Streamlined Strut Design



Wing/Strut Cavitation Suppression Streamlined Strut Design



Final streamlined strut design



QUADPAN solution on final streamlined strut

Body - Design Rules

An axisymmetric body can be defined by revolving a symmetric foil section about its chord line. The foil design methodology can thus be used to design a body of revolution.

All of the foil design parameters (except sweep) are retained, with the camber coefficients A_n set to zero (as in the strut design problem). The foil section is revolved and the 3-D co-ordinates are used for the potential flow analysis. A free surface grid is also created and used in the analysis. The computed wave drag and hydrodynamic lift are added to the friction drag and hydrostatic buoyancy, respectively, to obtain total drag and net weight (the friction drag includes an allowance for strut wetted area). A "tare" is employed to make the computed wave drag and lift more accurate when using a coarse grid.

Separate horizontal and vertical diameters can be used for non-axisymmetric bodies of elliptical cross-section.

The objective is to maximize the weight-to-drag ratio for a given speed and displacement, subject to the following constraints:

1. Cavitation-free operation
2. Minimum thickness ratio (for example, 10%).
3. Minimum leading edge radius.
4. Minimum range (using variation of structural weight with depth).

The limitations of the body design procedure are:

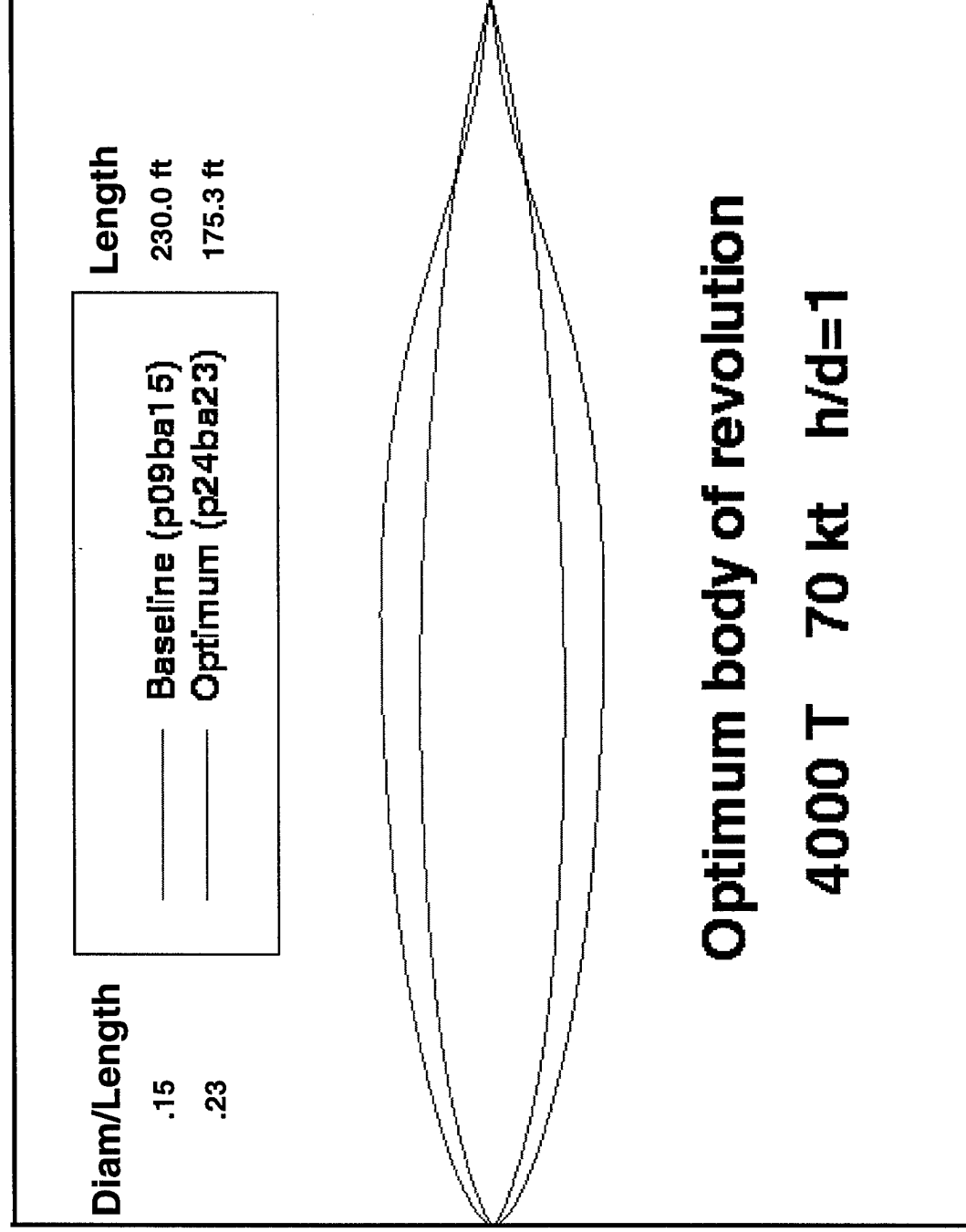
1. Inviscid analysis.
2. No strut interference.

These limitations, however, are later addressed by higher fidelity analysis.

- **Body Nomenclature :**

- METHOD / CAVITATION NUMBER / TYPE / VERSION / DIAMETER-TO-LENGTH RATIO
- method = "P" (POINTER)
- type = "B" (body), "T" (twin-body)
- version = "A", "B", "C", ...
- cavitation number and diameter-to-length ratio are in percent

Body - Design Rules



Havelock's Solution for Wave Drag of Submerged Ellipsoid

The wave drag of a submerged ellipsoid as computed by QUADPAN is compared to that calculated by a classical solution of Havelock. The ellipsoid is 130 meters long, with vertical diameter of 15 meters, and horizontal diameter of 19 meters; the displacement of the ellipsoid is 20,000 metric tons. The centerline of the ellipsoid is at a depth of 10 meters.

The ratio of buoyant lift to wave drag for the ellipsoid is plotted versus speed. The maximum drag occurs at a speed of about 40 knots. There is general agreement between the QUADPAN computations and the Havelock solution.

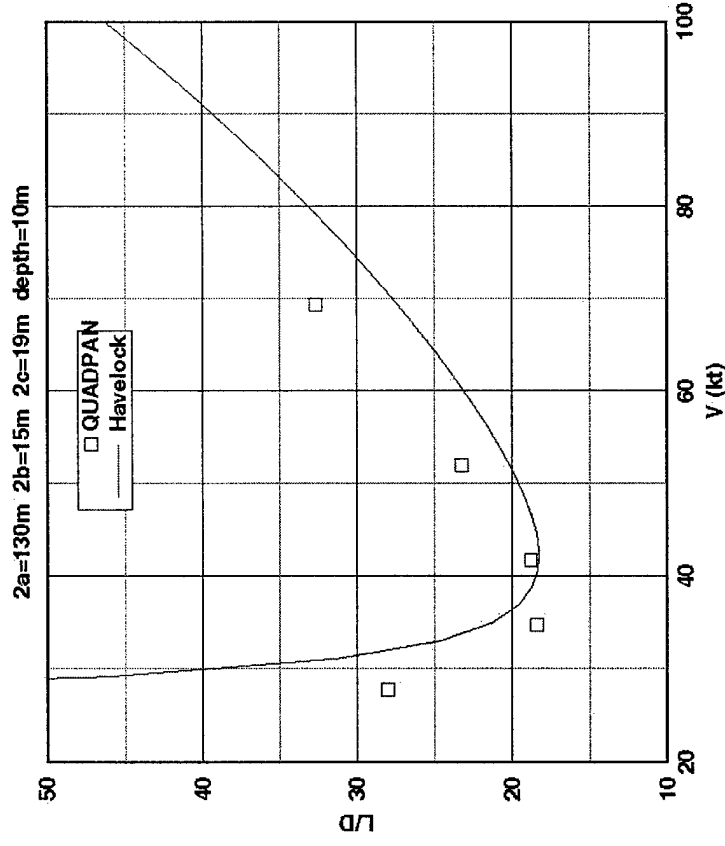
The Havelock solution is calculated by integrating the wave drag contribution of doublet singularities representing the ellipsoid. The strengths of the singularities, however, are those for the ellipsoid in an unbounded fluid. There is no modification of the singularity strength to account for the free boundary. As such, it is a first approximation for the resistance when the ellipsoid is not too close to the surface. The Havelock solution will deviate from the QUADPAN computed solution as the depth becomes shallower.

The low speed range is re-plotted in the inverse form, that is, as the ratio of wave drag to buoyant lift. The several small local maximum and minimum are characteristic of wave drag versus speed curves.

Havelock's Solution for Wave Drag of Submerged Ellipsoid

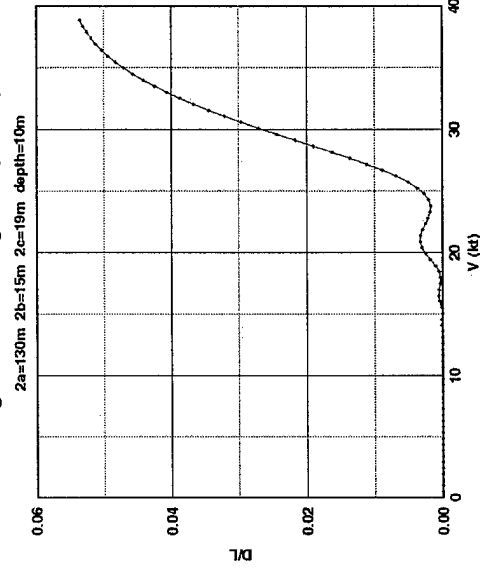
- Ellipsoid of 20000 tonne displacement (19400 cu.m.)
- Depth of centerline = 10 meters

Lift/Wave-Drag of submerged ellipsoid



Note local maxima and minima below 25 kt

Wave-Drag/Lift of submerged ellipsoid (Havelock)



Mutual Interference Effects for Catamaran

The mutual interference effects for a catamaran configuration are studied. The variation of the wave drag and hydrodynamic lift coefficients with Froude number of a single p11ba15 body is first computed (the body centerline is at one diameter depth). The results are doubled, and plotted as the line labeled "infinity", representing a catamaran with infinite spacing between the hulls. At a Froude number of 0.4 and 1.65, the coefficients are computed for varying spacing between the bodies ranging from 0.1 to 1.0 (the number represents half the distance between body centerlines divided by the body length).

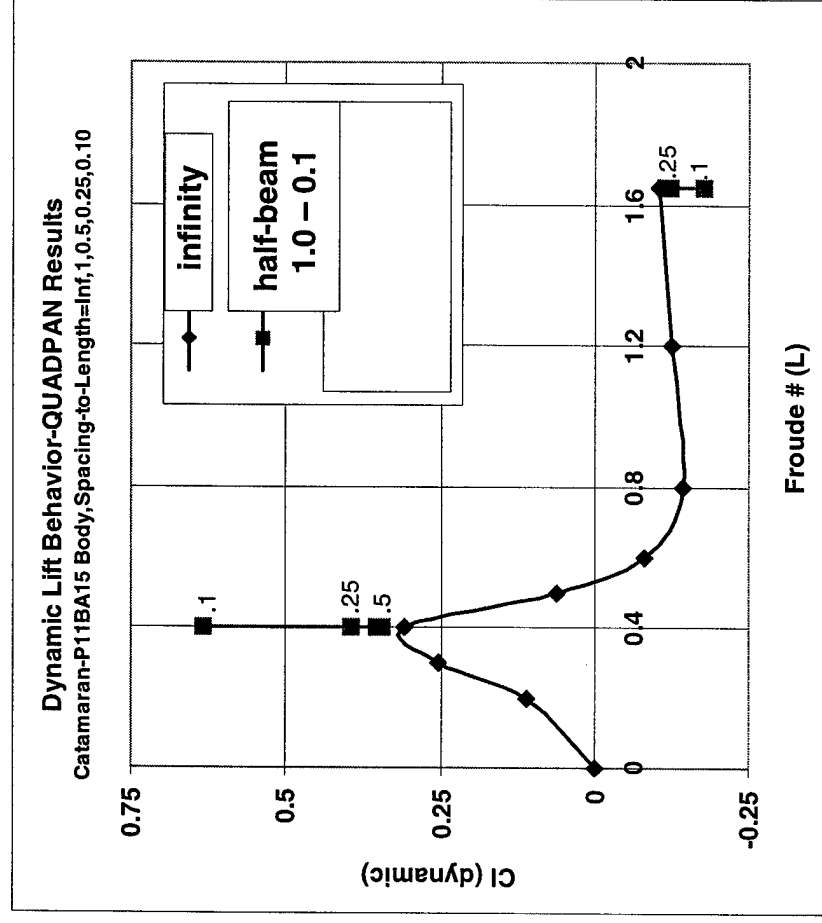
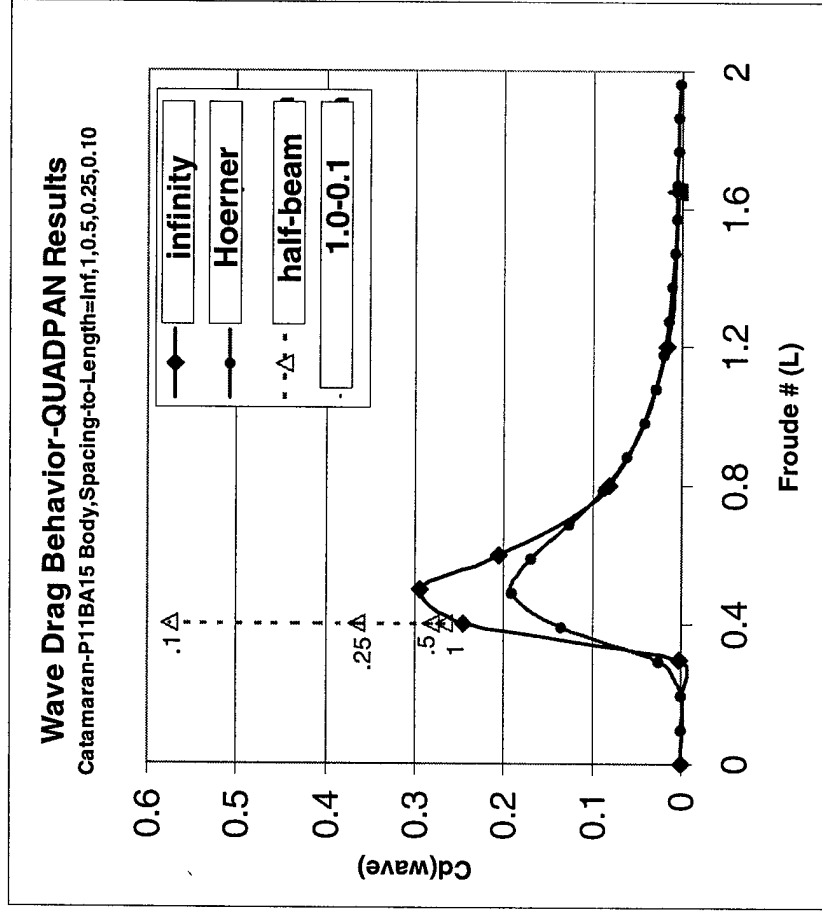
It is seen that the magnitude of the hydrodynamic lift and the wave drag are both increased as the bodies are brought closer together. The interference effect is slight until the bodies are fairly close together, say, at a half-beam to length ratio of 0.2. Further reduction of beam rapidly increases the amount of interference.

The variation of wave drag coefficient with Froude number, for infinite spacing between the hulls, is also plotted according to empirical data (for a generic body) from Hoerner for comparison.

The coefficients are referenced to the maximum frontal area of one body.

Note that the hydrodynamic lift switches from positive at low speed to negative at high speed. At low speed, the free surface behaves as if it were rigid, and suction produced by the "image" body results in positive lift. At high speed, a "negative image" produces the reverse effect. The "cross-over" point of zero lift seems to occur near the maximum of wave drag.

Mutual Interference Effects for Catamaran



Cavity Ship Design

The cavity ship is modeled by replacing the lower half of a body of revolution with a flat surface representing the cavity. Since the cavity is filled with air (at the ambient pressure for the depth of the bottom), the skin friction drag of the bottom surface is taken as zero. Otherwise, the cavity-water boundary can be regarded as a solid surface for the hydrodynamics calculations. The pressures on the flat-bottom surface representing the cavity will be the same as those on the actual structure containing the cavity (note that the cavity volume should be included in calculating the buoyancy of the ship).

In a potential flow solution, the water will go around the sharp edge dividing the bottom and top surfaces at infinite speed. A perfectly flat bottom surface will therefore produce an infinite suction on that edge. To prevent this, the lower surface is designed to be a one-tenth scale inverted version of the upper surface. This rounding of the bottom surface eliminates the sharp edge and associated infinite suction. Nevertheless, some high suction pressures are still evident near the edges of the lower surface.

A cavity ship may be either one half of a body of revolution, or one half of a body with unequal vertical and horizontal diameters (elliptical cross-section).

A comparison is shown between a body of revolution and a cavity ship at 4000 tons displacement and 70 knots speed. The depth of the top of the body is 17 feet for both ships. The cavity body is somewhat longer than the body of revolution, with a smaller frontal area. The cavity ship has somewhat more wave drag and (negative) hydrodynamic lift, but less friction drag.

Cavity Ship Design

Cavity Ship

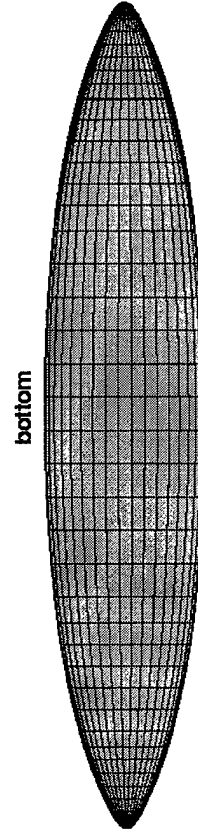
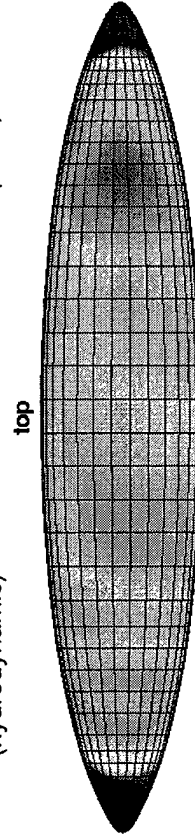
Length 257 ft.

Frontal area 792 sq.ft.

Froude No. = 1.30

Lift = -513 T
(hydrodynamic)

Drag = 71 T
(wave)



Body of Revolution

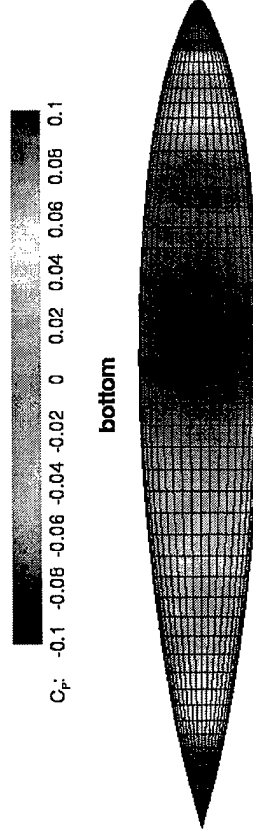
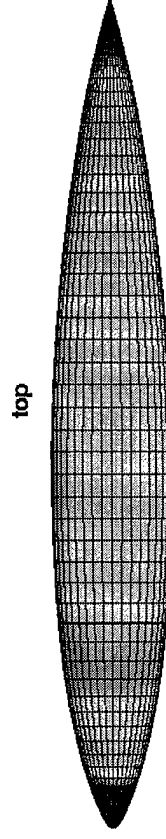
Length 231 ft.

Frontal area 910 sq.ft.

Froude No. = 1.37

Lift = -401 T
(hydrodynamic)

Drag = 48 T
(wave)



Catamaran Cavity Ship Design (no struts)

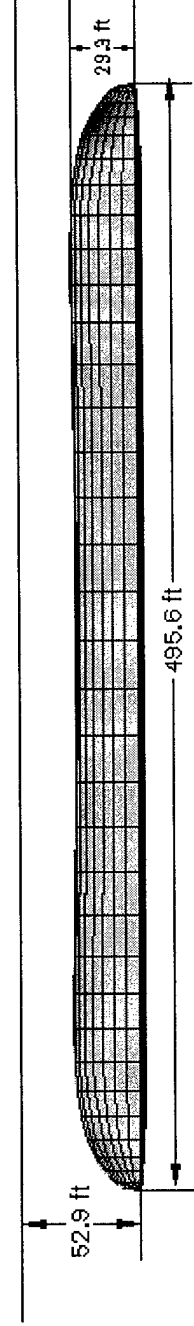
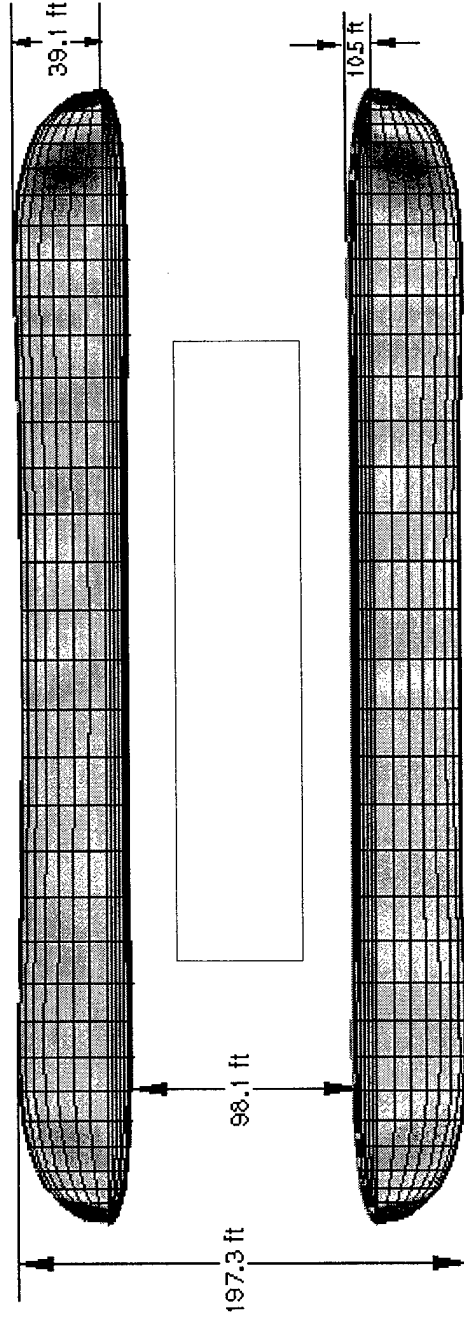
A twin-hull catamaran is designed similarly to a single body, except that:

1. The beam is constrained to a maximum of 200 ft.
2. The gap between the two bodies is a design variable.
3. The inboard and outboard sides of each hull are allowed to have different radii.

Some of the characteristics of the optimum catamaran cavity ship design (without struts) are listed in the table below:

Name	p29ta12
Speed	70 knots
Displacement	31500 tons
Hydrodynamic Lift	-1563 tons
Net Weight	29937 tons
Wave Drag	551 tons
Total Drag	1652 tons
Weight/Drag	18.1

Catamaran Cavity Ship Design (no struts)

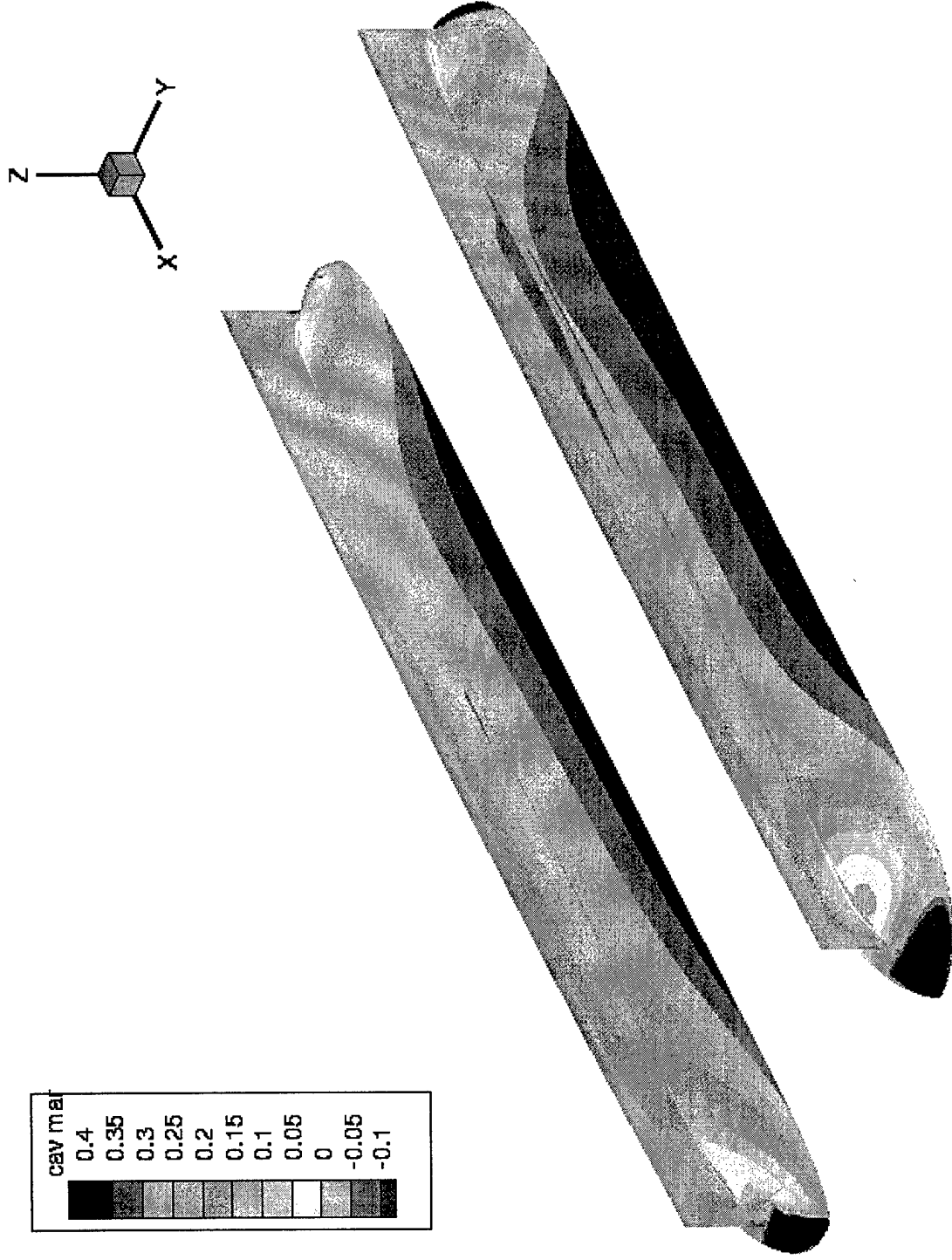


Catamaran Cavity Ship with Struts

The pressure distribution on the p29ta12 catamaran cavity ship with struts is plotted in terms of cavitation margin, expressed in units of cavitation number. The speed is 70 knots.

The bodies were designed to zero cavitation margin in isolation. With the addition of the struts, some small regions of cavitation are observed at the front and rear of the bodies, in the region just below the intersection with the strut. Nowhere does the amount of negative margin exceed 0.05.

Catamaran Cavity Ship with Struts

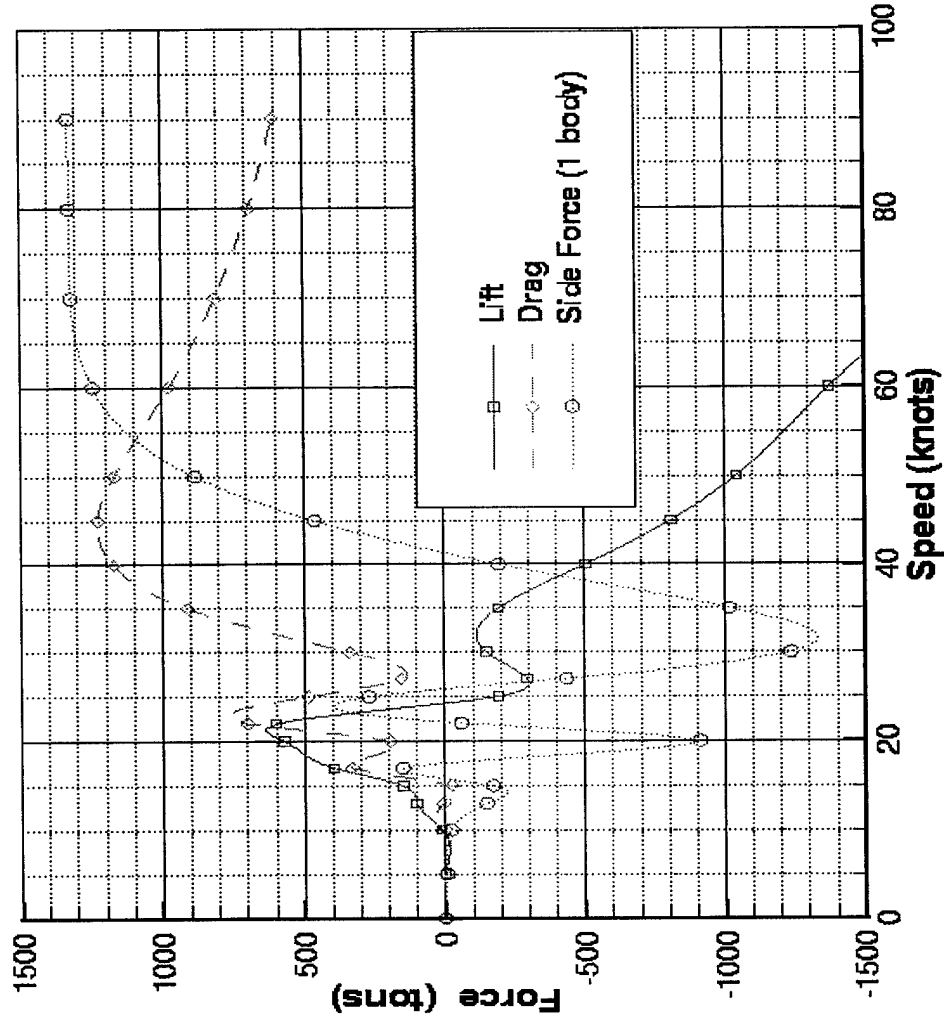


Catamaran Cavity Ship with Struts

The lift, drag, and side force characteristics versus speed for the p29ta12 catamaran cavity ship with struts are plotted. The ship's displacement is 31,500 tons.

The hydrodynamic lift is positive at low speed, and becomes negative at high speed. The wave drag maximum is at 45 knots. The side force (on one of the two bodies) is inboard at low speed, and outboard at high speed.

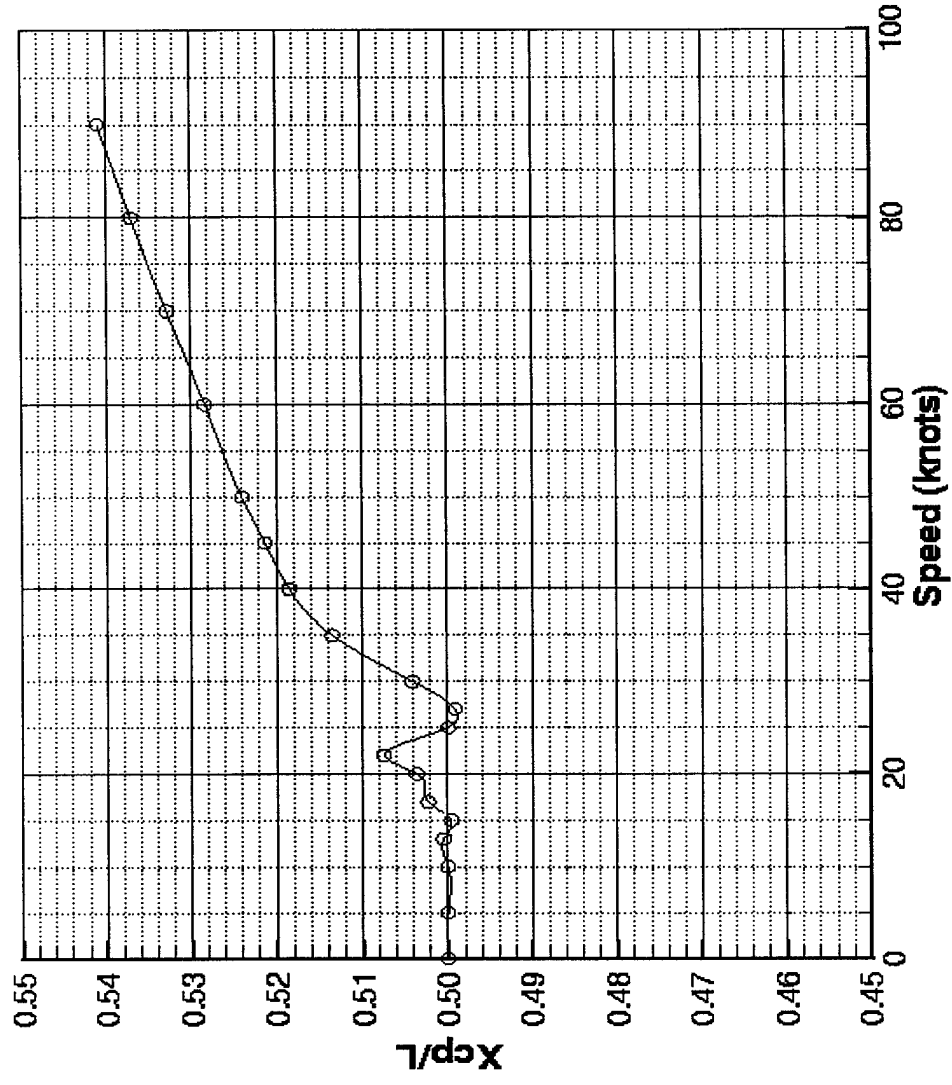
Catamaran Cavity Ship with Struts



Catamaran Cavity Ship with Struts

The center of pressure for the p29ta12 catamaran cavity ship with struts is plotted versus speed. Assuming that the center of buoyancy is at mid-body, it is seen that the center of pressure moves aft with increasing speed. This will require a re-trimming mechanism, such as a hydrodynamic control surface or shifting of the fuel volume.

Catamaran Cavity Ship with Struts



Stability and Trim Analysis

Introduction

In analyzing the static stability of the hydrofoil, the three issues of concern were the size of the horizontal tail (for longitudinal stability and trim), the longitudinal location of the center of gravity, and how much of a vertical tail was needed (for yaw stability and engine-out trim). Since the vertical struts that attach the horizontal tail to the ship could account for a vertical tail, the longitudinal trim and stability issues were tackled first. The bulk of this work was done with the assistance of Bob Coopersmith.

Hydrofoil Longitudinal Trim

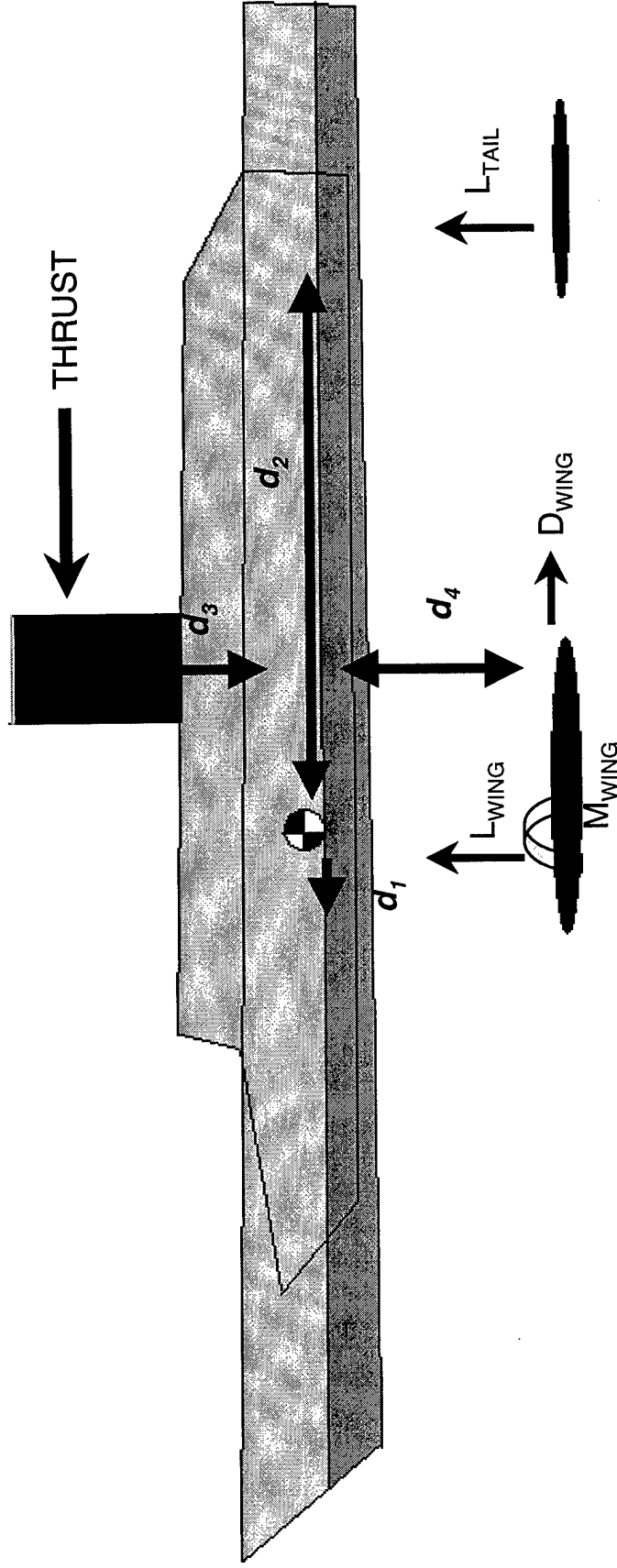
First of all, a trim equation needs to be developed by balancing the moments in the figure on the facing page. In this figure, the ship is reduced to a point mass acting at the center of gravity (CG). The thrust vector, resulting from the six propellers, acts at a distance h_a above the CG. The hydrofoil features a lift, which acts with a moment arm of x_a in front of the CG, a drag with a moment arm of z_a below the CG, and a zero lift moment that can be represented by the coefficient C_{Mac} . Finally, the horizontal tail has a lift with a moment arm of l_t . The drag of the tail is considered to be small enough to ignore. The trim equation is given below.

$$C_{M_{CG}} = C_L \frac{x_a}{C} - C_D \frac{z_a}{C} - T_C \frac{h_a}{C} - C_{L_t} \frac{HTV}{C} + C_{Mac} = 0$$

The next step is to assess what is known and what is unknown in the trim equations. First of all, h_a and z_a are set via a previous design iteration. The amount of thrust, T_C , is also known. Then Quadpan is used to calculate the lift, C_L , and the wave-drag/induced-drag combination at zero degrees angle-of-attack (α). To get the total drag, C_D , the drag due to skin friction, C_{Df} , needs to be added to this combination.

The only unknowns are the tail lift, the tail moment arm, and the longitudinal location of the CG, which also acts as the lift moment arm. However, since it is desirable that the system be trimmed without assistance from the horizontal tail, C_{L_t} is taken to be zero. This also eliminates the contribution of the tail moment arm to the trim equation, leaving only the lift moment arm, x_a . This results in the center of gravity needing to be 17.27 ft aft of the hydrofoil aerodynamic center.

Ship Hydrofoil



Hydrofoil Longitudinal-Moments Balance

Hydrofoil Longitudinal Static Stability

Longitudinal Static Stability

It is known that although no horizontal tail is needed to longitudinally trim the system, one will probably have to be added to make the system statically stable. Taking the derivative of the trim equation with respect to C_L produces the longitudinal static-stability equation. That equation is given below.

$$\frac{\partial C_{M_{CG}}}{\partial C_L} = \frac{x_a}{c} - \frac{1}{C_{L_\alpha}} \left(C_{D_\alpha} - \frac{\pi}{180} C_L \right) \frac{z_a}{c} - \frac{C_{L_{\alpha\alpha}}}{C_{L_\alpha}} \left(1 - \frac{d\varepsilon}{d\alpha} \right) HTV = 0$$

C_{L_α} and C_{D_α} are the derivatives of C_L and C_D with respect to α , and $d\varepsilon/d\alpha$ is the rate of change of downwash. The latter quantity was calculated via an elliptical wing lift distribution assumption. The aerodynamic derivatives were calculated via Quadpan.

The only unknown in the stability equation is the horizontal tail volume, HTV, which is comprised of the ratio between the tail and wing areas multiplied against the ratio between the tail moment arm and wing chord. Thus, once HTV is determined, a definite relationship between the tail area and moment arm is established. This analysis yields an HTV value of 1.30. The tail moment arm is taken to be 151.25 ft due to a previous design iteration. This results in a horizontal tail area of 544 sq ft.

Stability Criteria for the Hydrofoil

Lateral Trim

In the lateral-trim analysis, the desire was to determine if a vertical tail was needed to combat an engine-out situation. Since the horizontal tail is attached to the ship via vertical struts, these can be thought of as a vertical tail. So, the real question is whether any additional vertical tail area will be needed to laterally trim the system in an engine-out situation.

The engine-out situation is illustrated by the figure on the facing page. In this figure, the hydrofoil is at the top, with the system center of gravity directly behind it. This is balanced by the horizontal tail at the far rear. The system also has six propellers, 24 ft in diameter, spanning a distance of 214.8 ft. The moment arm of the horizontal tail 151.25 ft and the propellers are 40 ft aft of the CG. It is assumed that the moment arm of the vertical tail is the same as that of the horizontal tail.

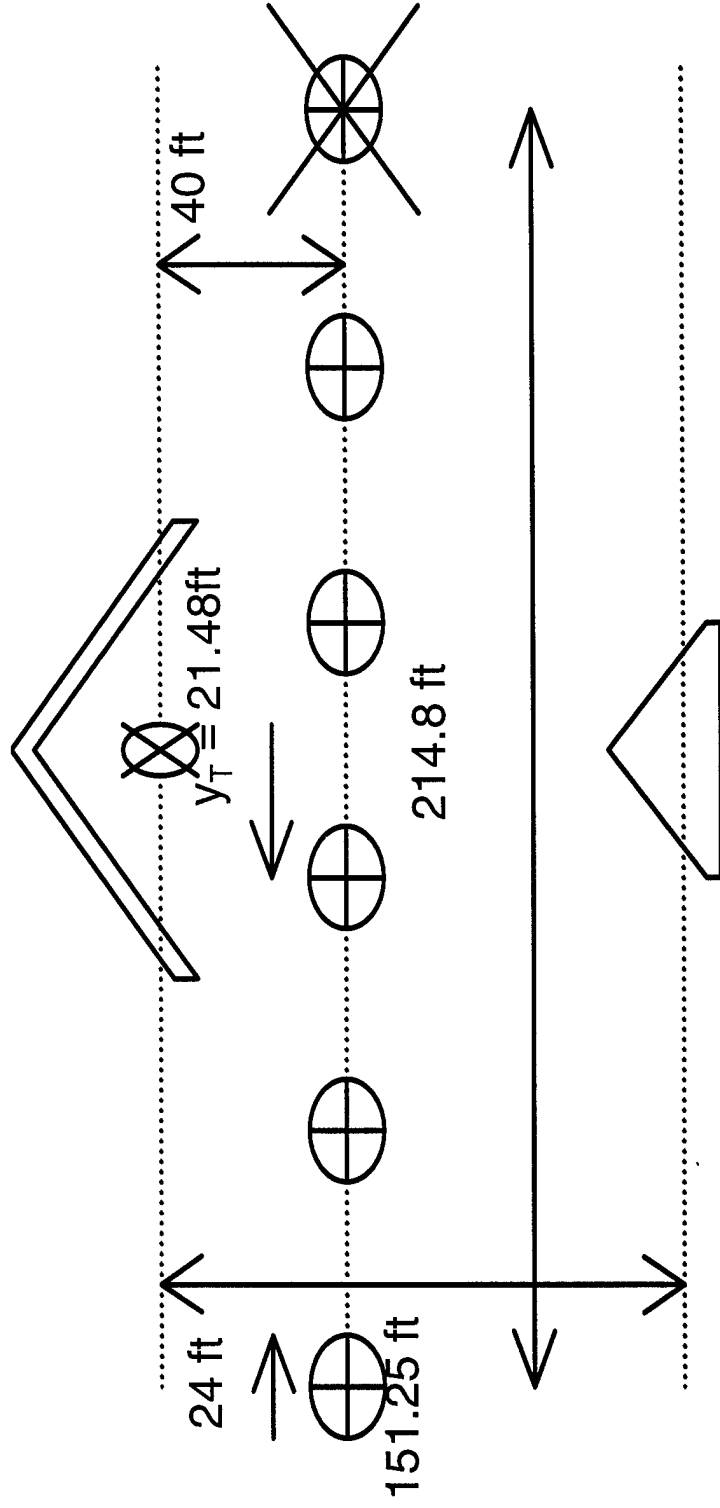
To assess the engine-out situation, it is assumed that the engine furthest to the right fails, forcing the center of thrust to move 21.48 ft to the left. This creates an unbalanced lateral moment about the CG equal to the resultant thrust multiplied by the 21.48 ft moment arm. This is the moment that must be combated by the vertical tail.

The lateral-trim equation is given below.

$$C_N = C_{N_{\beta_w}} \beta + C_{N_{\delta_a}} \delta_a + C_{N_{\beta_{fus}}} \beta + C_{N_{\beta_v}} \beta - C_T \frac{y_T}{b} - C_{F_p} \frac{x_T}{b}$$

The term C_N is the resultant yawing moment, which must be forced to zero. The terms $C_{N_{\beta_w}}$, $C_{N_{\delta_a}}$, $C_{N_{\beta_{fus}}}$, and $C_{N_{\beta_v}}$ are the change in yawing moment with respect to sideslip for the wing, fuselage, and vertical tail, respectively. The change in yawing moment with respect to aileron deflection is given by $C_{N_{\delta_a}}$. It is assumed that the fuselage and aileron contributions are negligible. The last two terms involve the propellers. The first is thrust coefficient, C_T , and its associated moment arm, y_T/b , where y_T is the lateral distance between the center of gravity and the center of thrust, and b is the span of the hydrofoil. The final term is the unbalanced side force induced by the propellers, C_{F_p} , and its moment arm x_T/b . The term x_T is the longitudinal distance between the center of gravity and the center of thrust, which is about 40ft. The span of the hydrofoil is 125 ft. The thrust is taken to be five-sixth the drag and the wing-moment derivative is calculated via Quadpan. This leaves the tail-moment derivative as the only unknown.

Stability Control Tri-Hydrofoil



Hydrofoil Engine-Out Situation

Hydrofoil Lateral Control and Stability

Lateral Trim (continued)

Now, the question is whether the vertical struts supporting the horizontal tail are enough of a trim device. In attempting to answer this question, it is useful to consider the effect of the vertical tail volume, VTV , via the following equation.

$$C_{N_{\beta_v}} = C_{F_{\beta_v}} VTV$$

In this equation, $C_{F_{\beta_v}}$ represents the change in vertical-tail side-force coefficient with respect to sideslip. Similar to the horizontal tail volume, VTV is given as the ratio between the vertical tail and hydrofoil planform areas multiplied against the ratio between the tail moment arm and the hydrofoil span (instead of the chord). The ratio of the strut area supporting the horizontal tail to the planform area of the horizontal tail is taken to be the same as the ratio of the strut area supporting the hydrofoil to the hydrofoil planform area. This results in a vertical "tail" area of 830 sq ft. Thus, VTV has a value of 0.357.

Taking these developments in association with the stability equation, there is now a relationship between side-force coefficient and sideslip, rather than the moment coefficient and sideslip. Thus, to determine whether or not additional area is needed, simply calculate the side force necessary to combat reasonable values of sideslip and decide if those side-force values are acceptable. Sideslip values of 1° and 5° result in necessary side-force coefficients of 0.0171 and 0.0114, respectively. Given that the hydrofoil lift coefficient is 0.2, it was determined that a side-force coefficient of 0.0171 should be well within the range of any vertical-strut device added to the horizontal tail. As a matter of fact, the design team is fairly confident that the struts will produce a C_F a good deal greater than 0.02, resulting in a system that easily trims, with engine out, at less than 1° sideslip.

Lateral Stability

As it turns out, in this situation, lateral trim will always imply lateral stability. If one takes the derivative of the trim equation with respect to sideslip, one finds that only the wing derivative and tail derivative terms remain. The tail derivative must be a positive value with a magnitude greater than the negative wing tail derivative to produce a stable system. This is assured, since in the trim equation the tail must combat the negative contributions of both, the wing and the propellers. For an example, if it is assumed that C_{F_v} will achieve of a paltry value of at least 0.02 at 1° sideslip, this implies a $C_{N_{\beta_v}}$ of 0.00714 per degree, which is much greater than 0.0035.

Stability of Conventional Hydrofoil

Conclusions

In conclusion, the longitudinal center of gravity needs to be placed 17.27 ft aft of the aerodynamic center of the hydrofoil to assure that the system will be trimmed in pitch without the assistance of the horizontal tail. The tail, with a moment arm of 151.25 ft, must have an area of at least 544 sq ft to produce a longitudinally stable system.

The vertical struts supporting the horizontal tail have an area of 830 sq ft, with a moment arm of 151.25 ft. This combination is more than enough to trim the system in an engine-out situation at less than 1° sideslip. Furthermore, a laterally-trimmed system automatically implies a laterally-stable system.

CATAMARAN Lateral Trim and Stability

CATAMARAN Lateral Stability

The first issue of concern was whether or not the CATAMARAN is stable in yaw. A quick analysis seemed to suggest that it would be unstable. The center of gravity (CG) of the CATAMARAN resides at the center of buoyancy, by necessity. This is located at the longitudinal midpoint of the underwater strut-body combination. However, it was determined that the center of pressure of the side forces would probably reside in front of the CG, thereby producing a laterally unstable system. A Quadpan analysis of the ship at 1° sideslip confirmed these suspicions. This condition produced a negative yawing moment about the CG, thereby implying that the rate of change of yawing moment with sideslip is negative. Thus, the CATAMARAN is unstable in yaw.

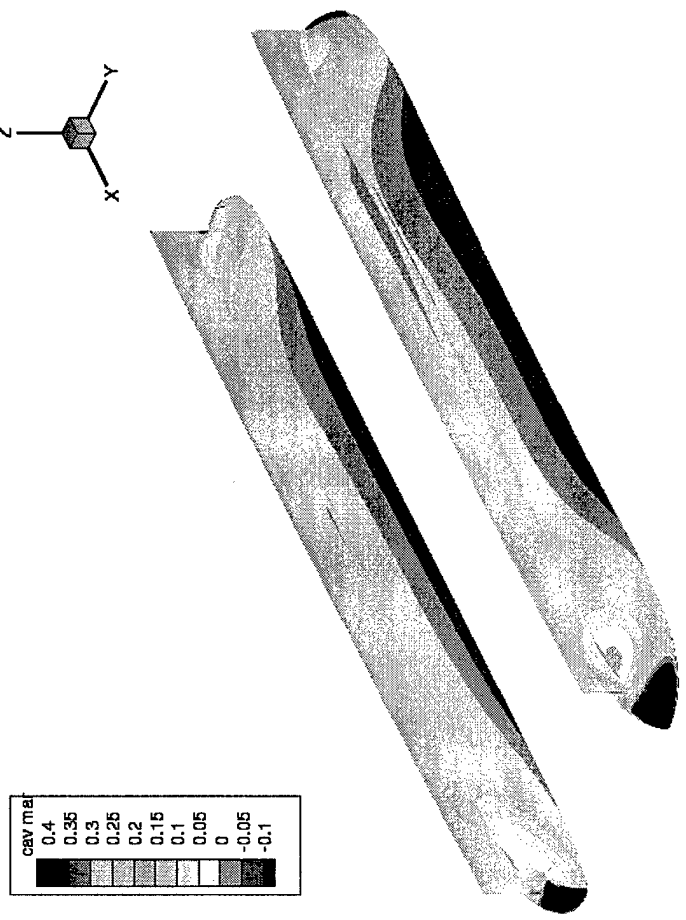
However, a quick, qualitative analysis of ships in general revealed that most ships are probably unstable in yaw. These ships are able to control their courses, though, through rudder corrections of induced sideslip. Thus, if it could be shown that the CATAMARAN could handle moderate sideslip angles with a reasonably-sized rudder, the issue of instability would be no cause for concern.

CATAMARAN Lateral Trim

First of all, it was decided that the rearmost 10 percent of each strut would act as rudders. This just seemed a reasonable strut area. Next, the strut-body combo was run through Quadpan at 1° rudder-angle deflection to determine the change in yawing moment with respect to rudder deflection. Having already determined the change in moment with respect to sideslip, it was now possible to quantify the amount of rudder deflection necessary to trim the ship at a particular sideslip. The ratio of rudder-deflection angle to sideslip angle was around 1.8.

However, the rudder is only effective if it is operating in a relatively cavity-free environment. Thus, Quadpan runs were done at 0° through 10° rudder-deflection angle in 1° increments. A contour plot of cavitation margin for the body-strut combination at 0° rudder deflection is shown on the facing page. Negative contour values indicate regions where the body is experiencing cavitation. Positive values indicate cavitation-free zones.

STABILITY AND DYNAMICAL BEHAVIOR



Cavitation-Contour Plot at 0° Rudder Deflection

Stability and Control Batch

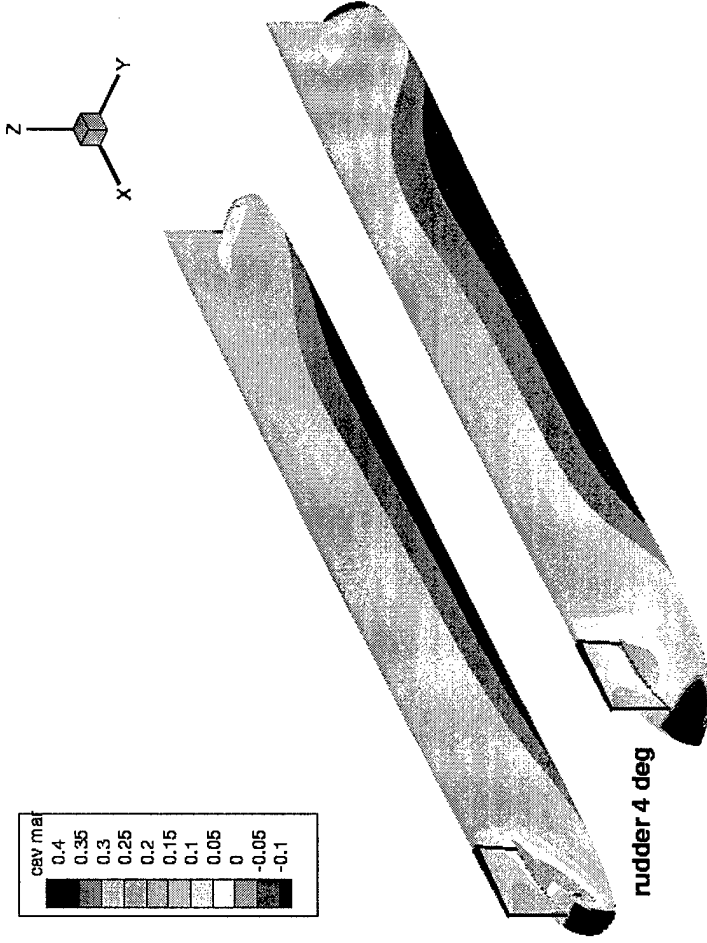
CATAMARAN Lateral Trim (Continued)

It can be seen that at no rudder deflection, the body is relatively cavity-free. There are some areas, indicated by orange, in the front and rear that experience cavitation. However, the opinion is that these areas are sufficiently small that they can be ignored. Now, it is important to determine at what rudder deflection do these areas become large enough to cause concern.

After visually inspecting the Quadpan cases of 1° through 10° rudder deflection, it was decided that 4° would be the maximum amount of deflection that one could achieve and be reasonably confident that the level of cavitation is not affecting rudder performance. This case is shown on the facing page. As can be seen, there is a good deal more cavitation area at the 4° case than there was at 0°. However, we have two reasons to be confident that this is not an issue. First of all, despite the fact that there is more cavitation area, there is still not a lot of area. The cavitation area is confined to a relatively small space on body and below the rudder. The second reason for hope is that there isn't actually any cavitation on the rudder. That gives reason to believe that the rudder will act as it should up to 4° deflection.

A 4° rudder deflection will enough to counteract 2° of sideslip.

Statistical Analysis of BWTCH



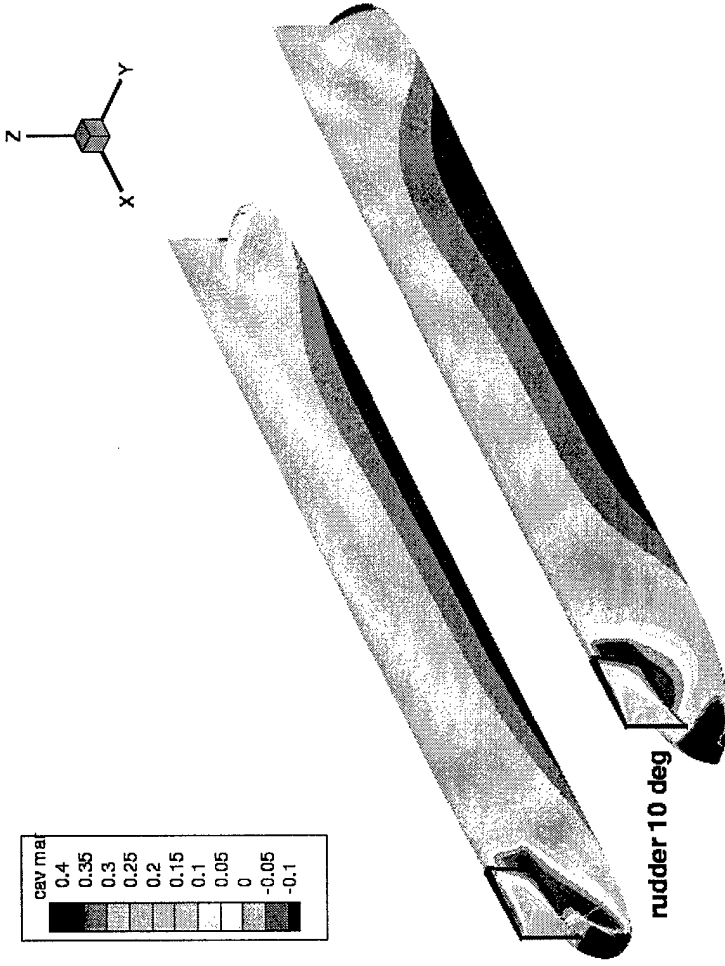
Cavitation-Contour Plot at 4° Rudder Deflection

Stability and Control BWATCH

CATAMARAN Lateral Trim (Continued)

Though 4° does seem to be limit for which one can be reasonably confident that the rudder will act with cavitation-free effectiveness, there is good reason to believe that it will have some decent level of effectiveness at much higher rudder deflection angles. The 10° case is given on the facing page to illustrate this reasoning. It can be seen that though the cavitation region is much larger in this case than at 4° , it is *still* primarily confined to the body. Some of it does reach the rudder, and a good portion has crept into the area in front of the rudder. However, the majority of the rudder itself is cavitation-free. Though it is unlikely that the rudder will act with near-cavitation-free effectiveness, it is quite possible that it will produce quite a bit of restoring moment. This would create a situation in which the ship could trim out anywhere from 2° to 5° sideslip. Though the 5° would be a bit optimistic, there is great confidence that the two-rudder system could handle much greater than 2° .

Stability and Operational BWATCH



Cavitation-Contour Plot at 10° Rudder Deflection

Static Margin Analysis

Conclusions

A Quadplan analysis showed that the CATAMARAN is unstable in yaw. However, analyses have shown that with two rudders that comprises the rearmost 10 percent of each strut, the ship should be able to trim out at least 2° of sideslip, potentially much more. This means that as long as the ship does not diverge from zero sideslip too quickly, it should be a relatively easy task to bring the ship back to zero. Four degrees of rudder deflection should be enough to trim out the 2° sideslip.

Furthermore, a statically unstable system may be preferable. The instability would make turning much easier. If the rudder is effective enough to keep the ship under control, instability would be a blessing rather than a curse.

Future Considerations

One thing a future design team might want to do is a dynamic-stability analysis of the CATAMARAN. This would answer the question of whether the statically-unstable ship is damped in yaw. This, of course, is the preferable situation because even though the ship wishes to diverge from zero sideslip, that attempt to diverge would lessen with time. This situation, coupled with an effective rudder, would ease any fears relating to the static instability of the system.

If the fact that the system is statically unstable in yaw is still a cause for concern, a future design team could investigate the impact of placing a vertical tail in the rear portion of the ship, between the two struts. This tail would improve the stability of the system, and could be used as a very powerful control surface if it is an "all-moving" tail. That is, if the entire tail rotates as one piece, it would act as a very large rudder. The tail would provide two causes for concern. First of all, it adds wetted area to the system, thereby increasing drag. Second, there may be some interference impact between the vertical struts and the tail.

Structures -Objectives, Approach, and Methodology

Structures Objectives, Approach, and Methodology

Objectives and Overall Approach

The original primary objectives of the hydrofoil structures effort on this program were to: 1) determine the feasibility of various hydrodynamics-driven designs, and 2) to quantify the wing and strut structural weights associated with each design in order to support the overall ship design optimization. More detailed objectives included determining preferred materials and quantifying sensitivities to parameters such as number of struts, side load, vertical load, minimum skin thickness, strut length, strut taper, strut location, and wing span.

Initially, the objectives dealt only with hydrofoil concepts. As the program evolved, the scope expanded to include similar analyses on submerged buoyant body designs. The additional objectives and tasks performed that pertained to these vehicles are discussed later in this report.

To accomplish the primary objective of generating conceptual/preliminary design level structural sizing of the Hydrofoil Fast Ship struts and wing, the approach taken needed to include as much flexibility as possible with regard to accommodating the many loading, geometry, and other parameters whose effects needed to be examined. A physics-based Excel spreadsheet solution employing a built-in optimizer (Solver) was developed and used to derive minimum total strut and wing weight solutions. Some of the initial trades were performed with incremental variations of several parameters to determine trends and to derive reasonable values at which to fix some parameters to reduce the total variable count during optimization runs.

The final hydrofoil structures task was to both validate and refine the preliminary wing and strut sizings through the use of higher order methods. A finite element model representing the wing and strut structure of the preferred design configuration was created and used to accomplish this.

Structures Objectives, Approach, and Methodology - Hydrofoil

- **Determine preferred materials**
- **Derive preliminary wing and strut sizings and weights for different wing designs and numerous geometry and loading parameters**
 - Develop spreadsheet with physics-based methodology
 - » Geometry, loading, and other parametric input
 - » Section properties
 - » Internal loads
 - » Analysis and optimized sizing
 - » Strut/wing total and net weights
- **Determine feasibility of different wing and strut design configurations**
- **Quantify sensitivities to number of struts, side load, vertical load, minimum skin thickness, strut length, strut taper, strut location, wing span**
- **Determine “optimum” strut configurations for several wing sections, areas, and spans**
- **Use finite element analysis to validate physics-based solutions and to produce refined sizing of the preferred design**

Structures Approach and Methodology - Hydrofoil

Approach and Methodology – Hydrofoil

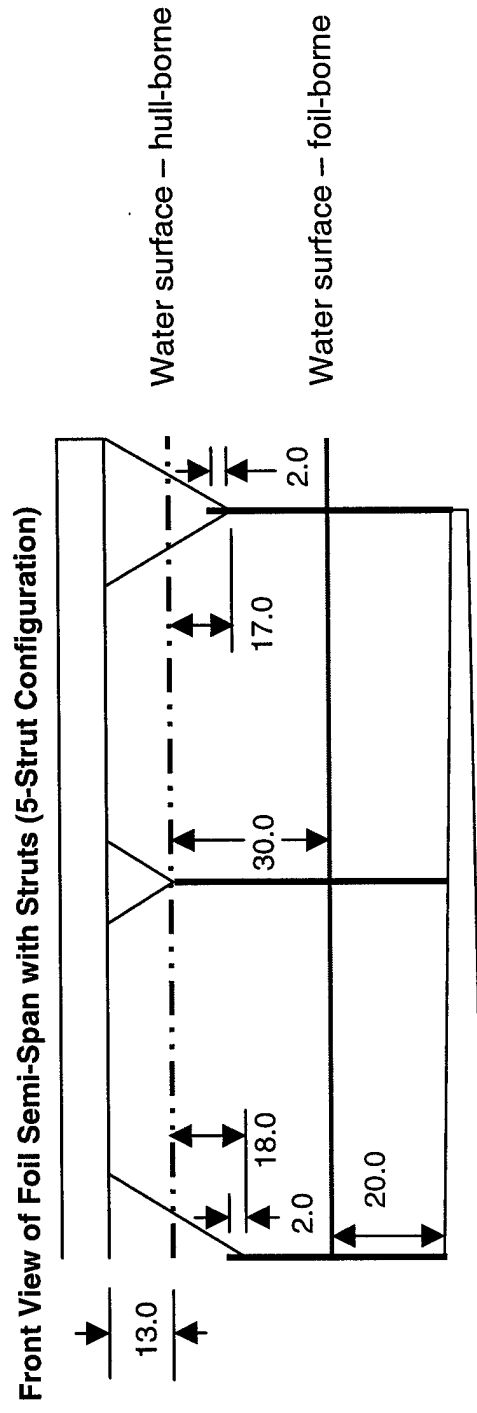
Several basic assumptions were made early in the program regarding the ship, strut, and wing configurations that affected wing and strut structural sizing. The ship was assumed to be a trimaran for hull-borne efficiency. The struts were assumed to extend/retract vertically for practical purposes. Both of the end struts would tie in to the outer hulls, with the middle strut tying in with the center hull for an odd-number-of-struts configuration. This hull tie-in would serve to effectively decrease the strut moment arm and hence increase the structural efficiency. “Mini-hulls” were assumed to be located where the intermediate struts attached to the ship in order to aid in reacting the strut loads and to at least somewhat reduce the strut moment arm at these locations. The lowest point on these mini-hulls were set so as to not penetrate the water surface during hull-borne operation.

Initially, all strut spacings were made equal to simplify the sizing methodology. This assumption was eliminated when the capability was added to allow the strut spacing to vary during the optimization process.

Structures Approach and Methodology - Hydrofoil

Strut Location Assumptions

- **Three-hull design**
- **Struts retract vertically**
- **Middle and end struts penetrate hull structure**
- **Outboard struts coincident with ends of wing**
- **Evenly spaced, constant chord struts for generating preliminary results (pre-April 2000)**
- **“Optimized” strut spacing and strut taper for latest results**



Structures Approach and Methodology - Hydrofoil

Approach and Methodology – Hydrofoil (Cont'd)

The vehicle size, loading, and wing geometry/sizing assumptions for the primary hydrofoil sizing trade studies are shown below. The vehicle size was set at 4000T which was determined to be the size that allowed the greatest payload over the given design range. The G-loadings came from historical ship design criteria. The assumed material was 15-5PH stainless steel, heat treat H1150M. Since the wing sizing methodology produced identical upper and lower surface skin stress magnitudes (opposite sign), and since the estimated tension and compression stress cutoffs could be considered to be the same magnitude, those cutoffs were indeed made the same to simplify the methodology. The tension cutoff took into consideration low cycle-to-failure S-N fatigue data with some knockdown for weldments. The compression and shear cutoffs were nominal values that took into account stiffened panel instability.

Structures Approach and Methodology - Hydrofoil

Loading, Geometry, and Sizing Assumptions

- **AUW = 4000 tons**
- **Design G-loadings**
 - Vertical (lift) force = **2.0G** (Used for wing and strut sizing)
 - Side force = **0.5G** (Used for strut sizing only)
 - Aft force = **0.5G** (Considered for strut sizing only)
- **Wing sizings**
 - 200-foot wing span, 2-10 struts; **125-200-foot span with 3, 5, 7, and 9 struts**
 - 5 wing sections (**1750 - 3000 psf wing loading, 35° - 45° leading edge sweep**)
 - Constant pressure loading - running load proportional to local planform area
 - Mid-segment running load calculated and assumed constant between struts
 - Fixed-end beam bending/shear/torsion analysis for inner wing segments
 - **Inner-end-fixed, outer-end-pinned** for most outboard wing segments
 - Mid-segment section properties based on skin t-bar, spar caps and webs
 - Skin t-bar + spar weights factored up to account for rib structure
 - Stainless steel -- 55 ksi tension/compression stress cutoff, 40.5 ksi shear cutoff
 - Min. skin thickness = **0.5** in. nominal, min spar web thickness = **0.25** in. nominal

Structures Approach and Methodology - Hydrofoil

Approach and Methodology – Hydrofoil (Cont'd)

Additional assumptions pertaining to the strut sizings are shown below.

Structures Approach and Methodology - Hydrofoil

Loading, Geometry, and Sizing Assumptions (Cont'd)

- **Strut sizings**

- 200-foot wing span, 2-10 struts; **125-200-foot span with 3, 5, 7, and 9 struts**
- 60-foot effective nominal strut lengths (28-29 feet shorter for hull-penetrating struts)
- 10-30-foot wing depth; **20-foot nominal depth**
- Chord lengths at strut tops/bottoms specified as percentage of local wing chord
- Strut-to-wing connection: pinned end
- Strut-to-hull connection: fixed-end
- Analysis: Bending/compression + column buckling + shear
- Skin t-bar + spar weights factored up to account for rib structure
- Stainless steel -- 55 ksi tension/compression stress cutoff, 40.5 ksi shear cutoff
- P70-40SA0 (symmetric) strut section

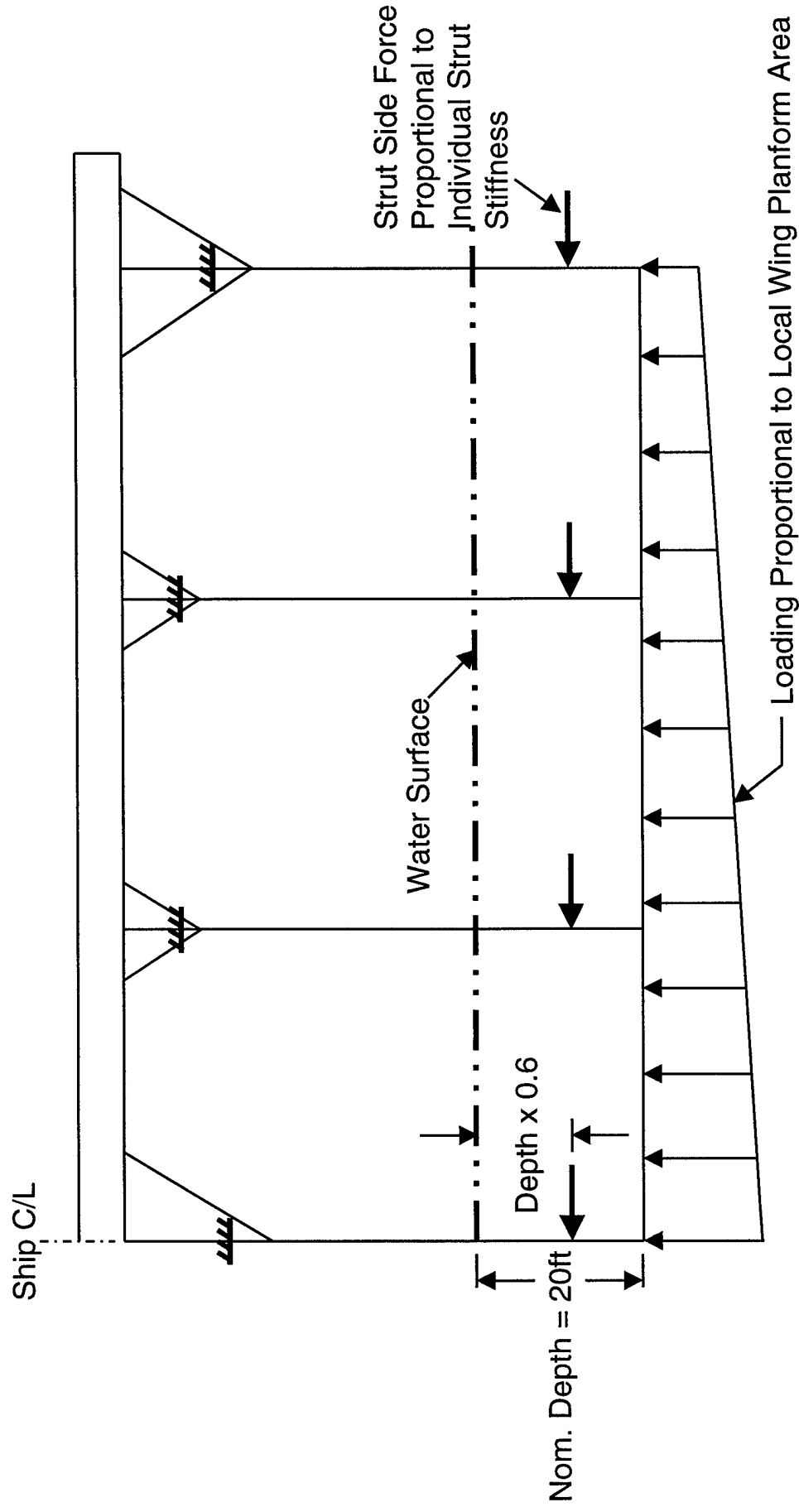
Structures Approach and Methodology - Hydrofoil

Approach and Methodology – Hydrofoil (Cont'd)

The figure below shows graphically some of the previously mentioned applied loading assumptions used in the structural sizing analyses.

Structures Approach and Methodology - Hydrofoil

Applied Loads Assumptions



Structures Approach and Methodology - Hydrofoil

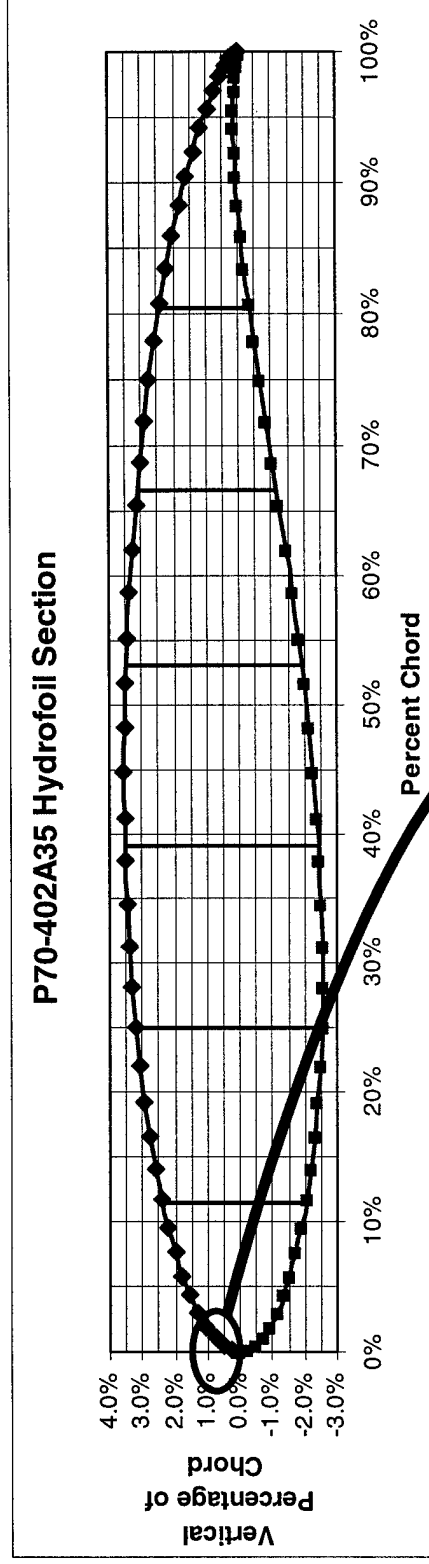
Approach and Methodology – Hydrofoil (Cont'd)

Where possible, sizing methods were geared toward obtaining a high degree of fidelity. Accurate wing and strut section properties were considered to be of primary importance. A large number of ordinates were obtained that provided a detailed definition of the OML of the wing and strut sections. These ordinates represented a streamwise section, and were converted to actual x and y coordinate values based on the local chord length of the location at which the section properties were needed. In the case of the swept wing, these coordinates were converted to a section perpendicular to the elastic axis, assumed to be at the 40% chord. Discrete elements were produced at each OML coordinate, the center of which was offset half the skin t-bar for more accurate section property calculations, as seen in the figure below. The section properties to compute bending and shear stress levels for each wing segment were then calculated for the section normal to the neutral axis midway between strut attachment locations (or in the case of an even number of struts, midway between the inner strut location and the wing centerline).

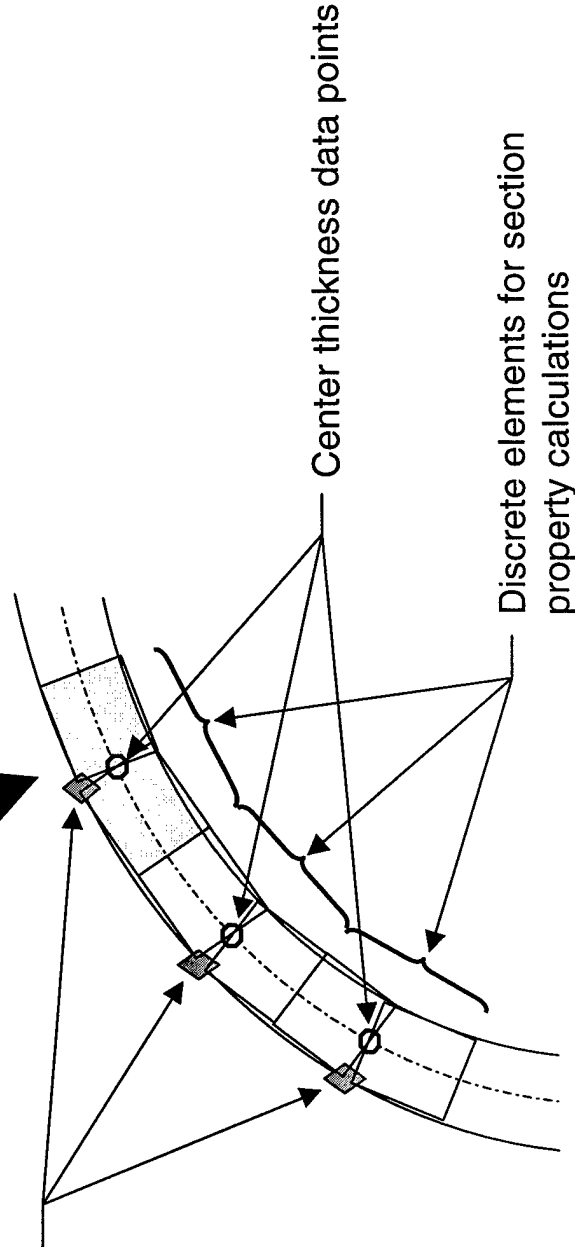
Once all the various parameters and geometric relationships were set, the inputs to the calculations performed by the spreadsheet were reduced to the skin t-bar and spar web thickness. The weight for the skins, spar webs, and spar caps were derived based on computed material volume and specified density. The rib weights were factored off of the spar web weights based on historical aircraft relationships. Finally, the water displacement volumes of the submerged structure was generated to compute the “net” weight of the wing and strut structure.

Structures Approach and Methodology - Hydrofoil

Shell Section Property Calculations



OML geometry data points



Structures Approach and Methodology - Hydrofoil

Approach and Methodology – Hydrofoil (Cont'd)

To simplify the applied and internal load/stress calculations for each wing segment, a uniform running load, w , was assumed that was equal to the wing loading, W/S , divided by the mid-segment chord length of each wing segment. Also, to avoid the programming complexity associated with a continuous beam solution that would accommodate a variable number of support struts, the wing was discretized into a number of segments (equal to the number of struts minus one). For the intermediate wing segments, bending moment equations for a both-ends-fixed restraint system were used. For the end segments, bending moment equations for an inner-end-fixed, outer-end-pinned restraint system were used.

The wing structure was sized primarily to meet maximum and minimum spanwise skin bending stress and spar web shear stress cutoffs. In the case of an even number of support struts in conjunction with a swept wing, the torsional moment, resulting from the load being applied to the center segment of the wing at a location forward of its reaction points, was taken into account. That wing segment was also sized to satisfy the torsional stress cutoff at the intersection with the most inboard strut.

The struts were sized to meet maximum and minimum axial and shear stress cutoffs using the section properties at top of each strut, as well as column buckling requirements using the section properties at the strut mid-length. The struts were sized primarily by the vertical and side loads. While fixity was assumed at the ship attach point of the struts, the wing attachment was assumed to be a lug arrangement capable of free rotation about the longitudinal axis (pin end).

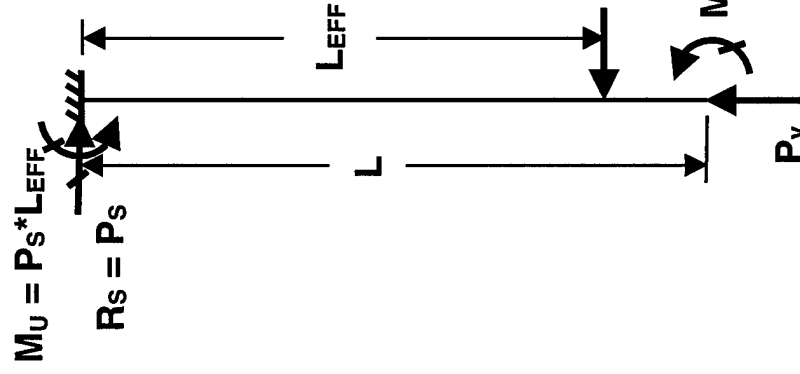
The vertical load on each strut was straightforward and was proportional to the strut chord length at the ship attachment point. Rather than assuming equal distribution of side load on the struts to determine their sizings, the load that each strut reacts took into account the relationship to its effective stiffness (based on a uniform skin and spar web thickness). This stiffness is directly proportional to the moment of inertia of the strut section (whose geometry is set by the percentage of the local wing chord (L.W.C.) at both the top and bottom of the strut, and inversely proportional to the cube of the effective moment arm (the distance from the effective load application point to the effective fixity point at the top). With a tapered wing whose centerline chord is twice that of the tip chord (a parameter that was held constant throughout the trade studies), the much larger cross-section and lesser length of the middle strut results in its reacting a significant percentage of the total side load.

Structures Approach and Methodology - Hydrofoil

Internal Loads and Analysis Assumptions

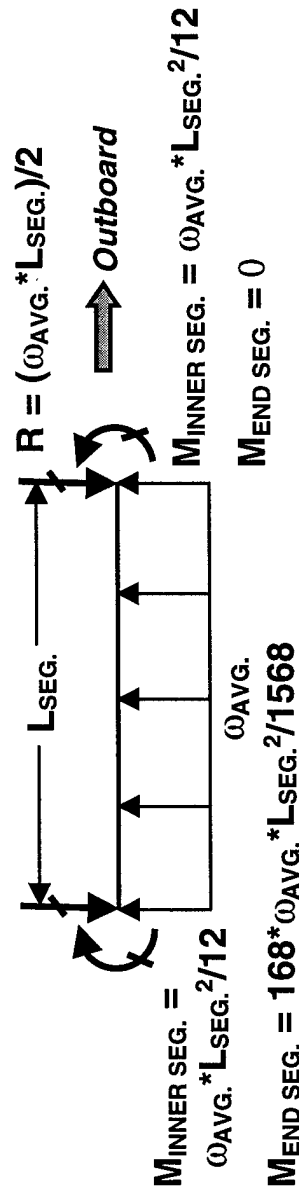
Strut Sizing

- Axial/bending stress ($P_v/A_{TOTAL} + M \cdot c/I$)
- Shear stress ($P_s/[A_{SPAR\ WEB} + EFEC. SKIN/CAP]$)
- Column buckling stress ($\pi \cdot E / [(L/c^{0.5})/\rho]^2$, $c = 2.05$)



Wing Sizing

- Bending stress ($M_x \cdot c/I$)
- Shear stress ($\omega_{AVG.} \cdot L_{SEG.} / [A_{SPAR\ WEB} + EFEC. SKIN/CAP]$)
- Torsional stress ($M_y / [2 \cdot A_{INT.} \cdot t]$)



Structures Approach and Methodology - Hydrofoil

Approach and Methodology – Hydrofoil (Cont'd)

As stated previously, the structural analyses and sizings needed to enable the overall design of the hydrofoil ship had to include as much flexibility as possible to be able to quantify the effects of numerous loading and geometry parameters. A physics-based model with optimizer was used to derive minimum total strut and wing/body weight solutions. The list below contains the primary parameters included in the sizing efforts. Accounting for the fact that each wing segment has two thickness variables (skin and spar web thickness), as many as 16 parameters are allowed to vary, subject to over 60 constraints, while optimizing the wing and strut design for minimum combined weight.

Two variables in particular that were shown to have a significant effect on structural weight were design loads and minimum skin thickness. Although some rationale was employed to arrive at the values used in the trade studies, the values derived from actual water tank or prototype testing in addition to impact testing could be significantly different. To at least maintain consistency throughout the trade studies, the values were held constant.

Structures Approach and Methodology - Hydrofoil

• Automated Structural Sizings

– Independent variables used by optimizer to derive minimum wing/strut weight

- » Skin thicknesses (up to 4 for wing, 5 for struts)
- » Spar web thicknesses (up to 4 for wing, 5 for struts)
- » Spanwise location of intermediate struts
- » % local wing chord at lower end of strut
- » % local wing chord at upper end of strut

– Constraints

- » Minimum skin thickness
- » Minimum spar web thickness
- » Spanwise range of spar locations (up to 3)
- » Min/max % local wing chord at lower end of strut
- » Min/max % local wing chord at upper end of strut

- » Max/min bending/axial stress cutoffs
- » Max/min shear stress cutoffs
- » Column buckling stress allowable

– Independent variables held constant

- » Mat'l prop./allow. (***55ksi ten./comp., 40.5ksi sh.***)
- » Vertical, side, and aft G-load factors (***2,0.5,0.5G***)
- » All-up weight (***4000T***)
- » Wing section geometry
- » Wing span (***125,150,175, or 200-ft***)
- » Wing leading edge sweep (***35°,40° or 45°***)
- » Wing centerline and tip chords (***2:1 taper***)
- » Wing anhedral/dihedral (***0°***)

- » Outboard strut distance from end of wing
- » Number of struts (***3, 5, 7, or 9***)
- » Strut length parameters
- » Nominal wing depth (***20-ft***)
- » Number of spars (***6***)
- » % chord location of front and rear spars
- » Numerous geometric relationship assumptions used in sizing calculations

Structures Approach and Methodology - Hydrofoil

Approach and Methodology – Hydrofoil (Cont'd)

Below are the dependent variables generated during the sizing optimization process.

Structures Approach and Methodology - Hydrofoil

- **Automated Structural Sizings (Cont'd)**
 - Dependent variables generated by optimizer
 - » % chord of wing section neutral axis
 - » Wing neutral axis sweep
 - » Wing section properties normal to wing neutral axis
 - » Wing t/c (streamwise and normal to neutral axis)
 - » Wing area and loading
 - » Wing aspect ratio
 - » Ship height above water (hullborne and foilborne)
 - » Strut locations
 - » Strut leading edge sweeps
 - » Strut thickness factor at water surface
 - » % side load taken by each strut
 - » Weight of each strut
 - » **Total wing and strut weight**
 - » Submerged wing/strut volumes (water displacement)
 - » **Net wing and strut weight** (total less buoyancy)
 - » Average foil and strut % solidity
 - » Max/min skin and spar web thicknesses
 - » Strut critical failure modes
 - » Maximum strut trailing edge compression stress
 - » Wing and strut wetted areas
 - » Theoretical L/D
 - » **Theoretical Zero-Payload (Breguet) Range**

Structures Trade Study Results - Hydrofoil

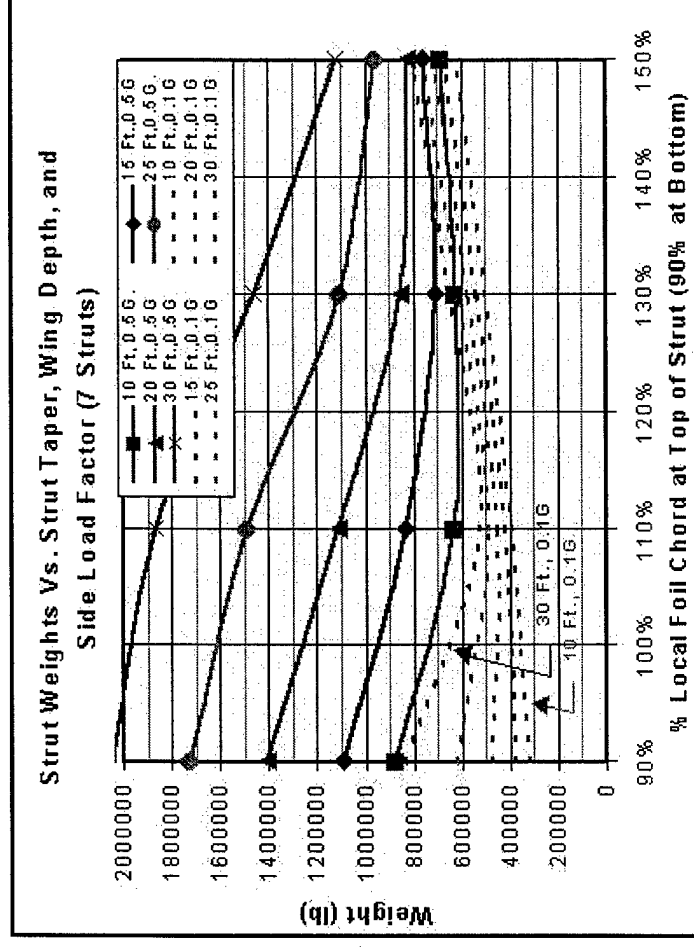
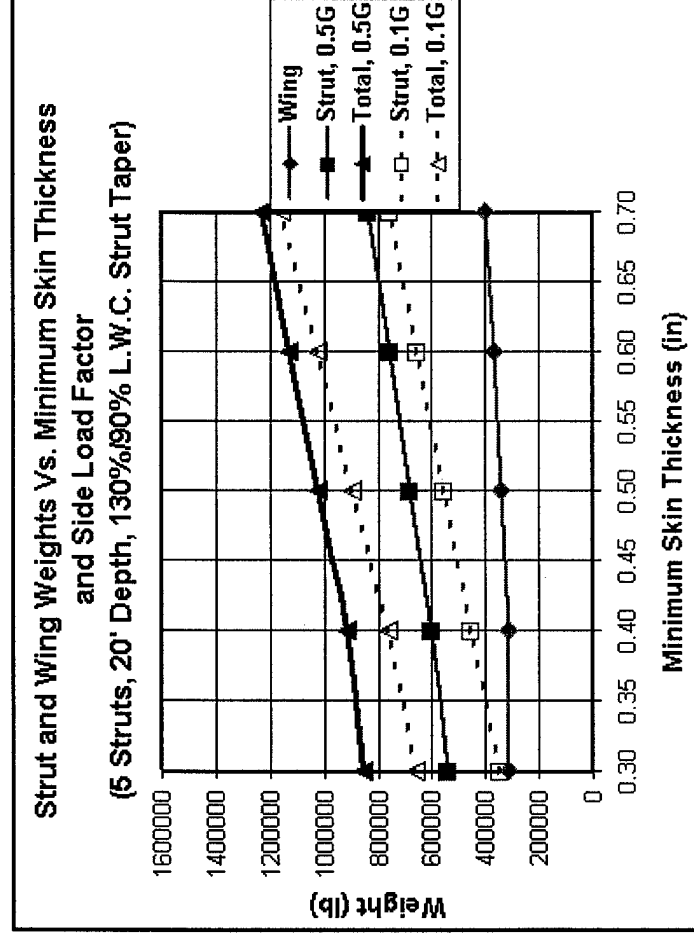
Trade Study Results – Hydrofoil

As mentioned previously, two variables in particular that were shown to have a significant effect on structural weight were design loads and minimum skin thickness. Therefore, a trade study was run to attempt to quantify the effect of these variables, the results of which is shown in the figure on the left below.

A trade study to quantify the effects of strut taper, wing depth, and side load on the weight of the struts was also performed. The results for this study are shown in the figure on the right below. The results pertaining to wing depth were factored in to the overall performance evaluation to come up with the “optimum” depth of 20 feet for the 4000T vehicle.

Structures Trade Study Results - Hydrofoil

Trade Study Results for Minimum Skin Thickness, Design Side Load, Strut Taper, and Wing Depth



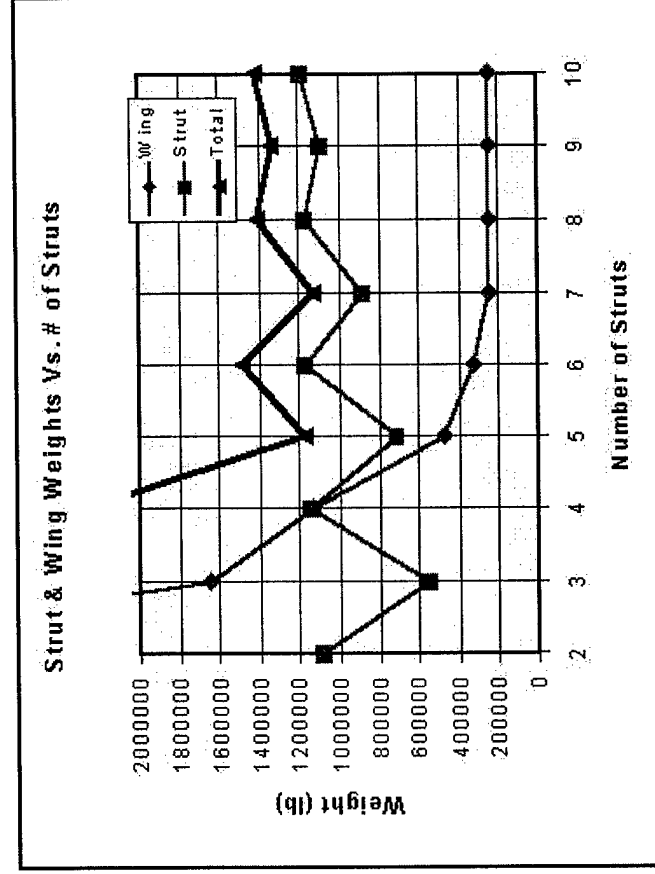
Structures Trade Study Results - Hydrofoil

Trade Study Results – Hydrofoil (Cont'd)

All of the structural trade studies performed assumed a 3-hull configuration. The trimaran hulls permit shorter struts, and hence shorter moment arms, for the middle and the two end struts that penetrate the hulls. The strut length must span the distance from the above water keel height to wing operating depth. Without having a shorter strut tied to the center hull with an even number of struts, the two longer struts that essentially take the center strut's place are less efficient. Also, if the spacing is wide enough between these two inner struts, there can be an additional penalty paid in the wing structural weight to react the torsional load that would develop between those struts in a swept-wing configuration. The typical effect of the number of struts can be seen in the plot shown below for a preliminary wing geometry/loading and even strut spacing, where the efficiency of the shorter struts resulted in a relatively lower strut overall weight. It was therefore concluded from this that only odd-number-of-strut configurations would be considered with the tri-hull arrangement.

Structures Trade Study Results - Hydrofoil

Trade Study Showing the Effect of the Number of Struts on Wing and Strut Weight



Structures Trade Study Results - Hydrofoil

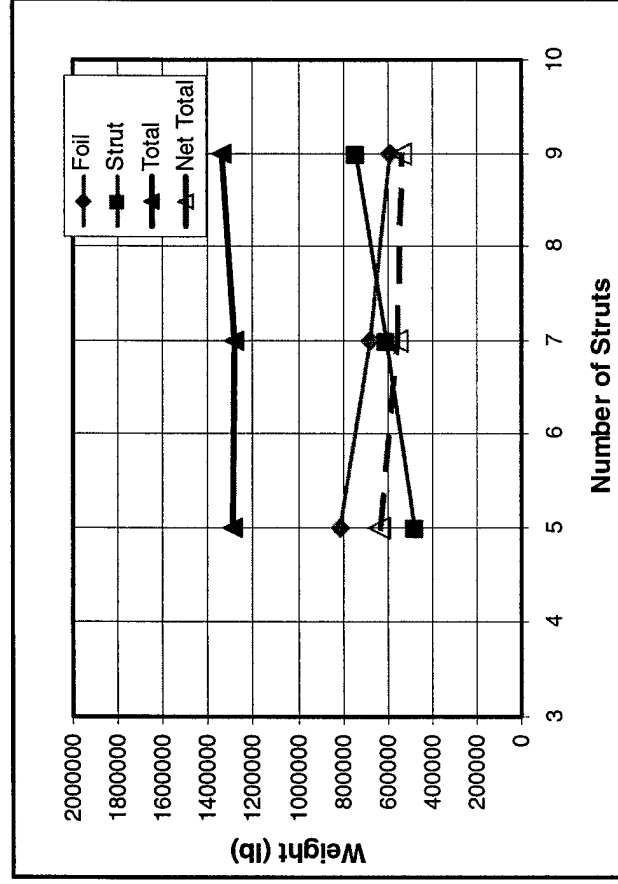
Trade Study Results – Hydrofoil (Cont'd)

As mentioned previously, the original wing and strut sizings were done with evenly spaced struts for analysis simplicity. When that parameter became a variable to include in the optimization process and the results were generated, a comparison between the evenly versus the optimally spaced struts was made and is shown in the figures below. The wing structural efficiency was the primary driver in determining the optimum spacing. Hence, the effect on the wing weight was dramatic, while the effect on the total strut weight was minimal. The fact the the wings were tapered is believed to have been a major factor in this finding.

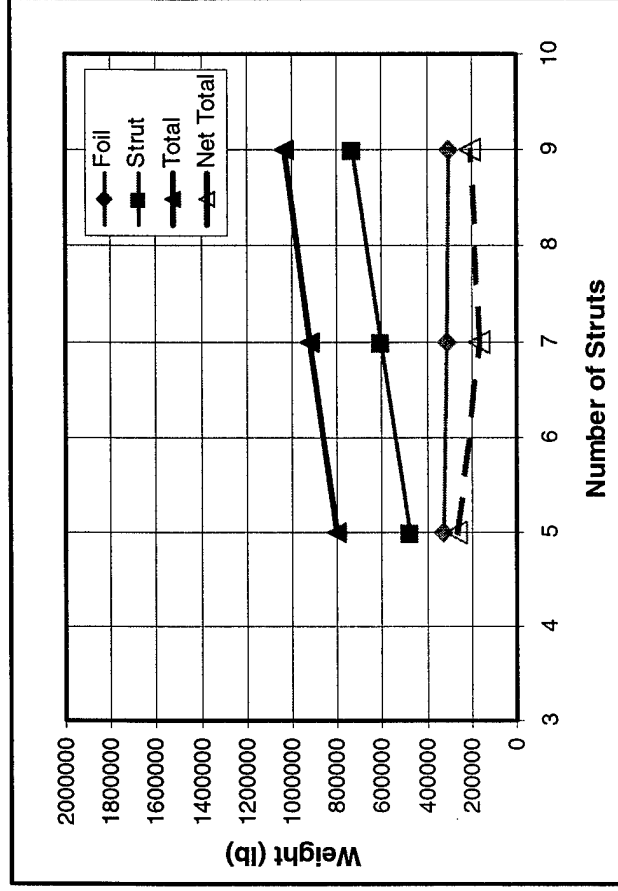
Structures Trade Study Results - Hydrofoil

Trade Study Results for Even Versus Optimum Strut Spacing

Even Strut Spacing



Optimum Strut Spacing



Structures Trade Study Results - Hydrofoil

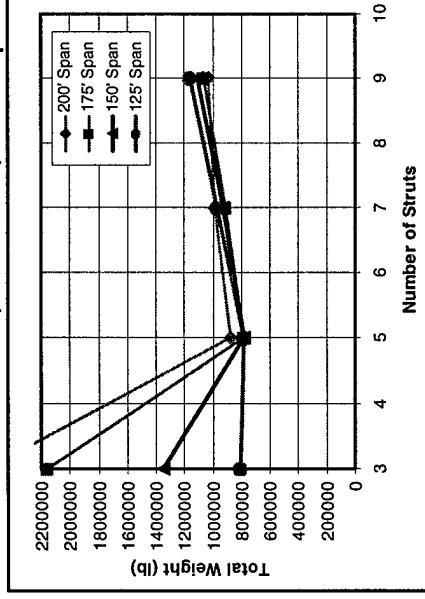
Trade Study Results – Hydrofoil (Cont'd)

Up to this point, the wing span used in the trade studies was set at 200 feet to capture the performance benefits of a higher aspect ratio wing. In that more highly loaded wings may be excessively heavy or structurally unfeasible, consideration was given to reducing the span to arrive at a more achievable design solution. The primary structures trade studies performed showed the effect of wing span and number of struts on wing and strut weight for several wing section geometries and associated wing loadings. The results shown below are for the actual structural weight, and do not include any buoyancy effects. As can be seen, there is a general increase in wing structural efficiency as the wing span decreases. This is due to the wing sections becoming “stubbier” (more efficient in bending) as the planform area is necessarily held constant. However, as the span decreases and the chord increases, since the strut chord lengths are tied to the local wing chord length, their weight begins increasing past the point at which the minimum skin thickness constraint is met.

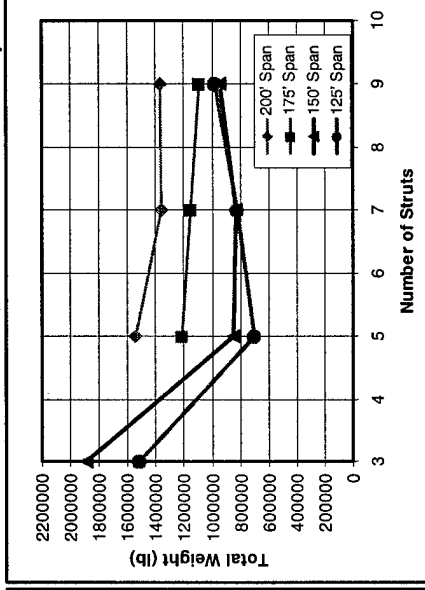
Structures Trade Study Results - Hydrofoil

Total Wing/Strut Weight Vs. Number of Struts and Wing Span

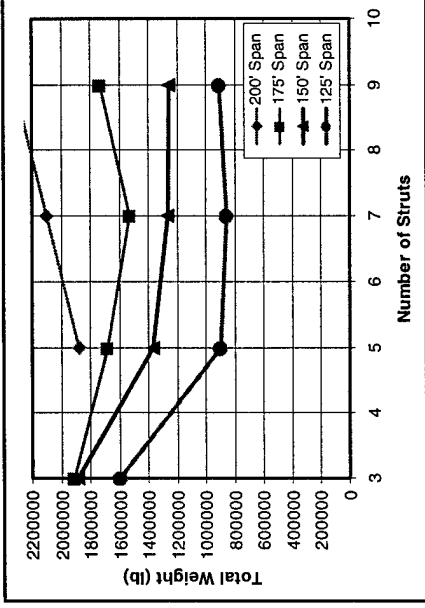
P70/40/2.0H35, 4600 ft², 1750 psf



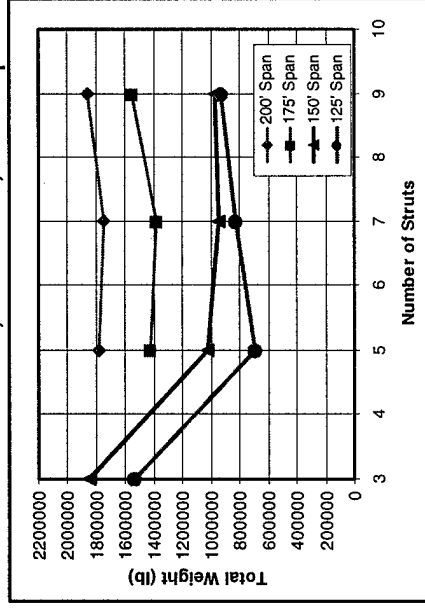
P70/50/2.0H40, 3265 ft², 2450 psf



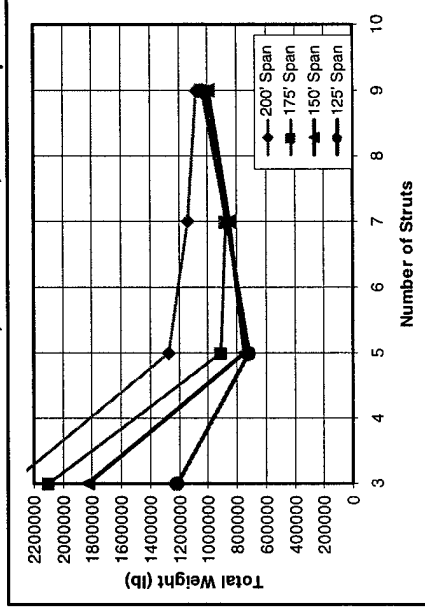
P70/55/2.0H45, 2666 ft², 3000 psf



P70/55/2.0D40, 2910 ft², 2750 psf



P70/50/2.0H35, 3720 ft², 2150 psf



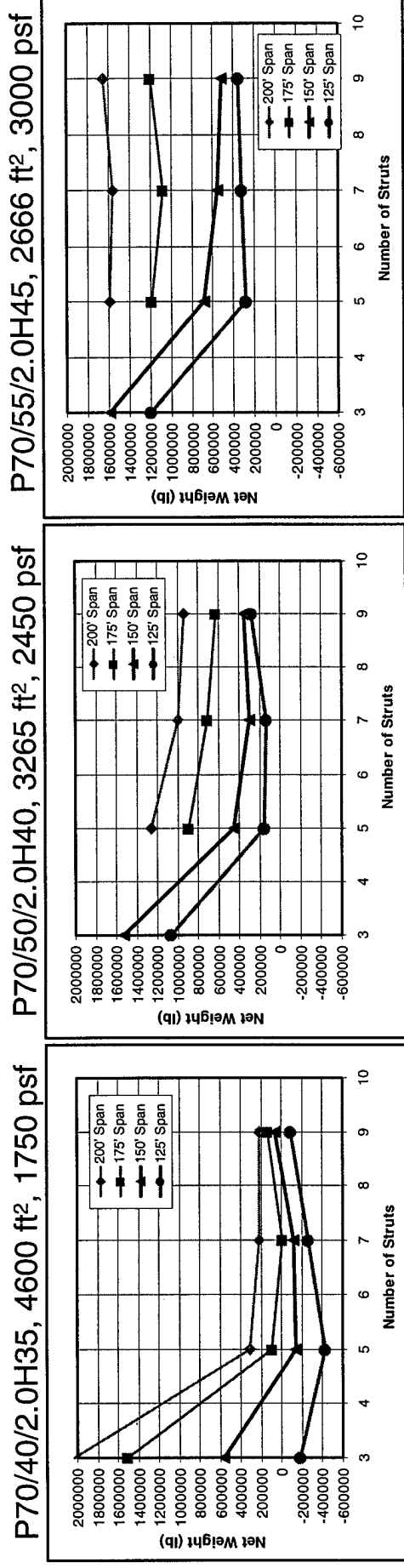
Structures Trade Study Results - Hydrofoil

Trade Study Results – Hydrofoil (Cont'd)

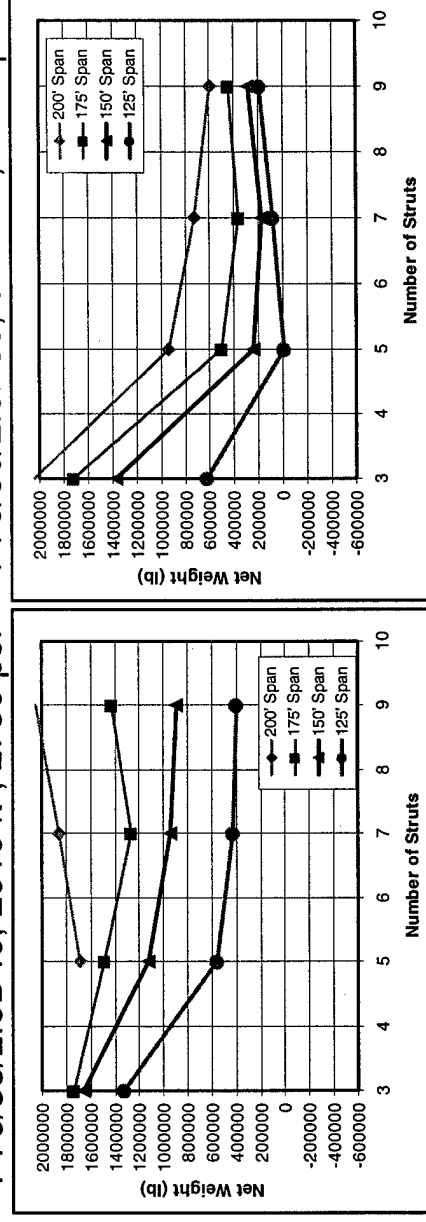
When the buoyancy effects of the wing and submerged portion of the struts were taken into account, the benefits of reducing the span became more pronounced due to the effect of net weight reduction caused by the increase in the displaced water volume by the wing and struts. The results of this trade study are shown in the figures below.

Structures Trade Study Results - Hydrofoil

Net Wing/Strut Weight Vs. Number of Struts and Wing Span



P70/55/2.0D40, 2910 ft², 2750 psf P70/50/2.0H35, 3720 ft², 2150 psf



Structures Trade Study Results - Hydrofoil

Trade Study Results – Hydrofoil (Cont'd)

In order to capture the effects of the various structural weight trades on the vehicle range during the optimization process, range was added as a dependent variable by incorporating the Breguet range equation shown below for zero-payload and a fixed-weight fraction of 0.45. The results were then used as a screen to determine which configurations would be looked at more thoroughly during the overall vehicle performance assessments.

Structures Trade Study Results - Hydrofoil

- **Performance estimation incorporated into sizing runs**

- Determine range using weight as a *dependent* variable (Breguet Equation)

$$R \approx \left(\frac{V}{TFSC} \right) \cdot \left(\frac{L}{D} \right) \cdot \ln \left(\frac{W_i}{W_f} \right)$$

$$V \approx 70 \quad TSFC \approx 0.12$$

$$W_i \approx 4000T \quad W_f \approx 45\% \cdot 4000T + \text{Strut \& Foil}_{Net_Weight}$$

$$L/D \approx \frac{0.35 \cdot b^2 \cdot V^2 \cdot (W/S)}{0.0088 \cdot k_2 \cdot b^2 \cdot V^4 + 125 \cdot (W/S) \cdot W_i}$$

$$b \approx \text{Wing Span} \quad W/S \approx \text{Wing Loading}$$

- » function of wing section (sweep and loading)
 - » function of number of support struts
 - » function of wing span
- Summary of other variables for select configurations
 - » weight, wetted area, strut spacing, skin thickness, etc.

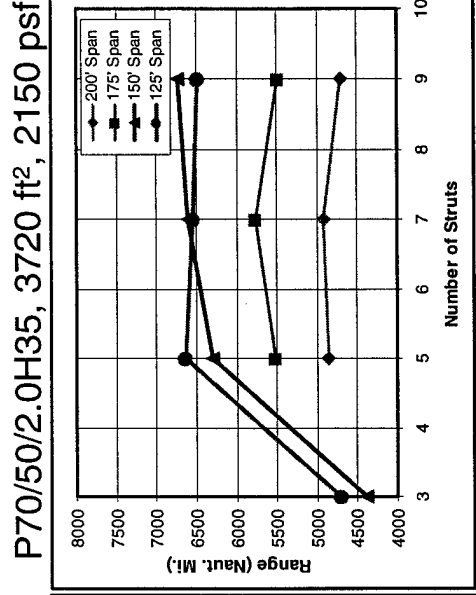
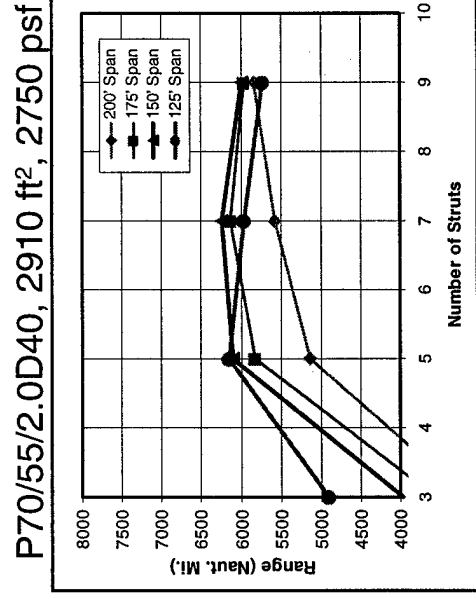
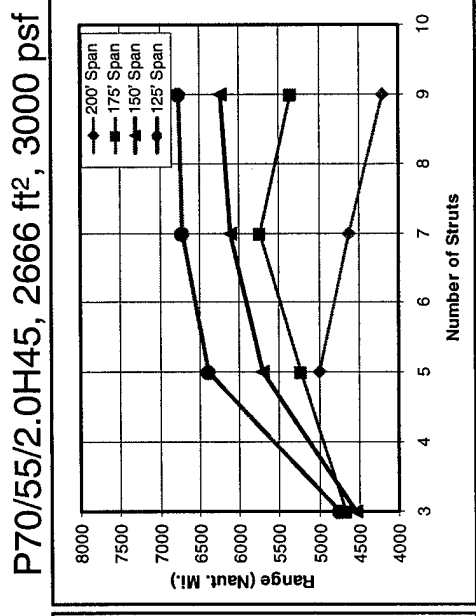
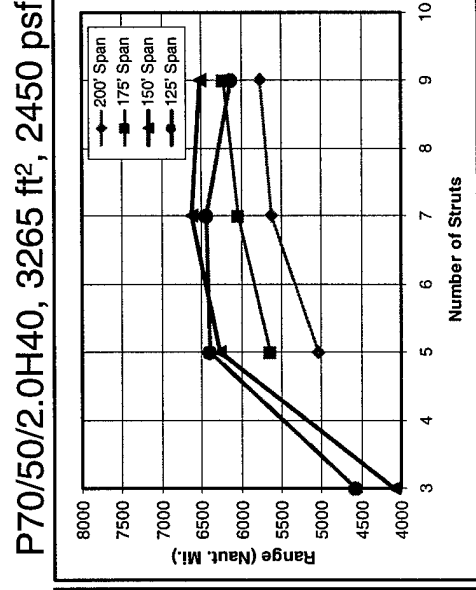
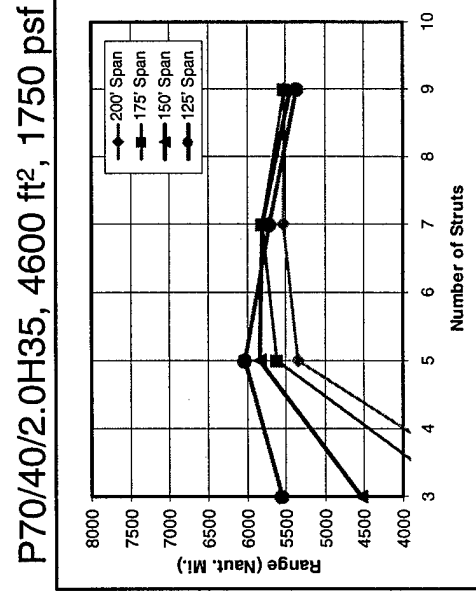
Structures Trade Study Results - Hydrofoil

Trade Study Results – Hydrofoil (Cont'd)

The effect of the those previously assessed configurations on theoretical range is shown in the figures below. The positive effects of decreasing span coupled with the increasing buoyancy were readily apparent. It was also evident that there tended to be an optimal span and number of struts for a given wing section and loading. From the results shown, the two candidate configurations producing the best range were: 1) the 125-ft span, P70/55/2.0H45 section, 2666 ft², 3000 psf wing, with 7 struts, and 2) the 125-ft span, P70/50/2.0H35 section, 3720 ft², 2150 psf wing, with 5 struts. The most promising configurations were subsequently examined in a more accurate performance evaluation.

Structures Trade Study Results - Hydrofoil

Range Vs. Number of Struts and Wing Span



Maximum theoretical zero-payload range = 6767 nautical miles (FWF = 45%)

Structures Refined Sizing - Hydrofoil

Finite Element Analysis to Refine Sizing and Validate Physics-Based Solution

Finite Element Analysis was performed to validate and refine the physics-based solution for the 4000-ton AUW hydrofoil structure. MSC PATRAN and NASTRAN were used for this analysis. PATRAN is a pre and post processor and NASTRAN is the finite element solver. Typical Steel material properties of $E = 30\text{msi}$ and $\rho = .283\text{ lbs/in}^3$ were used. The physical properties for area and thickness were taken from the physics-based solution.

Finite Element Model of Hydrofoil Geometry

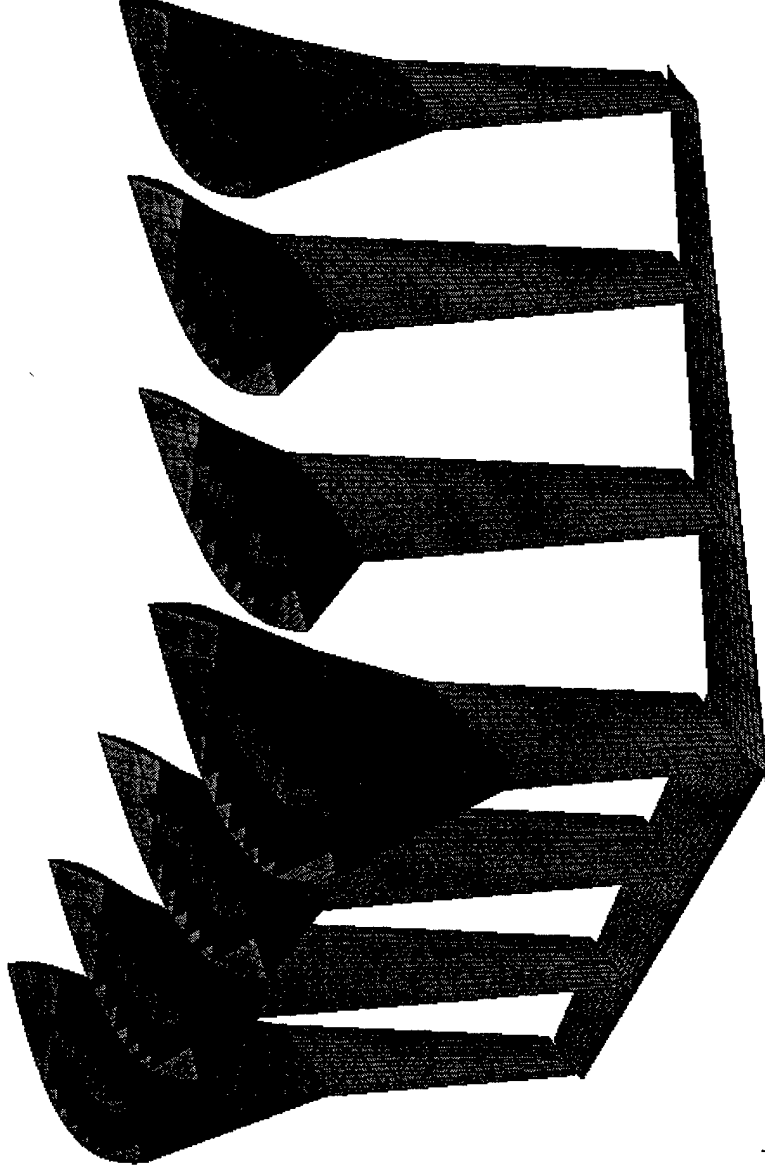
The figure below left shows the finite element model of the hydrofoil/strut geometry. The figure below right is a view of the ribs and spars of the hydrofoil and struts. Shell elements were used for all skin and web structure. One directional Rod element with axial stiffness were used for all spar caps. One direction Bar elements with axial and bending stiffness were used to connect the struts to the hydrofoil, simulating a fitting. The model consisted of 17,236 elements and 9781 nodes (or grid points). Representative hull structure was modeled at the top of the struts.

Boundary Conditions and Loads

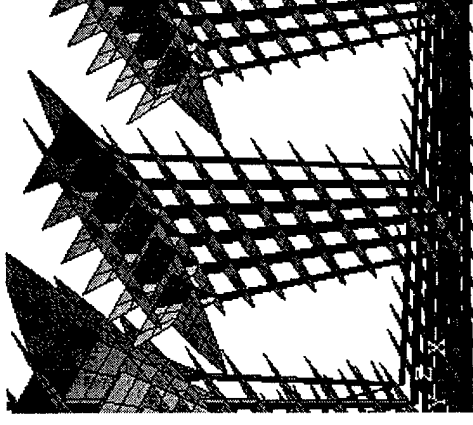
The top of the struts and the hulls were "fixed." The nodes at these locations were constrained from moving in any direction. Two different load cases were analyzed. The first load case was a 2.0G hydrodynamic load on the hydrofoil and the other load case was a combined 1.0G hydrodynamic load on the hydrofoil and a 0.5G side inertial load.

Structures Refined Sizing - Hydrofoil

Hydrofoil Finite Element Model



Overall Model



Internal Structure

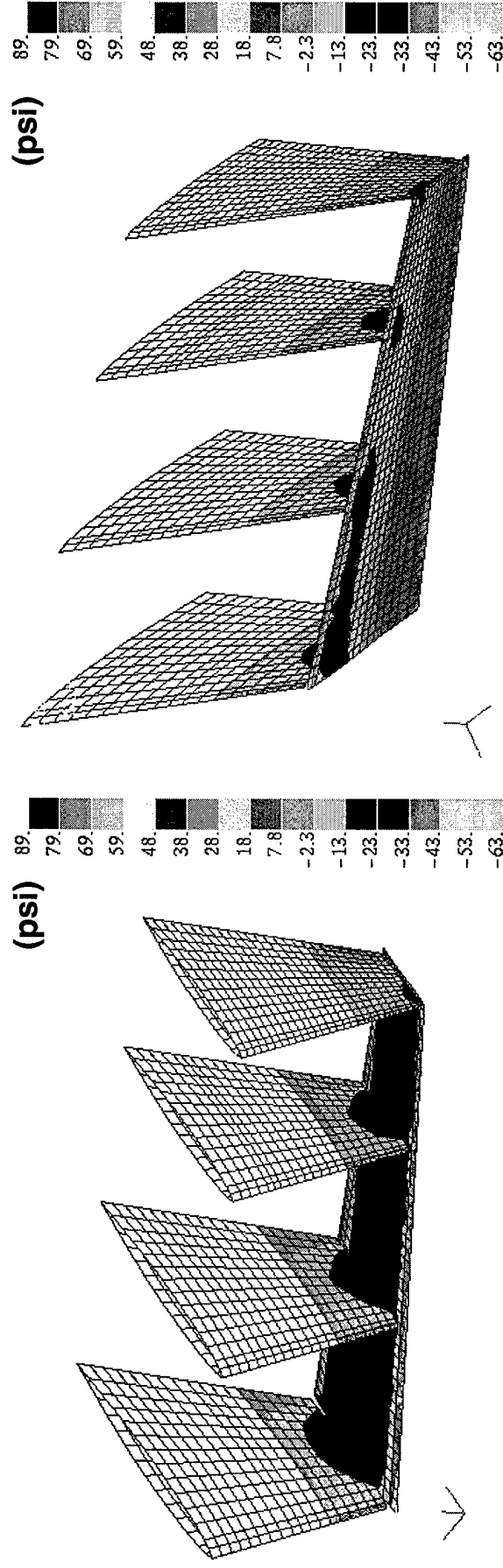
Structures Refined Sizing - Hydrofoil

Hydrodynamic Load

The main applied load on the hydrofoil / strut structure is due to hydrodynamic pressures on the hydrofoil. Hydrodynamic pressures generated by Computational Fluid Dynamics were imported into PATRAN and converted to structural pressure loads. The CFD hydrodynamic pressures correspond to 70 knots and a Froude Number of 4.4. The net resultant vertical load (lift) was 4000T, a 1.0G load. The figure below shows the pressure contour on the finite element model from the CFD analysis. The 2.0G hydrodynamic load is the 1.0G scaled up by a factor of two.

Structures Refined Sizing - Hydrofoil

Hydrodynamic Loads on Wing and Struts



Top View

Bottom View

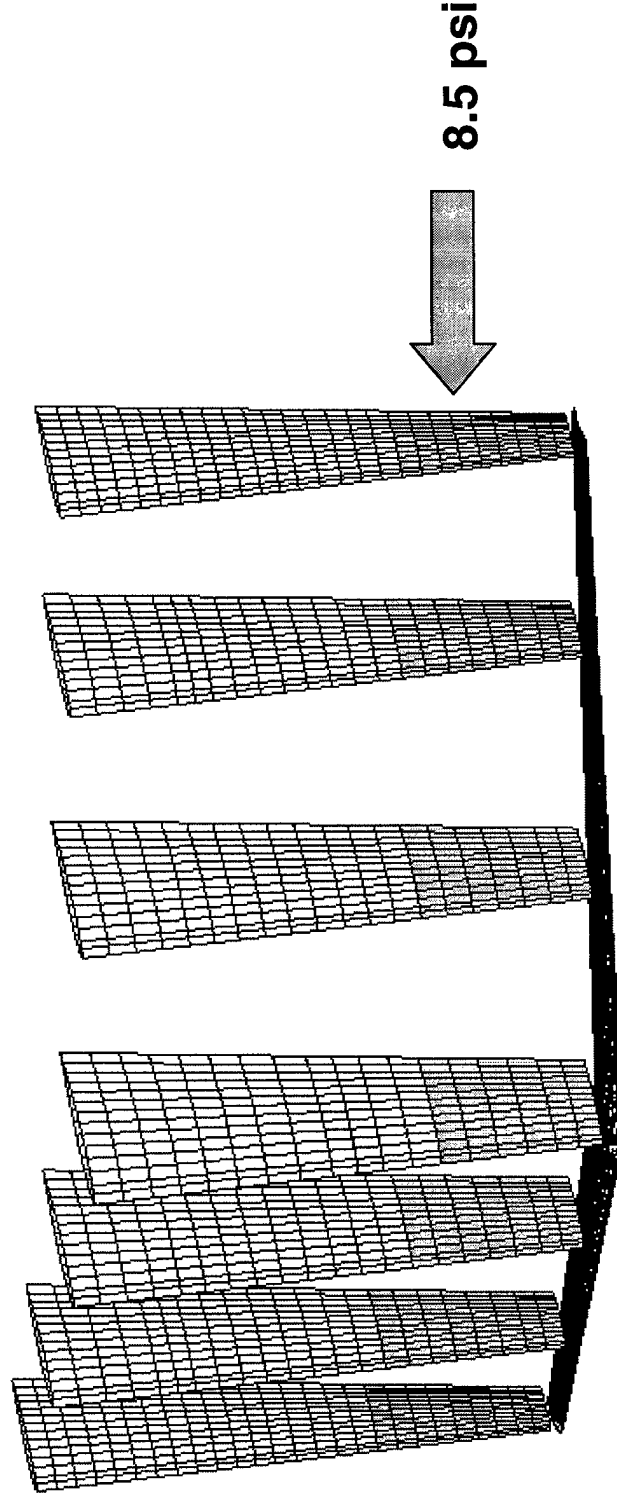
Structures Refined Sizing - Hydrofoil

0.5G Inertial Side Load

Another applied load was a 0.5G (or 2000 ton) inertial side load. This load was applied using a uniform pressure load laterally on one side the struts submerged under water. The surface area of one side of the struts submerged under the water was calculated. Knowing a 2000 ton side load was needed, the corresponding pressure was found to be 8.5 psi. The figure below shows the area on the struts where the 8.5 psi was applied.

Structures Refined Sizing - Hydrofoil

0.5G Inertial Side Load on Struts



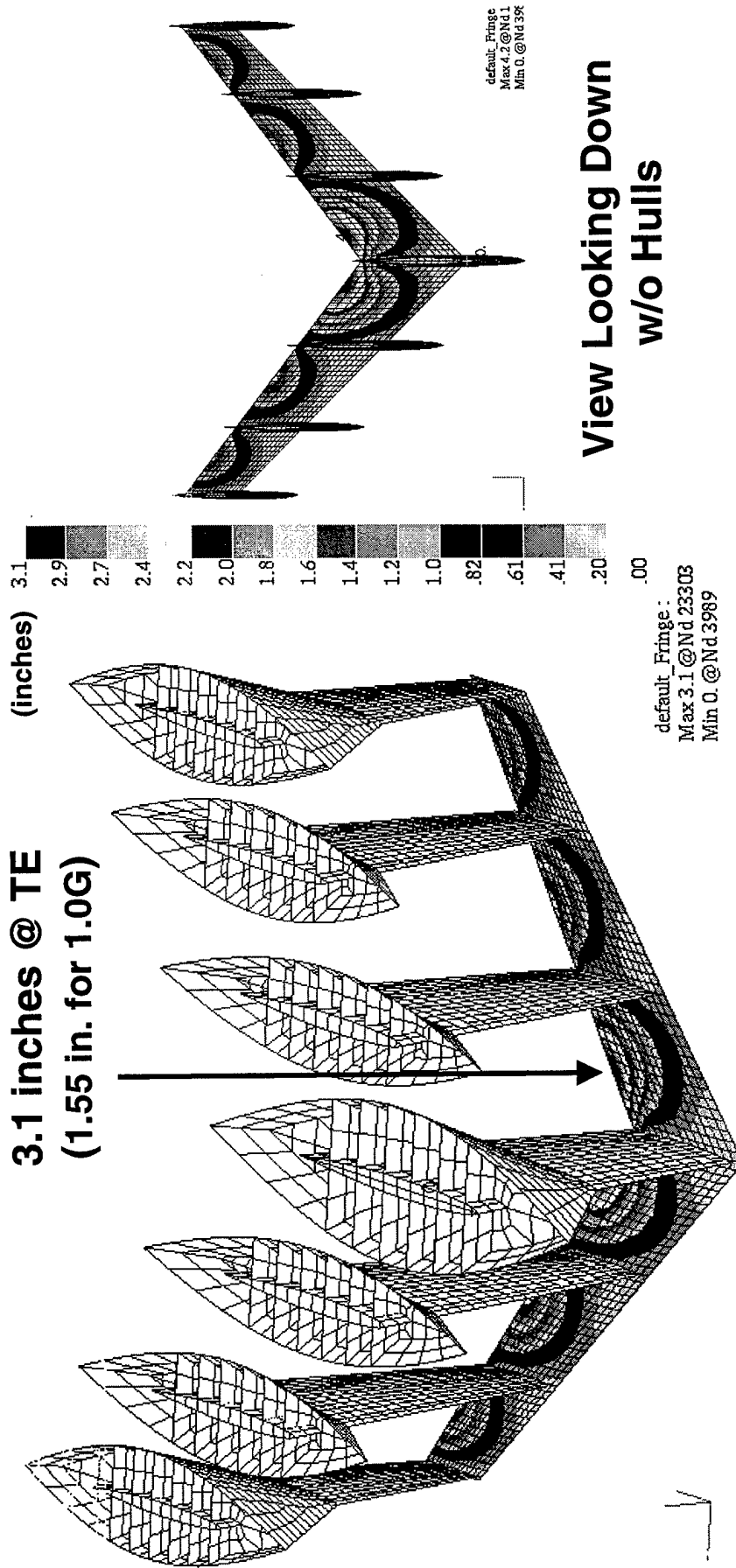
Structures Refined Sizing - Hydrofoil

1.0G Hydrodynamic Load Displacement Results

The figure below shows the displacement results for the 2.0G hydrodynamic load case. Representative structure of a flap system is not present in this model. Hence, the maximum displacement at the trailing edge of the hydrofoil would probably change if the flap structure was modeled.

Structures Refined Sizing - Hydrofoil

Displacement Results Using Spreadsheet Sizing Output



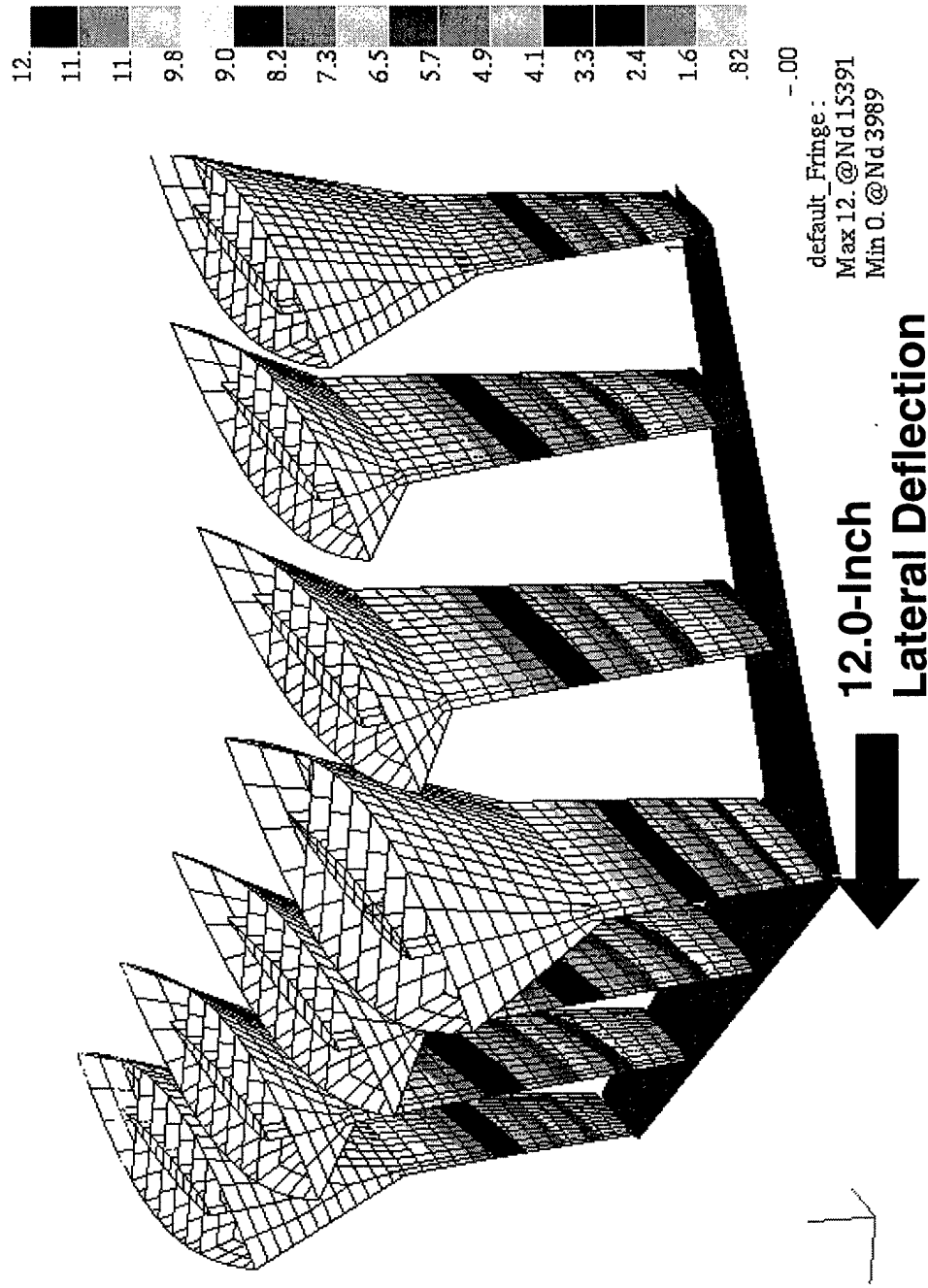
Structures Refined Sizing - Hydrofoil

1.0G Hydrodynamic Load plus 0.5G Side Load Displacement Results

The figure below shows the displacement results for the 1.0G hydrodynamic load plus the 0.5G side load. The lateral deflection was 12 inches.

Structures Refined Sizing - Hydrofoil

Displacement Results Using Spreadsheet Sizing Output (Cont'd)



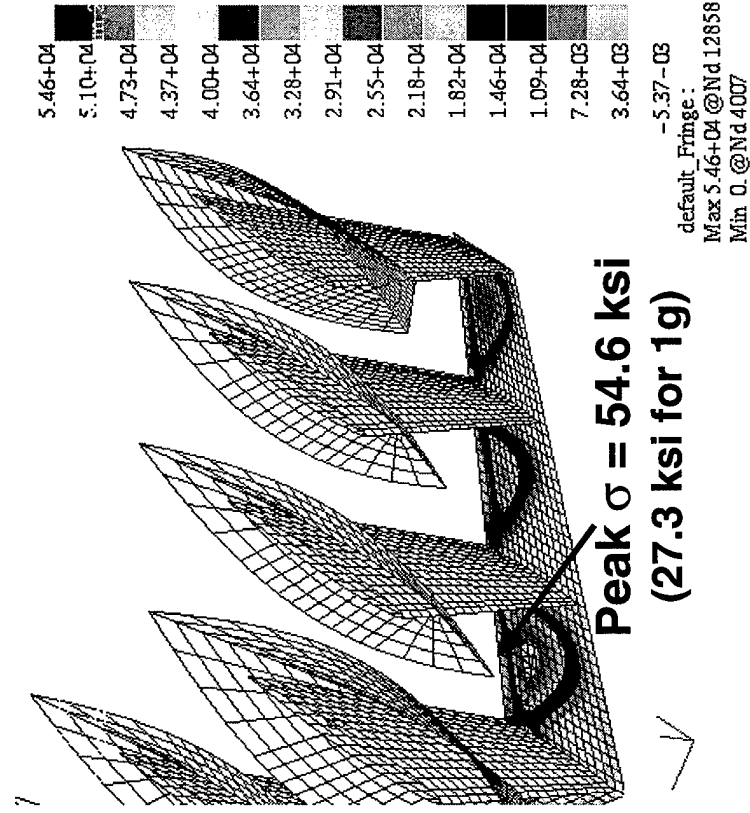
Structures Refined Sizing - Hydrofoil

2.0G Hydrodynamic Load Stress Results

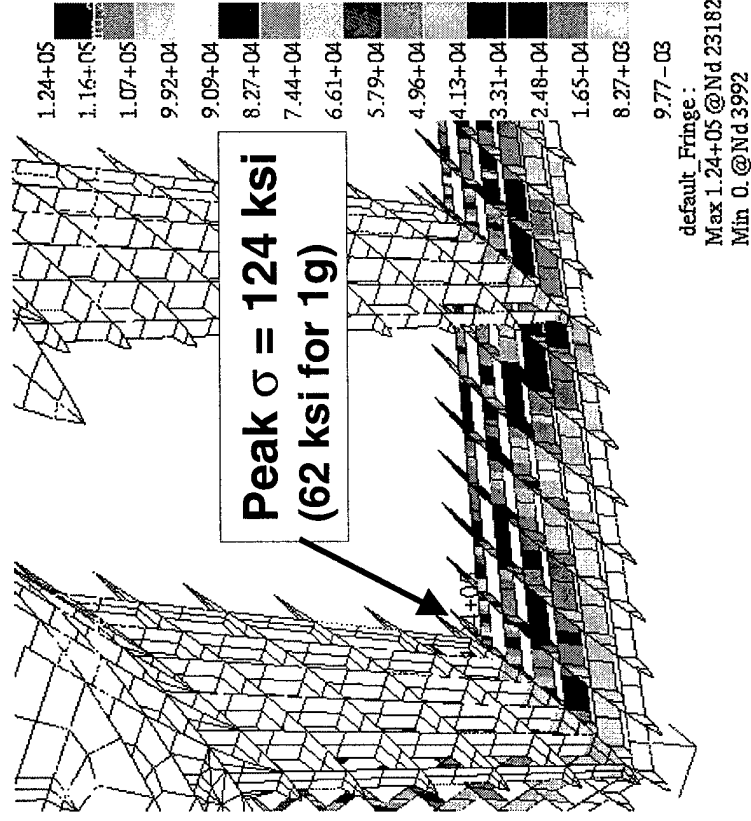
The figure below shows the maximum stresses found for the 2.0G hydrodynamic load. The maximum axial (1D elements) or normal (2D elements) stress allowable was 55 ksi and the maximum (in-plane) shear stress allowable was 44 ksi. The maximum stress in the foil skin was 54.6 ksi. A maximum stress in the rib / spar structure was found to be 124 ksi at the trailing edge spar near the center strut. This is the result of large bending loads at that location. Hence, there were locations in the rib / spar structure that had negative margins of safety.

Structures Refined Sizing - Hydrofoil

Stress Results Using Spreadsheet Sizing Output



Skins



Ribs and Spars

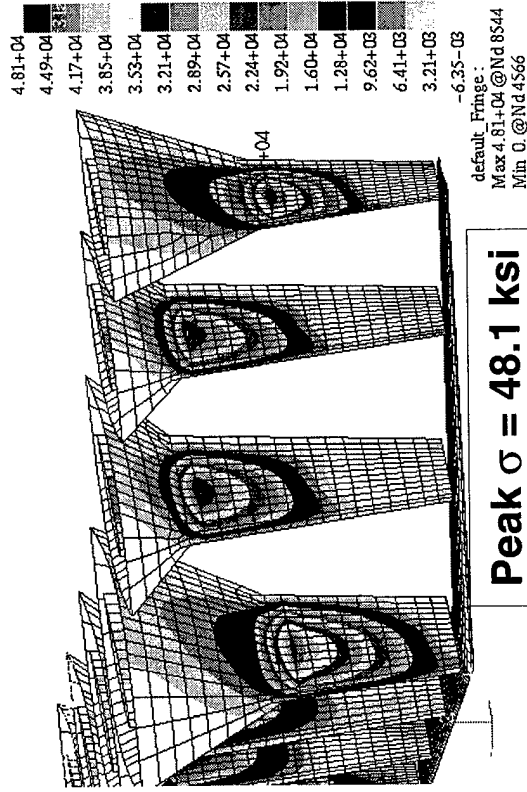
Structures Refined Sizing - Hydrofoil

1.0G Hydrodynamic Load Plus 0.5G Side Load Stress Results

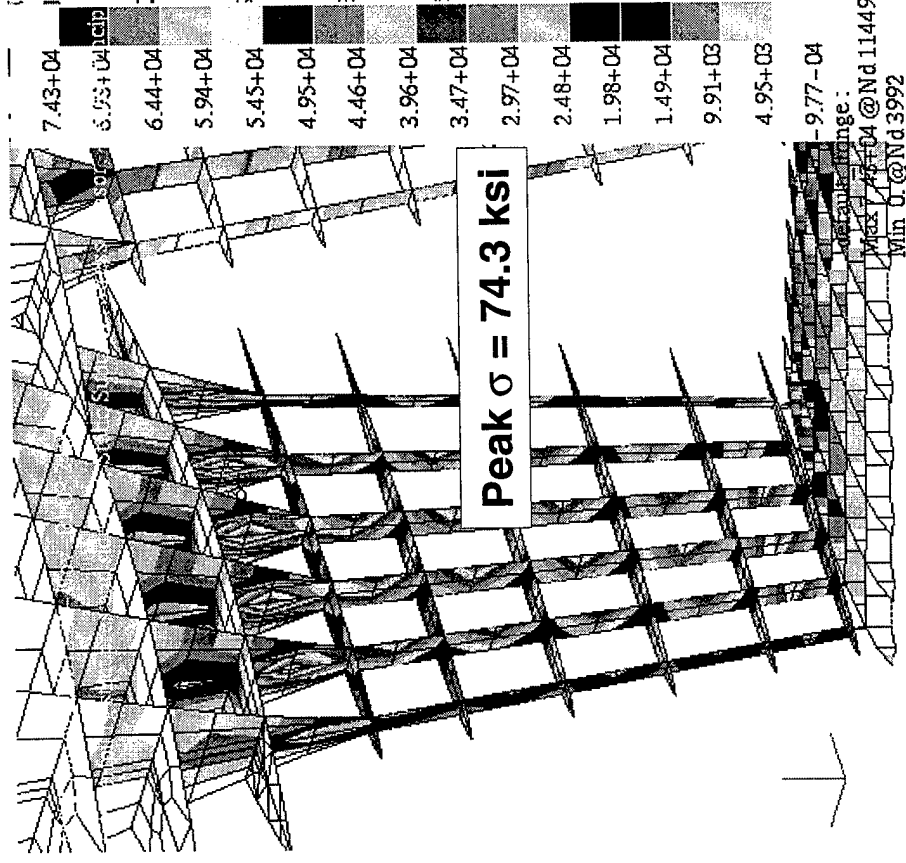
The figure below shows the maximum stresses found for the 1.0G hydrodynamic load plus side load. The maximum stress found in the skins was 44 ksi, which is below the allowable. A maximum stress in the rib / spar structure was found to be 74.33 ksi at the top of the center strut spars. This is the result of large bending loads at that location from the side load. Again, there were locations in the rib / spar structure that had negative margins of safety.

Structures Refined Sizing - Hydrofoil

Stress Results Using Spreadsheet Sizing Output



Skins



Ribs and Spars – Center

Structures Refined Sizing - Hydrofoil

Comparison to Physics-Based Solution

The results from the FE model validate the physics-based solution. The properties used in the model originated from the physics-based solution. Only in several local regions were stresses higher than the allowed stresses. Furthermore, the two methods resulted in structural weights with a very small difference in values. The physics-based solution computed a structural weight of 861,000 lbs. The finite element model computed a structural weight of 883,000 lbs. The difference between the two solutions was only 2.5%.

It should be noted that the hull structure was not included in the structural weight.

Structures Refined Sizing - Hydrofoil

Finite Element Model - Resizing

The finite element analysis indicated that resizing should be performed. There were some areas that had negative margins of safety and other areas were over-designed. Therefore, additional finite element analysis was performed primarily to remove the negative margins of safety and second to try to decrease weight. Instead of manually altering properties to remove the negative margins of safety it was decided to use NASTRAN's optimization analysis. The two load cases and boundary conditions previously used were again applied to the model.

The optimization analysis has three main components. First is the Design Objective. This application had a Design Objective of minimum weight. Next, is the Design Variables. These are components that are allowed to change over some assigned range or bounds. Thirty eight groups of structure were setup as design variables. Thickness and area were allowed to fluctuate with appropriate lower and upper bounds assigned. Hull structure was held constant. The next component to setup is Design Constraints. The design constraints for this analysis were the allowable stresses. The maximum axial (1D elements) or normal (2D elements) stress allowable was 55 ksi and the maximum (in-plane) shear stress allowable was 44 ksi.

Initial values have to be assigned for the design variables. Three runs were made with different initial values. The first run had the physics-based solution as the initial values. The second run had the lower bound for the initial runs and the third run had the upper bounds for initial values. All three runs found acceptable solutions. Each run converged to a solution while not violating any of the constraints. The second run resulted in the minimum design and it's results will follow.

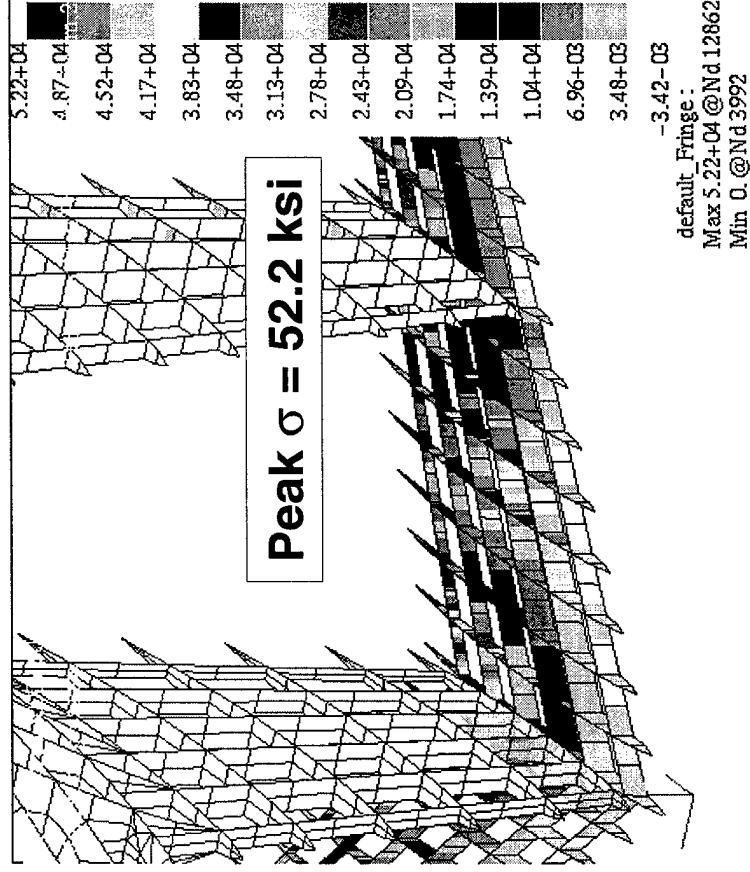
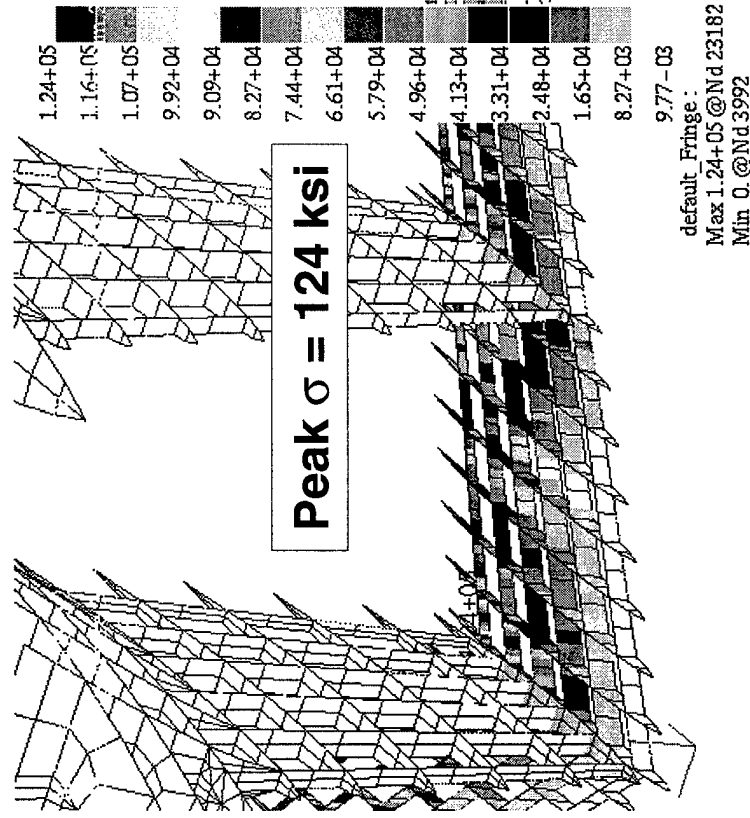
Structures Refined Sizing - Hydrofoil

2.0G Hydrodynamic Load Stress Results

The figure below shows the maximum stresses found for the 2 g hydrodynamic load before and after the resizing. The stresses in trailing edge spar web were reduced from 124 ksi to 52.2 ksi which is below the allowable.

Structures Refined Sizing - Hydrofoil

Stress Results Before and After Resizing - Wing



Before Resizing

After Resizing

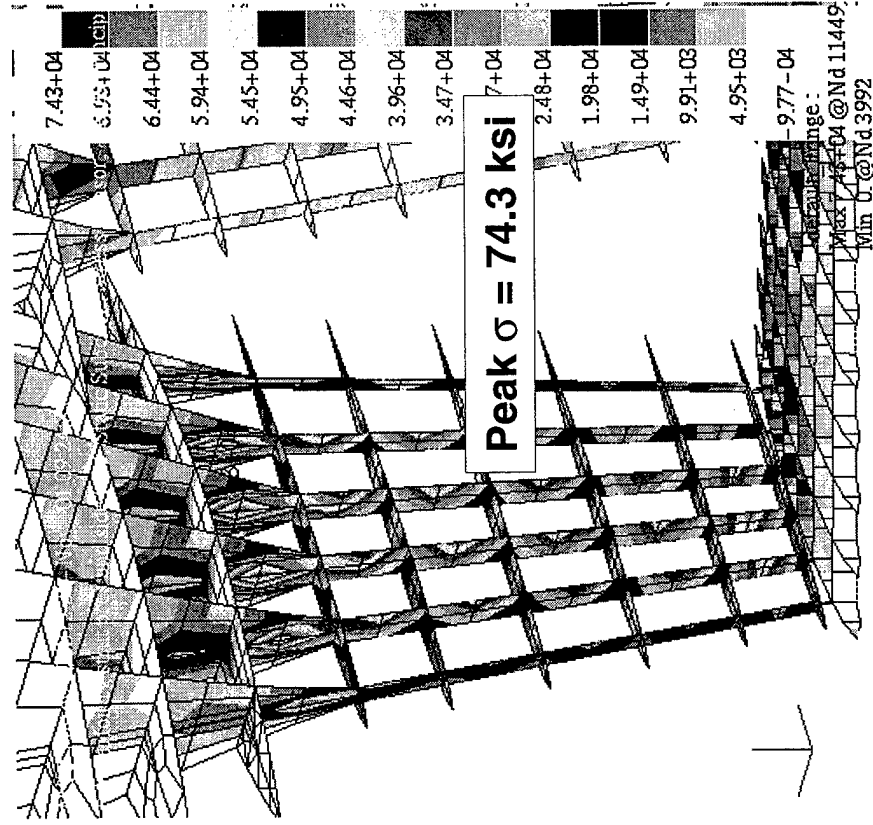
Structures Refined Sizing - Hydrofoil

1.0G Hydrodynamic Load Plus 0.5G Side Load Stress Results

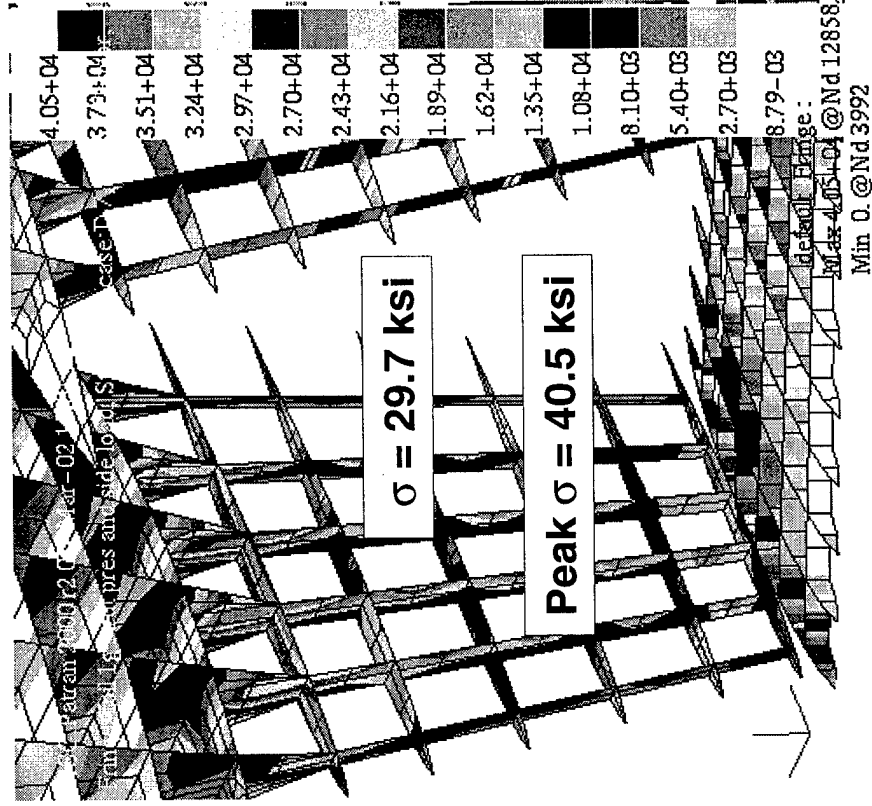
The figure below shows the maximum stresses found for the 1 g hydrodynamic load plus side load before and after resizing. The previous analysis had a maximum stress in the rib / spar structure was found to be 74.33 ksi at the top of the center strut spars. The redesign reduced this stress to 29.7 ksi. The maximum stress from this load case with the redesign is now located in the rib / fitting below the center strut. This stress is 40.5 ksi and below the allowable.

Structures Refined Sizing - Hydrofoil

Stress Results Before and After Resizing - Spars



Before Resizing



After Resizing

Structures Summary and Conclusions - Hydrofoil

Summary and Conclusions – Hydrofoil

In summary, various parametric structural sizing and optimization trade studies were performed using a physics-based methodology to examine the effect of various design perturbations on structural weight. These trade studies were carried one step further to include the effect on theoretical range as an aid to narrowing down the number of possible design configuration options to be more thoroughly evaluated. Overall, these higher fidelity trade studies showed how important the structure of the wing and strut system is to the total vehicle synthesis process.

A change in one design feature which would likely have a beneficial effect on wing and strut weight (and possibly performance) is the reduction or elimination of wing taper. Since each struts chord length is tied to the local wing chord, the more outboard (shorter-chord) struts are having to inefficiently make up for a lack of section size through increased skin thickness. From a manufacturing point of view, also, all struts and wing sections could likely be made the same, thus realizing a significant relative cost savings.

The determination of what may be more realistic design loadings, and also a practical minimum skin thickness constraint, should be considered a necessary steps to be taken before any effort is made to refine the wing and strut structure sizing. The resizing exercise resulted in a working design that validated the physics-based solution, has no negative margins of safety, and results in a slight decrease in weight.

Physics-Based Solution Weight = 861,000 lbs

FE Model Weight of Physics-Based Solution = 883,000 lbs

FE Model Weight after Resizing = 879,600 lbs

Structures Summary and Conclusions - Hydrofoil

Summary and Conclusions

- Parametric sizings runs made to determine structural feasibility of numerous wing/strut configurations and to provide guide for further studies
- Coupled structural sizing and estimated range studies indicate a significant benefit to reducing span
- Refined sizing exercise proved preferred design to be workable structurally; validated physics-based solution approach, methodology, and results
- **Alternate design assumptions**
 - Effect of reducing wing taper
 - » More even distribution of side load on struts, weight reduction
 - Effect of relaxing G-load and tension stress cutoff requirements
 - » Potential weight reduction

Structures Objectives, Approach, and Methodology - Buoyant Lift

Objectives and Overall Approach – Buoyant Lift

The primary objectives of the buoyant lift vehicle structures effort on this program were to: 1) determine the feasibility of various designs driven by hydrostatic lift, and 2) to quantify the buoyant body and strut structural weights associated with each design in order to support the overall ship design optimization. More detailed objectives included quantifying structural weight trends and sensitivity to parameters such as all-up vehicle weight, number of bodies, number of struts per body, strut thickness and chord length, and fore/aft strut attachment location on the body.

To accomplish the primary objectives of generating conceptual/preliminary design level structural sizing of the body and strut weights of the various buoyant body configurations, a similar approach to the hydrofoil solution was taken employing a physics-based Excel spreadsheet methodology including optimization (Solver). The initial buoyant body concept focused primarily on minimizing structural weight, with three submerged bodies each supported by either one or two pairs of struts oriented in a “V” fashion for efficiently reacting both vertical and side loads. This configuration was proven to be unfeasible from a ship stability standpoint, and was subsequently eliminated. However, even though the original sizing results directly using the methodology discussed in the following pages were not considered useful, the basic methodology was still applicable with certain modifications made as needed to accommodate other configurations. The methodology discussions in the pages that follow are geared toward the original concept, but will include discussion of those required modifications. (This portion of the report is necessarily constructed in this manner to take advantage of existing figures and text from previous program briefings.)

The rapid evolution of buoyant body configurations coupled with the additional geometric complexity of the cavity body designs prevented the setting up of a physics-based solution beyond that capable of sizing the initial tear-drop shaped body of revolution. Only the capability to factor that calculated baseline body weight up or down was added to enable using results potentially obtained from other sizing methods. Therefore, the various structural weight trade study results that were generated necessarily used only the original buoyant body section, sized according to the total vehicle weight requirement, since time constraints did not permit the calculation and incorporation of subsequent body design sizings. The trends displayed in these results which were used in the vehicle performance assessments, however, should still be valid.

Structures Objectives, Approach, and Methodology - Buoyant Lift

- **Derive preliminary buoyant body and support strut sizings and weights for several designs and various geometry and loading parameters**
 - Develop spreadsheet with physics-based methodology
 - » Geometry, loading, and other parametric input
 - » Section properties
 - » Internal loads
 - » Analysis and optimized sizing
 - » Strut/body total and net weights
- **Provide structures input to develop preferred configuration for buoyant body design**
- **Use finite element analysis to validate physics-based solutions (strut sizings only) and to size preferred body design**

Structures Approach and Methodology - Buoyant Lift

Sizing Assumptions and Methodology – Buoyant Lift

Several basic assumptions were made to size the initial configuration of buoyant bodies and support struts. These assumptions are shown below. Again, the primary consideration behind this initial design configuration was to minimize structural weight.

Structures Approach and Methodology - Buoyant Lift

Initial Strut Geometry Assumptions for Parametric Sizings

- Two pairs of struts per body (“V” configuration)
- Strut lines intersect at center axis of buoyant body
- Inboard and outboard struts have same orientation
- Struts have no taper

Structures Approach and Methodology - Buoyant Lift

Sizing Assumptions and Methodology – Buoyant Lift (Cont'd)

The various loading and geometry assumptions are listed below (initial trade study conditions in regular text, later trade study preferred conditions in italics). Initially, the vehicle weight used was 4000 tons for comparison to the hydrofoil design. The same vehicle design load conditions were also assumed.

The P11BA15 was the designation for the original body design geometry, which was used to generate all of the physics-based structural sizings for the body. While the initial configuration contained three bodies, the trade studies were performed primarily on both one or two-body (catamaran) configurations, and primarily one strut per body. A limited number of 4-strut-per-body sizings were performed on a single-body design; however, it appeared that at least the strut weights were coming out higher than those for the single-strut configuration. It may be that this could be offset by a reduced body weight due to having a better distribution of support points on the body, but since time constraints did not permit accurately quantifying this, it was decided to only generate the matrix of trade study results for the single strut configurations.

Structures Approach and Methodology - Buoyant Lift

Loading and Geometry Assumptions

- **AUW = 4000 tons (2000T – 60,000T)***
- **Design G-loadings**
 - Vertical (lift) force = 2.0G (Used for body and strut sizing)
 - Side force = 0.5G (Used for strut sizing only)
 - Aft force = 0.5G (Used for strut sizing only)
- **Buoyant body sizings**
 - P11BA15 body configuration (*FEM sizing of final body configuration only*)*
 - 3-body configuration (*1 & 2-body configurations preferred*)*
 - 4 struts per body (2 fore/aft attach locations) (*1 strut per body preferred*)*
 - Buoyancy loads proportional to incremental H₂O displacement volumes
 - Hydrodynamic pressure distribution provided by Aero
 - Bending, shear, normal pressure load analysis
 - Section properties based on skin t-bar only
 - Skin t-bar weights factored up to account for internal structure
 - Stainless steel -- 55 ksi tension/compression stress cutoff, 40.5 ksi shear cutoff
 - Min. skin thickness = 0.5 inch nominal

**** Pertains to those trade studies following the initial trade study***

Structures Approach and Methodology - Buoyant Lift

Sizing Assumptions and Methodology – Buoyant Lift (Cont'd)

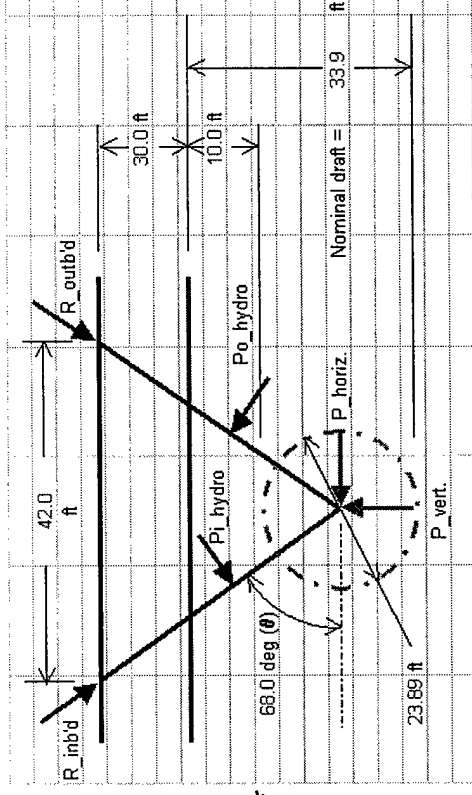
Additional assumptions pertaining to the strut sizings are shown below. The figure on the right shows graphically some of the original applied loading and geometry assumptions, with modifications for the preferred designs addressed in the text.

Structures Approach and Methodology - Buoyant Lift

Loading and Geometry Assumptions (Cont'd)

- **Strut sizings**
 - 4 struts per buoyant body (1 or 2)*
 - Strut lengths function of angle with horiz.
 - Two pairs of struts per body ("V") (vertical)*
 - Strut lines intersect at center axis of body
 - Inbd. & outbd struts have same orientation
 - Struts have no taper
 - Distance from ship hull to water surface = 30 ft. (12 ft. to match hydrofoil)*
 - Other dimensions/loading as shown (strut angle 90°, body depth variable)*
 - Side loads (0.5G) correspond to 2.5° side angle of attack
 - Strut section properties empirically derived
 - End connections are fixed
 - Analysis: Bending/compression + column buckling + shear
 - Skin t-bar + spar weights factored up to account for rib structure
 - Stainless steel -- 55 ksi tension/compression stress cutoff, 40.5 ksi shear cutoff

*** Pertains to those trade studies following the initial trade study**



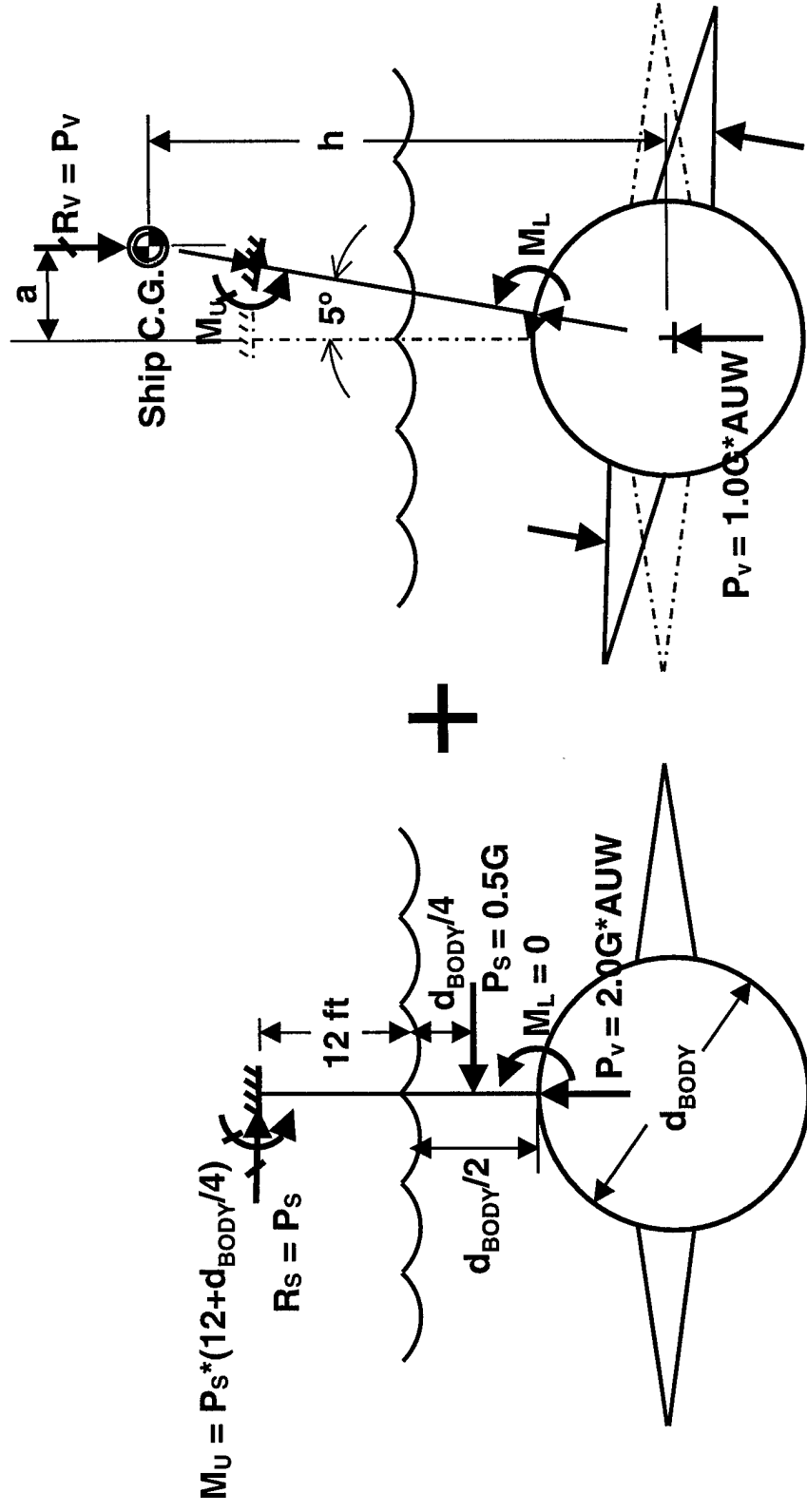
Structures Approach and Methodology - Buoyant Lift

Sizing Assumptions and Methodology – Buoyant Lift (Cont'd)

Some of the special methodology and unique loading assumptions directly related to the single strut, single body configuration are illustrated below. In particular, roll stability requirements peculiar to the single body design resulted in an additional bending moment that the strut needed to react.

Structures Approach and Methodology - Buoyant Lift

Single Strut and Body Internal Loads and Sizing Assumptions



Basic Design Loads on Strut

5° Righting Moment Loads on Strut

Structures Approach and Methodology - Buoyant Lift

Sizing Assumptions and Methodology – Buoyant Lift (Cont'd)

A summary of the methodology and sizing assumptions unique to the single strut, single body configuration are shown below.

Structures Approach and Methodology - Buoyant Lift

Single Strut and Body Internal Loads and Sizing Assumptions

Strut Sizing

- Axial/bending stress ($P_v/A_{TOTAL} + M \cdot c/I$)
- Shear stress ($P_s/[A_{SPAR WEB} + EFEC. SKIN/CAP]$)
- Column buckling stress ($\pi \cdot E / [(L/c^{0.5})/\rho]^2$, $c = 2.0$)
- Aft 0.5G loading check (long chord provides more than adequate bending and shear capability)
- Struts are not tapered
- Uniform skin thickness for entire strut
- Section properties empirically derived using curve fit formula generated from multiple hydrofoil strut sizings (reduced to a function of strut t/c , strut thickness, and skin thickness)
- Internal structure equal to 25% of skin weight

Body Sizing

- Carried over from past V-strut configuration body of revolution sizings that considered bending and shear resulting from forward and aft strut attachment locations
- No cavity body sizings performed (presumed similar to bodies of revolution – could be slightly higher)

Structures Approach and Methodology - Buoyant Lift

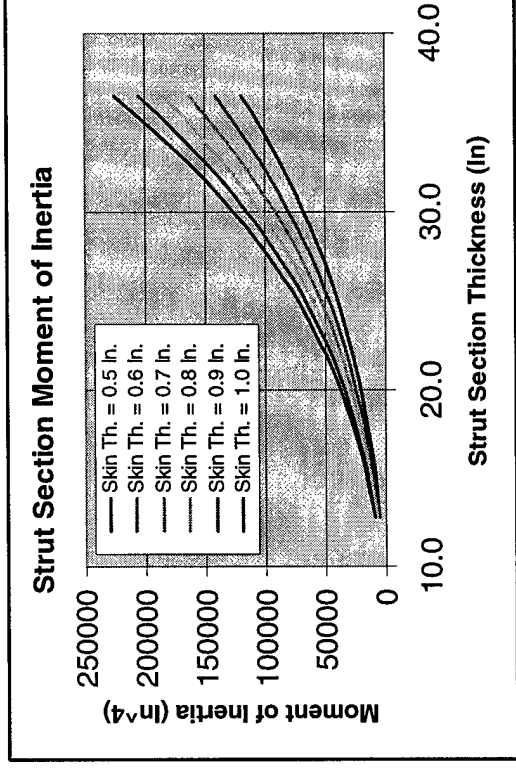
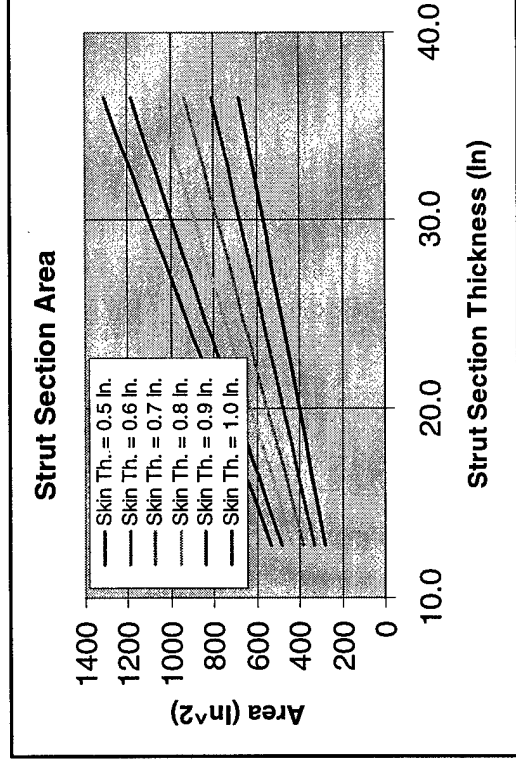
Sizing Assumptions and Methodology – Buoyant Lift (Cont'd)

The section properties for the strut were generated using empirical formulas derived from data obtained by making numerous runs of the hydrofoil strut parametric physics-based sizing method. The basic assumption made was that the strut section shape for the buoyant body designs would be similar to that of the hydrofoil struts. The three input variables required to generate the strut sizings were then strut thickness, strut t/c , and strut skin thickness. The parametric plots and associated curve-fit formulas are shown below.

Structures Approach and Methodology - Buoyant Lift

Strut Section Property Calculations

- Strut section properties were generated using empirical formulas derived from multiple runs of hydrofoil strut section properties



$$A = \left[(0.0519 * t_{skin}^3 - 0.1042 * t_{skin}^2 + 0.0527 * t_{skin} - 0.0088) * t_{strut}^2 + (32.422 * t_{skin} + 0.7517) * t_{strut} + (-20.893 * t_{skin}^2 + 130.23 * t_{skin} + 2.9396) \right] * (1 - (0.7 * (1 - t / C_{calc.} \div t / C_{actual})))$$

$$I_{N.A.} = \left[(4.3534 * t_{skin} - 0.0738) * t_{strut}^3 + (-0.0137 * t_{skin}^3 - 10.51 * t_{skin}^2 * 22.131 * t_{skin} + 0.0287) * t_{strut}^2 + (-12.704 * t_{skin}^3 + 170.34 * t_{skin}^2 - 3.019 * t_{skin} + 0.6489) * t_{strut} + (292.61 * t_{skin}^3 + 47.144 * t_{skin}^2 - 29.846 * t_{skin} + 6.287) \right] * (1 - (0.4 * (1 - t / C_{calc.} \div t / C_{actual})))$$

Structures Approach and Methodology - Buoyant Lift

Sizing Assumptions and Methodology – Buoyant Lift (Cont'd)

The list below contains the primary parameters included in the physics-based buoyant body and strut sizing efforts. Distinctions are noted for sizing parameters based on the original versus subsequently preferred design configurations.

Structures Approach and Methodology - Buoyant Lift

- **Automated Structural Sizings**
 - **Independent variables used by optimizer to derive minimum body weight and either minimum strut weight or thickness**
 - » Skin thicknesses (up to 4 for body, 1 for struts)
 - » Fore/aft location of struts (3-body configuration only)
 - » Strut angle with horizontal (V-strut configuration only)
 - » Strut thickness (fixed for 3-body configuration, variable for minimum weight runs)
 - » Strut t/c (for minimum thickness runs)
- **Constraints**
 - » Minimum skin thickness
 - » Fore/aft limits on strut locations (4-strut configurations only)
 - » Limits on strut angle with horizontal (V-strut configuration only)
 - » Maximum strut-chord-length-to-body-length ratio (95%)
 - » Max/min bending/axial and shear stress cutoffs (55.0 ksi axial, 40.5 ksi shear)
 - » Column buckling stress allowable
 - » Maximum % solidity (strut)
- **Independent variables held constant**
 - » Material properties/allowables
 - » Vertical, side, and aft G-load factors (2.0, 0.5, 0.5G)
 - » All-up weight (4000T – original, 2000T - 60,000T – subsequent)
 - » Body and strut section geometry
 - » Number of bodies (3 original, 1 or 2 subsequent)
 - » Number of struts per body (4 original, 1 subsequent)
 - » Height of ship above water
 - » Depth of body

Structures Approach and Methodology - Buoyant Lift

Sizing Assumptions and Methodology – Buoyant Lift (Cont'd)

Below are the dependent variables generated during the sizing optimization process.

Structures Approach and Methodology - Buoyant Lift

- **Automated Structural Sizings (Cont'd)**
 - **Dependent variables generated by optimizer**
 - » Length, maximum diameter, and weight of body (for fixed initial body shape)
 - » Chord, thickness, and weight of struts
 - » Strut angle with horizontal (original configuration only)
 - » Strut length
 - » Lateral distance between strut attach points on ship (original configuration only)
 - » Fore/aft location of strut attach points on body (4-strut configuration only)
 - » Body/strut volumes (water displacement)
 - » Max/min skin and spar web thicknesses
 - » Strut critical failure modes

Structures Trade Study Results - Buoyant Lift

Trade Study Results – Buoyant Lift

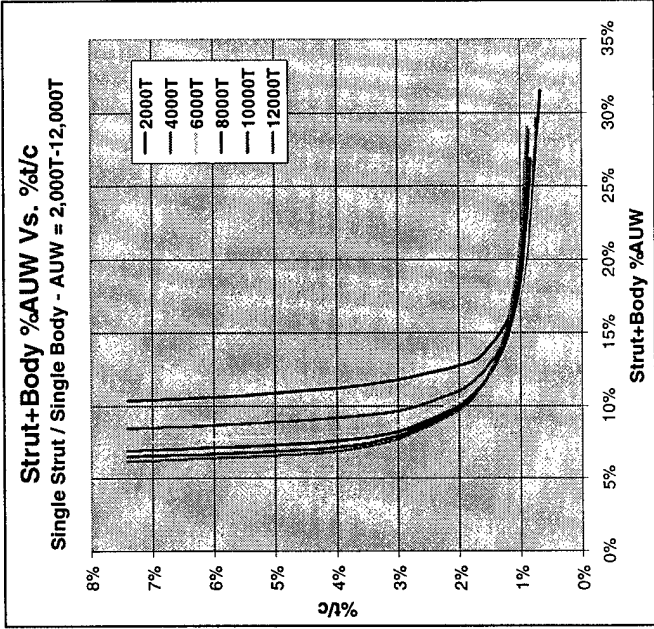
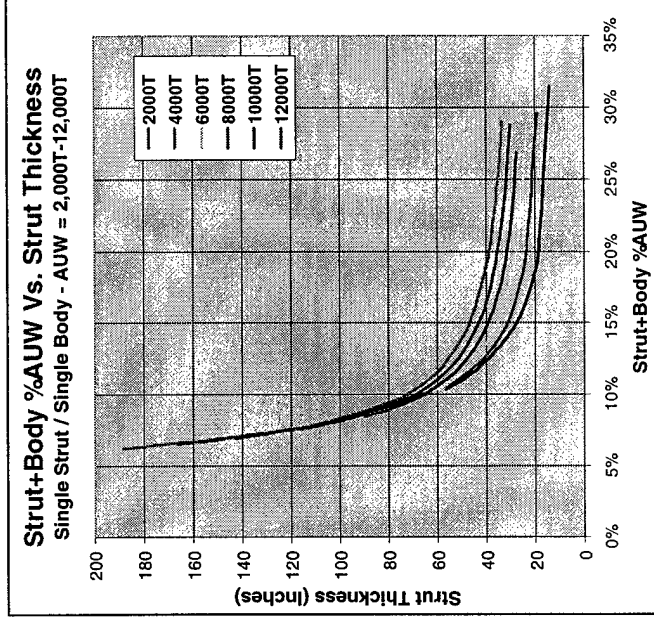
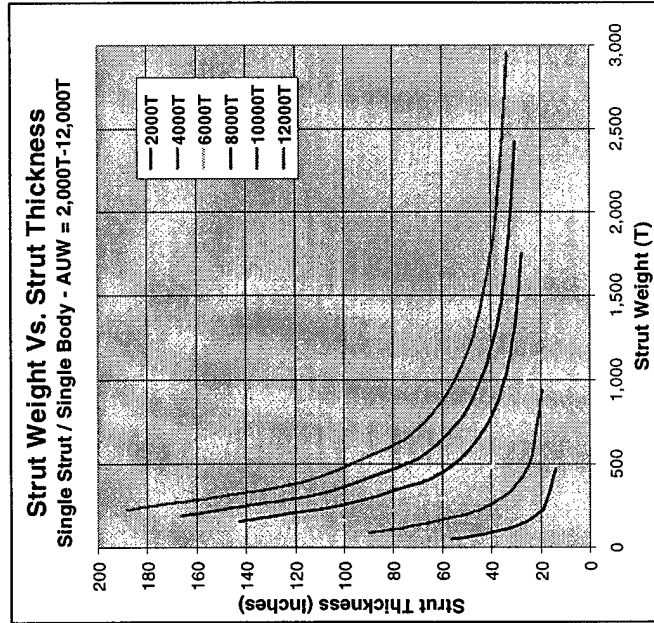
As mentioned previously, since the original V-strut configuration was deemed unfeasible due to hydrodynamic instability related issues, no sizing results are presented in this report.

One of the primary objectives of these trades studies was to determine the strut and body weight as a function of strut thickness. Since strut thickness is a critical factor related to hydrodynamic drag, it was necessary to quantify the tradeoff between the lower drag of the heavier thinner struts with the higher drag of the lighter thicker struts. These results were fed directly into the vehicle performance assessment.

There are two sets of structural weight trade study results. The first set is for the single body, single strut configuration, and is shown below. The range of vehicle weights examined in these trades was 2000 to 12,000 tons.

Structures Trade Study Results - Buoyant Lift

Strut Thickness Effects Single Body / Single Strut



Results used in quantifying strut weight versus spray drag tradeoff

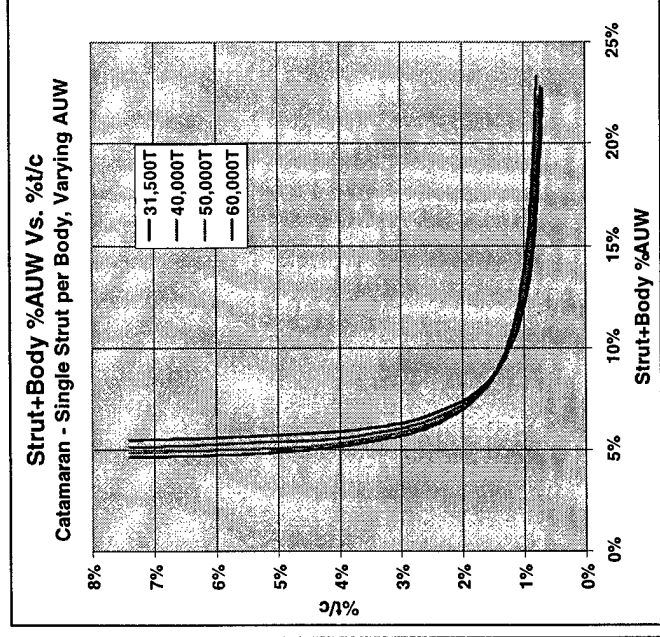
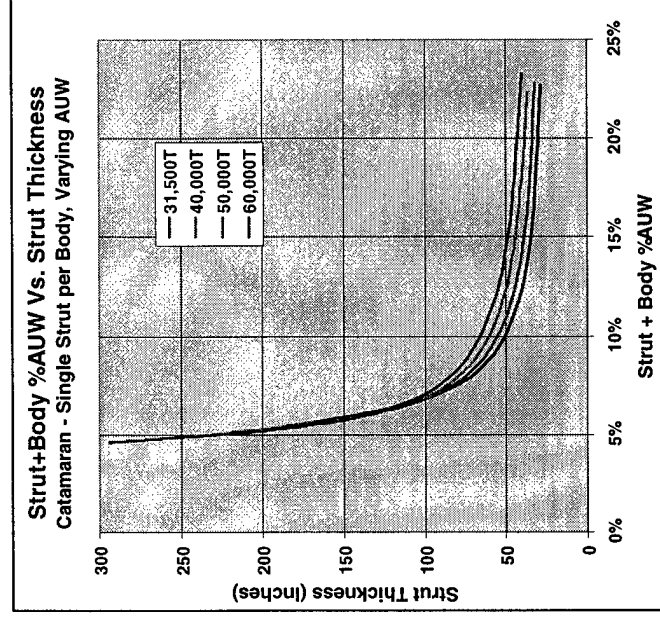
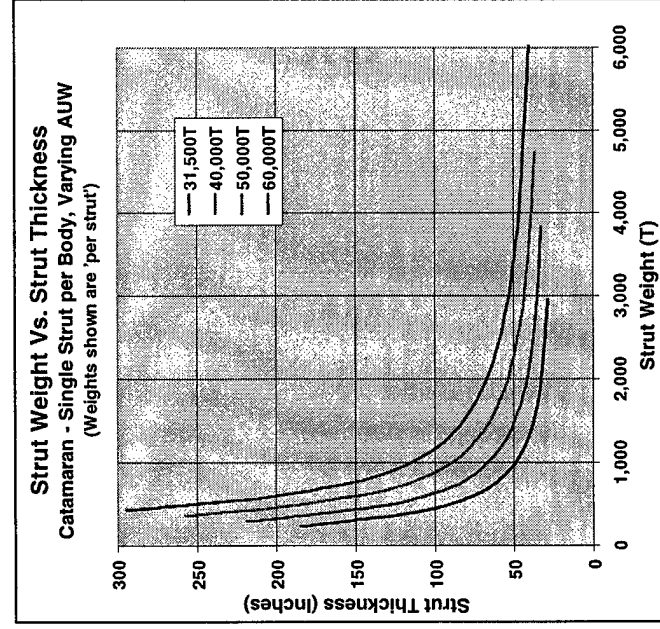
Structures Trade Study Results - Buoyant Lift

Trade Study Results – Buoyant Lift (Cont'd)

The second set of structural weight trade study results is for the two-body (catamaran) configuration with one strut per body. Since this configuration carried the advantage of reduced draft for the same displacement, larger sized vessels could be considered without exceeding the channel draft constraints. The range of vehicle weights examined in these trades was 31,500 to 60,000 tons.

Structures Trade Study Results - Buoyant Lift

Strut Thickness Effects Catamaran – Single Strut per Body



Results used in quantifying strut weight versus spray drag tradeoff

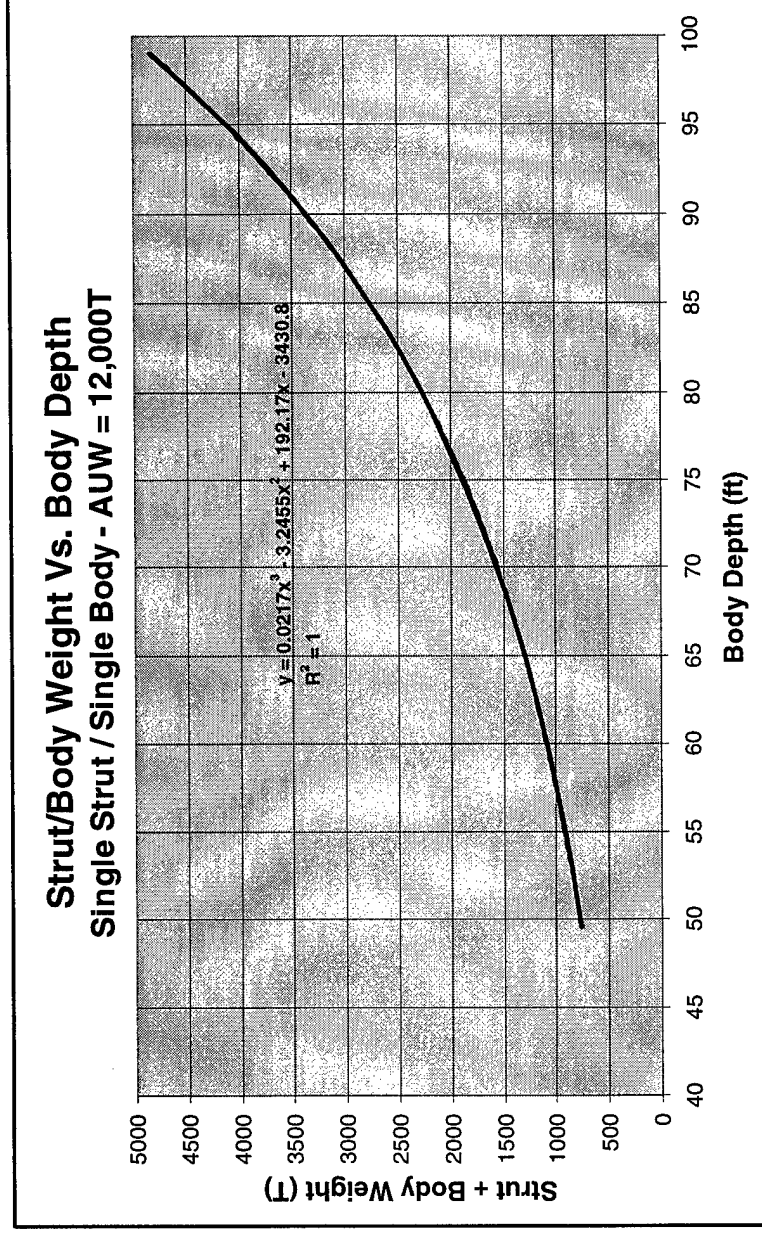
Structures Trade Study Results - Buoyant Lift

Trade Study Results – Buoyant Lift (Cont'd)

The other trade study needed was an assessment of the variation in strut and body weight with respect to body depth. The results of this study are shown below, and were used in the cavity body shape optimization process.

Structures Trade Study Results - Buoyant Lift

Body Depth Effects Single Body / Single Strut



Results used in cavity body shape optimization studies

Structures Refined Sizing – Buoyant Lift

Refined Sizing Using Finite Element Analysis

Finite Element Analysis was performed to estimate the cavity body and strut weight for the SWATCH 31,500-ton ship. The cavity body used was an optimum design derived for a catamaran configuration of this AUW. The cavity body had a length of 495.88 feet. The strut was 95% the length of the body and had a $t/c = 1.5\%$.

As mentioned previously, the rapid evolution of buoyant body configurations coupled with the additional geometric complexity of the cavity body designs prevented the setting up of a physics-based solution beyond that capable of sizing the initial tear-drop shaped body of revolution. Therefore, the body weight generated during this refined sizing assessment on the 31,500-ton vehicle is the only one that was made on a more advanced design. Also, the optimum body length and strut chord length turned out to be approximately 36% greater than that generated and analyzed using the physics-based method. Therefore, no direct comparison of actual strut weight could be made – only an assessment of the relative weight difference taking into consideration the known difference in the outer dimensions.

MSC PATRAN and NASTRAN were used for this analysis. PATRAN is a pre and post processor and NASTRAN is the finite element solver. Typical Steel material properties of $E = 30\text{msi}$ and $\rho = .283\text{ lbs/in}^3$ were used.

Finite Element Model of Body and Strut Geometry

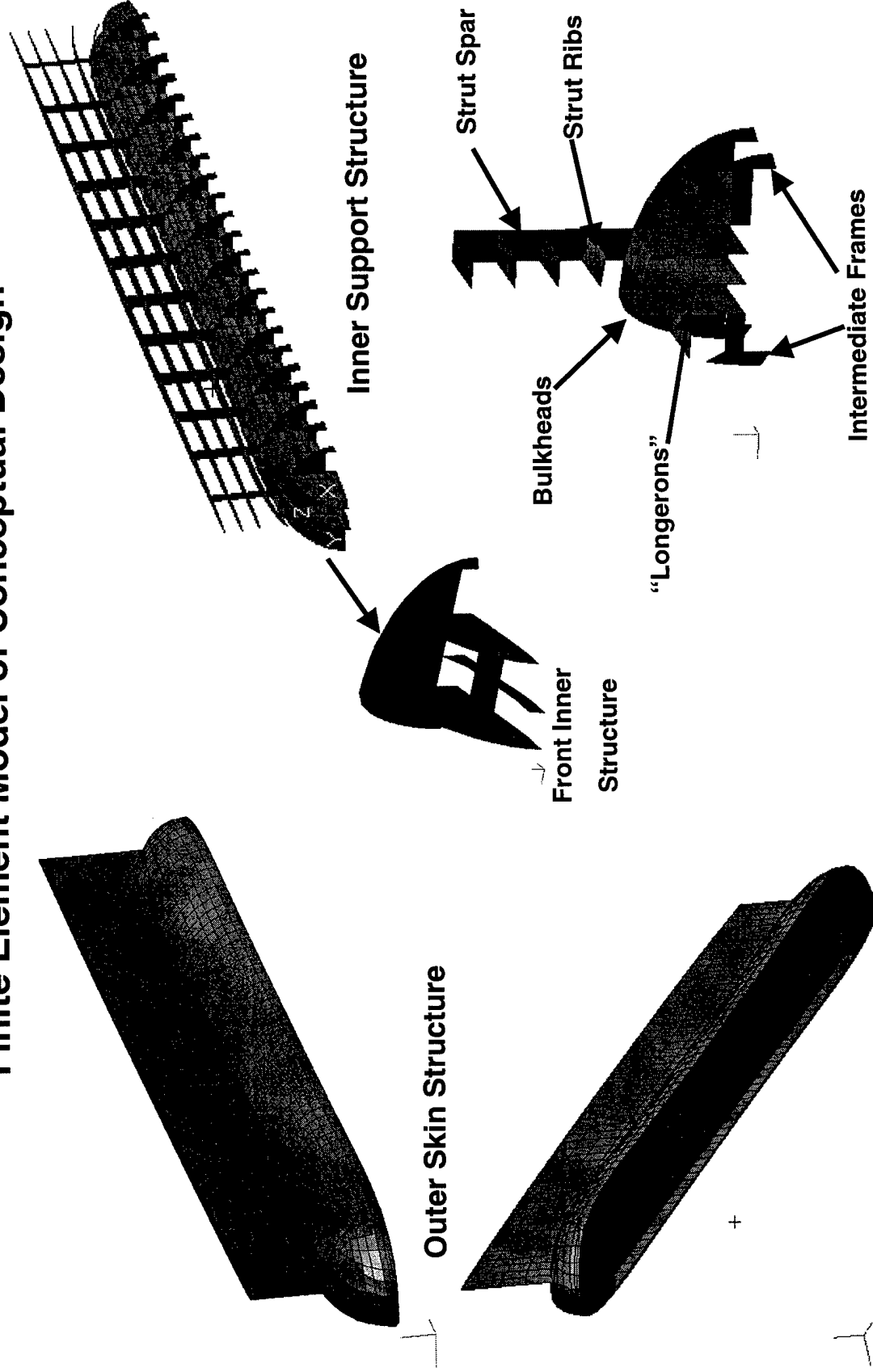
The figures below show the finite element model of the cavity body and strut geometry. The figures below left are views of the outer skin structure. The figures below right are views of the inner stiffening structure of the cavity body and struts. Shell elements were used for all skin and web structure. One directional Rod element with axial stiffness were used for all spar caps. The model consisted of 5718 elements and 3838 nodes (or grid points).

Boundary Conditions and Loads

The top of the strut was “fixed” simulating the restraint at the lower end of the retraction mechanism. The nodes at these locations were constrained from moving in any direction. A combined load of 1.0G hydrostatic vertical load (31.5e6 lbs on one cavity structure) and a 0.5G inertial side load (15.75e6 lbs) was investigated.

Structures Refined Sizing – Buoyant Lift

Finite Element Model of Conceptual Design



Structures Refined Sizing – Buoyant Lift

Applied Loads

The top figure below shows the 1.0 g hydrostatic pressure. This pressure was calculated as

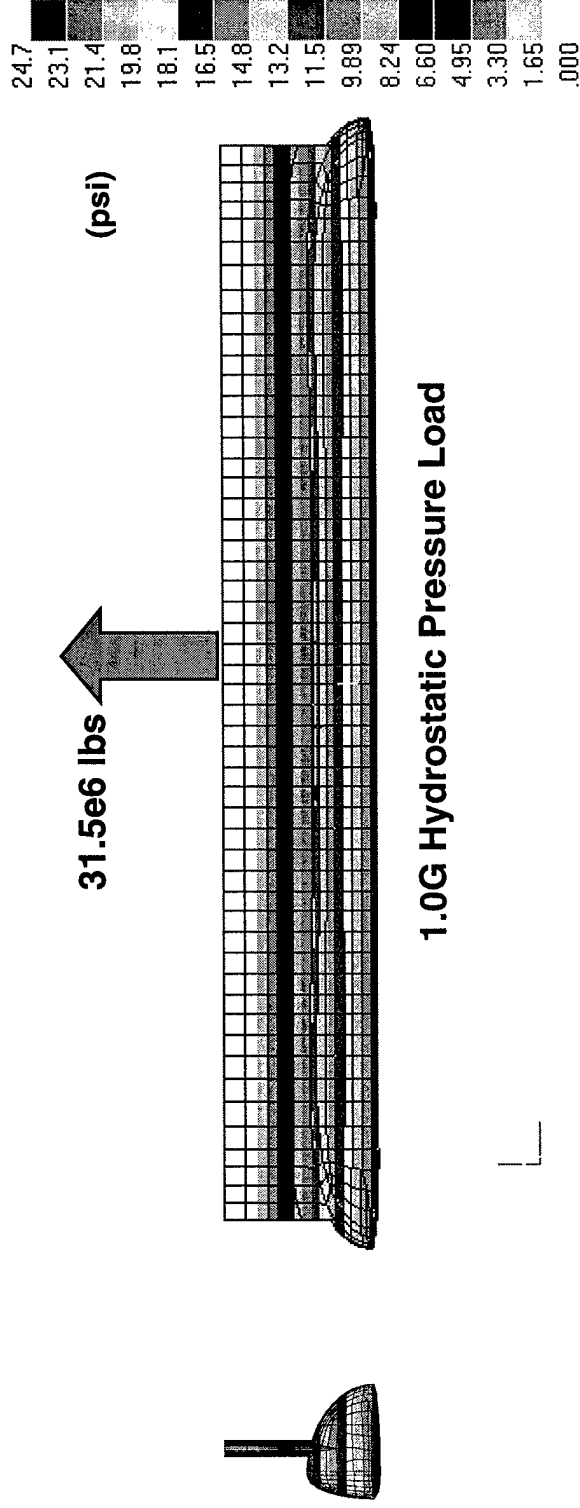
$$P = \rho * g * h$$

The total integrated load due to this pressure loading as applied to the structure below the water plane was 31.5e6 lbs vertical (buoyancy).

The bottom figure shows the 0.5 g side load. This load was applied using an RBE3 element in NASTRAN. The total force of 15.75e6 lbs is applied to one node. NASTRAN distributes this load over the chosen structure.

Structures Refined Sizing – Buoyant Lift

Applied Loads



1.0G Hydrostatic Pressure Load



0.5G Inertial Side Load

Structures Refined Sizing – Buoyant Lift

Analysis

A potential design was modeled and analyzed. Physics based analysis was not performed on this structure to the level of acquiring preliminary sizing of the structure. NASTRAN's optimization capability was used to size the structure. This application had a design objective of minimum weight. Twenty-nine groups of structure were setup as design variables. Thickness and area were allowed to fluctuate with appropriate lower and upper bounds assigned. The design constraints for this analysis were the allowable stresses. The maximum axial (1D elements) or normal (2D elements) stress allowable was 55 ksi and the maximum (in-plane) shear stress allowable was 40 ksi.

Initial runs were made with thickness (skins, webs, etc) set to 1.0 inch and area (caps, etc.) set to 20.0 in². These runs were made to perform model checkout and to see if there were any obvious deficiencies in the design. These runs indicated the need for further stiffening structure in the areas with flat skin surfaces due to large local displacements from the hydrostatic pressure. The intermediate frames and stiffeners on the bottom skin in the forward and aft sections were added. The figure below shows this additional structure.

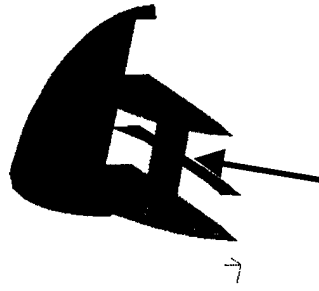
Optimization runs were made with the following bounds on the design variables:

- Thickness was allowed to vary from 0.25 inches to 1.5 inches.
- Area was allowed to vary from 10.0 in² to 30.0 in².

The lower bound of the design variables was used as the initial value. A converged solution that satisfied all of the constraints was found.

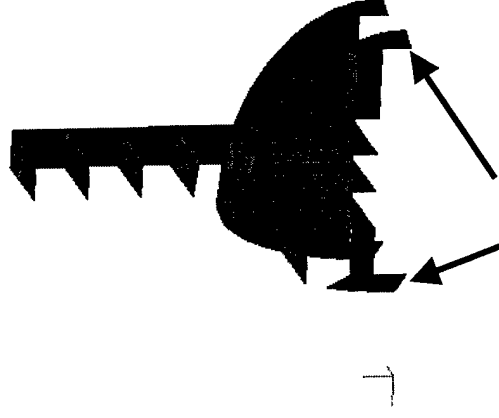
Structures Refined Sizing – Buoyant Lift

Results of Initial Analysis



Additional Stiffeners Added

Front Inner Structure



Intermediate Frames Added

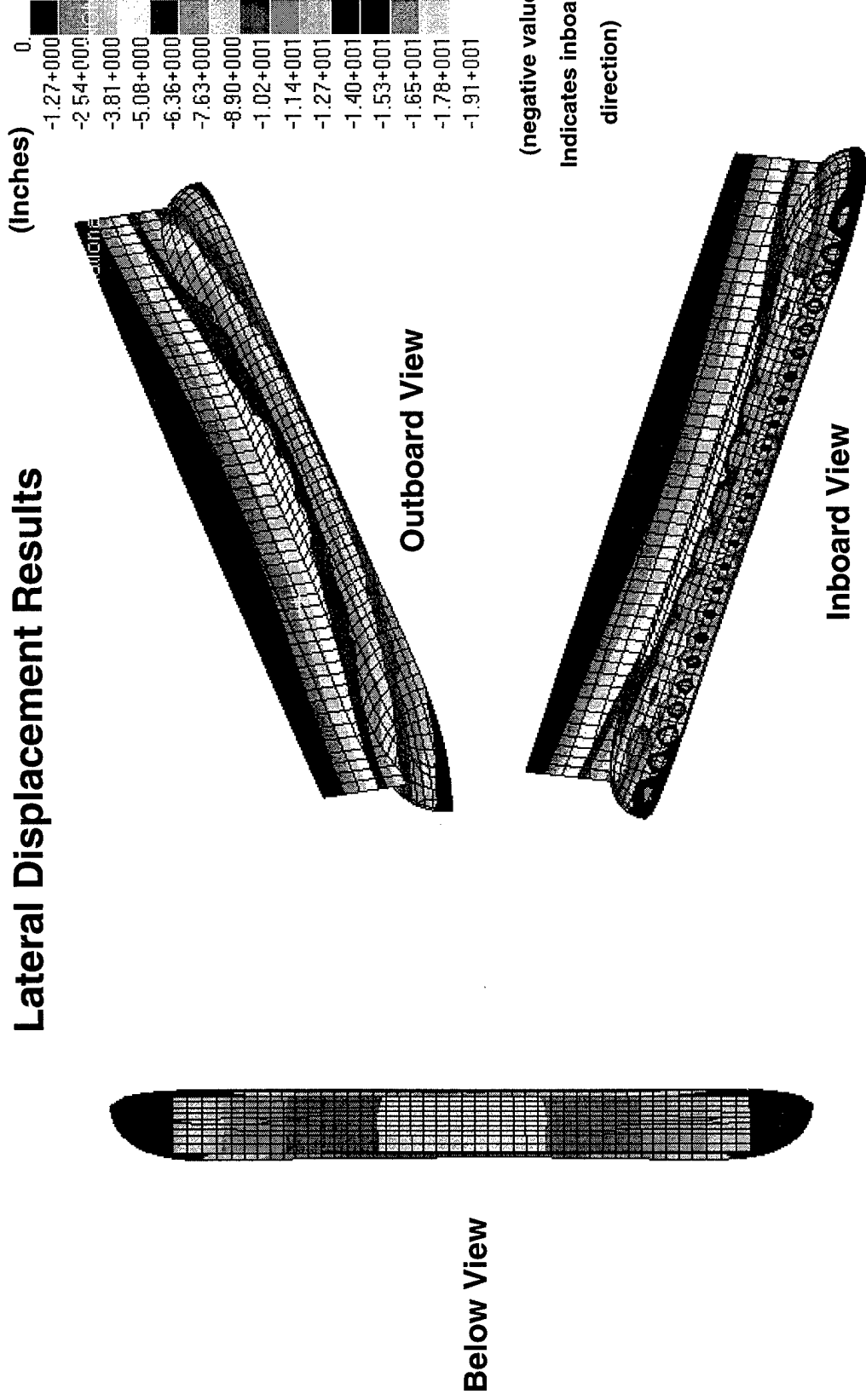
Structures Refined Sizing – Buoyant Lift

Displacement Results

The figure below shows the lateral displacement results. Some “pillowing” of the skin between internal supports was evident on the flatter inboard region of the cavity body.

Structures Refined Sizing – Buoyant Lift

Lateral Displacement Results

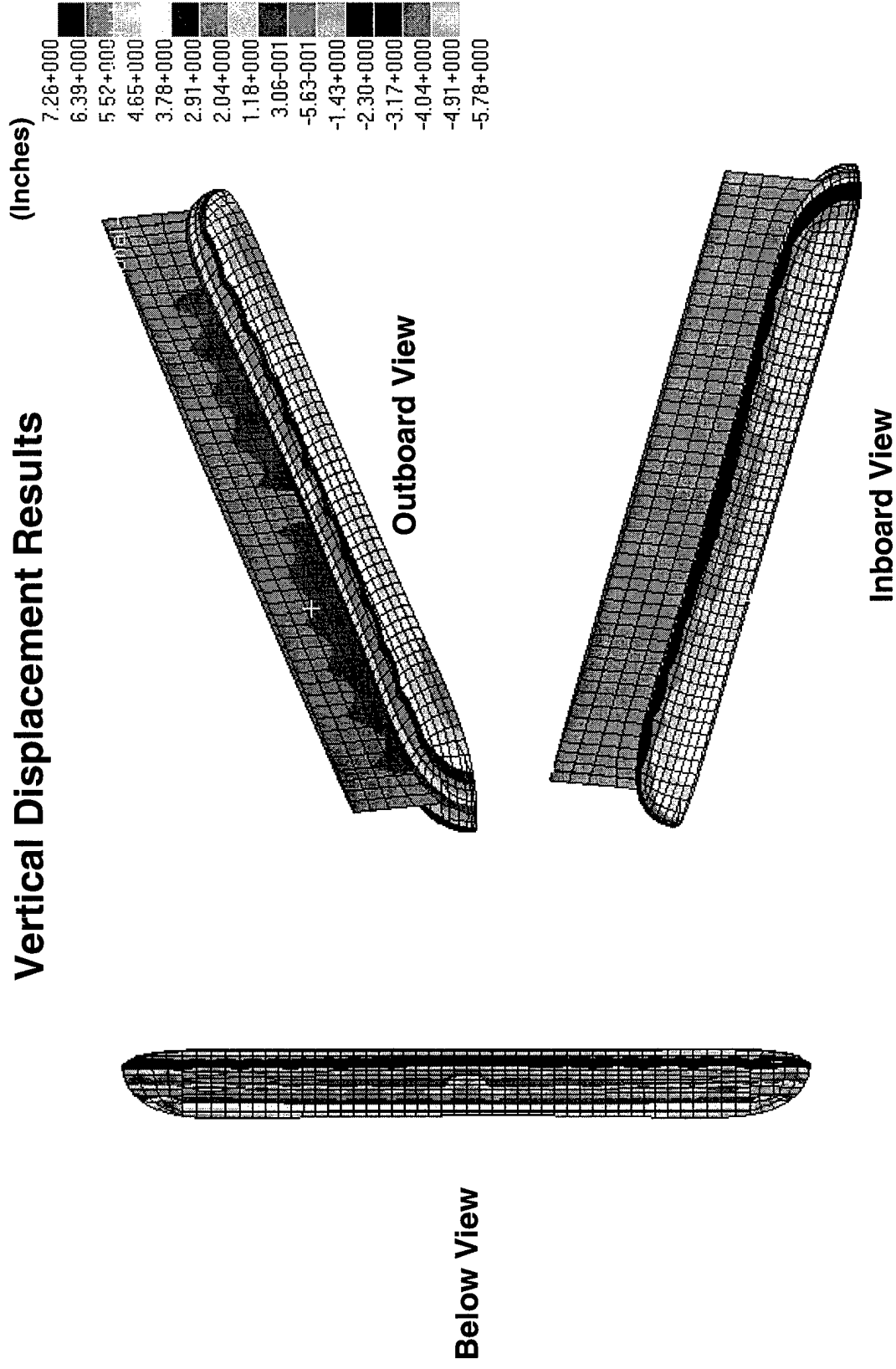


Structures Refined Sizing – Buoyant Lift

Displacement Results (Cont'd)

The figure below shows the vertical displacement results. The longitudinal displacements were very small and are not shown.

Structures Refined Sizing – Buoyant Lift



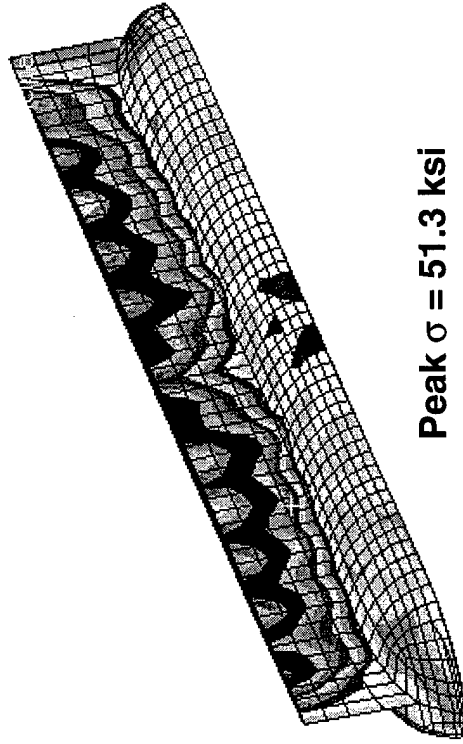
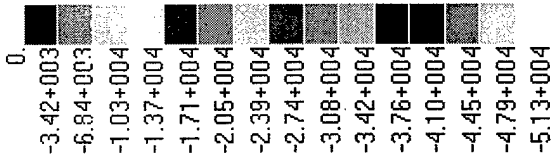
Structures Refined Sizing – Buoyant Lift

Stress Results

The figure below shows the peak stress results. The maximum stress in the skins was 51.3 ksi. This stress was located on the outboard strut skin. This area is highly loaded in compression due to the 0.5 g side load. The maximum stress found in the stiffening structure was on the bulkheads. This maximum value was 39.2 ksi. Both of these values are below the allowable of 55 ksi. The maximum shear stresses were acceptable.

Structures Refined Sizing – Buoyant Lift

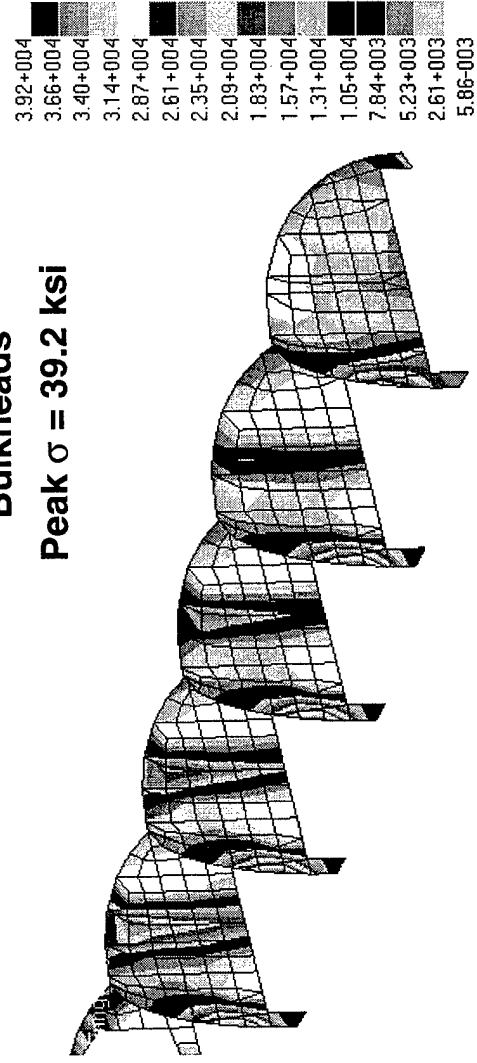
Stress Distribution Results



Skins

Bulkheads

Peak $\sigma = 39.2$ ksi



Structures Summary and Conclusions - Buoyant Lift

Summary and Conclusions – Buoyant Lift

In summary, various parametric structural sizing and optimization trade studies were performed using a physics-based methodology to examine the effect of various design perturbations on structural weight.

The weight of the structure (of one cavity body and strut) was 5.58e6 lbs. The weights broken down by component are as follows:

Strut Weight = 1.55e6 lbs

Cavity Body = 4.03e6 lbs

The strut weight for the same vehicle AUW and t/c generated by the physics-based method is 1.487e6 lbs. Considering the efficiency loss from the thinner strut (evident by a greater skin thickness than that generated by the FEM), this is considered to be as good a validation as possible of the physics-based methodology and trade study sizing results for the strut.

The body weight was relatively high compared to the baseline physics-based body weight (1.25e6), even considering the difference in length. Some of this difference can certainly be attributed to the highly structurally inefficient flat surfaces of the hydrodynamically optimized cavity body compared to the very structurally efficient body of revolution. However, additional optimization studies and different stiffening strategies (such as the use of truss structure) for the cavity body could result in a substantial reduced weight using the same FEM methods.

As with the hydrofoil, the determination of what may be more realistic design loadings, and also a practical minimum skin thickness constraint, should be considered a necessary steps to be taken before any effort is made to refine the body and strut structure sizing.

Structures Summary and Conclusions - Buoyant Lift

Summary and Conclusions

- **Structural weight trade studies performed**
 - Strut thickness effects
 - » Single body / single strut
 - » Two body (catamaran) / single strut per body
 - Body depth effects
- **Refined sizing performed using finite element analysis**
 - Physics-based strut sizing validated
 - FEM total strut and body weight = 5,580,000 lbs.
 - » FEM strut weight = 1,550,000 lbs.
 - » FEM cavity body weight = 4,030,000 lbs.
 - Working conceptual design with no negative margins
 - Further optimization / re-design would lower weight

Propulsion

Propulsion

Propulsion system design constraints imposed at the onset of the study require the capability of the vehicle to operate at all speeds. Therefore, a propulsion system is required:

1. for operation at low speeds as a buoyant ship (configuration and power requirements),
2. to attain minimum flight speed (configuration and power requirements), for take-off, and,
3. for cruise and dash speed capabilities as a hydrofoil (configuration and power requirements).

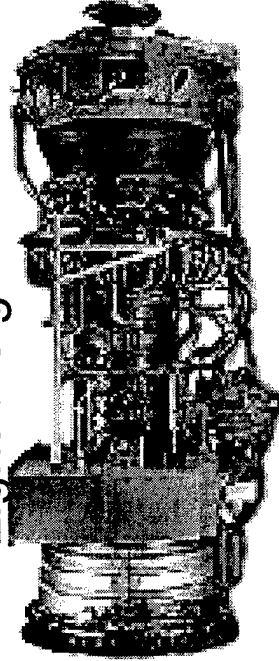
During the optimization process, the suitability of a variety of propulsion systems was considered. The key propulsion system development challenges to a large high-speed hydrofoil ship include:

1. minimizing the power needed to complete or satisfy the mission requirements,
2. reducing the adverse installation effects so as to keep the impact of weight, volume, and/or cost to a minimum, and,
3. maximizing the integration efficiency and hence the overall effectiveness of the system which in the end reduces the cost of the operation.

The objective during the effort was to identify key aero/hydro propulsion technologies and integration combinations using a trade study approach. For the purpose of simplification, the propulsion system was broken down into three identifiable subsystems, namely: power sources (power plant), propulsor and power distribution. Each subsystem was populated with a wide range of candidate propulsion system components that were traded in the study. The benefits and challenges that were identified with the implementation of each are listed in the following three slides

Initial Survey Results : Propulsion

- Candidate Propulsion Power Source Options
- Requirements :
 - High Efficiency
 - Light Weight



LM Preferred Option

<u>Power Sources</u>	<u>Benefits</u>	<u>Challenges</u>
Nuclear Electric	Well Known/Efficient Fuel Fraction Constant Clean/Low Emissions	High OWE Impact Political/Safety Refueling Downtime
Nuclear MHD	Distributed Power Low Emissions	Materials/Cryogenics Cavitation Impact
Diesel - Direct	Low Cost High Efficiency Reliable	High OWE Impact Speed/Emissions Large Envelope
Diesel- Electric	As Diesel-Direct but with Remote Prop.	Efficient Elec. Generation Lightweight Materials
Gas Turbine - Direct	Lightweight Generator Moderate-to-High Eff. Compact Envelope Multi-Fuel Capable	Environment/Safety Gearbox Weight/Size Efficiency-Part Power Thermal Emissions
Gas Turbine- Electric	As Gas Turbine Direct but w/ Remote Prop.	Generator Size/Efficiency Power Distribution Efficiency
Rankine/Stirling/Other	Thermo Efficiency Low Cost/Multi-Fuel	Envelope/Weight/Cost Emissions/Energy Density

Initial Survey Results: Propulsion (cont'd)

- Candidates :
 - Strut Mounted Water Jets
 - » pro: highest efficiency
 - » con: power distribution
 - Hull Mounted Air Propellers
 - » pro : simplest integration
 - » con: moderate efficiency

Candidate Propulsion System Propulsor Options

<u>Propulsors</u>	<u>Benefits</u>	<u>Challenges</u>
MHD	Low Emissions Minimum Interference Efficient Momentum Trans.	Energy Density vs. Length Materials and Cryogenics Efficient Integration
Propellers -Water sub/semi/super cavitating	Low Cost/Well Known Integration Potential Efficiency	Cavitation /Vibration/Erosion Structural Interaction Impact Draft/Fouling/Emissions Housing/Shaft Drag
Water Jets	Integration Flexibility High Efficiency/Low Noise Shallow Draft Potential	Internal Cavitation /Drag Fouling/Corrosion Low Thrust Directional Control
Air Jets/ Propellers Ducted Fans Constant/Variable Pitch	Ease of Integration Does Not Impact Draft No Marine Fouling	Bridge/Vessel Height Efficient Large Designs Lightweight Transmissions Noise/Thermal Emissions Safety/Corrosion/Spray

LM Candidate Solutions

Initial Survey Results: Propulsion (cont'd)

Candidate Propulsor Integration Options

<u>Integration/Layout</u>	<u>Benefits</u>	<u>Challenges</u>
Hull Integration - Water Driven	Minimum Power Transmission Dist. Maintainability Ease	Sea State/Speed/ Lift Inflow Quality/Efficiency
Strut/Tower Integration	Clean Entry Flow Tuned Speed/Height Draft	Power Transmission Dist. Drag/Lift Interference Prop/Strut Interaction Impact Fouling
Foil Integration	Minimum Induced Drag Sea State Capability	As Strut/Tower and Minimum Space Req.
Deck Integration-Air Driven Fore/Aft -Swiveled/Fixed	RM&S Ease Control Authority No Fouling Minimum Power Trans. Distance	Port Loading/Unloading Bridge Height Noise/Safety/Spray Ingestion Efficiency of Integration

Elements of the Propulsion System

The final quantitative measures of merit used to select the propulsion system were:

1. the net thrust,
2. the thrust specific fuel consumption (*TSFC*), and,
3. the installed weight.

The most promising subsystem elements are the Brayton Cycle (gas turbine) power source combined with an air-coupled propulsors in a mechanically distributed system. The power distribution logistics of a retractable underwater propulsor has been judged to pose a prohibitive weight penalty. The efficiency losses inherent to a hull borne pump-jet system have been judged excessive. For the high fidelity analysis system weights, sizes, thrust output and efficiencies have been developed for several candidate propulsion systems.

Elements of the Propulsion System

- **Power Generation**
 - Brayton Cycle is Efficient
 - Volume and Mass Properties Much Better Than Others
 - Cost-of-Ownership is Defined
- **Power Distribution / Management**
 - Mechanically Coupled is Most Efficient
 - Electrically and/or Hydro-statically Coupled are Fallbacks
 - High Torque Reduction Gearboxes Push Technology
- **Propulsor Selection / Integration**
 - Air-Coupled Fans/Propellers/Rotors Offer Reduced Cost-of-Ownership
 - Water-Borne Propellers/Pumps are Fallbacks
 - Installation Efficiency/Impact Will Be Key Issues

Propulsion System TPM's and Sizing

- **Propulsion TPM's**

- Thrust Specific Fuel Consumption
 - » pound of fuel burned per pound of thrust generated per hour (lb/lb-hr)
- Fixed Weight Fraction (FWF) Impact
- Cost-of -Ownership (Will Be Important)

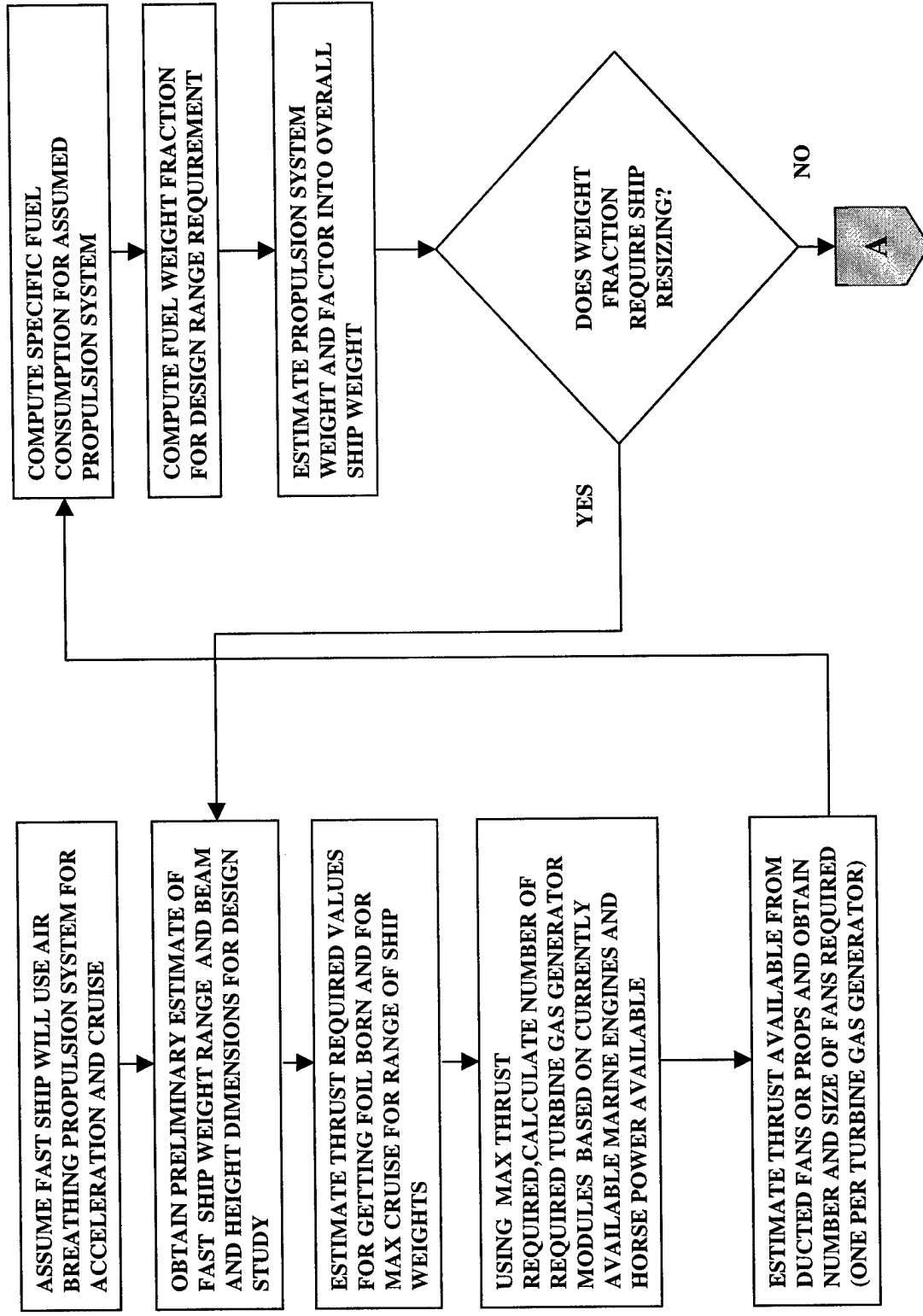
- **Propulsion System Sizing and Synthesis Process**

- Utilize Engine Company Data
- Process Defined in the Flowchart

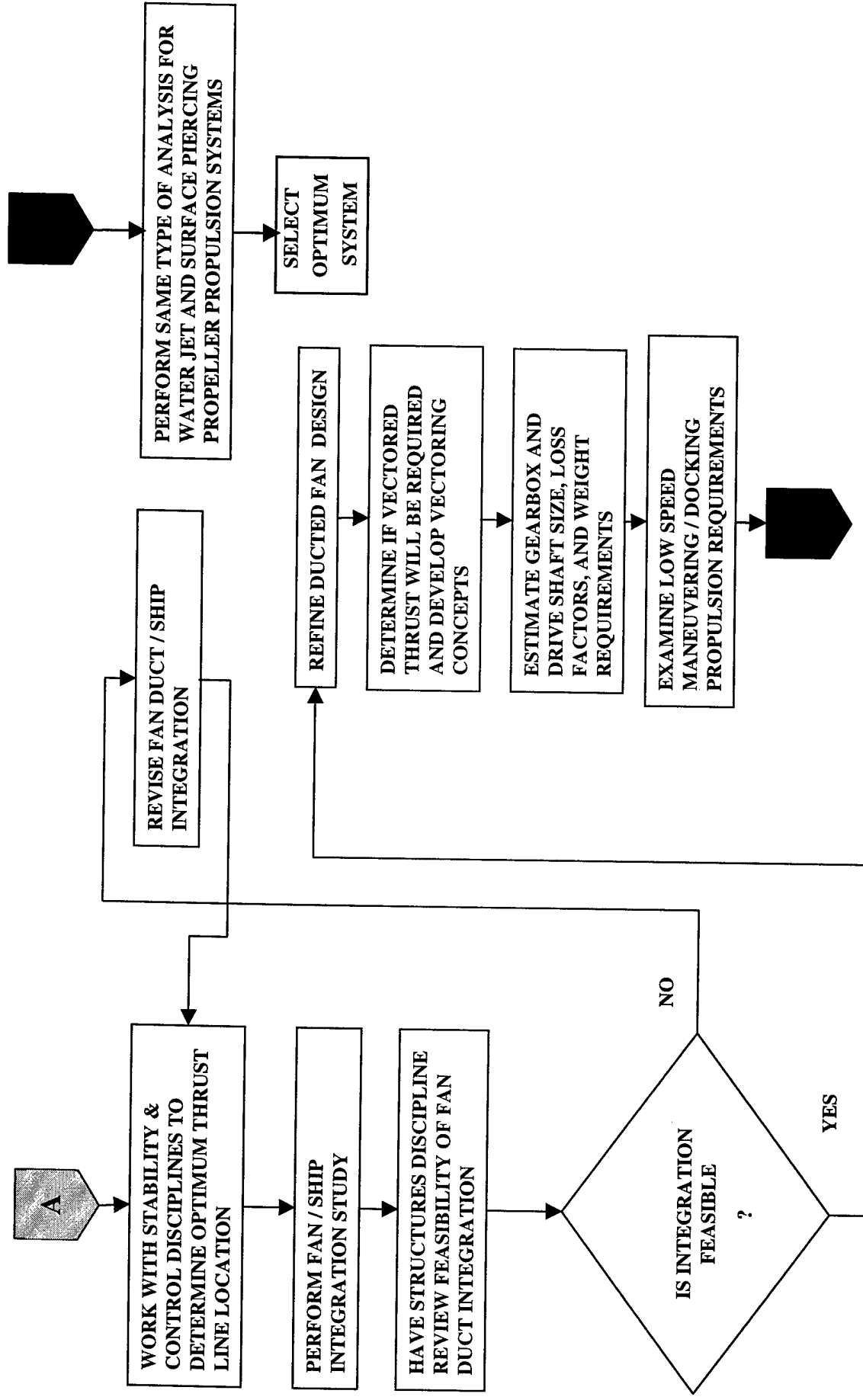
Propulsion System Sizing Process

The process used during the trade study invoked a variety of in-house tools and methods with were used to provide both qualitative and quantitative measures of merit. Initial constraints reduced the number of candidates in each of the three component categories. The flow chart that identifies the processes used in the propulsion system trade study is shown the following two slides

Propulsion System Sizing Process



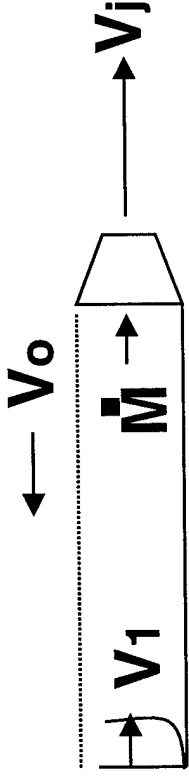
Propulsion System Sizing Process, cont.



Definition of Efficiencies-Propulsive

Propulsive efficiency can be calculated as is shown in the following slide. Note that no assumptions are made that limit the applicability and that the equations are left as being general. Furthermore, it should be understood that this is one part of the net efficiency of the complete propulsion system.

Definition of Efficiencies-Propulsive



$$\text{Propulsive Efficiency, } \eta_p = \frac{\text{Thrust Power}}{\text{Thrust Power} + \text{Power Loss}}$$

where Thrust Power = Force applied to Vessel times the distance moved per unit time, or

$$= F_{\text{net}} \cdot V_o$$

and Power Loss = Kinetic Energy of the Jet relative to the Vessel

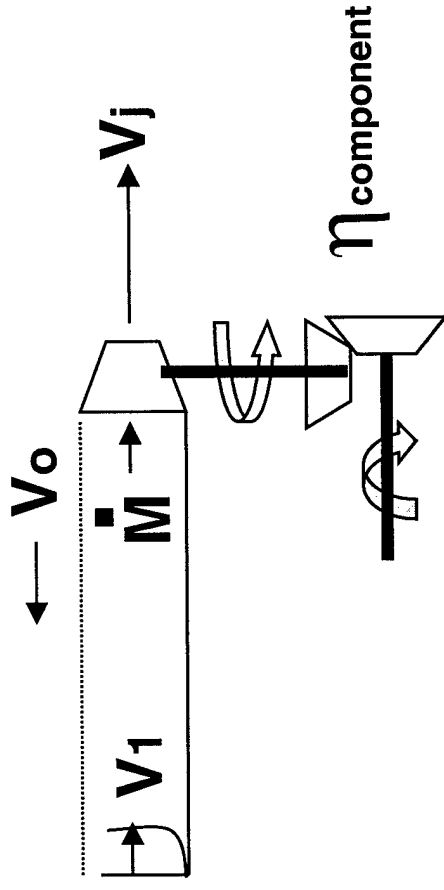
$$= \frac{1}{2} \dot{M} / g (V_j - V_o)^2,$$

so..... $F_{\text{net}} \cdot V_o = \dot{M} / g \cdot (V_j - V_1) \cdot V_o$, Therefore

$$\eta_p = \frac{1}{1 + \frac{1}{2} \frac{(V_j - V_o)^2}{V_o (V_j - V_1)}} \quad \text{if } V_1 = 0, \text{ then } \eta_p = \frac{2}{1 + V_j / V_o}$$

Definition of Efficiencies-Component & Net

Component Efficiency is used to define losses associated with a component in the propulsion system. It may include gearbox, drivetrain, and other losses in the system that may or may not be directly tied to the momentum efficiency (i.e. V_o , V_1 and V_j). In the case of propulsors, particular attention must be paid to the Control Volume and what is included in the thrust terms.



$$\eta_{\text{net}} = \eta_{\text{propulsive}} \times \eta_{\text{component}}$$

Disk Loading and Ideal Momentum Theory

The ideal efficiency of a propulsor is a function of its induced velocity, v . In other words, its efficiency is a function of the disk loading, T/A , the thrust, T , per propeller disk area, A

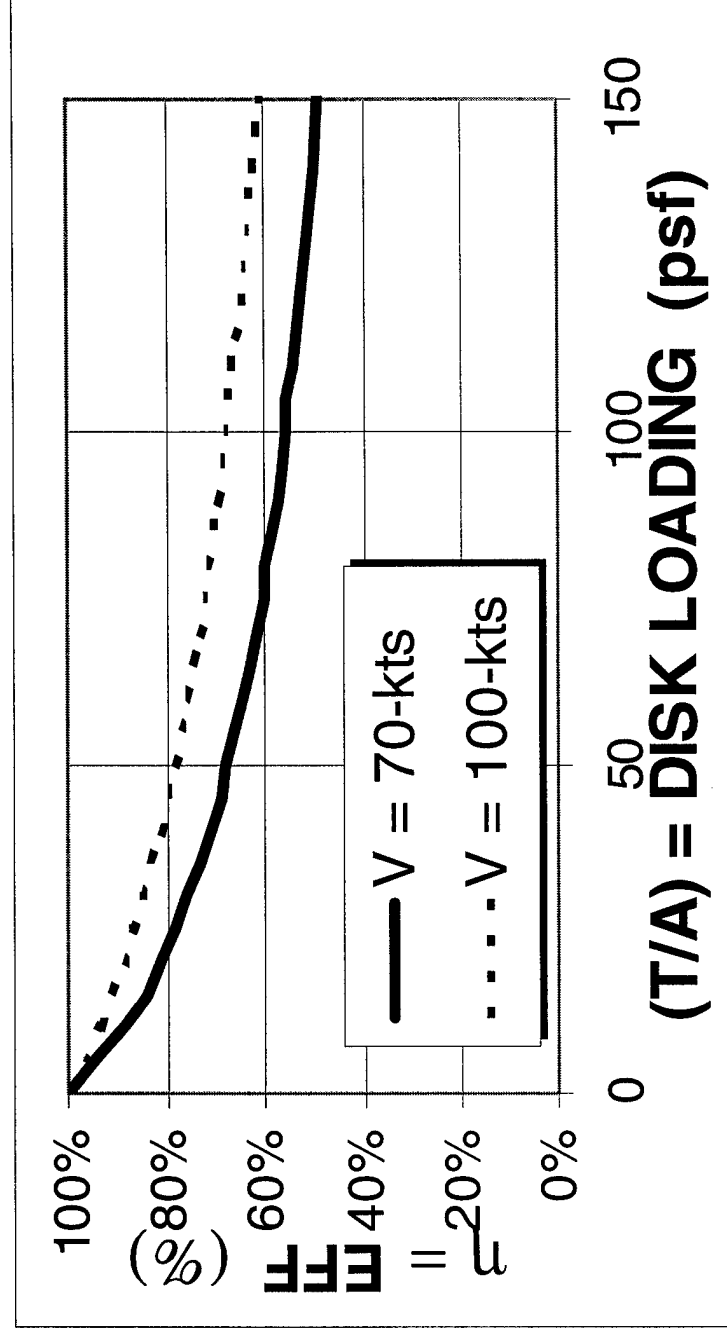
$$\eta = V / (V + v) = 2 / [1 + \sqrt{1 + (T / A) / q_{air}}]$$

, where $q_{air} = (1/2) \rho_{air} V^2$.

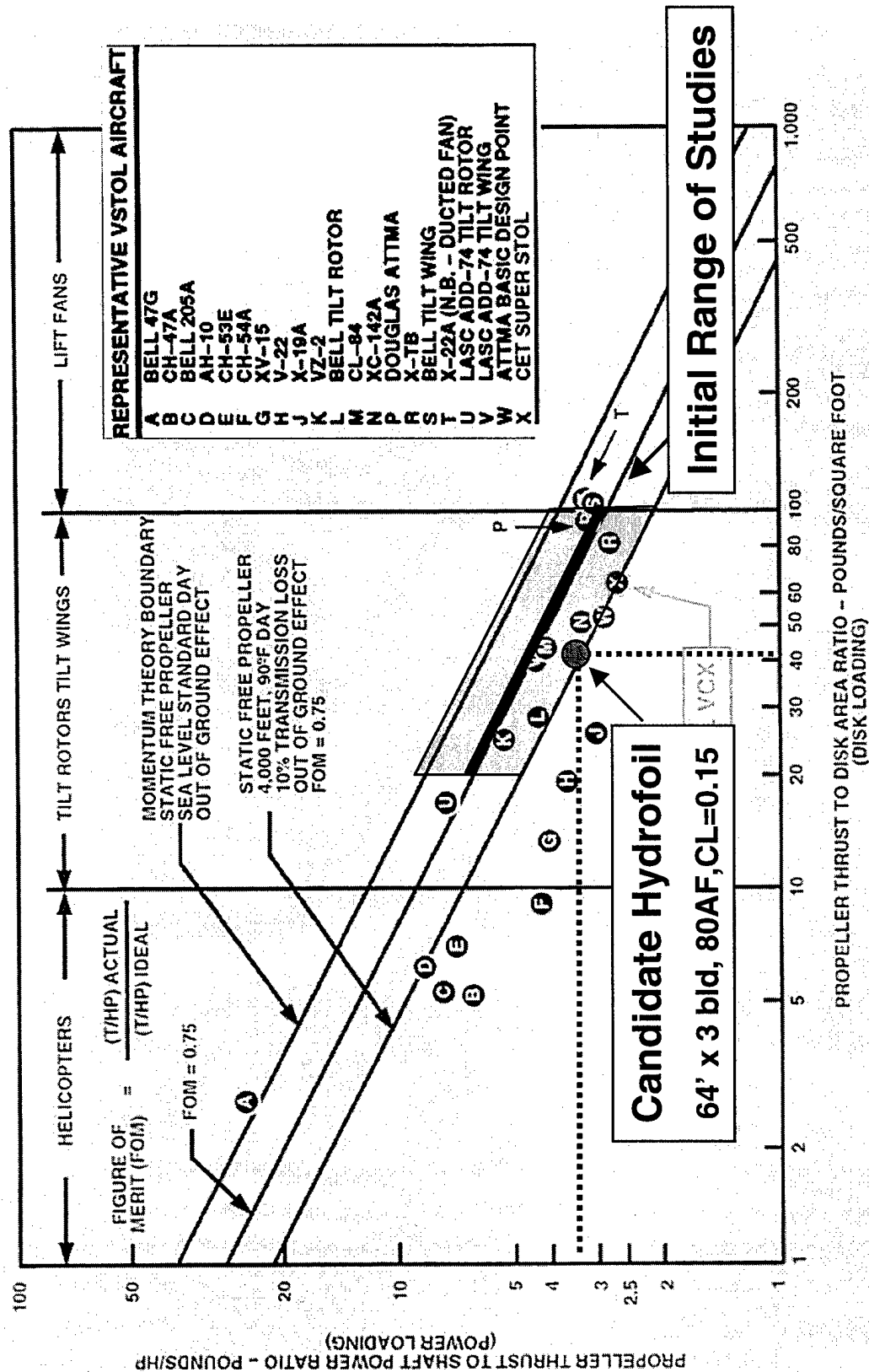
Contours of ideal momentum efficiency for an air coupled propeller as a function of cruise speed and disk loading are shown in following. A comparison of 70 and 100-kt cruise speeds demonstrates that air coupled propellers offer somewhat greater momentum efficiency with increasing design speed and that a momentum efficiency >70% requires a disk loading below ~50 lbf/ft². Also shown is a representation of the same momentum theory curve and how existing VTOL, STOL aircraft and the starting point for this study compares.

Disk Loading and Ideal Momentum Theory

Air Coupled Propulsive System Momentum Efficiency as a function of Disk Loading.



.....and provided the following starting point!



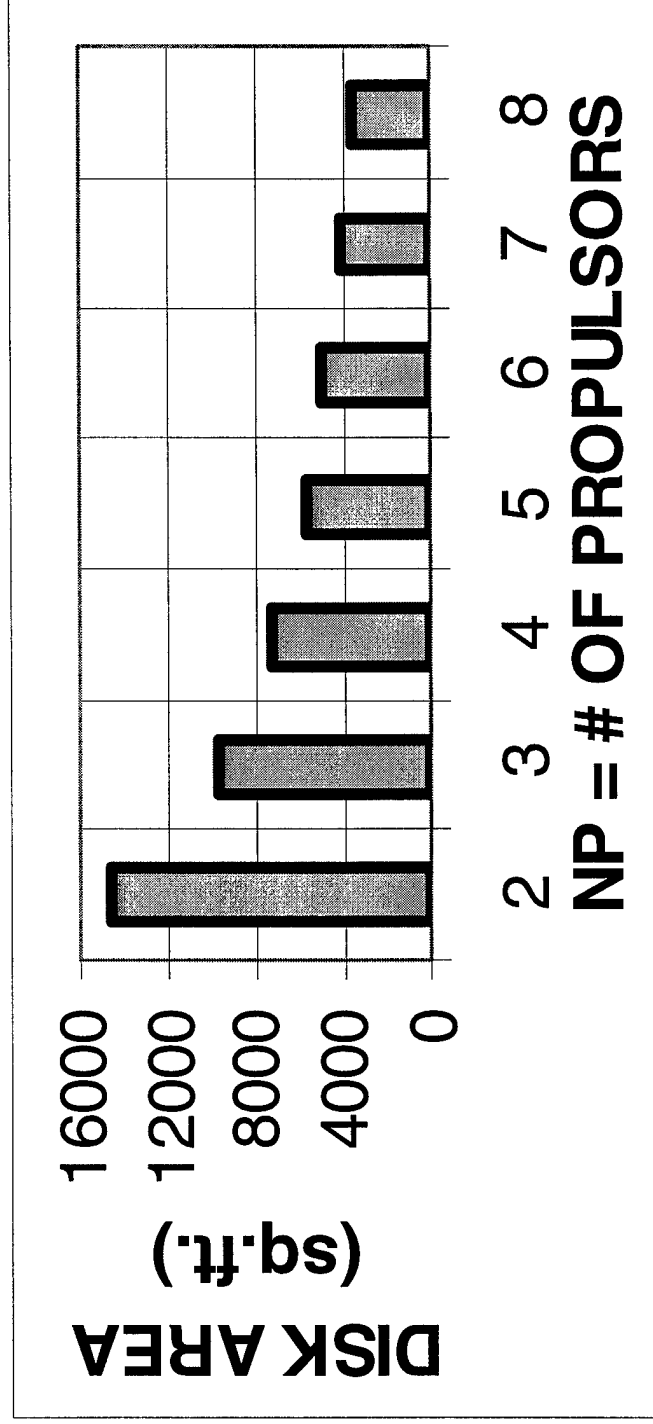
Disk Loading and the Beam Constraint

The Suez Canal transit requirement limits the width of the ship to be less than 65m (~213 ft). Thus it affects the permissible disk loading of an air coupled propulsion system. Design integration of a discrete number of propulsors, NP , (see Figure 6) leads to finite disk area availability for the propeller system (Figure 7). Similarly, these ideal equations may be used to estimate the thrust developed (Figure 8) and horsepower absorbed (Figure 9) for a discrete number of propulsors at a given cruise speed and cruise disk loading. From these idealized estimates of thrust and horsepower absorbed, noting that large gas turbine powerplants exhibit a brake specific fuel consumption, $BSFC$, of somewhat less than 0.4 lbm/hp-hr, the ideal thrust specific fuel consumption, $TSFC$, may be estimated as a function of disk loading (Figure 10).

Although the operational practicality of very large, very high thrust rotors is questionable, fewer and larger propellers enable greater propulsive thrust at lower disk loading than possible with smaller propellers. It appears that $TSFC$ s in the range of 0.12 to 0.16 lb-fuel/lb-thrust-hr are achievable with air coupled propellers. These may provide up to 1,000,000 pounds cruise thrust.

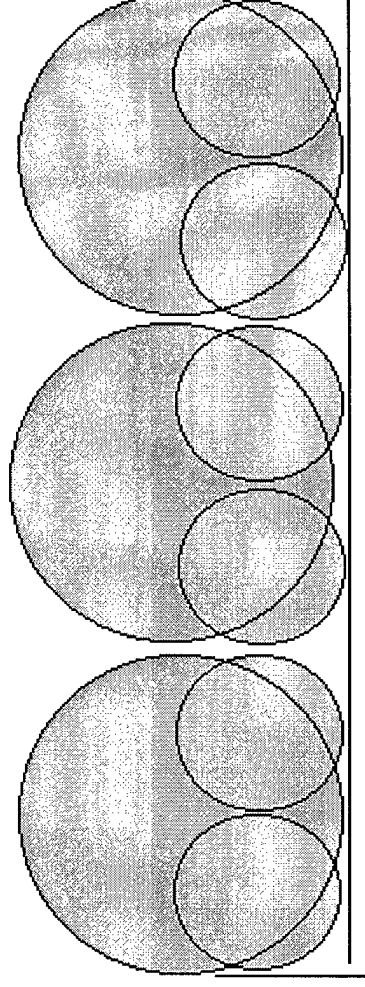
Disk Loading and the Beam Constraint

Axial Propeller System Disk Area, A , as a function of the Number of Propulsors, NP . 213-ft (65m) propulsion integration beam.



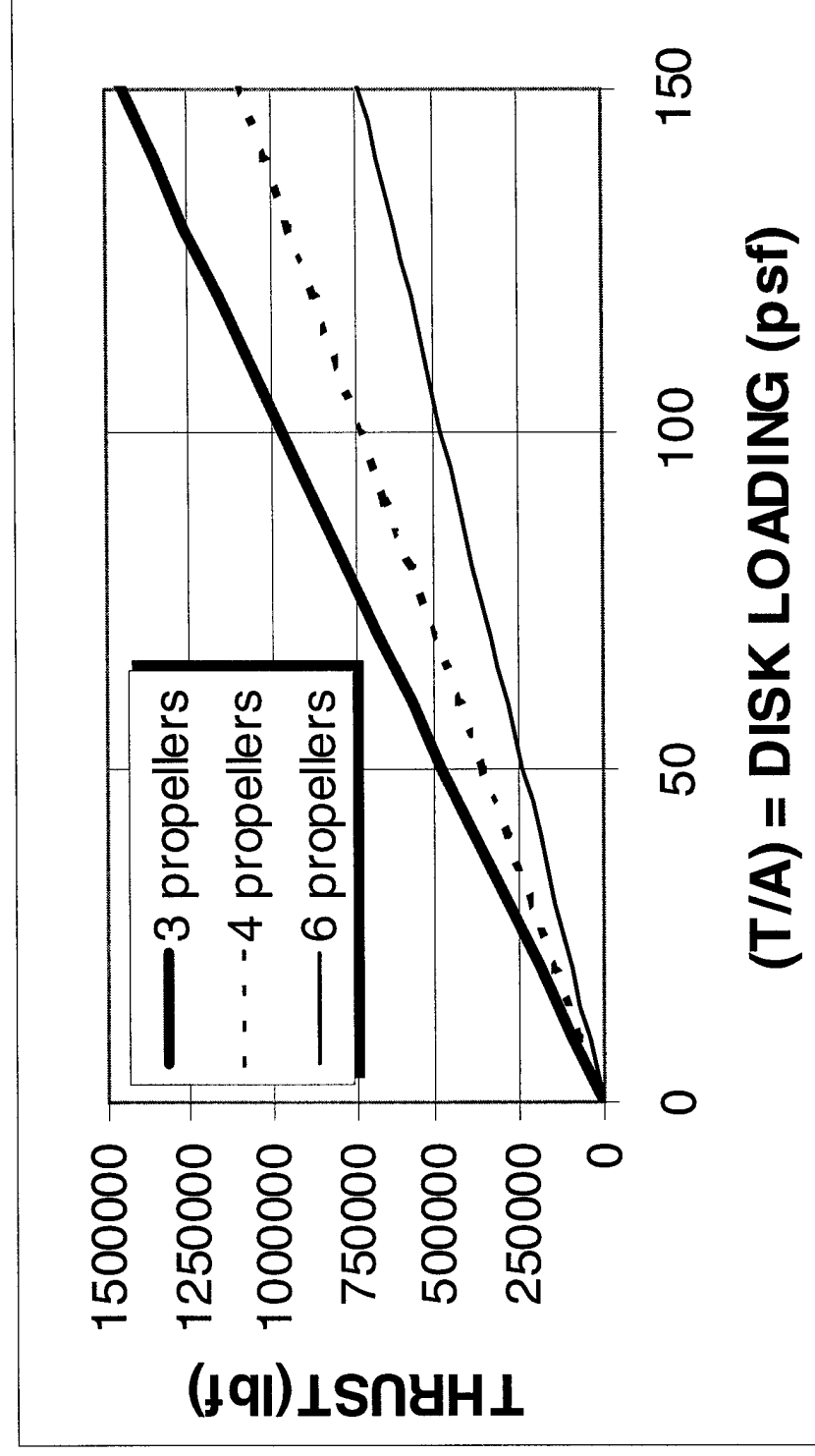
Disk Loading and the Beam Constraint

Air Coupled Propulsion System Integration Schematic. N.B. doubling the number of propulsors halves the propeller blade diameter and quarters the disk area.



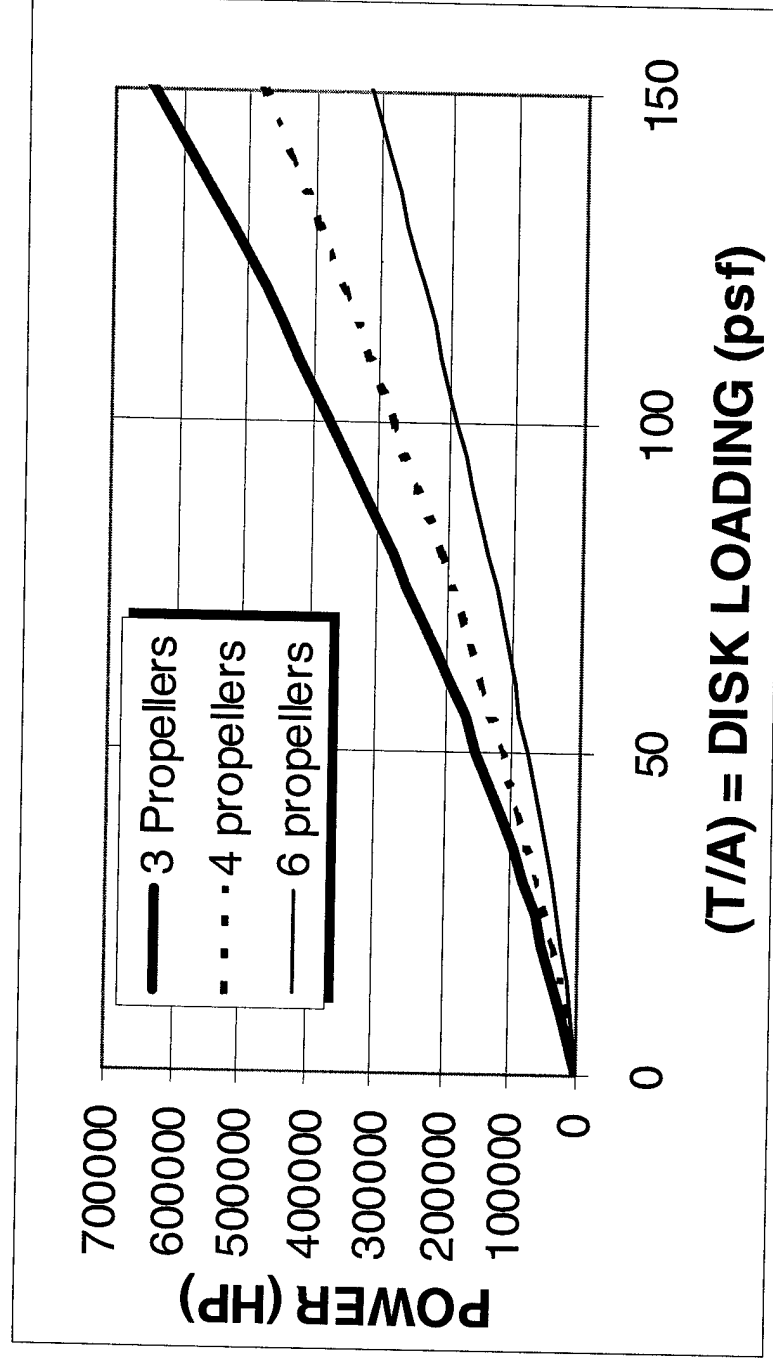
Disk Loading and the Beam Constraint

Idealized Thrust, T , Developed as a Function of Propeller Disk Loading,
(T/A) (Disk Loading computed @ 70-kts cruise speed; 213-ft (65m)
Propulsion Integration Beam)



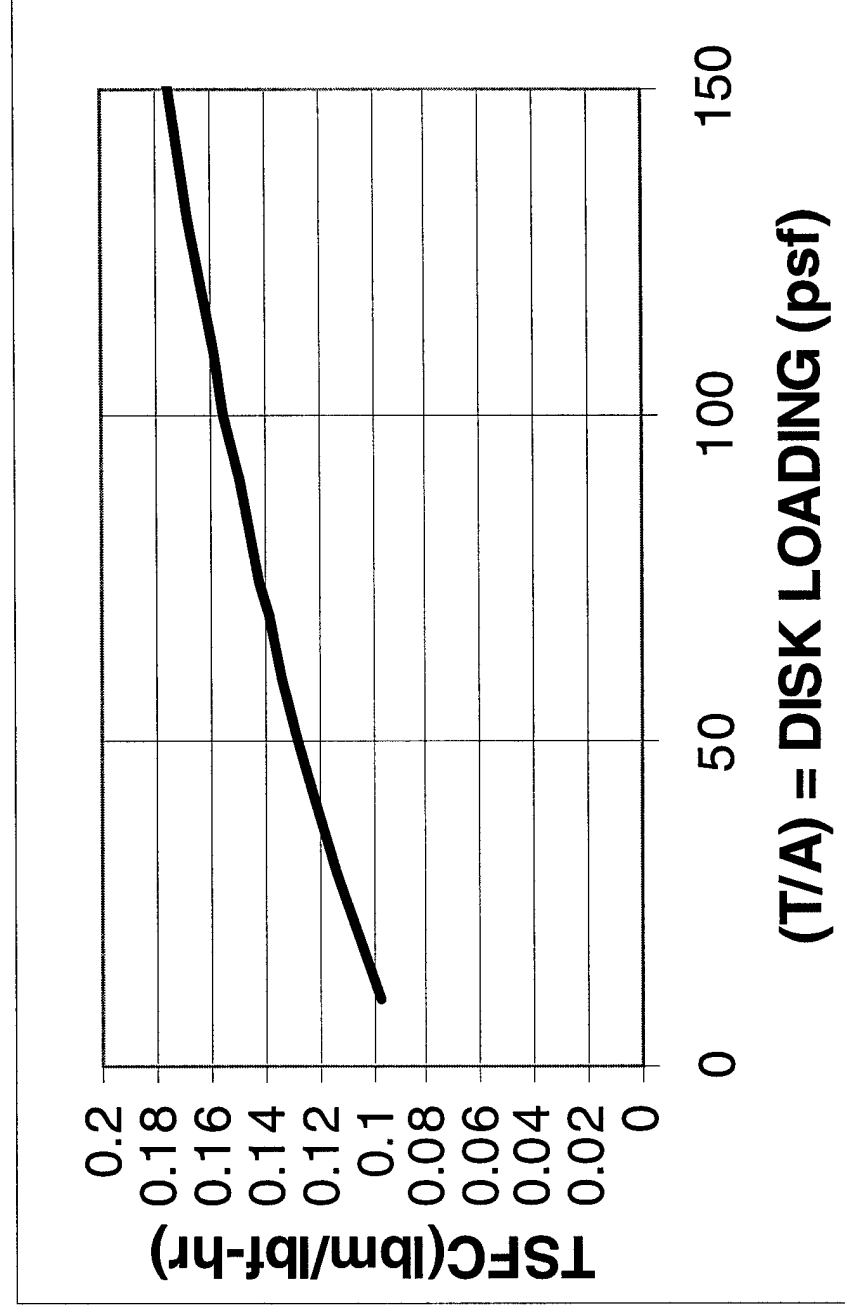
Disk Loading and the Beam Constraint

Idealized Horsepower Absorbed by Propeller System as a Function of Disk Loading, T/A . (Disk Loading computed @ 70-kt cruise speed; 213-ft (65m) Beam)



Disk Loading and the Beam Constraint

**Idealized TSFC as Function of Propeller Disk Loading, T/A .
Estimated Gas Generator Efficiency, $BSFC = 0.4$ -lbm-fuel / HP-hr.**

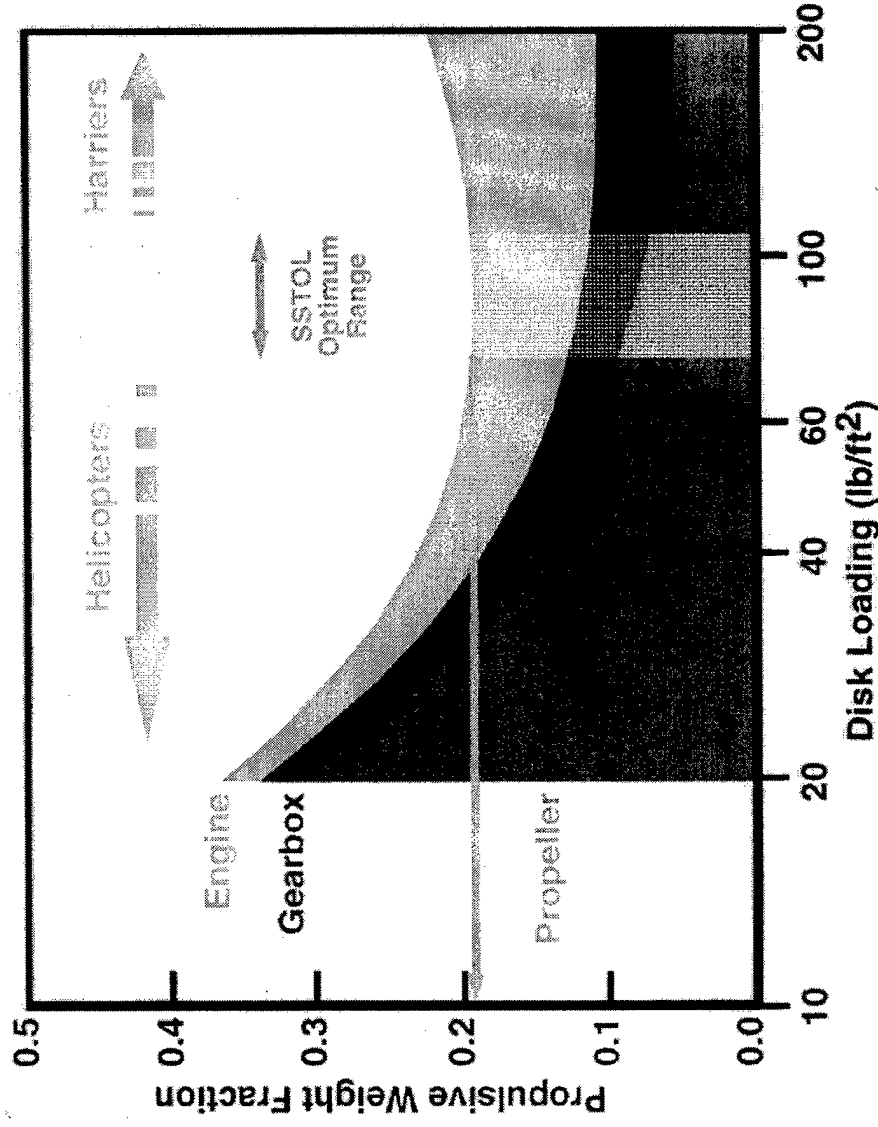


Historical Data - Mass Properties

Historical Database with respect to Disk Loading developed using flight weight hardware. The VTOL/STOL Database does not account for the higher structural weight fraction of this class of aircraft or in this case how it applies to a typical Ship Weight Breakdown Structure (SWBS). The mass fraction relative to the Lightship Weight as well as the individual components was extracted from this plot/database and used in the air-coupled propulsion assessments.

The individual pie charts on the follow slide show the relative breakdown of the varied disk loading cases.

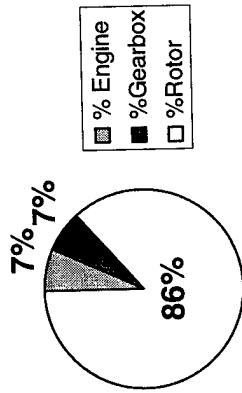
Historical Data - Mass Properties



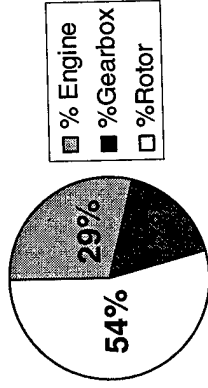
Historical Database with respect to Disk Loading developed using flight weight hardware. The VTOL/STOL Database does not account for the higher structural weight fraction of this class of aircraft or in this case how it applies to SWBS.

Historical Propulsion Mass Properties

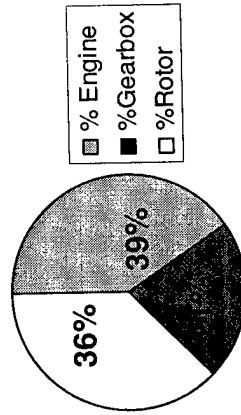
Weight Fractions at 20psf Disk Loading



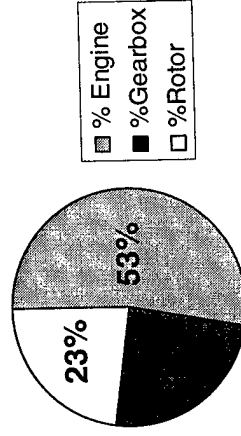
Weight Fractions at 60psf Disk Loading



Weight Fractions at 100psf Disk Loading



Weight Fractions at 200psf Disk Loading



Historical Data from V/STOL Aircraft

GE LM Gas Turbine Family-Mass Properties

The LM Gas Turbine Family mass properties are shown in following slide. For the scaling of the disk loading historical data to carried out it was important to remove those characteristics associated with marinization and relate the gas generator to a comparable aircraft system where it is of flight-weight construction. The LM6000 weight is heavily burden by sub-systems and required a break-out of components prior to disk loading scaling.

The discriminators to the selection of the appropriate size gas turbine is their specific output, or power output per pound mass and their specific fuel consumption. The second slide shows that the growth LM2500+ and the LM6000 have similar specific output, however the other two gas generators (LM2500 and LM1600) have reduced specific outputs. In the succeeding slides, the LM6000 has the definitive advantage with a 10% lower fuel consumption. At part power conditions it rivals the performance of the LM2500 with much reduced operating costs. Clearly it is the choice for use as the power production component of the propulsion system.

The LM6000 consists of:

- GE Large Marine/Industrial Gas Turbines*

- LM6000 Series - 2-Spool GE90-like core

- 50,000 SHP to 3600 rpm at 0.345 BSFC

- Volume= 36 ft. x 13 ft. x 12 ft., Weight = 25 Metric Tons

- 8550 KUSD per Unit

- 150-175 USD Maintenance Cost per Engine Hour

Package Includes:

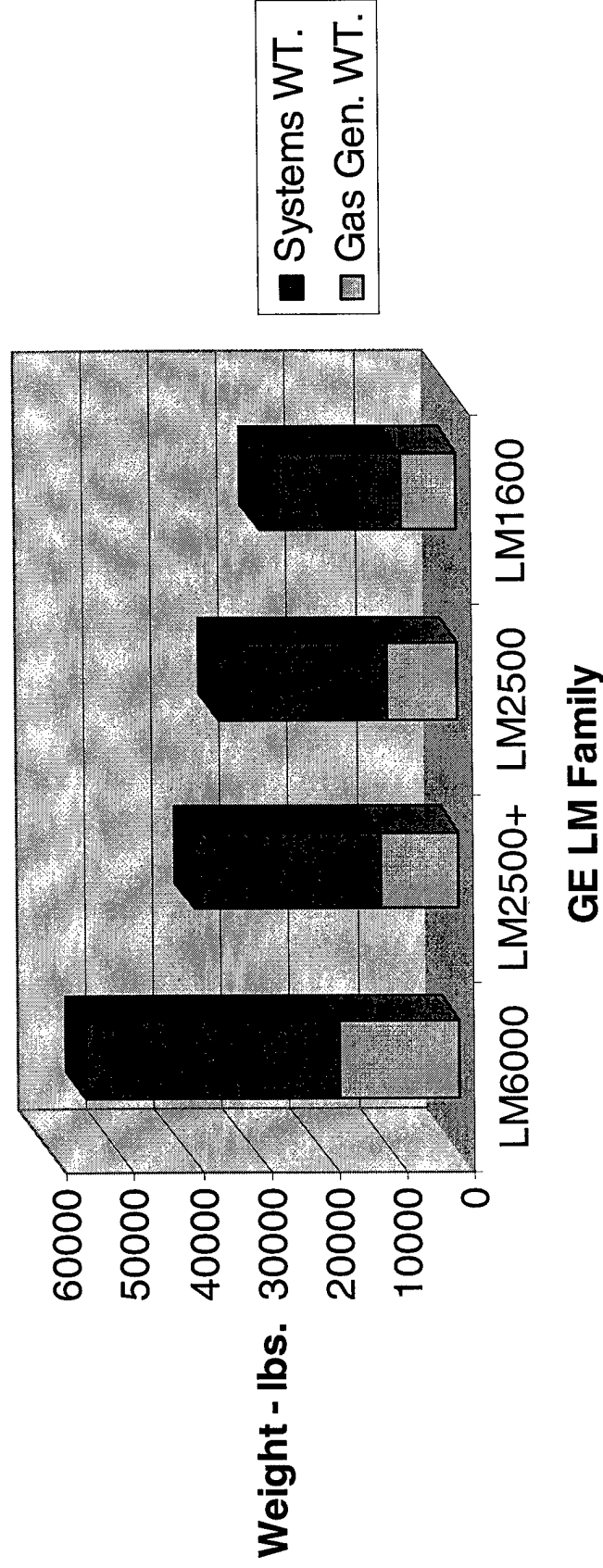
- Coalescing Inlet, Base / Enclosure and Auxiliary Support

- System (lube oil conditioning, fire protection, control system)

**It should be noted that the data from GE was provided au gratis by Mr. Dave Luck, GEAE*

GE LM Gas Turbine Family-Mass Properties

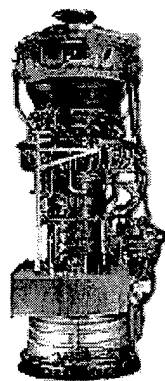
GE Marine Gas Turbine Weight Summary



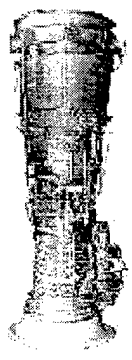
System Weight Includes: Coalescing Inlet, Base / Enclosure and Auxiliary Support System (lube oil conditioning, fire protection, control system)

GE LM Gas Turbine Family-Output Comparison

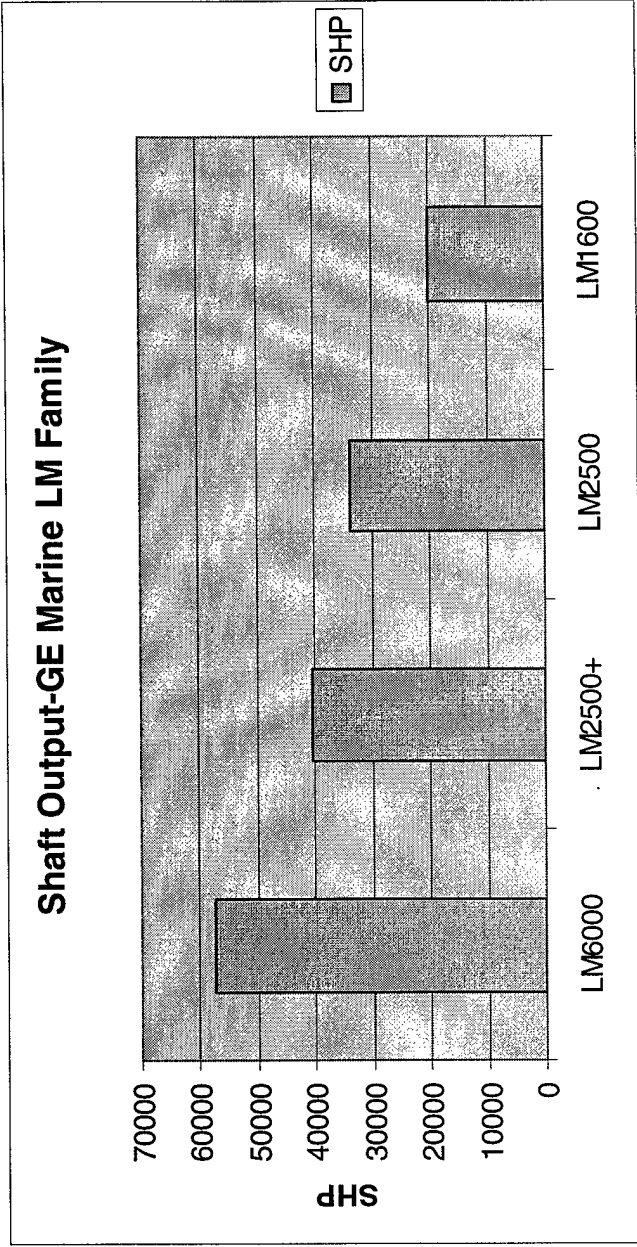
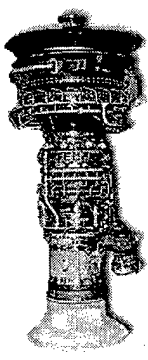
LM6000



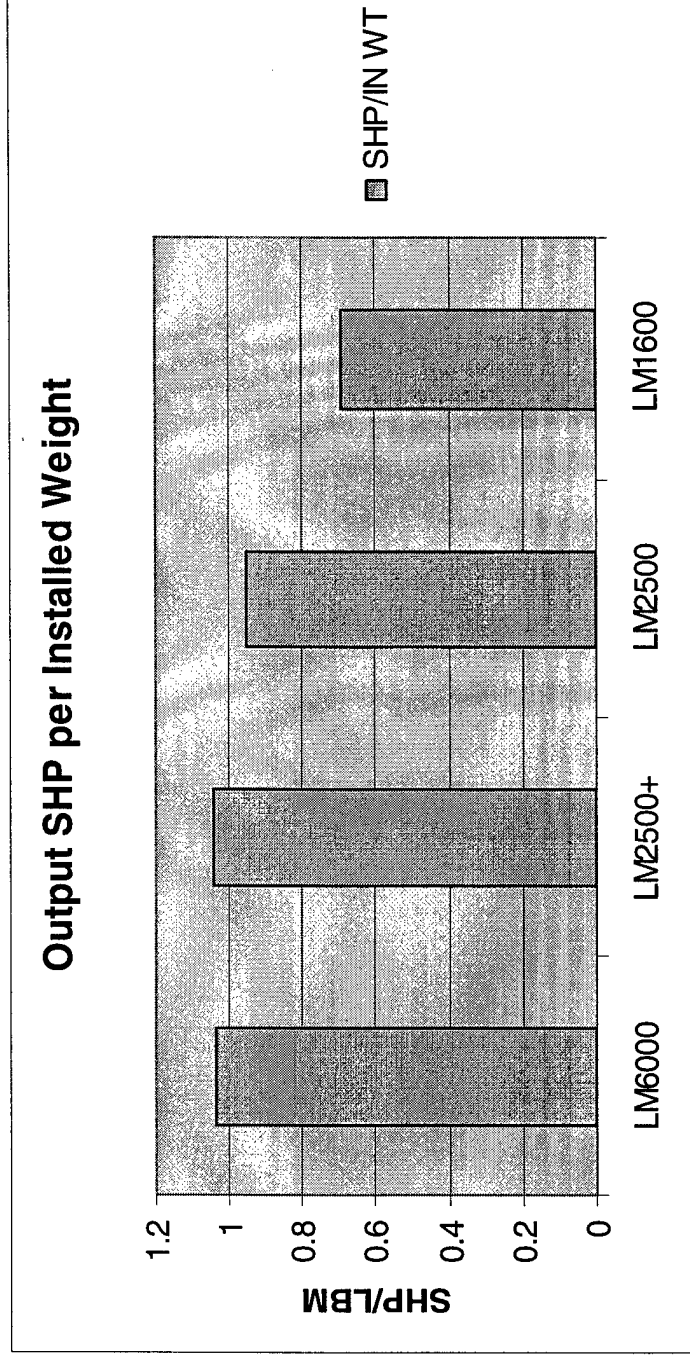
LM2500



LM1600

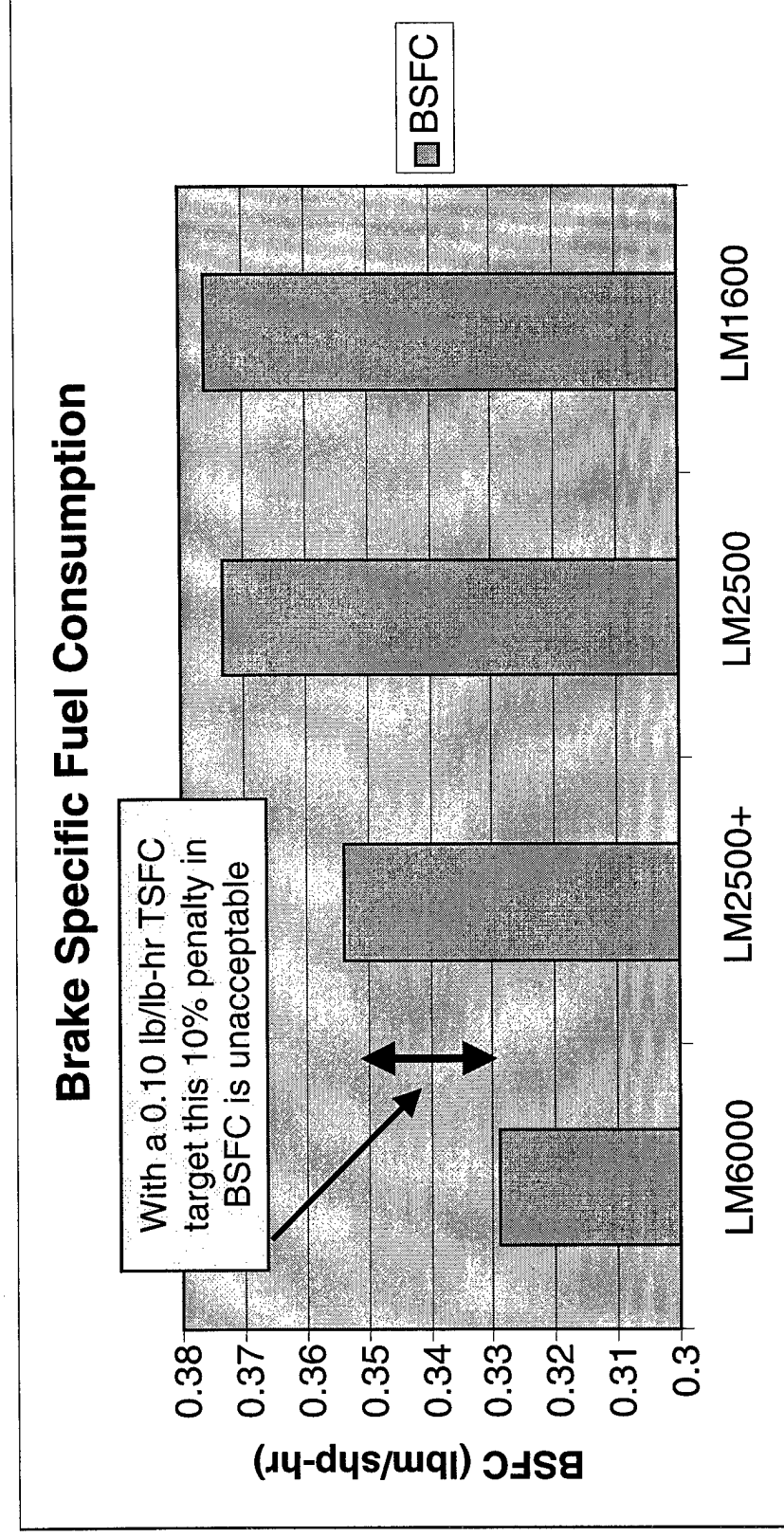


GE LM Gas Turbine Family-Mass Properties



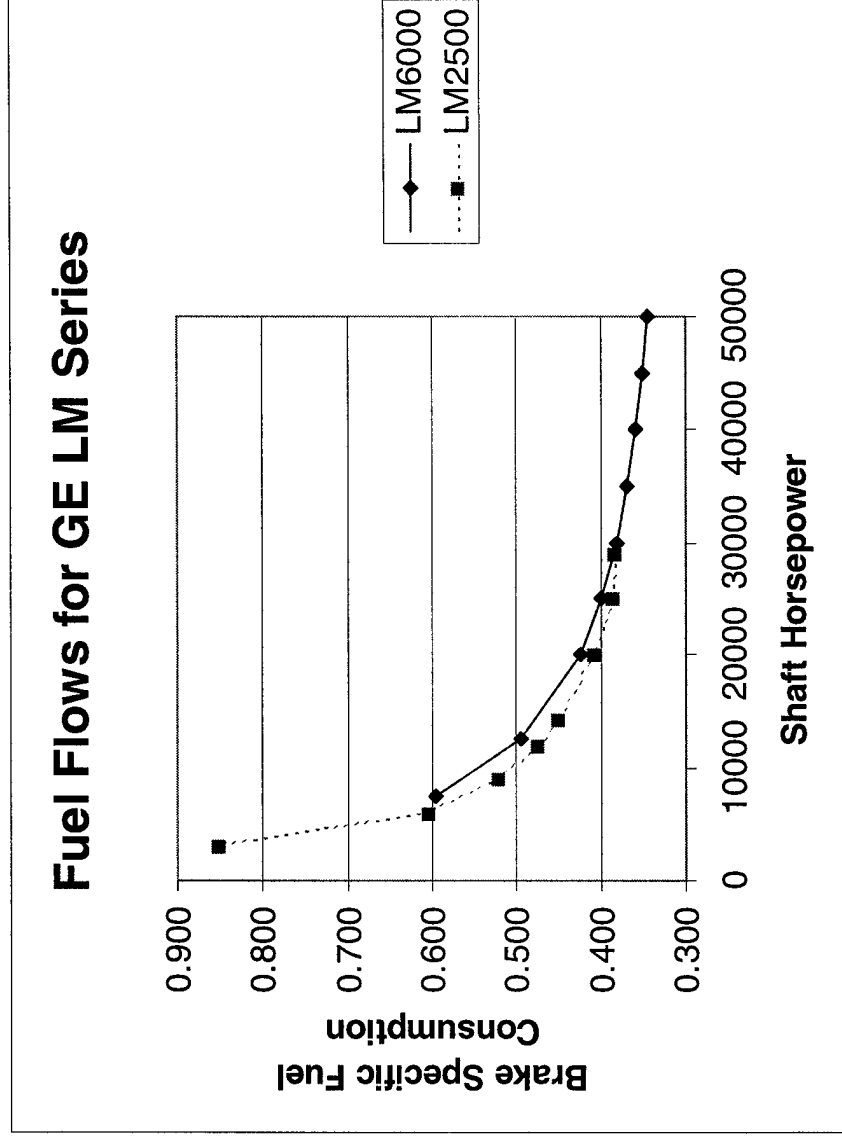
On an Installed Shaft Horsepower per Installed Weight Basis the LM6000 and LM2500+ are very comparable, however as previously shown....

GE LM Gas Turbine Family-Performance



.....there is a significant difference in Brake Specific Fuel Consumption.

GE LM Gas Turbine Families-Efficiency



Part-Power Performance of the LM6000 is comparable to the LM2500!

Fixed \$/hp are lower for LM6000

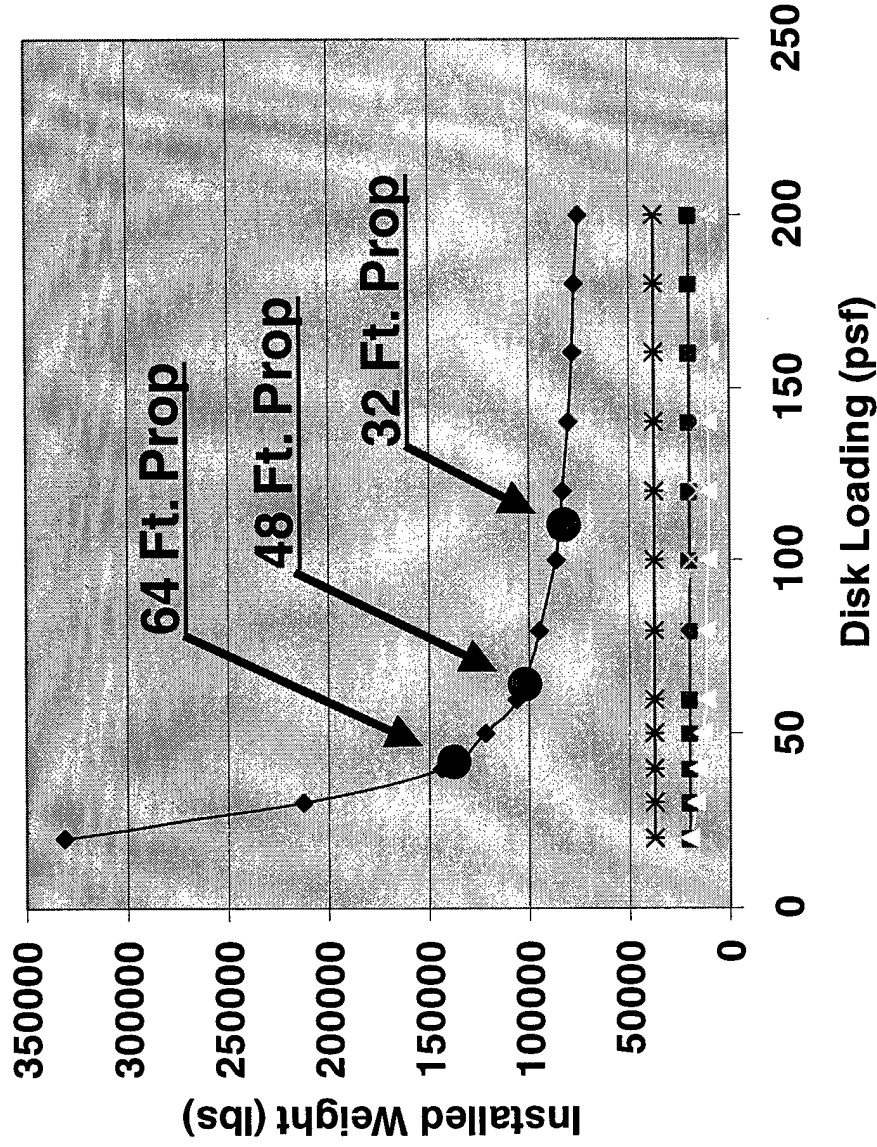
LM2500 → \$6,425,000 / \$75-90 per Engine Hour → \$215/hp
 LM6000 → \$8,550,000 / \$150-175 per Engine Hour → \$171/hp

GE LM6000 Air-Coupled Options

The LM6000 gas generator weight was used as a basis and the total weight for an air-coupled system was calculated using the historical data for varied disk loadings. Three propellers were examined, namely: 64-feet, 48-feet, and 32-feet in diameter. The following slide shows the breakdown of the varied systems and it is important to note that the key contributor is the propeller (or propulsor).

GE LM6000 Air-Coupled Options

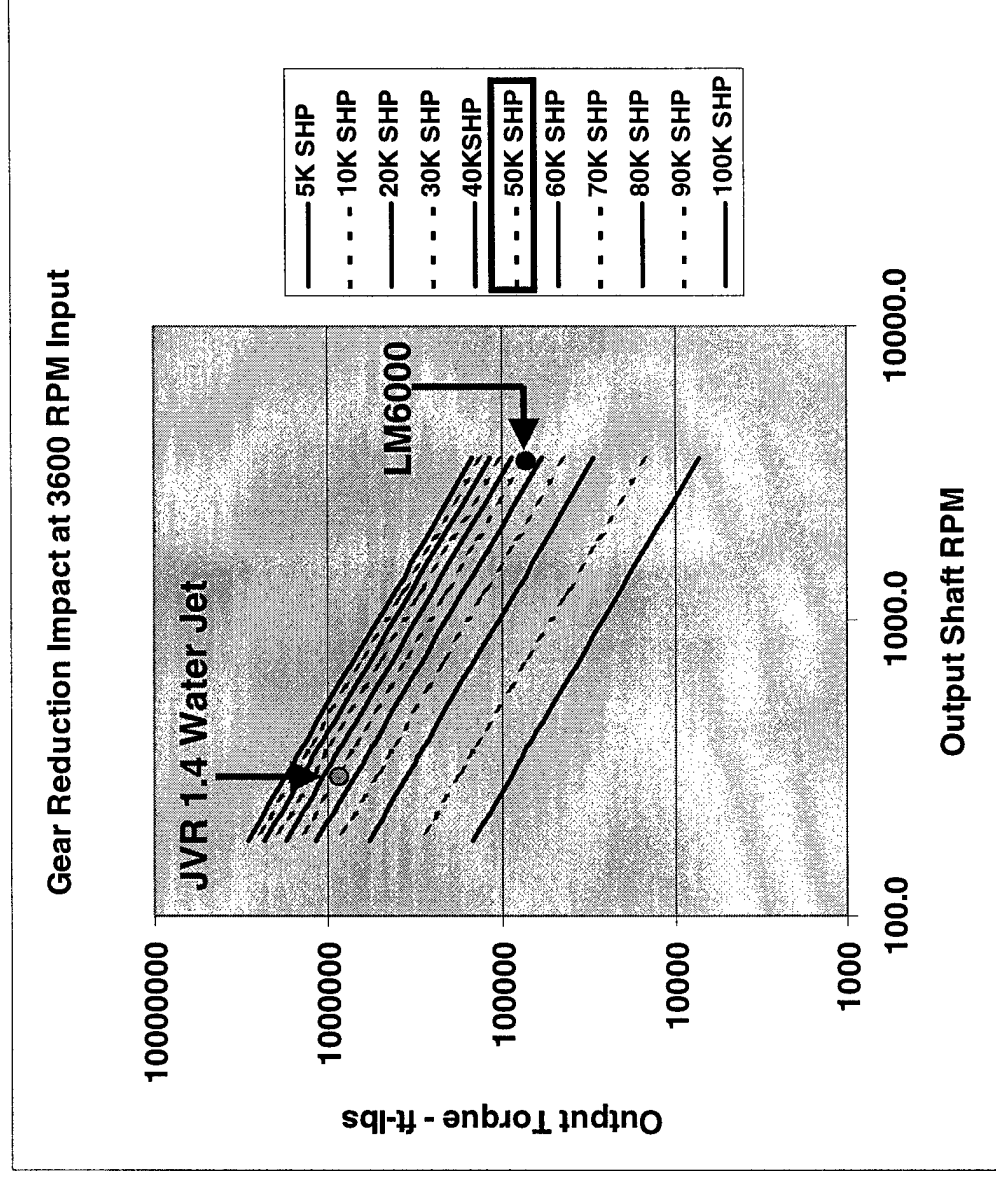
LM6000 System Mass Properties



Drive Shaft Torque Requirement Assessments

The following drive shaft sizing analysis was conducted to understand the minimum strut thickness potential of the candidate air and water coupled propulsors. For this the hydrofoil and SWA vessels, the minimum shaft diameter to transmit 50,000 shaft horsepower is approximately 13.2 inches in diameter. Support bearings will increase this diameter by a factor of two or three and suggest the minimum physical strut thickness to transmit power be on the order of 26 inches to 39 inches.

Drive Shaft Torque Requirement Assessments



Drive train requirements depend input/output peak torque values.

Higher shaft speeds keep torque lower and will minimize weight.

Drive Shaft Material Properties Assessments

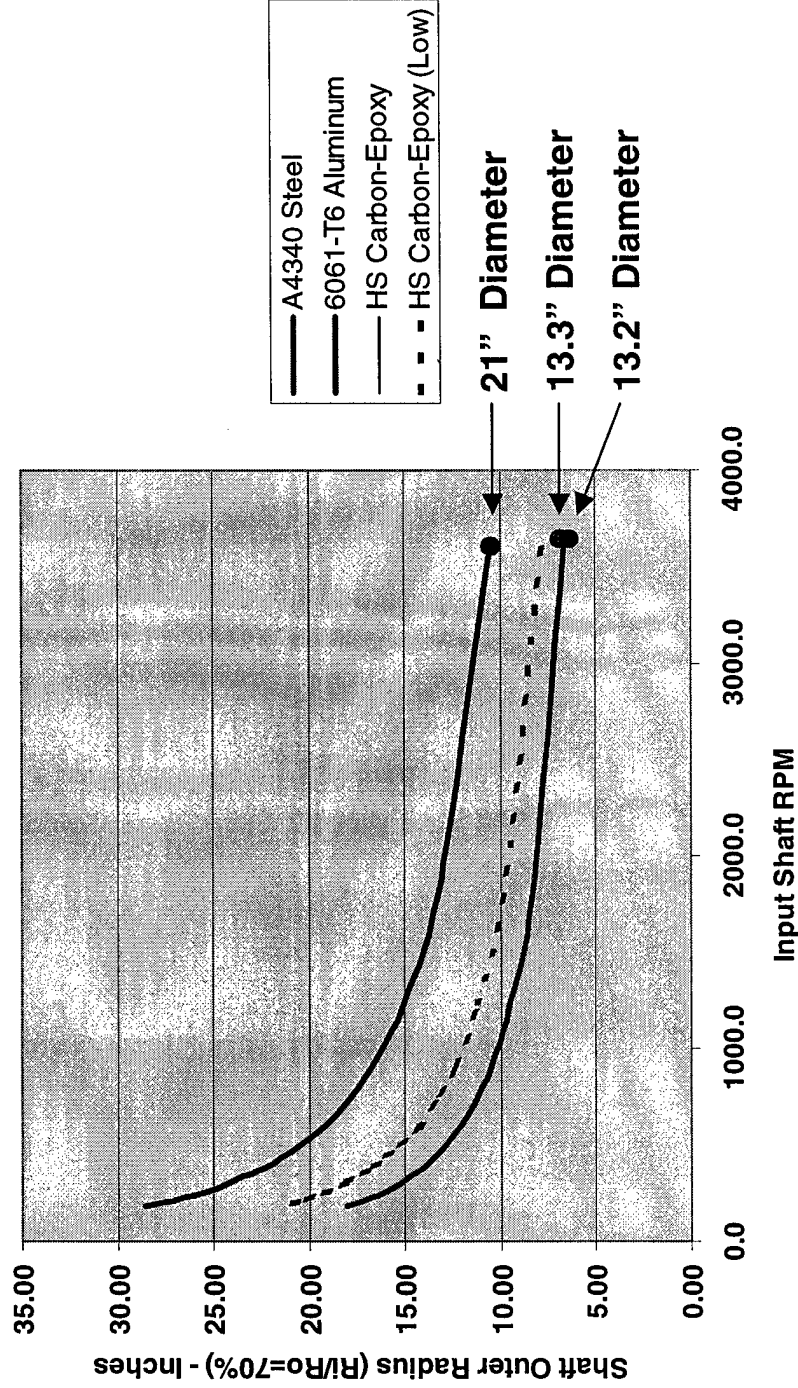
Type	Specification	Heat Treat	Density Pounds/ Cubic Inch	Yield Strength PSI	Shear Strength PSI	Endurance Limit PSI
CrMo Steel	A4140	Hot-Rolled	0.3	62000	15500	
CrMo Steel	A4140	Cold-Drawn	0.3	90000	22500	
NiCrMo Steel	A4340	Hot-Rolled	0.3	69000	17250	
NiCrMo Steel	A4340	Cold-Drawn	0.3	99000	24750	
NiCrMo Steel	A4340	Q1550F-D1000F	0.3	162000	40500	
Al	6061	T6	0.101	40000	10000	14000
Al	7075	O	0.101	15000	3750	17000
Al	7075	T6	0.101	73000	18250	22000
HS Carbon/Epoxy	Unidirectional		0.056	164000	41000	
Shear Stress = Yield Stress x 0.50 / Factor of Safety						
ASME Code for the Design of Transmission Shafting, B17c-1927						

“Kellog” Steel A4340 and High Strength Graphite/Epoxy are similar, However the density varies by a factor of almost 6:1. The Composite Drive Shaft will be durable, lightweight, a require minimal balance. Factor of Safety used in the Shear Strength is 2.

Drive Shaft Sizing Assessments

Shaft Size at 50KSHP Input

ASME Code for the Design of Transmission Shafting, B17c-1927

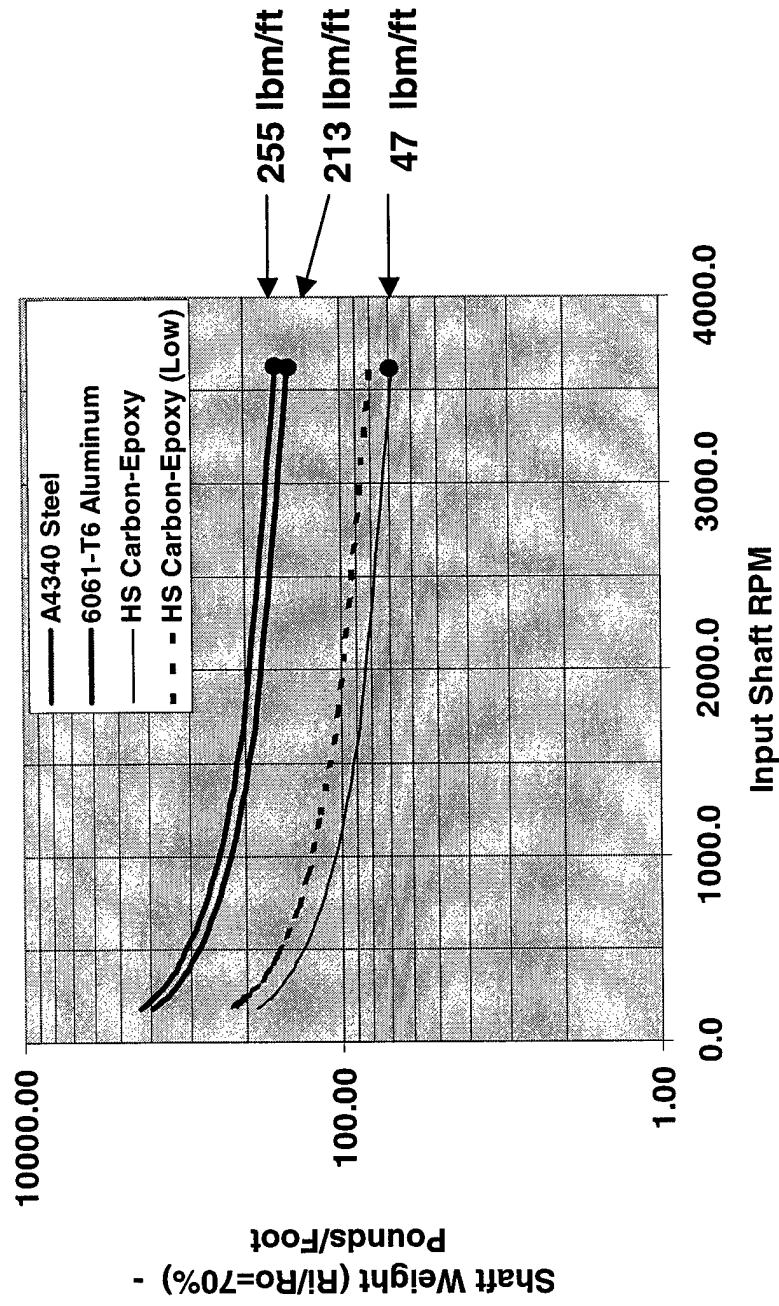


Loading assumed steady using a Safety Factor of 2!

Drive Shaft Mass Properties Assessments

Shaft Weight at 50KSHP Input

ASME Code for the Design of Transmission Shafting, B17c-1927

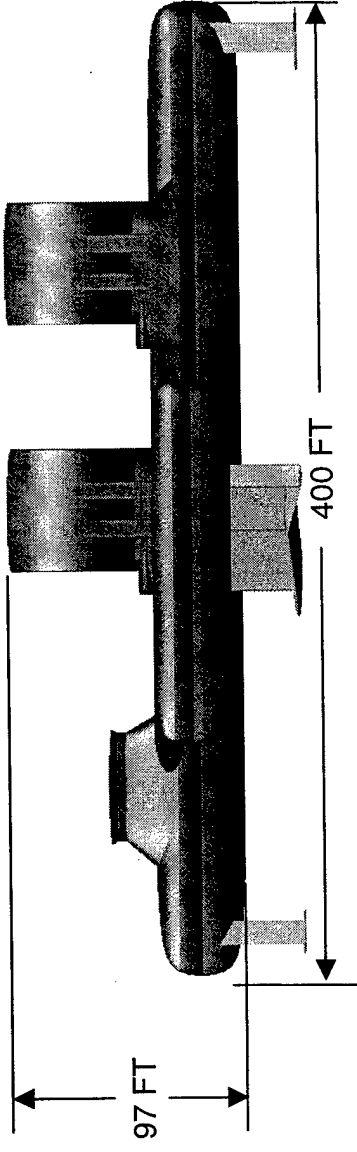
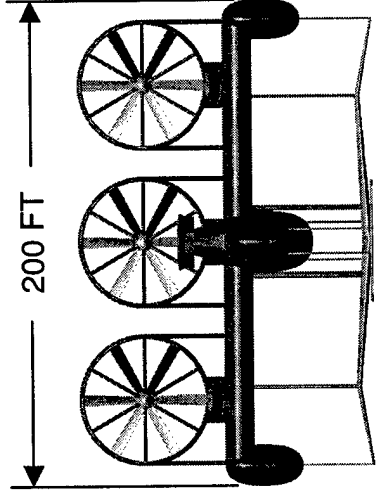


The Composite Shaft offers a significant weight savings !

11/99 Baseline - Propulsion Issues

Propulsion integration and technology application issues became immediately apparent when considering the use of large air-coupled propellers. In the following two slides, the issue are presented and are used to set the stage in the next phase of the study: propulsion component design, integration and installed performance estimation.

11/99 Baseline - Propulsion Integration Issues



Thrust Centerline is ~100 ft above Hydrofoil, > 50 ft above CG

Vessel Bridge Clearance is impacted and sea-state will impart dynamic loads

Ducting/Cowl subject to side-loads and will require substantial deck space.

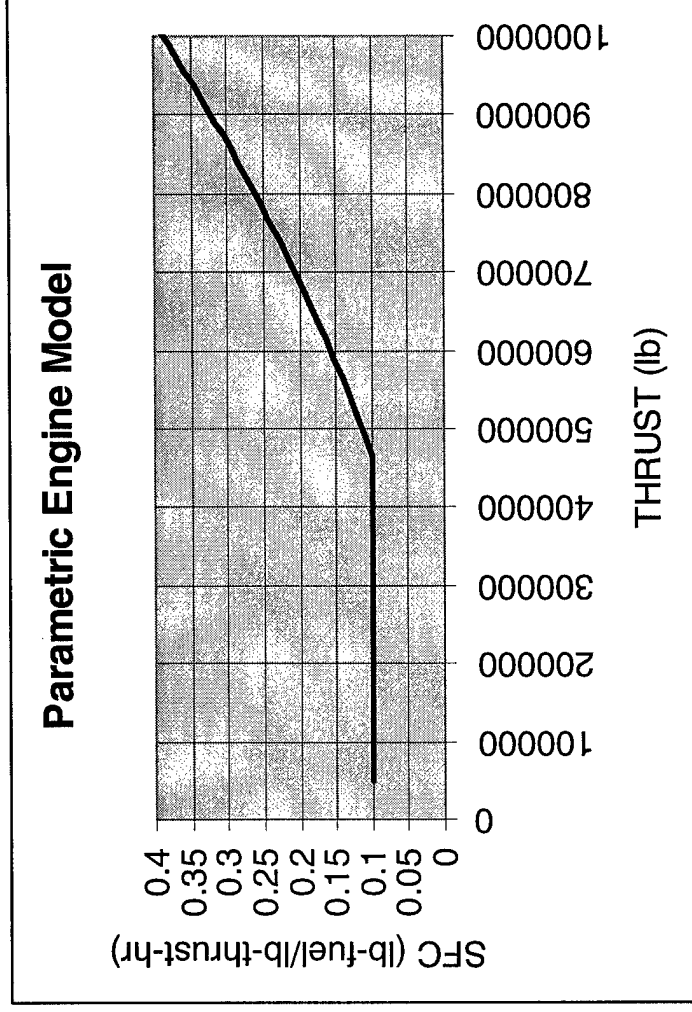
Vehicle boundary layer/cross-winds will impart varied disk loading.

Austere topside environment during full power operation (~150knots)

Strut/Rotor interaction will induce noise, vibration and high cycle fatigue

11/99 Baseline - Propulsion Technology Issues

“Knee” in the TSFC curve due to the 200’ beam propulsion integration constraint.
Location of the “knee” is dependent upon in-going assumptions database quality/depth
and analysis method fidelity!



Gearbox and Transmission - Flight Weight Hardware Currently Not Available.
Propeller and Pitch Control - HP Loading / Diameter beyond Current State-of-the-Art.
**Analysis Methods - Thrust-minus-Drag Prediction Accuracy is dependent upon
the availability of quality test data and/or calibrated analytical tools.**

Propulsor Integration & Performance Analysis Process

The next level of fidelity in the development of the propulsion system required the definition of the propulsor and how it could be coupled to the gas generator. It also requires that the propulsor be defined such that its component performance can be used in conjunction with the gas generator performance to create a system installation database.

At this point in time, the air-coupled and water-coupled system were considered viable. Power production was selected and considered to be equally applicable to either propulsor. Two air-coupled systems were examined as were two water coupled systems.

The design, integration and performance assessments are shown in the remaining slides in this section of the report.

Air-Coupled Propulsors Investigations

Candidates Include:

Conventional and Variable Pitch Axial Propellers

Requires State-of-Art Large Diameter Propellers

Large Lightweight Gearbox Required

Variable Pitch May Allow Constant Speed Shaft

Integration Effects Will Be Key Issues

Large Efficient Transverse Fan

Based on LM IRAD Studies of the 1980's

Fan Pressure Ratio Drives Net Propulsive Efficiency

Integration Effects and Fabrication Will Be Key Issues

Axial Propeller - Performance Analysis Process

Key Elements To Defining Propeller Installed Performance*

1. Characterize Additional Propeller Performance Parameters

Diameter, Number of Blades, Blade Activity Factor, Section CL

2. Calculate Power Coefficient, Advance Ratio at specified conditions

3. Determine Thrust Using Propeller Calibration Charts

Static Efficiency Charts,

Forward Velocity Efficiency Charts

4. Tabulate Thrust as a function of Input Horsepower, Speed, PALT

5. Examine Multiple Propeller/Core Combinations wrspt. TSFC optimization

may be iterative depending on the sustention thrust requirements.

****Hamilton Standard Methodology used***

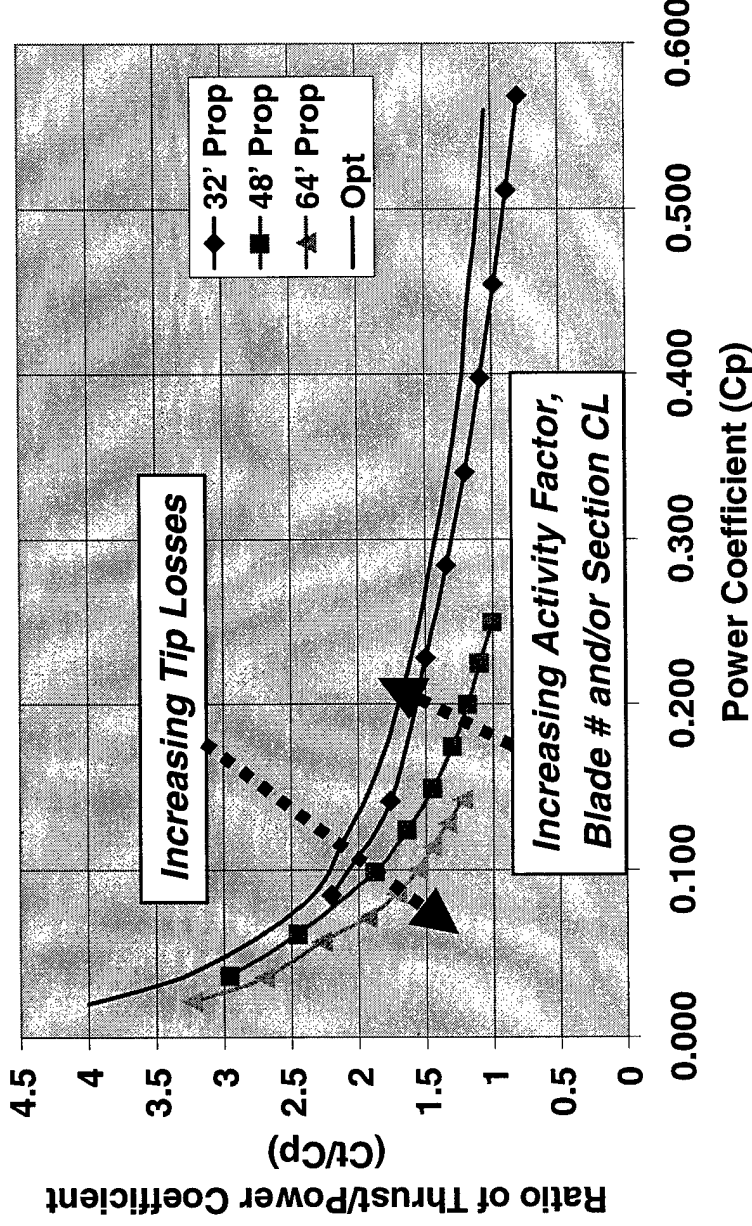
Axial Propeller Performance Analysis-Static

Performance is based on geometric characteristics of the propeller

$$C_p = \frac{bhp^* (\rho/\rho_o)}{2000^*(n/1000)^3*(d/10)^5}$$

$$T = \frac{(C_t/C_p)*bhp*33000}{nD}$$

Static Propeller Performance



$$CL(\text{design})=0.20$$

$$\text{Activity Factor (32' x 3 bld.)}=100$$

$$CL(\text{design})=0.15$$

$$\text{Activity Factor (48' x 3 bld.)}=100$$

$$\text{Activity Factor (64' x 3 bld.)}=80$$

Propeller Performance Analysis-Forward Flight

Propeller Operating Characteristics

Advance Ratio, $J = 0.0$ to $0.63 = V/nD$

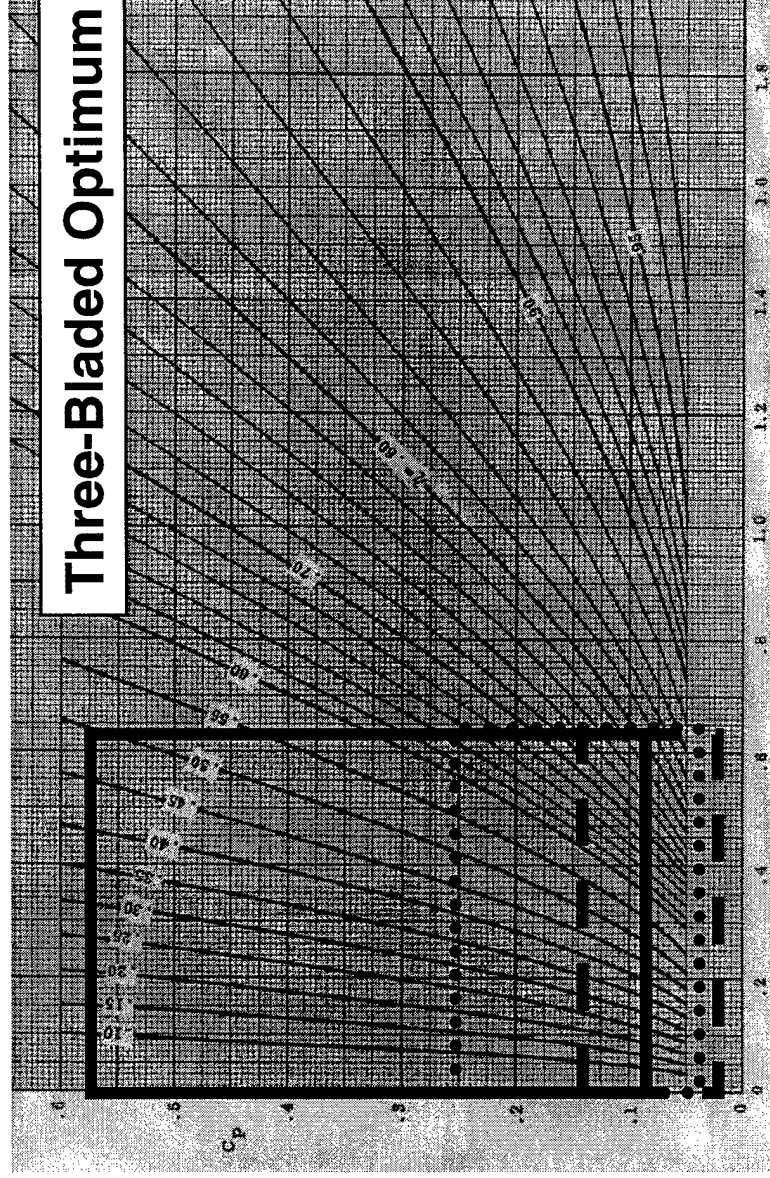
Power Coefficient, $C_p = 0.085 - 0.568$ @ 32 ft. —

$C_p = 0.037 - 0.250$ @ 48 ft.

$C_p = 0.021 - 0.143$ @ 64 ft. —

$$C_p = \frac{bhp^* (\rho / \rho_o)}{2000^* (n/1000)^3 (d/10)^5}$$

$C_p =$
Power
Coeff.

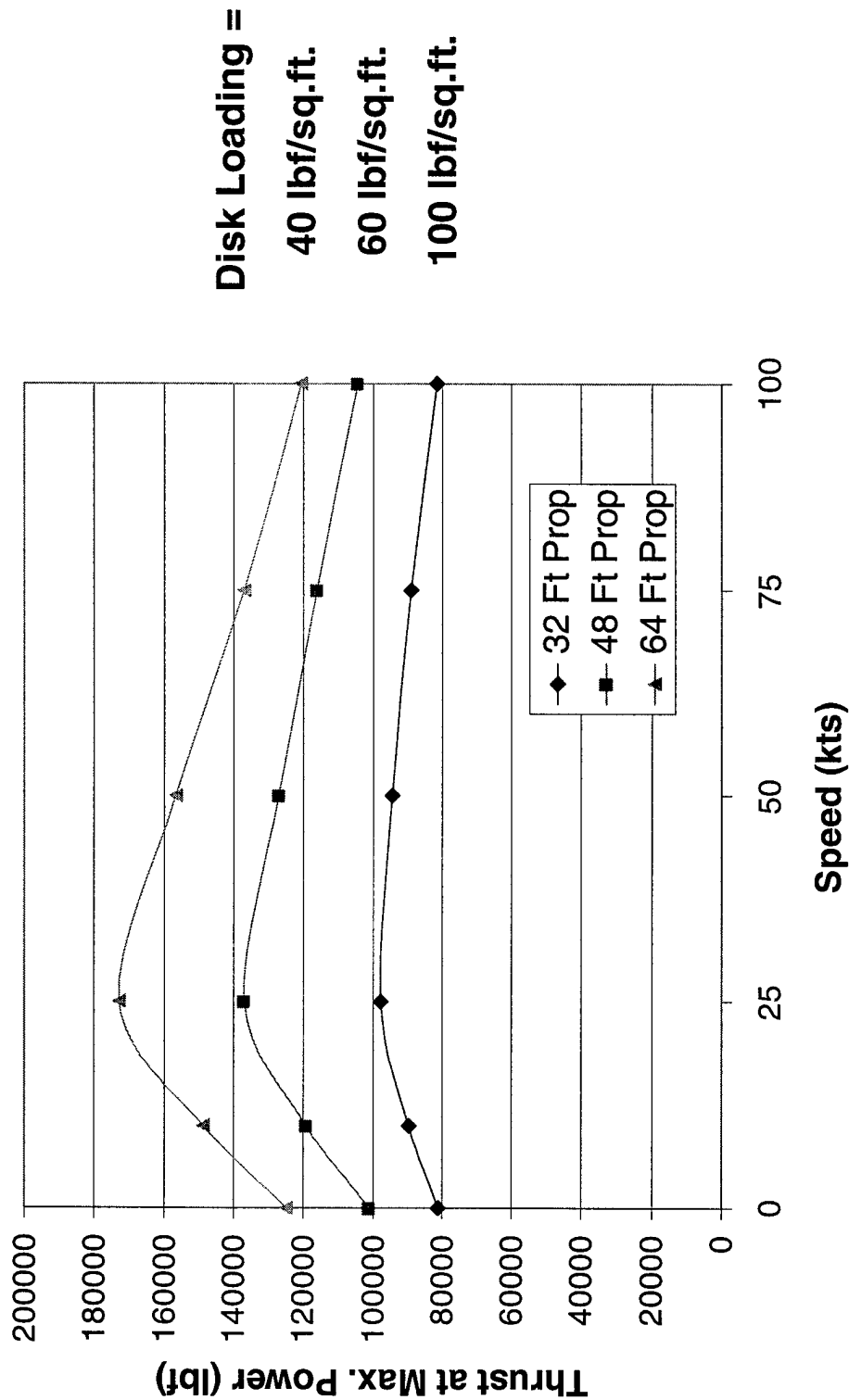


Three-Bladed Optimum Efficiency

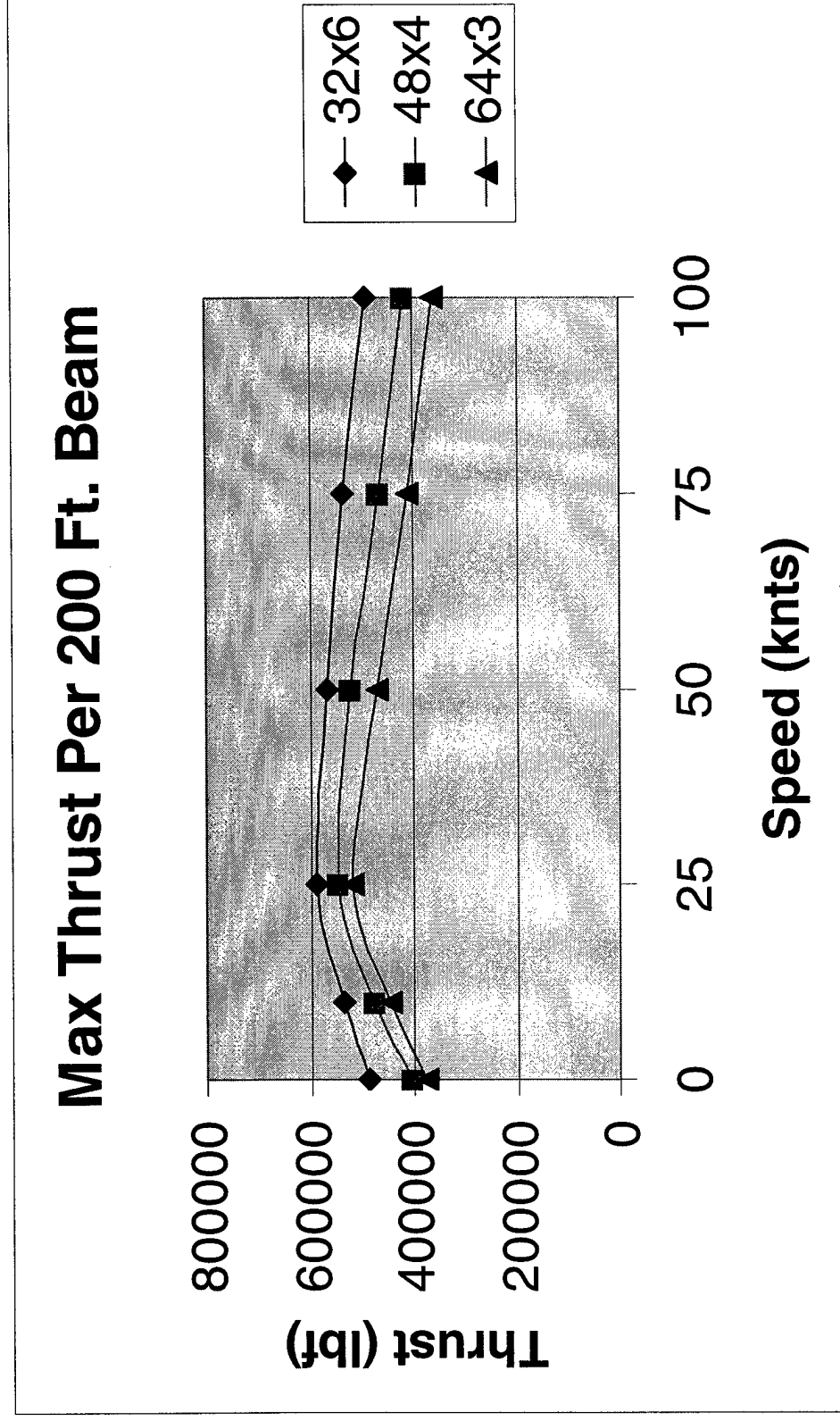
$$J = V/nD = \text{Advance Ratio}$$

Results for All Three Props using LM6000 Output

Maximum Available Thrust Per LM6000



200 Foot Beam Sets Maximum Available Thrust

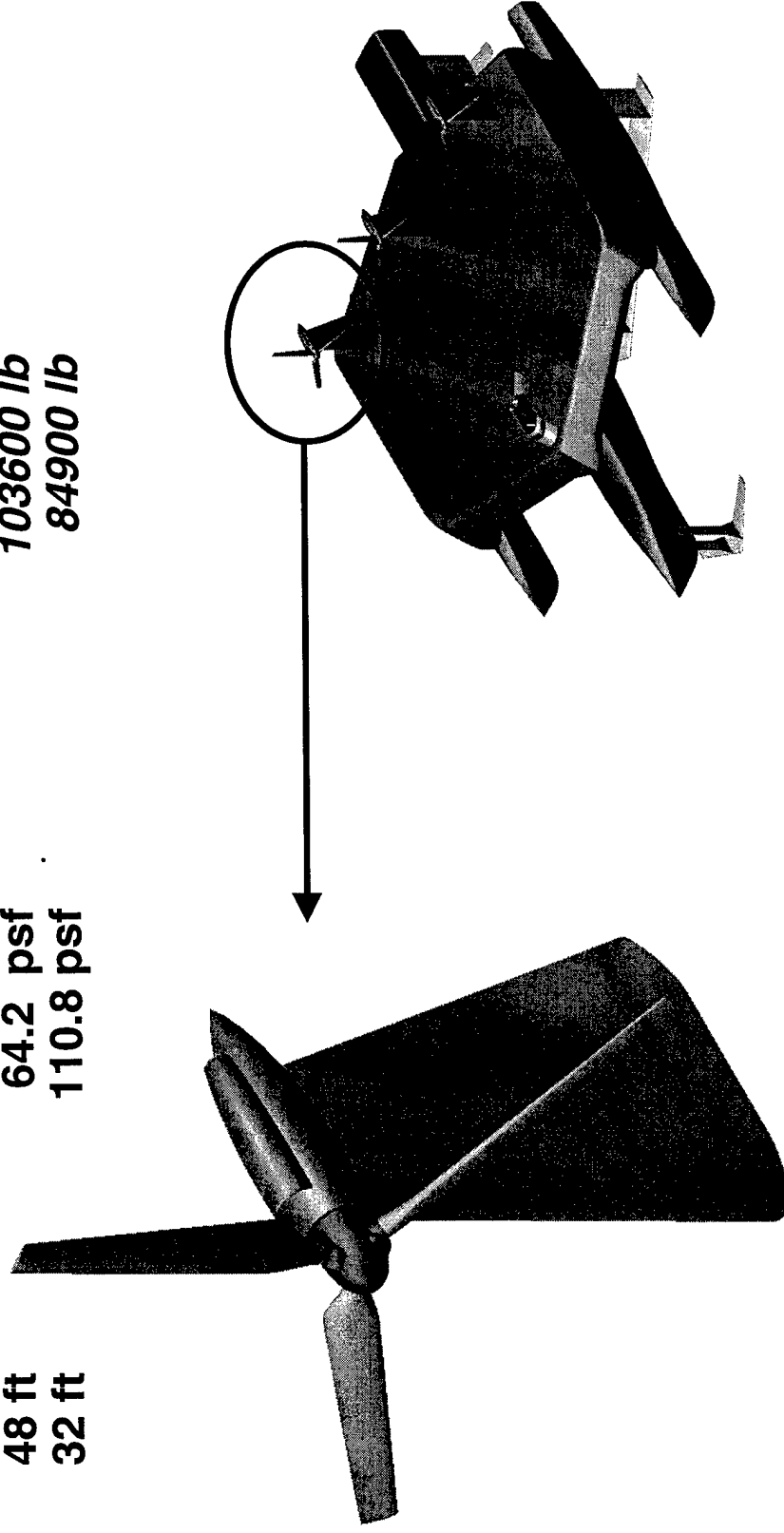


Revised Axial Air-Coupled System Weights

Current Baseline Design Criteria - 50000 SHP
Tip Speed ~ 850 fps (M0.76), $n \cdot D = 16,245$ rpm-ft
Peak Efficiency at Design Pt. ~ 0.84 (Goal)

Mass Property Estimates
revised using LM6000 gas
generator weights

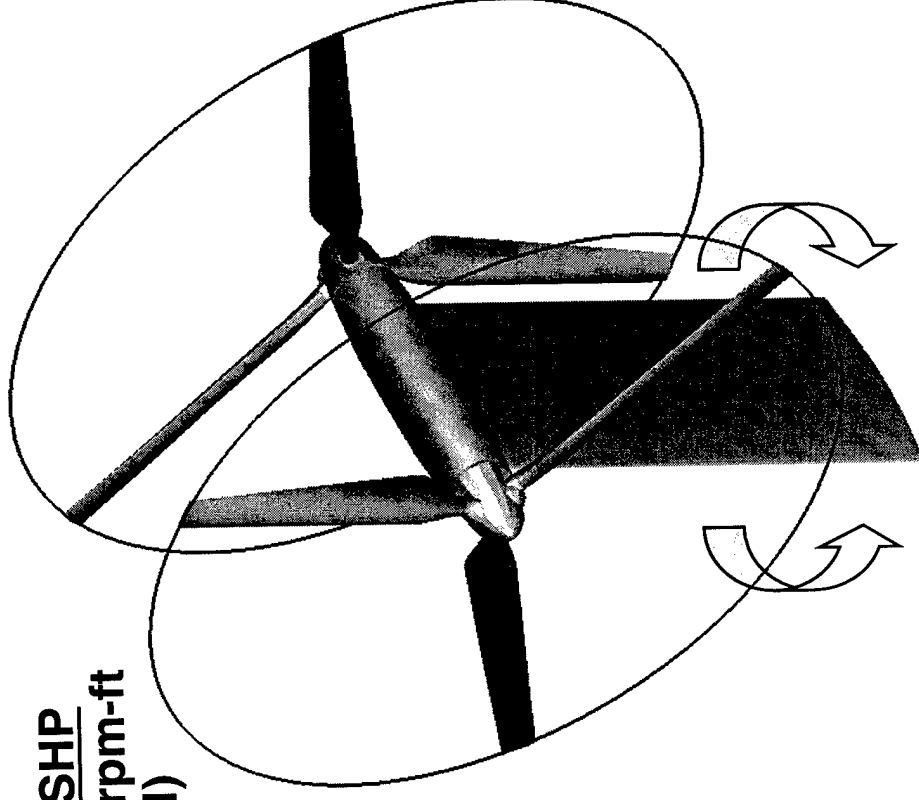
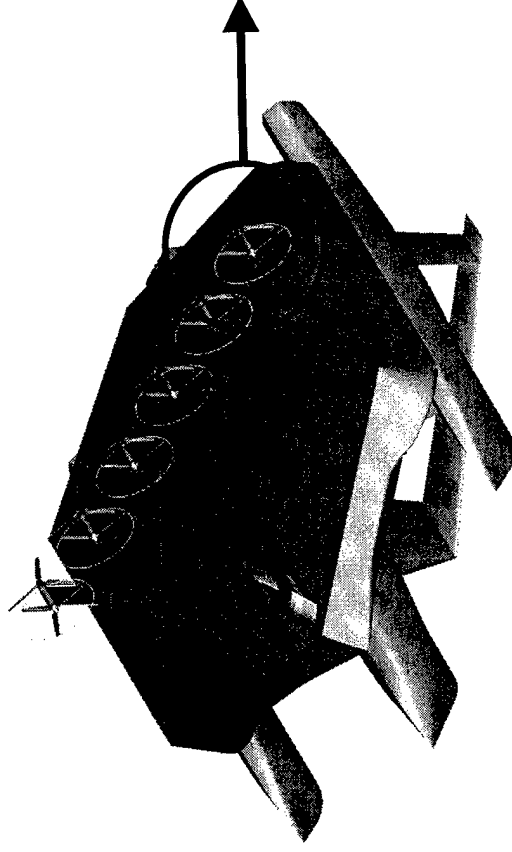
<u>Diameter</u>	<u>Disk Load</u>	<u>Weights</u>
64 ft	42.7 psf	139700 lb
48 ft	64.2 psf	103600 lb
32 ft	110.8 psf	84900 lb



Baseline Design - Asymmetric Thrust Loading

Current Baseline Design Criteria - 50000 SHP
Tip Speed ~ 850 fps (M0.76), $n \cdot D = 16,245$ rpm-ft
Peak Efficiency at Design Pt. ~ 0.84 (Goal)

<u>Diameter</u>	<u>Disk Load</u>
32 ft	110.8 psf / 221.6 psf

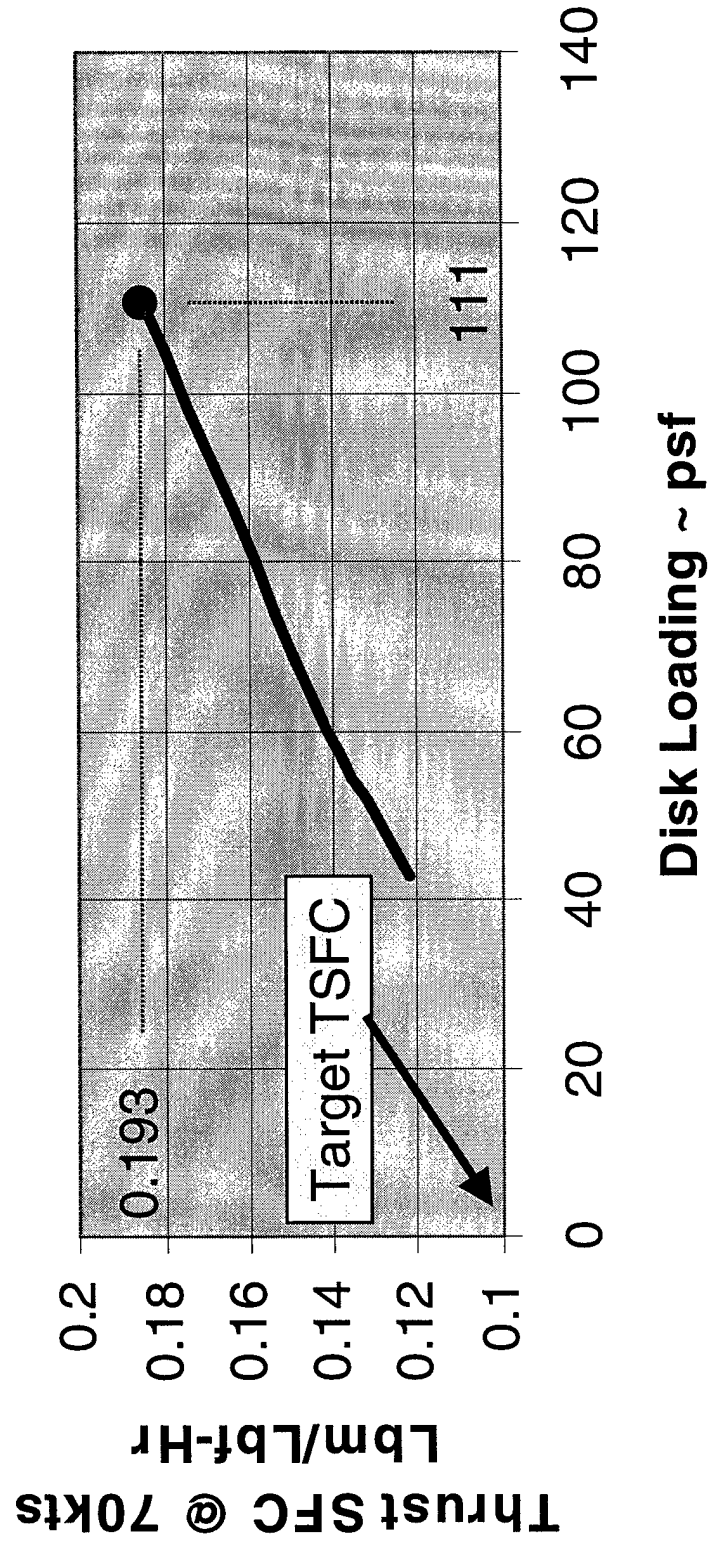


***Pusher Propeller May Be Used for Take-off Thrust Augmentation
or to Balance Engine Out Thrust Losses. Outboard systems
may be placed on deck swivels for beaching/docking.***

Disk Loading and TSFC-Baseline 32' Props

Efficiency as a Function of Disk Loading

LM6000 Gas Generator



Axial Propeller-Performance Analysis Risks

Key Issues with Respect to the Propeller Performance Estimates

- 1. Integration Aspects are completely neglected**
- 2. Static vs. Forward Velocity Efficiency Chart Interpolation**
- 3. Typically Propellers in the 40-70 foot diameter range are loaded much lighter (ie. Helicopters and Wind Turbines) and have lower Power Coefficients at static conditions.**

Transverse Fan Incorporates Design Constraints

The transverse fan became final attempt of air-coupling the propulsion system within the 200 foot beam design constraint. LM data from the 1980's was used in the assessment. The weakest link in the study was an accurate mass properties assessment. Performance was determined to be comparable to the axial flow propellers, however the concept was much more complicated and was deemed to be high risk.

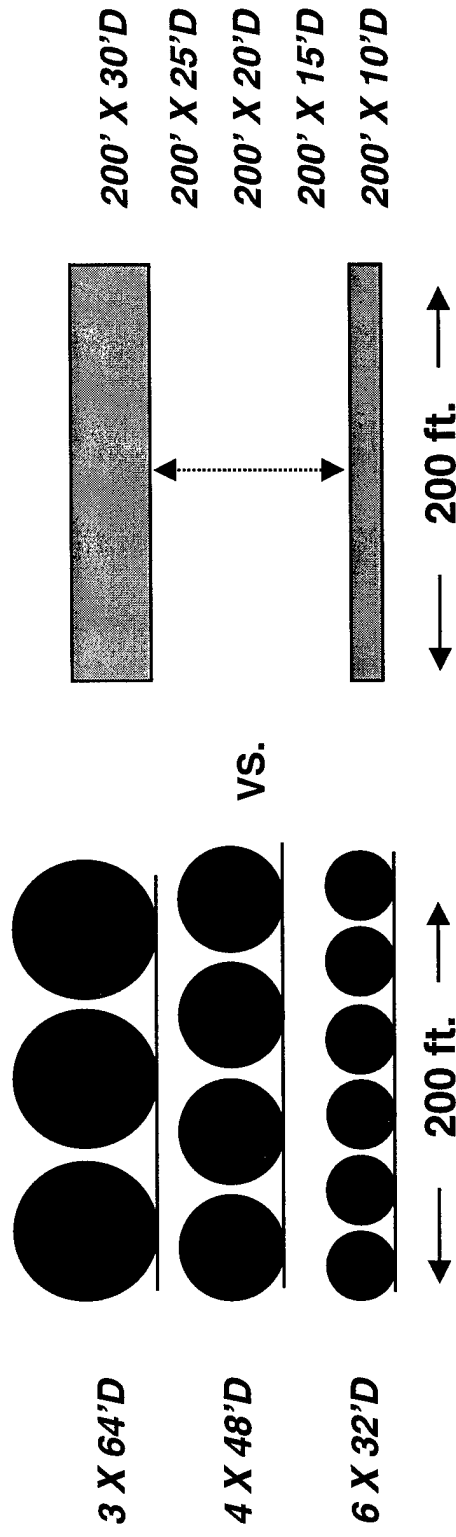
Transverse Fan Incorporates Design Constraints

Problem: Efficiently Convert the Gas Turbine Shaft Output to Propulsive Thrust by Transferring Momentum via. Transverse Fan

Approach: Amend simple momentum theory to incorporate

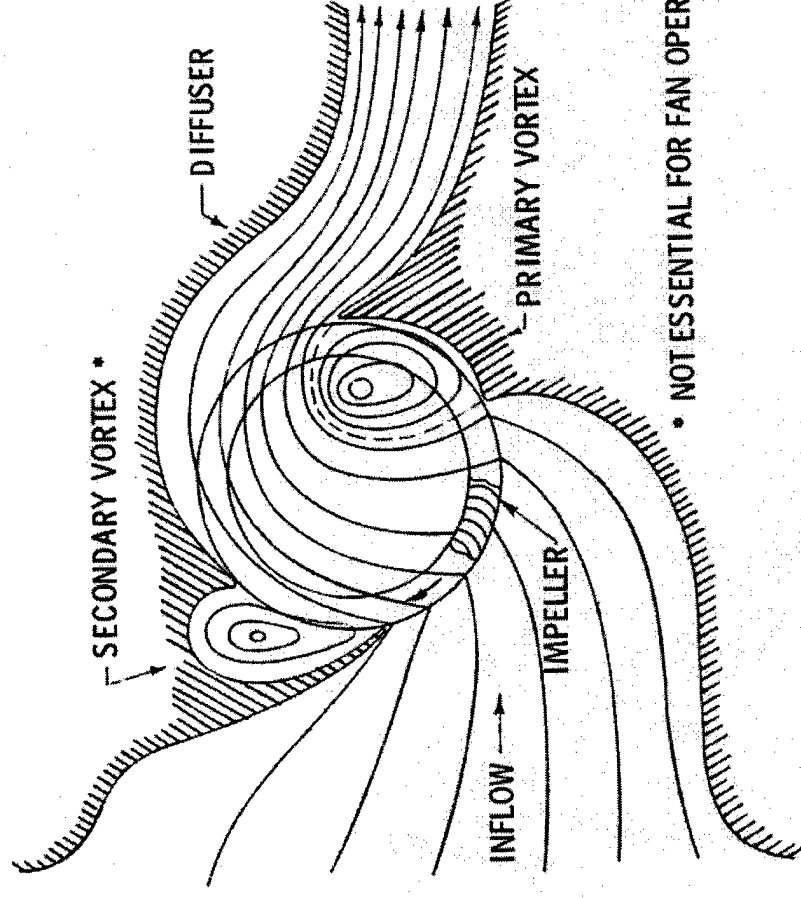
1. Axial Propeller Performance as Functions of Speed and Design,
2. Alternate Air-Coupled Momentum Transfer Methods,

and define the Propulsion System Installed Performance with the Propulsion TPM's. Provide Baseline Vehicle Design Input which is consistent with the analytical findings. Establish goal and status TPM's.



Alternate Propulsion Method-Transverse Fan

Previous IRAD Studies solved a significant number of technical challenges associated with this type of Low Pressure Ratio System



Alternate Propulsion Method-Transverse Fan

IRAD Studies Investigated Aspect Ratio 1.0 Fan Segment. Vought*under Navy Contract Investigated Aspect Ratio 0.083 and 1.0 Crossflow Fans

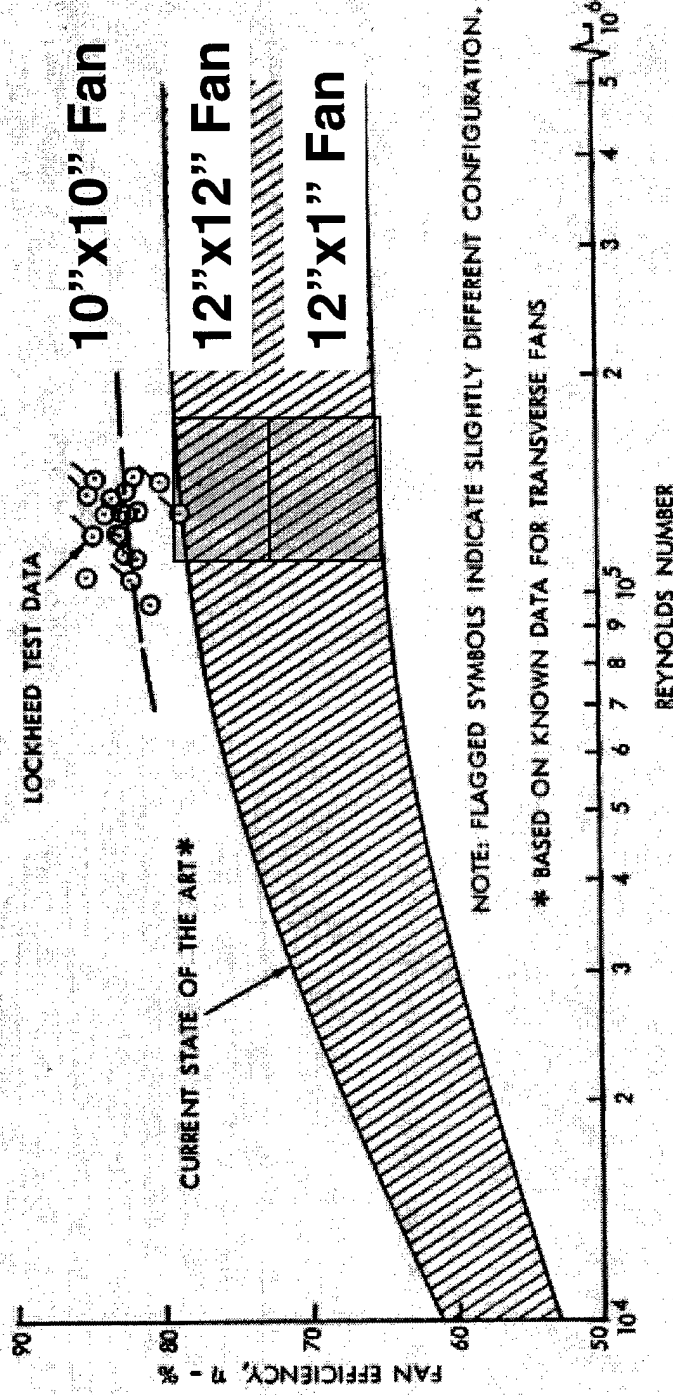
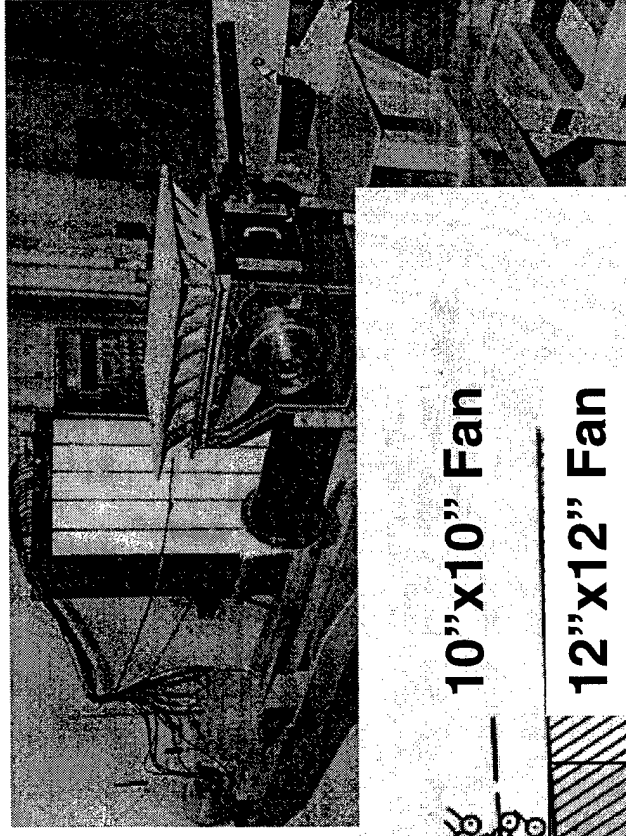


Figure 8. Fan Efficiency Comparison

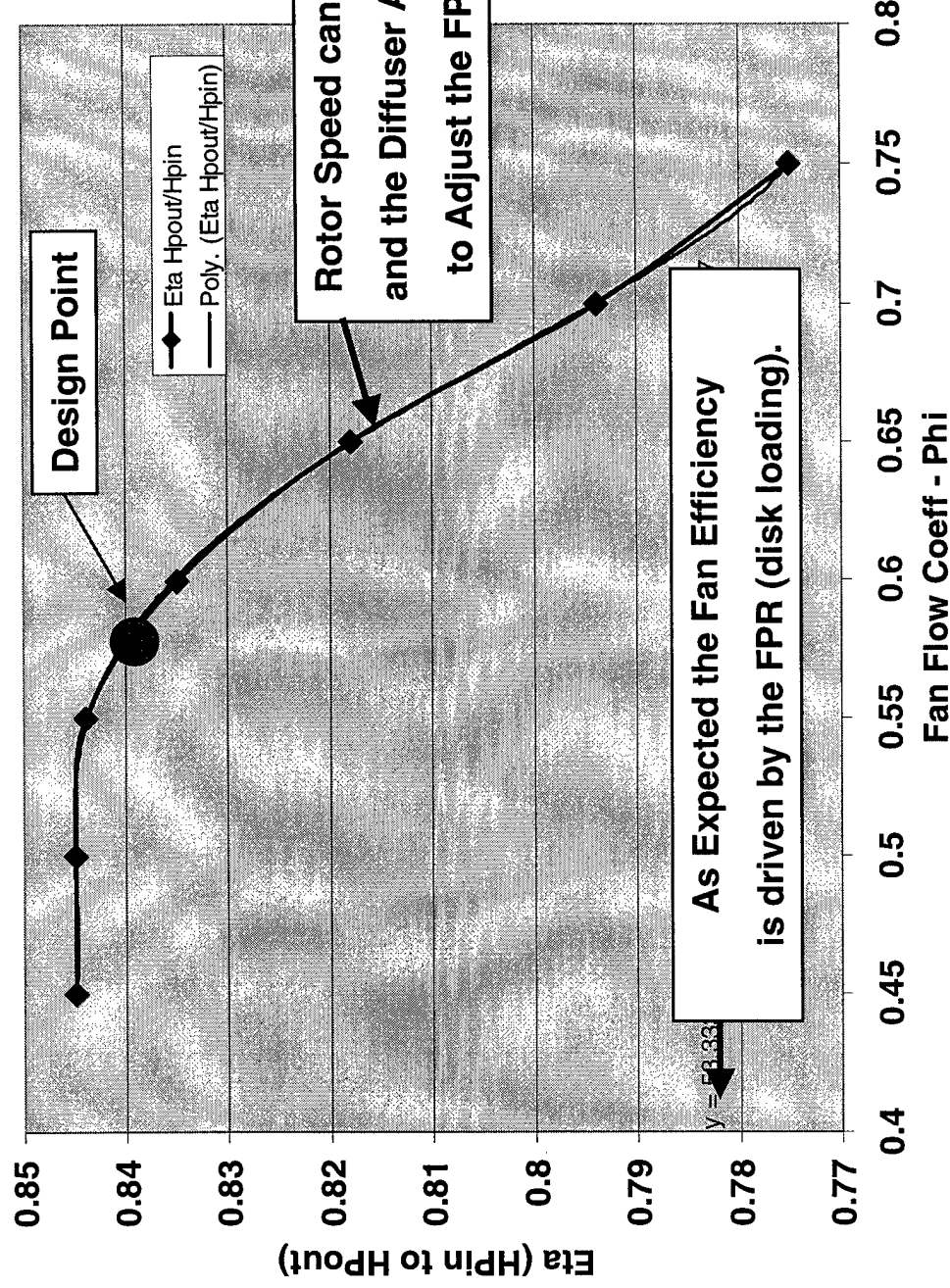
***N00019-74-C-0434**

Transverse Fan Performance Based on Test Data

Component efficiency of the transverse fan was on the order of 85% if it was design using the fan flow coefficients used during the 1980's tests. As expected, an equivalent disk loading was provided and the TSFC became a fallout of both fan drum diameter and the LM6000 gas generator.

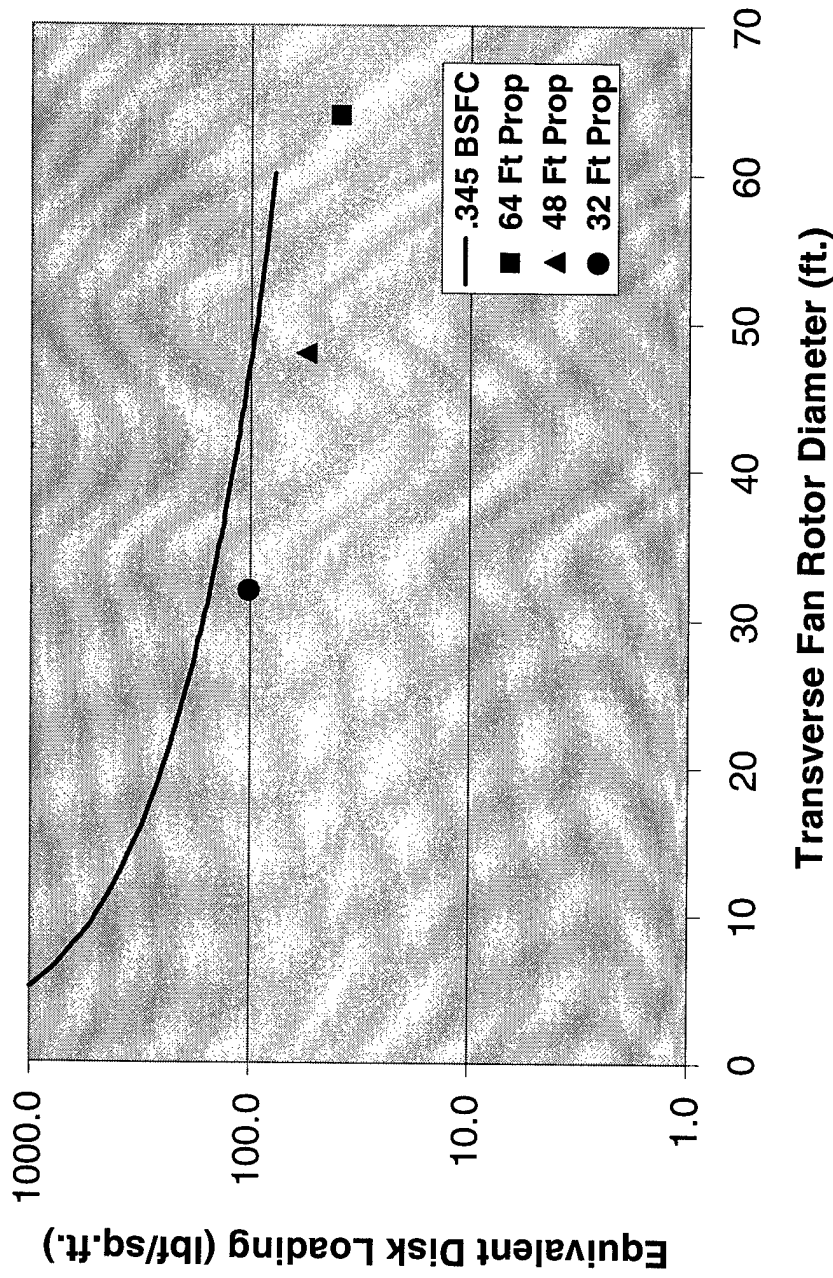
Transverse Fan Performance Based on Test Data

Transverse Fan Efficiency



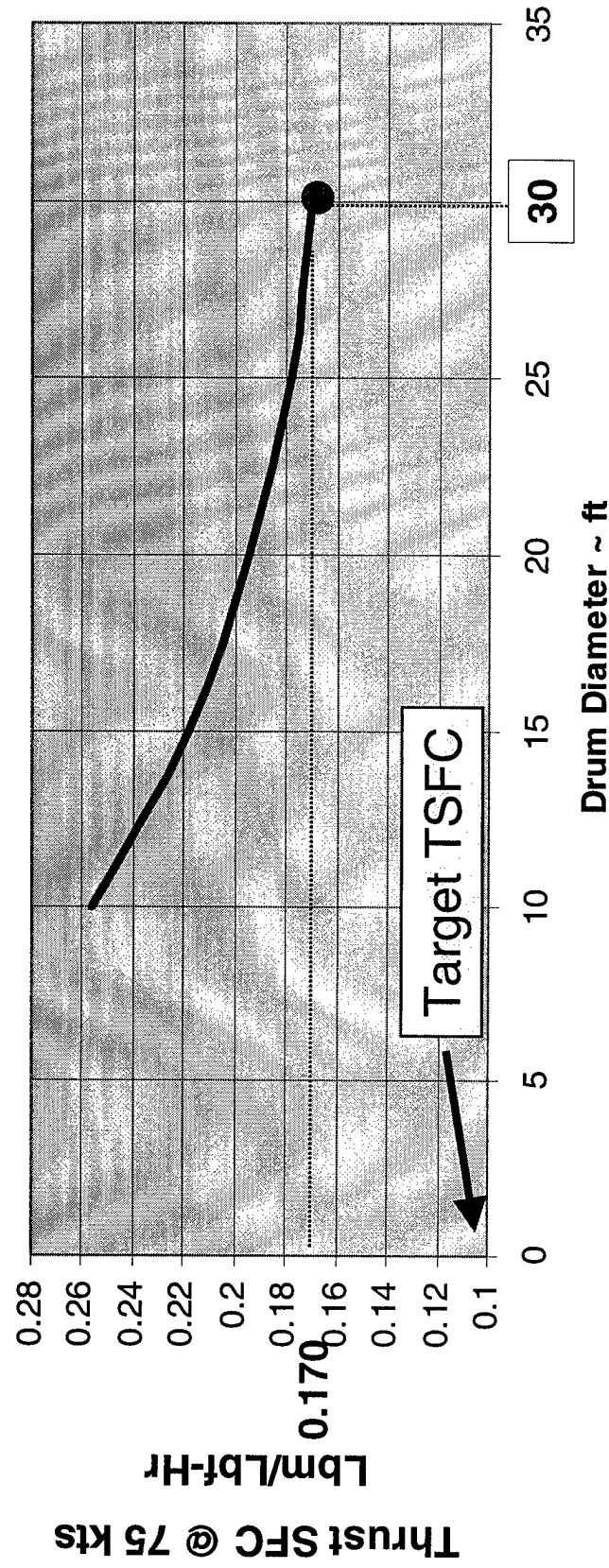
Transverse Fan Diameter Impact

Static Performance of a Single LM6000 Driven Transverse Fan with 85% Efficiency



Transverse Fan TSFC

TSFC as a Function of Propulsor Diameter LM6000 Gas Generator



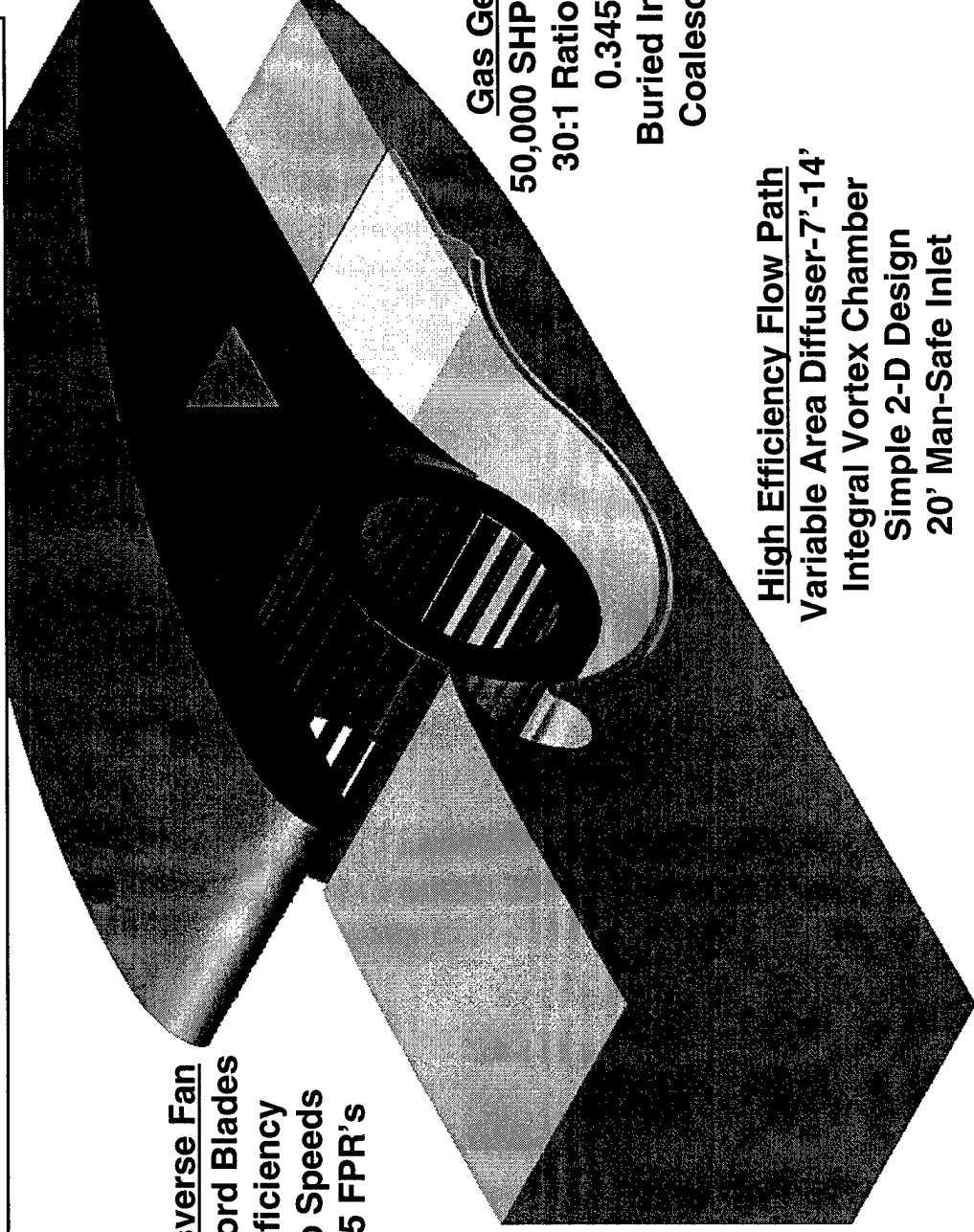
Alternate Propulsion Method-Transverse Fan

Three LM6000 gas generators were used to drive each of the fan segments. The output of each 66 foot fan segment was on the order of 135,000 pounds thrust. Integration aspects for this type air-coupled system were of high impact with respect to the inlet and nozzle placement.

Alternate Propulsion Method-Transverse Fan

Multiple Transverse Fan Segments are integrated across the Beam of the Fast Hydrofoil

30' Transverse Fan
30%R Chord Blades
85% Efficiency
Low Tip Speeds
1.05-1.5 FPR's



Gas Generator
50,000 SHP @ 3600 rpm
30:1 Ratio to 120 rpm
0.345 BSFC
Buried Installation
Coalescing Inlet

High Efficiency Flow Path
Variable Area Diffuser-7'-14'
Integral Vortex Chamber
Simple 2-D Design
20' Man-Safe Inlet

Alternate Configuration Integration-Transverse Fan

Specifications

3-30 ft. Rotors- 66 ft. Span each

4.5 ft Chord Blades at 4.5% t/c

ROM Rotor Weight ~ 1000 lb/ft-span

Fan Flow Coeff. =0.52 (Design Point)

Fan Pressure Coeff. = 2.81

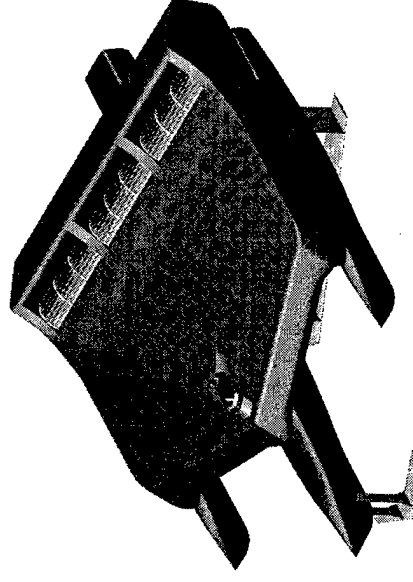
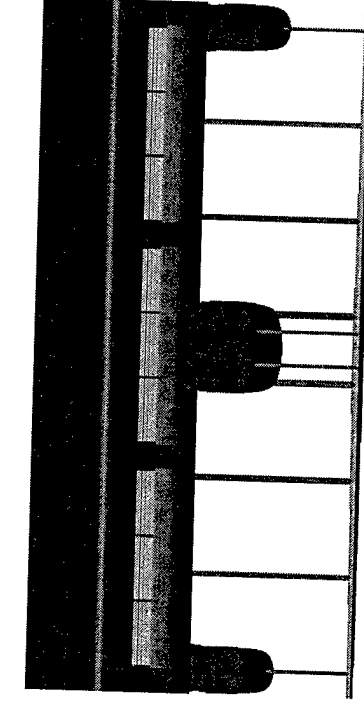
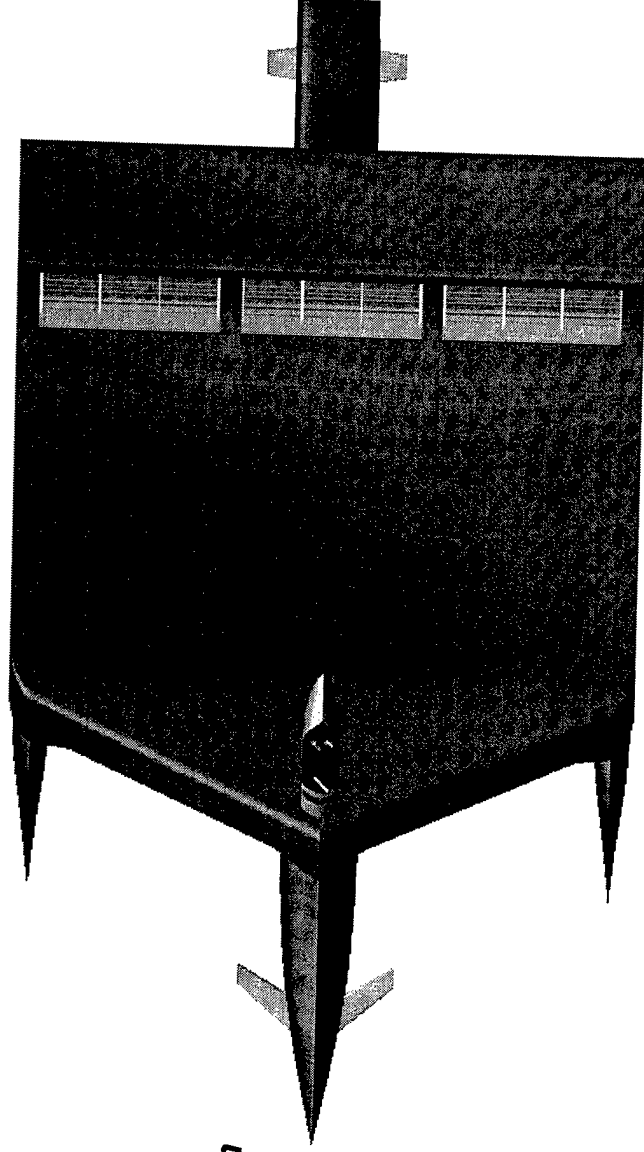
122 RPM, Tip Velocity = 192 ft/sec

Mass Flow Rate = 229 lbm/ft-span

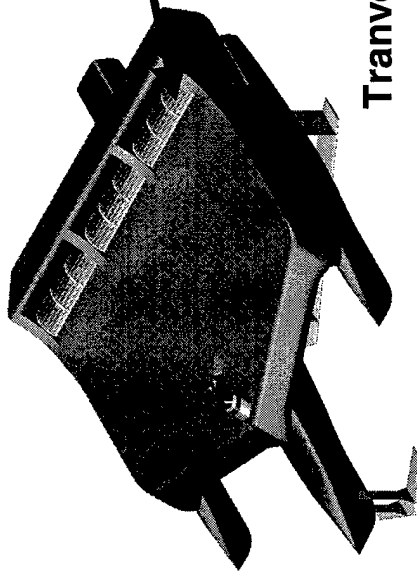
FPR=1.06, Exit Velocity=317.8 ft/sec

9.3' Nozzle Height, P=650 hp/ft-span

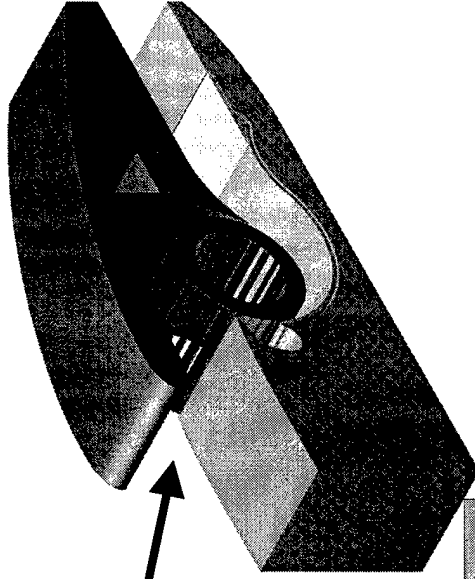
135,000 lbs thrust per Rotor.



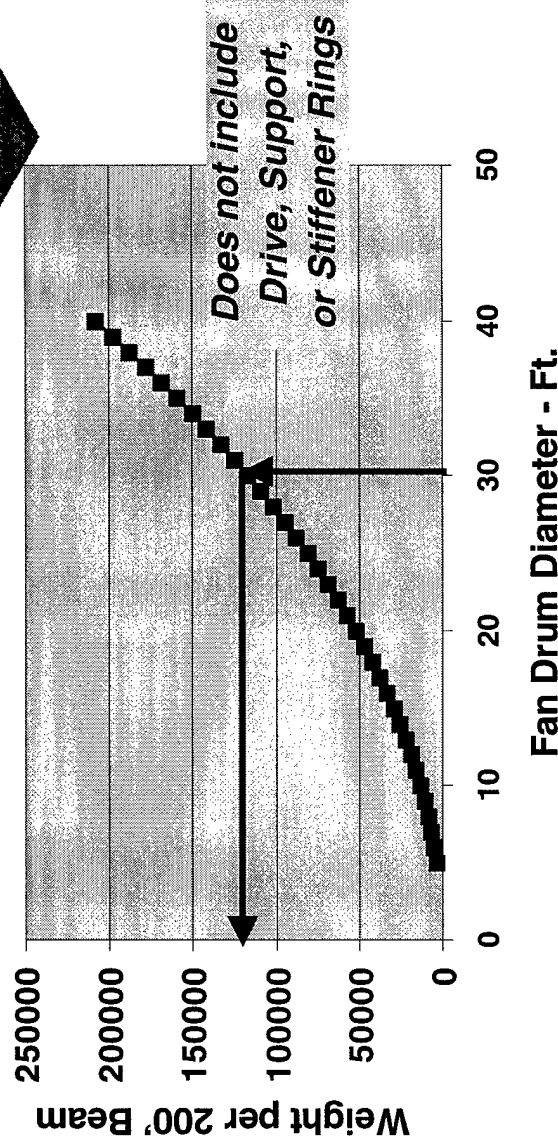
Transverse Fan Mass Properties Assessment



30' Transverse Fan
 30%R Chord Blades
 85% Efficiency
 Low Tip Speeds
 1.05-1.5 FPR's



Transverse Fan-Graphite/Epoxy Blades



Transverse Fan Segment Weights were estimated in the late 1970's with 30% solid Ti Blades. Current assessment makes use of graphite-epoxy strengths and densities.

Transverse Fan Development/Analysis Risks

Key Issues with Respect to the Transverse Fan

- 1. Integration needs a more thorough investigation.**
- 2. Lower Operating Range in FPR needs better definition.**
- 3. NASTRAN analysis conducted in the 1980's needs to be re-scaled and updated with modern materials/ fabrication techniques for a better understanding of its mass properties.**

Water-Coupled Propulsors Investigations

Candidates Include:

Conventional and Variable Pitch Propellers

**Requires State-of-Art Supercavitating Design Approach
Variable Pitch May Allow Constant Speed Shaft
Integration Effects and Fouling Will Be Key Issues**

Large Efficient Water Pumps

**Large Water Jets Being Developed-RR/Vickers/Kamewa
Jet Velocity Ratio Drives Net Propulsive Efficiency
Integration Effects and Fouling Will Be Key Issues**

Water-Coupled Propeller Performance*

Otto Scherer suggested that a water-coupled propeller could be in the 65% efficiency range for a 100,000 shp and 70 knot application. Performance tables were constructed using standard advance ratio and power coefficient data for candidate family of blade/sections. The propeller chosen for was of the Wageningen 4.55 B series designs and was used to provide throttle dependant thrust and fuel flows as coupled to a pair of LM6000 gas generators. At 70 knots approximately 300,000 pounds of thrust was developed using a 11.5 foot diameter screw rotating at 500 rpm. As expected the fuel flow went down appreciably to near goal type level, TSFC~0.113.

The following slides show the potential integrations with the hydrofoil ship. The issues are listed for each of the integrations.

***Otto Scherer Communication 5/25/00**

Water-Coupled Propeller Performance*

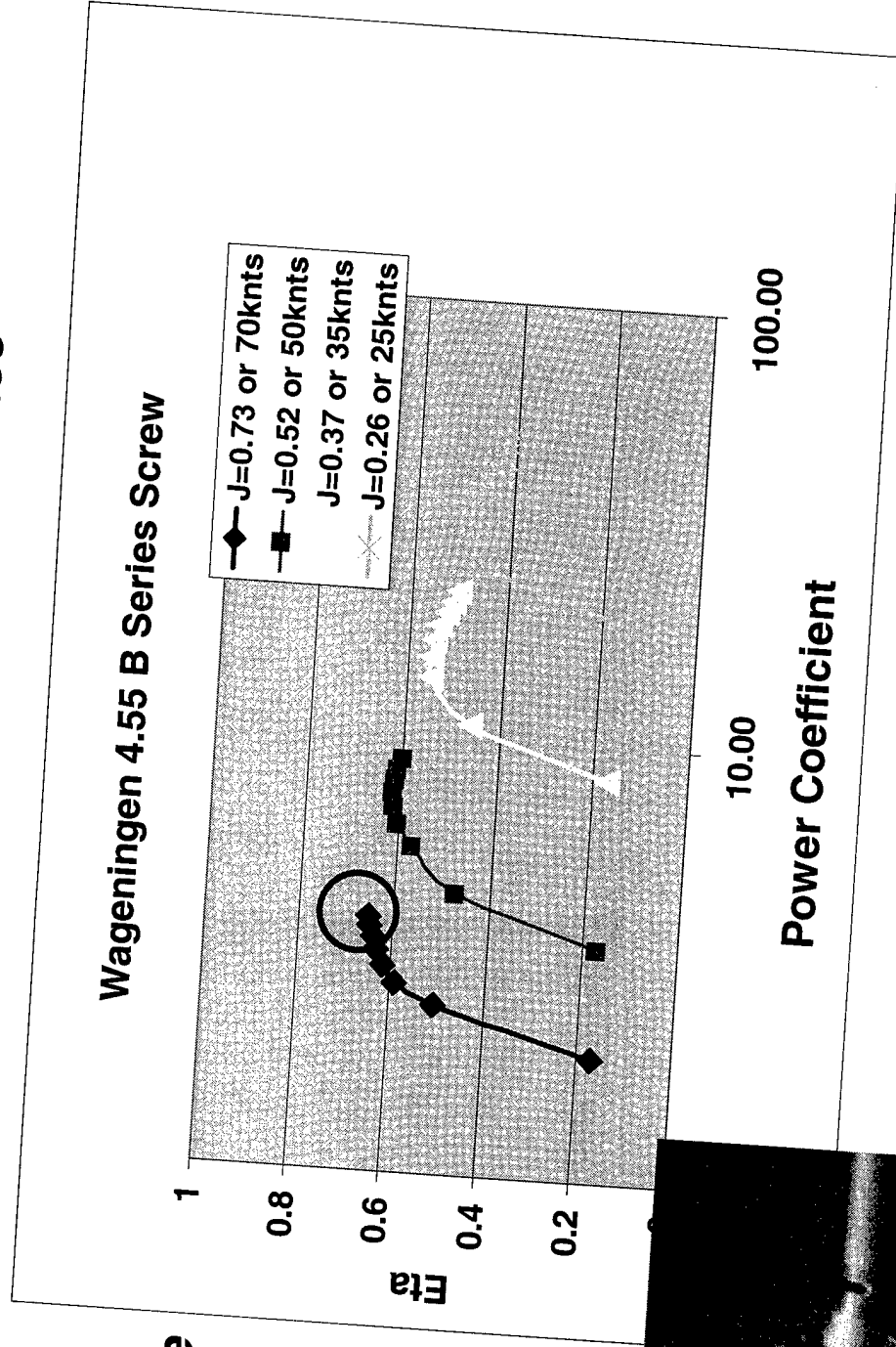
Example
Efficiencies are
derived from a

$B_p\text{-}\delta$
Diagram

$\eta_{net}=65\%*$



*Otto Scherer Communication 5/25/00

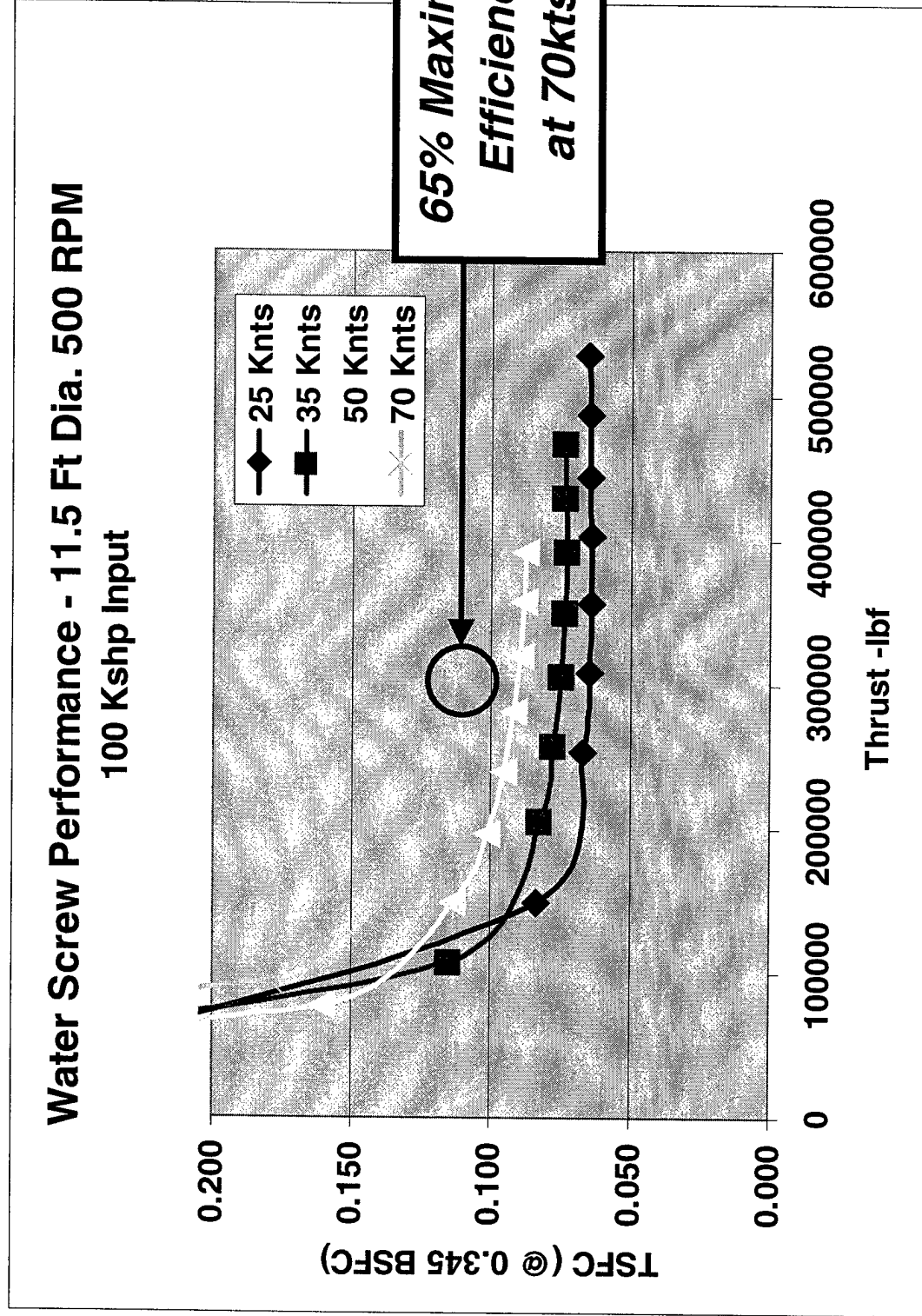


Power Coefficient, $B_p = nP^{1/2} / V^{5/2}$

Advance Ratio, δ (or J) = nD/V

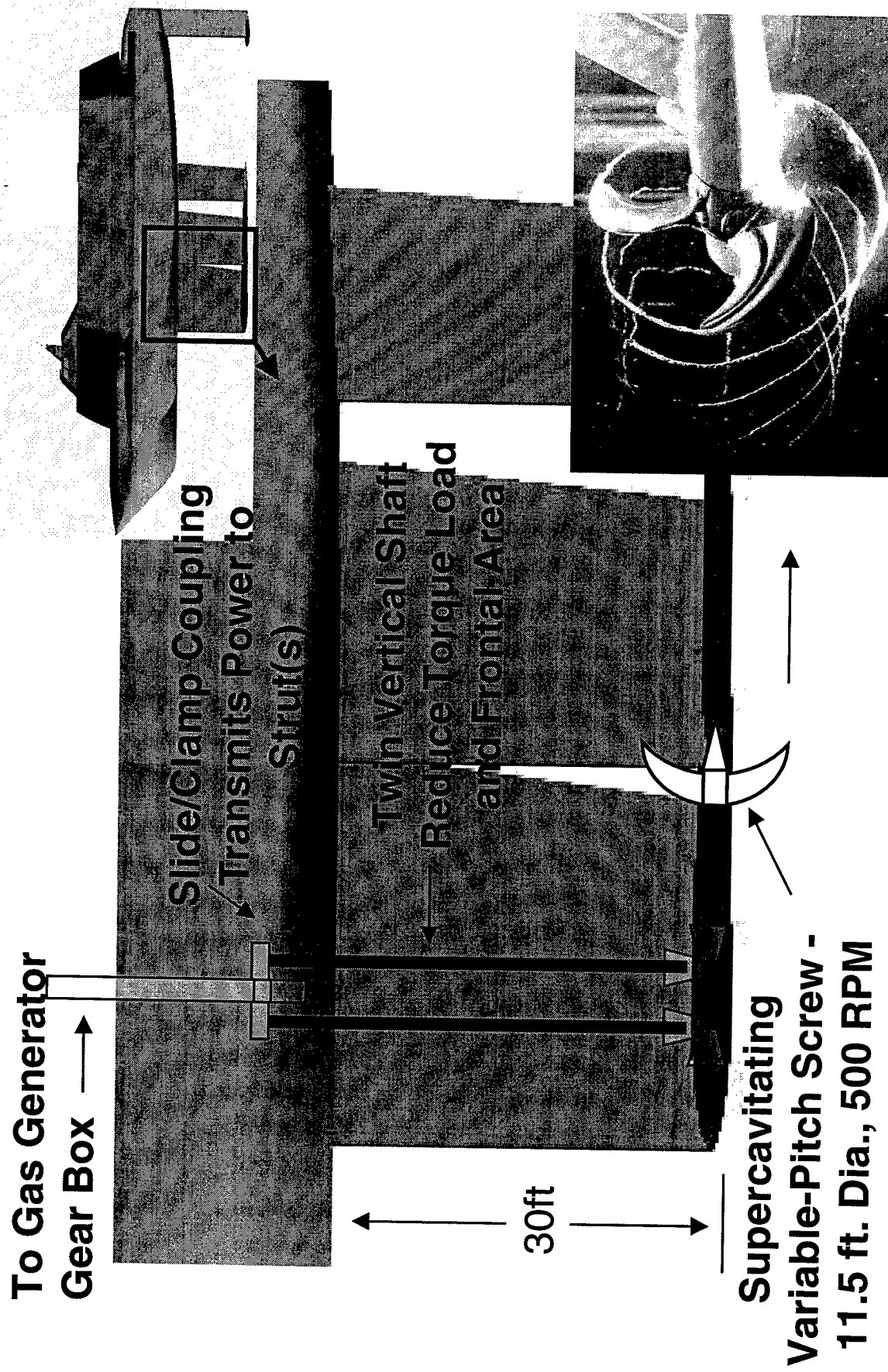
Eta = Net Efficiency = $\eta_{prop} \times \eta_{component}$

Water-Coupled Propeller Performance*

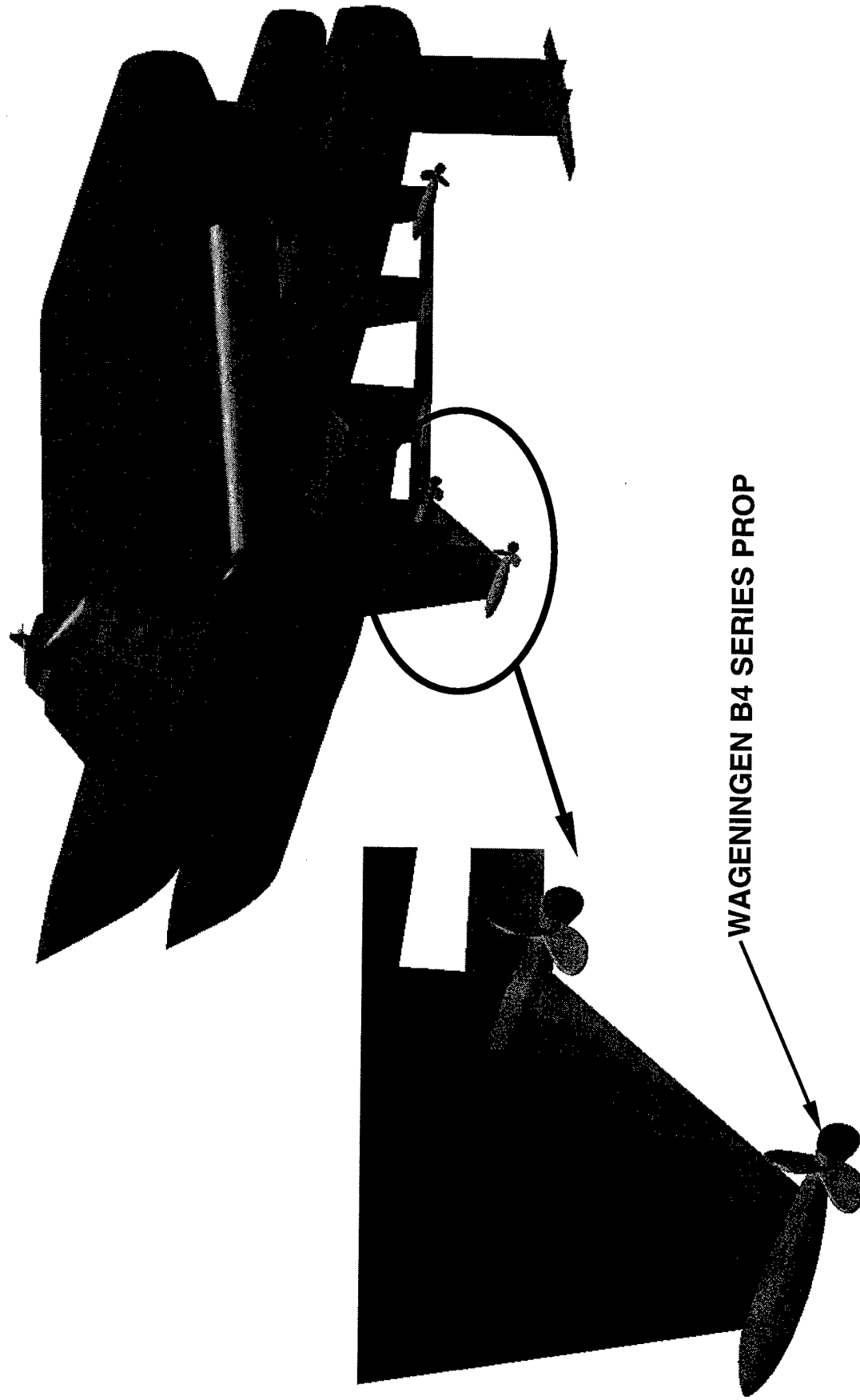


*Otto Scherer Communication 5/25/00

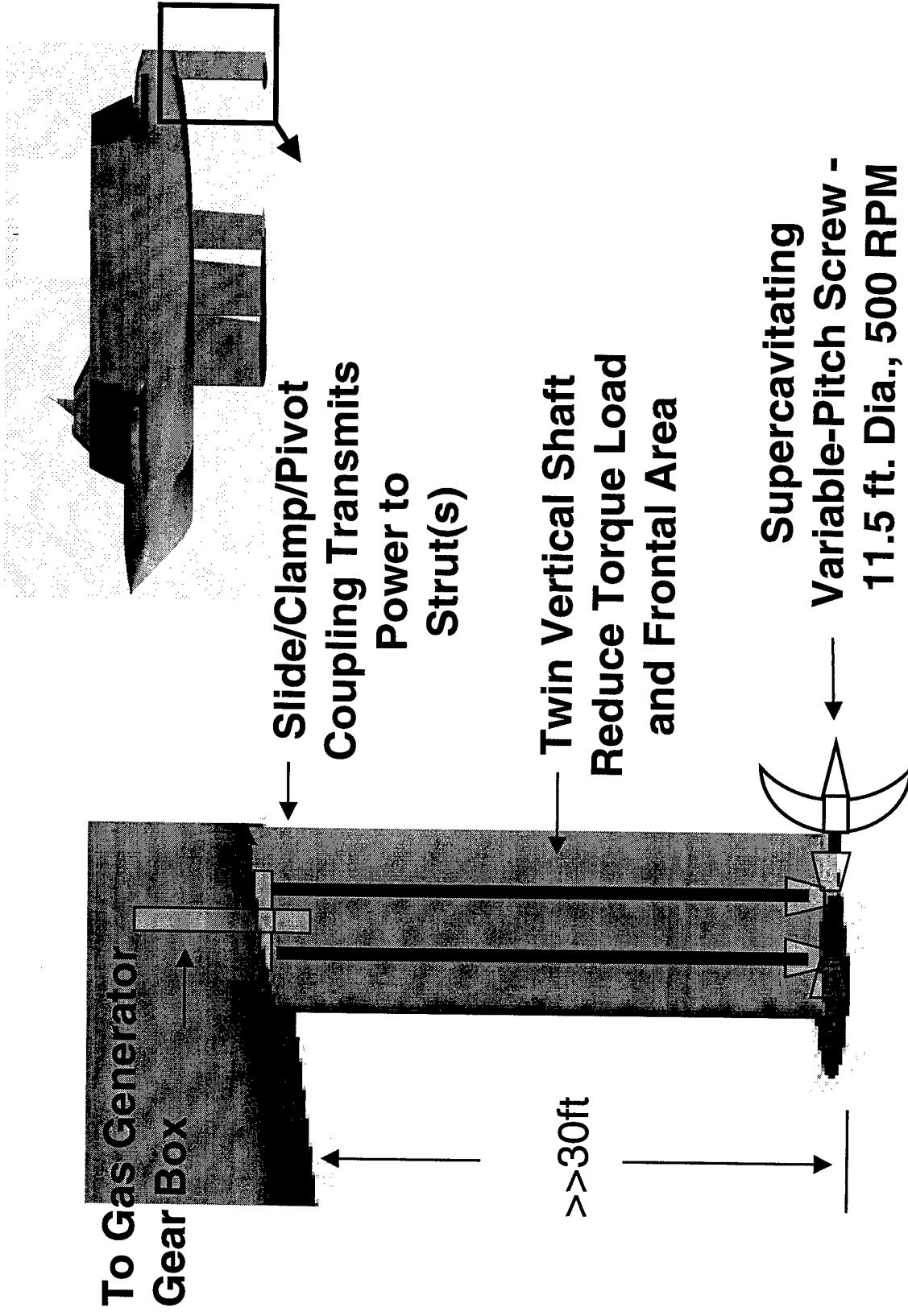
Water-Coupled Propeller Integration



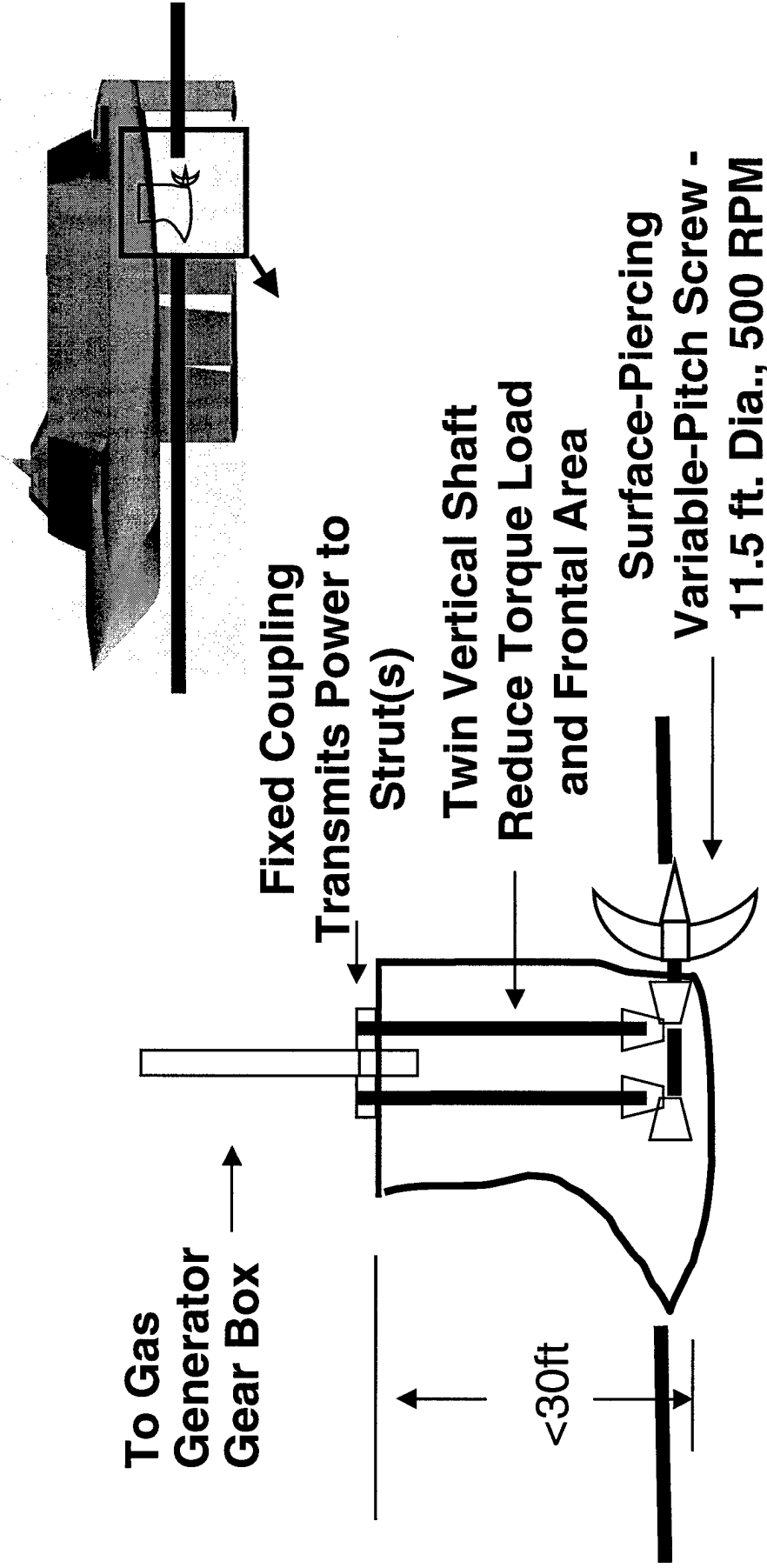
Hydrofoil Vessel – 4,000T – Water Screw



Propeller Alternate Integration-Stern



Propeller Alternate Integration-Dedicated Pod



The dedicated drive system operating with shaft near WL may be a minimum drag solution and lend itself to a fixed draft integration.

Water-Coupled Propeller Integration Impact

Increased Frontal /Base Area That Reduces System L/D

Localized Flow Acceleration at Foil/Strut Juncture Resulting in Possible Cavitation, Erosion and Vibration/Noise

Effects Due to the Increased Momentum of the Slipstream and the Interaction with the Hull/Strut/Foil.

Potential Stability and Control Implications

Operation in Shallow Draft Conditions

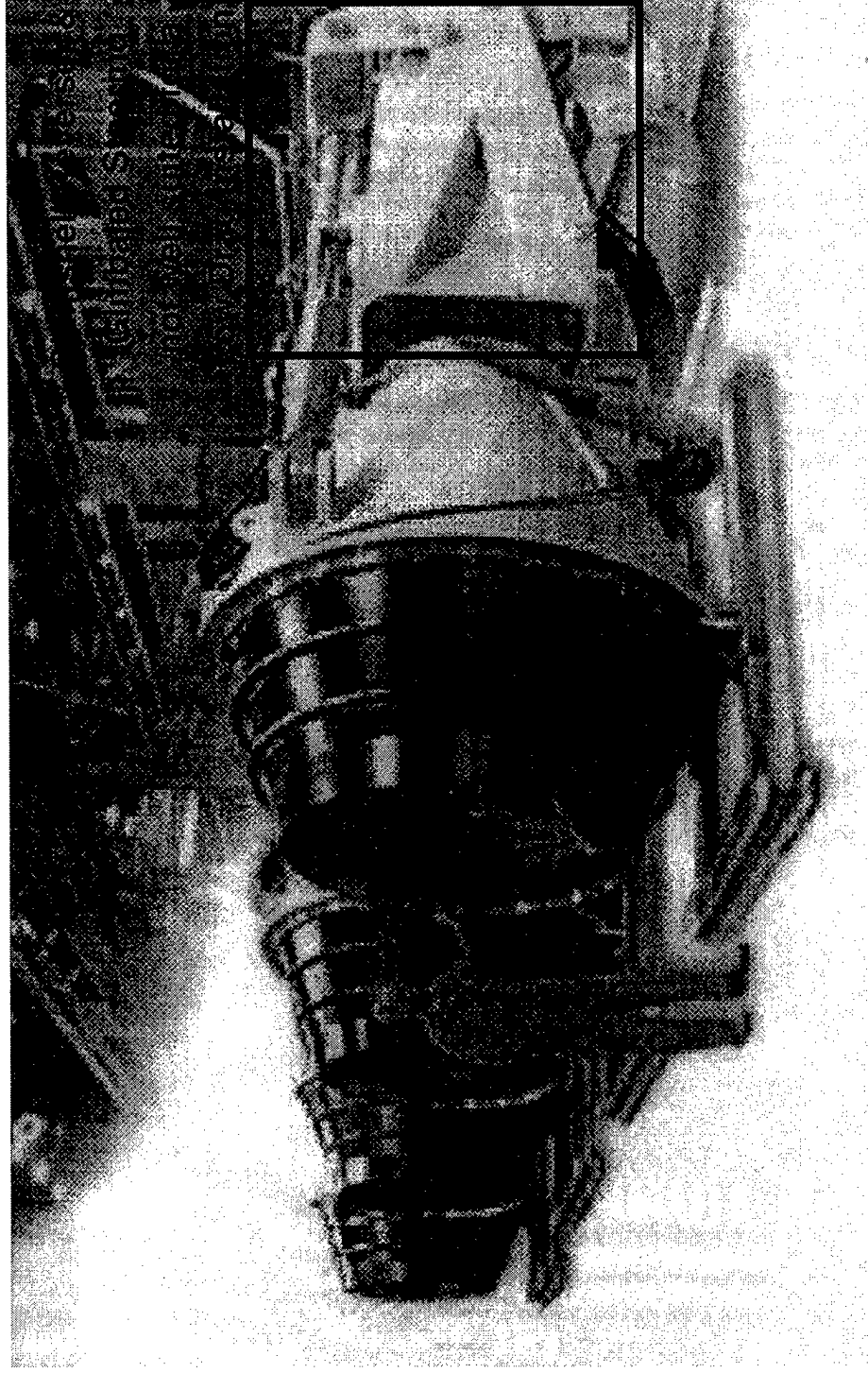
Water Jet Integration - Pump Characteristics

Large Efficient Water Pumps

Large Water Jets being developed by RR/Vickers/Kamewa for the FASTSHIP market are key candidates the hydrofoil and displacements ships for this study. As with any momentum transfer device, the jet velocity ratio sets the overall efficiency of the system. It is equivalent to disk loading and can be thought of as such. Up to this point in time the inflow velocity field has been assumed to be equal and opposite to the forward velocity of the vessel. This does not necessarily have to be true, and will be shown to have a favorable impact on the net propulsion efficiency and hence the thrust specific fuel consumption.

Water Jet Integration - Pump Characteristics

***This Large KAMEWA Pump is Sized for
the FASTSHIP Market and is Capable of
40 MW Power Input***



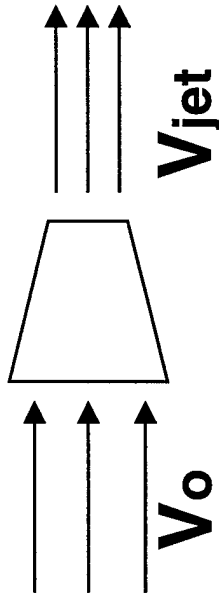
Water-Coupled Propulsors -Water Jets*

Data communicated to LM during this study* was used to develop candidate performance table and geometric integration. The Jet Velocity Ratios (JVR's) selected were in the range of 1.4 to 1.8. For a 100K shaft horsepower input the corresponding thrust and fuel consumption are shown. Note that the geometry of the pump, while not specified directly, is implied with respect to the inlet, nozzle and pump impeller rotational rate.

Note the high component efficiency of the pump and how a jet velocity ratio of 1.4 nearly achieves the goal of a 0.10 TSFC. Integration into the varied vessels became the emphasis of the effort with respect to the water coupled system design.

***Otto Scherer Communication 5/25/00**

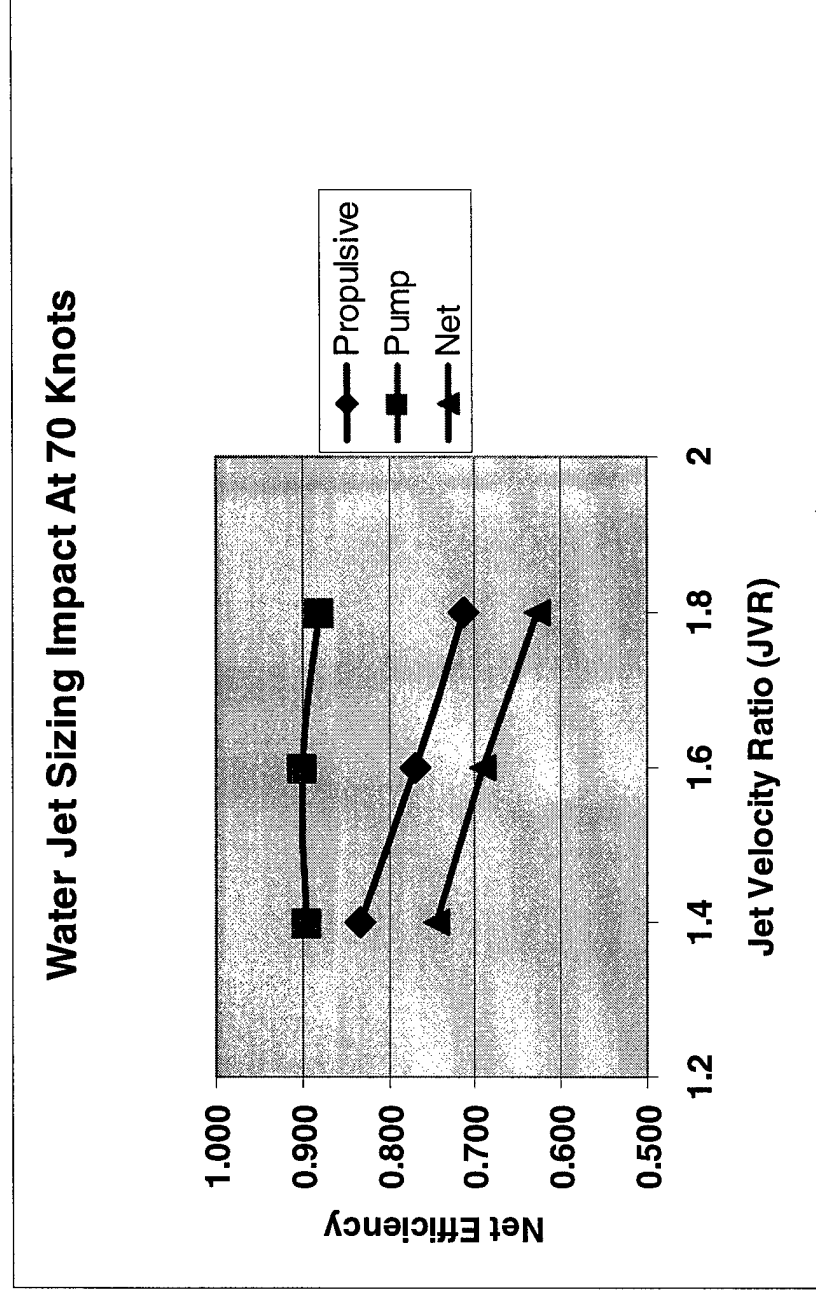
*Water-Coupled Propulsors -Water Jets**



Pump Efficiency
Defined by
Design / Type

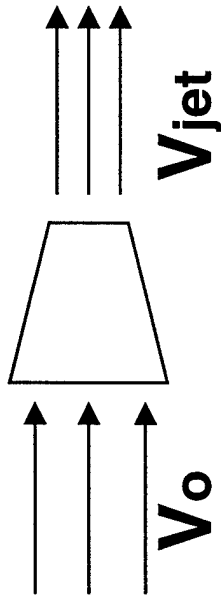
Propulsive Efficiency

$$\eta_{prop} = 2 / (1 + V_{jet} / V_o)$$



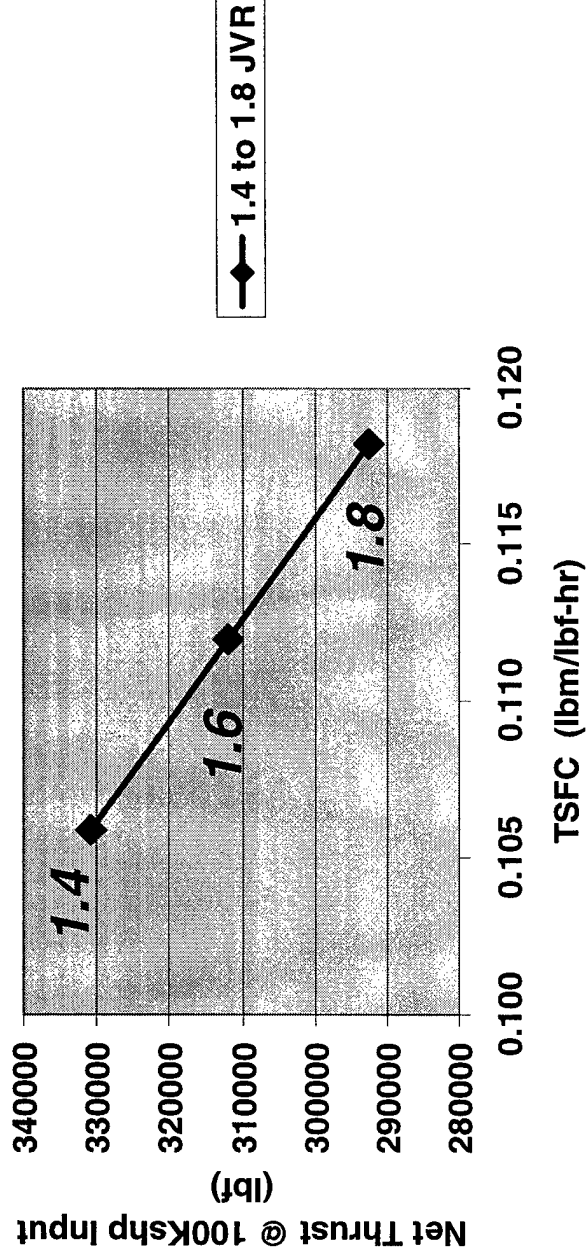
*Otto Scherer Communication 5/25/00

Water Jet Sizing Characteristics-100kshp



JVR	RPM	Dinlet	Drotor	Dnozz	CFS
1.4	316	7.77	9.32	5.16	3464.0
1.6	502	6.16	7.39	3.83	2178.0
1.8	650	5.45	6.54	3.03	1531.2

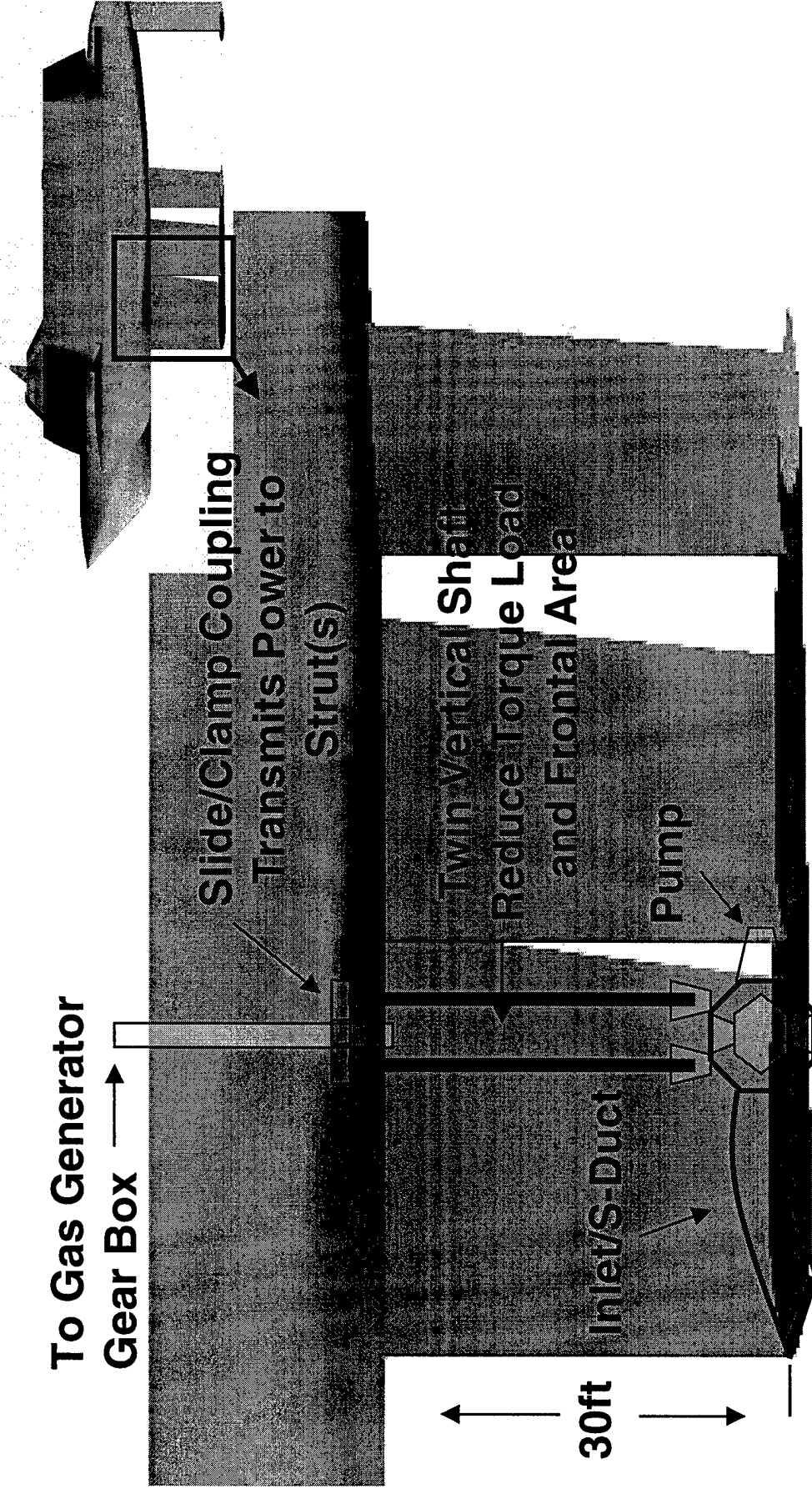
Water Jet Sizing Impact - 100 Khp Input
(2 x LM6000 @ BSFC=0.345 lbm/shp-hr)



Water Jet Integration - Pump-In- (Strut or Tail)

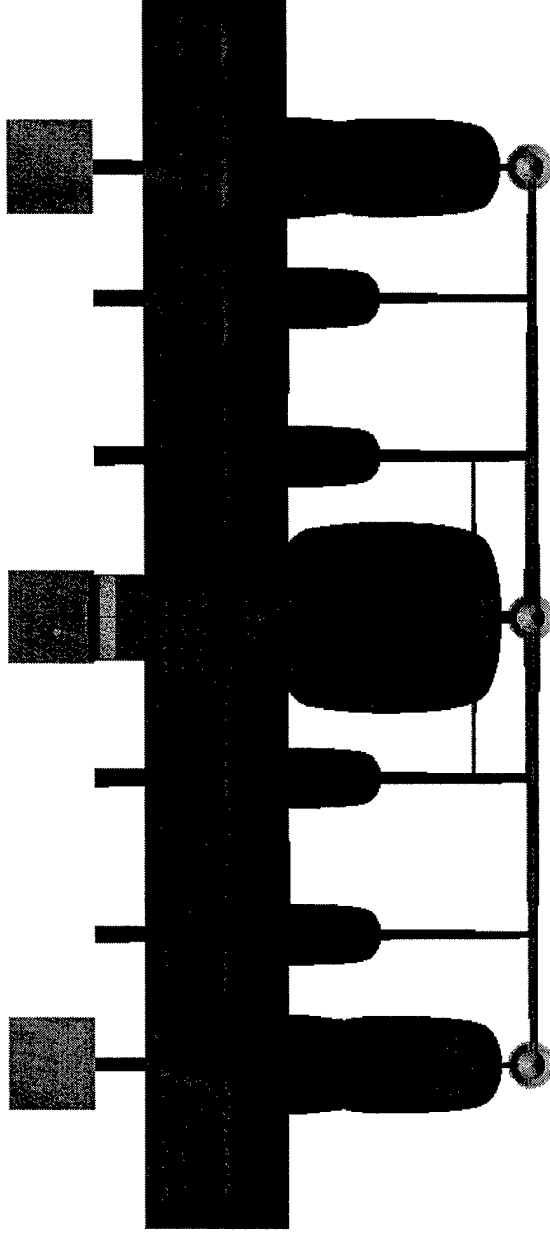
Two potential integrations of the water jet into the hydrofoil make use of the vertical support of the foil or horizontal tail. The key in each of the integrations is the need for reduced frontal area to keep strut wave, profile, and spray drag a minimum. Torque loads can be distributed across two vertical drive shafts and combined at the pump. Shaft speed from the LM6000 will be kept at 3600 rpm and then dropped at the pump with a gear reduction of 10:1 or 12:1. Slide and clamp couplings between the vertical drive shafts and the gas generator may allow both cruise and berthed pump operations.

Water Jet Integration - Pump-In-Strut



***Inlet, Transition Duct and Pump Translate with Foil
Powerplant Remain Fixed in Hull***

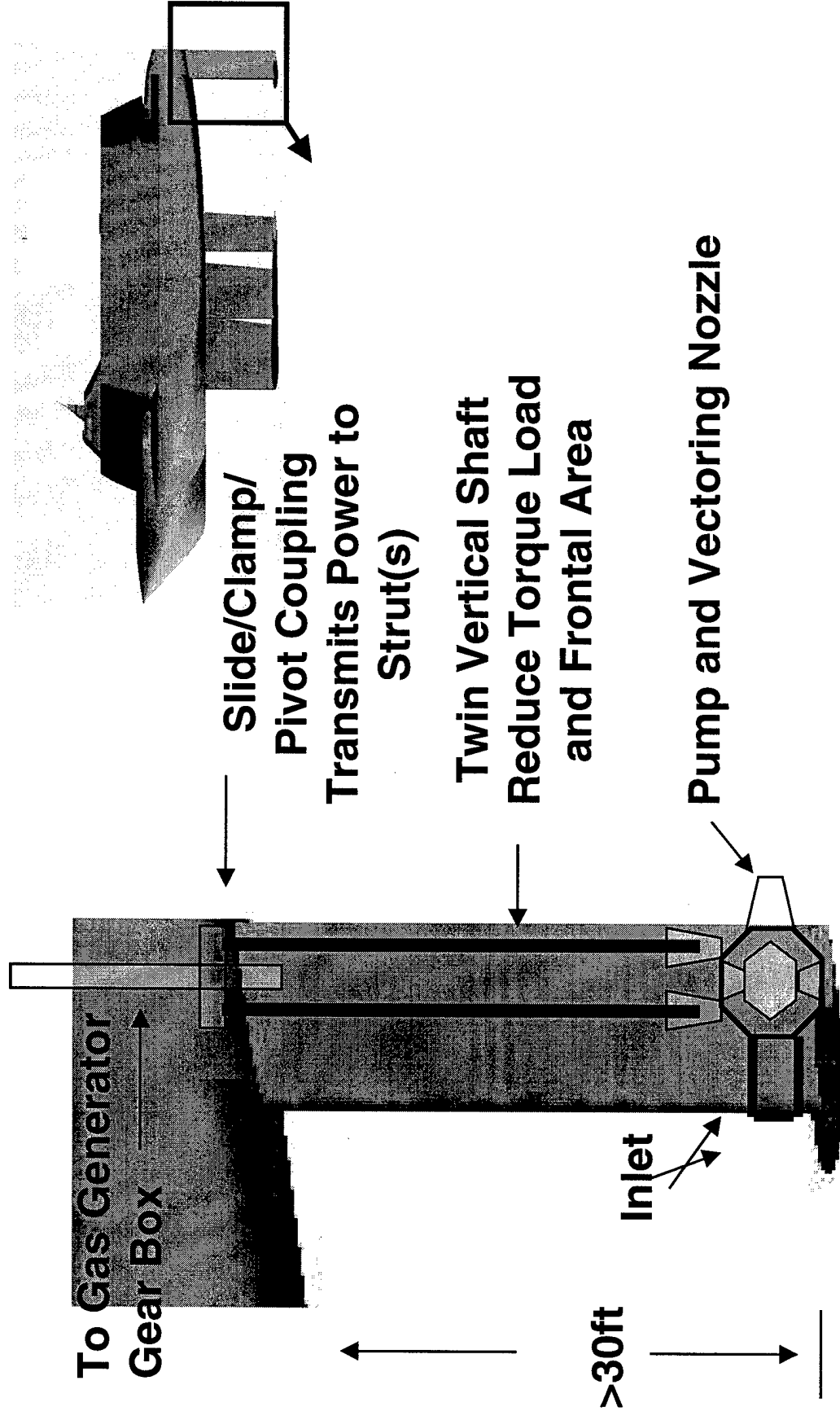
Hydrofoil Vessel – 4,000T – Jet Pump



LM6000 GAS TURBINES



Water Jet Integration - Pump-In-Tail



***Inlet, Transition Duct and Pump Rotate with Foil
Powerplant Remain Fixed in Hull***

Water Jet Integration - Pump-In-Strut Impact

Increased Frontal /Base Area That Reduces System L/D

Localized Flow Acceleration at Foil/Strut Junction Resulting in Possible Cavitation

Effects Due to the Increased Momentum of the Jet and Interaction with the Hull/Strut/Foil.

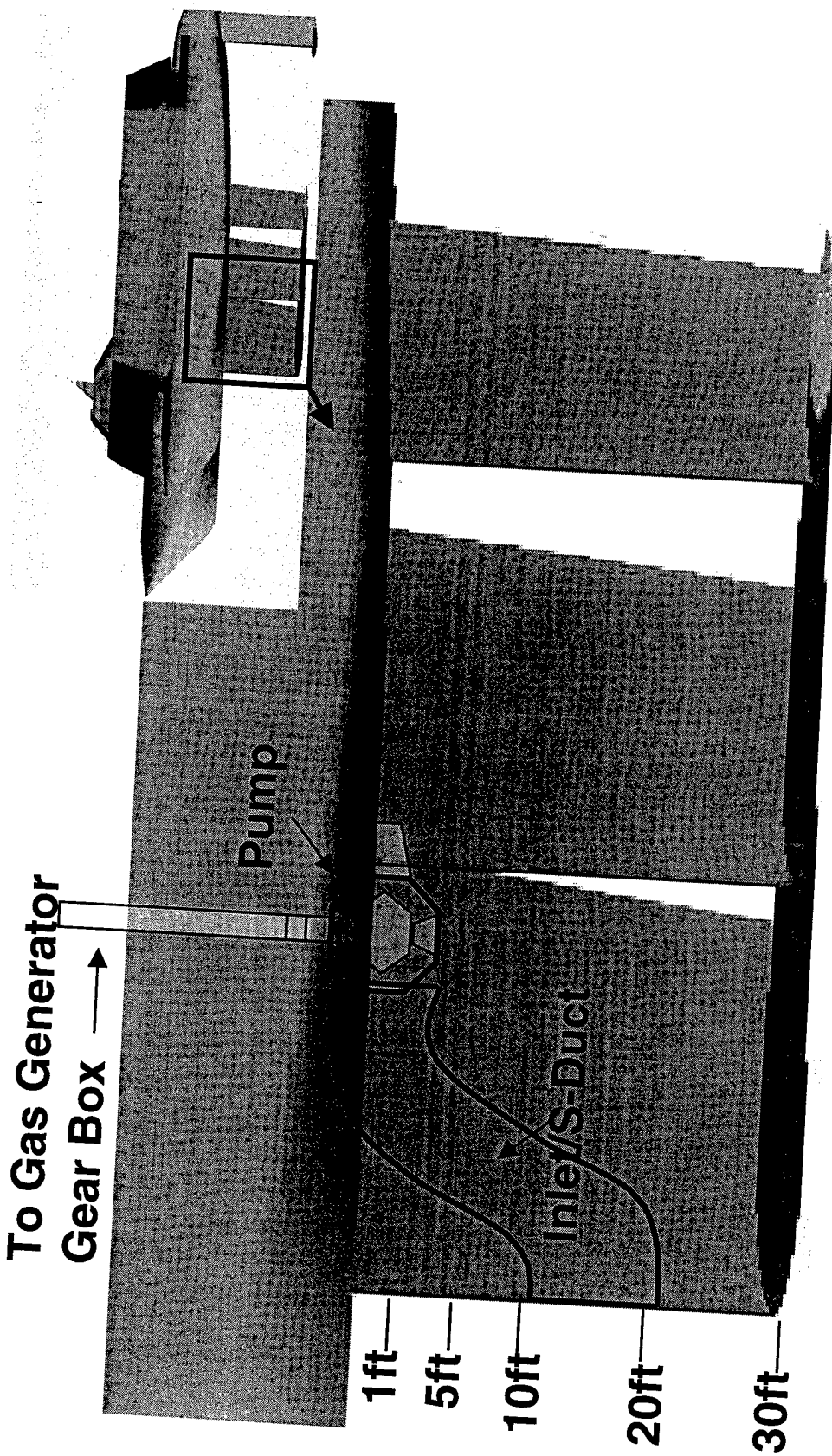
Potential Stability and Control Implications

Operation in Shallow Draft Conditions

Water Jet Integration - Pump-In-Hull

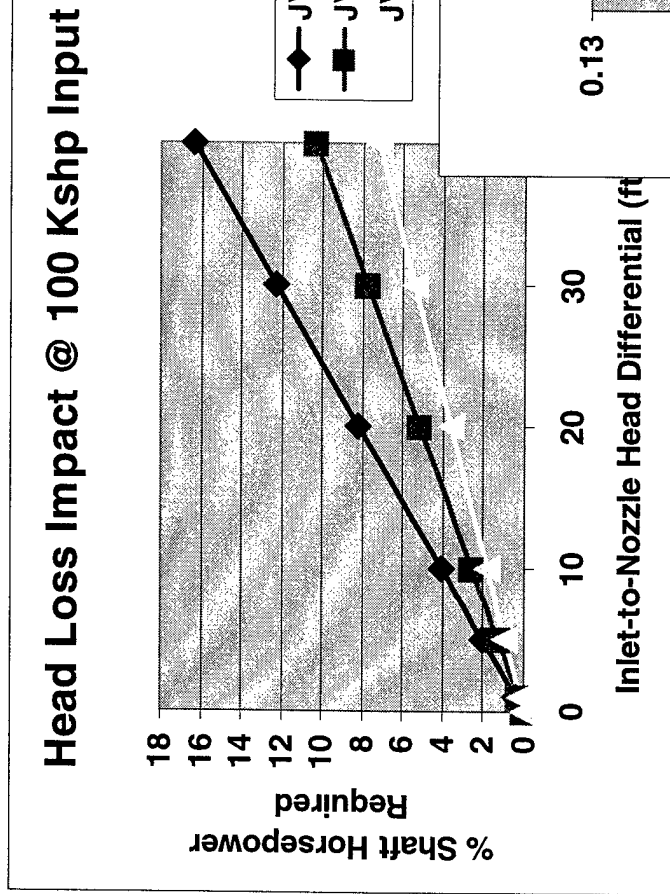
Analogous to the Boeing Hydrofoil concept, the water jet pump may be integrated into the hull and a fixed drive used to join it to the gas generator. Water is ingested from an inlet near or below the free surface and ducted to the pump. The impact of the loss in piezometric head was calculated for several elevation differences between the pump exit and the inlet capture waterline. At 20 foot variation in head, the variation in horsepower loss is from 2% to 8% for JVR1.8 to JVR1.4 respectively. Second order effects will include, but not be limited to, wave and spray drag impact associated with the modified strut shape and additional losses in the capture inlet flow.

Water Jet Integration - Pump-In-Hull

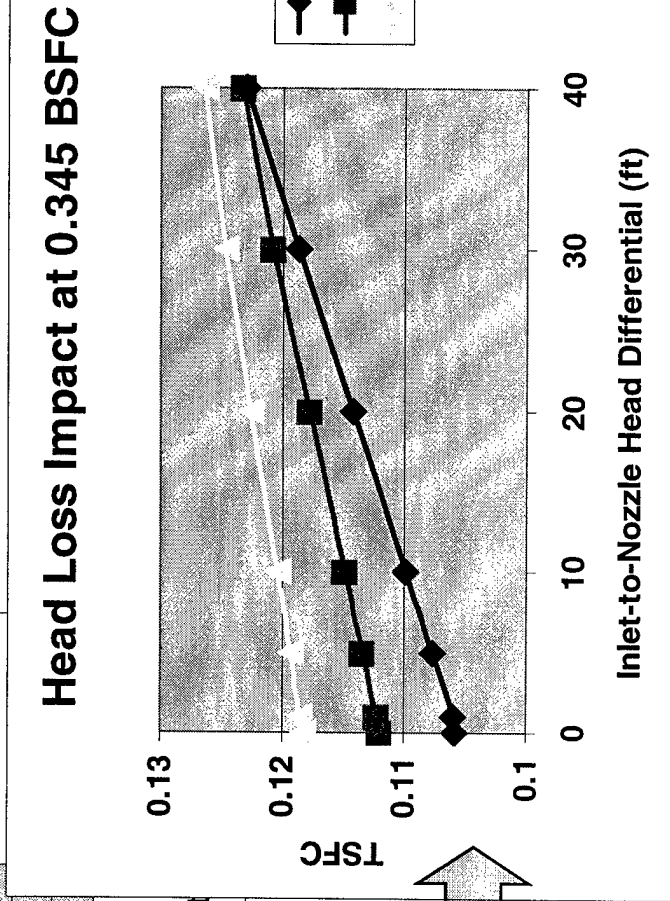


***Inlet and Transition Duct Translate with Foil
Pump and Powerplant Remain Fixed in Hull***

Water Jet Integration - Pump-In-Hull Impact



Higher JVR relates to Lower Head Loss due to Lower Jet Massflow



Momentum Loss by increasing the head is not recovered in Axial Thrust

Water Jet Integration - Pump-In-Hull Impact

Increased Frontal /Base Area May Reduce System L/D

Head Increase Results in Thrust Loss

Potential Inlet Seal Issues with Pump and the Pressurization of the Strut.

Effects Due to the Increased Momentum of the Jet and Interaction with the Hull/Strut/Foil.

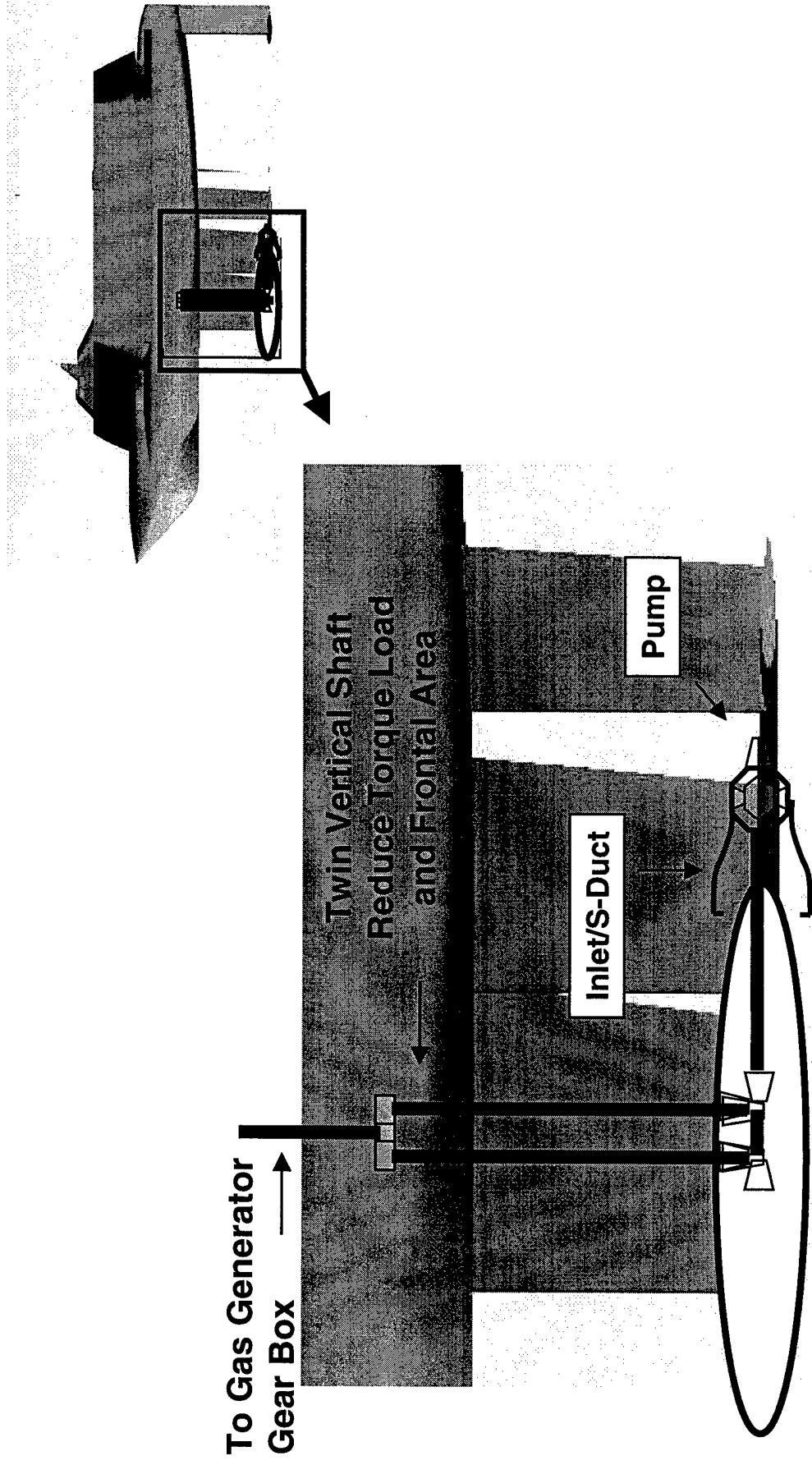
Potential Stability and Control Implications

Operation in Shallow Draft Conditions- Auxiliary Inlet System Needed.

Water Jet Integration - Pump In Body w/ Ingestion

The pump-in-body is adaptable to both the hydrofoil and the buoyant body design integrations. As shown in the following slide, the pump is placed in a shadow of a body of revolution and as such, removes the pump drive shaft from the flowfield. Boundary layer ingestion off of the body modifies the inlet capture flow momentum content as is shown in the successive slides. The result is surprising as the net propulsive efficiency increases and is reflected in a overall drop in fuel consumption (TSFC).

Water Jet Integration - Pump In Body w/ Ingestion



Powerplant, Inlet, Body and Pump Translate with Foil

Momentum Deficit Ingestion Impact

Propulsive efficiency is defined as the:

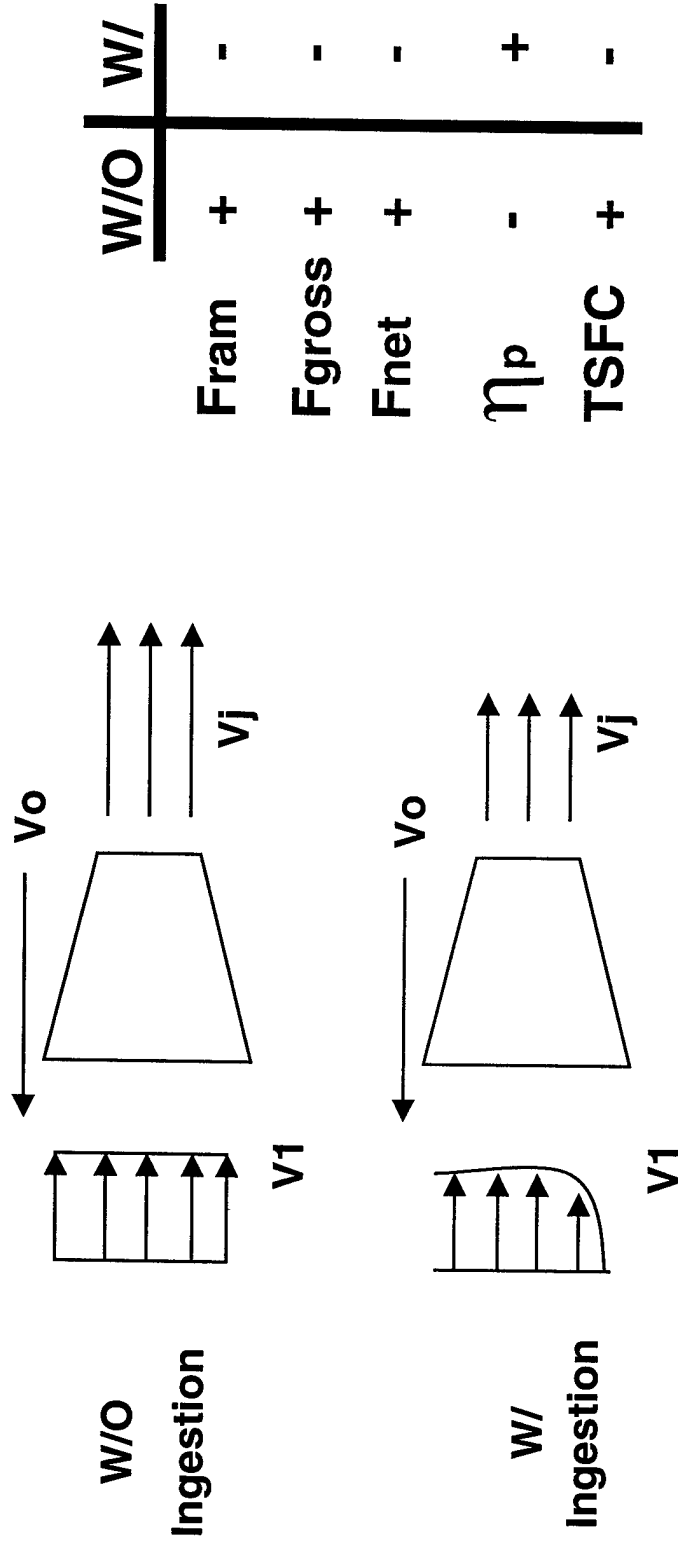
Thrust Power

Thrust Power + Power Loss

where the Thrust Power is the force applied to the vehicle times the distance moved per unit time and Power Loss is the kinetic energy of the jet relative to the vehicle.

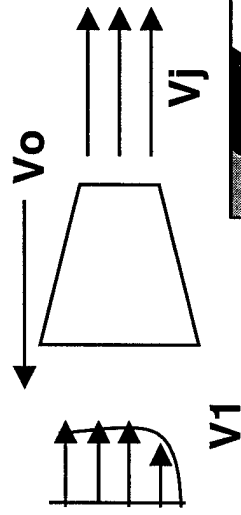
For a net decrease in the capture stream momentum the propulsive efficiency is enhanced. There is a potential for increased fuel economy provided the ingestion of the lower momentum does not adversely affect the component (pump) efficiency.

Water Jets with Momentum Deficit Ingestion



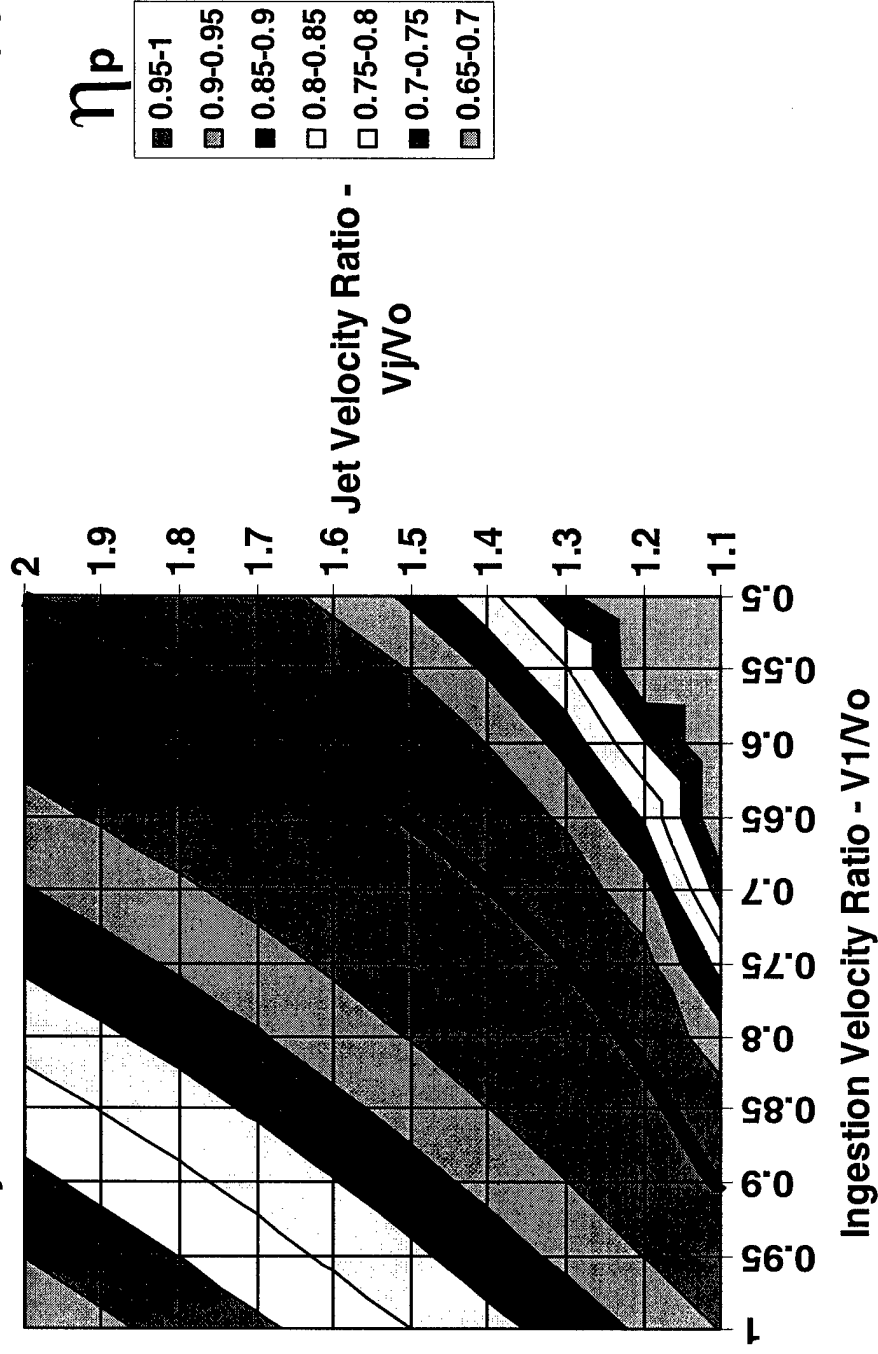
For a fixed jet velocity ratio the net thrust drops as the momentum of the inlet stream decreases. Horsepower required decreases and the trend is a decrease in TSFC.

Water Jets with Momentum Deficit Ingestion

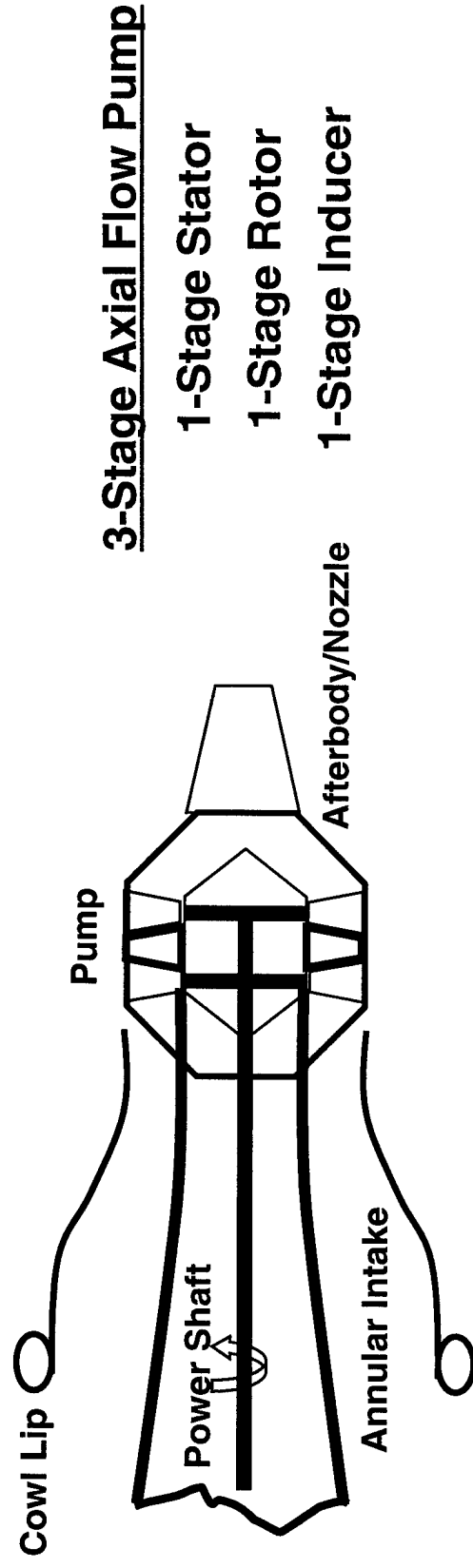


Propulsive Efficiency $\eta_p =$

$$\frac{1}{1 + \frac{1(Vj - Vo)**2}{2Vo(Vj - V1)}}$$



General Pump-in-Body Integration Considerations



- Intake to Water Pump will be Annular in Shape and Sized for Minimum Spillage and Momentum Loss at Cruise Point.
- Intake Cowl Lip may cavitate at high capture ratios.
- Removal of the Input Power Shaft from the Inlet will increase pump efficiency.
- Cowl and Pump Afterbody will need to be tailored for low drag.

General Pump Performance Considerations*

JVR	RPM	Dinlet	Drotor	Dnozz	CFS	Ns	NSS
1.4	316	7.77	9.32	5.16	3464.0	6869	6253
1.6	502	6.16	7.39	3.83	2178.0	6098	7876
1.8	650	5.45	6.54	3.03	1531.2	-	-

Ns – Pump Specific Speed

JVR1.4 JVR1.6

$$= \frac{N}{(Q)^{0.5}}$$

$$\text{Head} = 79 \text{psig} \quad 122 \text{psig}$$

$$H^{0.75}$$

N=Pump Shaft Speed

Q=Capacity in GPM

H=Total Head in Ft. at 70 Knots

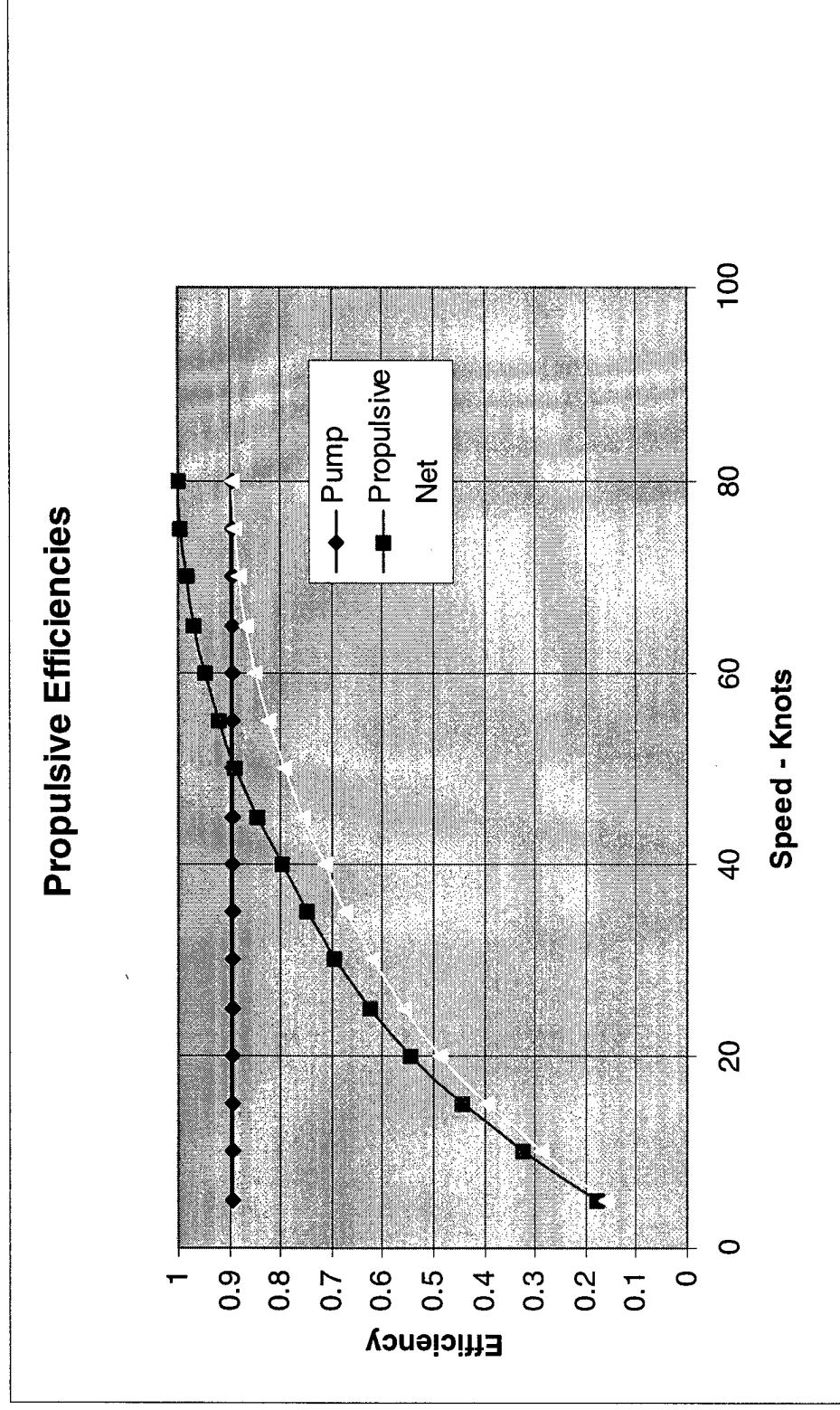
Nss – Pump Suction Specific Speed, as Ns

replacing H with NPSH- Net Positive Suction

Head necessary to preclude cavitation.

**Data Table Units in Feet and Sized to a 100KSHP Power Transmission*

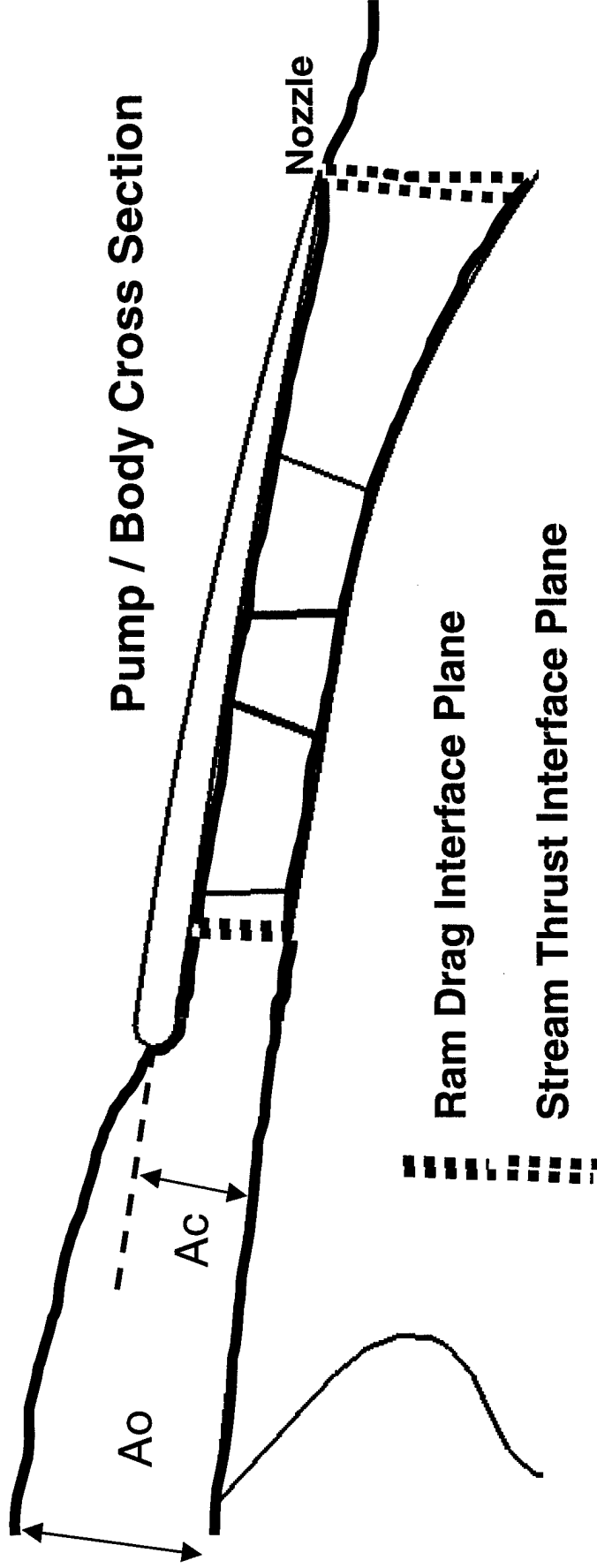
Efficiency Maximum is Set Near Maximum Desired Speed



Pump Component Efficiency will change with NS and NSS (specific speeds).

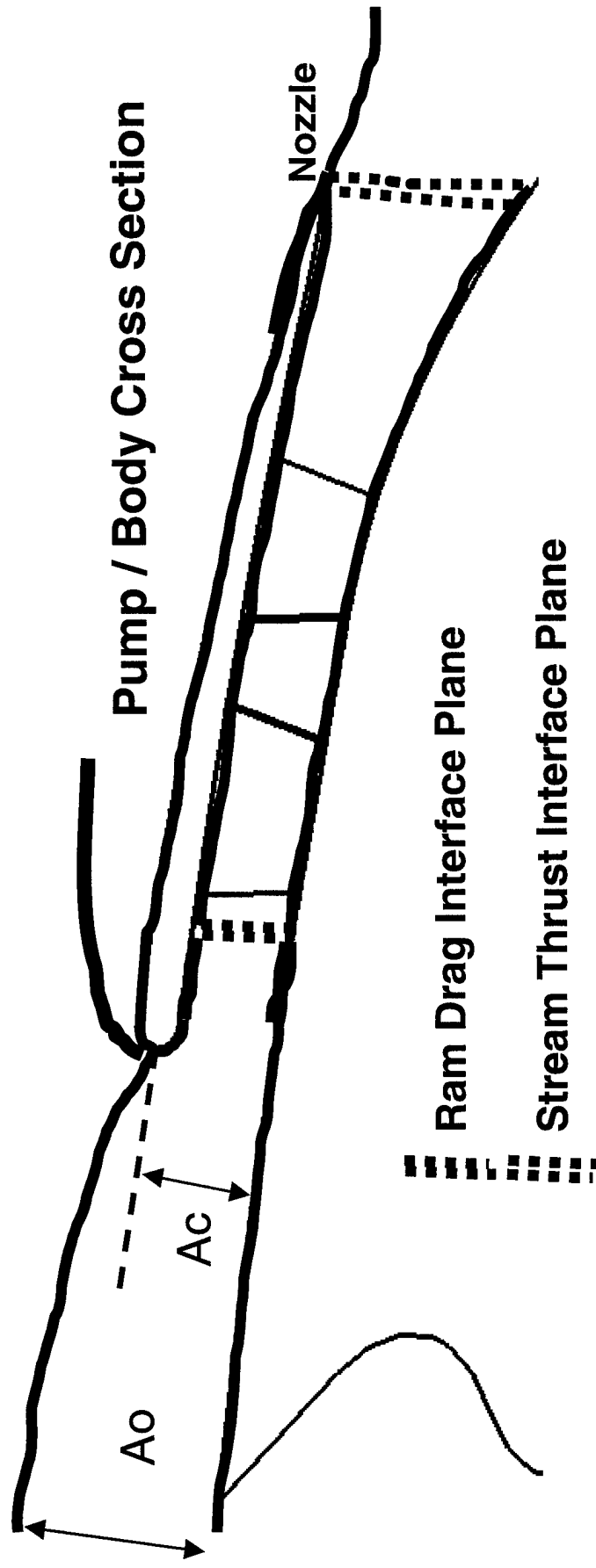
Goal is to Implement Actual Pump Data in Future Estimates.

Thrust-Minus-Drag Bookkeeping Considerations



- Propulsion Momentum Streamtube – Force Balance
- Assumes Hydrodynamic Reference Drag Conditions, $A_o=A_c$
- Pump Control Volume- Treated as a “Black Box” device.
- Assumed NS, NSS and internal efficiency.

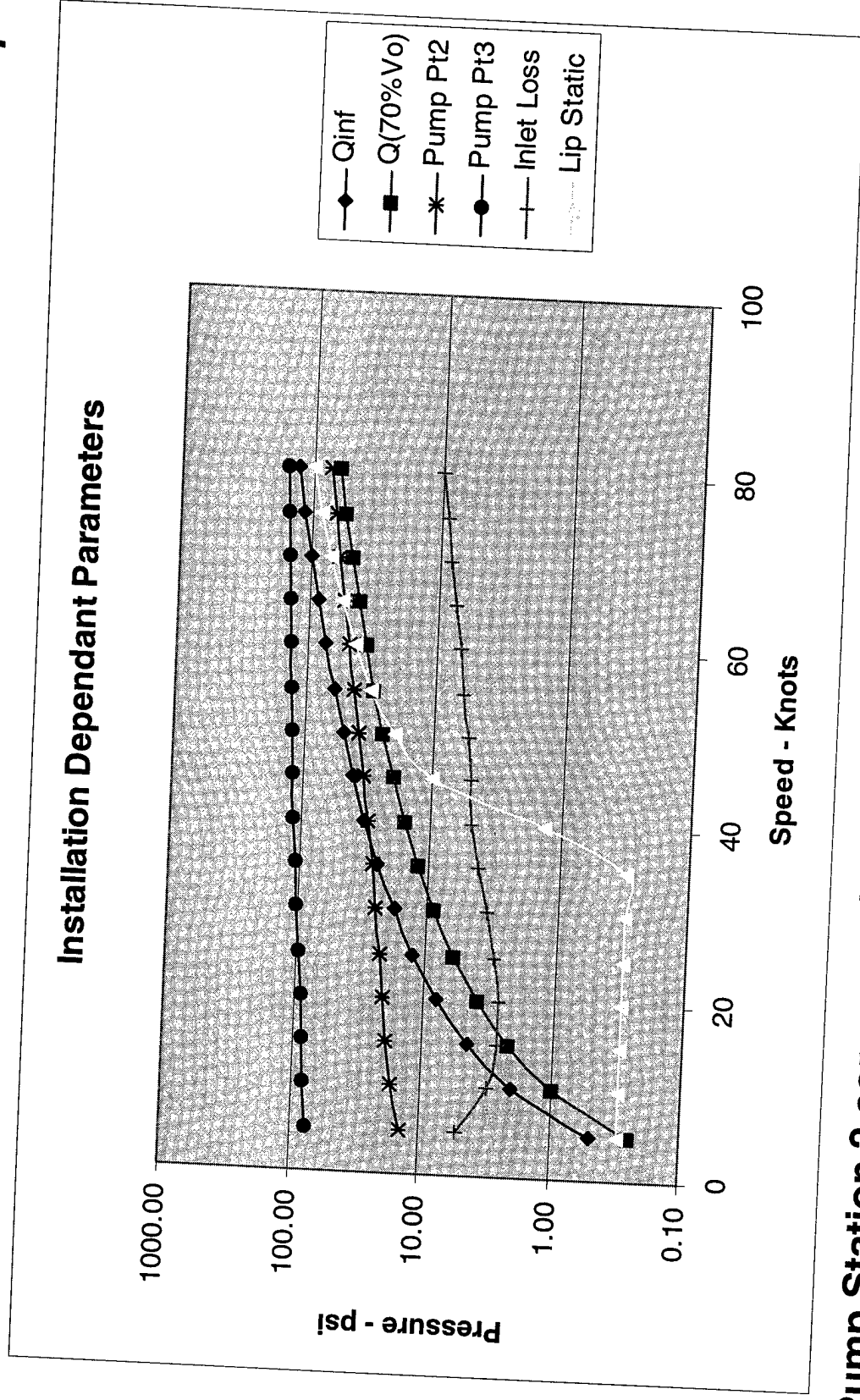
Thrust-Minus-Drag Bookkeeping Analysis Components



- Hydrodynamic Reference Drag Conditions, $Ao=Ac$
- Nozzle Boat Tail and Nozzle Throttle Dependant Forces
- Pump Component Efficiency
- Pump Inlet/Diffuser Total Pressure Losses
- Spillage Drag Increment for $Ac>Ao$
- Additive (or Approach) Drag and Lip Losses for Ao

Not Included
To Date

Pump Inducer Face Total Pressure Losses..Define Pump ΔP

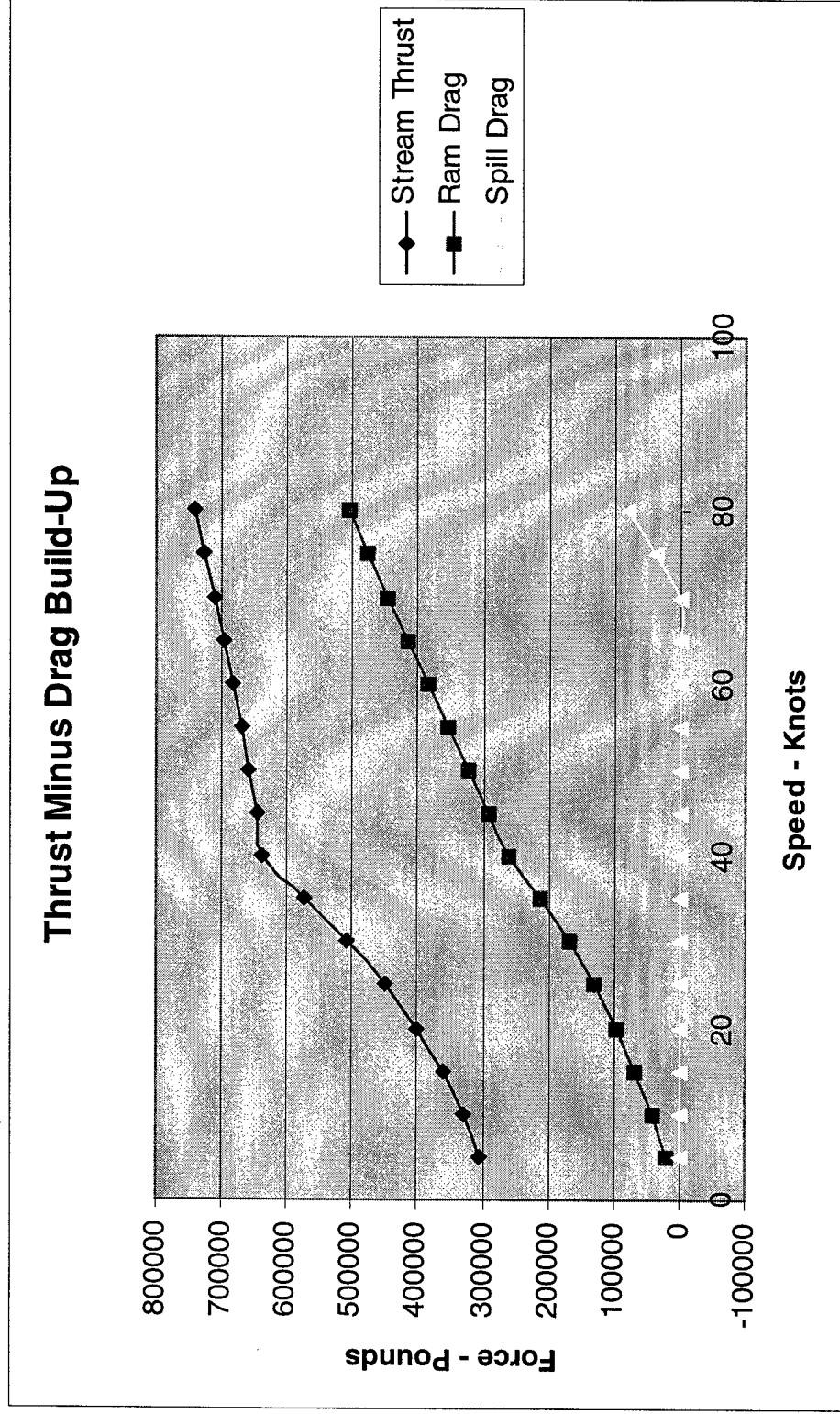


Pump Station 2 corresponds to Inducer Face and defines Ram Conditions

Pump Station 3 corresponds to Rotor Exit and defines Stream Thrust

...Results in the Following Thrust-Minus-Drag Build-up

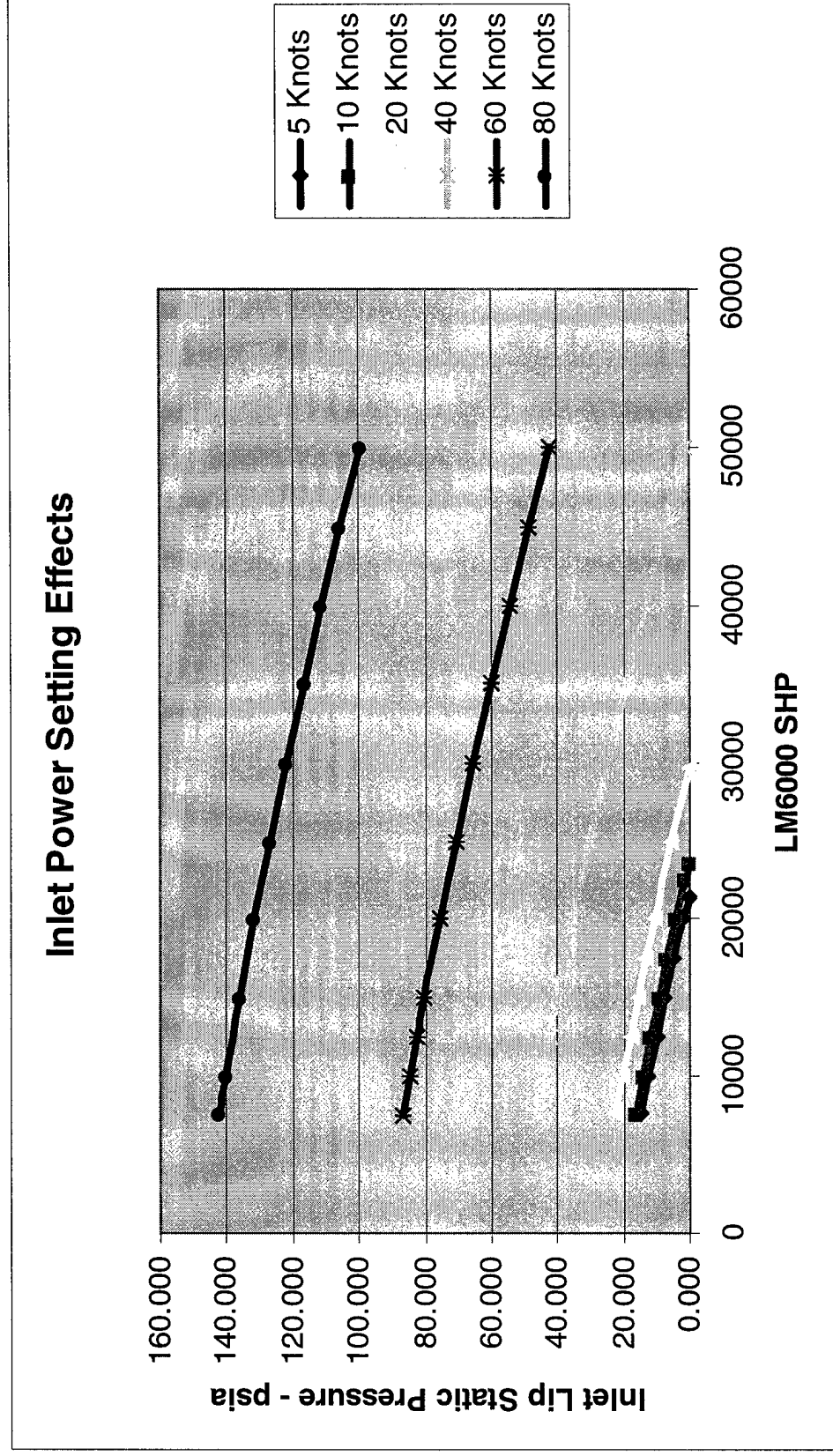
Below 40 knts the throttle is cut-back to prevent intake cavitation!



Above 70knts the inlet spills..resulting in a large increase drag increment.

Downsizing the inlet kills low speed performance at hump speeds!

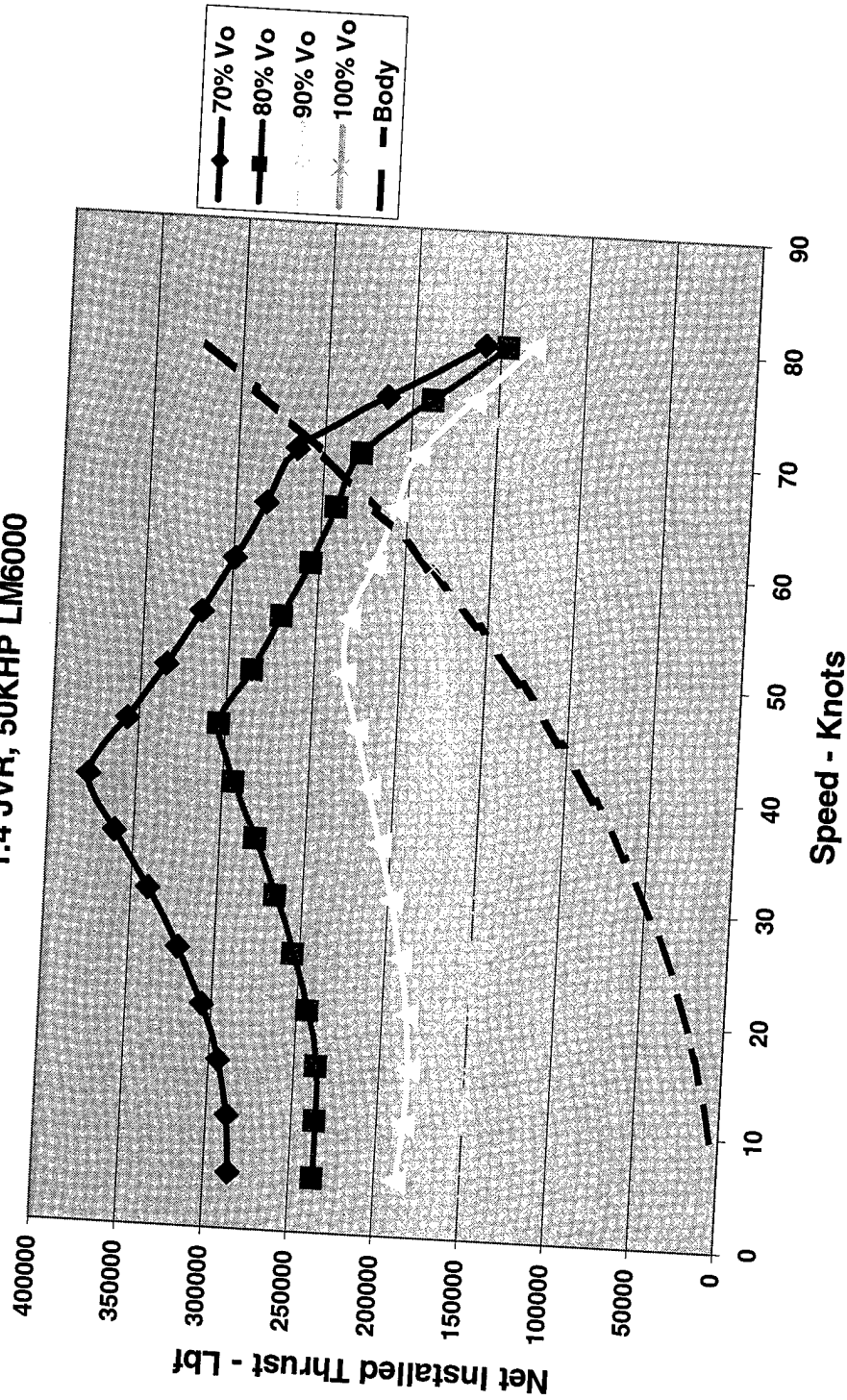
Power Setting Criteria Dependant on Integration



Throttle is Cut-Back for Low Speed and Acceleration. Lip Static Pressure nears Cavitation Critical Pressure at 10' Depth

Thrust Variation with Speed and Power Setting

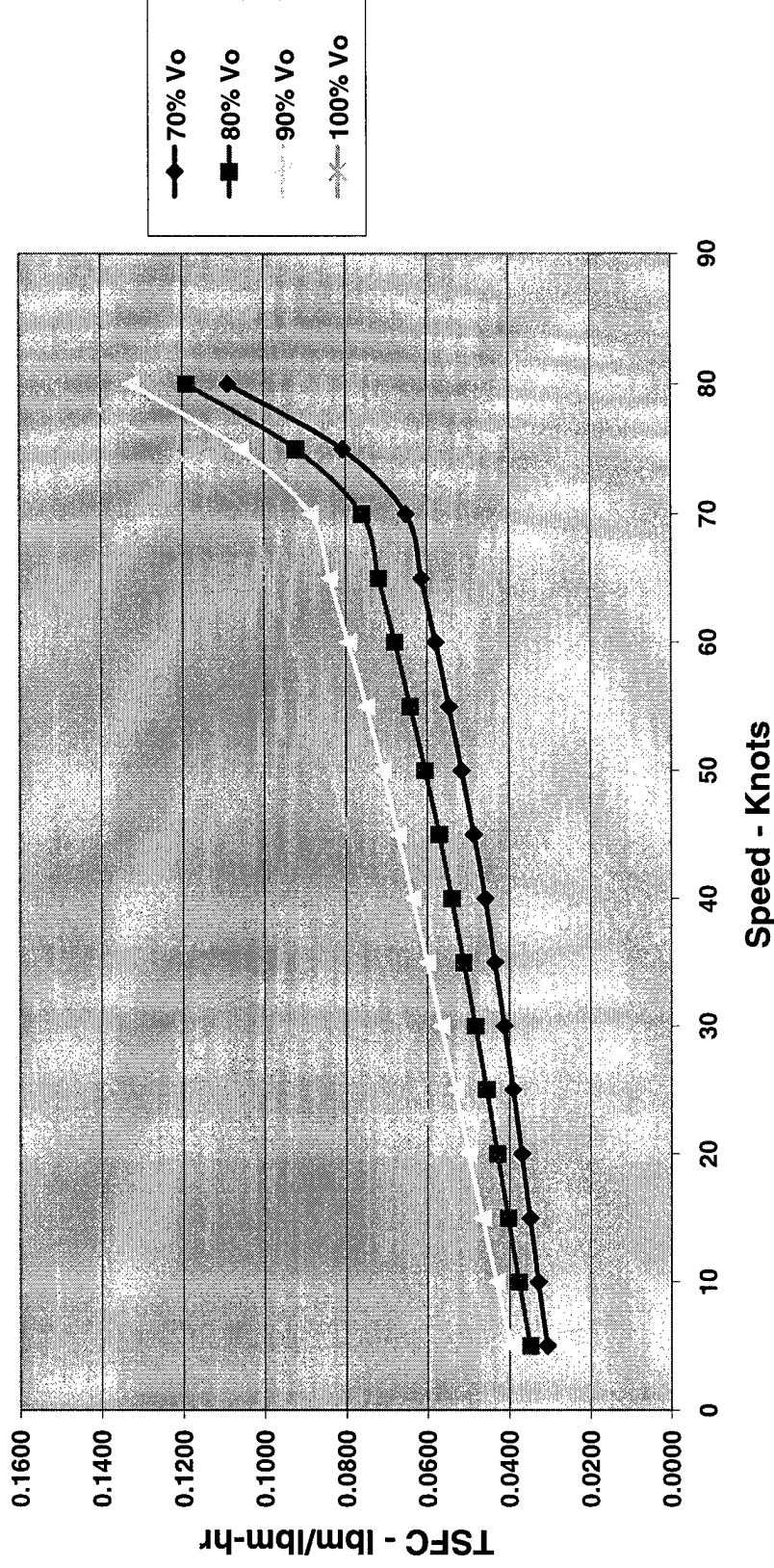
Impact of BL Ingestion
1.4 JVR, 50KHP LM6000



Reduction in Ram Drag elevates overall Installed Thrust

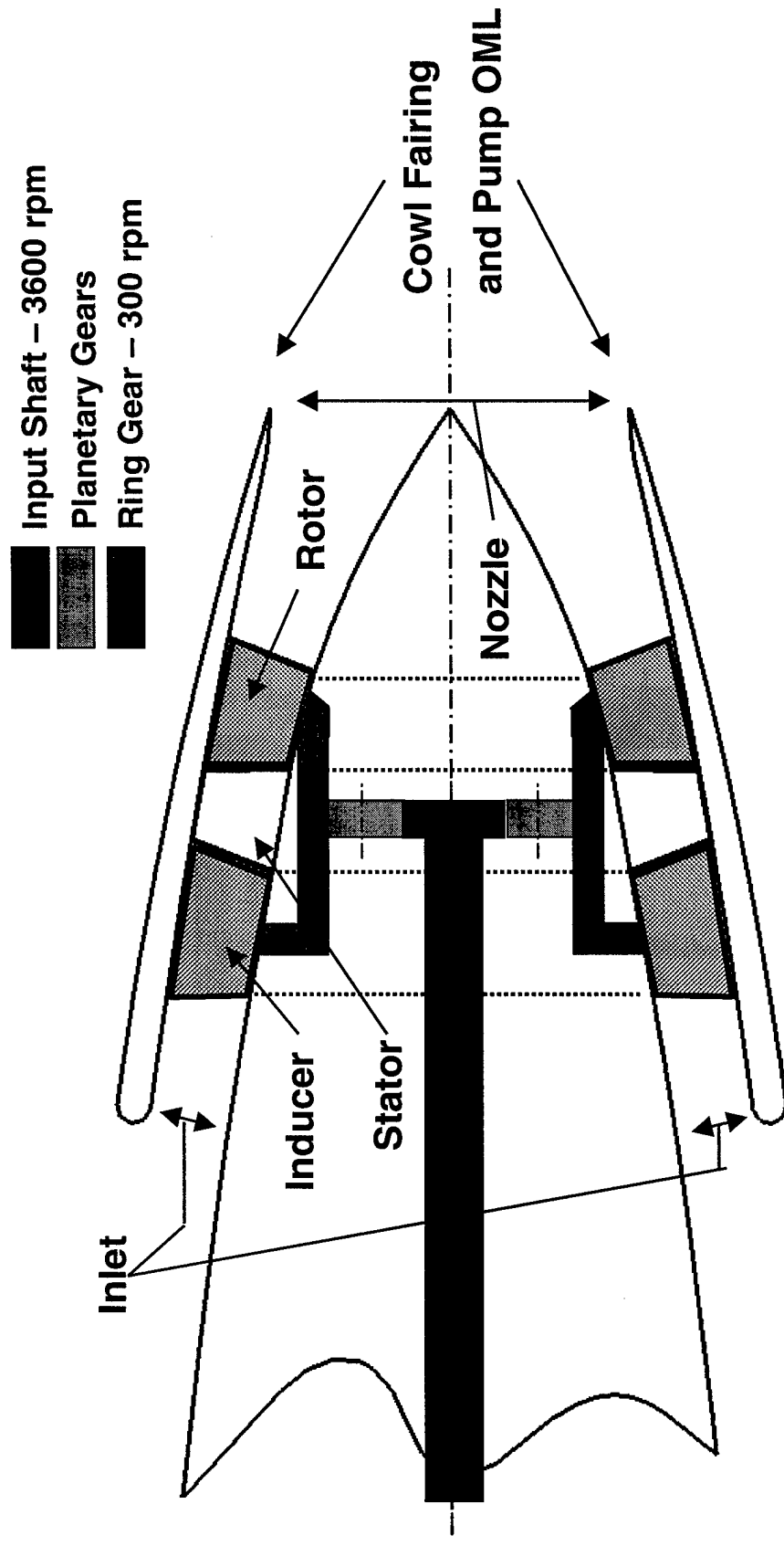
Fuel Flow Variation with Speed and Power Setting

Impact of BL Ingestion
1.4 JVR, 50KHP LM6000



The impact of Boundary Layer Momentum Ingestion is Appreciable as Speed and Relative Capture Increases!

Gas Turbine-to-Pump Gear Reduction Option

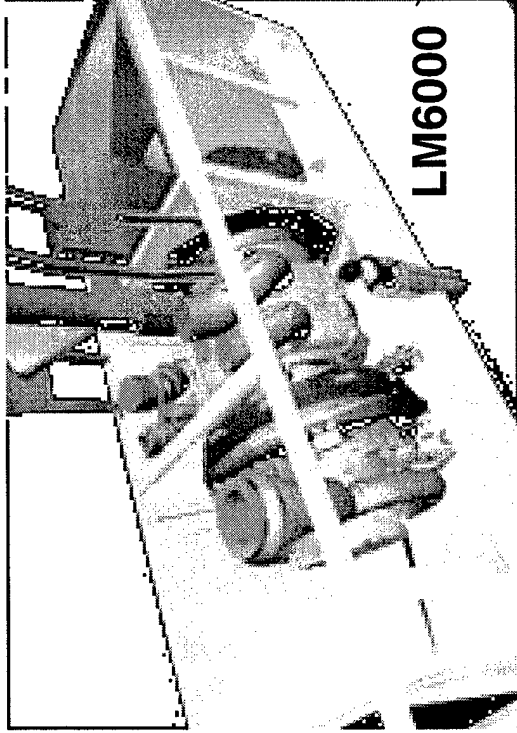


Pump Cross Section

Planetary system reduces final gear face pressures by ratio of planets.

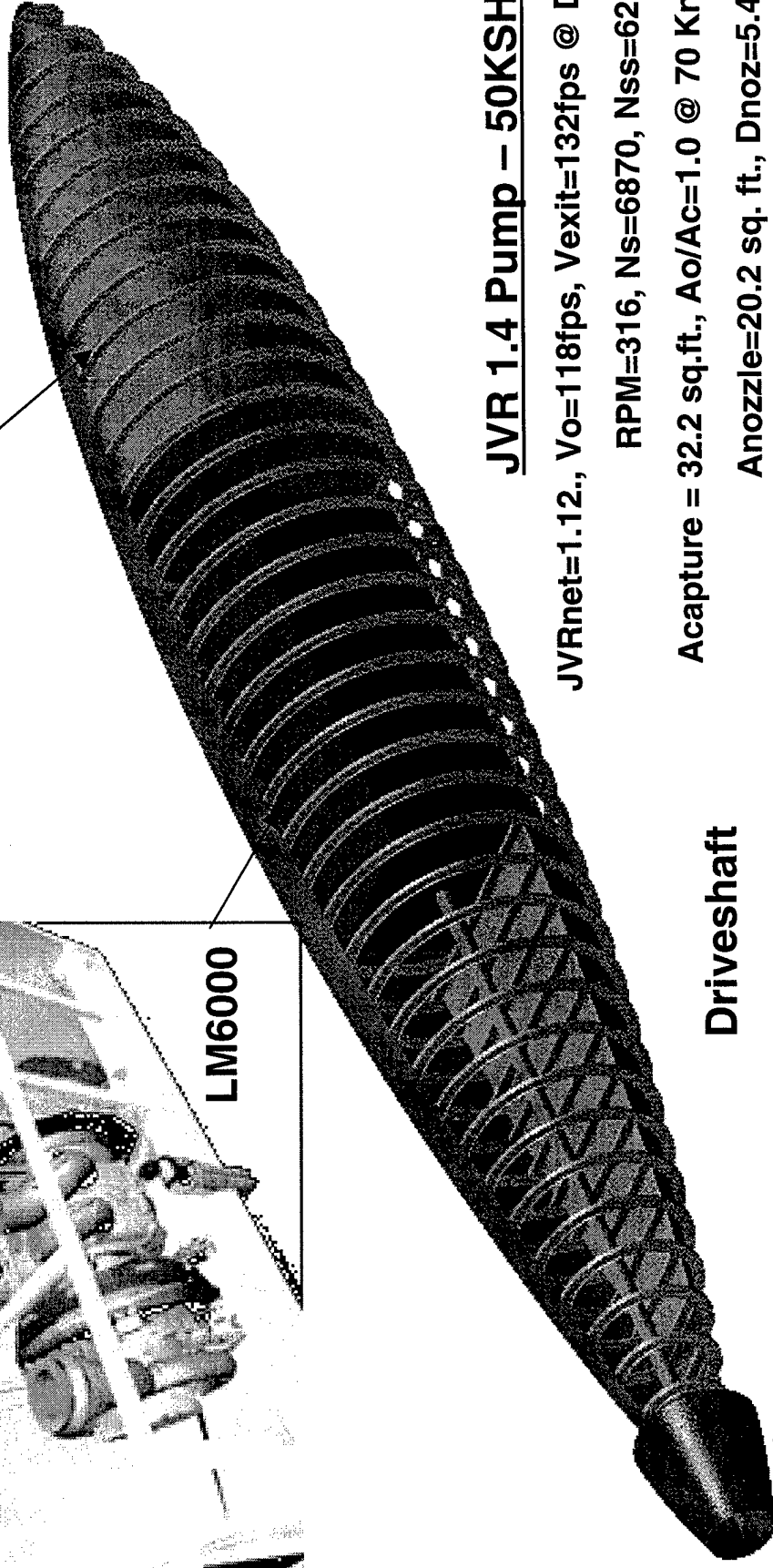
Torque multiplication factor is reduced by distribution.

Water Jet Integration - Pump-In-Body Design (BOR)



LM6000

Fuel



Driveshaft

Pump/Transmission

JVR 1.4 Pump – 50KSHP

JVRnet=1.12., Vo=118fps, Vexit=132fps @ DP

RPM=316, Ns=6870, Nss=6250

Acapture = 32.2 sq.ft., Ao/Ac=1.0 @ 70 Knts

Anozzle=20.2 sq. ft., Dnoz=5.4ft.

Volumetric Rate =2665.5 cu.ft./sec

Massflow Rate = 638.5 Tons/sec

Water Jet Integration - Pump-In-Cavity Body Design

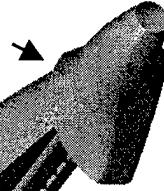
At berth the pump intake is placed favorably to avoid debris ingestion



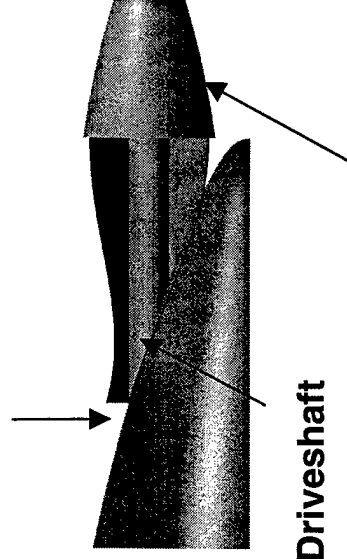
LM6000

High Speed Drive Shaft

Pump Intake



Annular Boundary Layer Ingestion Intake



Driveshaft

Pump/Transmission

JVR 1.4 Pump-100KSHP

JVRnet=1.12., Vo=118fps, Vexit=132fps @ DP

RPM=316, Ns=6870, Nss=6250

Acapture = 64.4 sq.ft., Ao/Ac=1.0 @ 70 Knts

Anozzle=40.4 sq. ft., Dnoz=7.2 ft.

Volumetric Rate =5331 cu.ft./sec

Massflow Rate = 1227 Tons/sec

Water Jet Integration - Pump-In-Body Issues

Increased Frontal /Base Area May Reduce System L/D

Effects Due to the Increased Momentum of the Jet and Interaction with the Hull/Strut/Foil.

Potential Stability and Control Implications

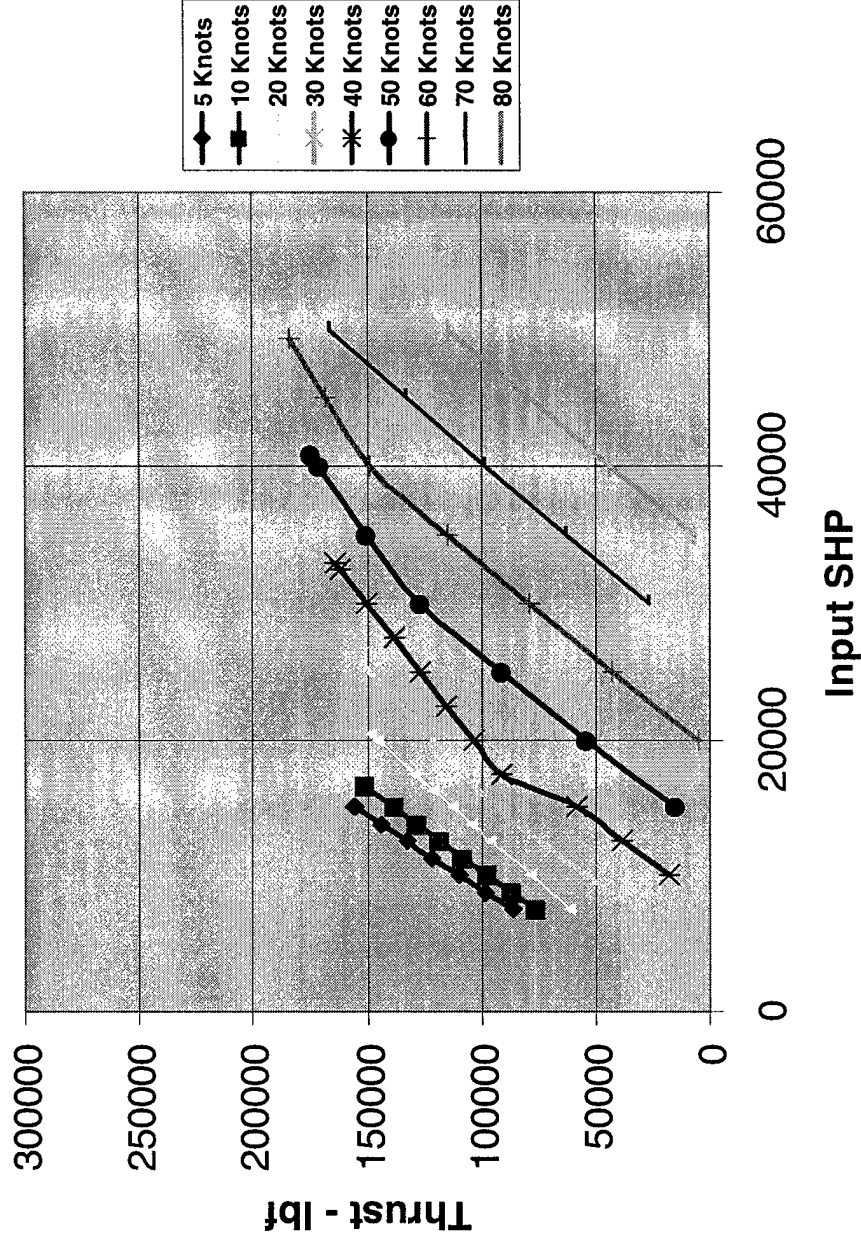
Capture Field Radial/Circumferential Distortion effects

Operation in Shallow Draft Conditions- Auxiliary Inlet System Needed?

Minimum BOR for integration into the Hydrofoil Strut System

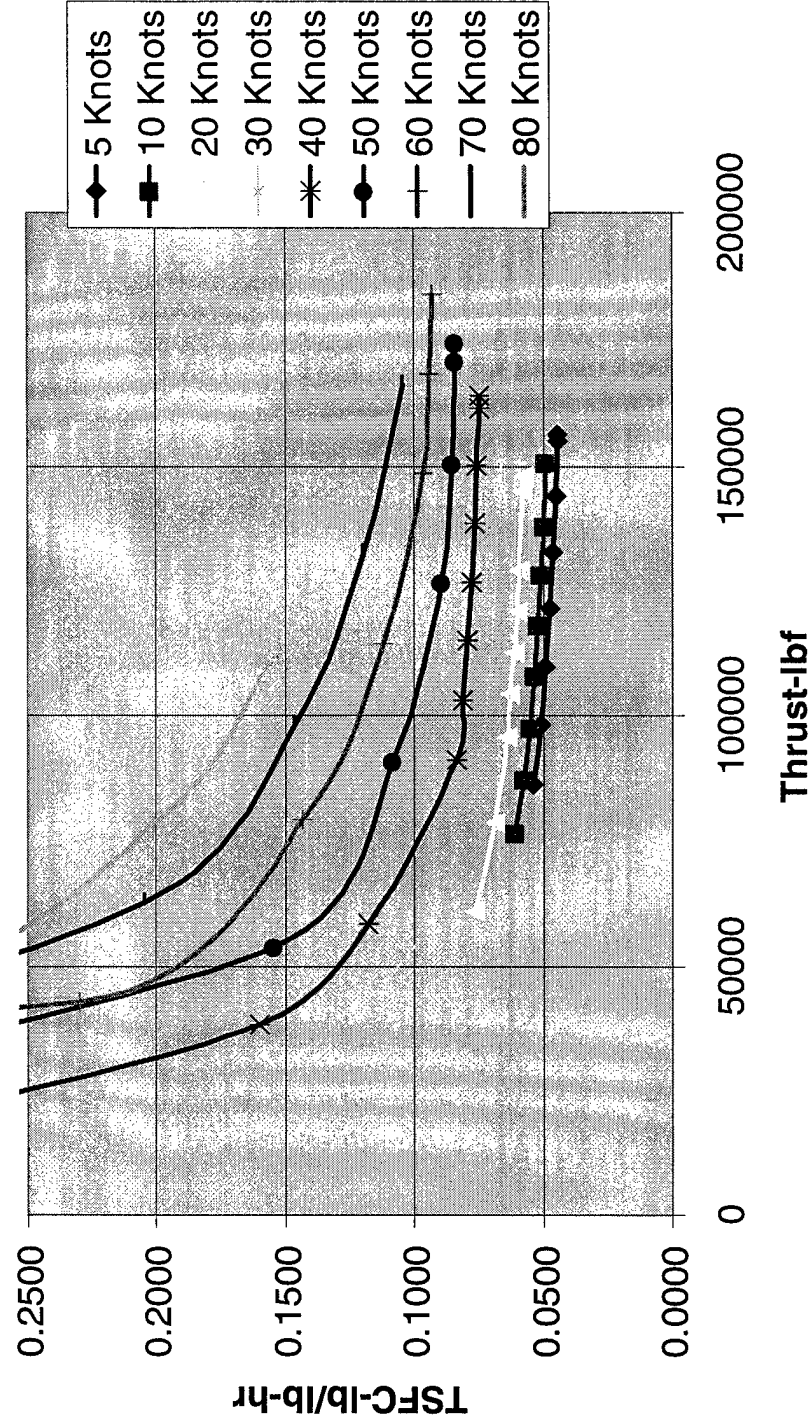
Thrust Variation with Speed and Power Setting

Horsepower vs. Thrust
JVR 1.4, Vo=100%, 50KSHP-LM6000



Fuel Flow Variation with Speed and Power Setting

Thrust vs. Fuel Flow
JVR 1.4, Vo=100%, 50KHP-LM6000

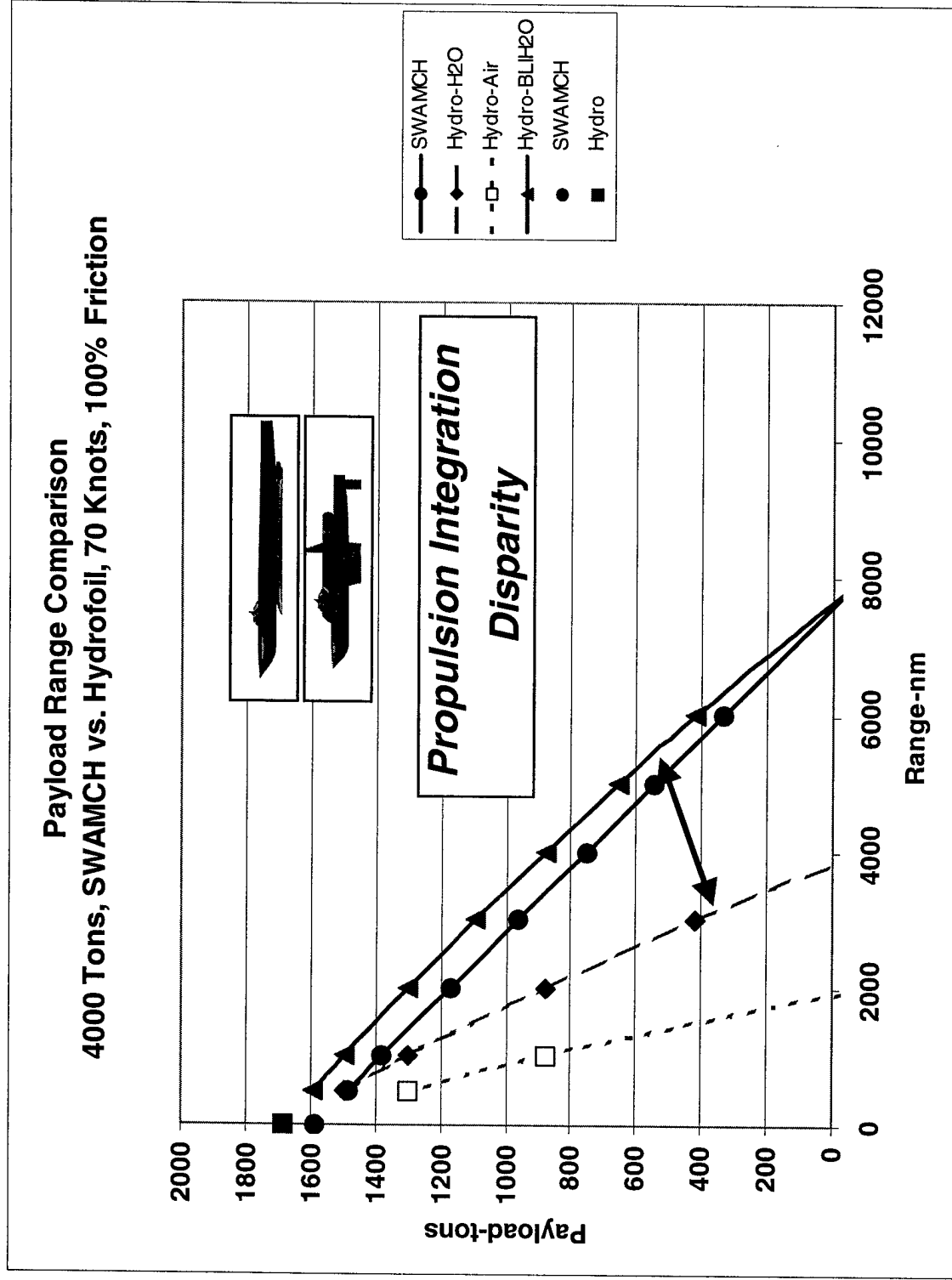


Propulsor Performance Summary

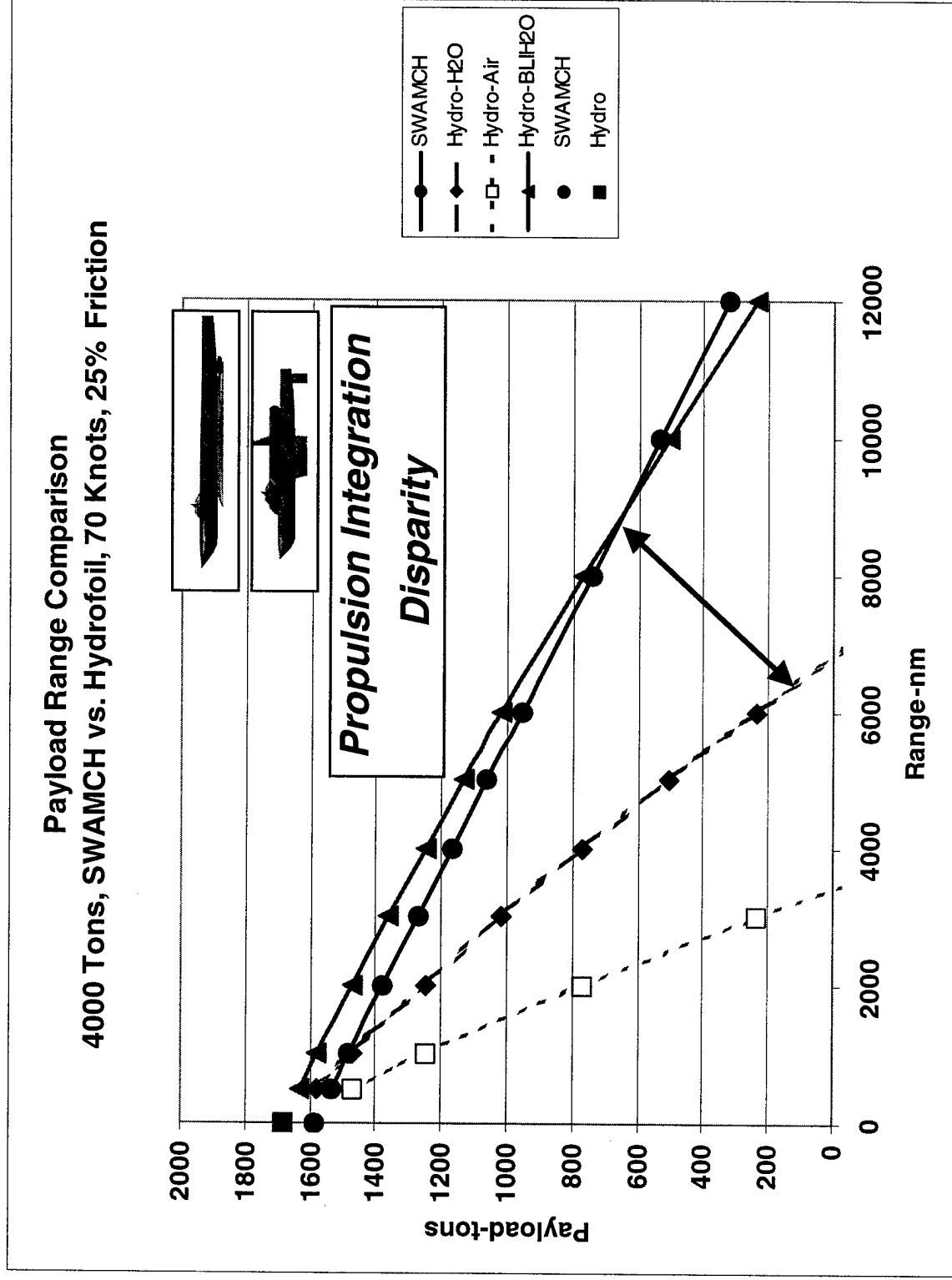
Air Coupled Systems (75knts)		<u>Size</u>	<u>Efficiency</u>	<u>TSFC</u>
Propellers		32'	41%	0.1930
		48'	54%	0.1480
Transverse Fan		64'	63%	0.1260
		40'	51%	0.1550
		10'	31%	0.2550
Water Coupled Systems (70knts)				
Propellers		11.5'	65%	0.113
Water Jets		JVR1.4	75%	0.1060 @ 100%
			87%	<u>0.0640 @ 70%U⁺</u>
		JVR1.6	69%	0.1120
			80%	<u>0.0790 @ 85%*</u>
		JVR1.8	63%	0.1180
			73%	<u>0.0870 @ 85%*</u>

* Implies that 15% Momentum Drag is from Body, +Implies Percent Freestream Velocity

Payload Range at Full Drag – Propulsion Comparison



Payload Range at 25%K2 – Propulsion Comparison



Propulsion System Summary

- **Future Considerations.**

Formal Engine Company Involvement in Powerplant and Power Distribution Definition when a preferred design direction is established.

- **Future Direction.**

Continued Definition of Candidate Propulsion System Options, considering Water-Coupled Propulsor Solutions.

Vehicle Design and Integration

Design Constraints

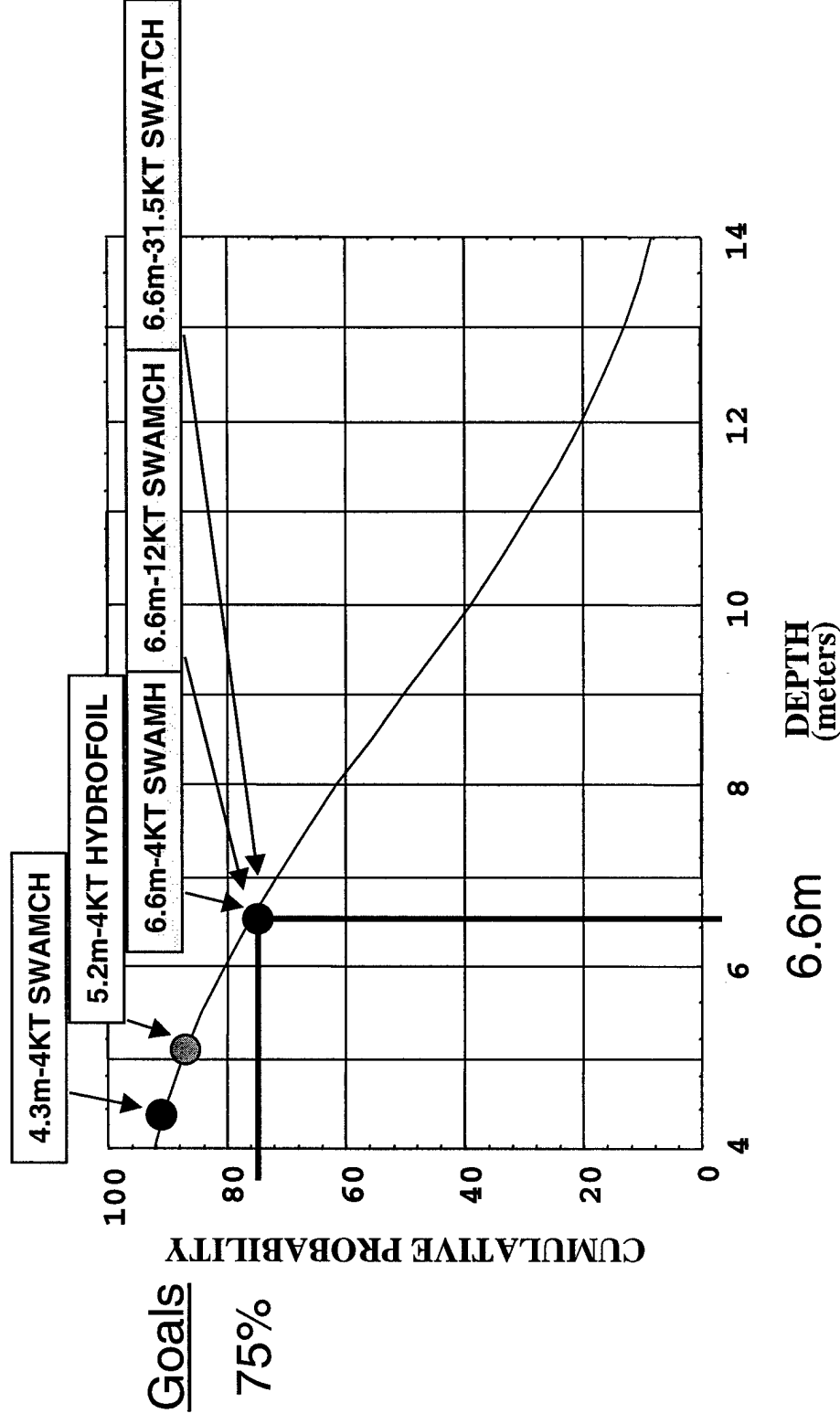
Ship configuration constraints were gathered from the DARPA Systems Analysis for length, beam and draft. Length is not to exceed 656 feet (200 meters) due to berthing size. Additional length will result in additional port charges and could possibly exclude the ship from some ports. Beam is not to exceed 200 feet (61 meters) due to canal and port widths. Draft is not to exceed 23 feet (7 meters) which will allow the ship entry into approximately 70% of the ports of the world. During the study, additional draft information was obtained from Lloyd's Ports of The World and was used as a goal. It was found that by limiting the draft to 21 feet (6.6 meters), 75% of the ports of the world could be accessed.

Payload was maximized within the 15,000 ton total vessel weight with provisions for up to 5000 tons of payload. A value of 100 lbs/sqft was used for cargo floor loading with on specific provisions for internal storage of outsized payloads.

Materials were selected from current technology data bases for the hull, struts, and foils. Standard ship building practices were assumed for fabrication.

From this, with inputs from hydrodynamics, structures and propulsion, configurations were explored that could achieve all of the constraints and goals. CATIA 3D software was used to loft the configurations and assess roll and pitch stability.

Port Depth* as a Design Constraint



Lloyd's Ports of the World

Line(s) = Gaussian Distribution: mean = 9.0 m; $\sigma = 3.55$ m

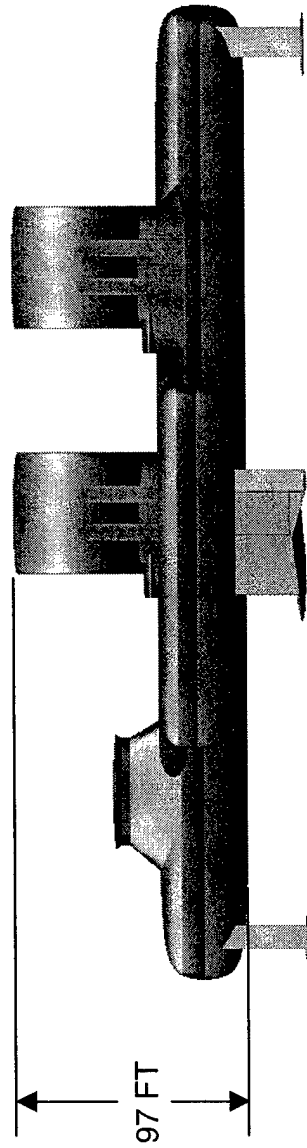
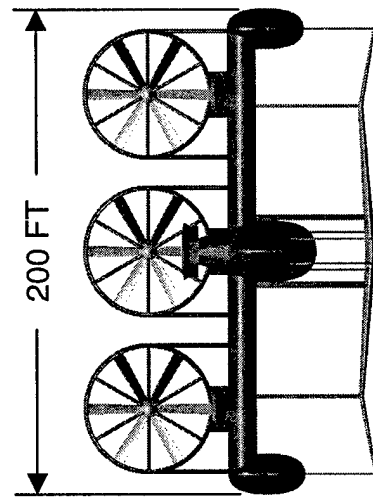
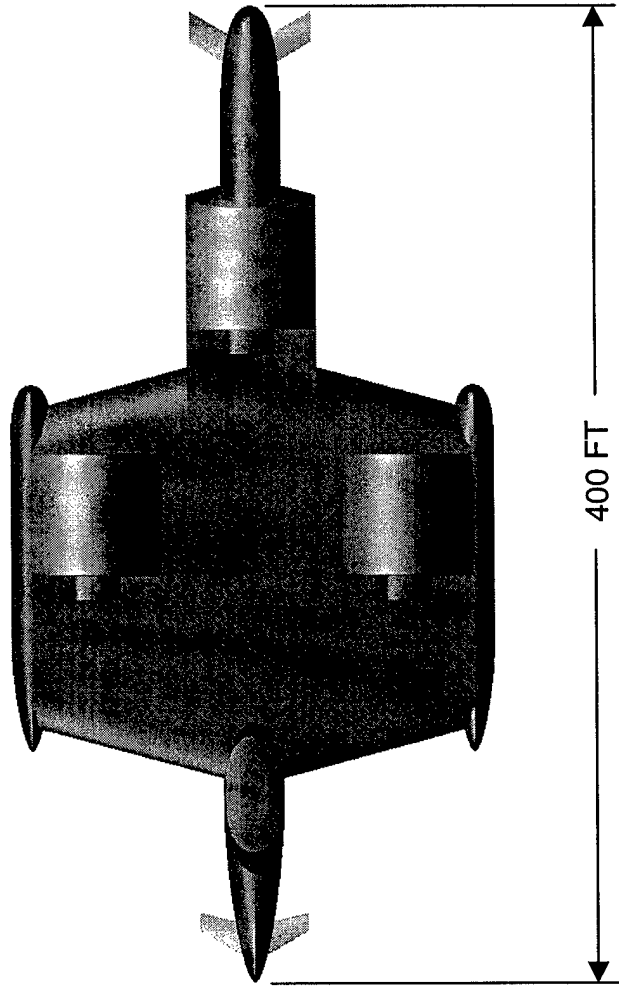
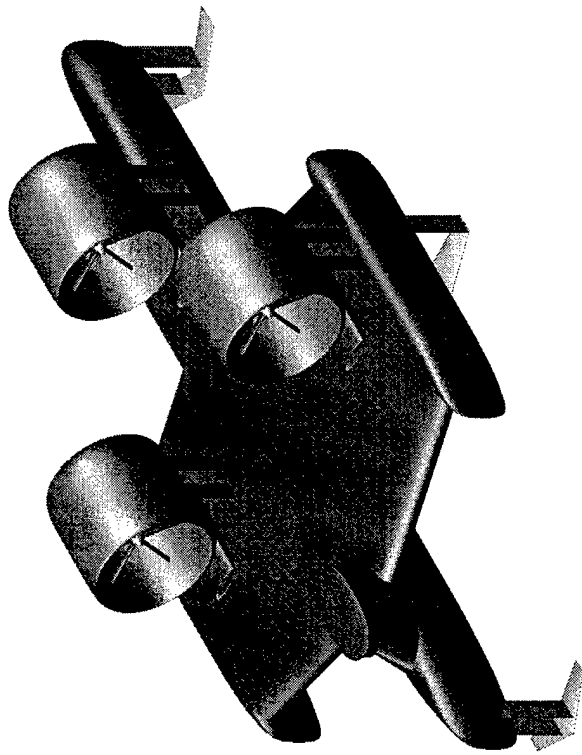
*Statistics and compilation received from A. Ellinthorpe

Hydrofoil Baseline Vessel

Given the design constraints, a baseline hydrofoil configuration was established. A trimaran hull was chosen and the wing, canard and stabilizer were integrated into the configuration. Deck mounted counter-rotating ducted fans driven by LM6000 gas turbines were added for propulsion. A foil retraction method was established to achieve the draft requirement.

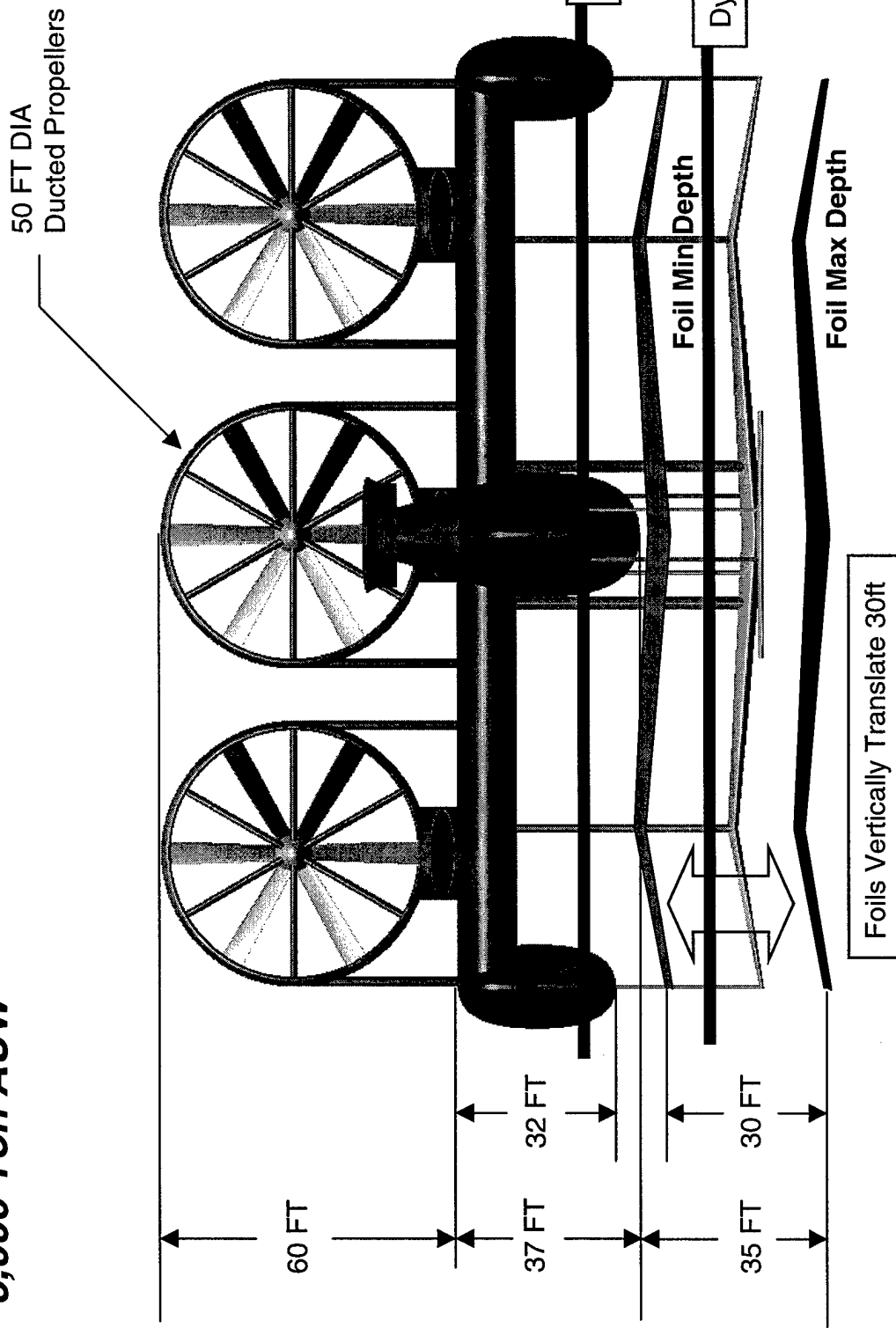
Hydrofoil Baseline Vessel

5,000 Ton AUW



Hydrofoil Baseline Vessel - Foil Retraction Scheme

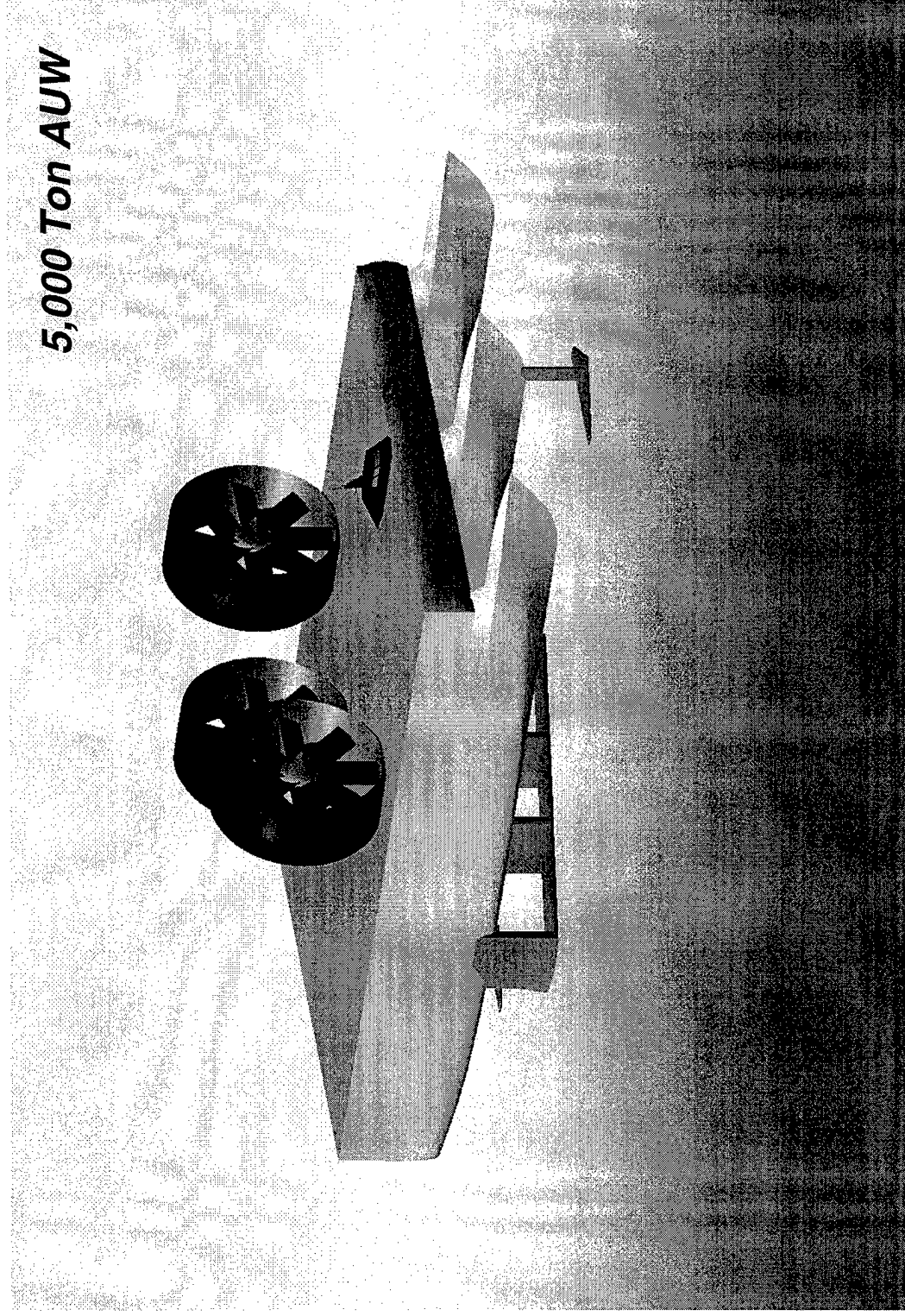
5,000 Ton AUW



Hydrofoil Baseline Vessel – CSC Advanced Marine

A study conducted by CSC Advanced Marine showed that three identical deep slender hulls needed to be added to the configuration. The new hull design would help support the transverse spans, reduce wave making resistance and reduce slamming loads in a seaway. The next slides show CSC design and the estimated vessel weight.

Hydrofoil Baseline Vessel – CSC Advanced Marine



5,000 Ton AUW

Estimated Vessel Weight - CSC Advanced Marine

SWBS GROUP	SWBS DESCRIPTION	WEIGHT (T)
1	HULL STRUCTURE	2,814
2	PROPULSION PLANT	463
3	ELECTRIC PLANT	114
4	COMMAND & SURVEILLANCE	11
5	AUXILIARY SYSTEMS	810
6	OUTFIT & FURNISHING	150
7	ARMAMENT	0
<hr/>		
	LIGHTSHIP	4,362
	FUEL	1,200
	FUEL OR CARGO	1,300
<hr/>		
	FULL LOAD CONDITION	6,862

Estimated Vessel Weight – Hull Structure

SWBS 100 Weight Elements

Shell Plating (615T)
Inner Bottom (1070T)
Stanchions (57T)
Transverse bulkheads (37T)
Cargo deck (663T)
Weather deck (254T)
Foundations (118T)

Estimated Vessel Weight – Propulsion Systems

SWBS 200 Weight Elements

Turbine / ducted propulsors (390T)

 Lube oil systems (59T)

Fuel transfer and service systems (14T)

Estimated Vessel Weight – Electric Power Systems

SWBS 300 Weight Elements

Power distribution cabling (57T)
Ships service power generation (42T)
Power conversion equipment (12T)

Estimated Vessel Weight – Command & Control Systems

Total SWBS 400 Weight Group is 11T

Estimated Vessel Weight – Auxiliary Systems

SWBS 500 Weight Elements

Struts and foil systems (~500T)
Cargo ramps and systems (85T)
Cargo space A/C system (82T)
Cargo space ventilation system (74T)
 Firemain system (43T)
Mooring and towing systems (16T)
Habitability spaces HVAC (10T)

Estimated Vessel Weight – Outfit & Furnishings

SWBS 600 Weight Elements

Hull Insulation (63T)

Painting (44T)

Cathodic Protection (20T)

Habitability Spaces (17T)

Deck Fittings (6T)

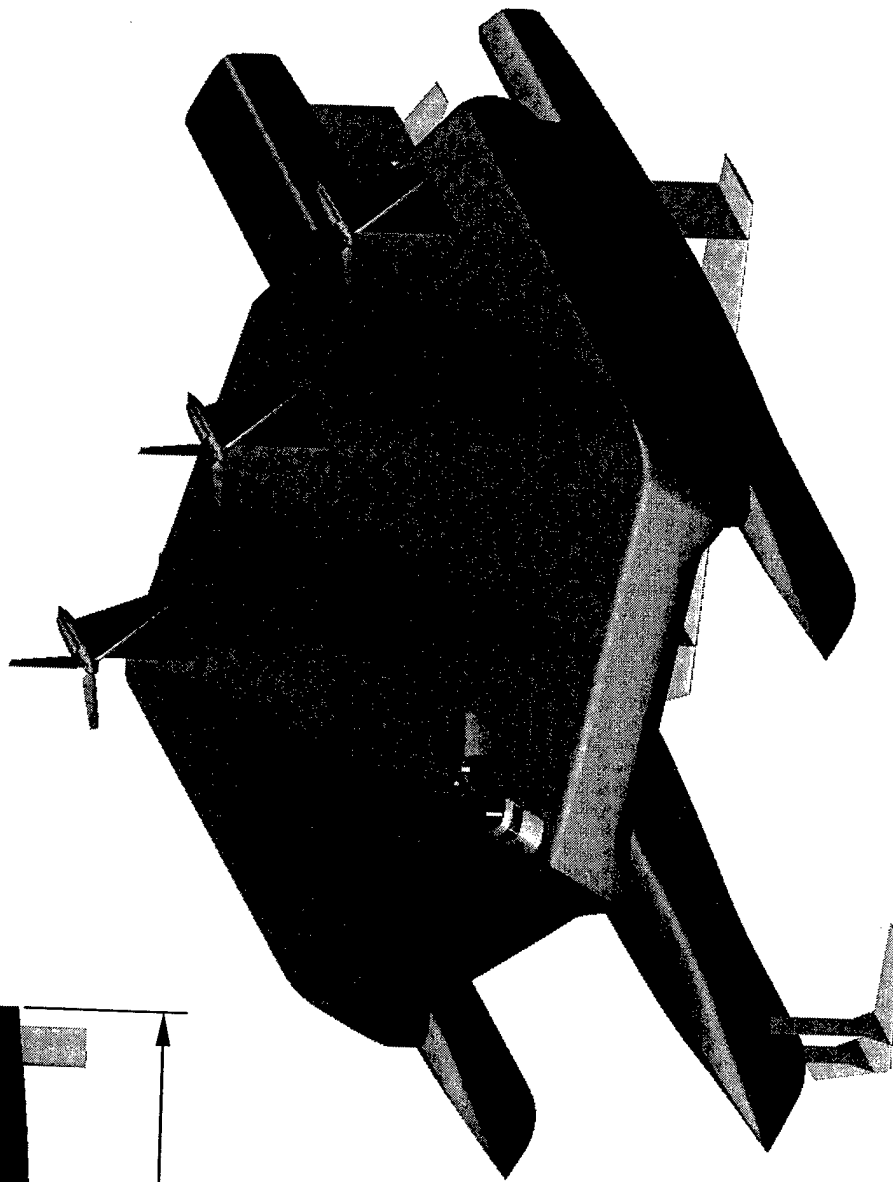
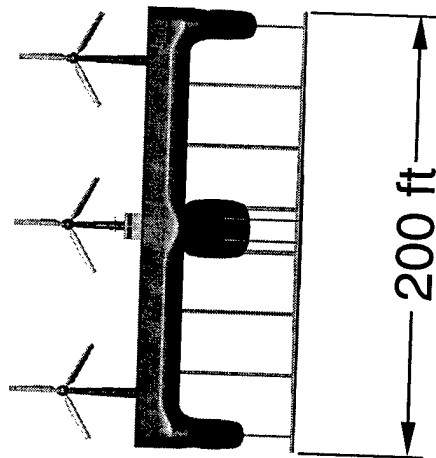
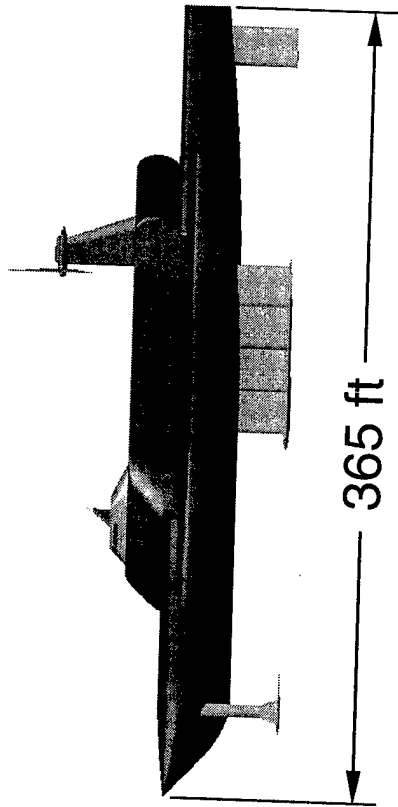
Hydrofoil Vessel – Concept II

Refinement of the hydrofoil wing section, structure, and propulsion models, along with input from CSC Advanced Marine, resulted in a new configuration. The new configuration utilized the three surface (wing, canard and stabilizer) configuration along with three unsymmetric hulls. Three blade axial propellers were integrated into the system along with the LM-6000 gas turbines.

The following slides show the new configuration and the weight breakdown.

Hydrofoil Vessel – Concept II

5,000 Ton AUW



Estimated Vessel Weight -- Concept II

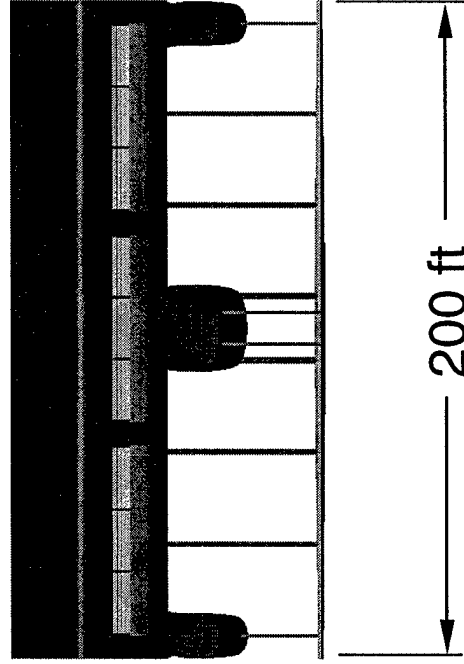
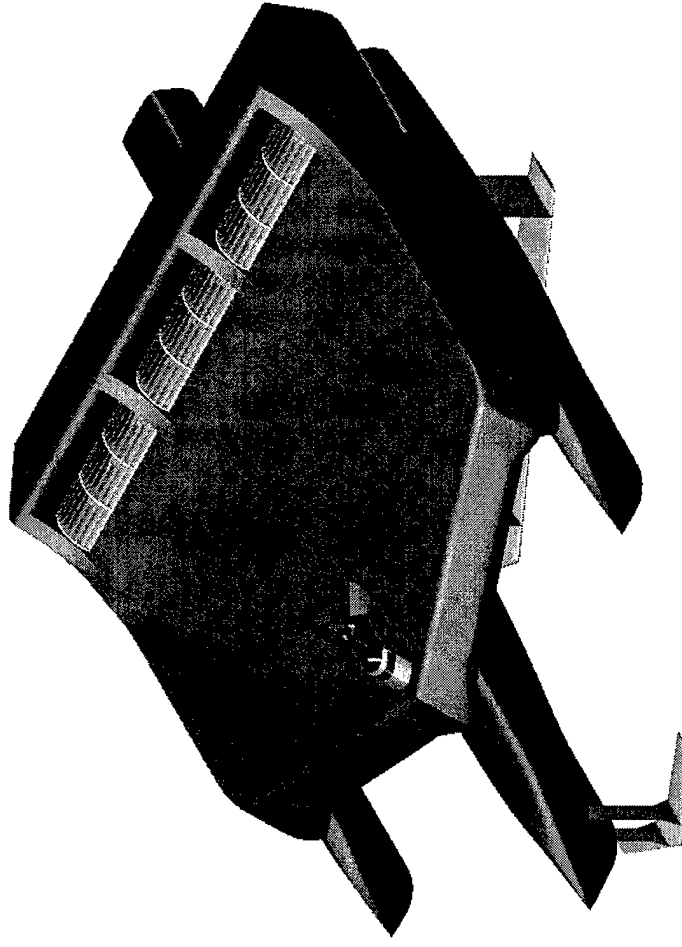
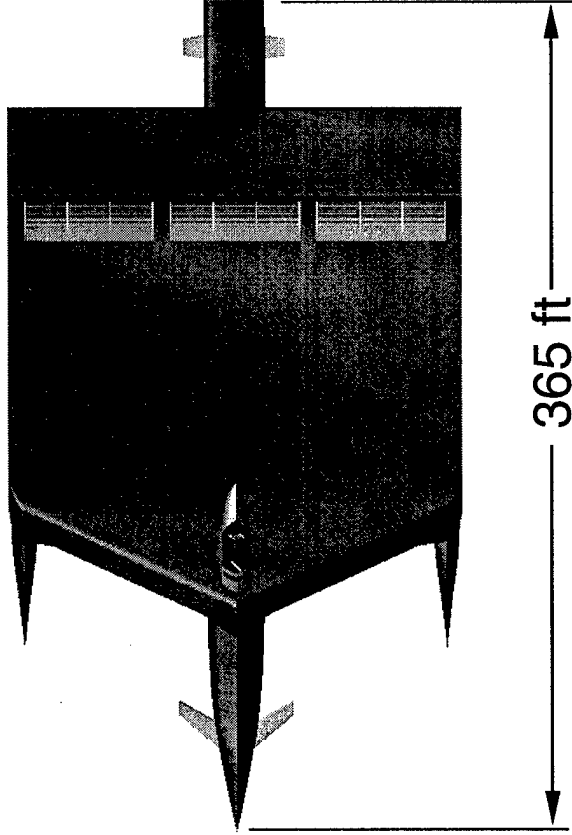
SWBS GROUP	SWBS DESCRIPTION	WEIGHT (T)
1	HULL STRUCTURE	1,600
2	PROPULSION PLANT	463
3	ELECTRIC PLANT	114
4	COMMAND & SURVEILLANCE	11
5	AUXILIARY SYSTEMS	728
6	OUTFIT & FURNISHING	75
7	ARMAMENT	0
<hr/>		
	LIGHTSHIP	2,991
	ACQ. MARGIN	224
	FUEL	1,000
	FUEL OR CARGO	1,000
<hr/>		
	FULL LOAD CONDITION	5,215

Hydrofoil Vessel – Concept II Alternate

The following slide shows the integration of the transverse fan propulsion system. This system utilizes three 30 foot diameter rotors that are 33 feet long. The rotor blades have a chord length of 4.5 feet and rotate at 122 rpm. Estimated rotor weight is approximately 1000 lbs/ft-span. The air exits out the stern through a 9.3 foot high nozzle to provide 650 hp/ft-span.

Hydrofoil Vessel – Concept II Alternate

5,000 Ton AUW

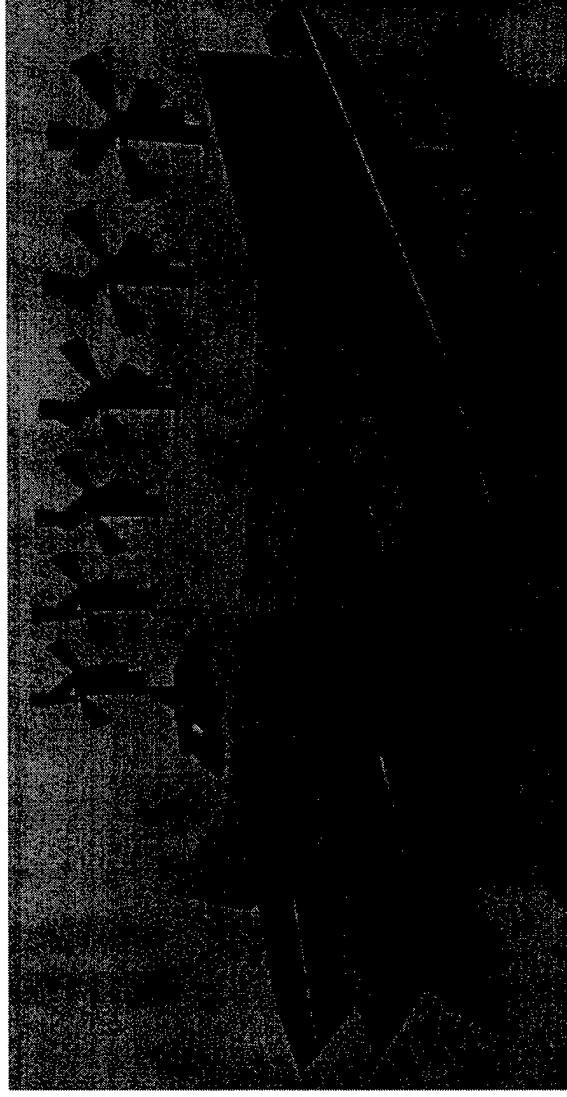


Hydrofoil Vessel Refinement

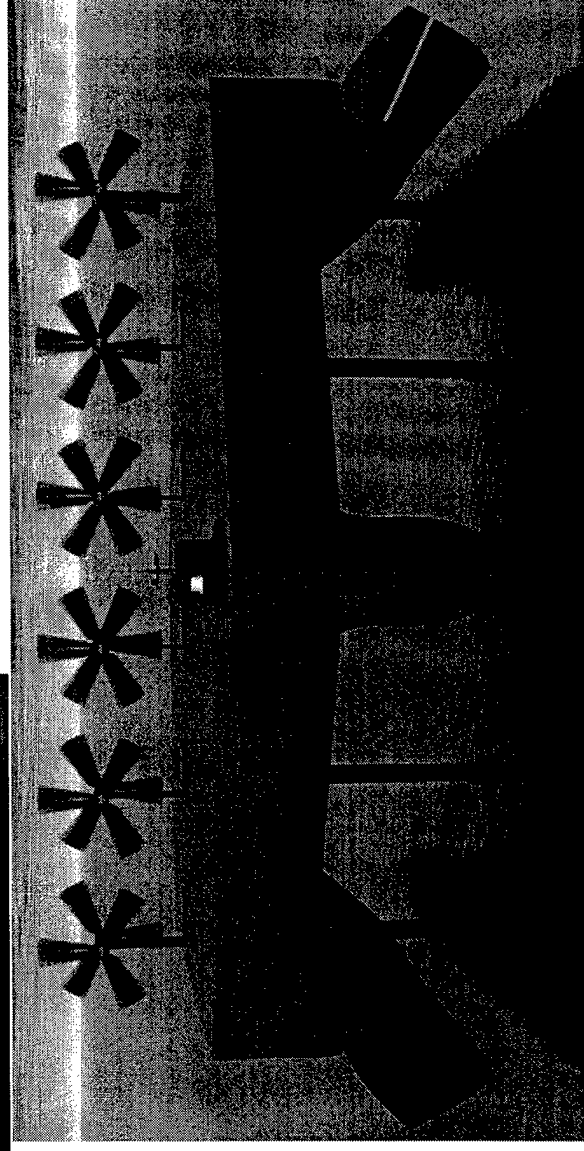
In this refinement, the configuration utilized only two underwater surfaces (wing and stabilizer) along with three unsymmetric hulls. Three blade "tractor-pusher" axial propellers were integrated into the system along with the LM-6000 gas turbines. The AUW was refined and reduced to 4000 tons.

The following slides show the integration of the "tractor-pusher" propellers, CSC Advanced Marine's hull refinement and weight estimate.

Hydrofoil Vessel Refinement



4,000 Ton AUW



Hydrofoil Vessel Refinement – CSC

Length overall = 250 feet

Beam overall = 213 feet

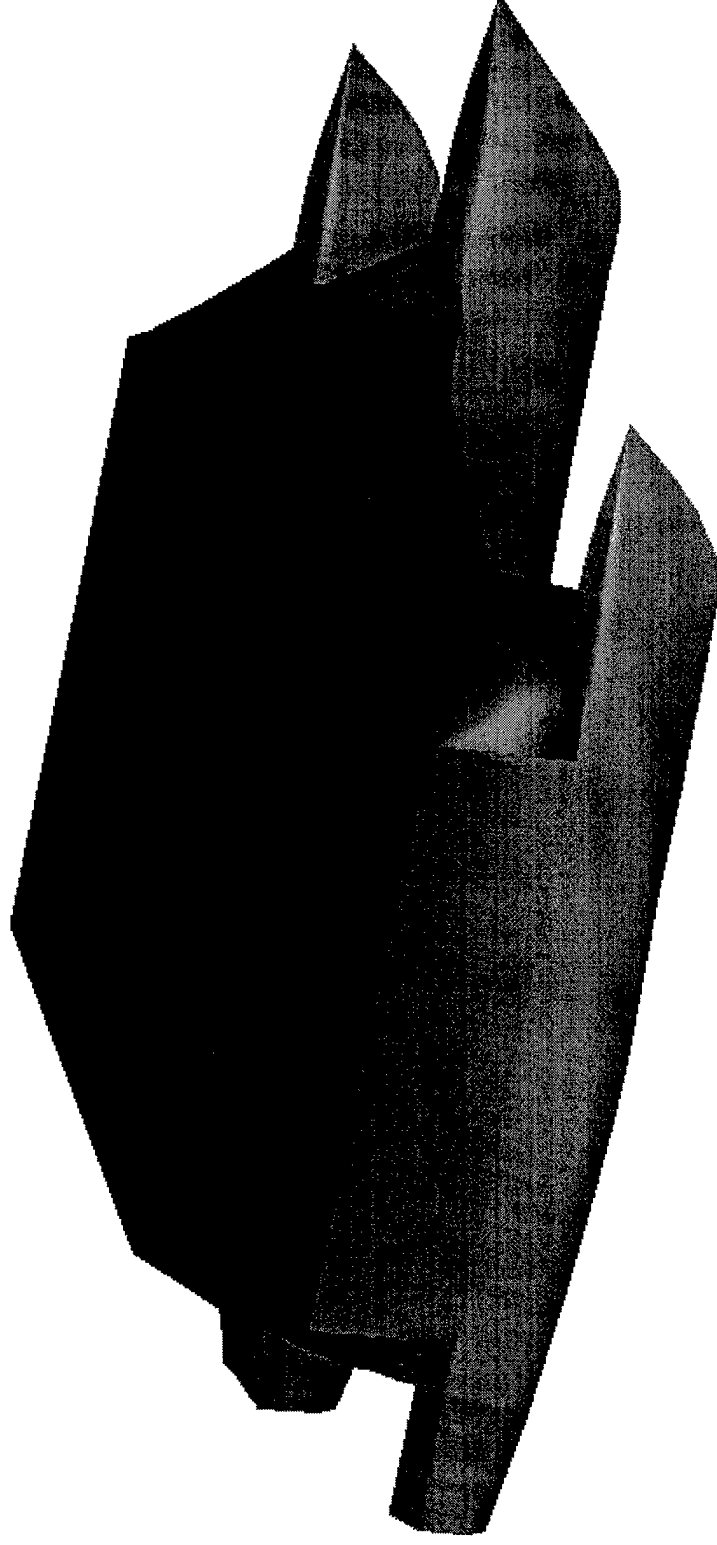
Static Draft at Full Load = 17.0 feet

Static Draft at Full Load = 47.0 feet

All aluminum hull

Structures to DNV high speed rules

4,000 Ton AUW



Estimated Vessel Weight - CSC

SWBS GROUP	SWBS DESCRIPTION	WEIGHT (T)
1	HULL STRUCTURE	1,297
2	PROPULSION PLANT	284
3	ELECTRIC PLANT	115
4	COMMAND & SURVEILLANCE	13
5	AUXILIARY SYSTEMS	370
6	OUTFIT & FURNISHING	18
7	ARMAMENT	0
<hr/>		
	LIGHTSHIP	2,097
	ACQ. MARGIN	158
	FUEL	1,013
	FUEL OR CARGO	1,000
<hr/>		
	FULL LOAD CONDITION	4268

Hydrofoil Vessel Refinement – Beaching Hull

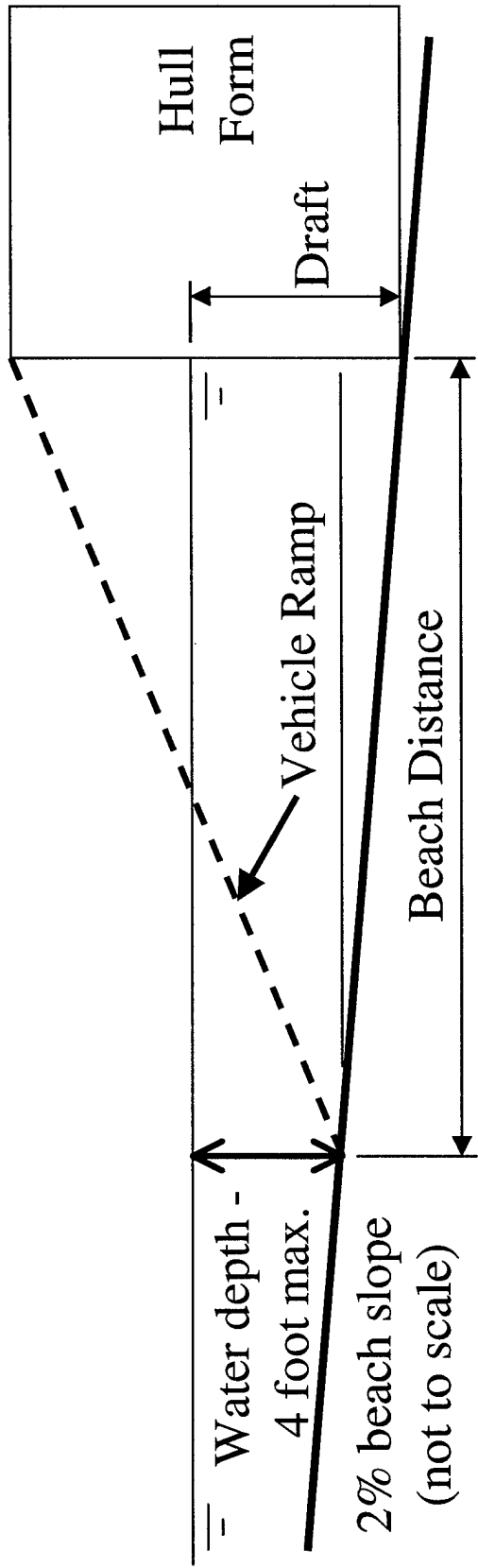
The ability to beach the vessel instead of in-stream cargo ops is highly desirable. This allows for unprepared beach landings and requires no secondary equipment. However, the vessel must have significant ballast capabilities and a rugged hull structure. It must also have mooring anchors and extraction anchors.

The following slides show results from the CSC Advanced Marine study of the “Beaching Hull”.

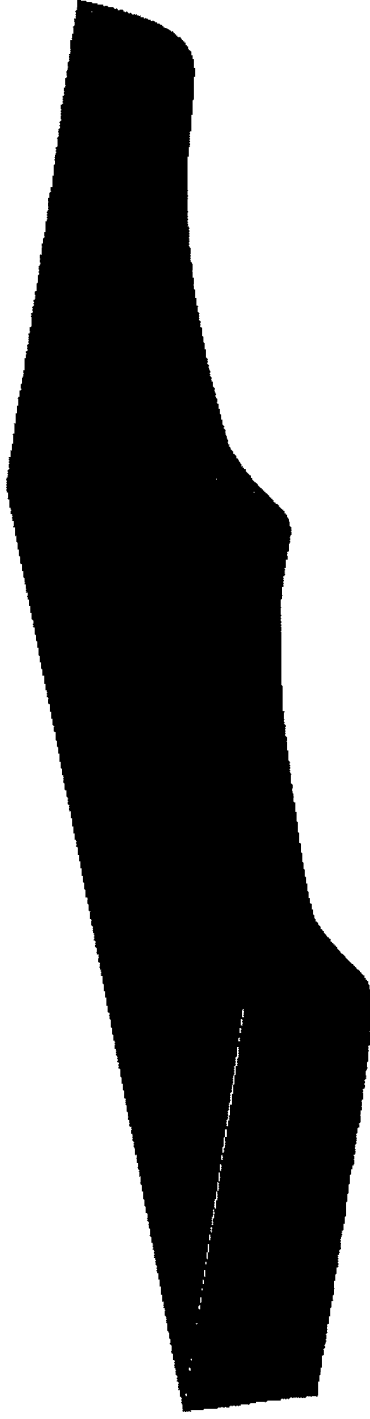
Hydrofoil Vessel Refinement – Beaching Hull

Beach Distance = (Draft - 4)/.02

Draft (ft)	Beach Distance (ft)
4	0
6	100
8	200
10	300
12	400
17	650



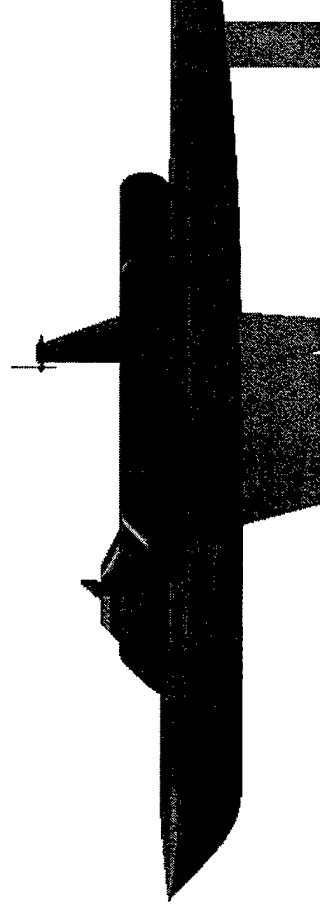
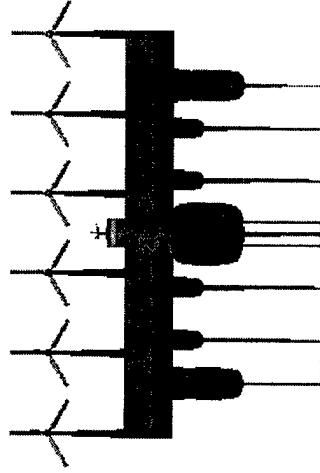
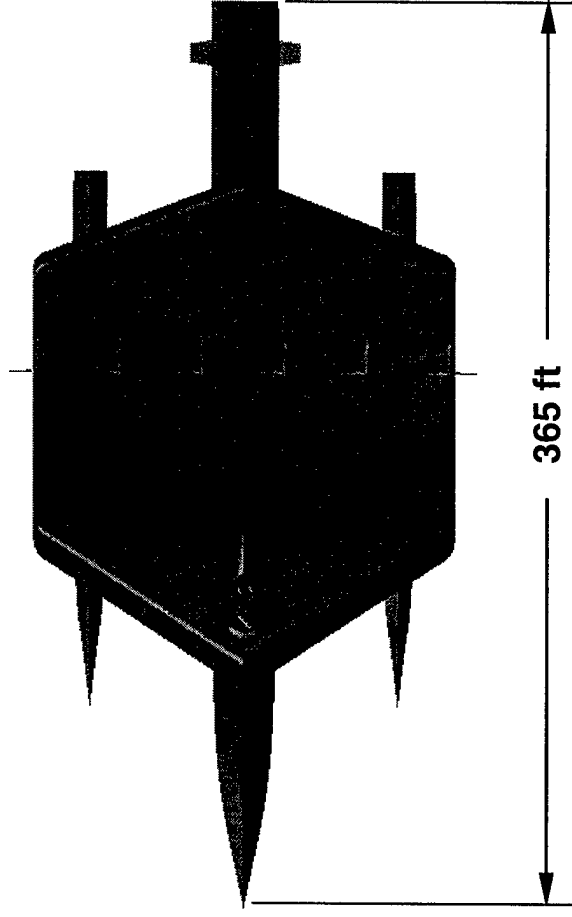
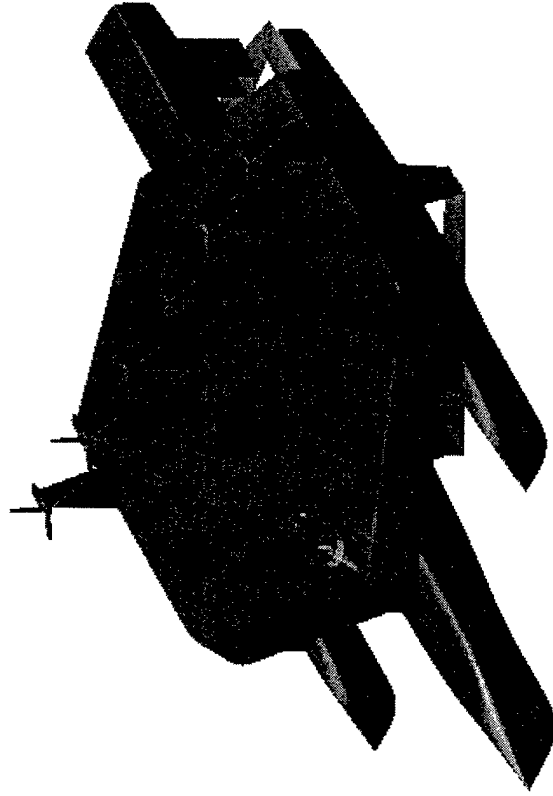
Beaching Hull Concept



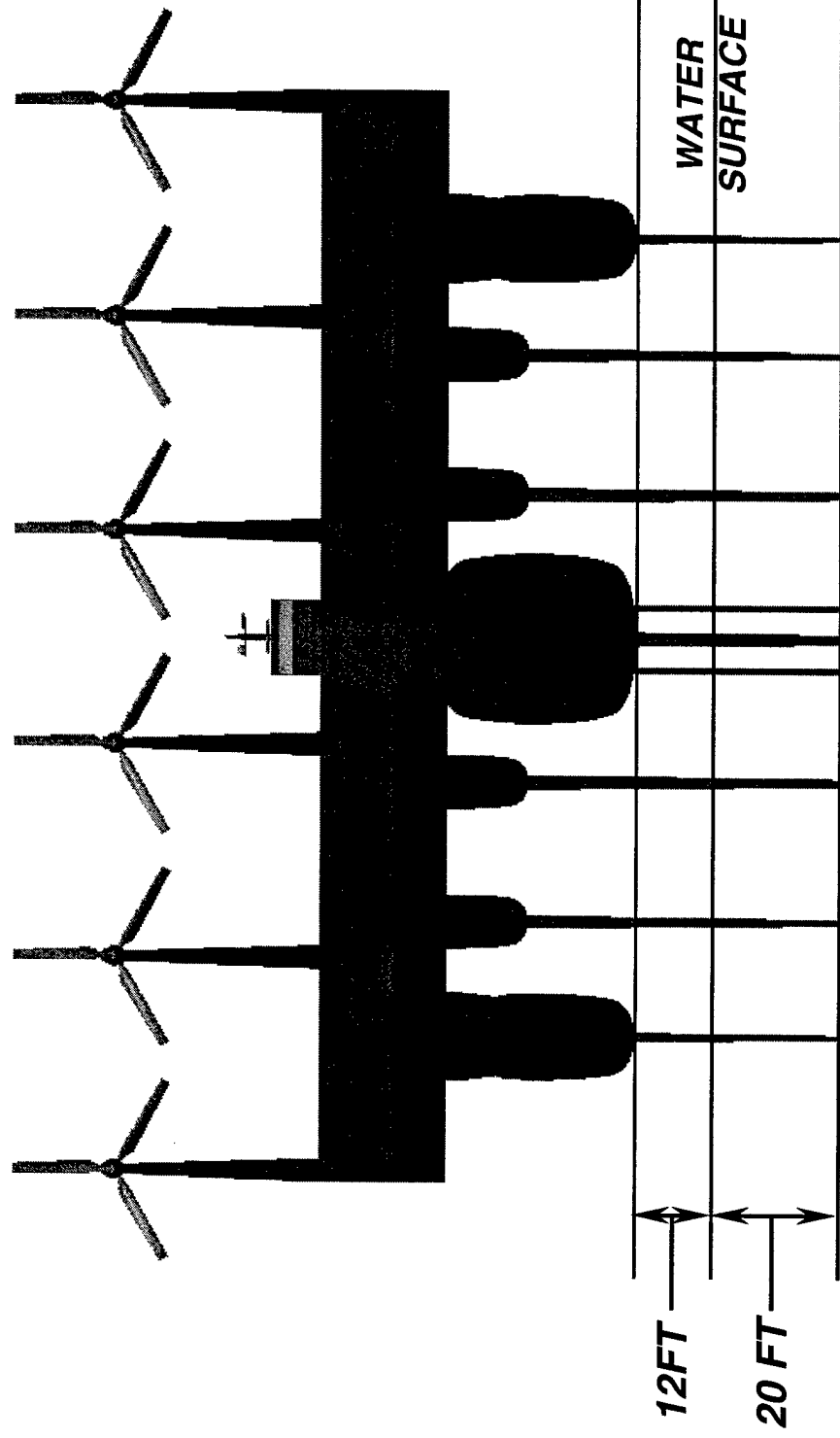
Hydrofoil Vessel – 4,000T

The following slides show three concepts for propulsion integration, air coupled propellers, jet pumps and water screws. All three systems utilize the LM6000 gas turbines for power generation. In the jet pump and water screw systems, the gas turbines will be mounted to and travel with the struts. This concept will utilize fixed drive shafts mounted inside of the struts for power transmission.

Hydrofoil Vessel – 4,000T – Air Coupled



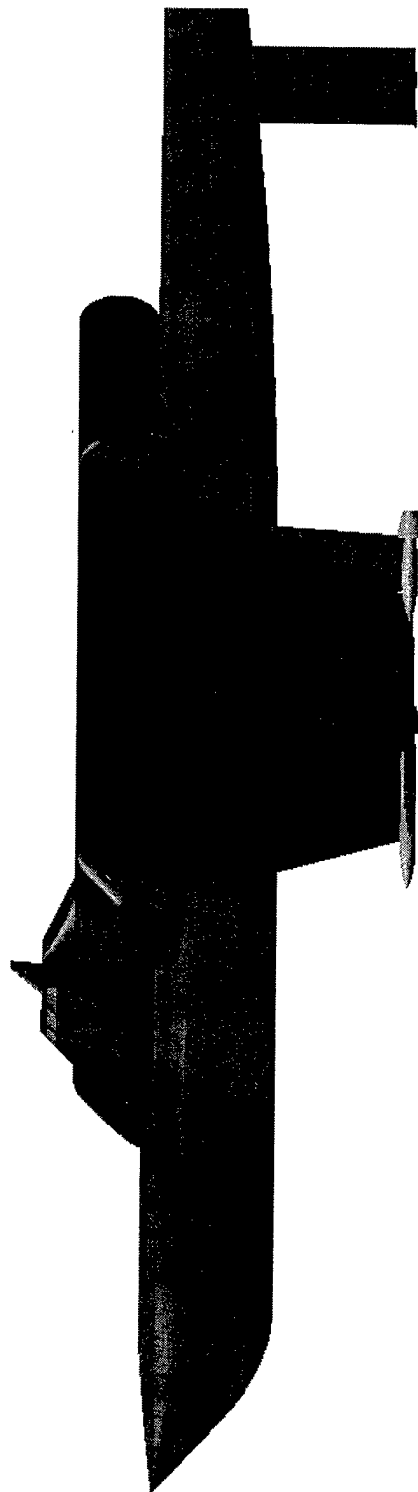
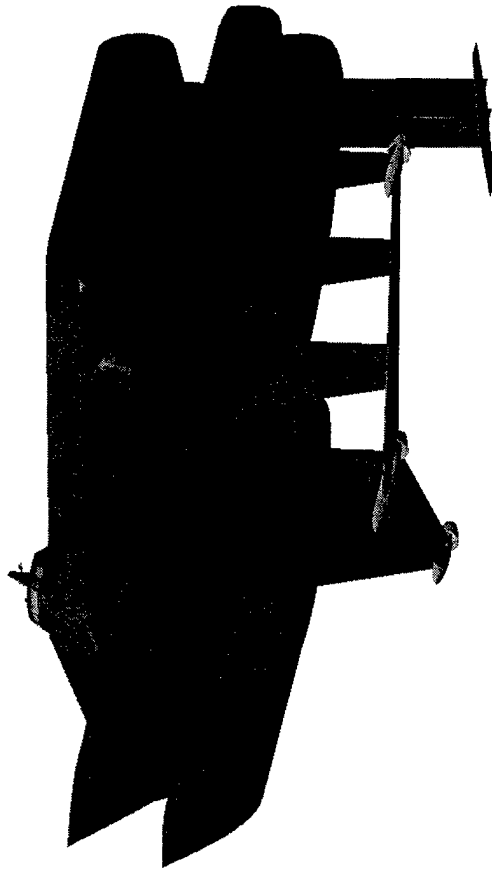
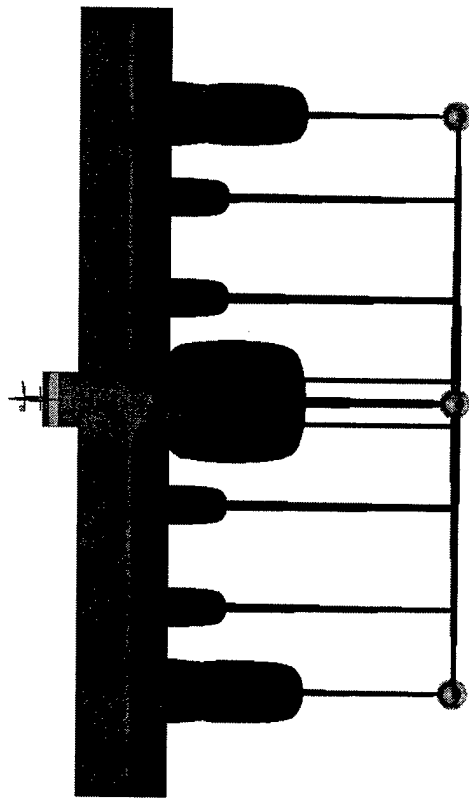
Hydrofoil Vessel – 4,000T – Air Coupled



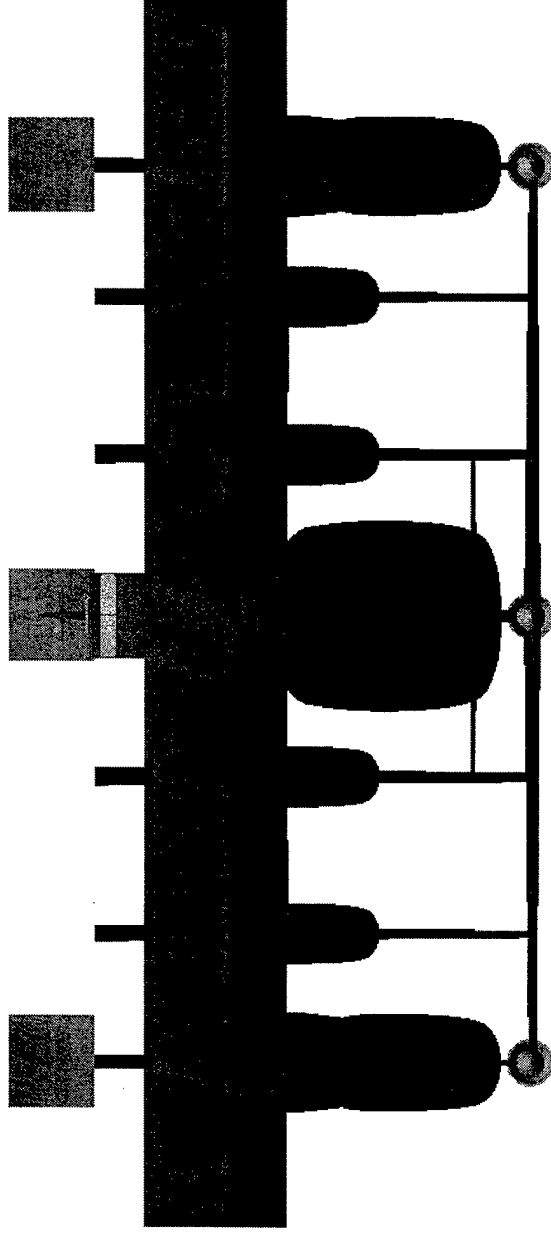
SHIP BODY BEAM = 214.8 FT

SHIP HULLS BEAM = 138.5 FT

Hydrofoil Vessel – 4,000T – Jet Pump



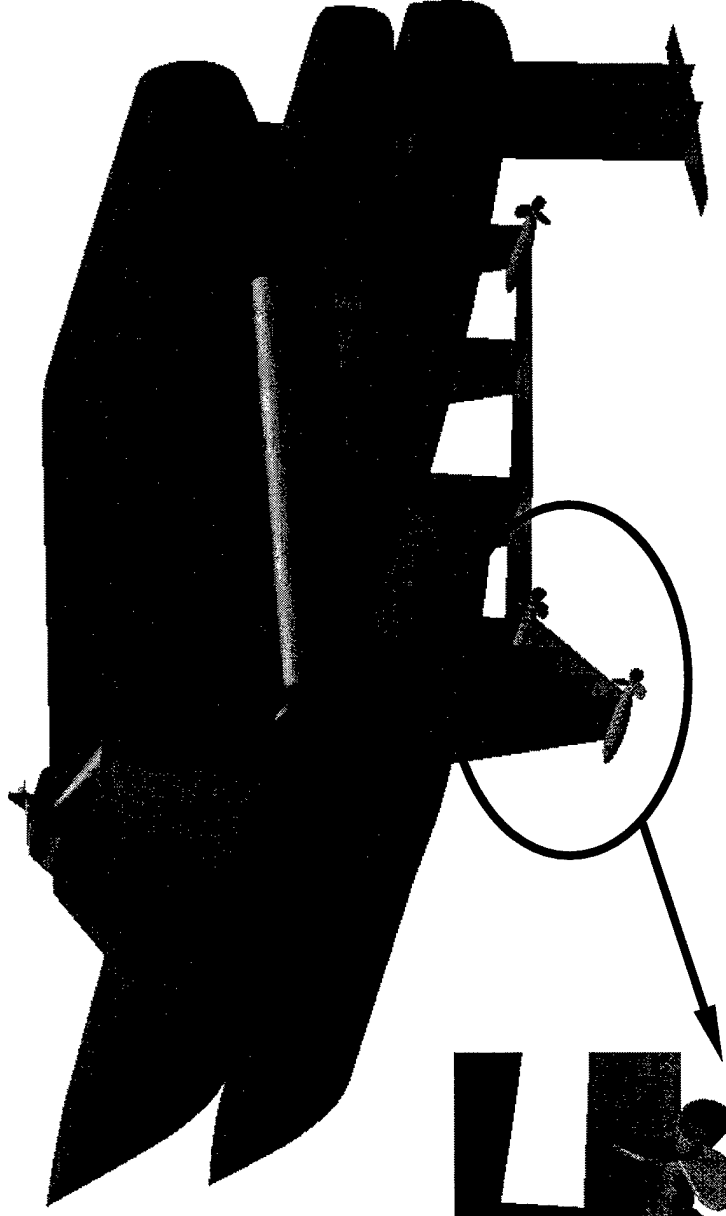
Hydrofoil Vessel – 4,000T – Jet Pump



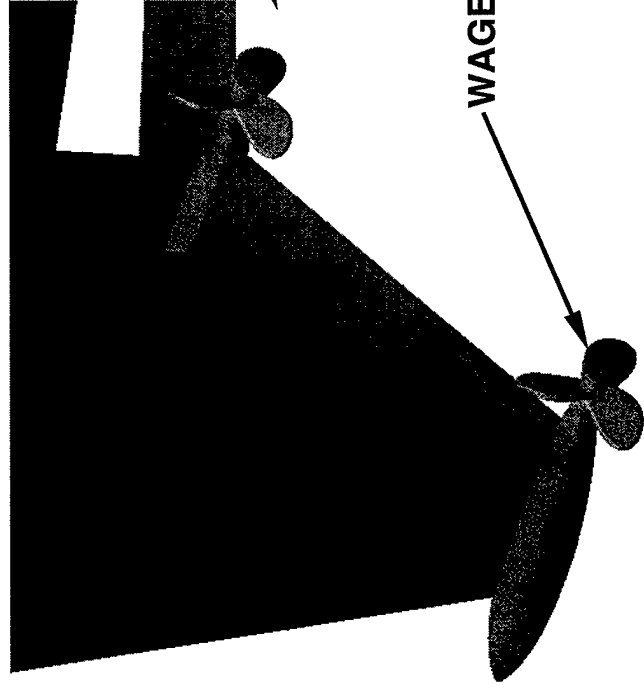
LM6000 GAS TURBINES



Hydrofoil Vessel – 4,000T – Water Screw



WAGENINGEN B4 SERIES PROP



Small Waterline Area Vessels

The next family of ships that were explored was the Small Waterline Area vessels. These vessels use submerged bodies mounted to struts for sustentation. In most cases, the body/strut system can be retracted into the main hull to achieve the 21 foot port depth. Propulsion for these vessels come from either jet pumps or water screws that are integrated into the submerged body.

Small waterline area vessels are divided into five configuration categories:

Small Waterline Area Tri Hull – SWATriH

Small Waterline Area Mono Hull - SWAMH

Small Waterline Area Mono Cavity Hull - SWAMCH

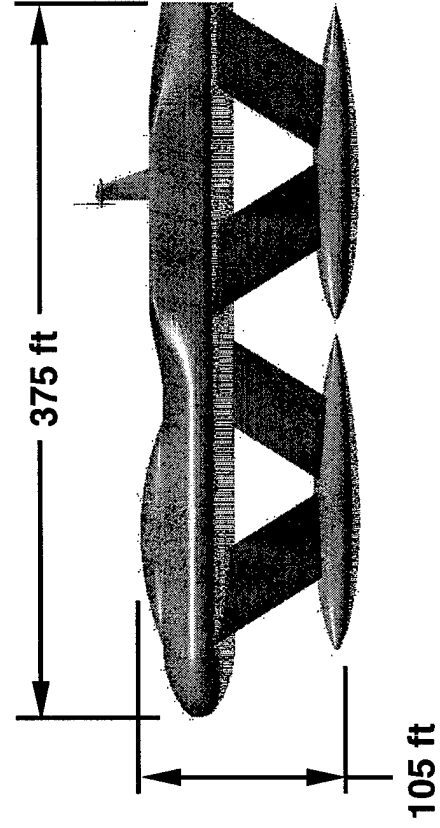
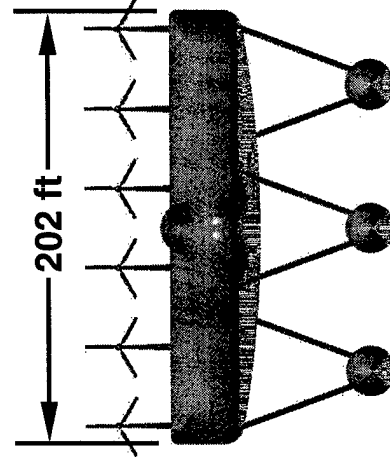
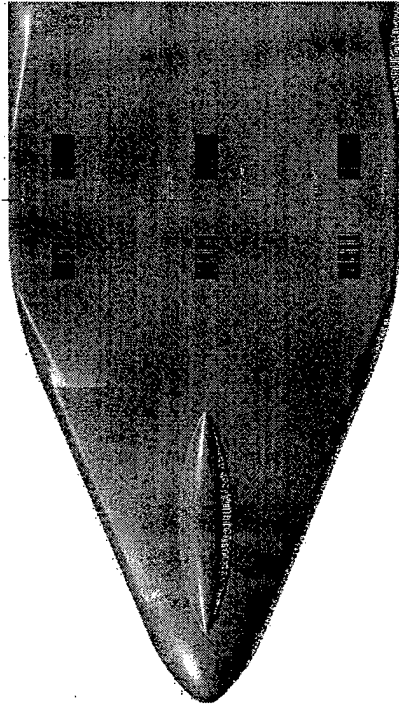
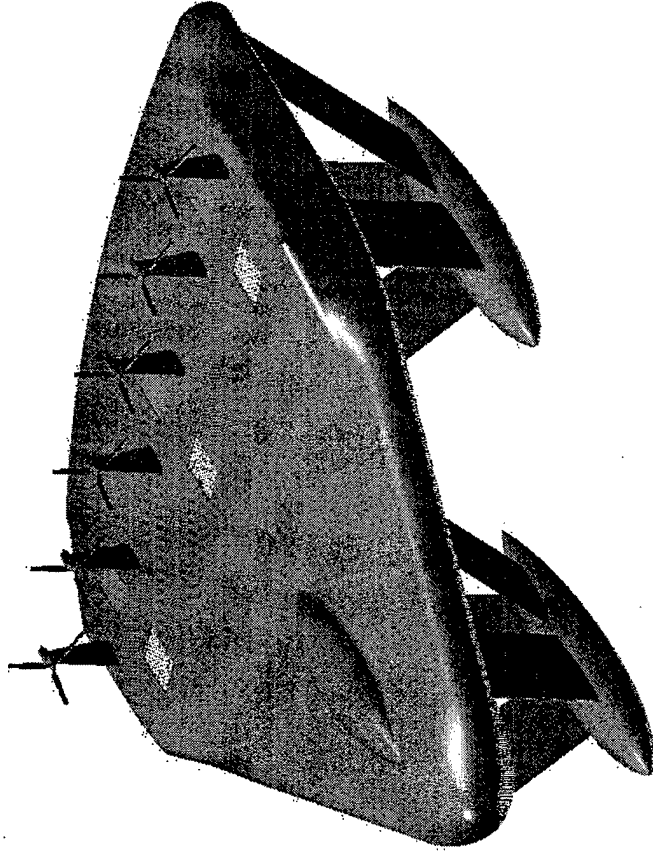
Small Waterline Area Twin Hull – SWATH

Small Waterline Area Twin Cavity Hull - SWATCH

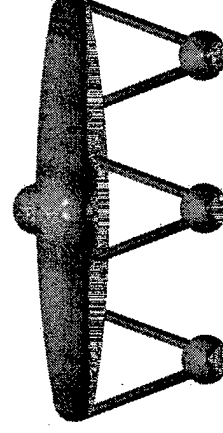
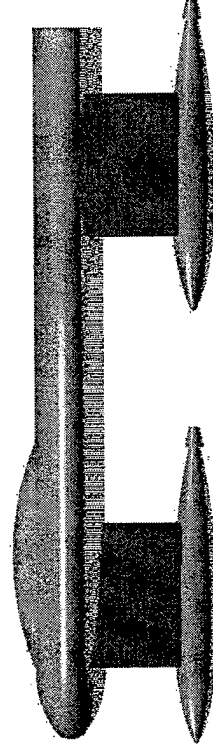
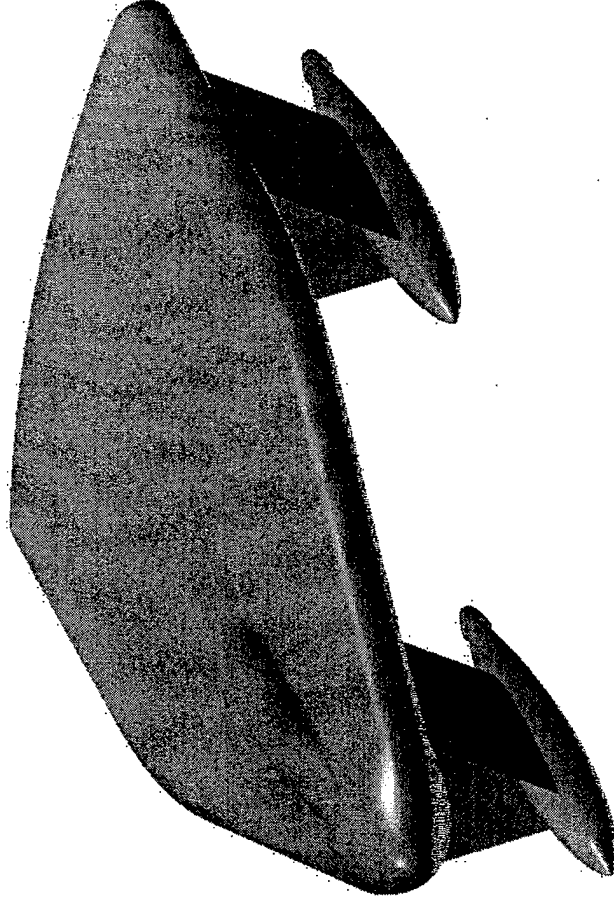
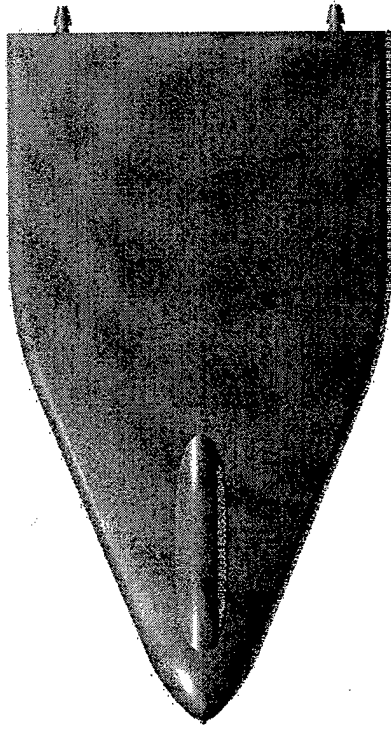
SWATriH Vessel – 4,000T

The following slides show the SWATriH vessel concepts. This system utilizes three submerged buoyant bodies for sustentation. The bodies were attached with four struts each to the main structure. Air coupled and jet pump systems were integrated for propulsion and LM6000 gas turbines were used to supply power. In the jet pump integration, the gas turbines were placed in the buoyant bodies because of the limited cross section of the struts.

SWATriH Vessel – 4,000T – Air Coupled



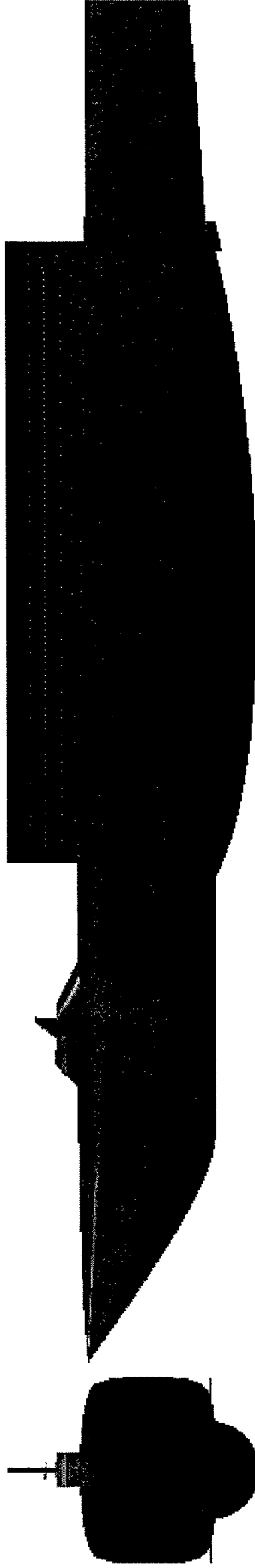
SWATriH Vessel – 4,000T – Jet Pump



SWAMH Vessel – 4,000T

The following slides show the Small Waterline Mono Hull (SWAMH) vessel concept. This system utilizes a single submerged buoyant body for sustentation which is attached to the main structure with a single retractable strut. The strut length is 95% of the body length and is 1.5% thick. It is raised and lowered by a direct drive gear system similar to what is used for power dam flood gates. Jet pump systems were integrated into the buoyant body for propulsion and a LM6000 gas turbine was used to supply power. The gas turbine could also be placed on top of the strut to enable the use of vertical drive shafts.

SWAMH Vessel – 4,000T



SWAMH Vessel – 4,000T

SHIP LENGTH = 477.8 FT

SHIP BEAM = 64.6 FT

SHIP HEIGHT = 67.3 FT

L/B RATIO = 7.4

BODY LENGTH = 231 FT

BODY DIAMETER = 34.2 FT

FINENESS RATIO = 6.75



CARGO BAY = 42.5 FT X 280 FT X 14 FT

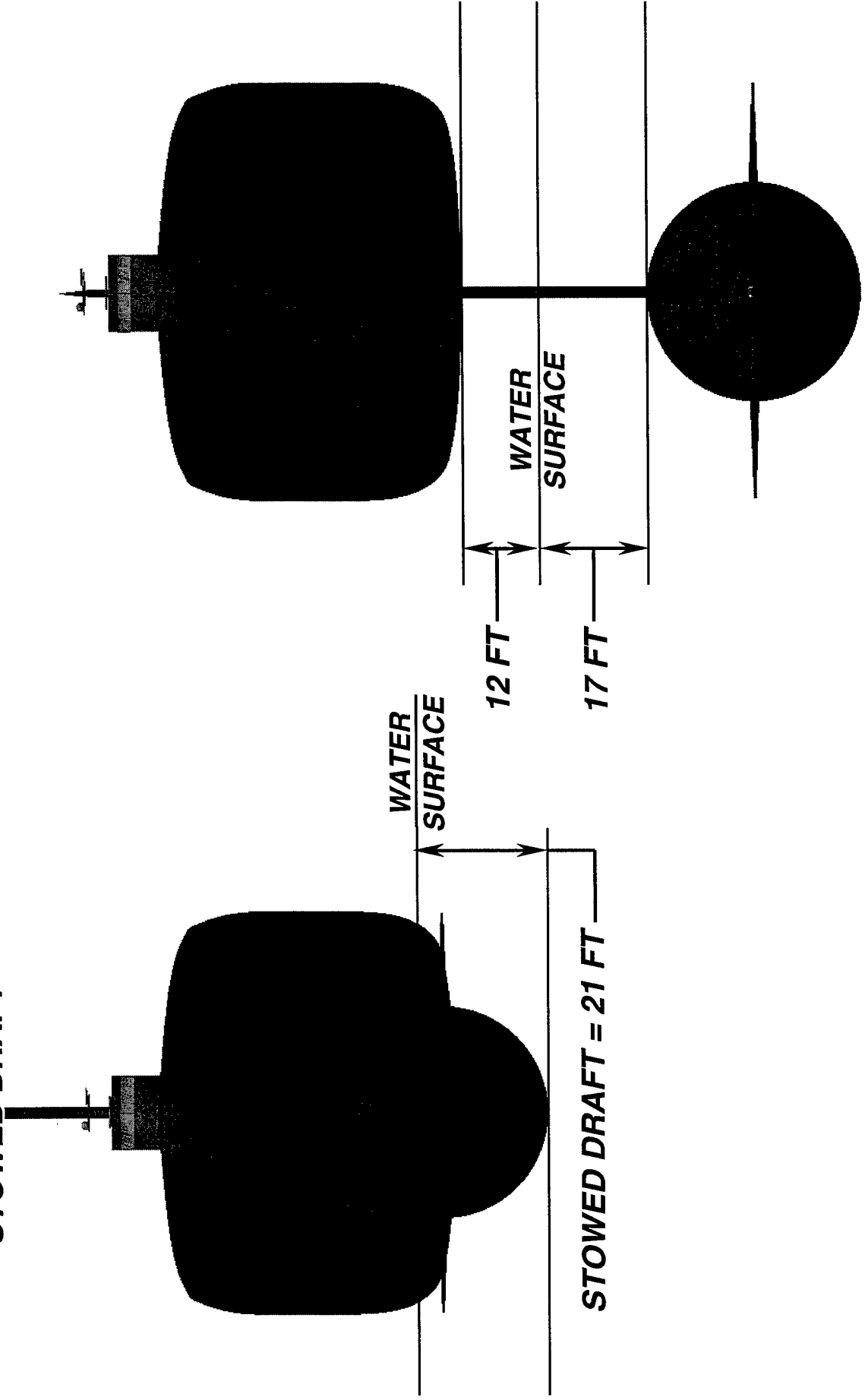
DRAFT = 21 FT

FLOOR AREA = 11,900 SQFT

SWAMH Vessel – 4,000T

STOWED DRAFT

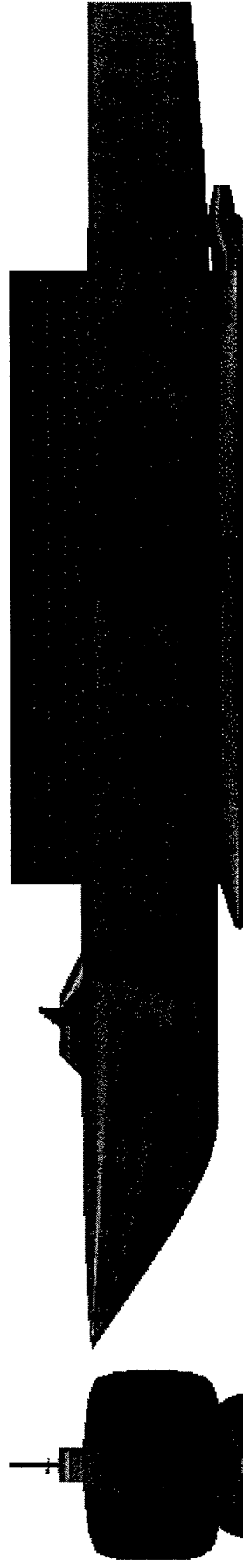
DEPLOYED DEPTHS



SWAMCH Vessel – 4,000T & 12,000T

The following slides show the Small Waterline Cavity Hull (SWAMCH) vessel concepts. This system utilizes a single submerged buoyant body for sustentation as before but, a large cavity has been added on the lower surface to help reduce skin friction. This cavity is pressurized with engine exhaust or air to provide the low friction surface. As before, the body is attached to the main structure with a single retractable strut. The strut length is 95% of the body length and is 1.5% thick. It is raised and lowered by a direct drive gear system as described previously. Jet pump systems were integrated into the buoyant body for propulsion and a LM6000 gas turbine was used to supply power. The gas turbine could also be placed on top of the strut as before.

SWAMCH Vessel – 4,000T



SWAMCH Vessel – 4,000T

SHIP LENGTH = 477.8 FT

SHIP BEAM = 64.6 FT

SHIP HEIGHT = 67.3 FT

L/B RATIO = 7.4

BODY LENGTH

= 256.8 FT

BODY HEIGHT

= 20.1 FT

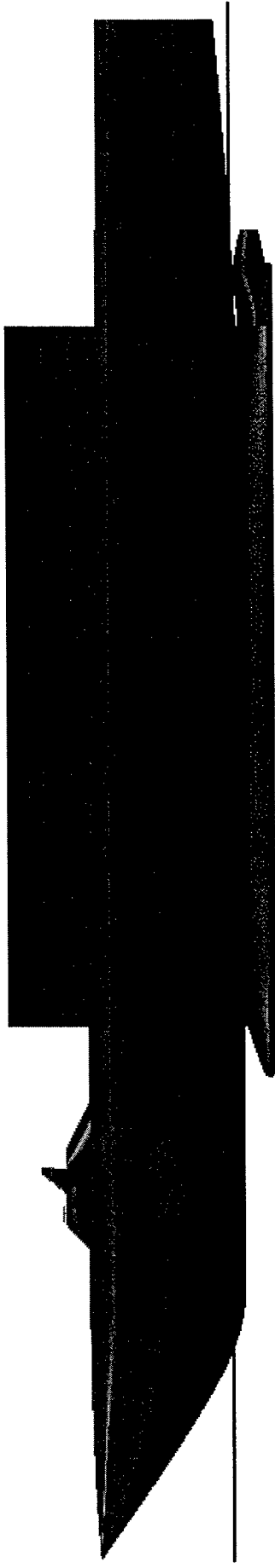
BODY WIDTH

= 50.1 FT

FINENESS RATIO

= 12.8

BODY ASPECT RATIO = 2.5



CARGO BAY = 42.5 FT X 280 FT X 14 FT

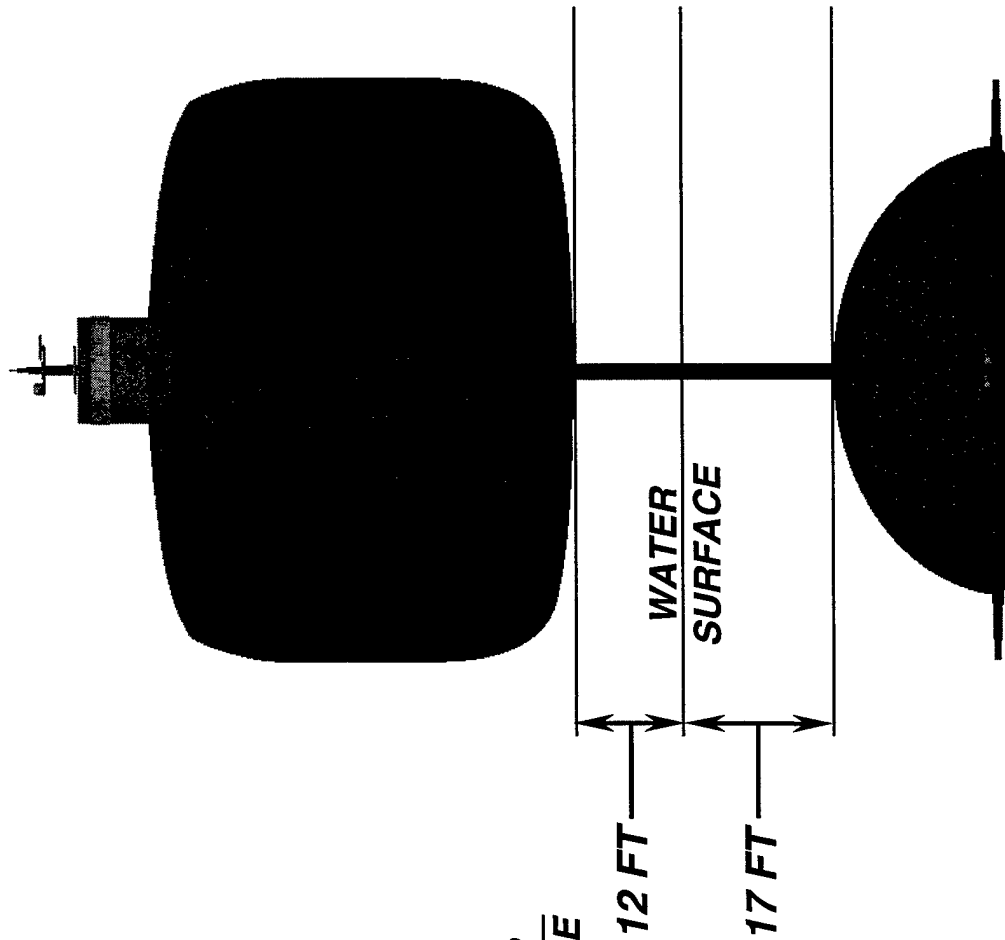
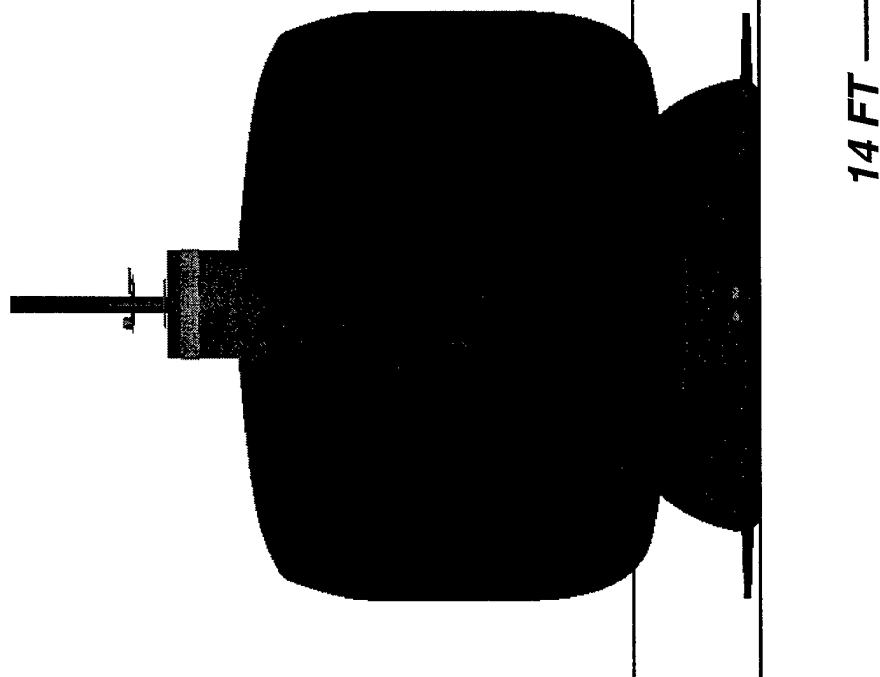
DRAFT = 14 FT

FLOOR AREA = 11,900 SQFT

SWAMCH Vessel – 4,000T

STOWED DRAFT

DEPLOYED DEPTHS



EDET.IN

* TTILE CARD
SYNTHESIZE TRAINING EXAMPLE PROBLEM

* KEYWORDS FOR SYNTHESIZE

* =====

* CLMAX0 1.5

* CLMAX30 1.8

* CLFLP30 0.0

* CDFLP30 0.0050

* CMFLP30 -0.01

* CLMAX60 2.7

* CLFLP60 0.8

* CDFLP60 0.0500

* CMFLP60 -0.50

* WEIGHT 200000.

* IXX 350000000.

* IYY 1800000000.

* IZZ 5000000000.

* OFFSET MACH 0.3

* OFFSET CL 0.0

* OFFSET CD 0.0

* OFFSET Cm 0.0

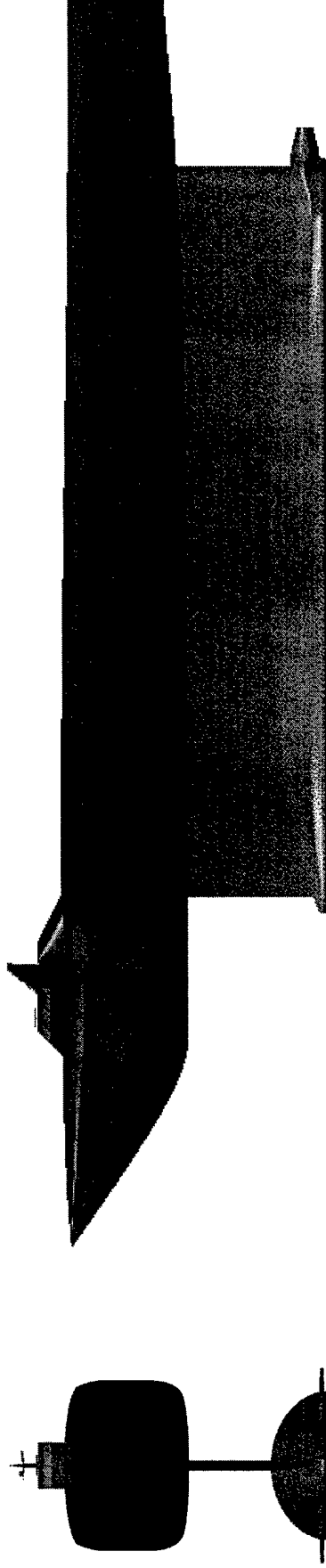
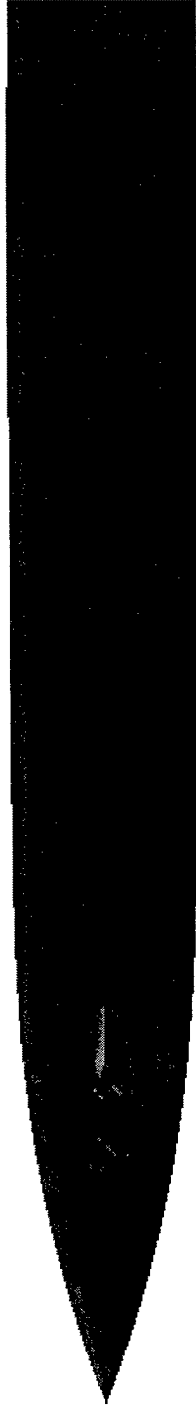
* OFFSET CnBETA 0.0

* ENTER DATA IN FIELDS OF 10. MARKS ARE IN TENTH LOCATION.

*WING T/C	AR	SWEEP	% CAMBER	SREF	TAPER
.12	8.00	20.0	0.0	1800.	.5
*BODY/SPAN	SPI	SBASE	BODY L/D		
0.10	115.	10.	10.0		
*MODE	ALTITUDE	RN/FT	TECHNOLOGY		
1.	30000.	1.	2.		
*NAME	SWET	LENGTH	L/D OR T/C	TRANSITION	X/C
				UPPER	LOWER
WING	3600.	15.	.12	0.	0.
FUSELAGE	4200.	120.	10.0	0.	0.
TAIL-HORZ	760.	10.	.12	0.	0.
TAIL-VERT	410.	10.	.12	0.	0.
NACELLES (2)	800.	10.	6.0	0.	0.
PYLONS (2)	300.	8.	.10	0.	0.

*
*FIXED COMP NAME | DELTA CD | | | |

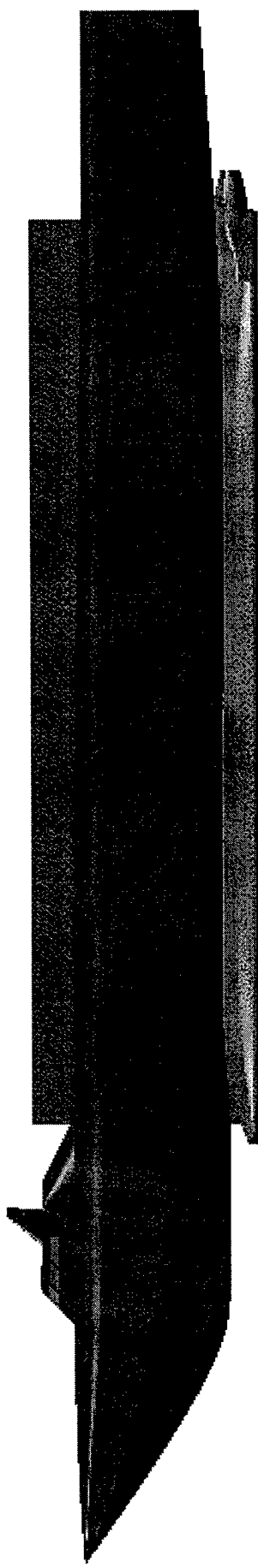
SWAMCH Vessel – 12,000T



SWAMCH Vessel – 12,000T

SHIP LENGTH = 650 FT
SHIP BEAM = 87.9 FT
SHIP HEIGHT = 88 FT
L/B RATIO = 7.4

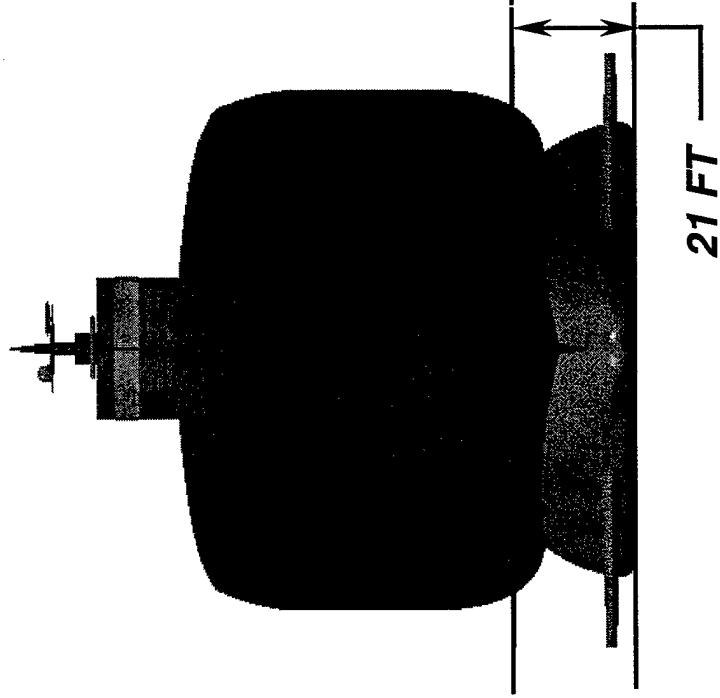
BODY LENGTH = 392.4 FT
BODY HEIGHT = 31.2 FT
BODY WIDTH = 77.2 FT
FINENESS RATIO = 12.6
BODY ASPECT RATIO = 2.5



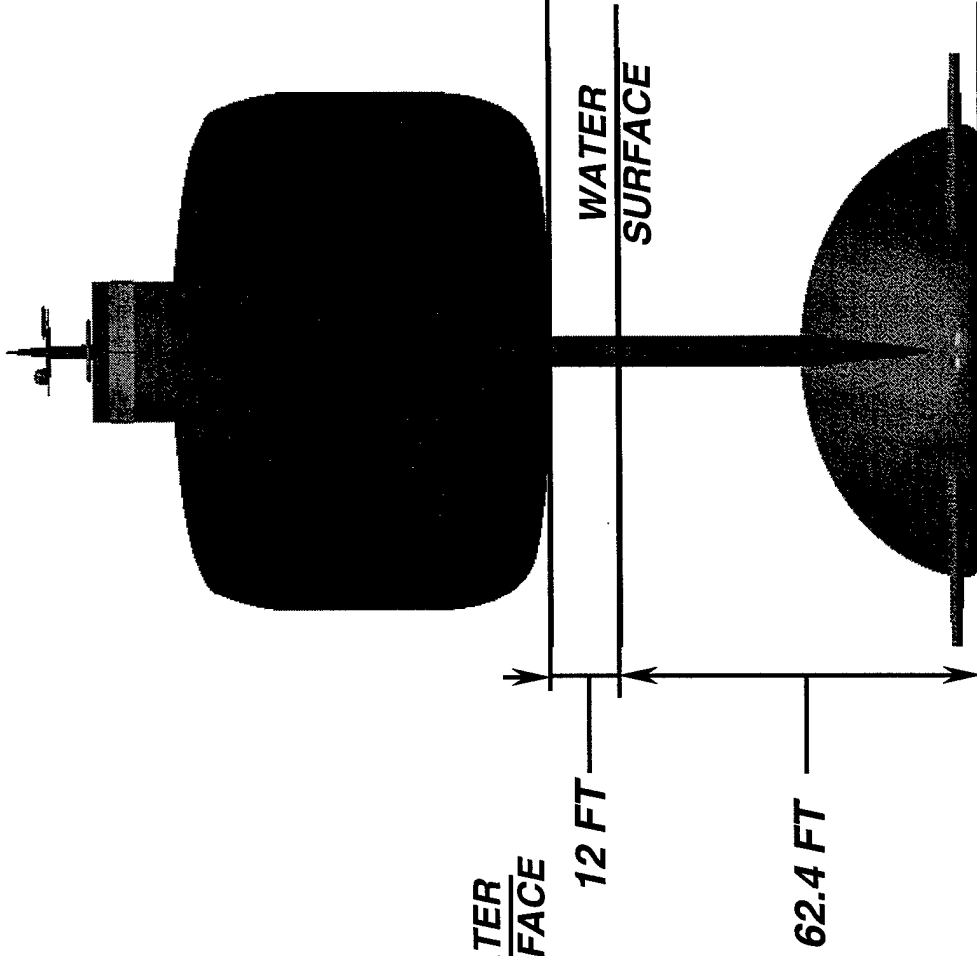
CARGO BAY = 70 FT X 320 FT X 14 FT
FLOOR AREA = 22,400 SQFT
DRAFT = 21 FT

SWAMCH Vessel – 12,000T

STOWED DEPTH



DEPLOYED DEPTHS



SWAMCH Vessel – 12,000T

The following slide shows the structural weight estimate for the SWAMCH vessel. Standard ship construction methods were followed in the structural modeling of the vessel in CATIA 3D solids. Once complete, the model was analyzed and the weight was obtained.

SWAMCH Vessel – 12,000T

SHIP STRUCTURAL WEIGHT BREAKDOWN 12,000 – 15,000 TON CLASS

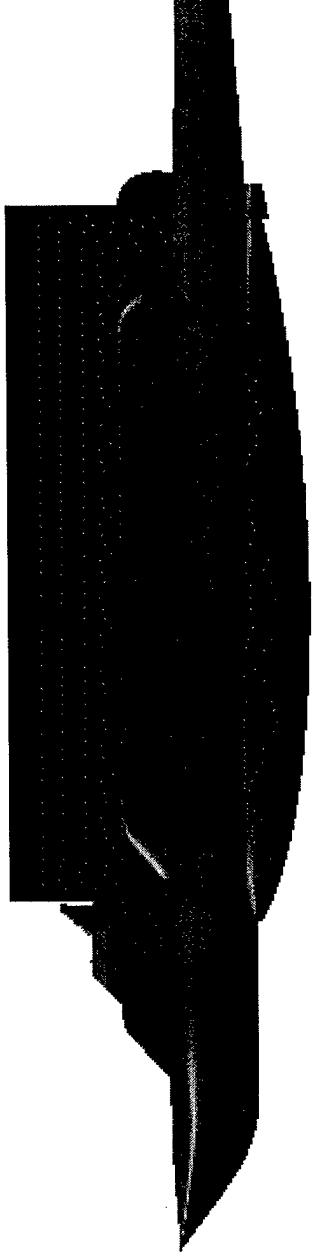
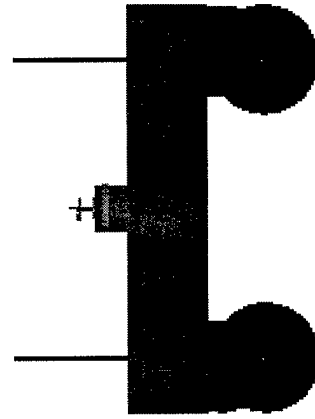
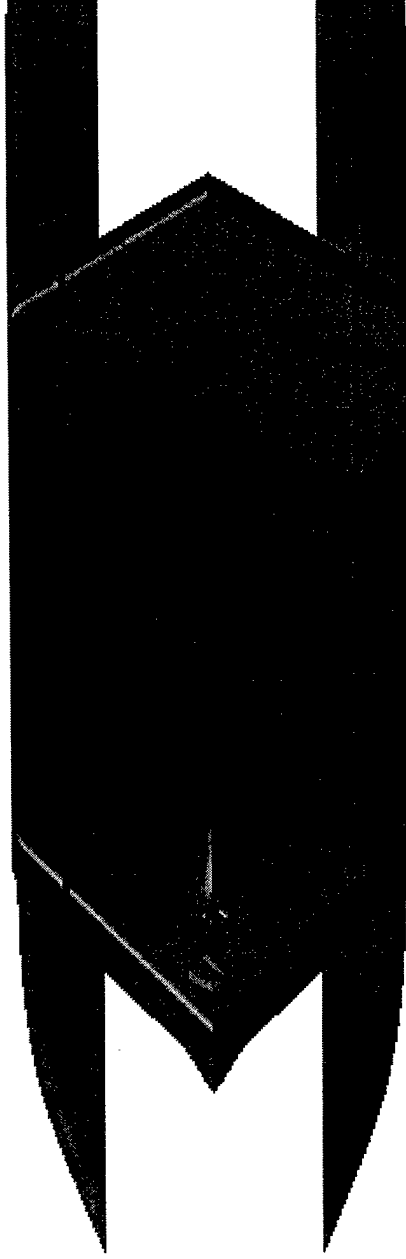
SUB STRUCTURE	3219 TONS
HULL	1563 TONS
DECKING	1008 TONS
STRUT CASION	<u>1128 TONS</u>
TOTAL	6918 TONS



SWATH Vessel

The following slides show the Small Waterline Twin Hull (SWATH) vessel concept. This system utilizes two submerged buoyant bodies for sustentation that are attached to the main structure with two retractable struts. The strut length is 95% of the body length and is 1.5% thick. It is raised and lowered by a direct drive gear system as described previously. Jet pump systems were integrated into the buoyant bodies for propulsion and a LM6000 gas turbine was used to supply power. The gas turbine could also be placed on top of the strut as before.

SWATH Vessel – 4,000T



SWATH Vessel – 4,000T

SHIP LENGTH = 314.8 FT

SHIP BEAM = 100.4 FT

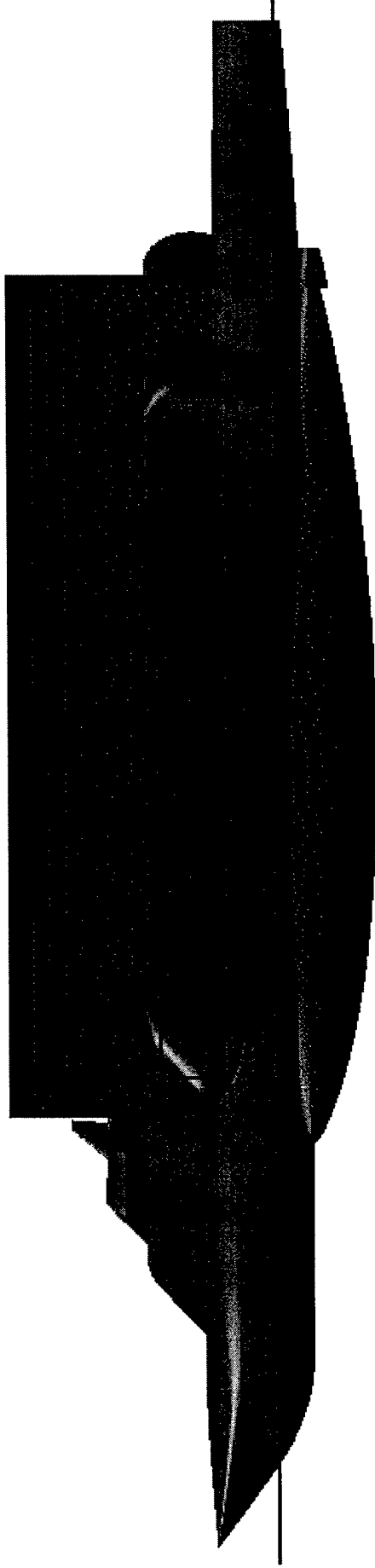
SHIP HEIGHT = 55.3 FT

L/B RATIO = 3.1

BODY LENGTH = 184.5 FT

BODY DIAMETER = 27.3 FT

FINENESS RATIO = 6.75



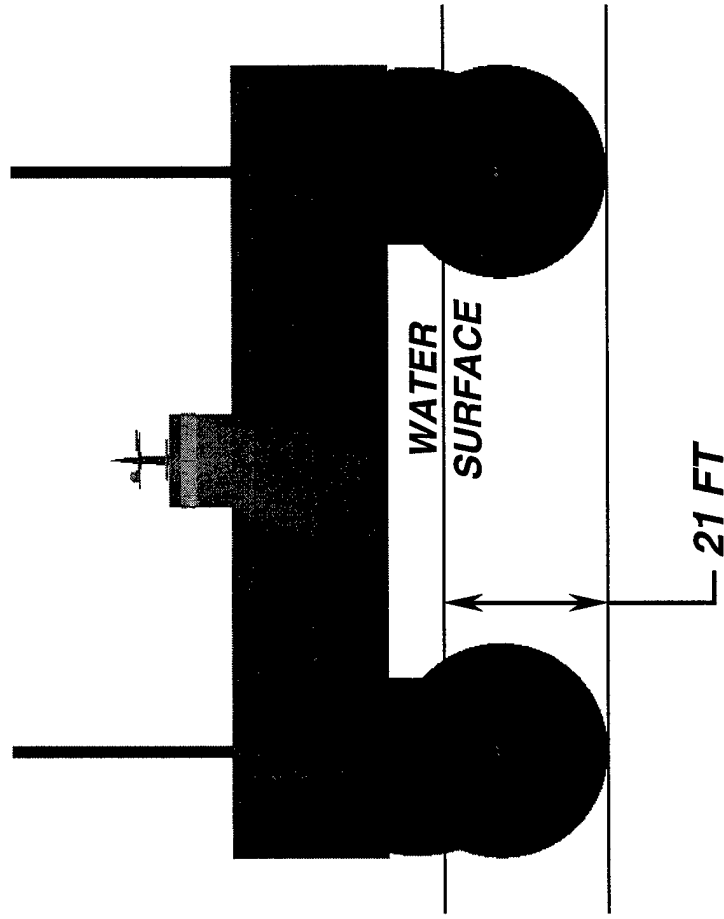
CARGO BAY = 80 FT X 140 FT X 14 FT

DRAFT = 21 FT

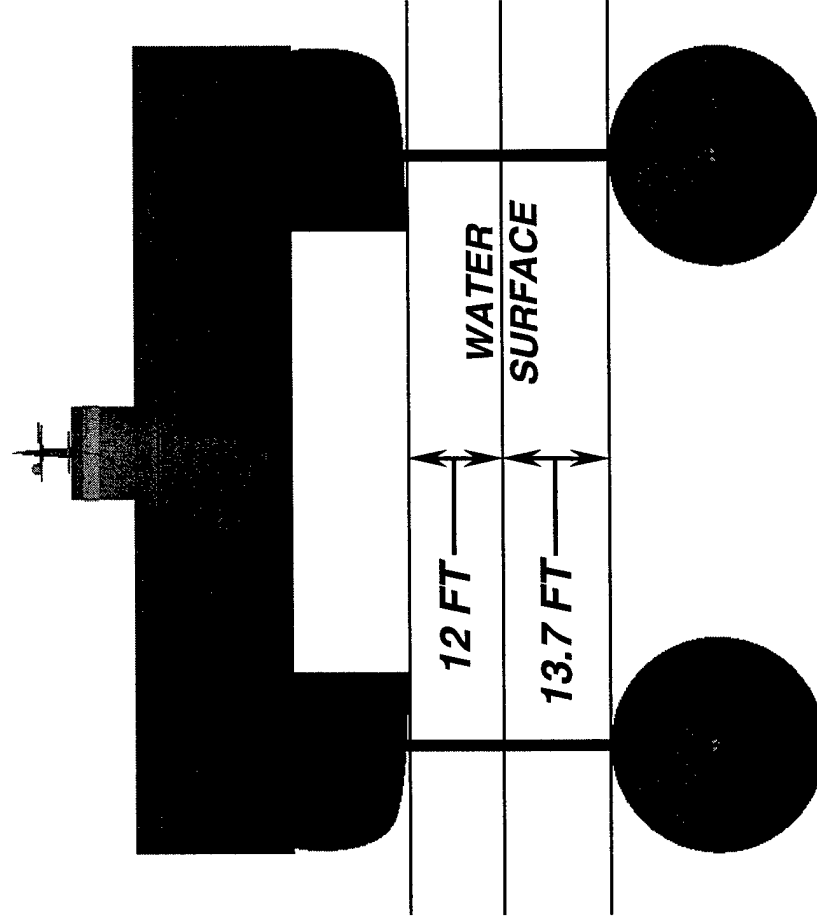
FLOOR AREA = 11,200 SQFT

SWATH Vessel – 4,000T

STOWED DRAFT



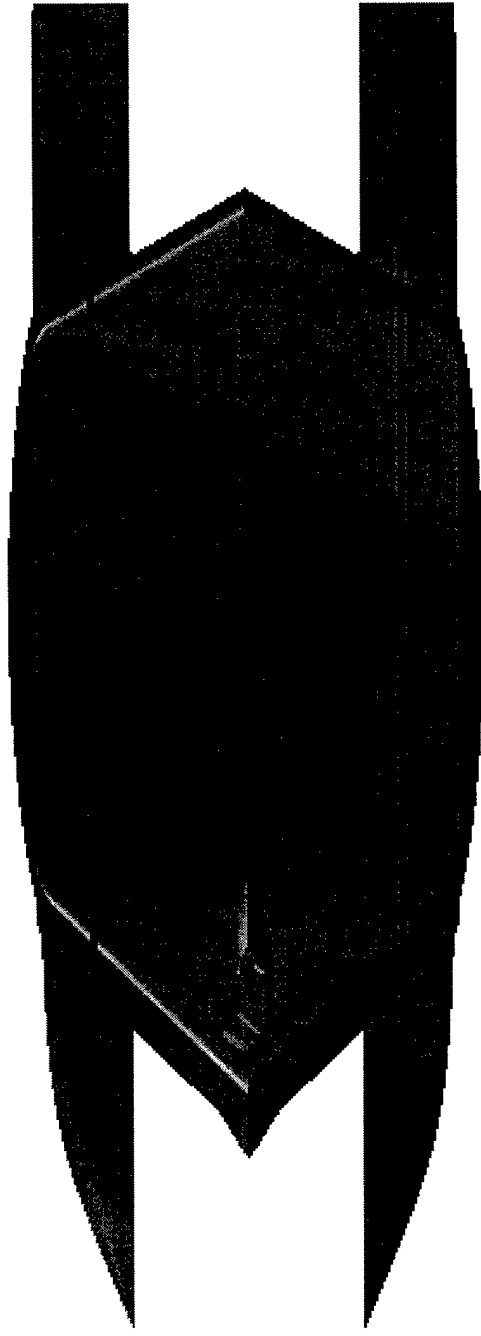
DEPLOYED DEPTHS



SWATCH Vessels – 4,000T & 31,500T

The following slides show the Small Waterline Twin Cavity Hull (SWATCH) vessel concepts. This system utilizes two submerged buoyant bodies for sustentation with the lower cavity that was described previously. As before, the bodies are attached to the main structure with two retractable struts. The strut length is 95% of the body length and is 1.5% thick. It is raised and lowered by a direct drive gear system as described previously. Jet pump systems were integrated into the buoyant bodies for propulsion and a LM6000 gas turbine was used to supply power. The gas turbine could also be placed on top of the strut as before. The 31,500 ton vessel is the maximum that could be achieved within the given constraints of length, beam and depth.

SWATCH Vessel – 4,000T



SWATCH Vessel – 4,000T

SHIP LENGTH = 314.8 FT

BODY LENGTH = 202.6 FT

SHIP BEAM = 100.4 FT

BODY HEIGHT = 16.1 FT

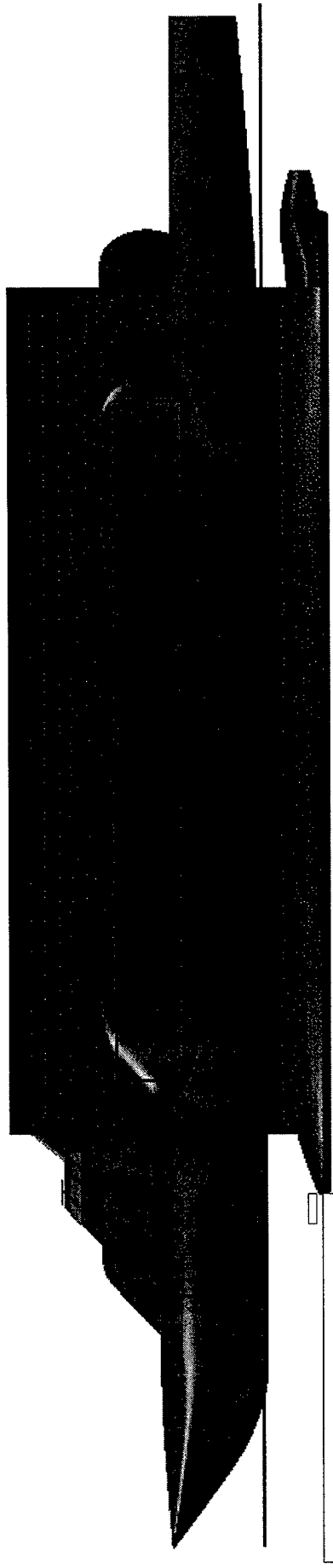
SHIP HEIGHT = 55.3 FT

BODY WIDTH = 40.1 FT

L/B RATIO = 3.1

FINENESS RATIO = 12.6

BODY ASPECT RATIO = 2.5



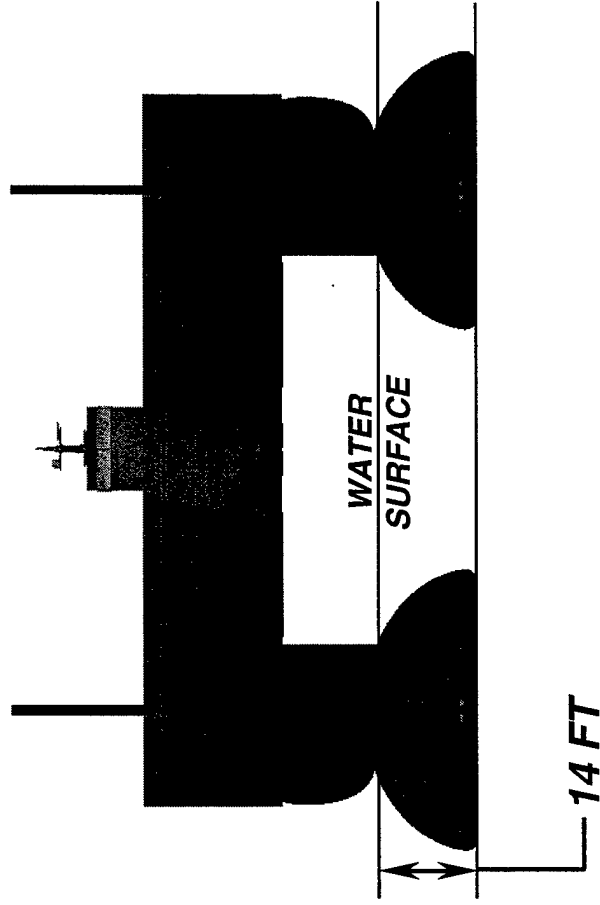
CARGO BAY = 80 FT X 140 FT X 14 FT

DRAFT = 14 FT

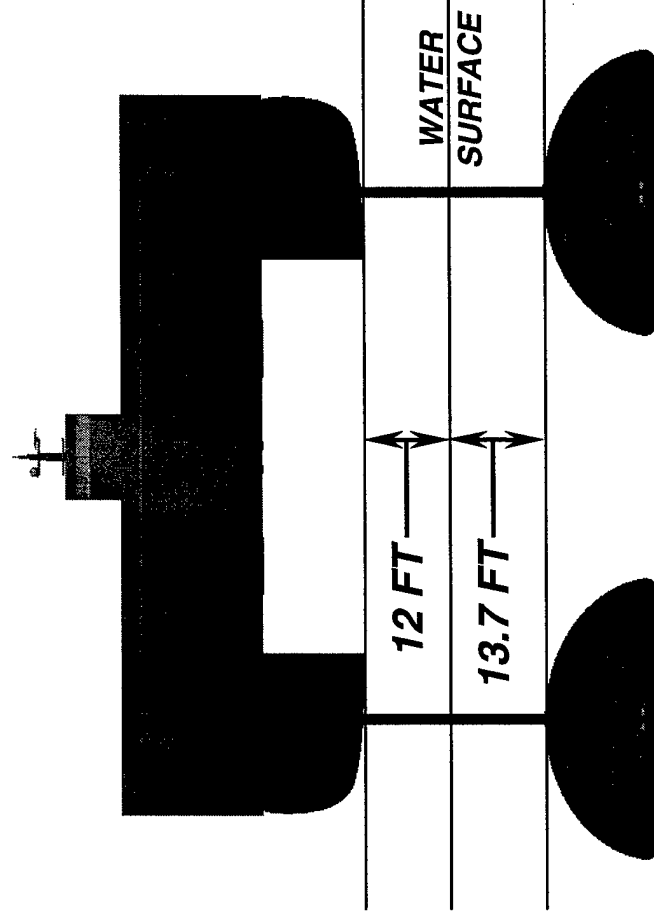
FLOOR AREA = 11,200 SQFT

SWATCH Vessel – 4,000T

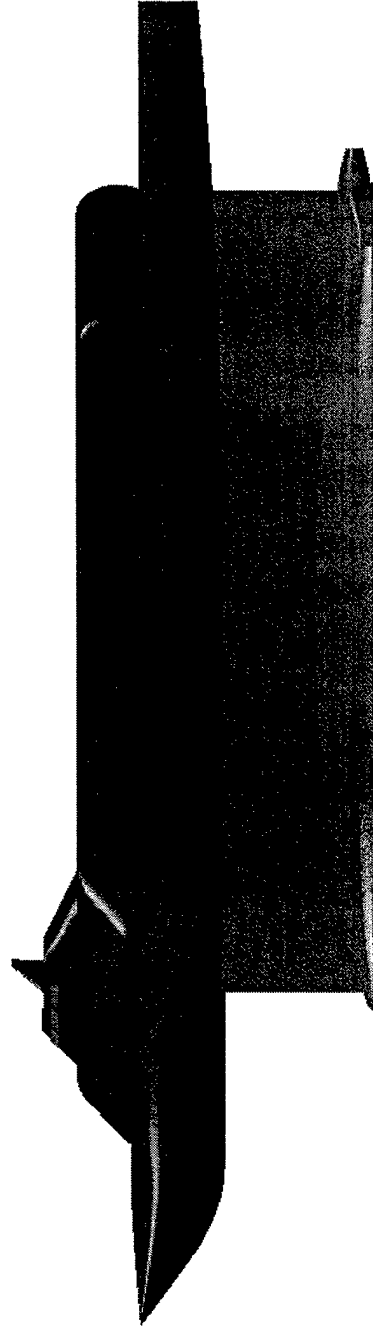
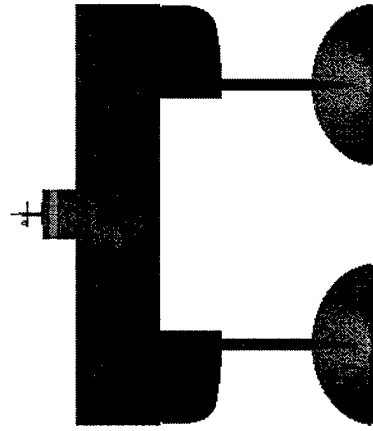
STOWED DRAFT



DEPLOYED DEPTHS



SWATCH Vessel – 31,500T



SWATCH Vessel – 31,500T

SHIP LENGTH = 629.6 FT

BODY LENGTH = 392.4 FT

SHIP BEAM = 200 FT

BODY HEIGHT = 31.2 FT

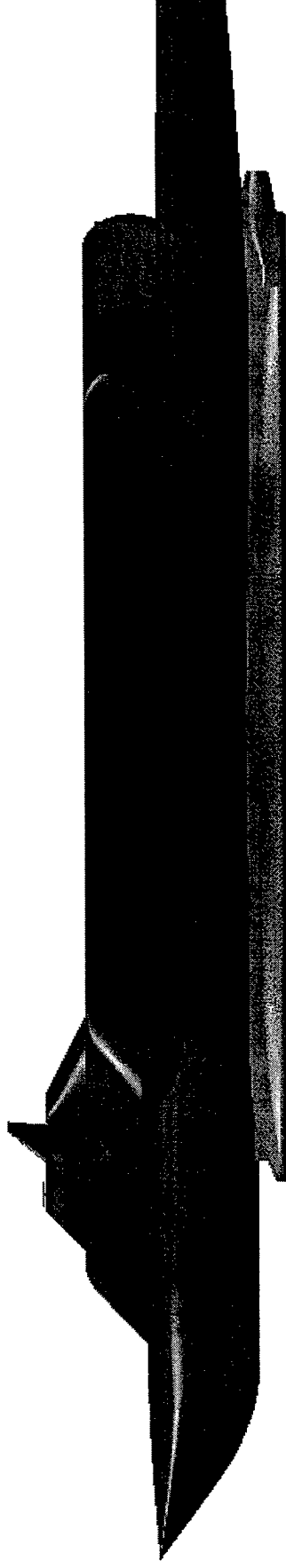
SHIP HEIGHT = 119 FT

BODY WIDTH = 77.2 FT

L/B RATIO = 3.15

FINENESS RATIO = 12.6

BODY ASPECT RATIO = 2.5



CARGO BAY = 160 FT X 280 FT X 14 FT

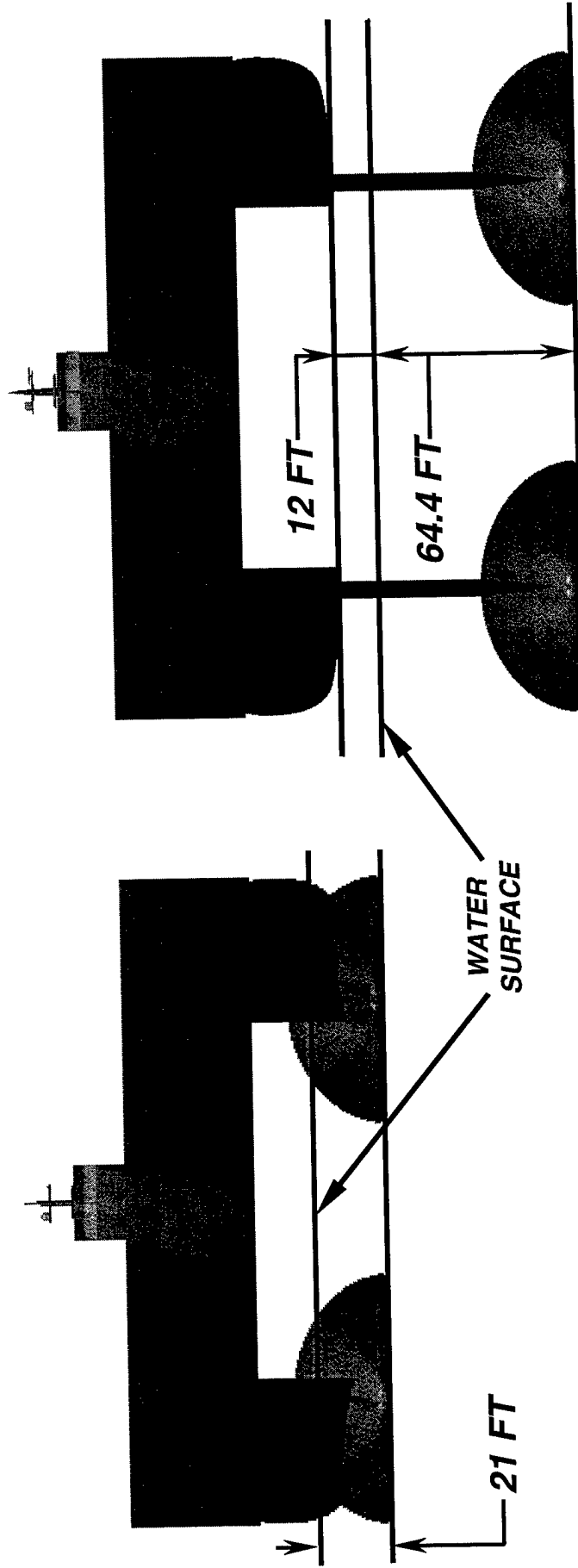
DRAFT = 21 FT

FLOOR AREA = 44,800 SQFT

SWATCH Vessel – 31,500T

STOWED DRAFT

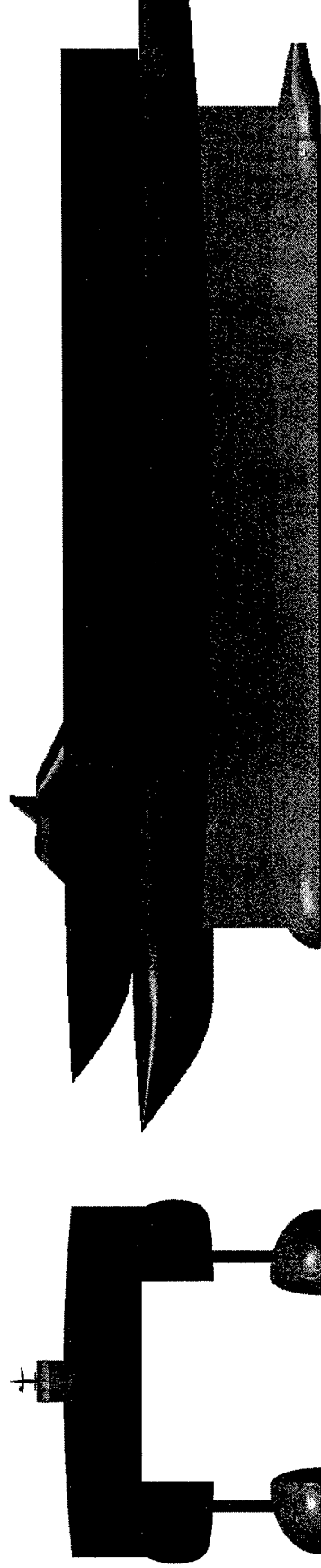
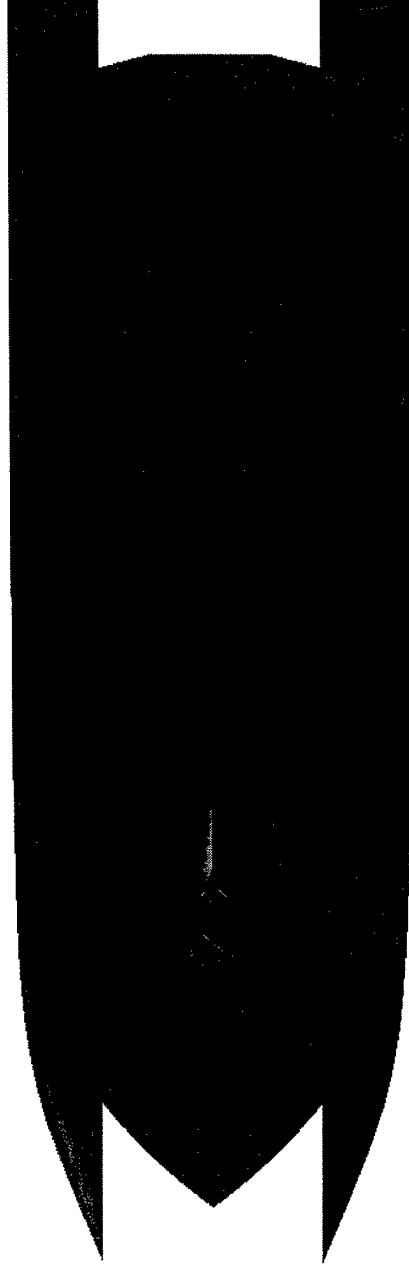
DEPLOYED DEPTHS



SWATCH Vessels – 31,500T

The following slides show the integration of the P29TA12 submerged body which was generated from the hydrodynamic optimizer. As before, the bodies are attached to the main structure with two retractable struts. The strut length is 95% of the body length and is 1.5% thick. It is raised and lowered by a direct drive gear system as described previously.

SWATCH Vessels – 31,500T



SWATCH Vessels – 31,500T

SHIP LENGTH = 650 FT

BODY LENGTH = 496 FT

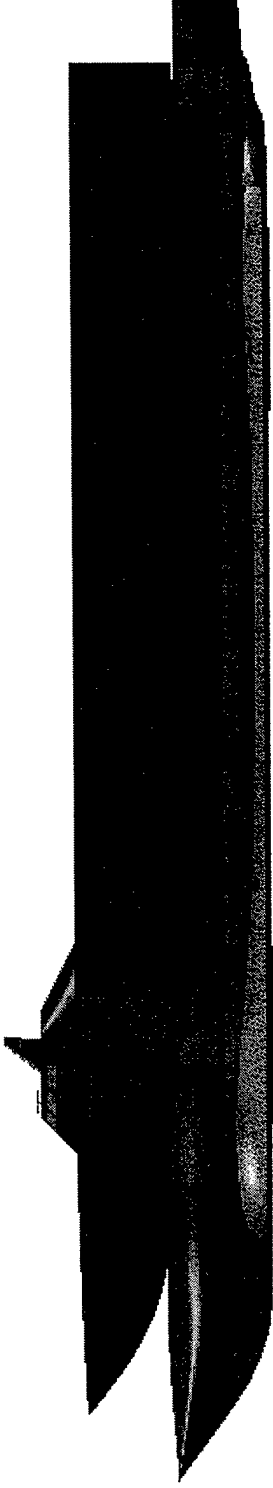
SHIP BEAM = 200 FT

BODY HEIGHT = 33 FT

SHIP HEIGHT = 97 FT

BODY WIDTH = 50 FT

L/B RATIO = 3.25



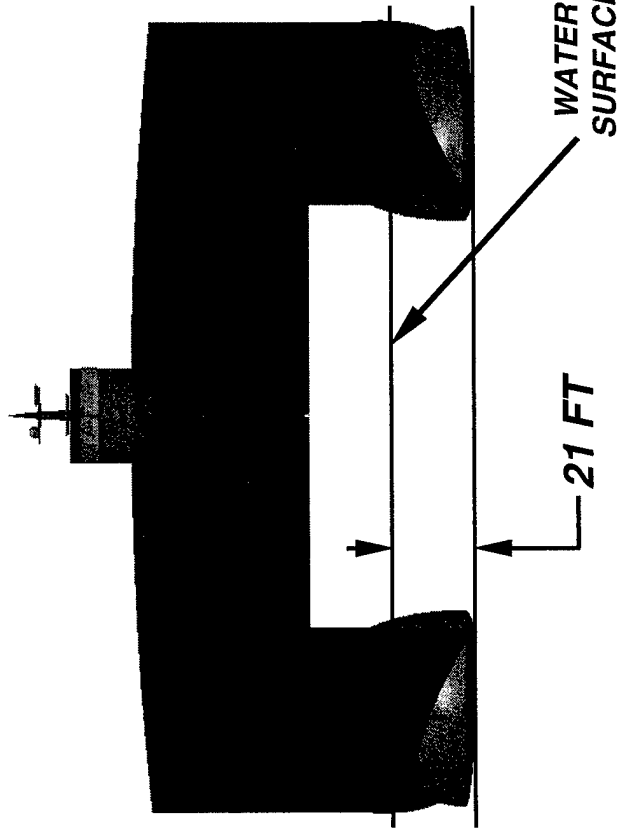
CARGO BAY = 160 FT X 380 FT X 14 FT

DRAFT = 21 FT

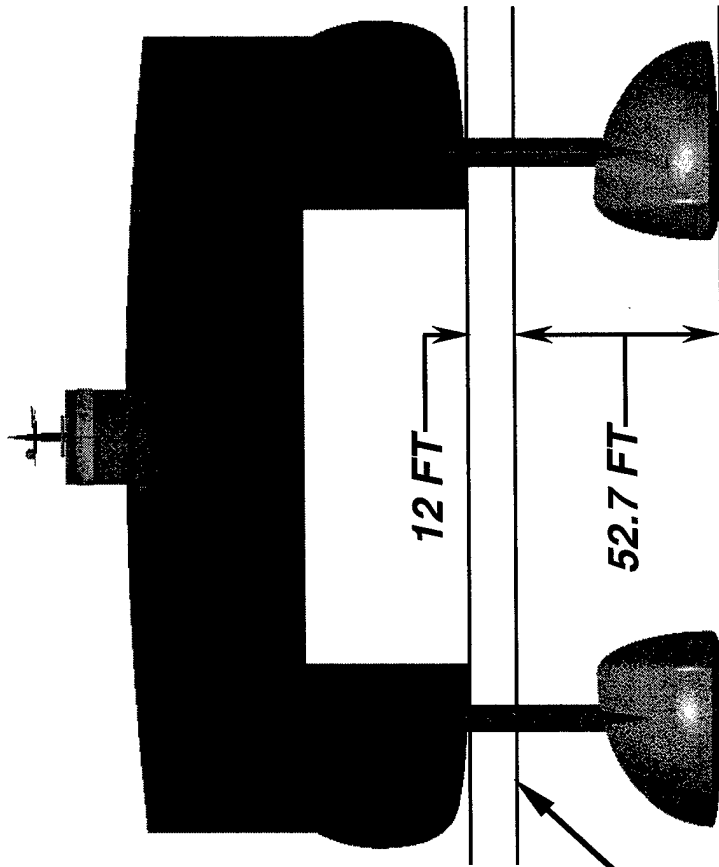
FLOOR AREA = 60,800 SQFT

SWATCH Vessels – 31,500T

STOWED DRAFT



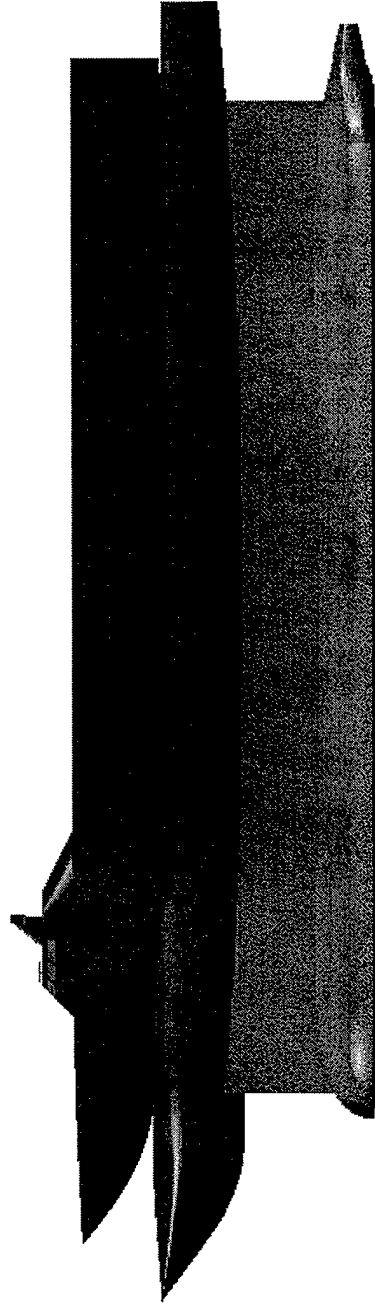
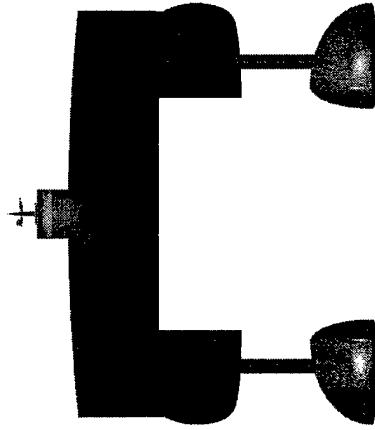
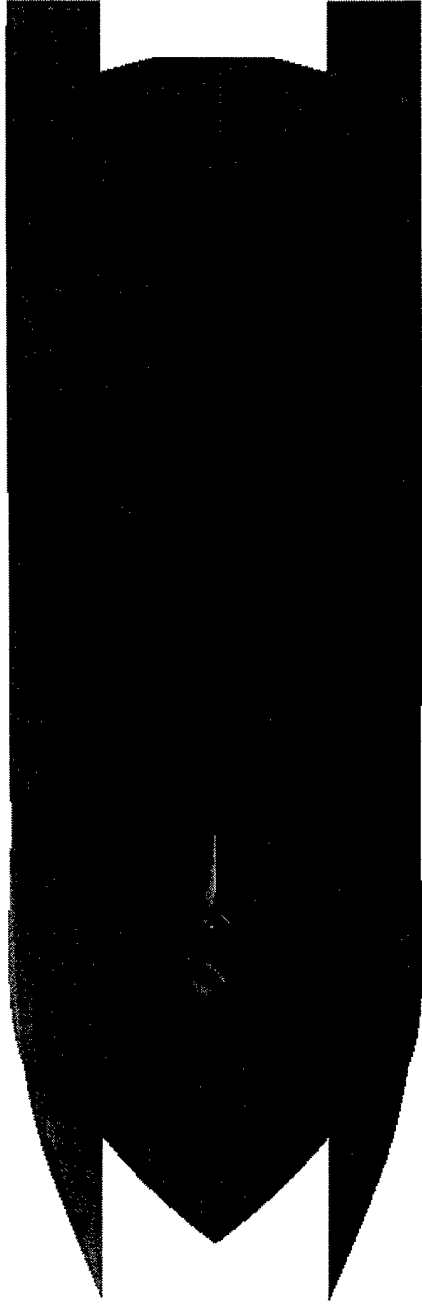
DEPLOYED DEPTHS



SWATCH Vessels – 40,000T, 50,000T & 60,000T

The following slides show three SWATCH vessel concepts that exceed the given design constraints, but incorporate the same design features for the struts and propulsion as the 4,000 ton vessel. These concepts were sized to show what could be achieved if the design constraints were relaxed.

SWATCH Vessels – 40,000T



SWATCH Vessels – 40,000T

SHIP LENGTH = 650 FT

BODY LENGTH = 523 FT

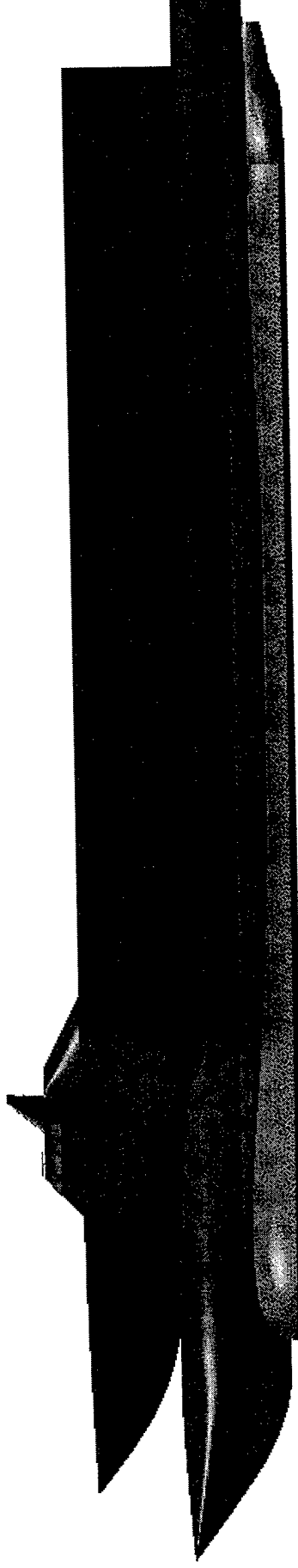
SHIP BEAM = 208 FT

BODY HEIGHT = 34 FT

SHIP HEIGHT = 97 FT

BODY WIDTH = 53 FT

L/B RATIO = 3.13



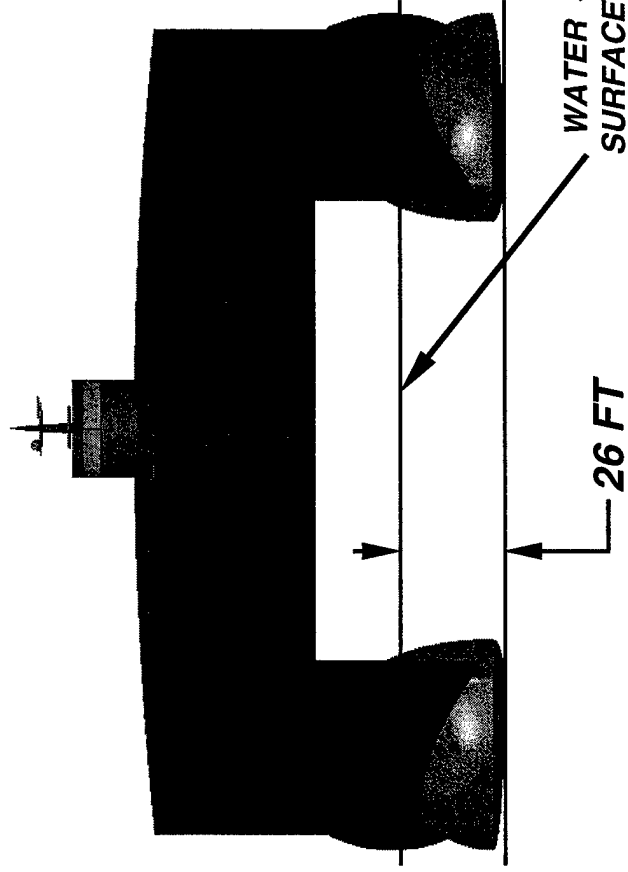
DRAFT = 26 FT

CARGO BAY = 160 FT X 380 FT X 14 FT

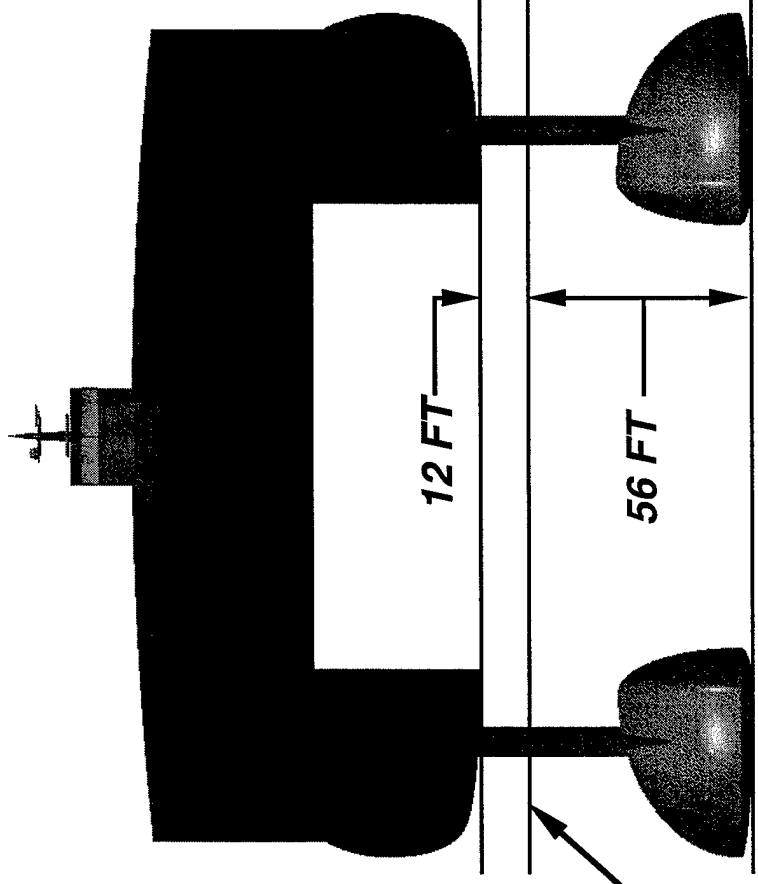
FLOOR AREA = 60,800 SQFT

SWATCH Vessels – 40,000T

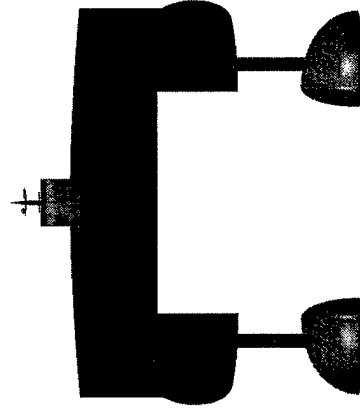
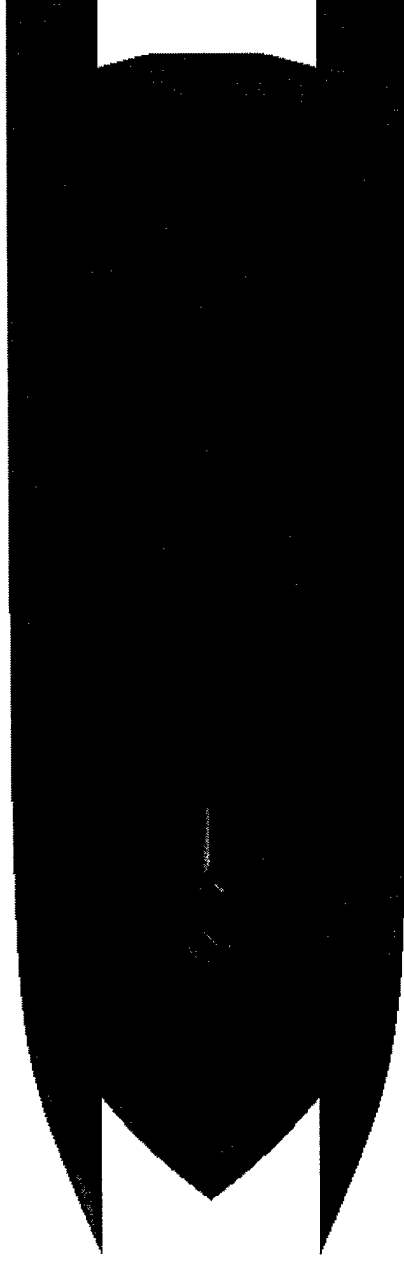
STOWED DRAFT



DEPLOYED DEPTHS



SWATCH Vessels – 50,000T



SWATCH Vessels – 50,000T

SHIP LENGTH = 739 FT

= 563 FT

SHIP BEAM = 236 FT

= 37 FT

SHIP HEIGHT = 118 FT

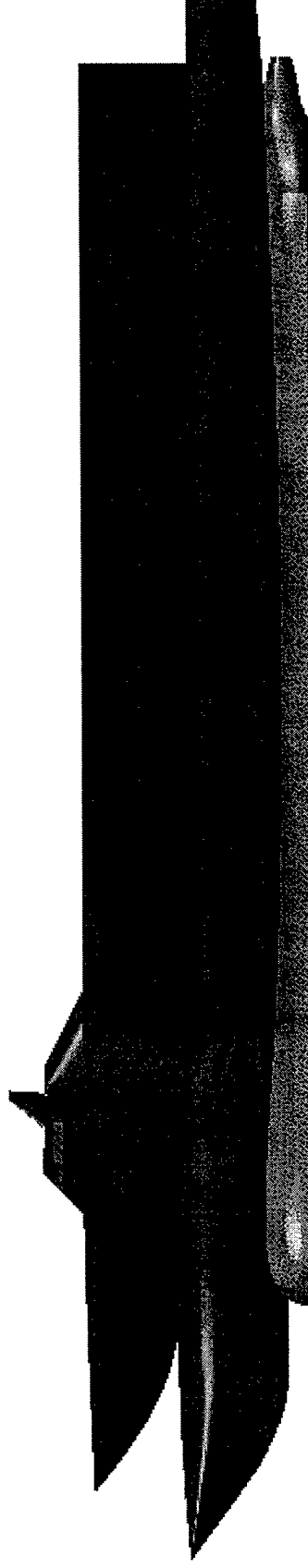
= 57 FT

L/B RATIO = 3.13

BODY LENGTH

BODY HEIGHT

BODY WIDTH



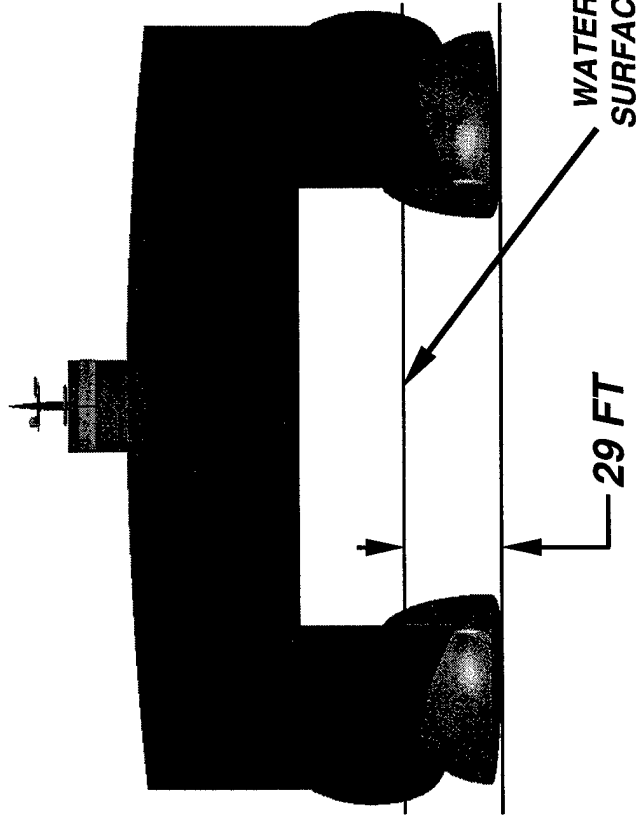
CARGO BAY = 190 FT X 430 FT X 14 FT

DRAFT = 29 FT

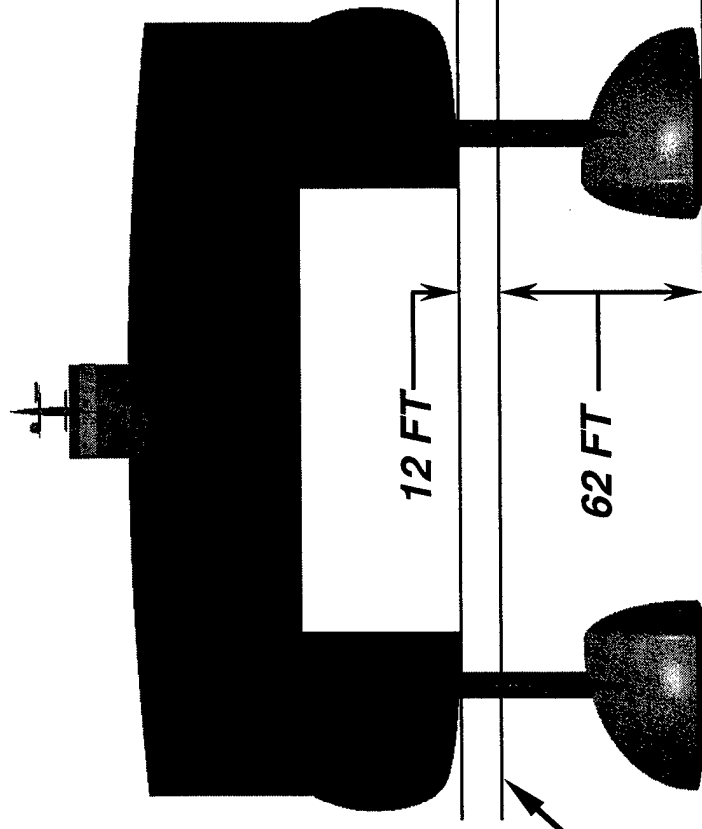
FLOOR AREA = 81,700 SQFT

SWATCH Vessels – 50,000T

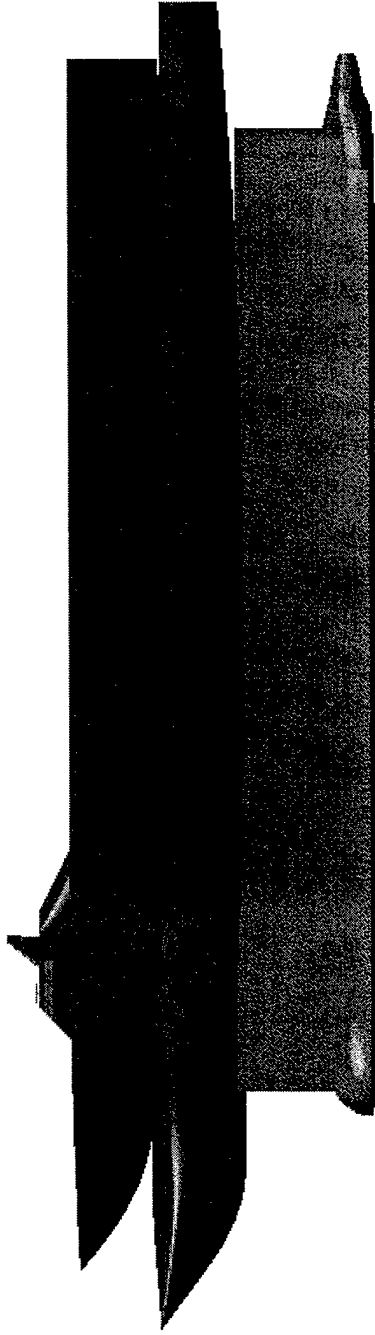
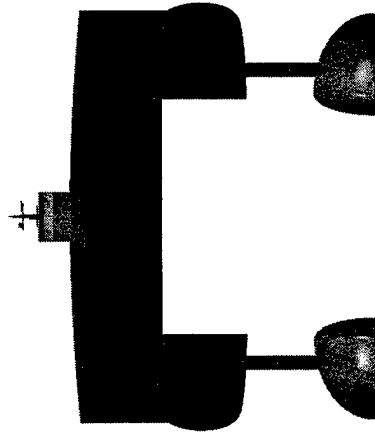
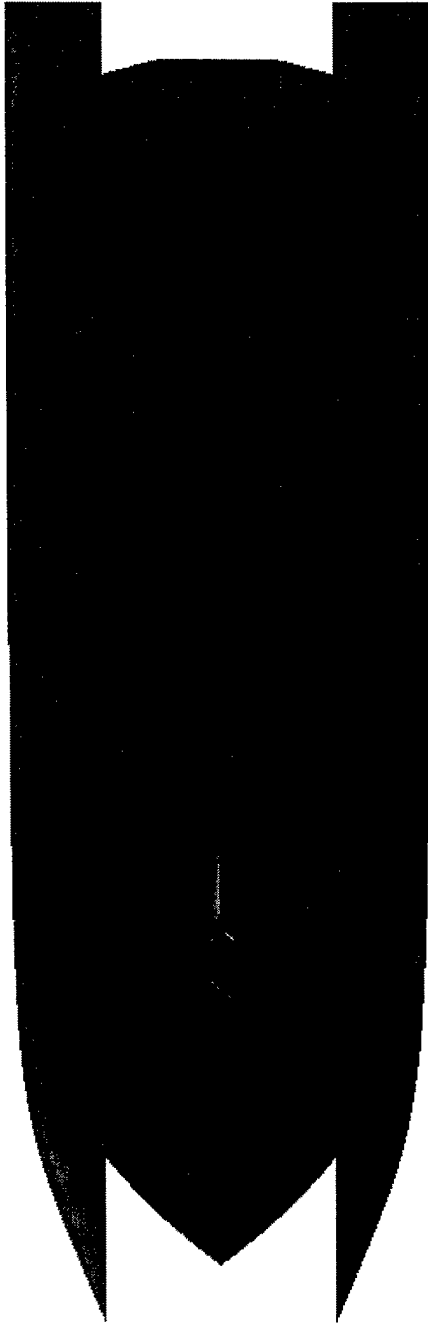
STOWED DRAFT



DEPLOYED DEPTHS



SWATCH Vessels – 60,000T



SWATCH Vessels – 60,000T

SHIP LENGTH = 785 FT

BODY LENGTH = 600 FT

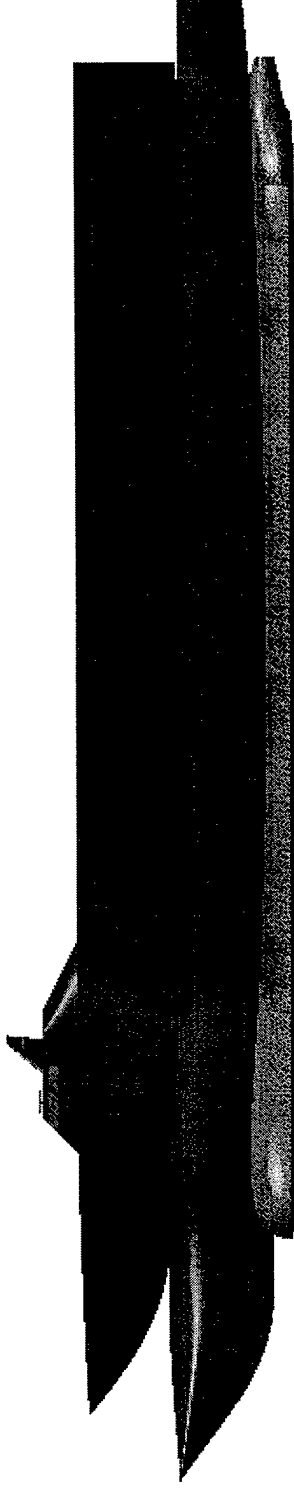
SHIP BEAM = 251 FT

BODY HEIGHT = 39 FT

SHIP HEIGHT = 125 FT

BODY WIDTH = 60 FT

L/B RATIO = 3.13



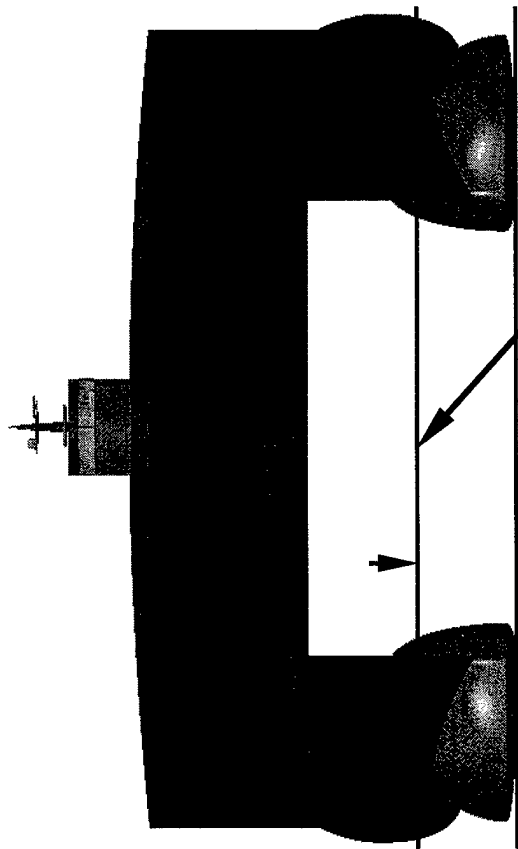
CARGO BAY = 200 FT X 455 FT X 14 FT

DRAFT = 30 FT

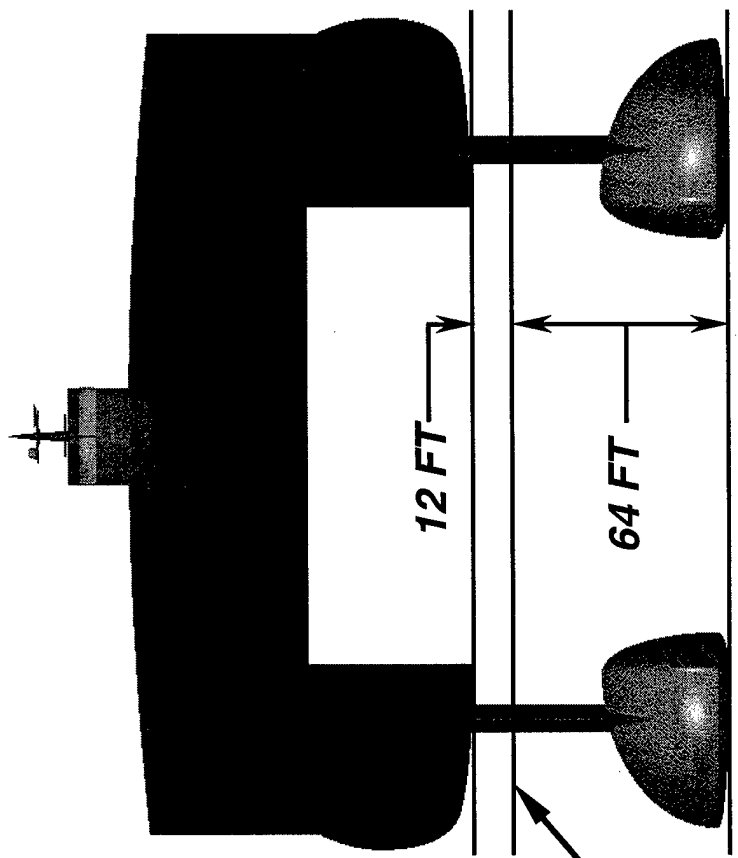
FLOOR AREA = 91,000 SQFT

SWATCH Vessels – 60,000T

STOWED DRAFT



DEPLOYED DEPTHS

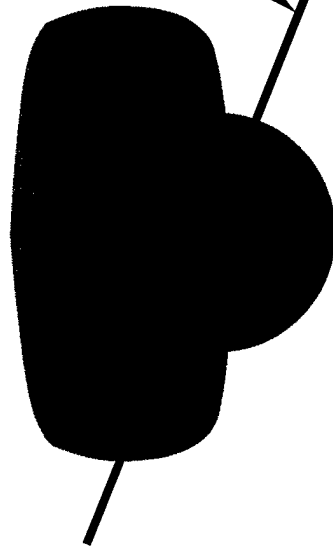


Static Stability Assessment of SWAxH Designs

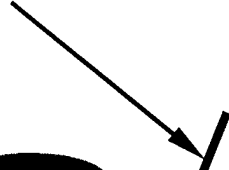
Static stability assessments were developed for the shallow draft geometry cases to show that they would be stable in the pitch and roll axis. The roll and pitch meta-centers were calculated using CATIA 3D solids and then plotted against the center of gravity and buoyancy.

The following slide shows a typical cut through a configuration as if it were rolled in the water.

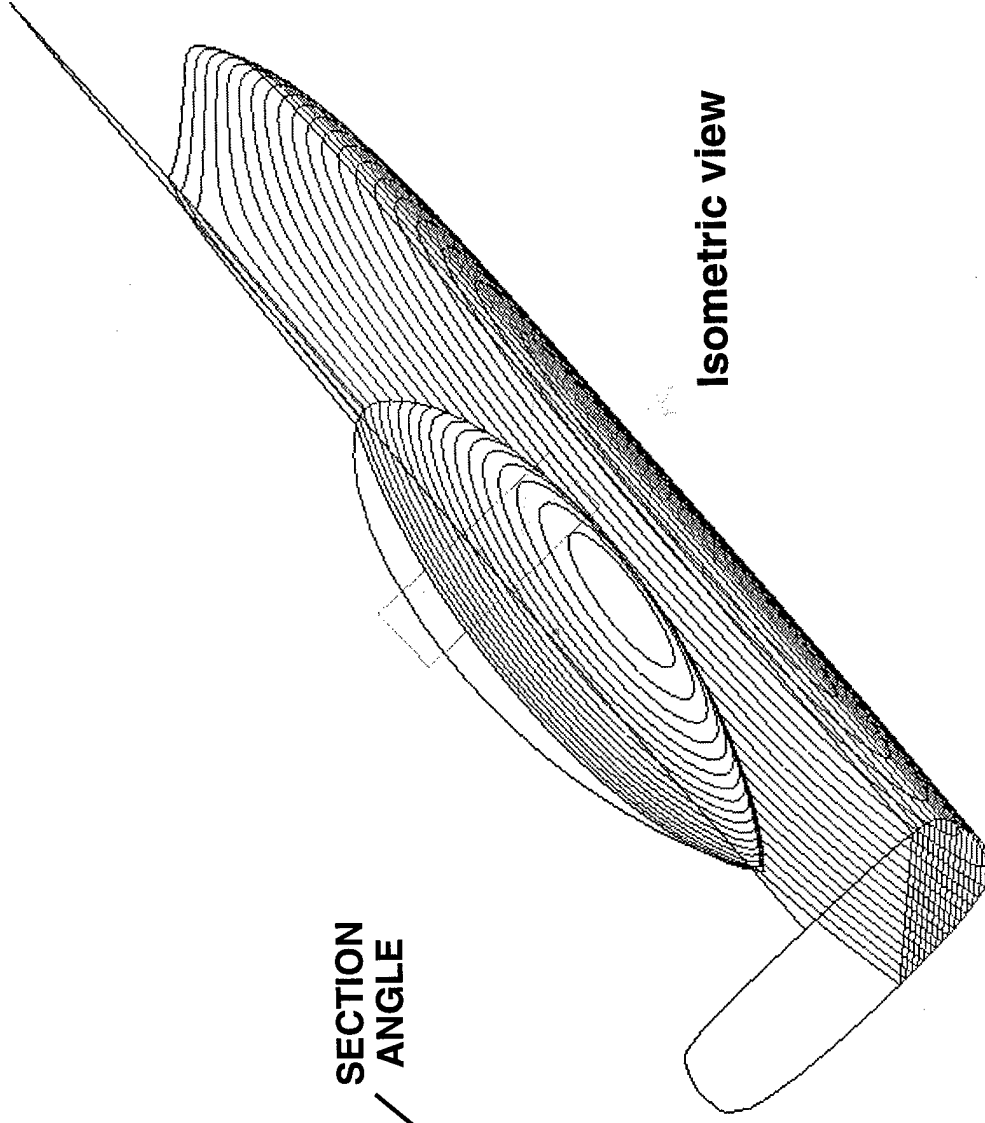
Static Stability Assessment of SWAxH Designs



SECTION
ANGLE



SWAMH Front View

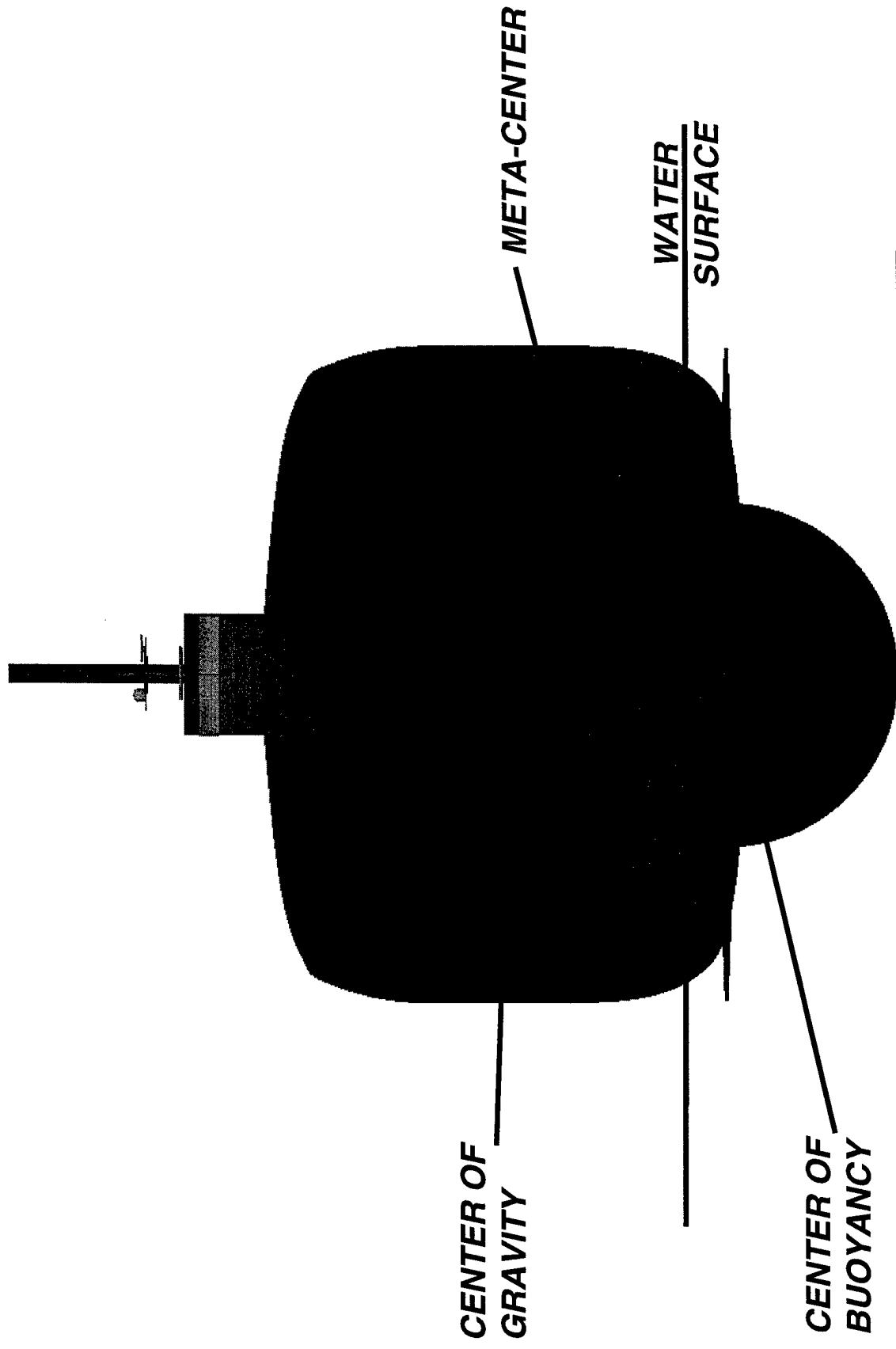


Isometric view

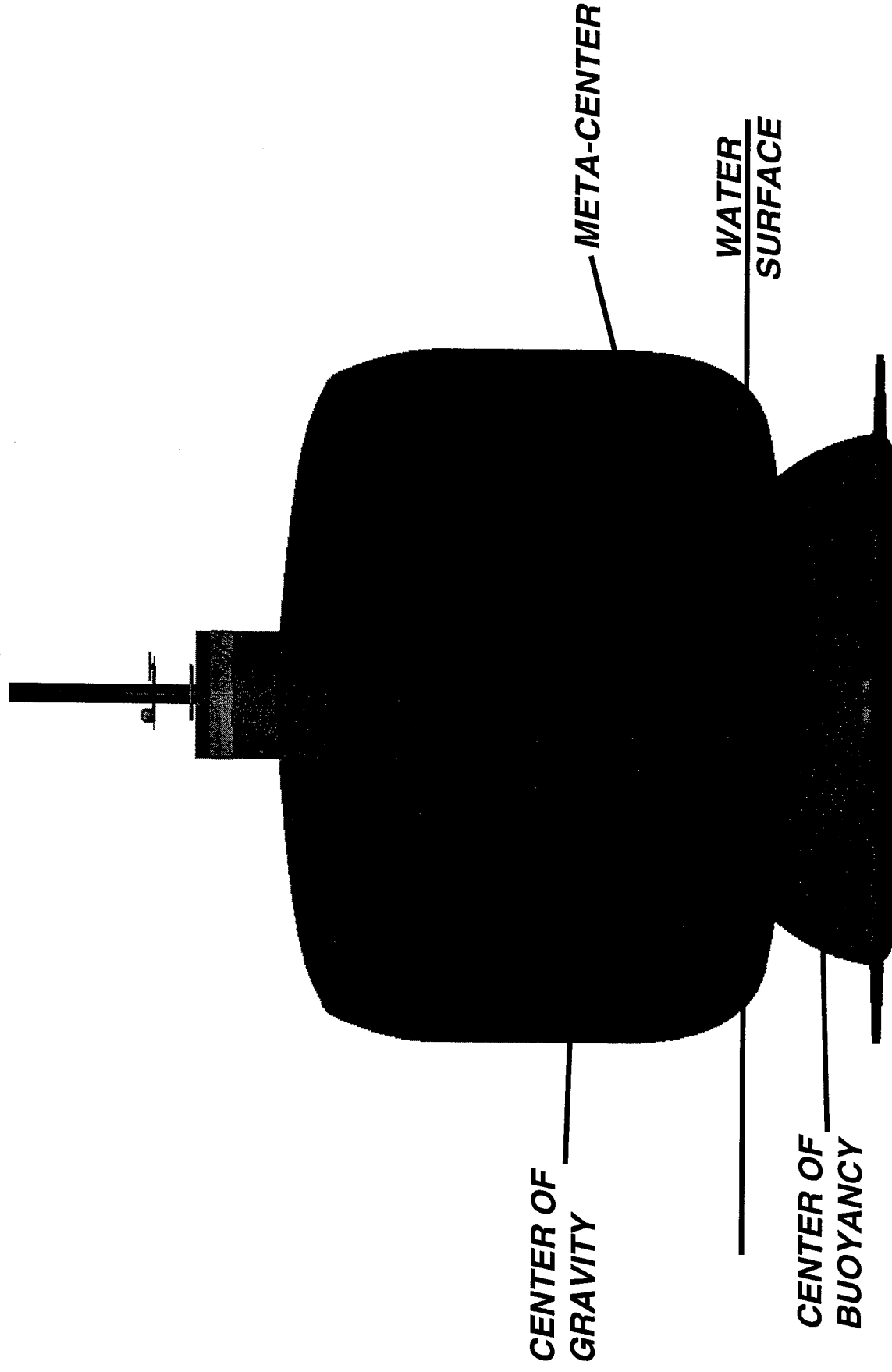
SWATH / SWATCH PITCH AND ROLL ASSESSMENT

The following slides show the roll assessment for the SWAMH and SWAMCH vessels. Each configuration was analyzed from 0 to 45 degrees, in 5 degree increments, and was found to be stable at all angles. For these configurations, pitch was not considered to be a problem due to the length to beam ratio. However, each configuration was analyzed from 0 to 25 degrees, in 5 degree increments, as a check. As suspected, both configurations were found to be stable.

SWAMH ROLL ASSESSMENT



SWAMCH ROLL ASSESSMENT



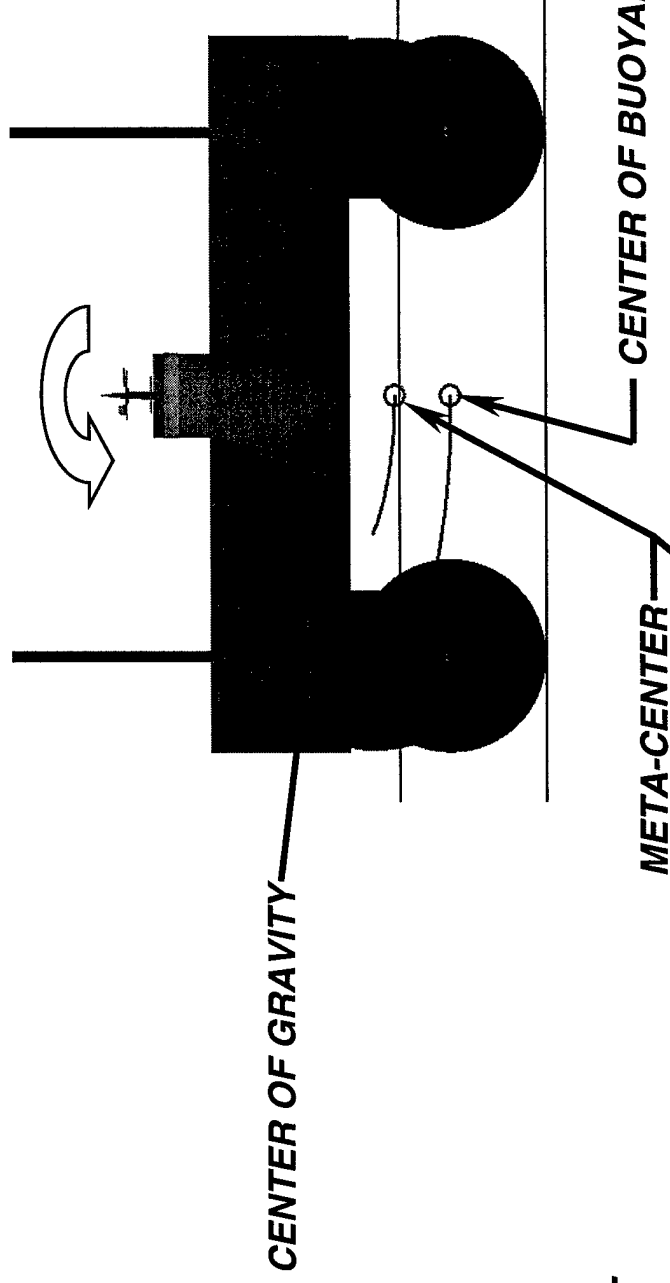
SWATH / SWATCH PITCH AND ROLL ASSESSMENT

The following slides show the pitch and roll assessment for the SWATH and SWATCH vessels. Each configuration was analyzed from 0 to 45 degrees in roll, in 5 degree increments, and was found to be stable at all angles.

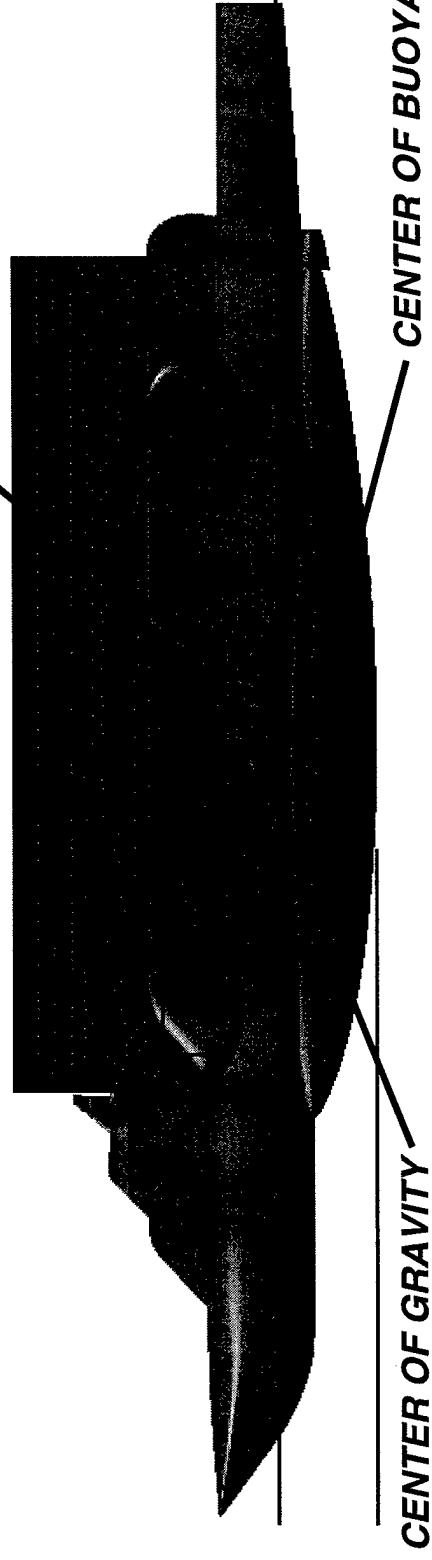
Each configuration was analyzed from 0 to 25 degrees in pitch, in 5 degree increments, and was found to be stable at all angles.

SWATH PITCH AND ROLL ASSESSMENT

ROLL ASSESSMENT

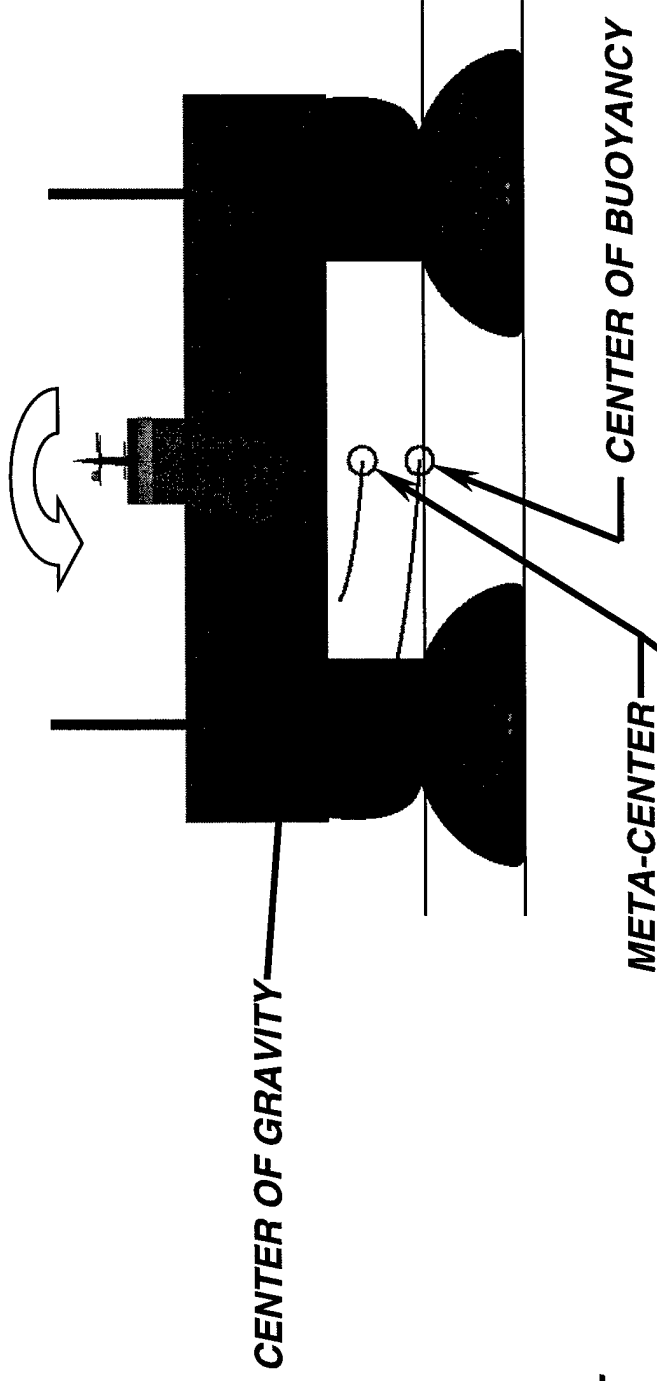


PITCH ASSESSMENT

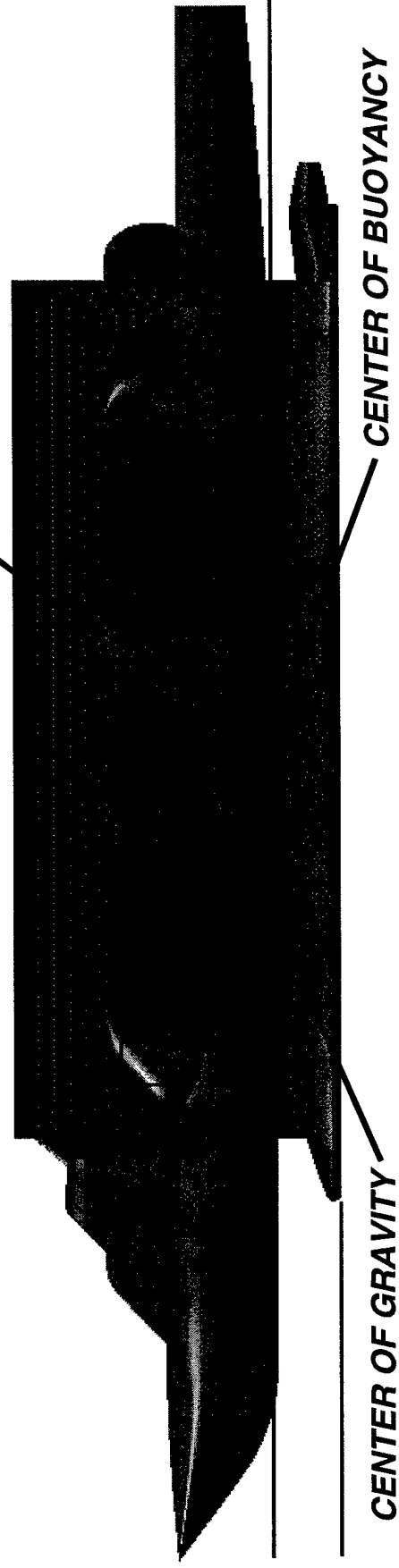


SWATCH PITCH AND ROLL ASSESSMENT

ROLL ASSESSMENT



PITCH ASSESSMENT



Vehicle Sizing and Synthesis

Multi-Disciplinary Assessments

Scope and Methods

This study seeks to establish feasibility and practicality constraints for a long-range hydrofoil transport ship. A hydrofoil fast ship, like an aircraft, is a dynamic lift vehicle. Unlike a conventional ship, at cruise speed it does not depend upon hull buoyancy for lift. This key distinction results in great kinship between this nautical design exercise and the aircraft sizing and synthesis process. This effort considers the interplay between hydrodynamics, structures, propulsion and stability & control disciplines.

Due to the unique nature of this vehicle and mission (high speed, large size and long range), the prior-art hydrofoil database is insufficient to base an empirical design optimization process. First, the design space must be bounded; a limited range of potential vehicles must be identified. Secondly, the sensitivity of performance metrics to the primary design variables must be shown. To build a useful knowledge base, the technical work is organized into a multi-tiered optimization process as shown in the following slide. Essentially, four parallel yet coupled multi-disciplinary design optimizations must exist:

1. hydrofoil wing sections must be designed subject to multidisciplinary (structural, mission performance, stability and control) constraints;
2. these sections must be used to develop finite hydrofoil wings, control surfaces and support struts;
3. these studies will provide the basis for optimized vehicle configurations that uphold structural and controllability metrics; and,
4. these configurations will be integrated with available propulsion options and sized to achieve mission requirements.

This monograph focuses on the top two priorities: bounding the design space and documenting the design sensitivity to perturbations of the primary design variables.

Multi-Disciplinary Assessments

- **Design Tiers - from specific to general :**

- 2-D Hydrofoil Section Element
- Hydrofoil “Wing/Strut” Components
- Underwater Hydrofoil Configuration
- Overall Vehicle Size / Configuration



- **Multidisciplinary Analysis used to reinforce synthesis at each tier.**

- High-fidelity tools used to substantiate design at the detailed level
- Analysis produces empirical relations used at higher levels
- Detailed high-fidelity analysis of final candidate design(s)



- **Design variables**

- Chosen for optimization appropriate to each tier
- Large number of overall design variables
- Reduced number of design variables at any given tier

Requirements and Design Constraints

The requirements in the following slide became the bounds for the design space during the study. At onset to the program, the anticipated sustentation system of choice was the hydrofoil, however as the performance of hybrid static lift systems were exploited the upper limits to displacement, LOA and Beam were pushed so that the bounds of the sustentation triangle could be better understood.

Additional data was required and LM Aero subcontracted CSC-Advanced Marine for support in the area of ship mass properties and hydrodynamic expertise. Mr. Andrew Kondracki and Mr. J. Otto Scherer supported this effort.

Requirements from DARPA Study

- **Design Requirements :**
 - DARPA Fast Ship Technology Study, May 28, 1997
 - LMAS/ONR Phase I Study

Parameter	Minimum	Target	Bonus	Comment
Sustained Transit Speed	50 kts	70 kts	75 kts	Operations
Un-refueled Range at Transit Speed	5000 nM	6000 nM	10000 nM	Global Reach
Payload	1000 MT	1500 MT	2000 MT	One Fully Equipped Infantry Company
Fully Loaded Displacement	<15,000 T	12,000 T	<10,000 T	Economy
Overall Length	< 650 ft		< 500 ft	Berthing Size
Overall Width	< 213ft		115 ft	Panama Canal
Overall Draft	< 23 ft		<16 ft	Port Entry
Ride Quality	<0.1g RMS		<0.03g RMS	Personnel Fatigue
Propulsion Power @ speed	<200khp		<100khp	Economy

- **Implications**
 - Payload Fraction : $1,500T/12,000T = 12\%$
 - Design Feasible if
 - » Mean $L/D = 20$, $SFC = 0.10 \text{ lb/lb-thrust-hr}$, Fuel Fraction = 35%
 - » Mean $L/D = 25$, $SFC = 0.10 \text{ lb/lb-thrust-hr}$, Fuel Fraction = 29%
 - » Mean $L/D = 30$, $SFC = 0.10 \text{ lb/lb-thrust-hr}$, Fuel Fraction = 25%

Requirements from BAA

- **Design Requirements :**
 - BAA 98-023

Parameter	Minimum	Target	Bonus	Comment
Sustained Transit Speed		70 kts		Operations
Un-refueled Range at Transit Speed		6000 nM		Global Reach
Payload		5000 MT		

- **Implications**
 - Payload Fraction : 5,000T @ 12% -> 40,000T Ship!
 - Other sizing restrictions from DARPA operations research not addressed
 - Additional information required to define design
 - » payload volume
 - » sea state capability
 - » powerplant limitations/restrictions
 - » materials limitations/restrictions
 - » 'technology factors'

Identified Specifications

- **LM Interpretation of Customer Requirements**
- **Vehicle Configuration (per DARPA Systems Analysis)**
 - Fully laden displacement : not to exceed 15,000T
 - Length: not to exceed 650 feet
 - Beam (foils retracted) : not to exceed 200 feet
 - Draft (foils retracted) : not to exceed 23 feet
- **Payload**
 - Maximize payload within 15,000T total vehicle mass limitation
 - Provisions for up to 5000T payload
 - 100 pound per square foot average payload density
 - No specific provision for internal storage of outsized payloads.
- **Range**
 - Un-refueled range : 6000nM @ >1500T payload
- **Speed**
 - Mean transit speed : not less than 70kts in calm seas
 - Operation in sea state 5, speed not specified.
- **Materials (for hull, foils and struts)**
 - Current technology engineering materials (metallic and composite)

Addition Design Data Required

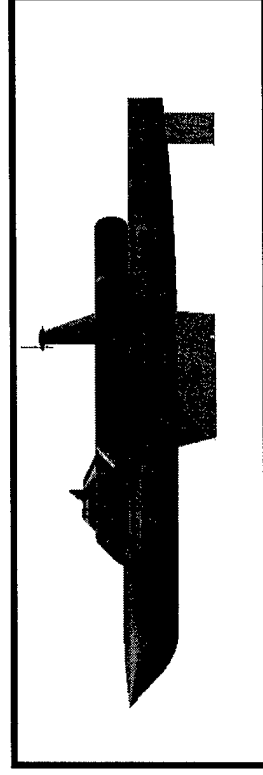
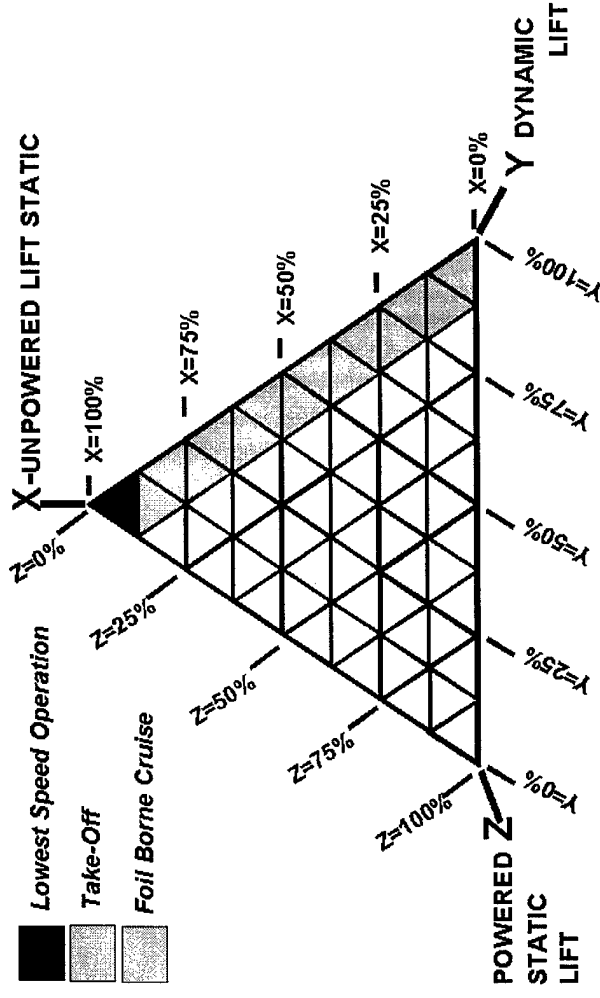
Additional information required for vehicle design, but outside LM Aero Databases include:

- **Hull Structural Design**
 - preferred MIL-STD guidelines?
- **Hull Mass Properties**
 - preferred references for empirical relations?
- **Subsystems Requirements**
 - preferred references
 - » subsystem identification
 - » subsystem power requirements
 - » subsystem space requirements
 - » subsystem mass properties
- **Handling Qualities**
 - preferred MIL-STD guidelines?
- **Sea State Model**
 - preferred model
 - model must address wave height, velocity distribution both at the surface at up to 20-ft depth

Hydrofoil Design Space – Sustention Triangle

- General Theory of Static Lift Payload Performance

- Understand how to trade hydrodynamic performance for fuel fraction through the choice of submerged body sections and propulsion integration in order to maximize mission performance

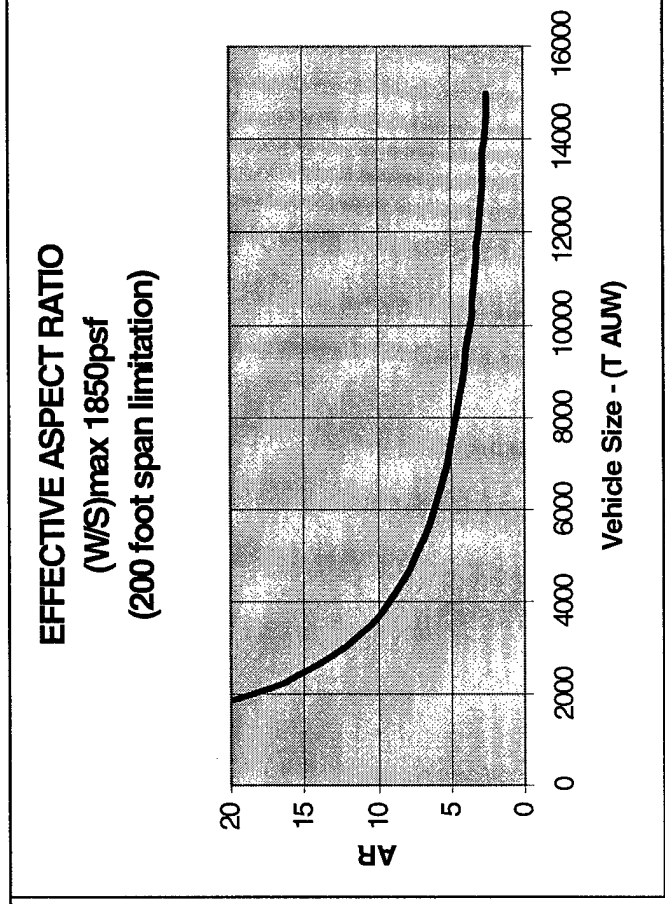
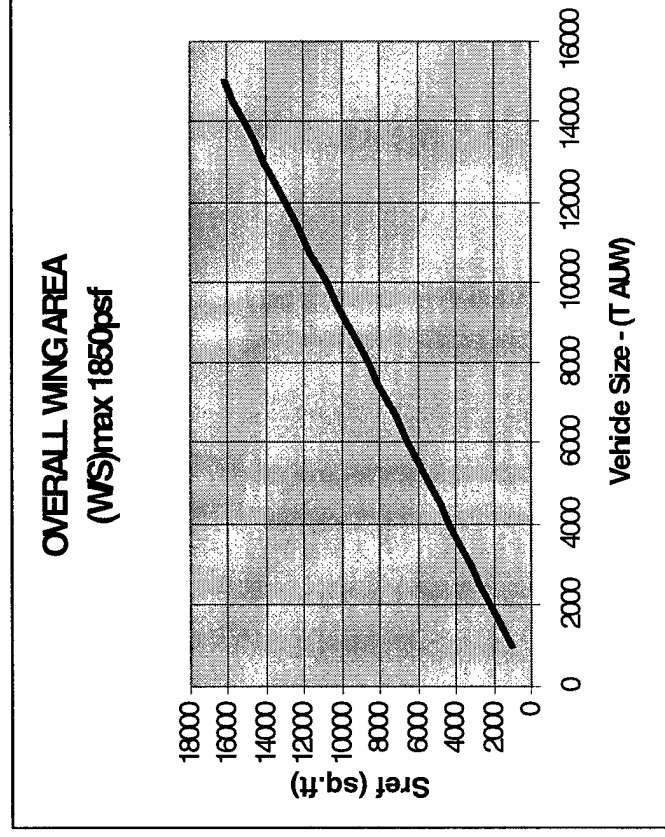


Hydrofoil Sustention System Design Space Defined

Upper and lower bounds to the problem were established using the maximum beam constraint of 200ft. As is shown in the following slide, the wing reference area and aspect ratio can be determined if the; cavitation-free lift characteristics of the wing section are chosen, and displacement of the ship is selected.

Hydrofoil Sustention System Design Space Defined

- **Untrimmed 3DOF Database Used for Sizing Exercise**
- **Trade Study Space :**
 - Overall Vehicle Size : 3000 -> 15000T AUW
 - Wing Area : appropriate for vehicle size and 200ft span limit
 - Cavitation Limitation : per P70/40/2.0A35 section
 - CD0 : 0.0050 (no drag mitigation) to 0.0010 (80% viscous reduction)



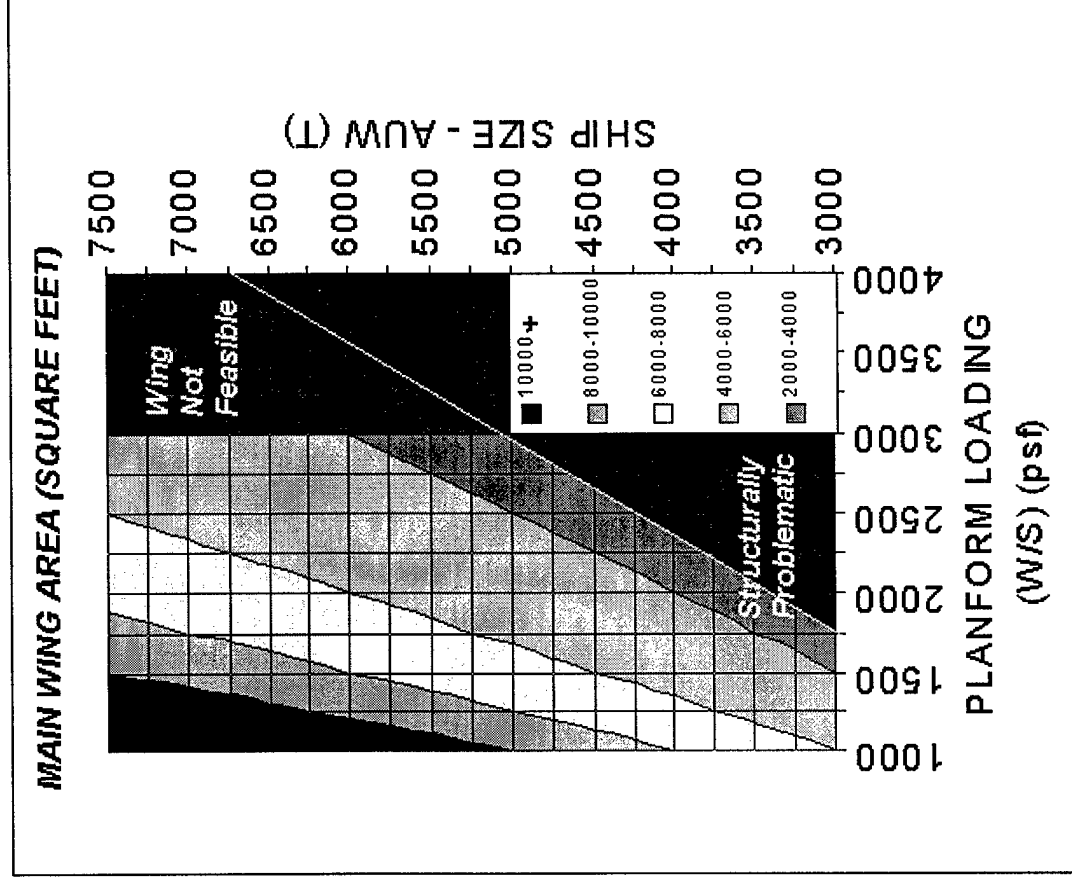
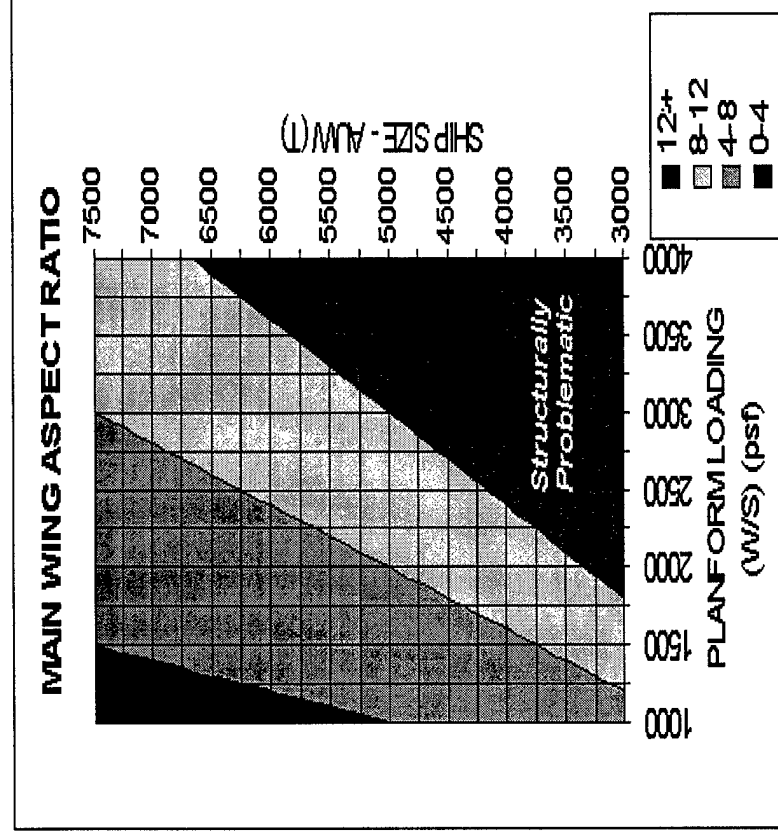
and is related to Wing Loading/Aspect Ratio...

If the combination of wing loading and aspect ratio are both high, the structural design and integration problem becomes problematic. The upper bounds for the design space was set at aspect ratio 12. At wing loading at and above 3000 pounds per square foot, the design was considered unfeasible. This made the large hydrofoils (>7500 Tons) impractical (structural solidity greater than what practical fabrication techniques would allow). As the study continued, the impact of the fixed beam with a air-coupled propulsion system set the upper bounds of the hydrofoil All-Up-Weight (AUW).

and is related to Wing Loading/Aspect Ratio...

- **Wing Size and Aspect Ratio as function of W/S_{max} & AUW**

- Very High AR wings shown to have structural difficulties



L/D and von K Efficiency Estimates

Performance estimates early on suggested that without viscous drag reduction the trimmed Lift-to-Drag ratios (L/D) were less than 25 and for the range of cruise speeds in which cavitation could be precluded, the von Karman efficiency parameter (Velocity times L/D) would be on the order of 1000, or significantly below the goal value of 5000.

L/D and von K Efficiency Estimates

Trimmed L/D Estimates and
Von Karman Efficiency
Estimates.

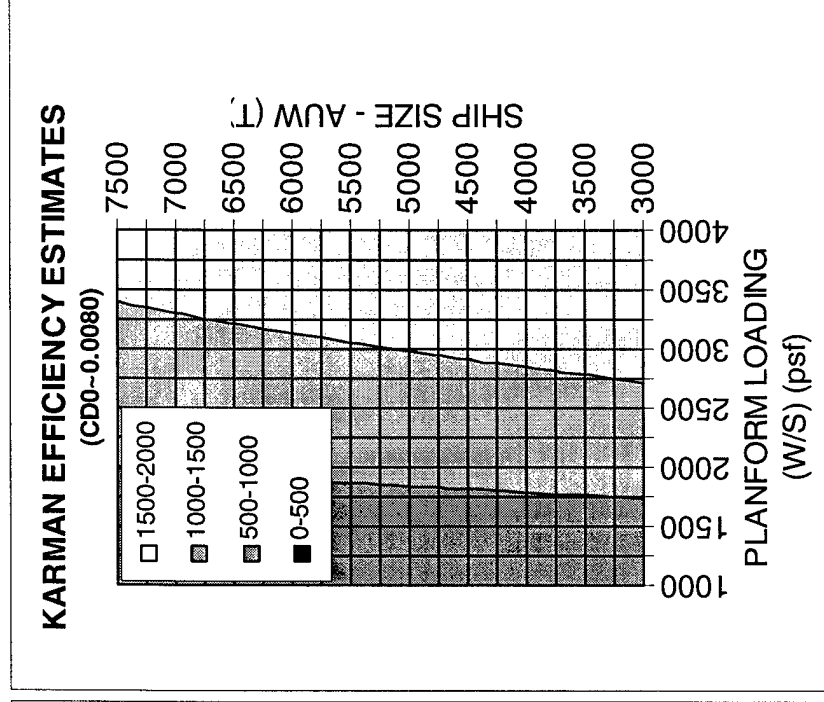
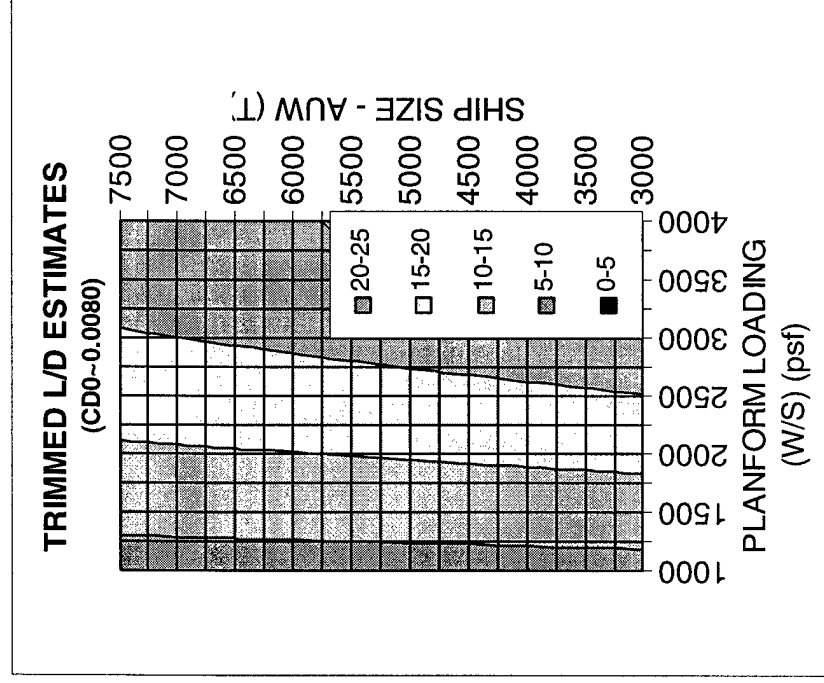
Without Viscous Drag

Mitigation

CD0 ~ 0.0080

Trimmed L/Ds < 25

vonK < 1000



L/D and von K Efficiency Estimates

If viscous drag is reduced through some type of drag reduction technology, the efficiency of the system in terms of L/D and von Karman parameter increases. Reducing the viscous drag to 50% of its original value elevates the L/D to less than 40. Note that the full elimination of the viscous drag would require an L/D of 70+ at 70 knots to meet the von Karman efficiency goal. In that case, the key is to have a very low inviscid (wave and induced) drag.

L/D and von K Efficiency Estimates

Trimmed L/D Estimates and
Von Karman Efficiency
Estimates.

With 50% Viscous Drag

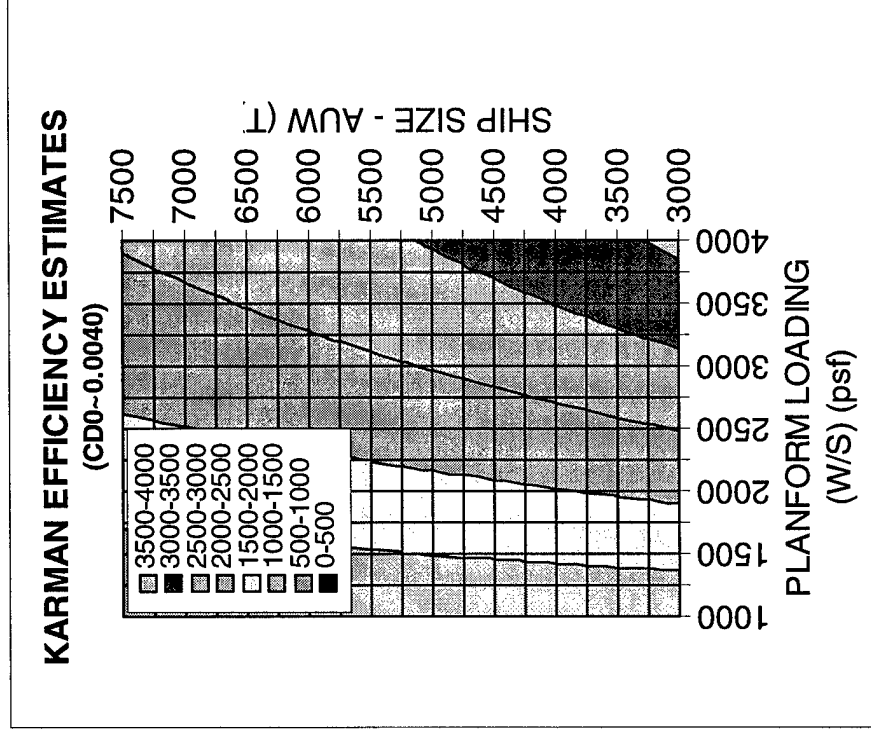
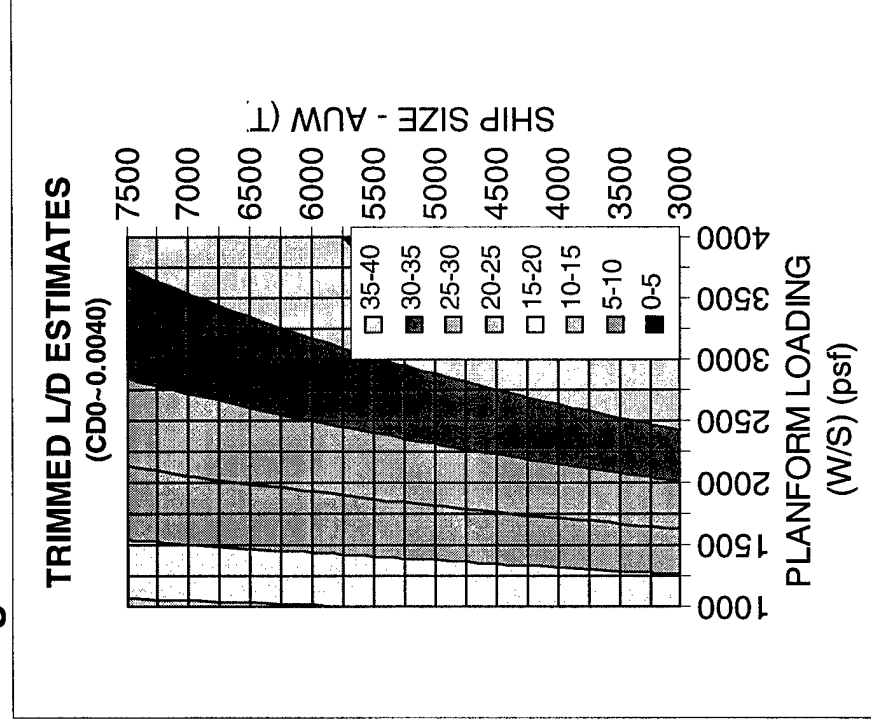
Mitigation

CD0 ~ 0.0040

Trimmed L/Ds

~25 to 40

vonK ~ 2000's



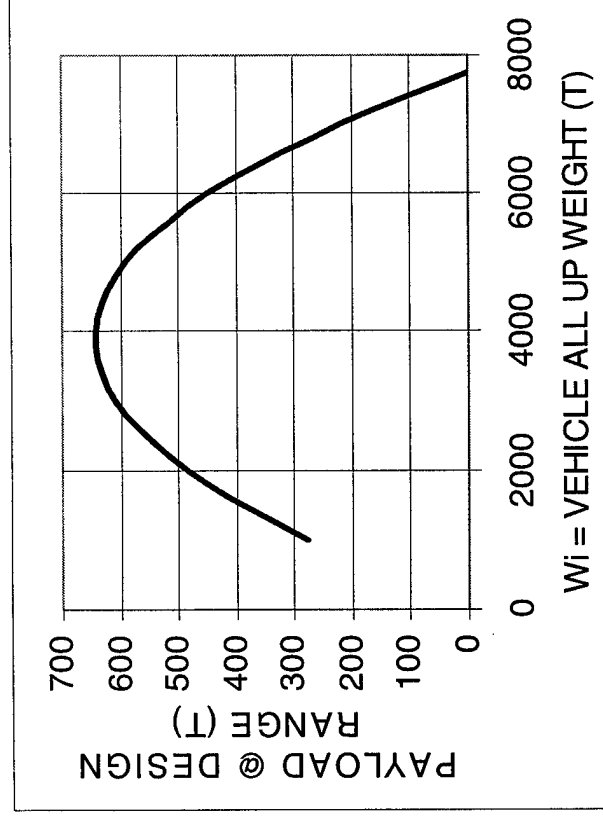
Optimum Size

The optimum sized ship was a key consideration with respect to the constraints of the study. Operationally, the hydrofoil ship behave like a transport aircraft. As fuel is burned off, the required lift decreases, and the integration of fuel burned over the mission becomes the Breuget integral.

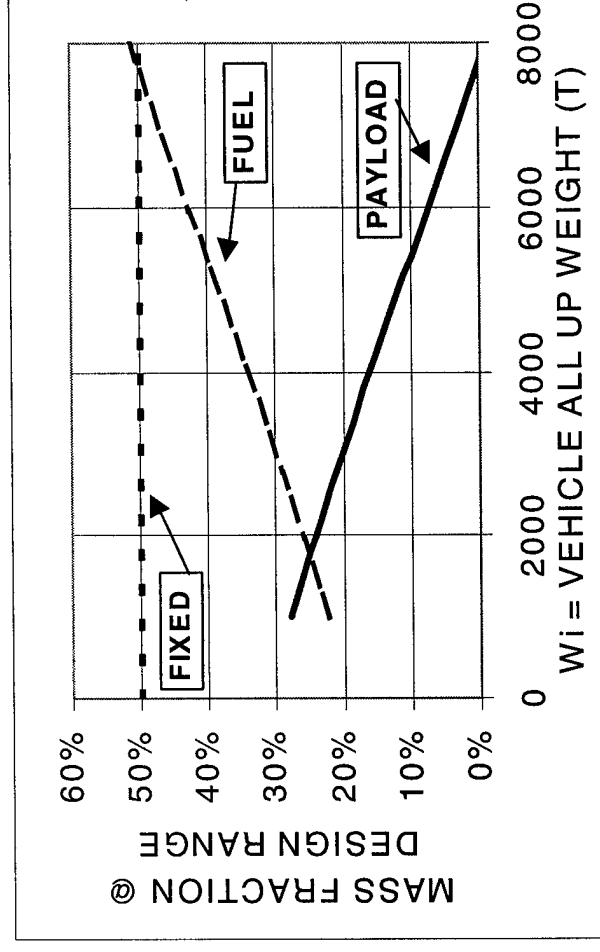
Initially, the fixed weight fraction was treated as an independent variable and the optimal ship size fell out from the combination of the type of propulsion system, and the L/D of the selected ship as constrained by the 200 foot beam and the 6000 nautical mile range goal. As the ship increases in size, the L/D decreases due to the decreasing aspect ratio of the wing. In addition, the thrust specific fuel consumption for an air coupled propulsion system decreases also due to the increase in disk loading. The results of the Breuget range study is shown in the followign slide. Note that maximum payload does not occur at the maximum payload range!

Optimum Size

- “First-Principles” Sizing Exercise shows existence of “Optimum” Ship Size
 - Fixed Weight Fraction (FWF) is an *Independent Variable*
 - Increasing ship size leads to : declining L/D and increasing TSFC (for air coupled propellers).
 - Payload fraction declines. Absolute Payload reaches peak at intermediate vehicle size.
- Higher Fidelity Solutions add realism in key areas :
 - Fixed Weight Fraction (FWF) is a *Dependent Variable*
 - Effects of wing geometry/configuration on mass fraction, wetted area, L/D
 - Propulsion system details : efficiency at cruise thrust, sizing and weights for peak thrust requirements.



Vehicle Sizing. Payload Capacity at Design Range, $R=6000\text{nM}$, as a Function of Vehicle All-Up Weight, W_i .
 $b=200\text{-ft}$; $h=20\text{-ft}$; $t/c=5\%$; $k_2=100\%$; $V=70\text{-kts}$;
 $FWF=50\%$.



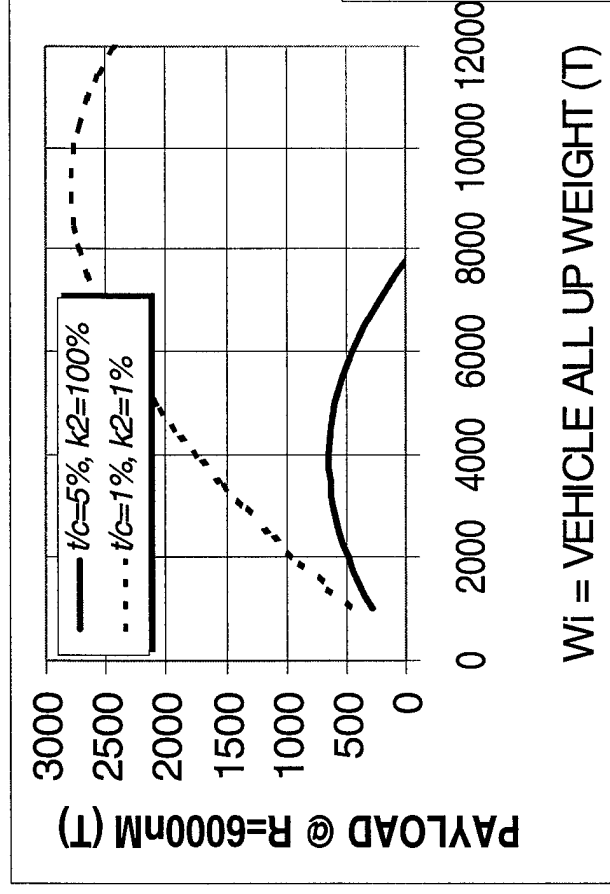
Vehicle Sizing. Mass Fraction for Payload and Fuel at the Design Range, $R=6000\text{nM}$, as a Function of Vehicle All-Up Weight, W_i . $b=200\text{-ft}$; $h=20\text{-ft}$; $t/c=5\%$; $k_2=100\%$;
 $V=70\text{-kts}$; $FWF=50\%$.

Optimum Size (cont'd)

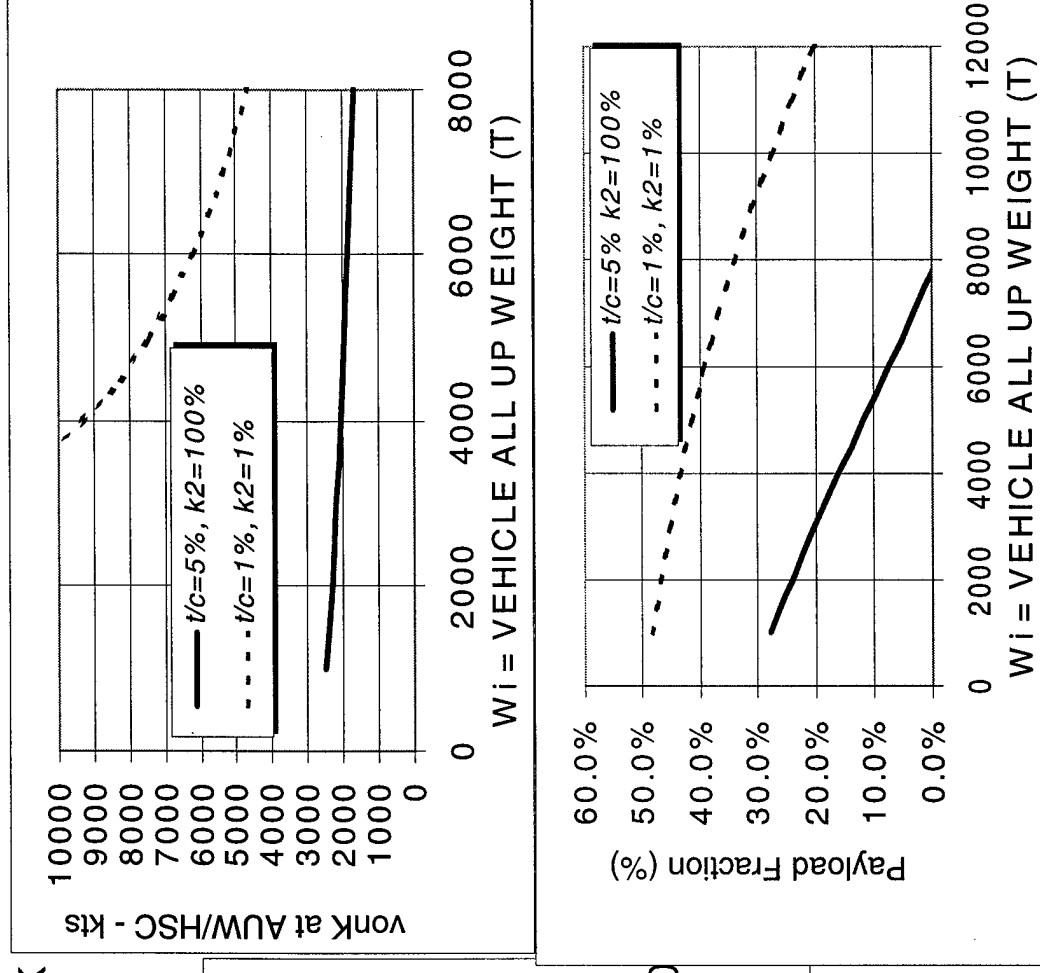
The ingoing parameters for the optimal size study were initially chosen to be the full viscous drag and a realistic wing thickness. Goal values for viscous drag reduction (1% Schoenherr k2) and profile drag (foil thickness to chord, t/c , 1%) were examined and the results showed for a fixed propulsion system, that the maximum von Karman efficiency parameter did not occur at the maximum payload at range condition. Clearly a reduction in drag at zero lift (Cdo) favors a larger ship.

Optimum Size (cont'd)

- “First-Principles” Sizing Exercise shows existence of “Optimum” Ship Size
 - Compare representative design from paper with “Theoretical Limit” design ($k_2=1\%$, $t/c=1\%$, $FWF=50\%$)
 - Optimum Payload @ Range not at peak vonk



Vehicle Sizing. Payload Capacity at Design Range,
 $R=6000\text{nm}$, as a Function of Vehicle All-Up Weight, W_i .
 $b=200\text{-ft}$; $h=20\text{-ft}$; ($t/c=5\%$; $k_2=100\%$ and $t/c=1\%$;
 $k_2=1\%$); $V=70\text{-kts}$; $FWF=50\%$.

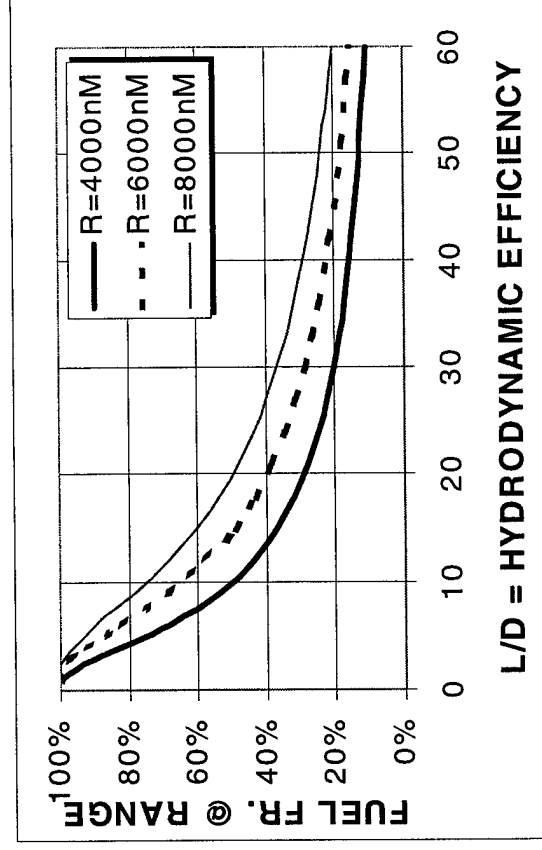


Performance Limitations on Range

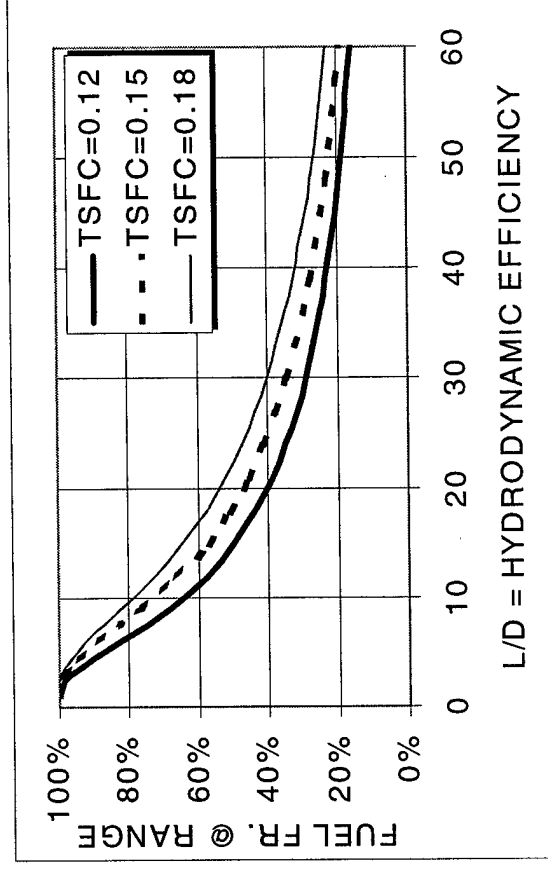
The propulsion system efficiency sets the relative amounts of fuel versus payload at a given range value. Using a 50% FWF as a starting point, the thrust specific fuel consumption was varied between 0.18 for a air coupled system to a 0.12 for a possible water coupled system. This show that the minimum L/D required to meet the mission must be between 20 and 30.

Performance Limitations on Range

- Previous "Bottoms up" Zero Payload Fixed Weight Fraction likely to be ~50%
- 10% Payload Fraction requires < 40% Fuel Fraction.
- Minimum acceptable mean L/D for 6000nM mission must be between 20 and 30 depending upon propulsion choices
- August 2000 work substantiates feasible L/D ~ 15.



Required Fuel Fraction, FF , for Design Range, R , as a function of Hydrodynamic Efficiency, (L/D) , and Design Range. $TSFC=0.12$ -lb/lb-hr. $V=70$ -kts.



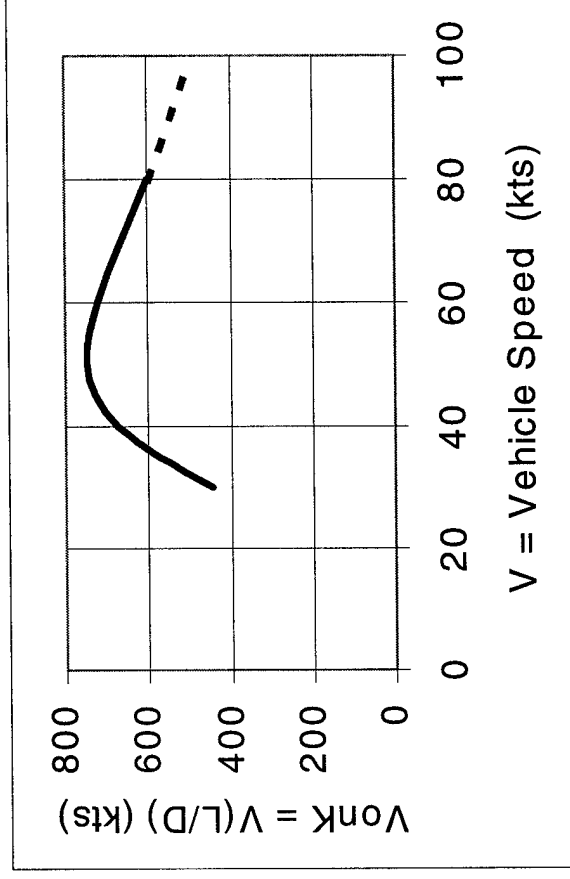
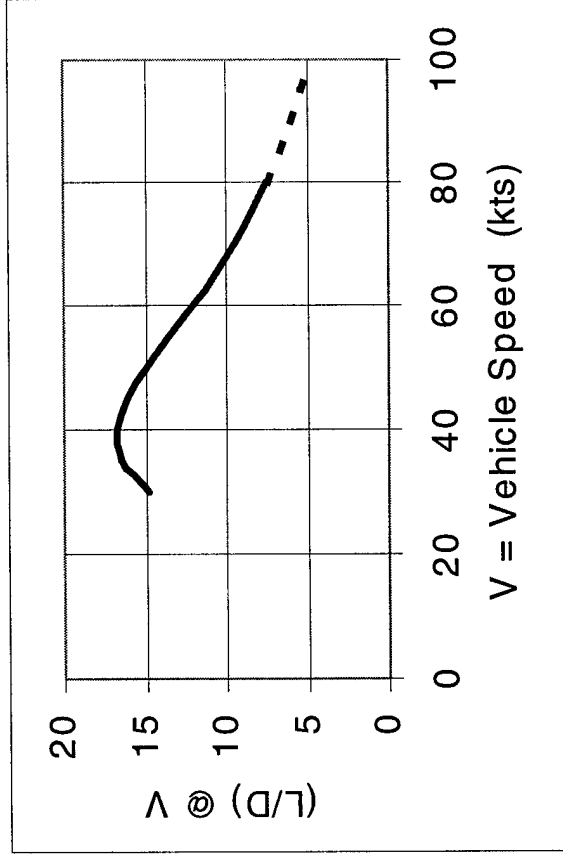
Required Fuel Fraction, FF , for Design Range, $R=6000$ nM as a function of Hydrodynamic Efficiency, (L/D) , and Thrust Specific Fuel Consumption, $TSFC$. $V=70$ -kts.

von Karman Efficiency and Range

The speed of the peak von Karman efficiency is difficult to align with the design cruise speed of the hydrofoil. If the peak is at less than the design speed, there is a moderate range penalty at high speed cruise, and for long-range cruise near the peak von Karman efficiency. If the speed of the peak von Karman efficiency is greater than the design cruise speed, there is a range penalty at the high speed cruise and operation at lower speed further reduces the range.

von Karman Efficiency and Range

- **Speed of Peak Karman Efficiency difficult to align with Design Cruise Speed.**
- **If Speed of Peak Karman Efficiency is less than Design Cruise Speed**
 - moderate range penalty at high speed cruise, long-range cruise speed near speed of peak vonK
 - cruise drag dominated by VISCOUS drag
- **If Speed of Peak Karman Efficiency is greater than Design Cruise Speed**
 - range penalty at high speed cruise, operation at lower speeds further reduces range.



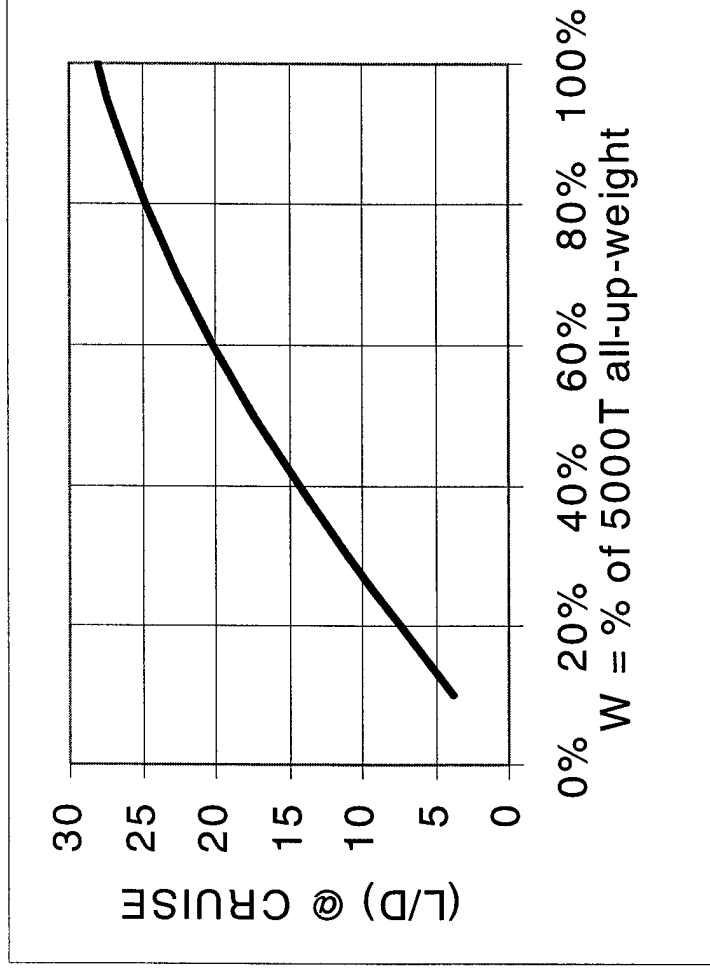
Effect of Fuel Consumption on Mean L/D

Fuel consumption rate also enters into the determination of the mean L/D . If the fuel fraction is decreased, the hydrofoil system is more able to stay near the optimal design point L/D . Again if the speed of the peak von Karman efficiency is above the design speed a consumption of 40% fuel leads to almost a 30% reduction in L/D .

Effect of Fuel Consumption on Mean L/D

- If Speed of Peak Karman Efficiency is less than Design Cruise Speed

- operation on “front side” of L/D curve (in angle of attack)
- L/D diminishes as fuel is consumed
- speed of peak Karman Efficiency declines as fuel is consumed.
- Example figure : consumption of 40% fuel fraction leads to ~30% decline in L/D .



Effect of Vehicle Load, W/W_i , upon Theoretical Hydrodynamic Efficiency. $W_i=5000T$; $b=200$ -ft; $t/c=5\%$; $h=20$ -ft; $V=70$ -kts, $k_2=100\%$.

- High L/D solutions favorable synergy

- Smaller fuel fraction for given range
- Larger payload fraction for given range
- More efficient operation (higher L/D) with most of the mission operating near the maximum design weight.

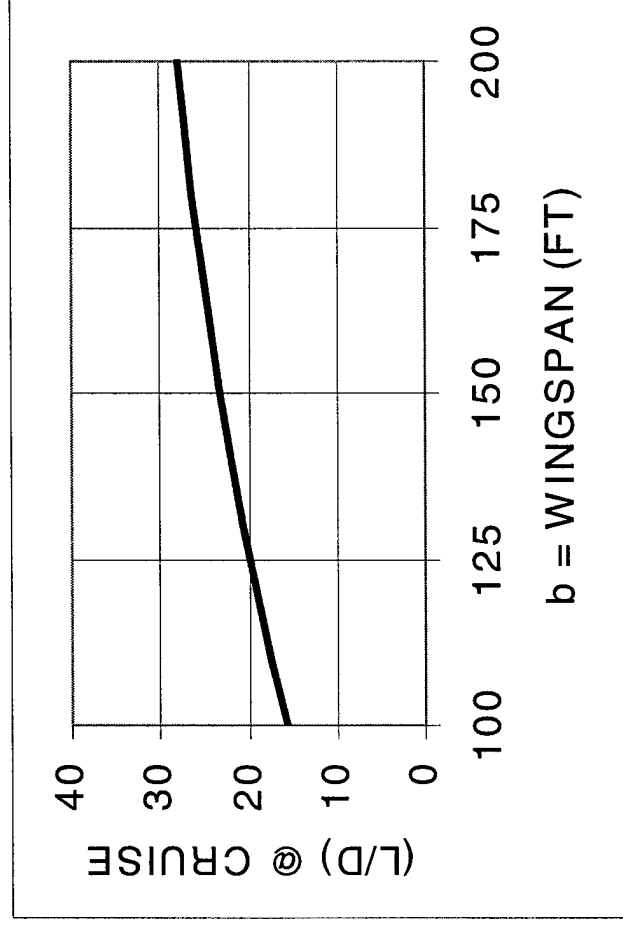
Effect of Wingspan on L/D

The effect of the wingspan on the L/D is shown in the following slide. The viscous drag decreases with span reduction, however the induced drag increases. The overall net benefit may in fact be favorable with respect to the structural weight and the the number of required struts needed that also act to impact the drag at zero lift.

Effect of Wingspan on L/D

- If Speed of Peak Karman Efficiency is less than Design Cruise Speed

- operation on “front side” of L/D curve (in angle of attack)
- hydrodynamic drag dominated by the viscosity of water
- reductions in wingspan increase induced drag (reduce L/D)
- but may have favorable structural implications!



Effect of Wingspan, b , upon Theoretical Hydrodynamic Efficiency. $W=5000T$; $t/c=5\%$; $h=20\text{-ft}$; $V=70\text{-kts}$; $k_2=100\%$.

Theoretical Limits to Wing Loading

The theoretical limits on developing lift were examined for a non-cavitating system. Note that performance of the hydrofoil ship in this study is based on this design approach.

Theoretical Limits to Wing Loading

- Theoretical Maximum Wing Loading function of design depth and design speed

– ideal theoretical wing would have upper and lower surface pressures of $-\sigma$ and $+\sigma$ over respective surfaces.

$$\gg W/S_{\max} = 2\sigma q$$

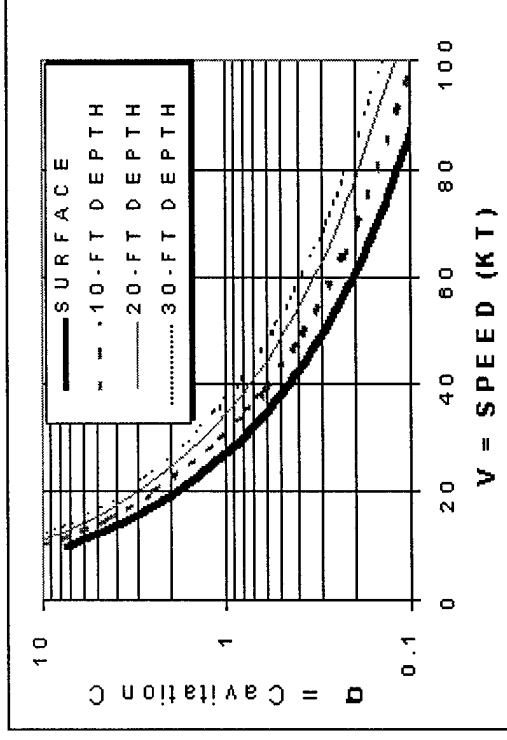
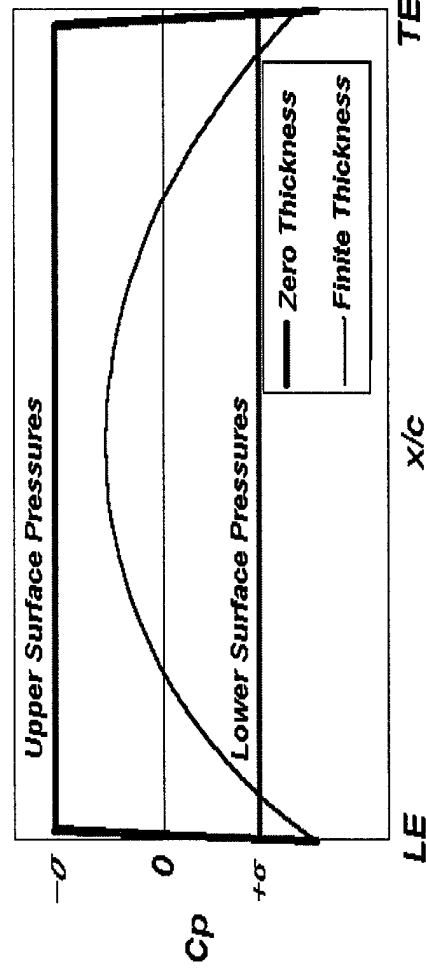
– pressures due to thickness diminishes theoretical loading

$$\gg W/S_{\max} = 2(\sigma - k_t(t/c))q; \text{ where } k_t \sim 1.5 \text{ (NACA)}$$

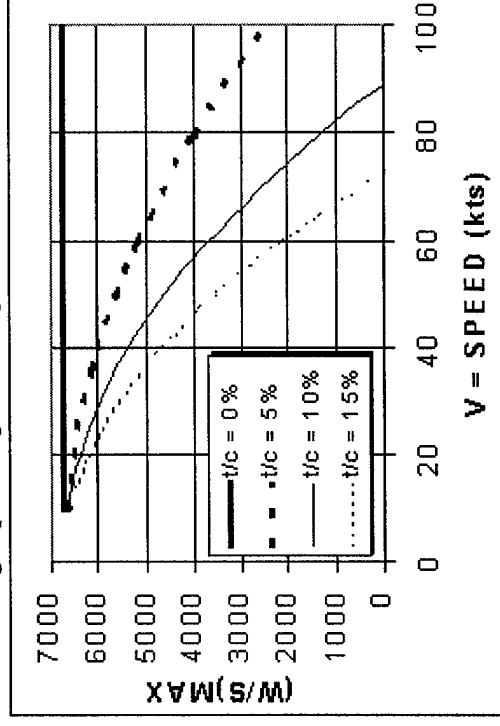


Airfoil Lift = Pressures due to Camber + Pressures due to Thickness
Incidence

IDEALIZED WING PRESSURE DISTRIBUTION



Cavitation Coefficient, σ , as a function of Speed, V , and Wing Operating Submergence Depth, h .



Effect of Wing Thickness upon Maximum Wing Loading
(from Thin Airfoil Theory : $h=20\text{-ft}$, $k_t=1.5$).

Practical Limits to Wing Loading

Realistic wing performance is compared theoretical limits. At finite thickness, the lift developed on LM sections is very close to maximum theoretical limits for the P70-55 section family. Note that the reduction is due to the combination of viscous effects, and how they must be managed with the requisite pressure gradients.

Practical Limits to Wing Loading

- Practical Wing Loading less than Theoretical Maximum Wing Loading

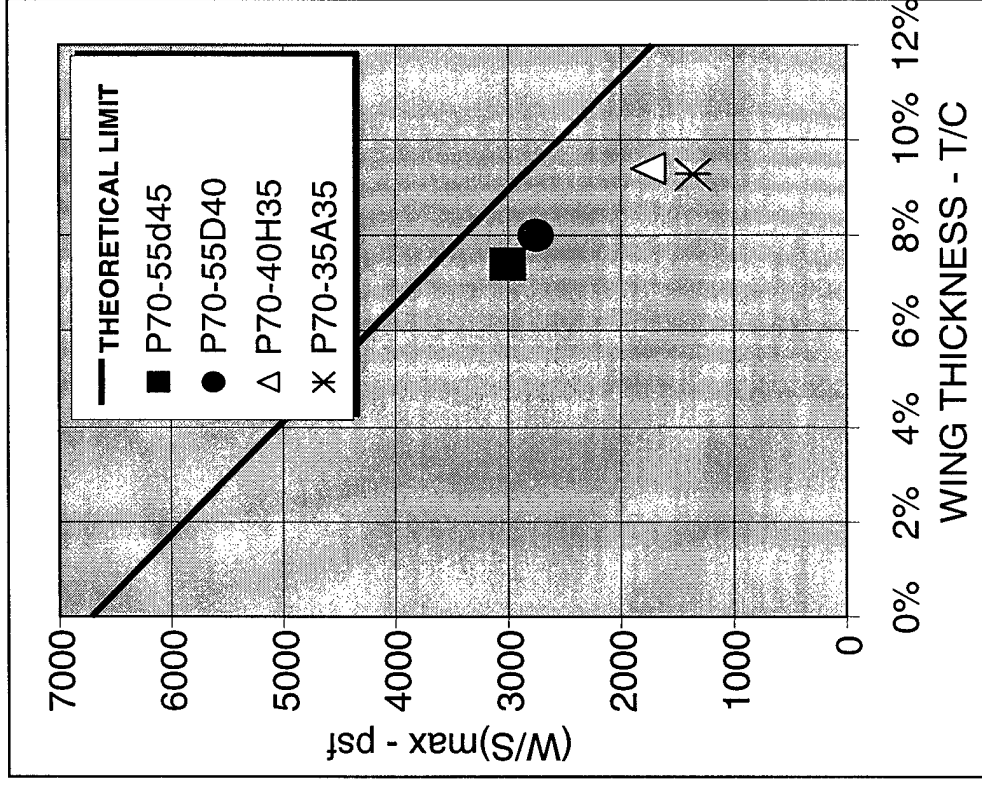
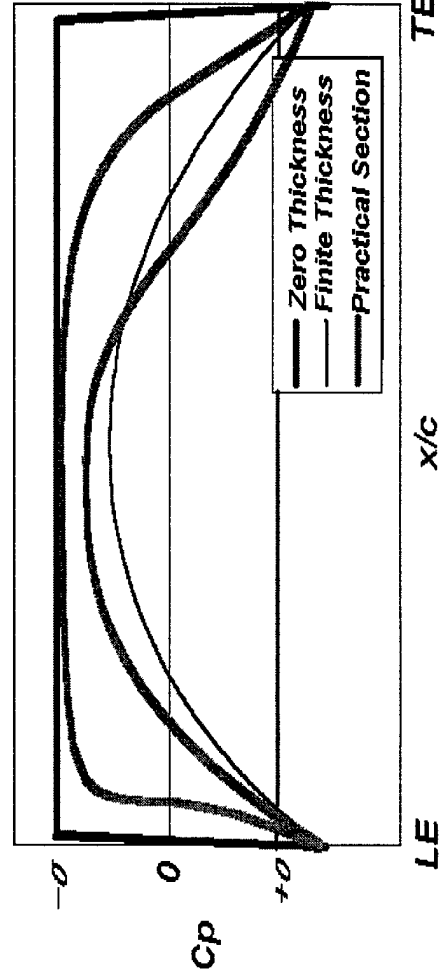
- practical limitations reduce wing loading
 - » non-cavitating operation of range of speed
 - » non-cavitating operation of range of weight (W/S)
- viscous considerations mandate trailing edge pressure recovery. Flow will separate if adverse pressure gradient is too steep.

W/S of practical sections 20%-50% below theoretical limit



Airfoil Lift = Pressures due to Camber + Pressures due to Incidence + Pressures due to Thickness

IDEALIZED WING PRESSURE DISTRIBUTION



Comparison of Practical Wing Performance to Theoretical Maximums. (from Thin Airfoil Theory : $V=70$ -kts, $h=20$ -ft, $k_t=1.5$).

Optimum Wing Depth - Trade Study

The depth at which the hydrofoil was optimum was examined using both a combined hydrodynamic and structural analysis. For the fixed AUW of 4000 Tons, the optimal depth was 20 feet.

Optimum Wing Depth - Trade Study

• Multidisciplinary Trade of Hydrodynamics and Structures

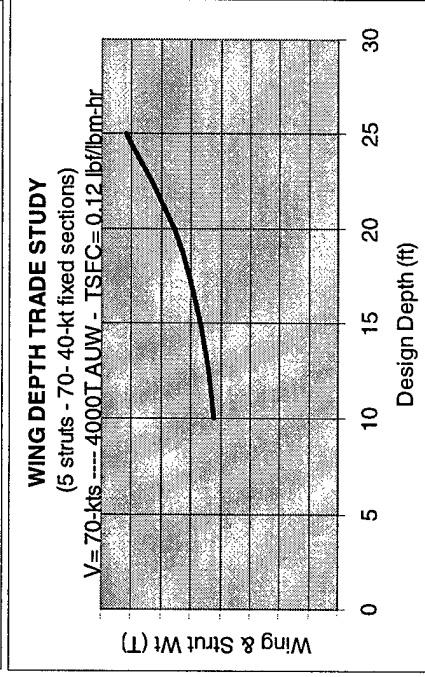
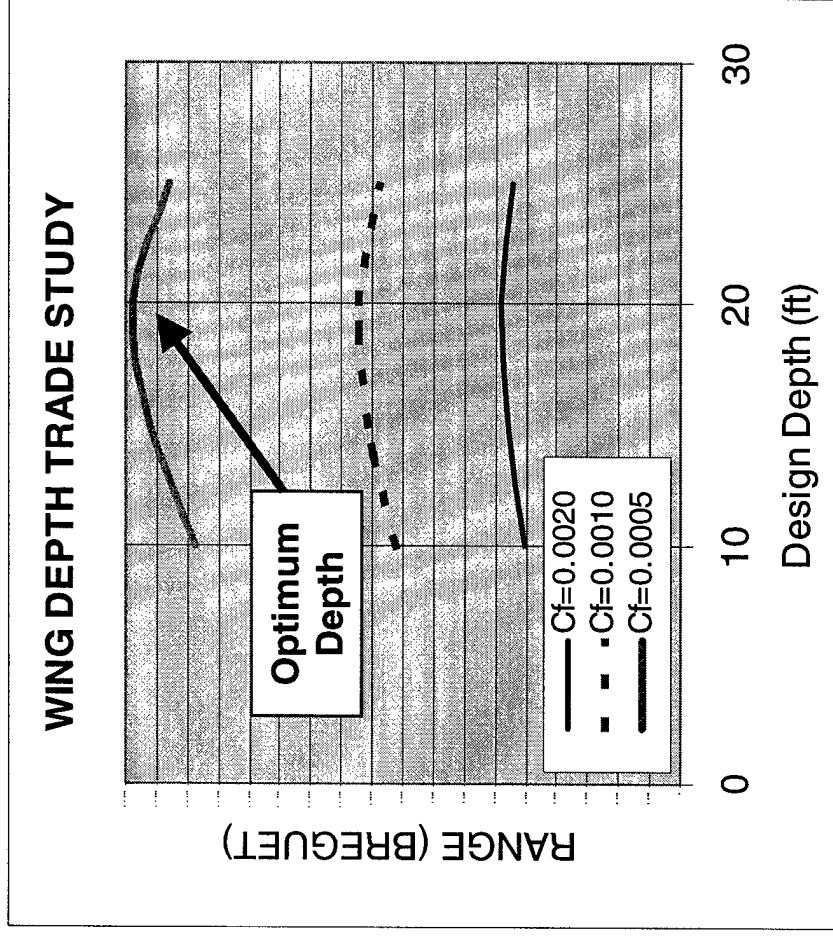
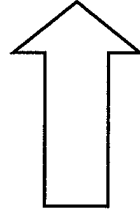
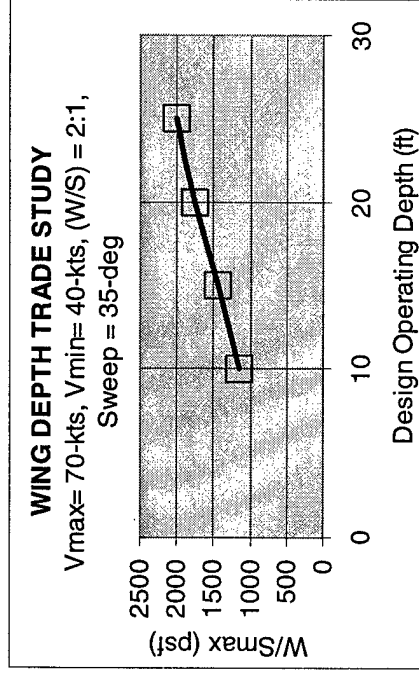
Breguet Equation :

$$\text{RANGE} = (V / \text{TSFC}) (L/D) \log_e (W_i/W_f)$$

$$V = 70 \text{ kt; TSFC} = 0.12; W_i = 4000T; W_f = 2000T + \text{WING\&STRUT WT}$$

$$L/D = L/D @ V=70 \text{ kt, } b=200\text{-ft, } W/S_{\text{max}}(\text{depth}), AR(W/S_{\text{max}}), CD0 (\text{wetted area and } C_f)$$

OPTIMUM DEPTH ~ 20-ft

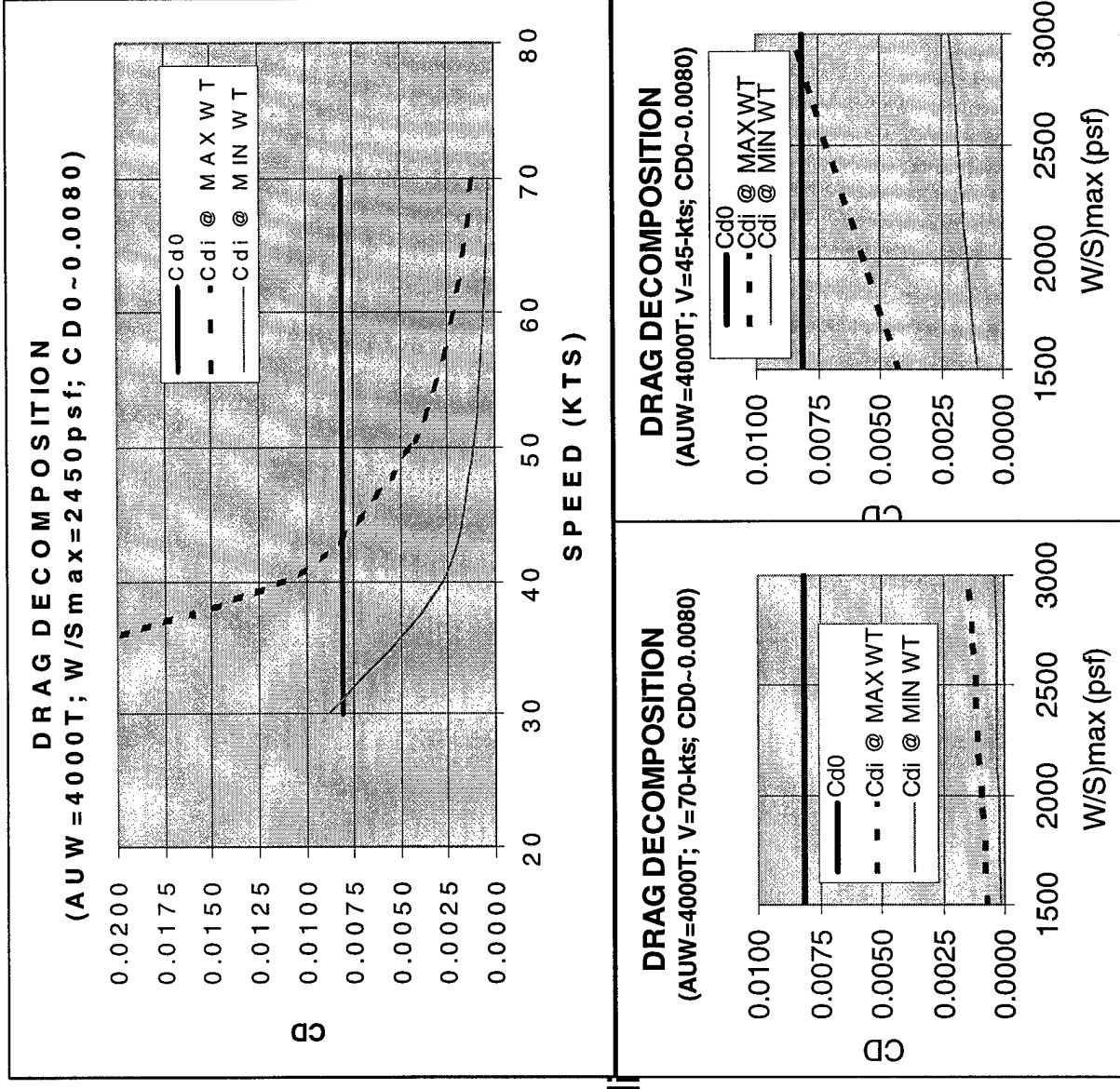


Drag Component Decomposition

The competing issues with the hydrofoil design are the viscous drag at high speed and the induced drag at or near takeoff. They act to push the power requirements to opposite end of the performance envelope.

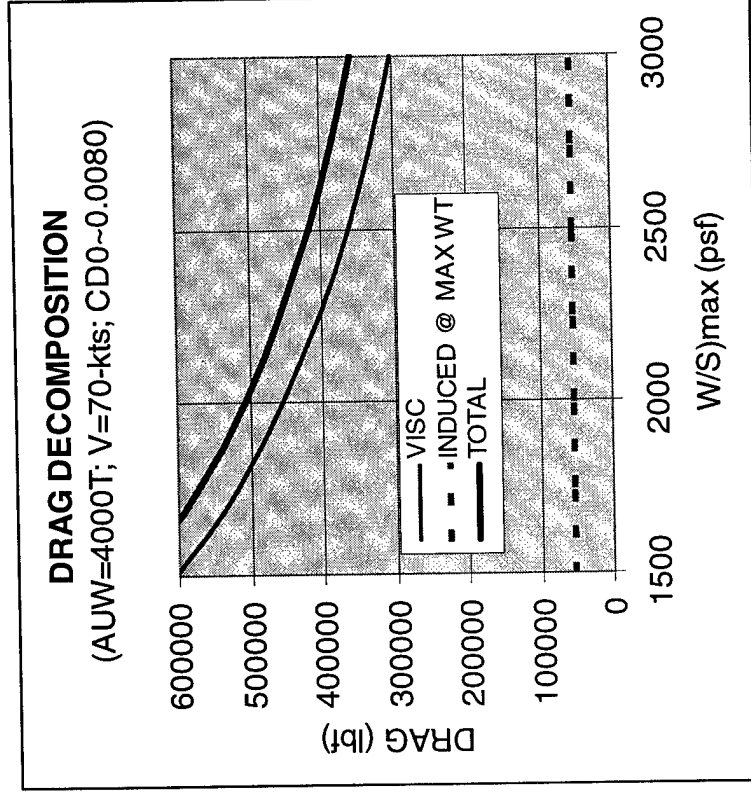
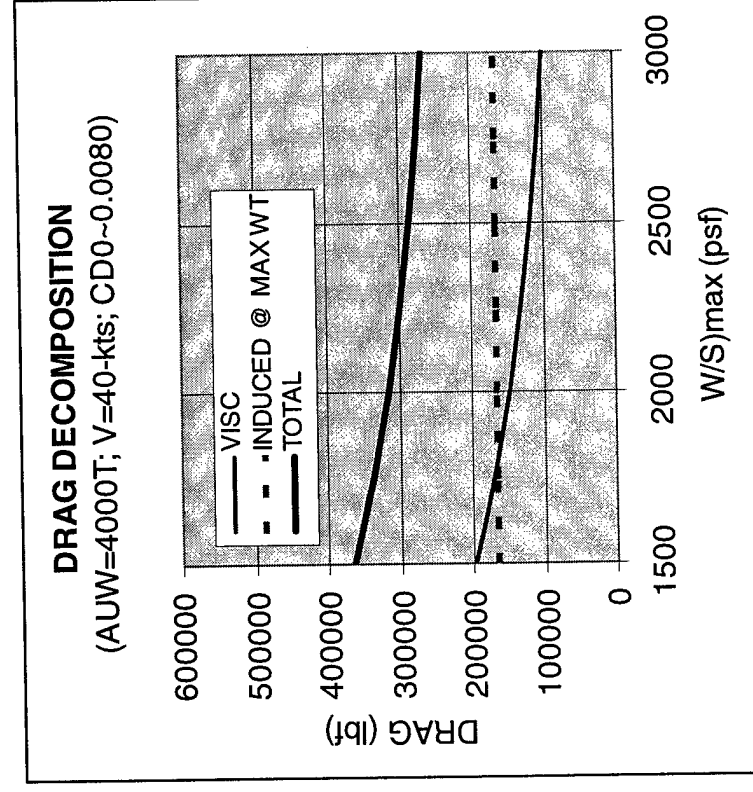
Drag Component Decomposition

- **Viscous Drag dominates total drag at high speeds**
- **Induced Drag dominates total drag at take-off**
- **Competing issues :**
 - high W/S_{max} wing
 - » higher take-off speeds
 - » proportionately more C_{Di}
 - low W/S_{max} wing
 - » lower take-off speeds
 - » proportionately less C_{Di}



Drag Component Decomposition (cont'd)

- **Recall that Dimensional Drag sizes Powerplant**
 - dimensional induced drag function of span and weight, not W/S_{max} !
- **Competing issues - cruise thrust @ spec TSFC limits design**
 - high W/S_{max} wing --- cruise thrust \sim T/O thrust
 - low W/S_{max} wing --- cruise thrust \gg T/O thrust

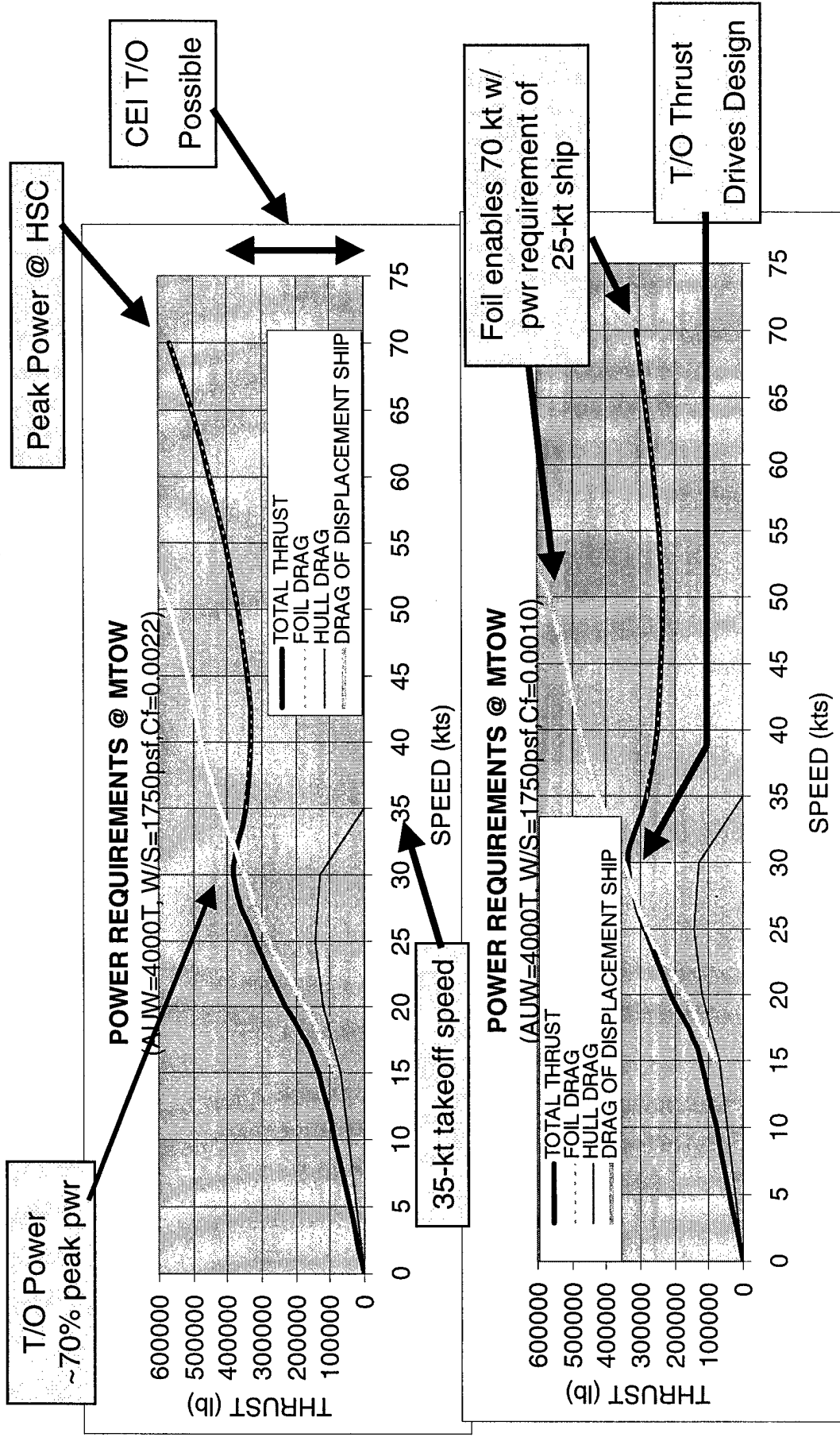


4KT Hydrofoil Take-Off Thrust Requirement

For the 4000 Ton Hydrofoil, the ship hull resistance is combined with the foil drag and the take-off power requirement is determined. The air-coupled system restricted to 400000-500000 pounds total thrust due to the beam constraint. A water-coupled system is not beam restricted and could produce 150000 pounds thrust per LM6000 with a water jet from 5 knots through 70 knots. Reducing viscous drag will reduce overall cruise power needs, the take-off will then be the pinch point in the power speed curve.

4KT Hydrofoil Take-Off Thrust Requirement

- Recall that Dimensional Drag sizes Powerplant



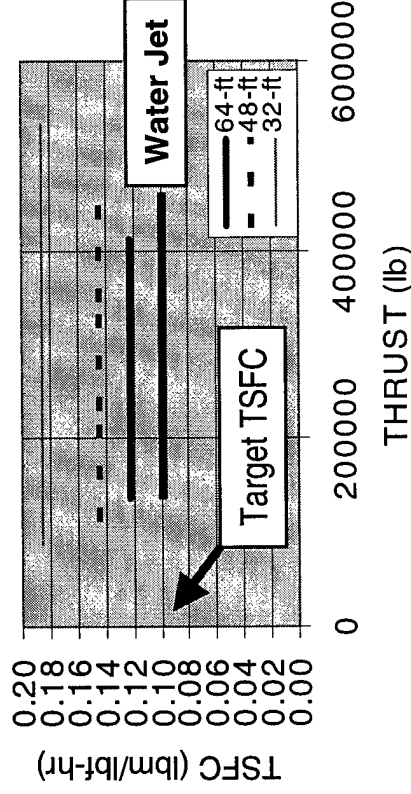
4KT Hydrofoil Propulsion System Summary

Various means of provided thrust-required were examined. The air-coupled systems resulted in large, high risk propellers with TSFC's ranging from 0.12 to 0.18. The water coupled systems, either super-cavitating propellers or water pumps, were capable of similar thrust levels at TSFC's of 0.10 to 0.12. For the 4000 Ton hydrofoil, three 50KSHP LM6000 gas generators would be needed. Auxiliary thrust could be provided with a commercial turbo-fan engine for a small FWF penalty is hump speed drag is higher than expected.

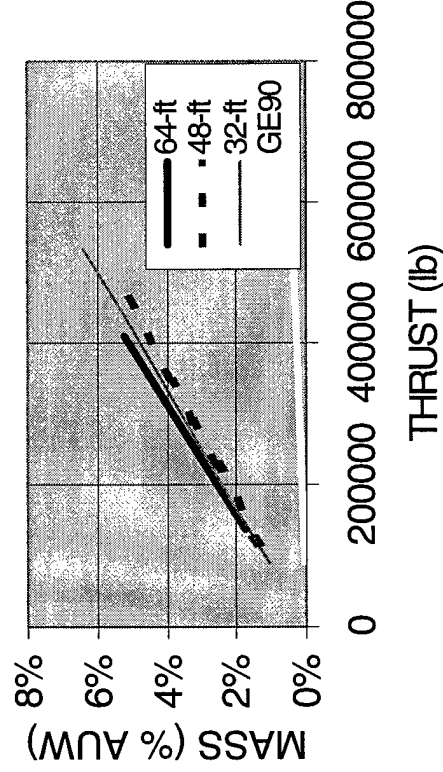
4KT Hydrofoil Propulsion System Summary

MOTOR	PROP DIA (ft)	WT (T)	THRUST @ 70-kts	TSFC @ 70-kts
LM-6000	64	70	136920 lb	0.122
LM-6000	48	52	116273 lb	0.145
LM-6000	32	43	89107 lb	0.185
LM-6000	9.0	70	150000+ lb	0.10
MOTOR	FAN DIA (ft)	WT (T)	THRUST @ 70-kts	TSFC @ 70-kts
GE-90	12	3	92000 lb	>0.3

PROPULSION SYSTEM TSFC
(LM6000 Gas Generator)

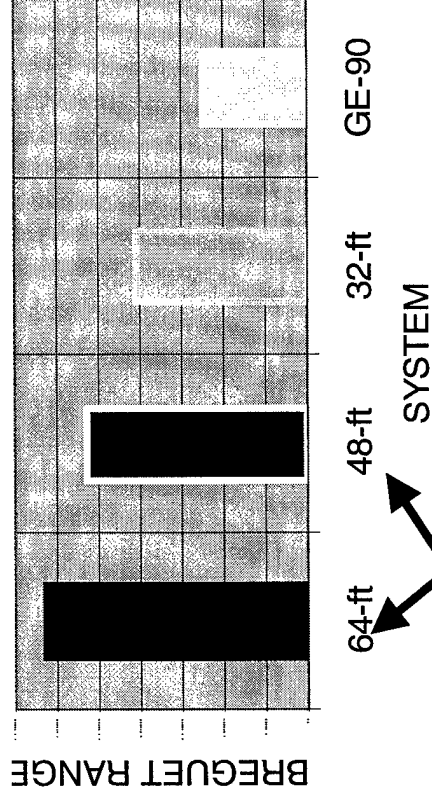


PROPULSION SYSTEM MASS
(NORMALIZED TO 4000T AUW)



PROPULSION SYSTEM TRADE STUDY

(NORMALIZED TO 4000T AUW, ~50% FWF, 400,000-lb Thrust)



Efficient Options limited to 400000-500000 lb Thrust

Feasible Vehicle Sizes - Effect of Viscous Drag Mitigation

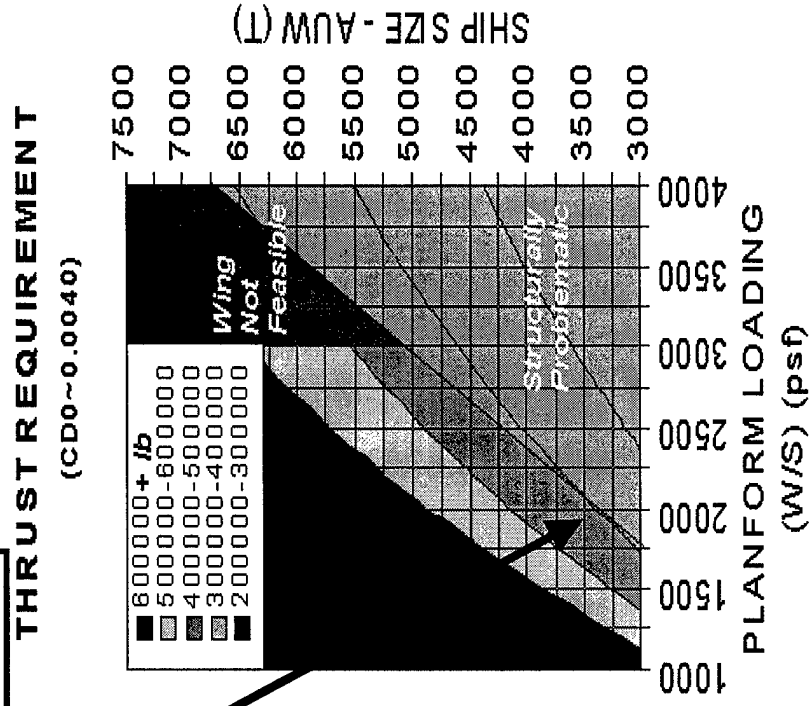
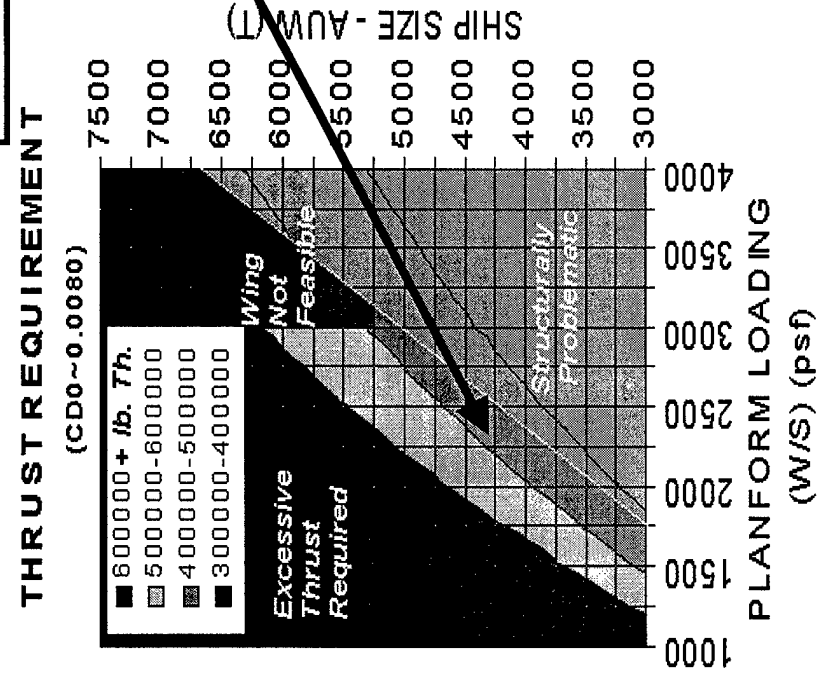
The range of feasible hydrofoil sizes is limited, largely to the combinations of the design constraints, propulsion system integration (air and water coupled propulsors) characteristics, structural material currently available and the amount of viscous drag reduction. If three water jets with total thrust near 900000 pounds were available, the largest hydrofoil that could be scaled off of the 4000T, 125 ft beam system would be in the range of 10KT to 12KT total displacement.

Feasible Vehicle Sizes - Effect of Viscous Drag Mitigation

Without Viscous Drag Mitigation, the practical vehicle size is severely constrained by low TSFC Thrust Limitations, Wing Planform Limitations and Structural Feasibility Concerns.

Optimum TSFC solutions are for ~400,000 lb cruise thrust, leading optimum sized ships to 4000T-6000T for $W/S=2450\text{psf}$; 3500T-5000T for $W/S=1750\text{psf}$ (depending upon CD0)

Feasible Design Space



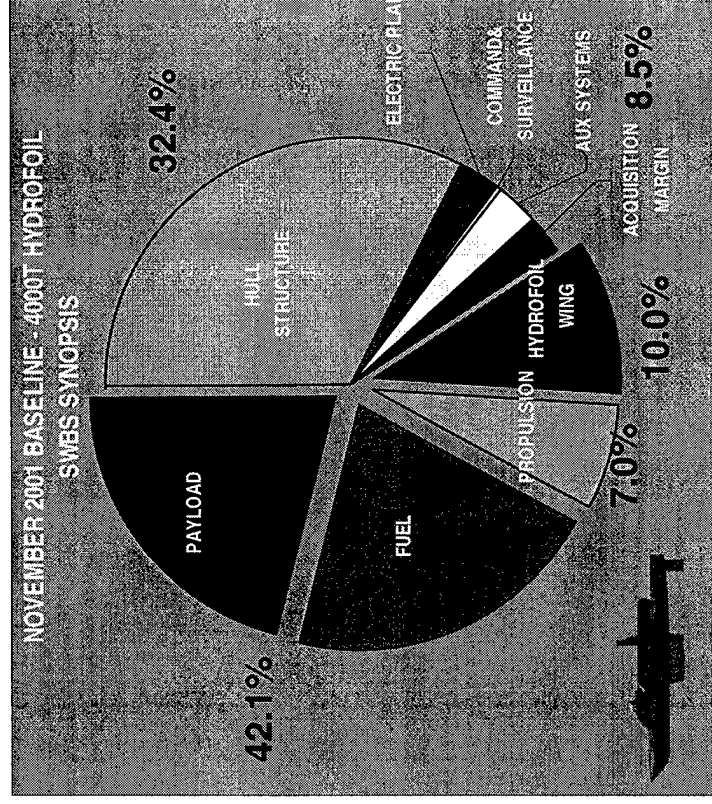
Hydrofoil SWBS – CSC-based Assessment

Bottoms-Up type payload range estimates were needed as well. It is important to realize that a high von Karman efficiency is not a guarantee to economic feasibility. The fraction of the system weight that can be used for economic purposes should be the real indicator of usefulness or practicality.

Nonetheless, the mass fraction of the ship that was used for sustentation was only as good as the estimates of the other on-board systems and their fraction of the total. Since the technical background of LM Aeronautics was largely aero-structural, CSC-Advanced Marine was brought on board to support the development of a Ship Weight Breakdown Structure (SWBS) and identify candidate hull designs and resistance estimates. The results of the that effort are shown in the following pie-chart. Sustentation weight is directly estimated and added to the SWBS. At 4000 tons the hydrofoil wing contributes to 10% of AUW. Propulsion estimates are based on a air-coupled approach and the remaining payload/fuel fraction is on the order of 42%. The Fixed Weight Fraction (FWF) is then 58%. At the onset of the study, the goal was for a FWF of no greater than 50%.

Hydrofoil SWBS – CSC-based Assessment

4000T Hydrofoil



The fraction of the All Up Weight (AUW) for the Foil and Strut System is approximately 10% and the Payload/Fuel is on the order of 42%

Hydrofoil Sizing/Synthesis Closure

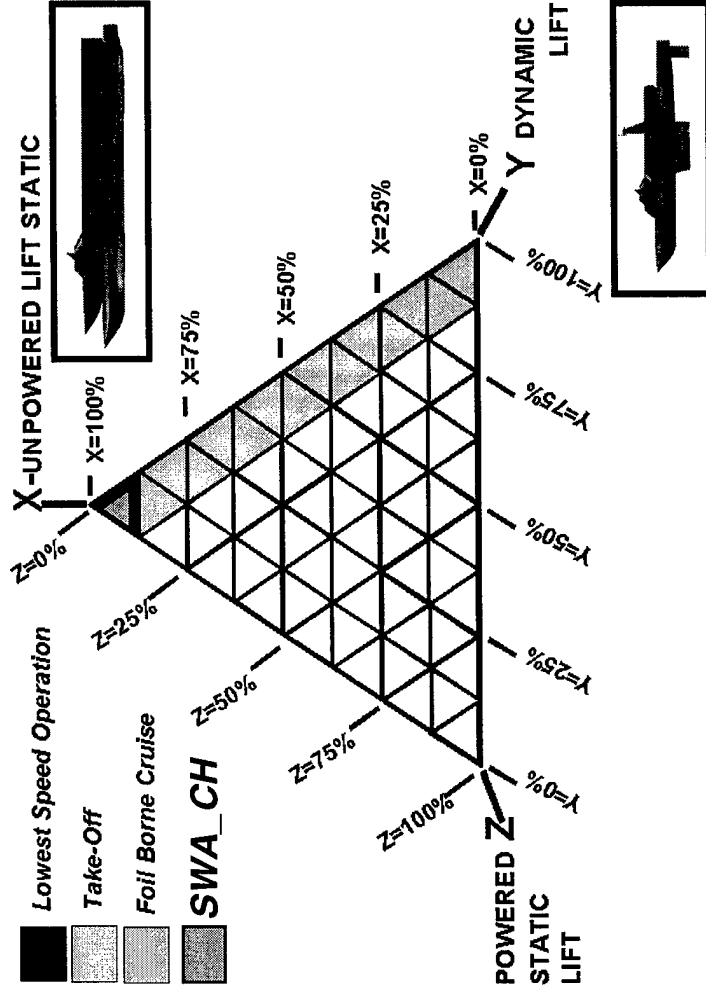
- What really is the “Optimum”?
 - Meets the primary requirement
 - » Payload @ Range
 - Balance wing weight, wing buoyancy with hydrodynamic efficiency
 - “Reduced sweep” wing section options are not markedly better than the optimum performance wing sections
 - Meets the secondary requirements
 - » 65-m / 213-ft Beam & “Reasonable” Power
 - Balance induced drag at take-off, wing-section takeoff speed and hull drag
 - Water Coupled system – 900,000 lbs thrust, Air-Coupled System-450,000 lbs thrust
 - Maximizes the tertiary requirement
 - » High von Karman Efficiency
 - » $k_2=100\%$ solutions --> $L/D \sim 15$, $\text{vonK} = (70\text{-kt})(15) = 1050\text{-kt}$
 - » $k_2 = 50\%$ solutions --> $L/D \sim 30$, $\text{vonK} = (70\text{-kt})(30) = 2100\text{-kt}$

Hydrofoil Payload Range Conundrum

- **Design Space Broadens**
 - Many different solutions provide similar range performance!
- **“Best” and “Runners Up” Dependent upon “Goodness Criterion”**
 - Best Range @ Zero-Payload not Best Range @ 1000T Payload
 - Best Range @ Payload not necessarily Highest Karman Efficiency
- **Contributing Factors to Payload-Range Behavior**
 - Trade-off between FWF and L/D
 - Configuration insensitivity is due to :
 - » improvements in L/D occur at an expense in weight
 - » reductions in foil system weight tend to reduce L/D
- **Effect of Viscous Drag Mitigation ($k_2 < 100\%$)**
 - » CD0 less important » Buoyancy more important » Induced Drag more important
 - » $k_2 < 100\%$ drives design to high buoyancy, high wetted area designs
- **1000+T payload capacity @ 6000nM requires $k_2 < 50\%$**
- **With little payload-range difference between top candidates secondary effects become design discriminator (i.e. Take-Off Power)**
- **The Next Step is to Investigate the Mixed Buoyancy System to determine if there is a Optimum!**

Design Space Revisited – Sustention Triangle

- General Theory of Static Lift Payload Performance
 - Understand how to trade hydrodynamic performance for fuel fraction through the choice of submerged body sections and propulsion integration in order to maximize mission performance



NOTE : *if dramatic viscous drag reduction* is feasible, static lift may ultimately prove to be competitive with dynamic lift. (I.e. a SWA_CH ship becomes the preferred solution above 12 KT.)*

***This is to specific and should be generalized to read:**
dramatic viscous drag reduction and the cavity hull approach

Mixed Buoyancy Range Equation

- The most complex situation occurs where we have a mixed-buoyancy vehicle, in particular one where the vehicle's buoyancy exceeds its structural weight.
- For the general case, the vehicle would begin its flight operating as a dynamic lift vehicle - burning off fuel, and, consequently demanding less lift until, perhaps, so much fuel is burned off so that the vehicle reverts to operating as a displacement hull.
- Excess theoretical buoyancy resulting from further fuel consumption would be offset by taking on ballast
- The total lift of the vehicle is the sum of the static and the dynamic lift....

$$Lift4 := LiftStatic + LiftDynamic$$

Mixed Buoyancy Range Equations

- The total weight of fuel at the beginning of the mission is...
 - $Fuel_i := AUW - ZFW$
- The requirement for dynamically supported lift, therefore, is....
 - $LiftDynamic := ZFW + FUEL - LiftStatic$
- So the range problem becomes more complicated depending upon whether or not your burn off so much fuel that you revert to a static lift vehicle. The crossover point is represented by a fuel load of $F1$...
 - $F1 := \max(LiftStatic - ZFW, 0)$
- During the portion of flight where lift derives from both dynamic and static effects, the range equation looks like the constant V , variable L/D equation.
- During the portion of the flight where lift derives solely from static sources, the range equation looks like the constant V , fixed CD equation.

Mixed Buoyancy Range Equations (cont'd)

- The overall range of the vehicle, is the sum of the range under static+dynamic lift flight and the range under static lift flight.
– **RANGE4 = RANGE4A + RANGE4B.**
- Where

$$\begin{aligned}
 \text{RANGE4A} &:= 1.772453851 \text{ V}kts \text{ AR} \left(\arctan \left(\frac{.3961075261}{\rho \text{ V}kts^2 \text{ Sref} \sqrt{CD_0 \text{ AR} k}} \frac{k (FUELi - \text{LiftStatic} + ZFW)}{\rho \text{ V}kts^2 \text{ Sref} \sqrt{CD_0 \text{ AR} k}} \right) - \right. \\
 &\quad \left. \arctan \left(\frac{.3961075261}{\rho \text{ V}kts^2 \text{ Sref} \sqrt{CD_0 \text{ AR} k}} \frac{(\max(\text{LiftStatic} - ZFW, 0.) - \text{LiftStatic} + ZFW)}{\rho \text{ V}kts^2 \text{ Sref} \sqrt{CD_0 \text{ AR} k}} k \right) \right) \\
 &\quad / (TSFC \sqrt{CD_0 \text{ AR} k})
 \end{aligned}$$

- and

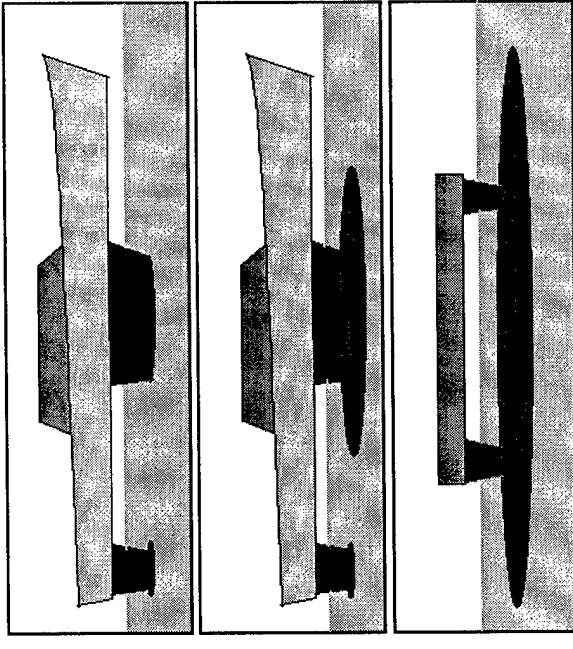
$$\text{RANGE4B} := .7020823101 \frac{\max(\text{LiftStatic} - ZFW, 0.)}{\text{V}kts \text{ TSFC} CD_0 \rho \text{ Sref}}$$

Mixed Buoyancy Trade Study

- **Design Trade**
 - Document Effect of Buoyancy Fraction,
 $BF = \text{Lift_Static} / (\text{Lift_Static} + \text{Lift_Dynamic})$
 - » impact on underwater configuration
 - » impact on hydrodynamic efficiency
 - » impact on payload/range
 - » “optimum” buoyancy fraction
 - for a given vehicle size
 - for underwater viscous drag reduction (**k_2** factor)

Examples:

- Dynamic Lift Hydrofoil
- Mixed Static/Dynamic Lift (HYSWAS)
- Static Lift (Small Waterline Area)



Important Nomenclature

- **Traditional Hydrodynamic L/D**
 - » $L/D = \text{Lift_Dynamic} / \text{Drag}$
 - » Buoyancy of wing system book-kept as a reduction in “all up weight”
- **System L/D**
 - » $L/D_{\text{system}} = (\text{Lift_Dynamic} + \text{Lift_Static})/\text{Drag}$
 - » Buoyancy of wing system book-kept as static lift
- **Payload over Range**
 - » Not a function of buoyancy book-keeping
- **Karman Efficiency**
 - Metric depends upon buoyancy book-keeping

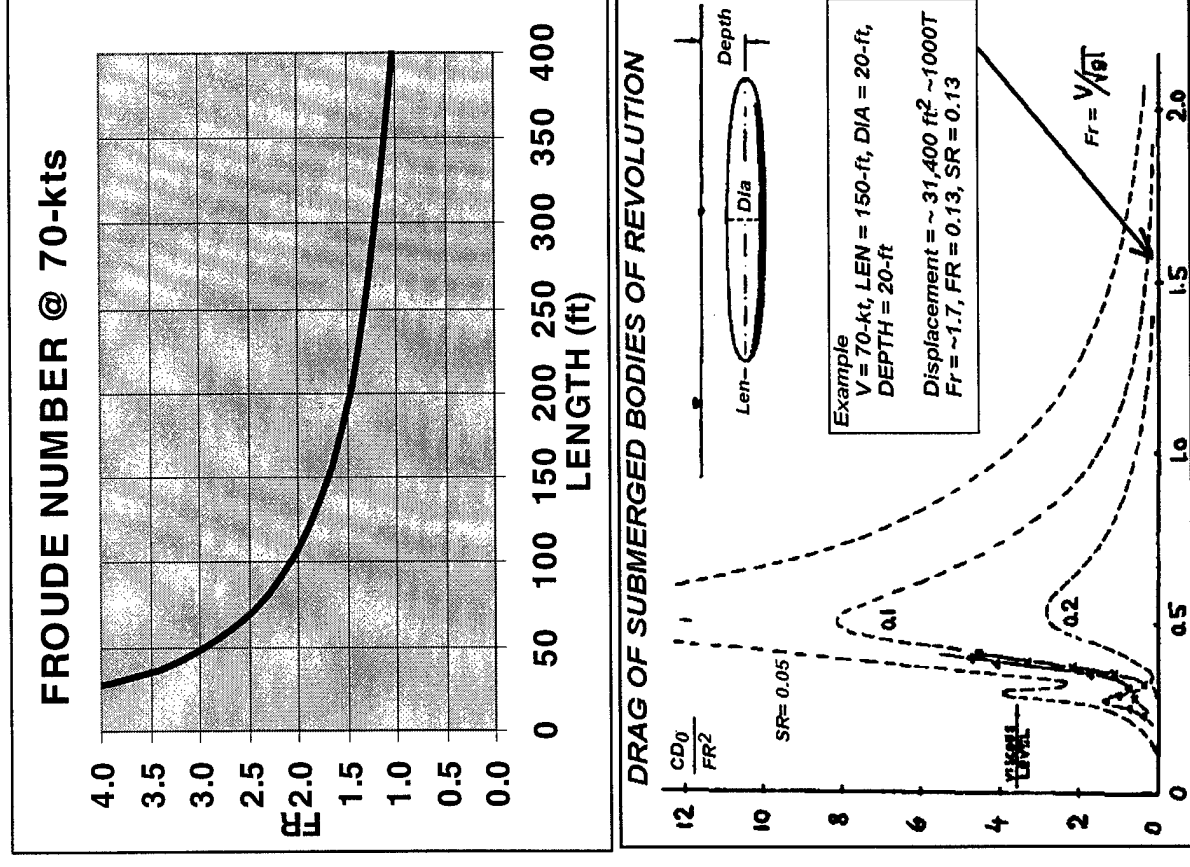
Drag of Fully Submerged Buoyant Bodies

- Drag :
 - Viscous Drag :
 - » Skin Friction on Wetted Area
 - » Base Pressure Drag due to Separated Flow
 - Inviscid Drag :
 - » Induced Drag (Drag due to Lift)
 - » Wave-making Drag (due to proximity to free surface)

- Froude Number
 - $Fr = V / (g L)^{1/2}$

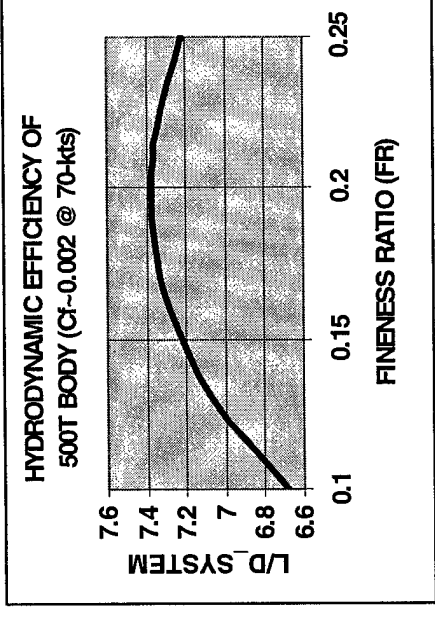
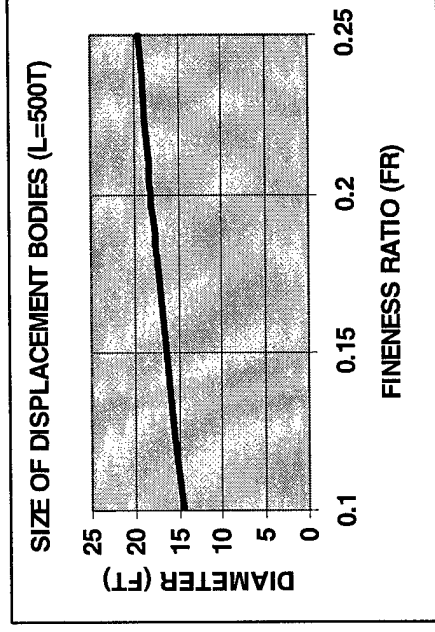
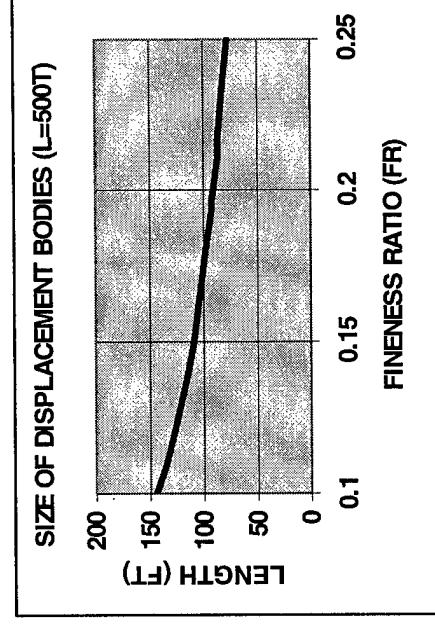
- Fineness Ratio
 - $FR = DIA / LEN$

- Submergence Ratio
 - $SR = DEPTH / LEN$



Drag of Fully Submerged Buoyant Bodies (cont'd)

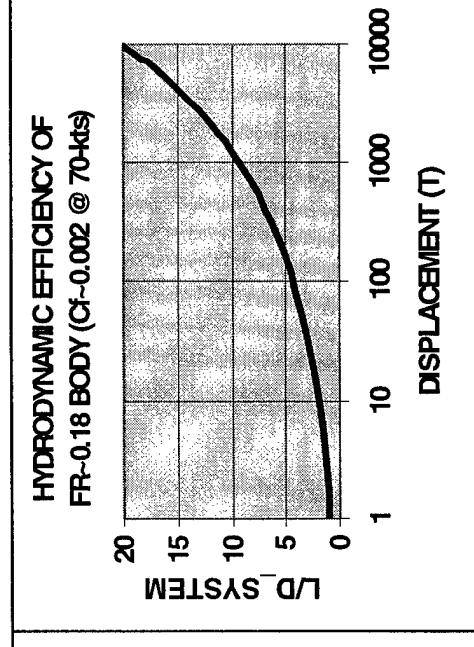
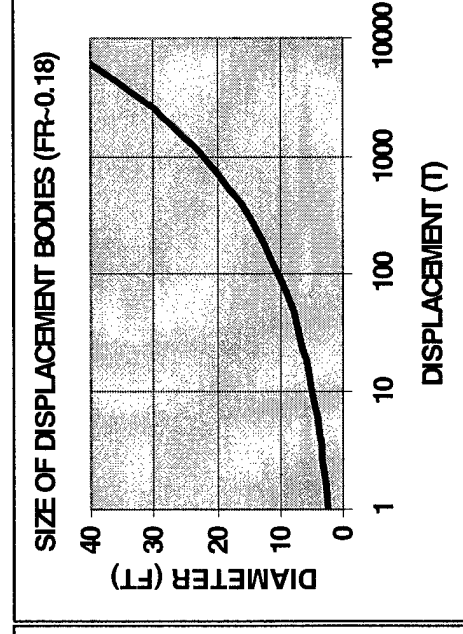
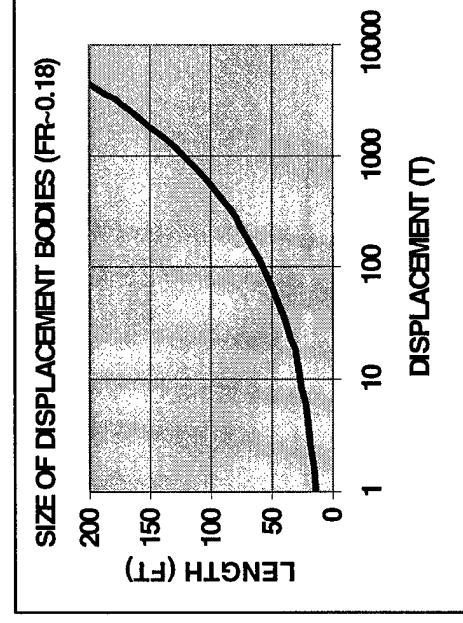
- Total Drag Estimate (after Hoerner)
 - Drag $\sim C_f \text{ Swet } q (1 + 1.5 \text{ FR}^{3/2} + 7 \text{ FR}^3)$
 - Swet $\sim 2\pi (DIA/2)^2 + 2\pi ((DIA) (LEN) / (4e)) \arcsin(e)$
 - $e = \text{sqrt}(1 - \text{FR}^2)$
- Buoyancy Estimate
 - Lift_Static $\sim 33.5 (\text{FR}^2 \text{ LEN}^3) (\text{lbs}) \sim 0.0168 (\text{FR}^2 \text{ LEN}^3) (T)$
- System L/D
 - $L/D_{\text{system}} = \text{Lift_Static}/\text{Drag}$



Efficiency of Submerged Buoyant Bodies

• Trade Study Results

- Displacement Hulls Favor Very Large Vehicle Sizes
 - » Wetted Area scales proportional to length squared
 - » Displacement scales proportionally to length cubed
- A single hull of ~ 5000T displacement has an L/D @ 70-kts ($C_f \sim 0.002$, $k_2 = 100\%$) roughly similar to the hydrofoil ($L/D_{system} \sim 15$)
- To maintain low wave drag, the submergence ratio (SR) must be > 0.1 .
- Competitively efficient vehicles must utilize large buoyant structures
- Vehicle draft becomes an issue when buoyant bodies are sized for high L/D



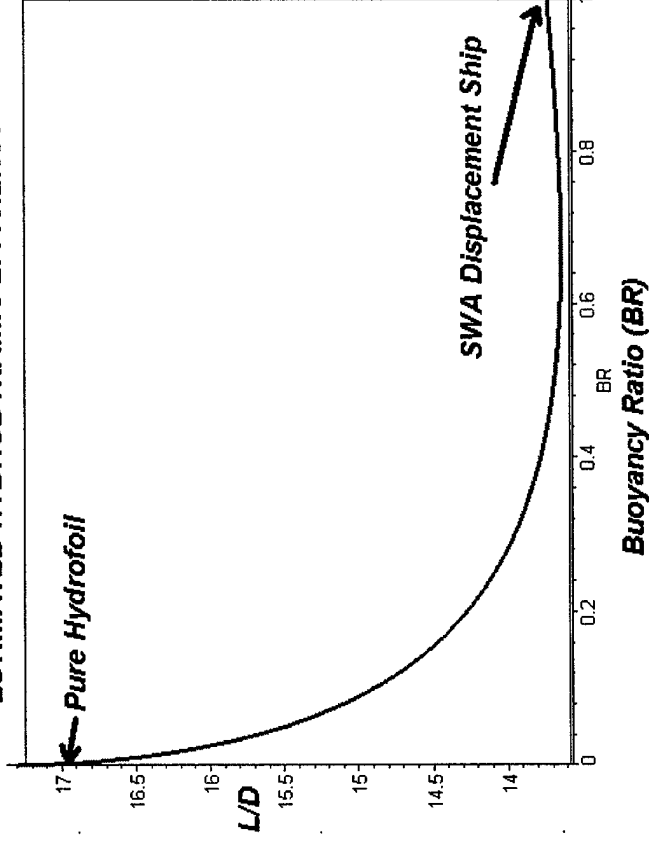
Mixed Static/Dynamic Lift Vehicles at 4000 T

- **Trade Study :**
 - **Two paradigms....**
 - » Payload-range effects for fixed total lift
 - i.e. Trade wing size and buoyant body size
 - » Payload-range effects for fixed wing size, variable buoyant body
 - i.e. Buoyant body increases overall system lift (but not hull size)
- **Assumptions :**
 - Vehicle Configuration :
 - » $AUW=4000T$, $C_f=0.002$, $k_2=100\%$
 - » Buoyant Body = Single; $FR=0.18$
 - » Wing $W/S_{max} = 3000\text{-psf}$, $b=200\text{-ft}$, $h=20\text{-ft}$
 - » Fuel_Fraction = 50%
 - » TSFC = 0.15 lb-fuel/lb-thrust-hr

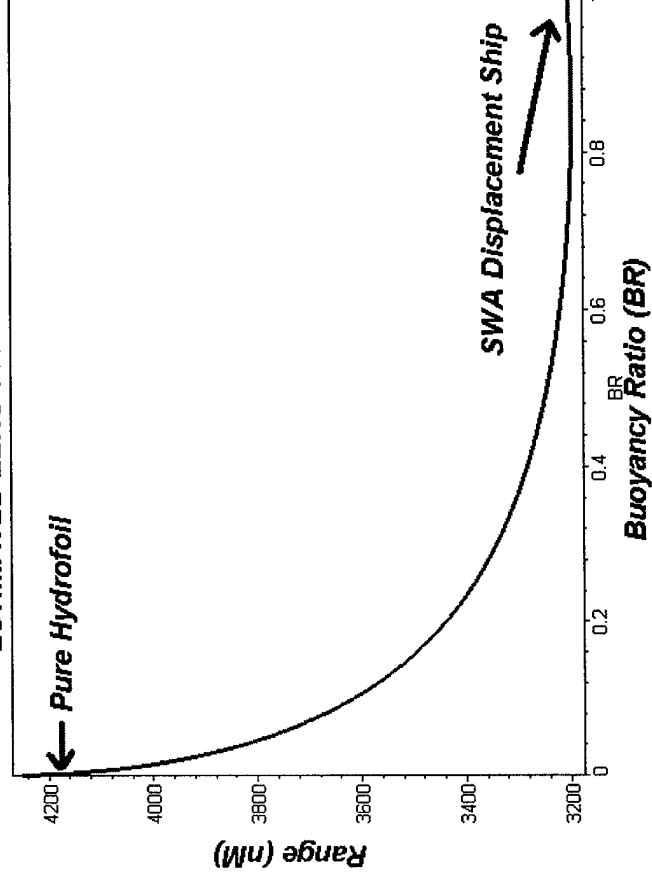
Mixed Static/Dynamic Lift Vehicles at 4000 T

- Paradigm # 1 :
 - Buoyant Body traded for wing area at Fixed 4000T Displacement
 - » For these assumptions the pure Hydrofoil has better L/D than an equivalent sized SWA displacement ship
 - » Small buoyant bodies dilute overall L/D
 - » Reduced wing area for fixed span may pose structural problems
 - » SUMMARY : Mixed Buoyancy has negative impact on range

ESTIMATED HYDRODYNAMIC EFFICIENCY



ESTIMATED ZERO-PAYLOAD RANGE



Mixed Static/Dynamic Lift Vehicles at 4KT (cont'd)

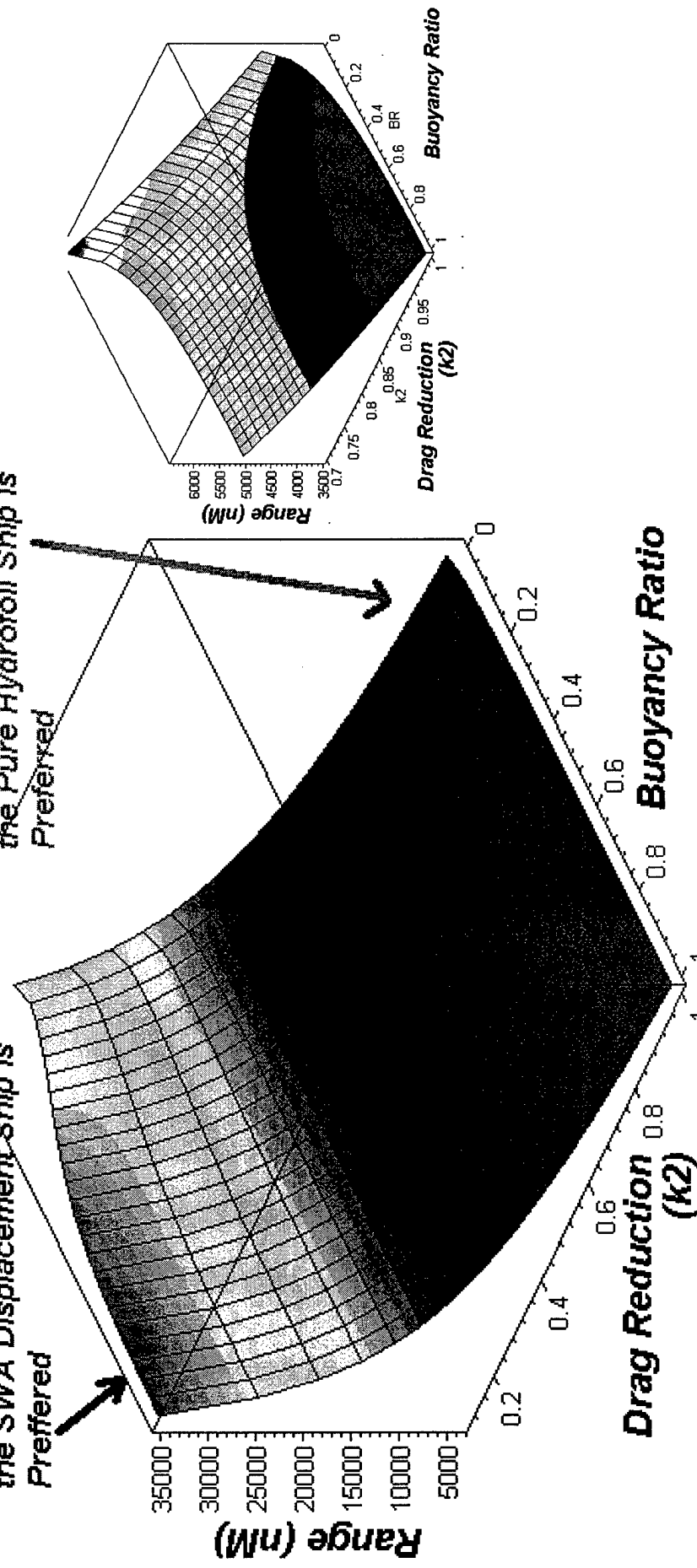
- Paradigm # 1 :

- Effect of Viscous Drag Reduction (4000T)

Effect of Viscous Drag Reduction upon Zero-Payload Range

For reduced drag ($k_2 < 25\%$)
the SWA Displacement Ship is
Preferred

For full drag ($k_2 = 100\%$)
the Pure Hydrofoil Ship is
Preferred

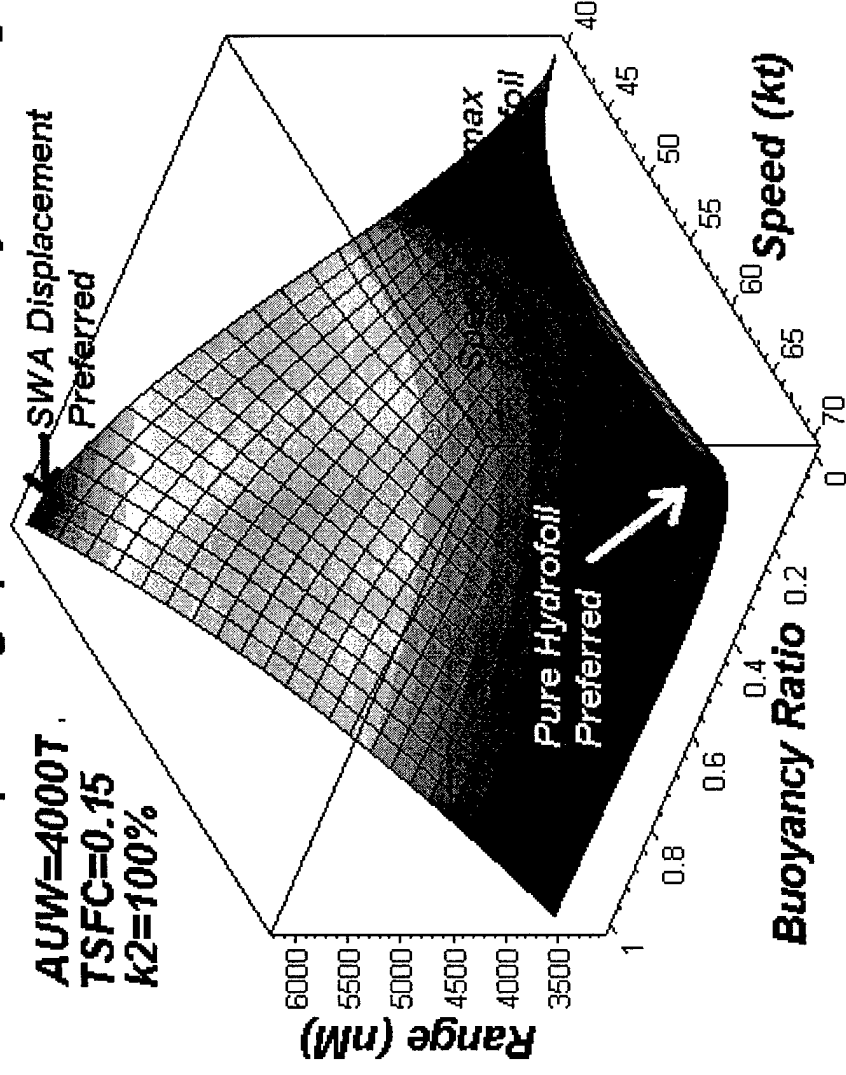


Mixed Static/Dynamic Lift Vehicles at 4KT (cont'd)

- **Paradigm # 1 :**
 - Effect of Vehicle Design Speed at Fixed 4000T Displacement
 - » Mixed Buoyancy can improve performance of Low Speed Hydrofoils
 - » SWA Displacement Ship is Preferred Solution @ Lower Design Speeds

Effect of Operating Speed on Zero-Payload Range

***AUW=4000T,
TSFC=0.15
k2=100%***



Mixed Static/Dynamic Lift Vehicles at 4KT (cont'd)

• Paradigm # 2 :

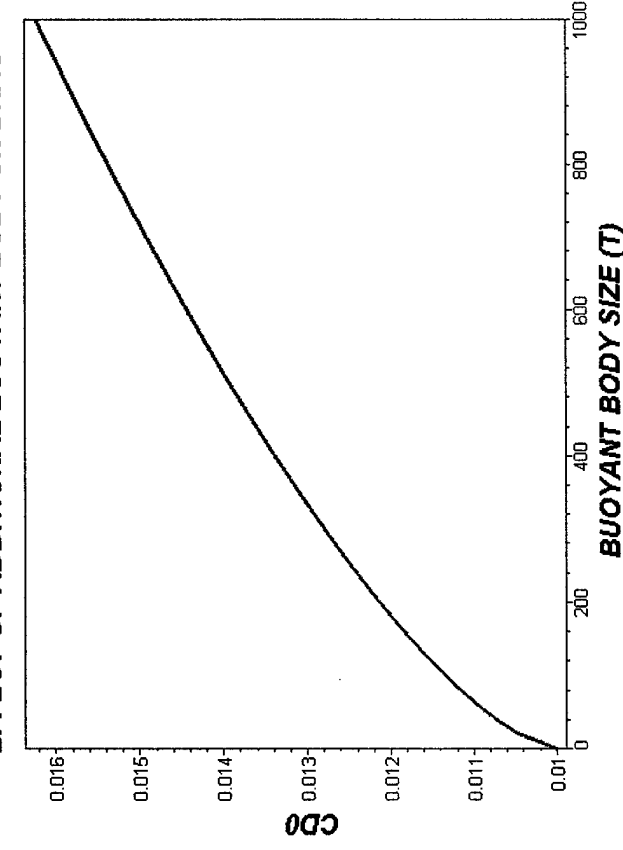
– Add Single Buoyant Body to Fixed Wing Area Hydrofoil

- » Assume basic vehicle : 50% fuel fraction
- » Assume 90% of Buoyant Body usable for fuel
 - (i.e. the body has zero structural mass)
- » Assume $k_2=100\%$

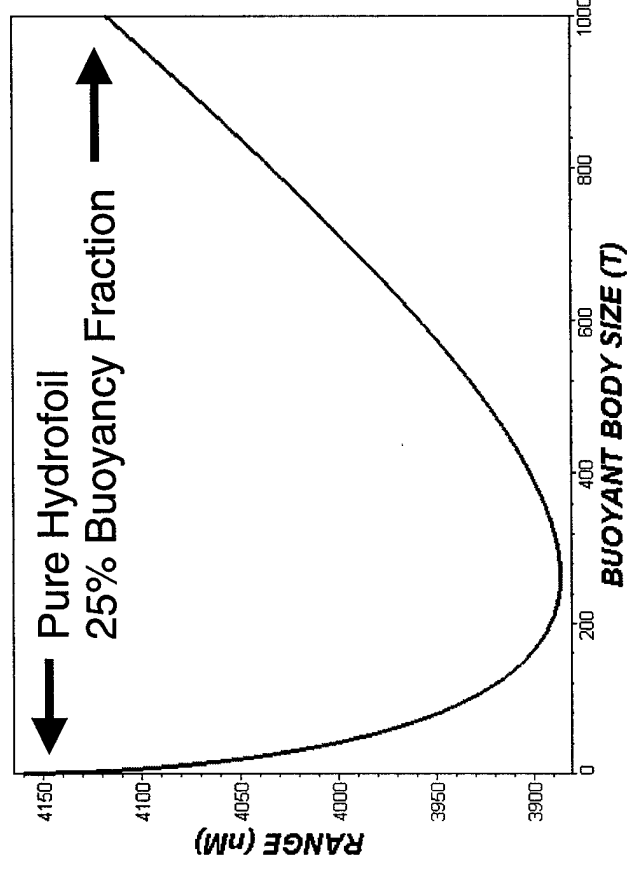
» Mixed Buoyancy Increases Drag Significantly

» Moderate Size Buoyant Bodies have Negative Impact on Range

EFFECT OF ADDITIONAL BUOYANT BODY ON DRAG



EFFECT OF BUOYANT BODY SIZE ON ZERO-PAYLOAD RANGE



Mixed Static/Dynamic Lift Vehicles at 4KT (cont'd)

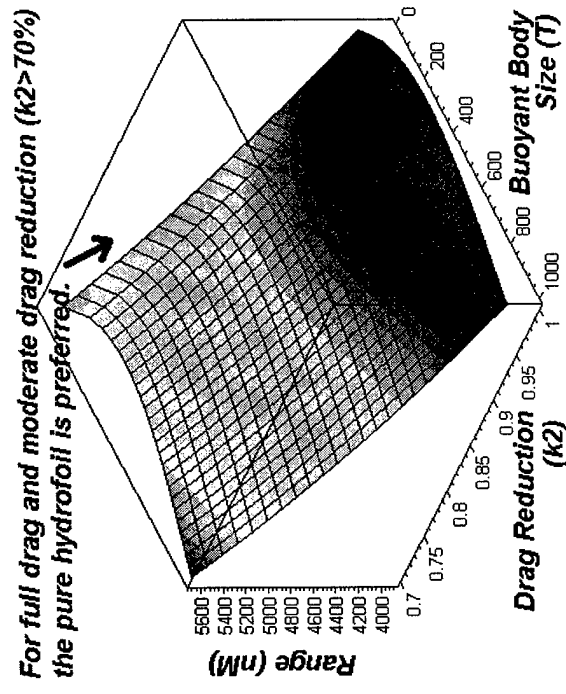
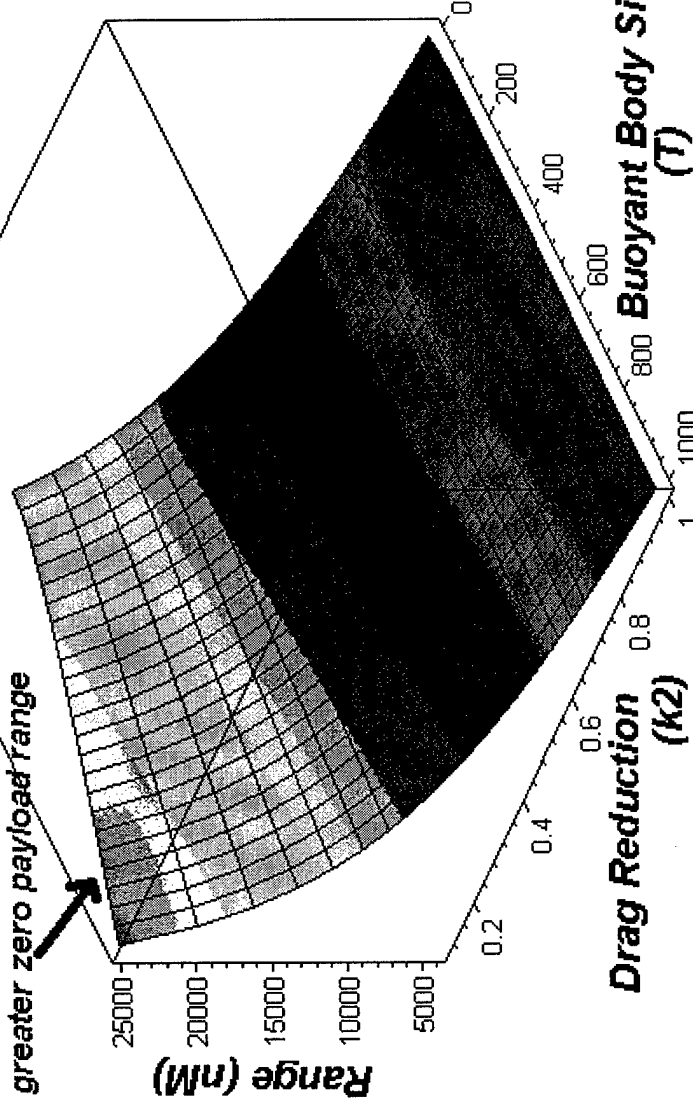
• Paradigm # 2 :

- Effect of Viscous Drag Reduction
 - » pure hydrofoil generally preferred
 - » for very low drag solutions, buoyancy improves range (see Paradigm #1)

Effect of Viscous Drag Reduction upon Zero Payload Range

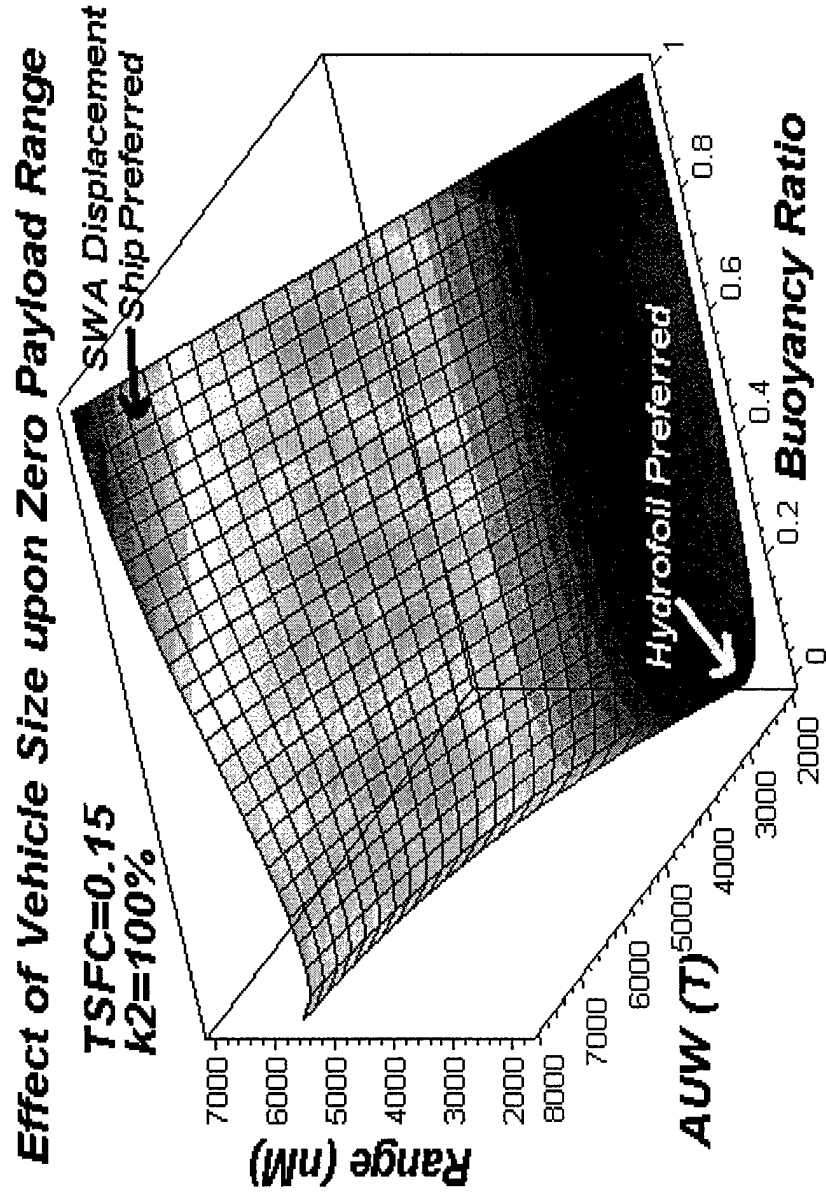
4000T Baseline

For reduced drag, the mixed buoyancy solution offers greater zero payload range



Mixed Static/Dynamic Lift Vehicles at Varied AUW

- A small Hydrofoil Ship has greater hydrodynamic efficiency, hence greater range than a small SWA displacement ship. L/D of hydrofoils declines with increasing size. L/D of SWA ship increases with increasing size. Crossover around 5000T AUW.



Drag Sources for the Varied Vessel Type

Vessel	Wave Drag	Induced Drag	Friction & Form	Spray Drag	Propulsion Drag
Hydrofoil	1-Foil, 9-Vert. 1-Horz.	1-Foil 1-Horz.	1-Foil, 9-Vert. 1-Horz.	9-Vert.	3-Pumps
SWAMCH	1-Body, 4-Horz. 1-Vert.		1-Body, 4-Horz. 1-Vert.	1-Vert.	1-Pump 1-Cavity
SWATCH	2-Bodies 2-Vert.		2-Bodies 2-Vert.	2-Vert.	2-Pumps 2-Cavities

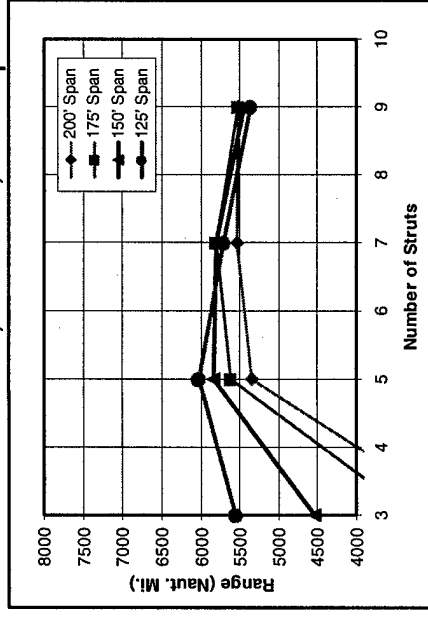


***QUADPAN/POINTER Performance Roll-Up**

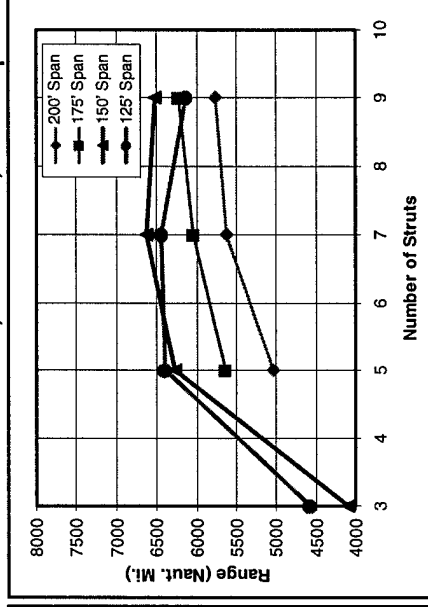
Hydrofoil Structural Sizing Results

Range Vs. Number of Struts and Wing Span

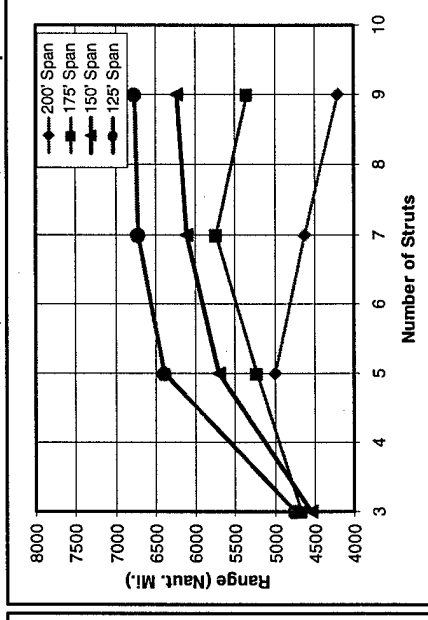
P70/40/2.0H35, 4600 ft², 1750 psf



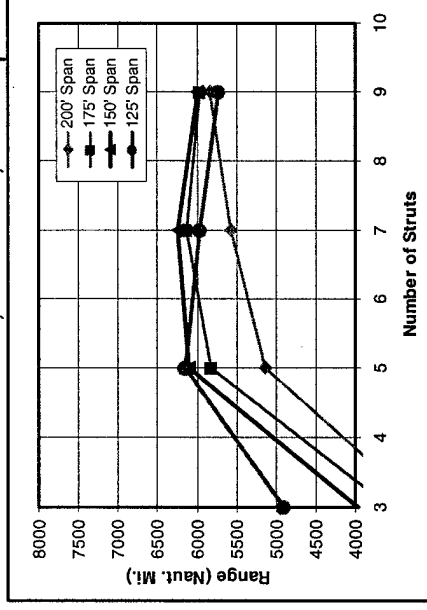
P70/50/2.0H40, 3265 ft², 2450 psf



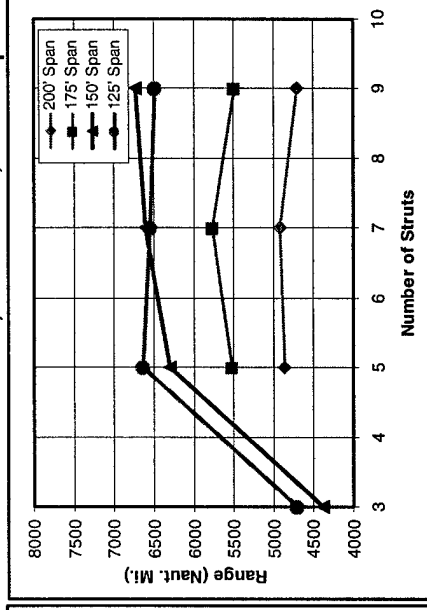
P70/55/2.0H45, 2666 ft², 3000 psf



P70/55/2.0D40, 2910 ft², 2750 psf

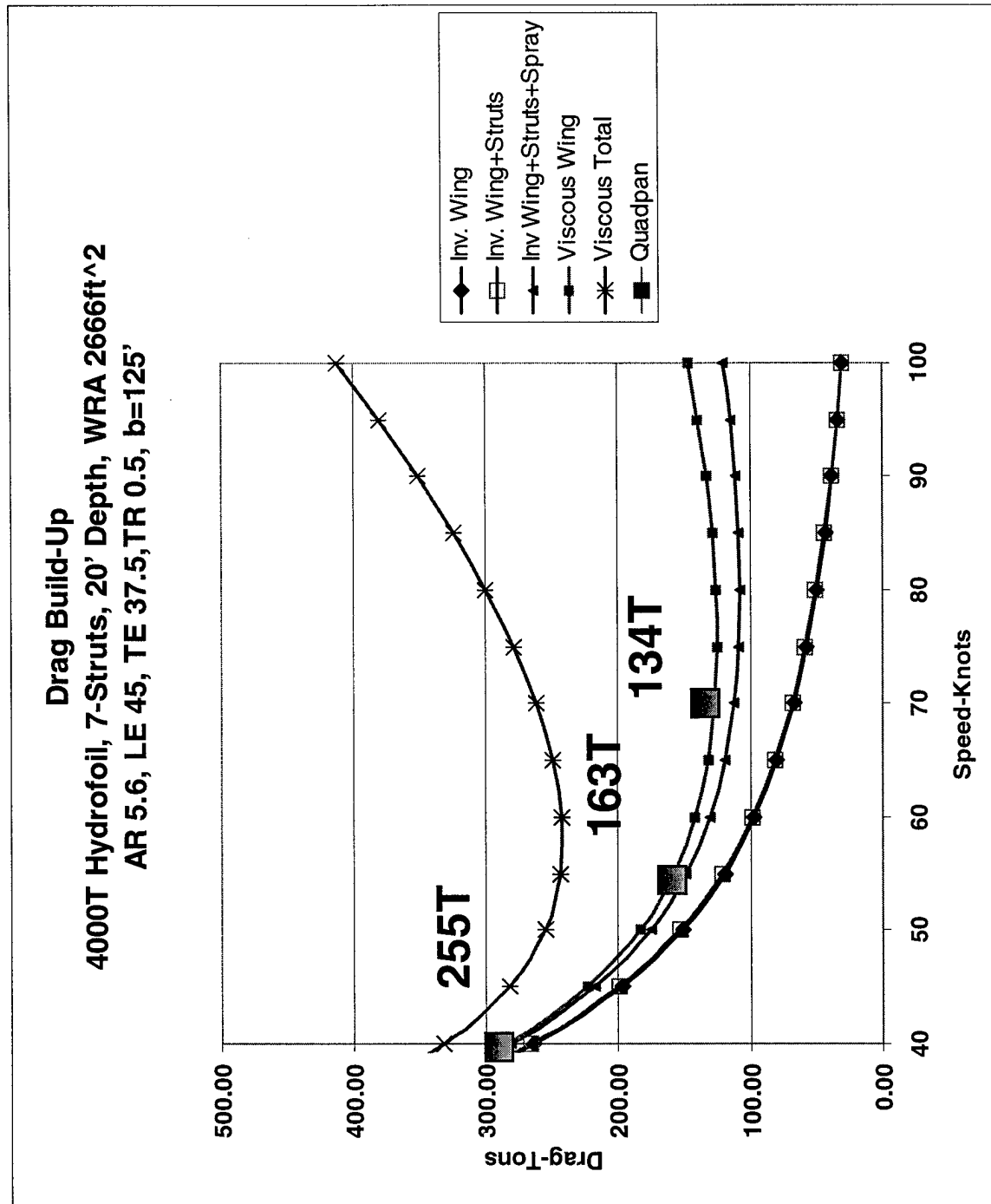


P70/50/2.0H35, 3720 ft², 2150 psf



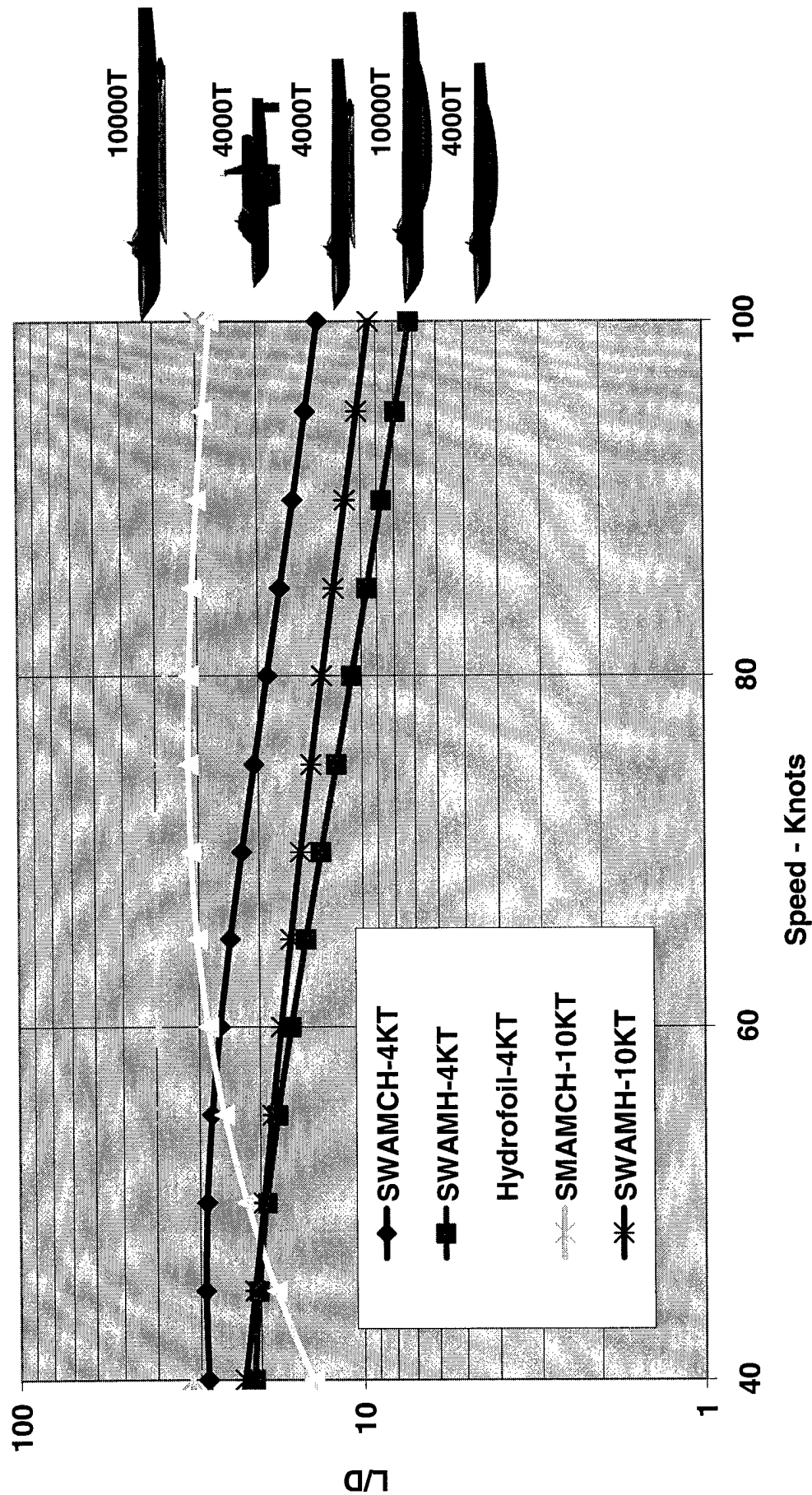
Maximum theoretical zero-payload range = 6767 nautical miles (FWF = 45%)

Hydrofoil Drag Assessment Comparison



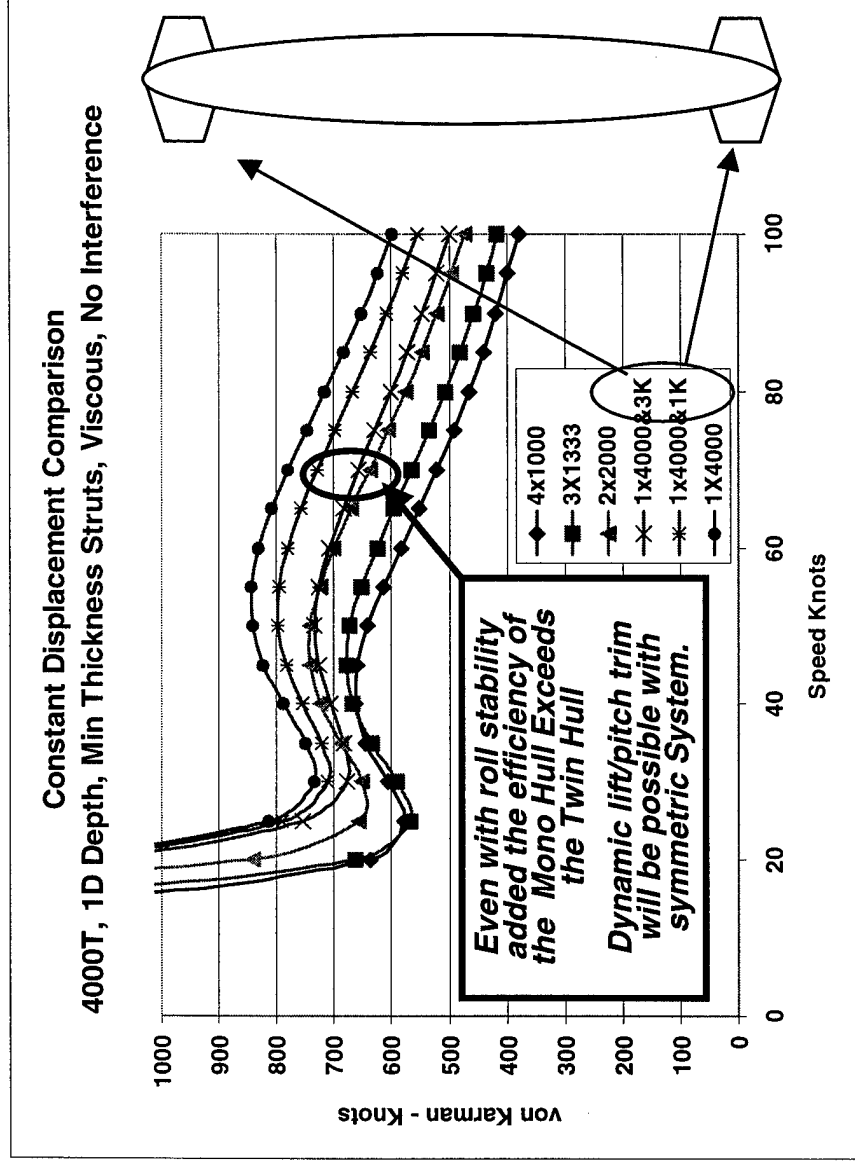
Hydrodynamic Efficiency – Summary*

Component Efficiencies
Varied Size Sustention Systems, 100% Drag



*Drag Values Determined Using 1st Order Methods

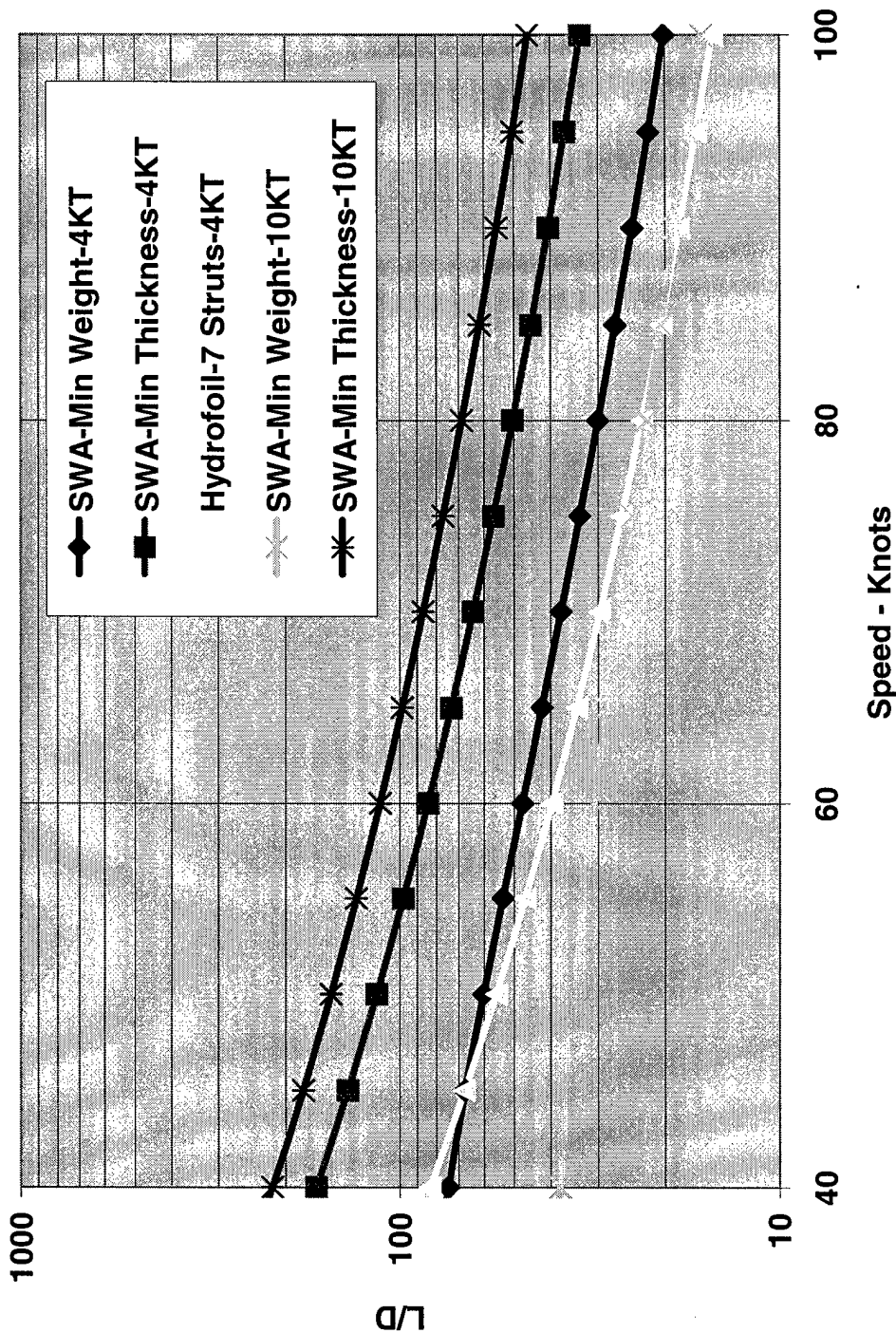
SWAMCH Roll Stability System Impact – 4000T



This chart was shown in November and is being revisited to show the impact that the roll control effectors have on the overall hydrodynamic efficiency. The intent at this point is to show how close the twin hull and mono-hull performance may in fact be!

Hydrodynamic Efficiency – Summary*

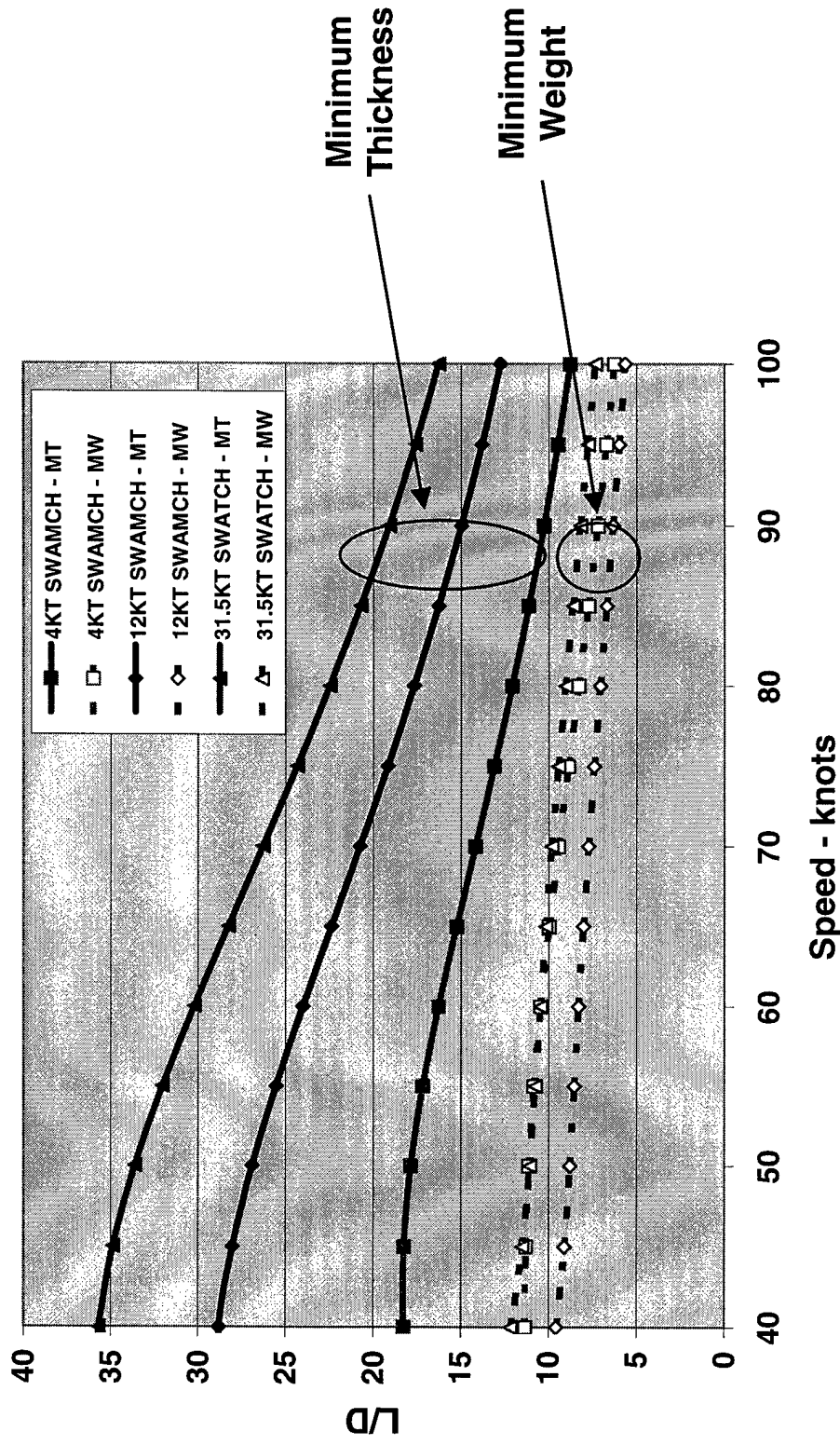
Component Efficiencies
Varied Support Systems, 100% Drag



*Drag Values Determined Using 1st Order Methods

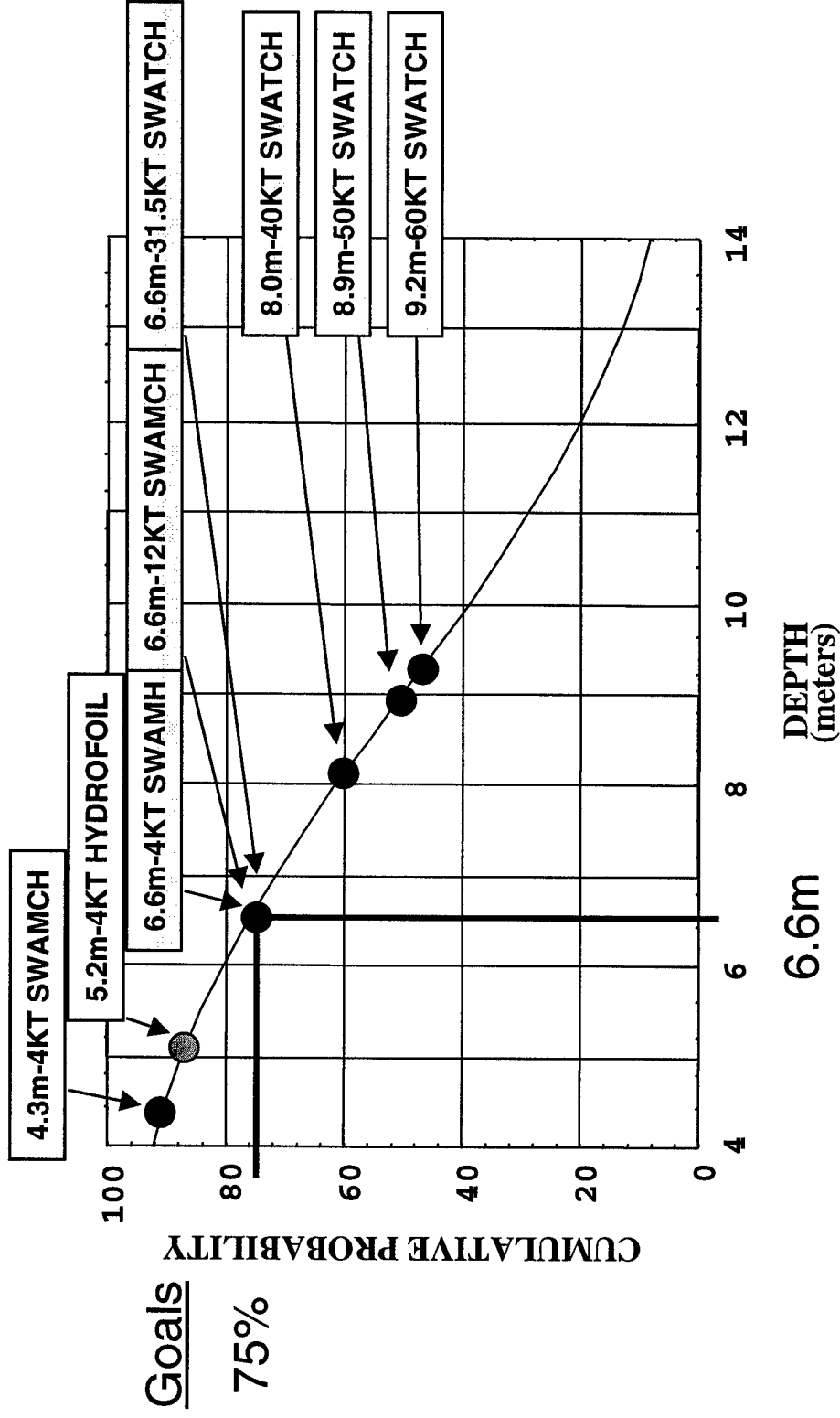
Variation of Strut Thickness and L/D Impact

Strut Design Impact on Integrated Hydrodynamic Efficiency
Thickness Varied From Minimum Thickness to Minimum Weight



This information must be combined with the %AUW of the sustention system to find the Optimum Strut Thickness for a given range.

Port Depth* as a Design Constraint

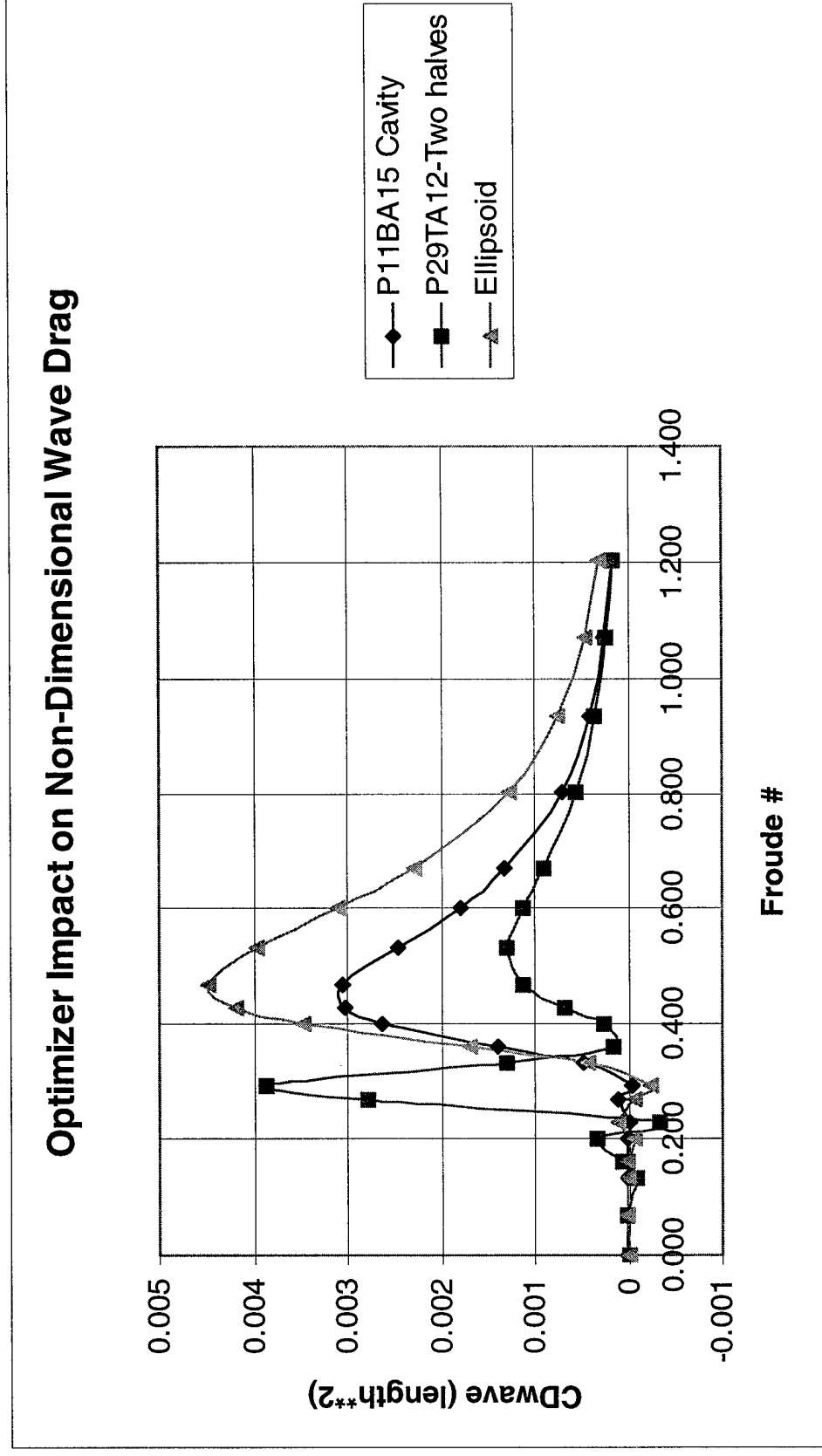


Lloyd's Ports of the World

Line(s) = Gaussian Distribution: mean = 9.0 m; $\sigma = 3.55$ m

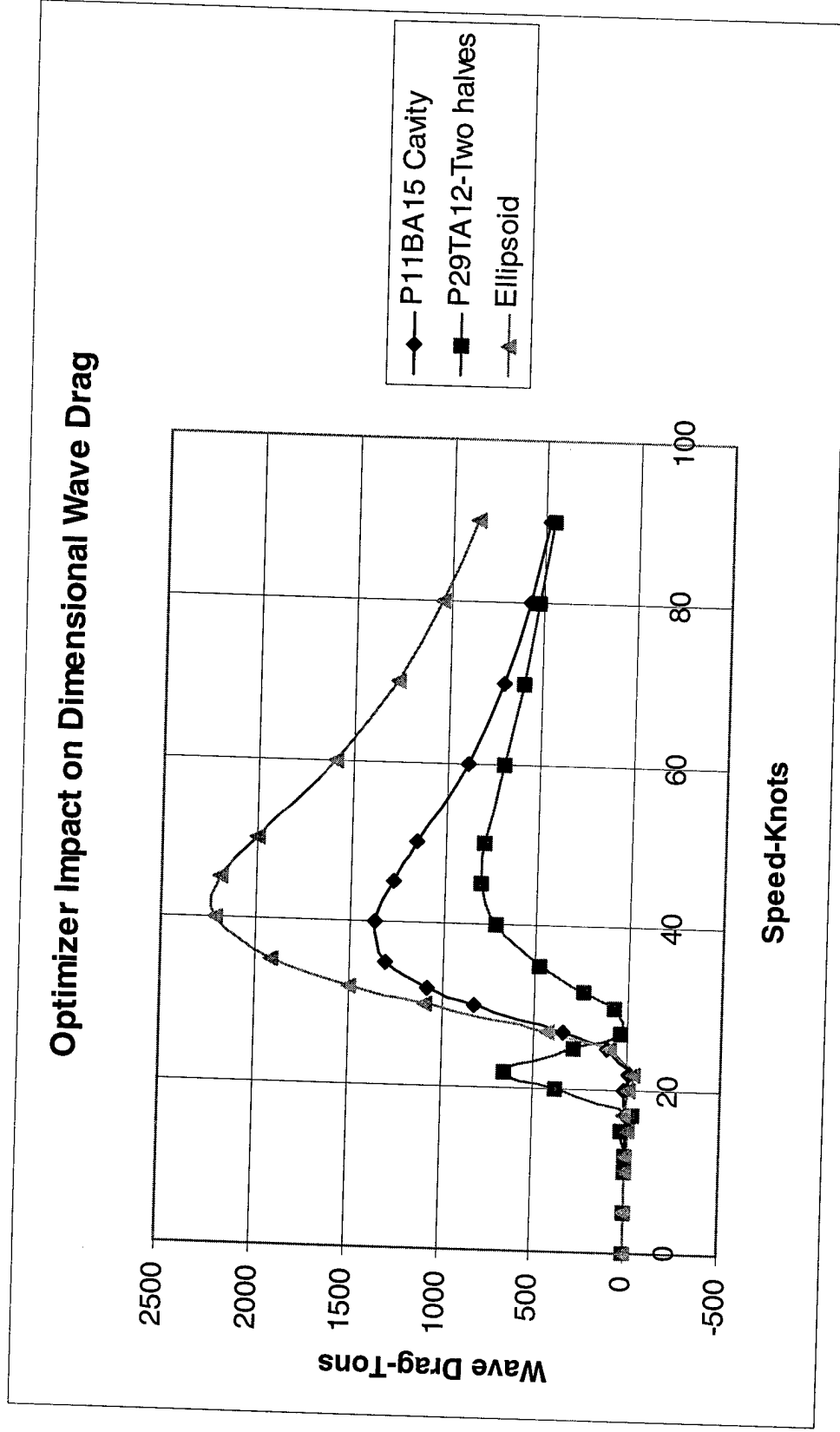
*Statistics and compilation received from A. Ellinthorpe

SWAMCH Body Design Comparison



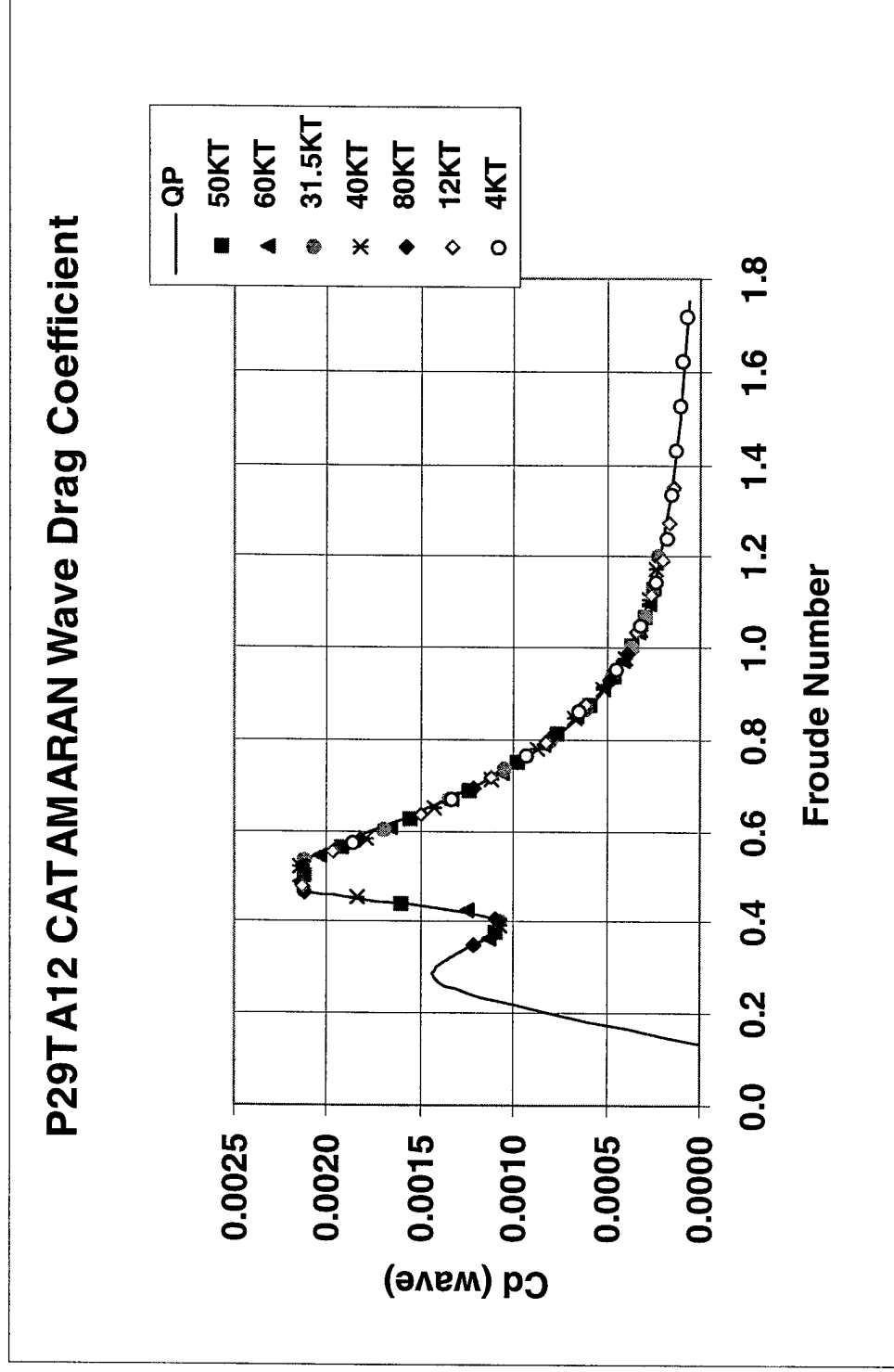
QUADPAN/POINTER results for the varied body design drags were calculated as a function of Froude Number and referenced to length2.**

SWAMCH Body Wave Drag Comparison



QUADPAN/POINTER results for the varied 12 KT body design wave drags.

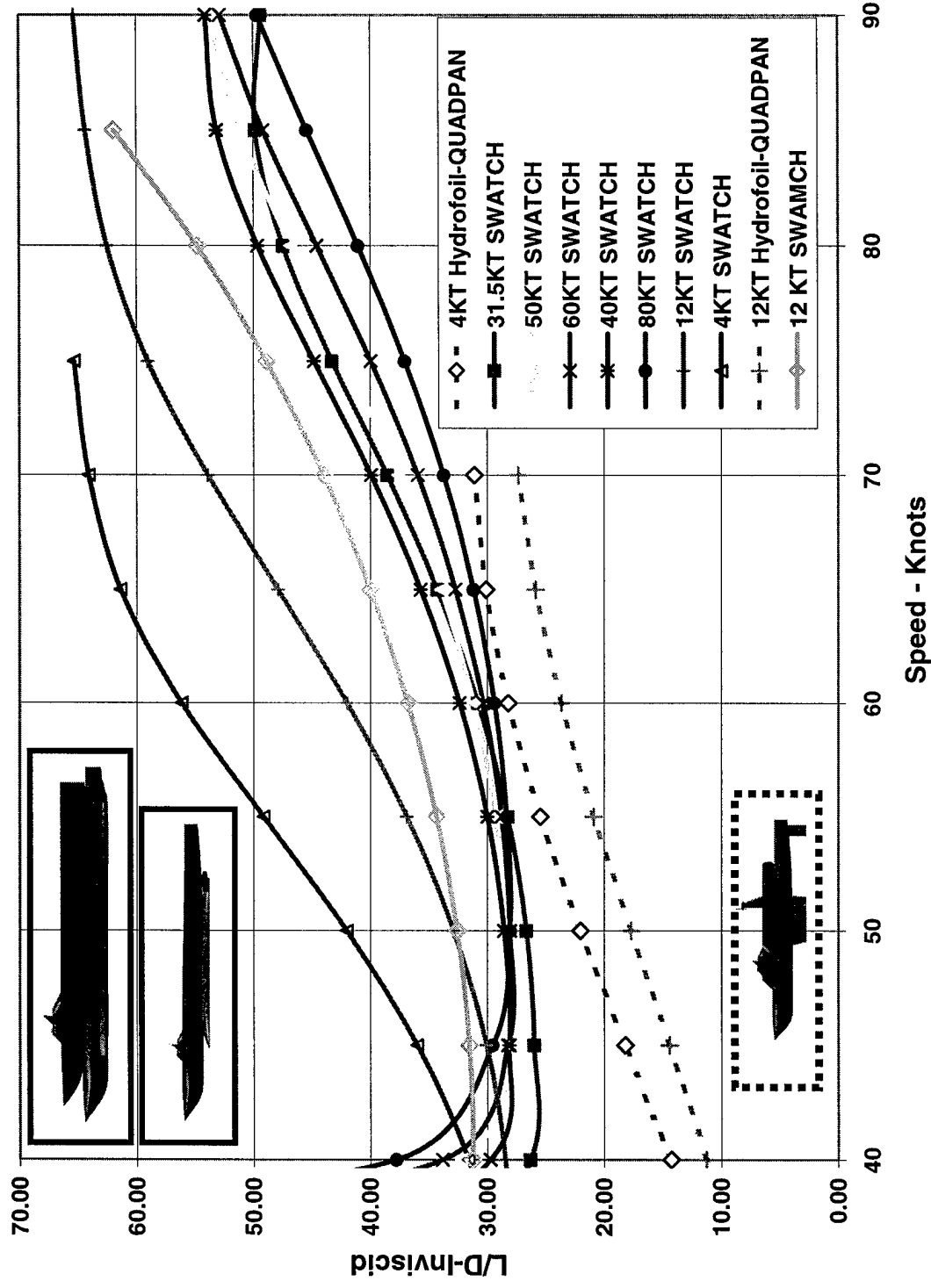
SWATCH Body Displacement Comparison



QUADPAN/POINTER results were curve fit and the varied displacement drags were calculated as a function of Froude Number and referenced to length2.**

Inviscid Hydrodynamic Efficiency – Varied Designs

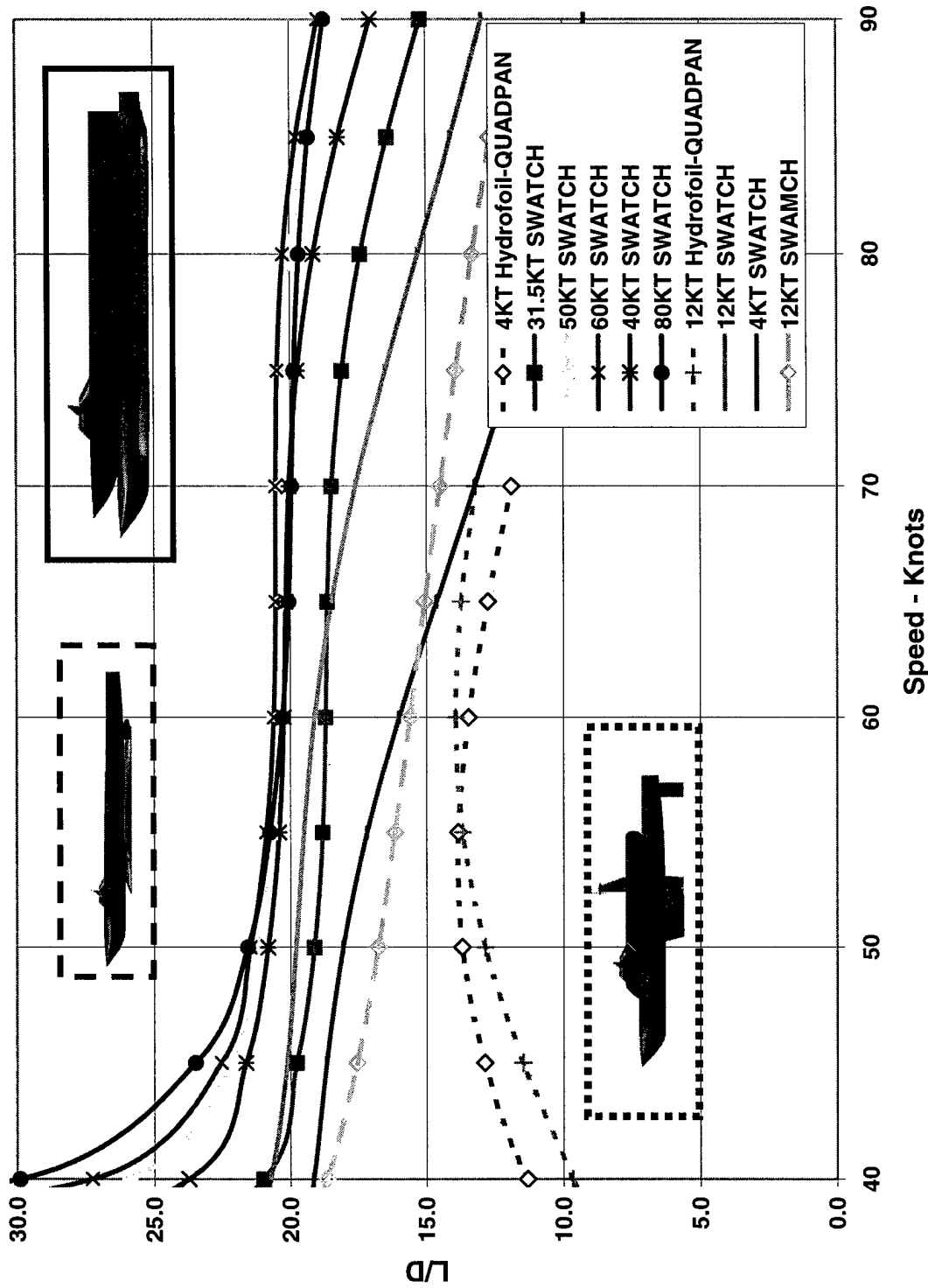
Ship Lift-to-Inviscid Drag Ratio



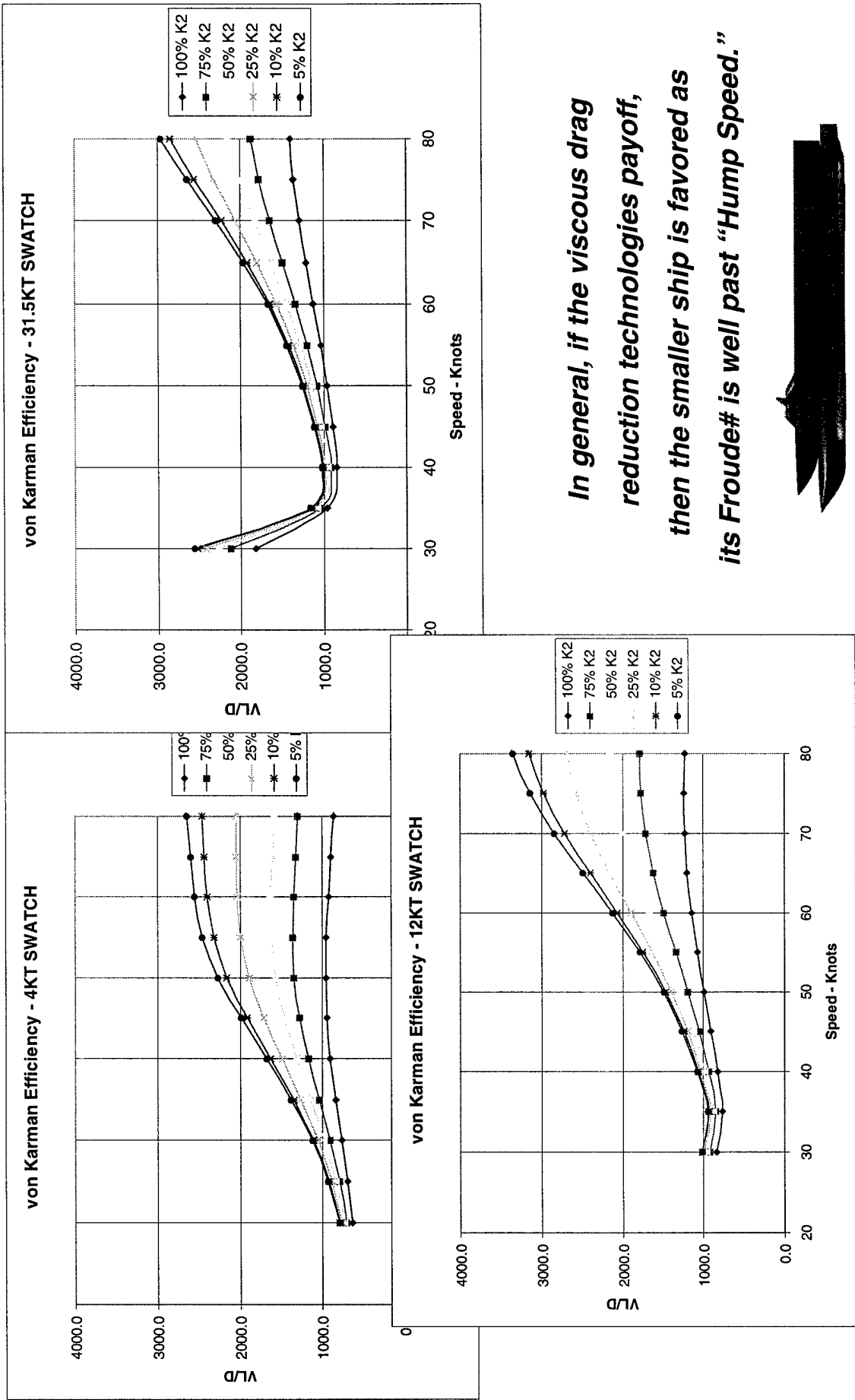
Hydrodynamic Efficiency – Varied Designs

Ship Lift-to-Drag Ratio

Full Skin Friction, 1.5% t/c SWATCH Struts, P29TA12 Bodies



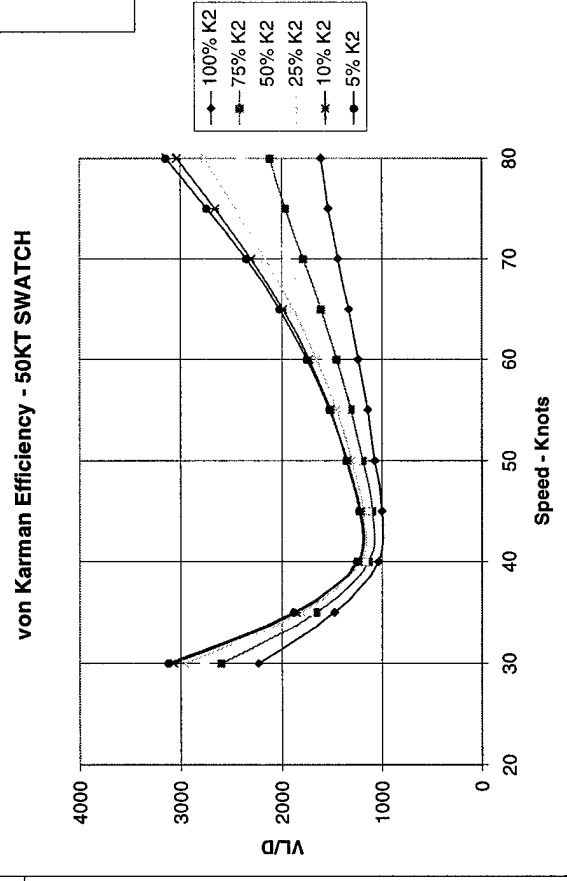
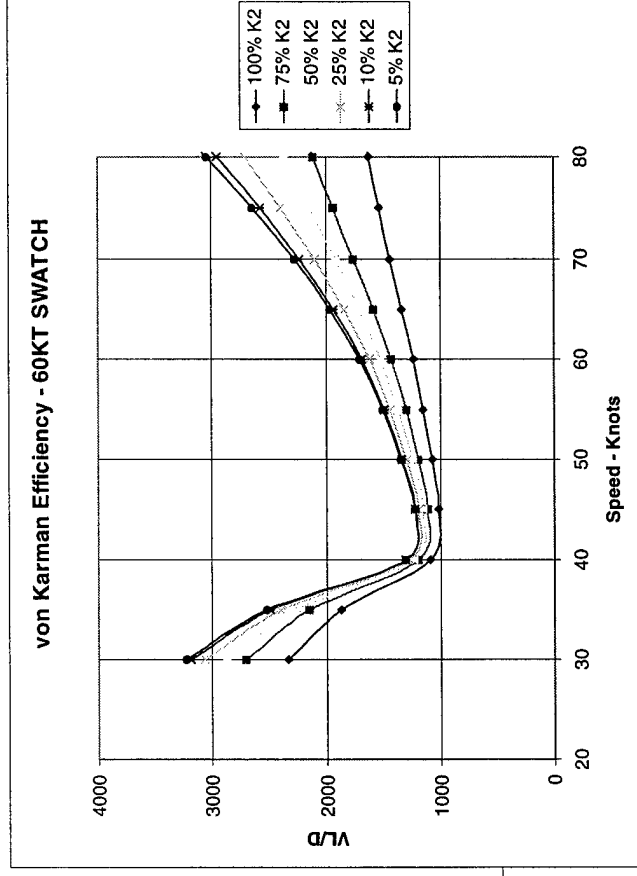
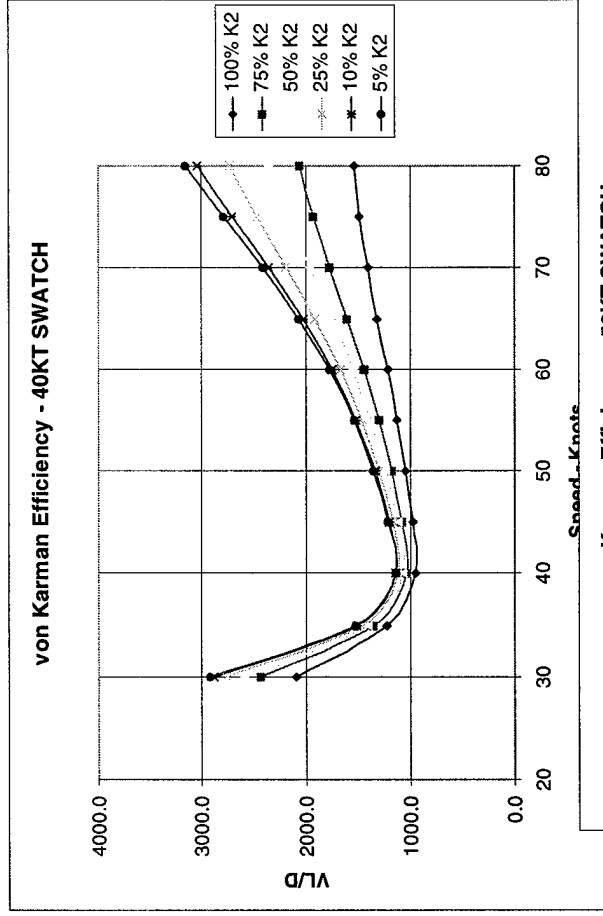
Karman Efficiency – 4KT,12KT & 31.5KT SWITCH



In general, if the viscous drag reduction technologies payoff, then the smaller ship is favored as its Froude# is well past "Hump Speed."

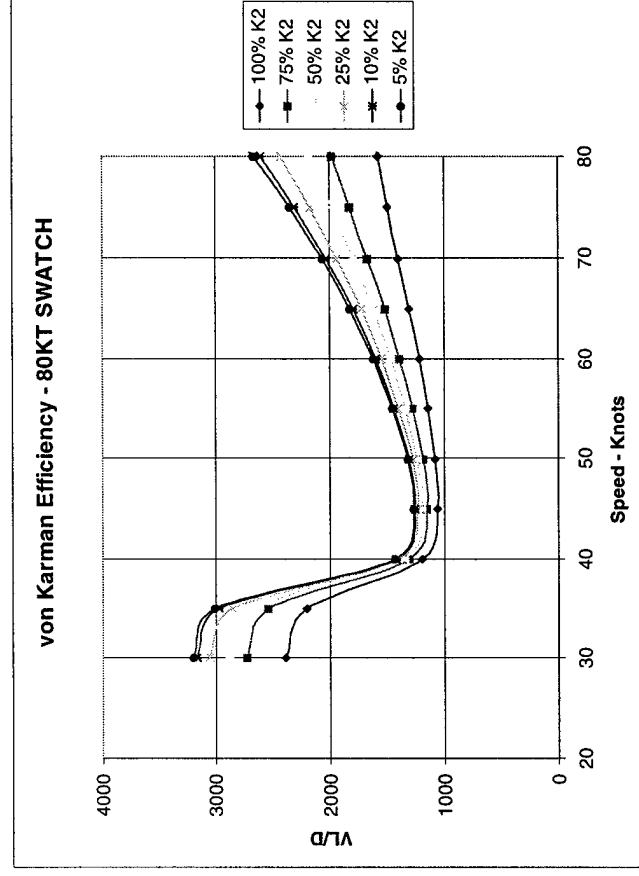
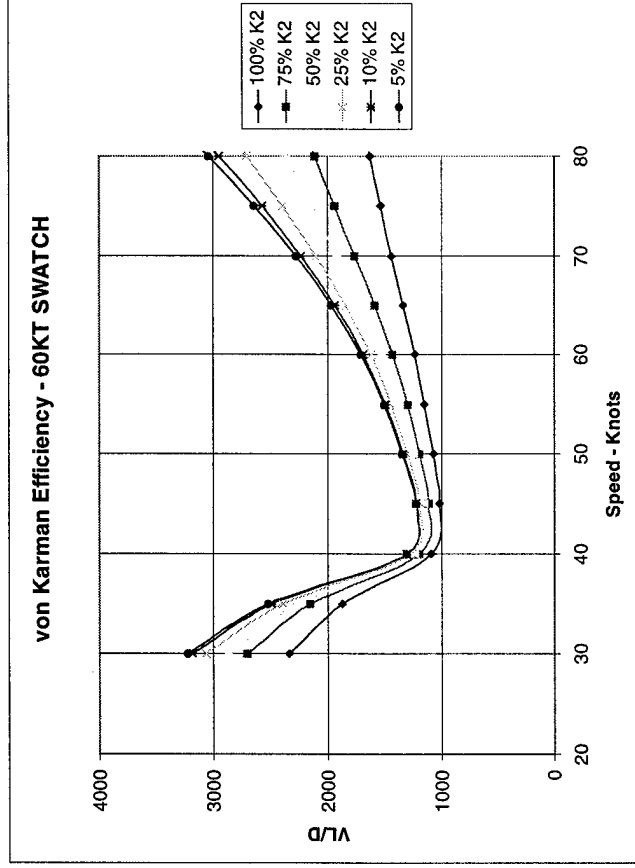


Karman Efficiency – 40KT,50KT & 60KT SWATCH



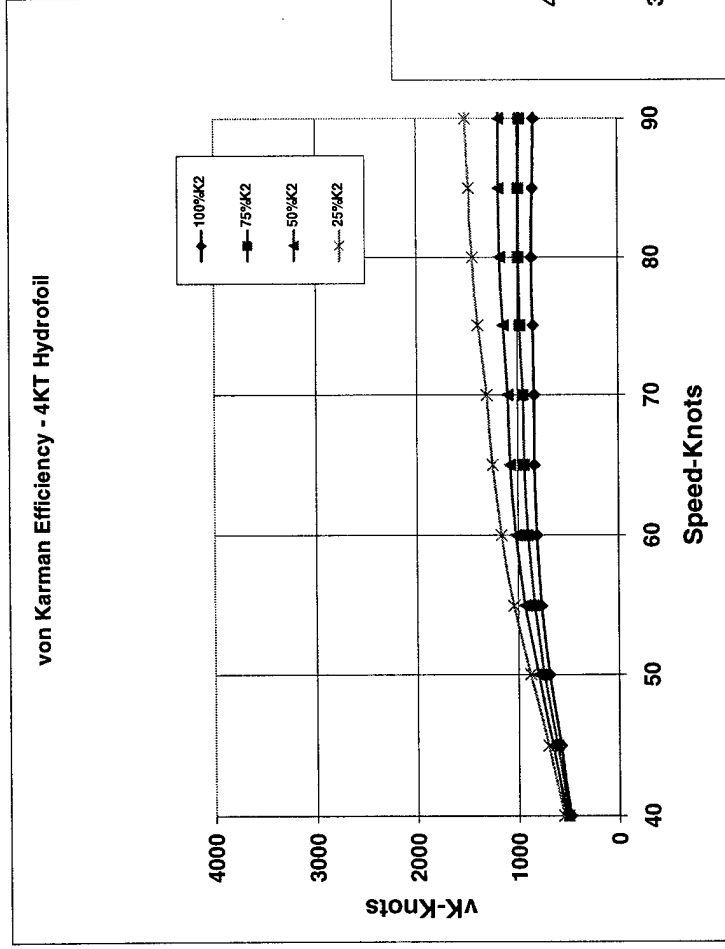
If viscous drag reduction technologies do not pan-out, the larger ship is favored as with its higher volumetric efficiency.

Karman Efficiency – 60KT & 80KT SWATCH

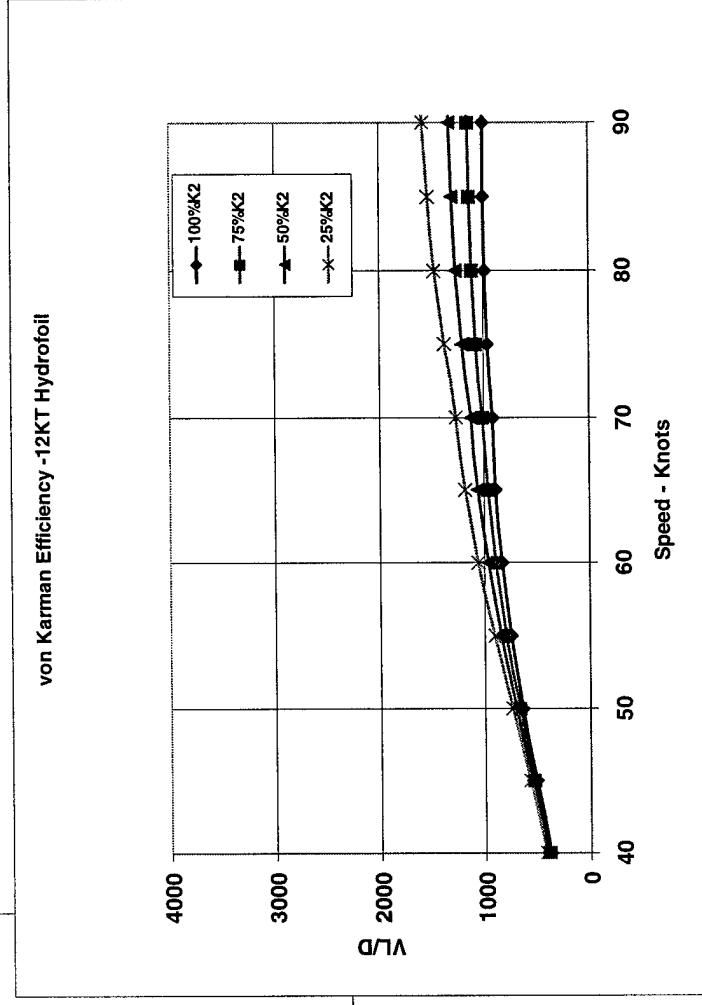


*If the ship size is pushed to 80KT, the
Wave drag becomes the limiting factor
Note that with the “Double Hump” Froude
number behavior – two efficient modes of
operation may be possible!*

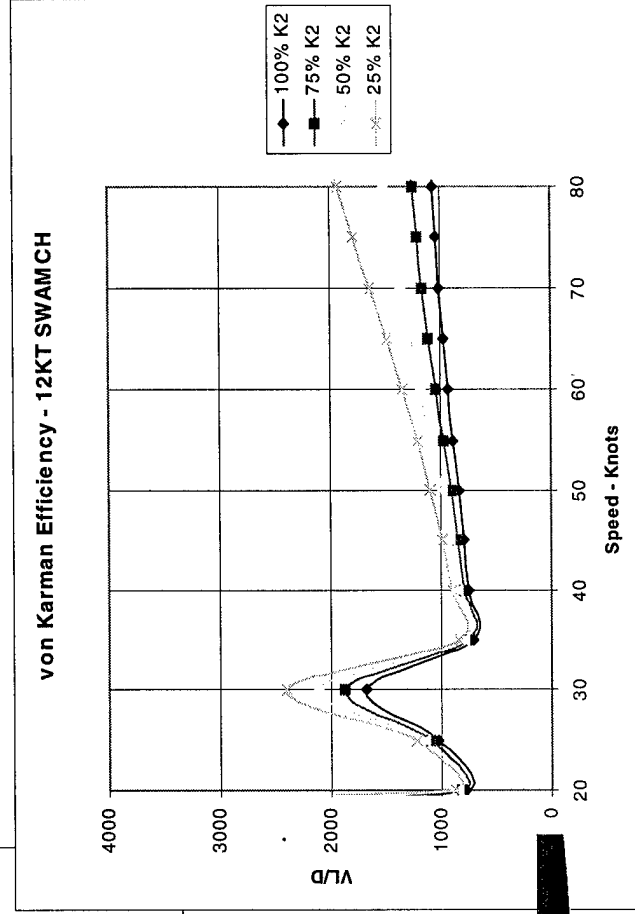
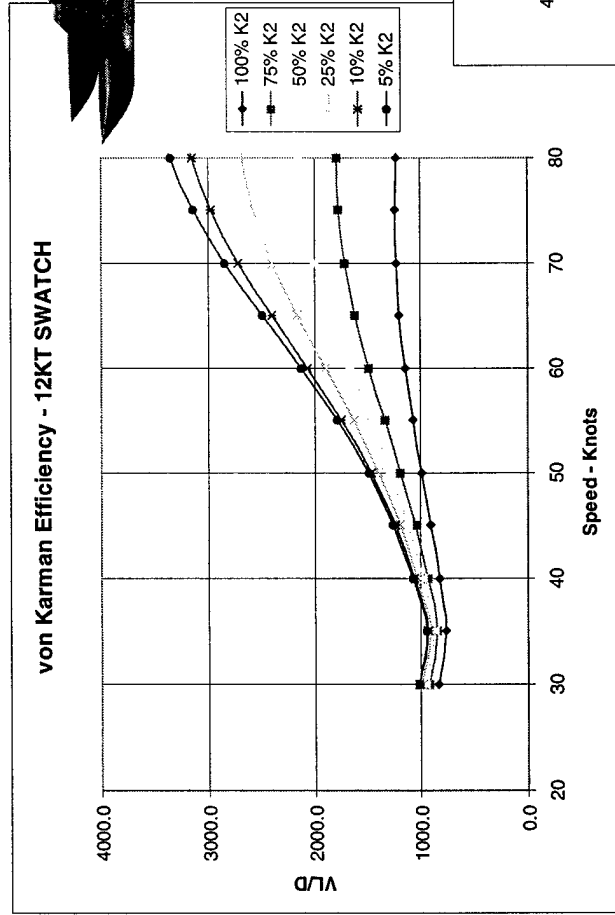
Karman Efficiency – 4KT and 12KT Hydrofoils



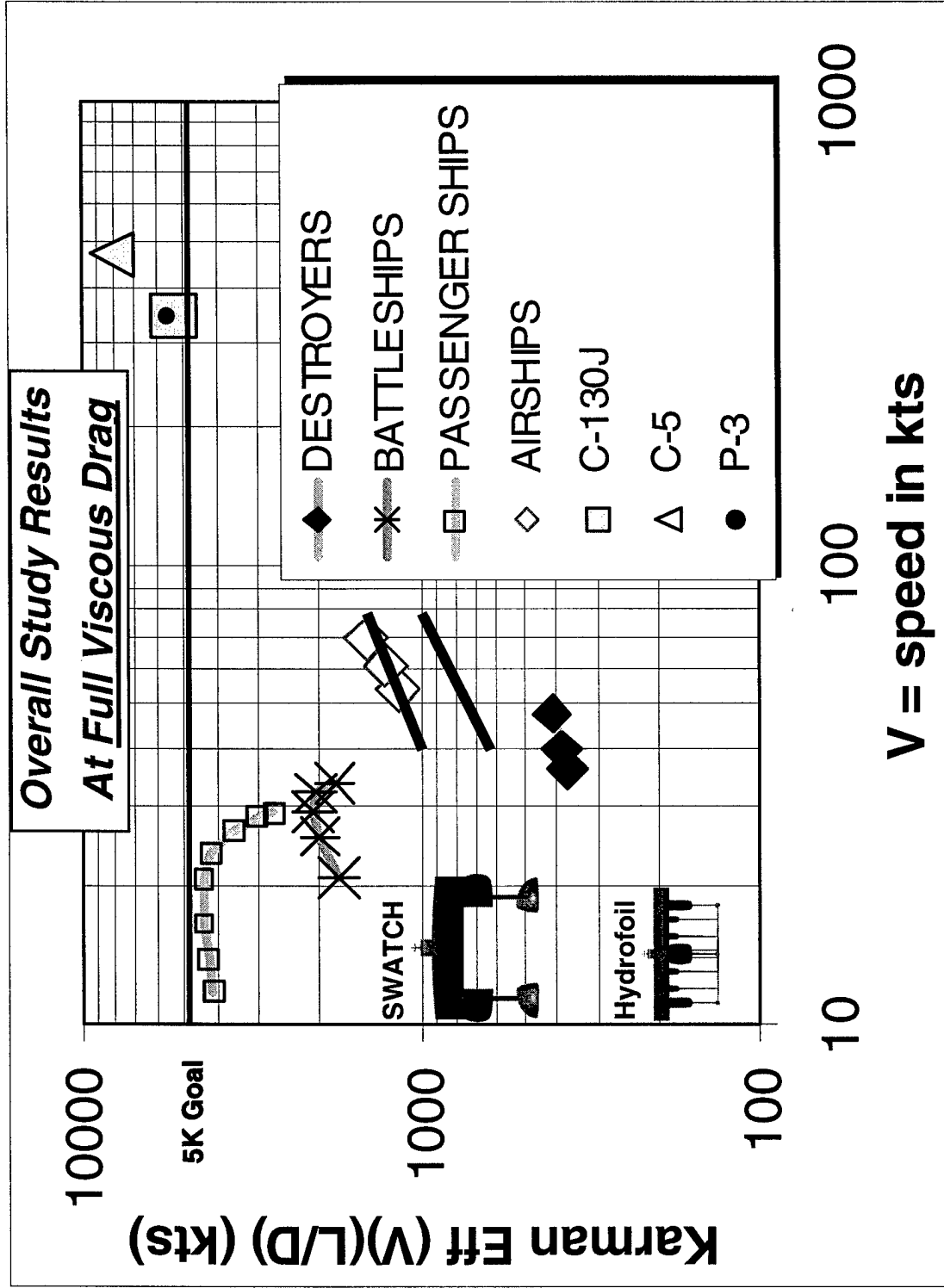
For the Hydrofoils at a fixed Wing Aspect Ratio, there is very little advantage of going to a larger vessel from a von Karman basis. Trim-related and spray drag are key limiters to higher performance.



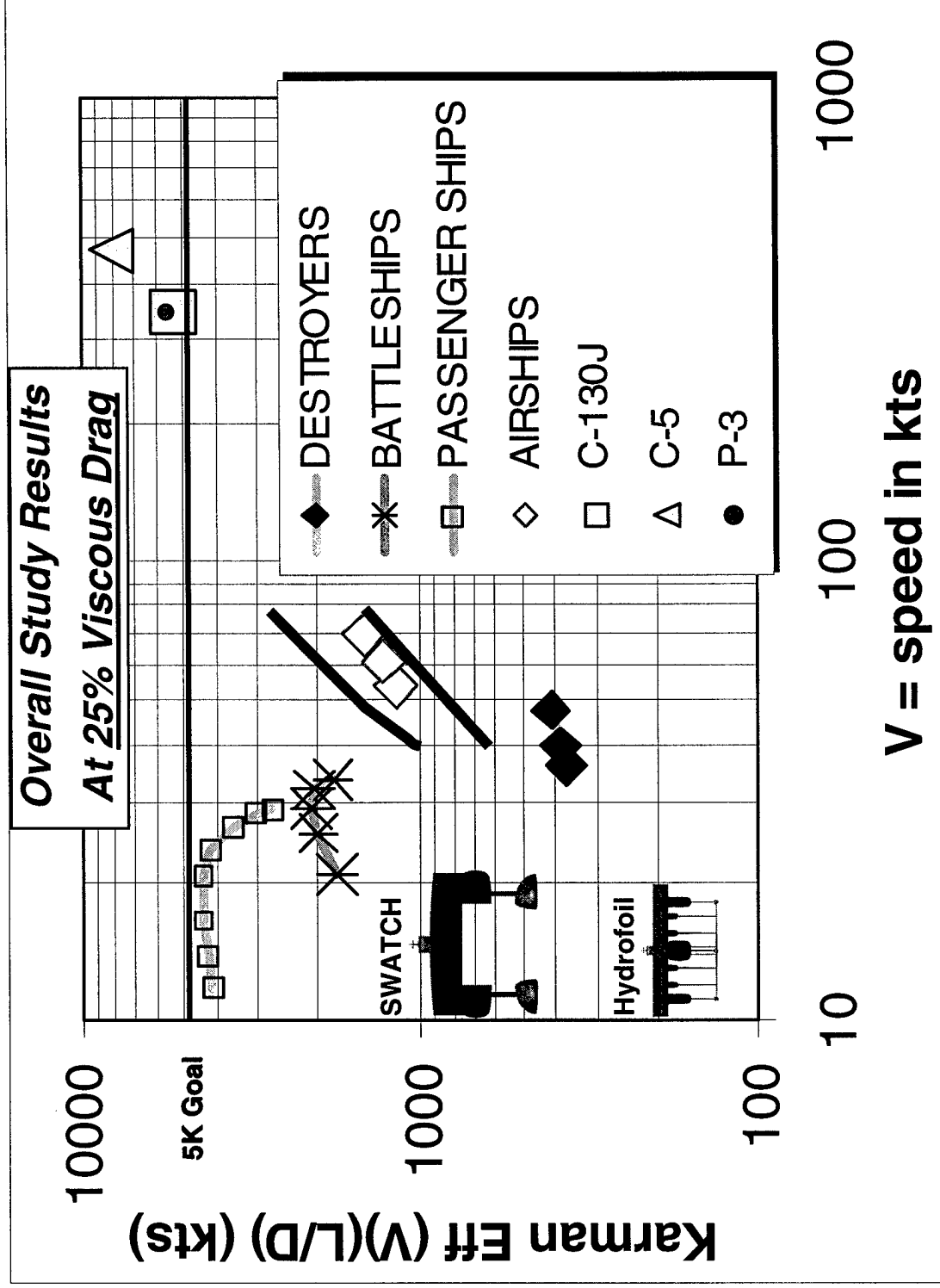
Karman Efficiency -12KT Cat and Mono SWA Cavities



Hydrodynamic Efficiency – Comparison

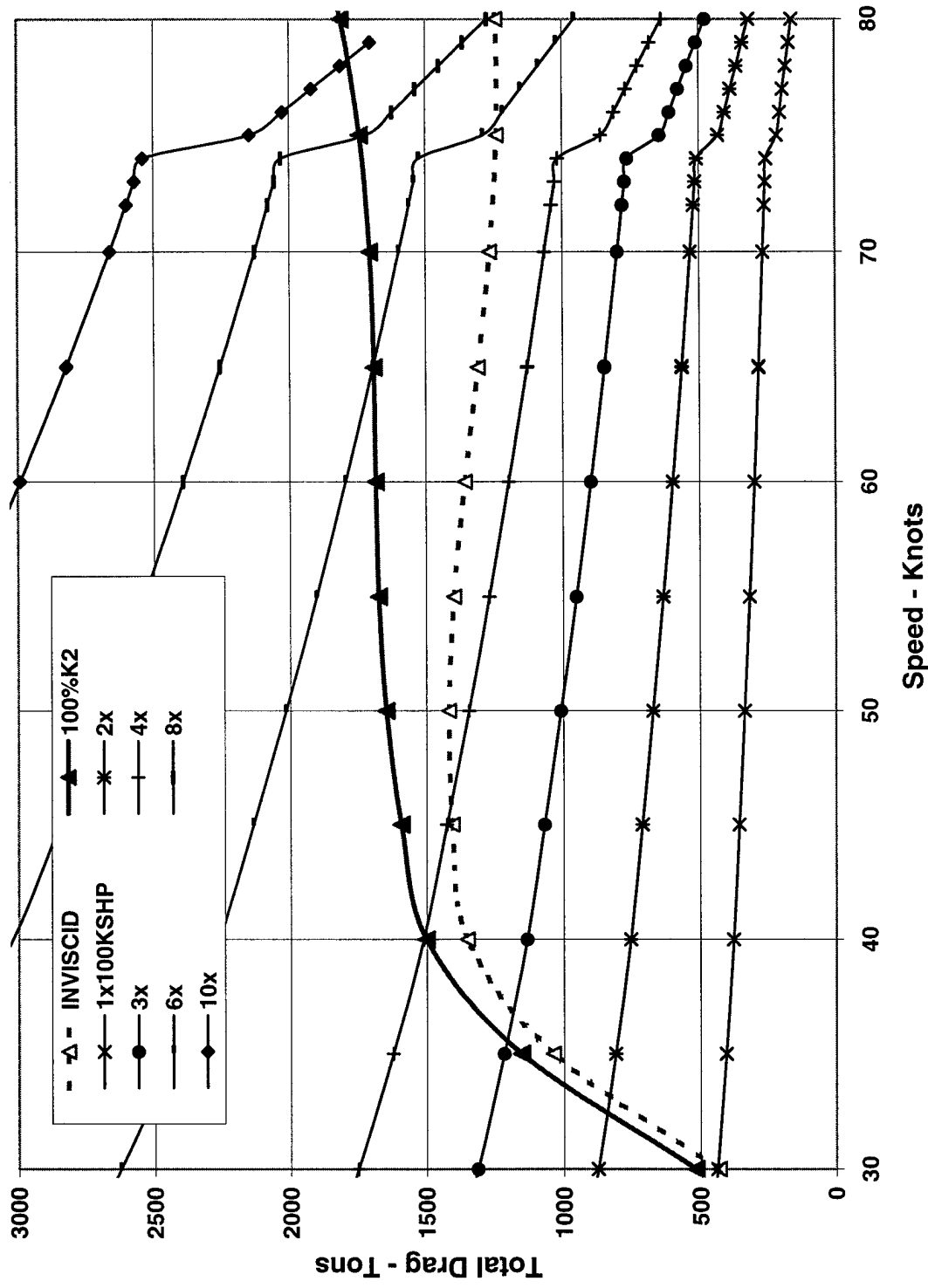


Hydrodynamic Efficiency – Comparison w/ VDR

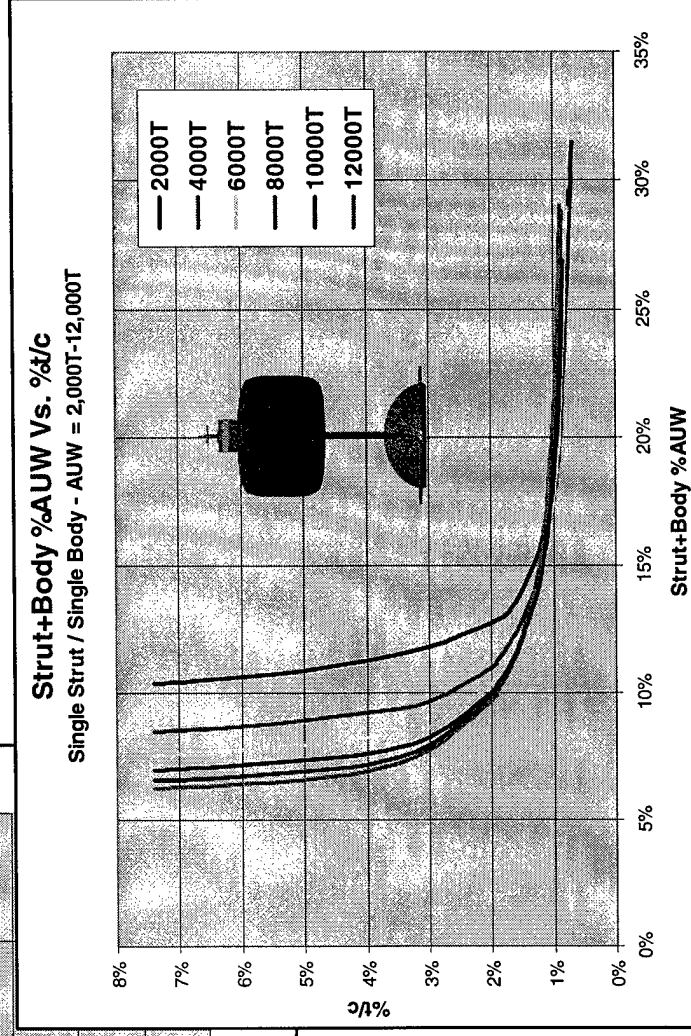
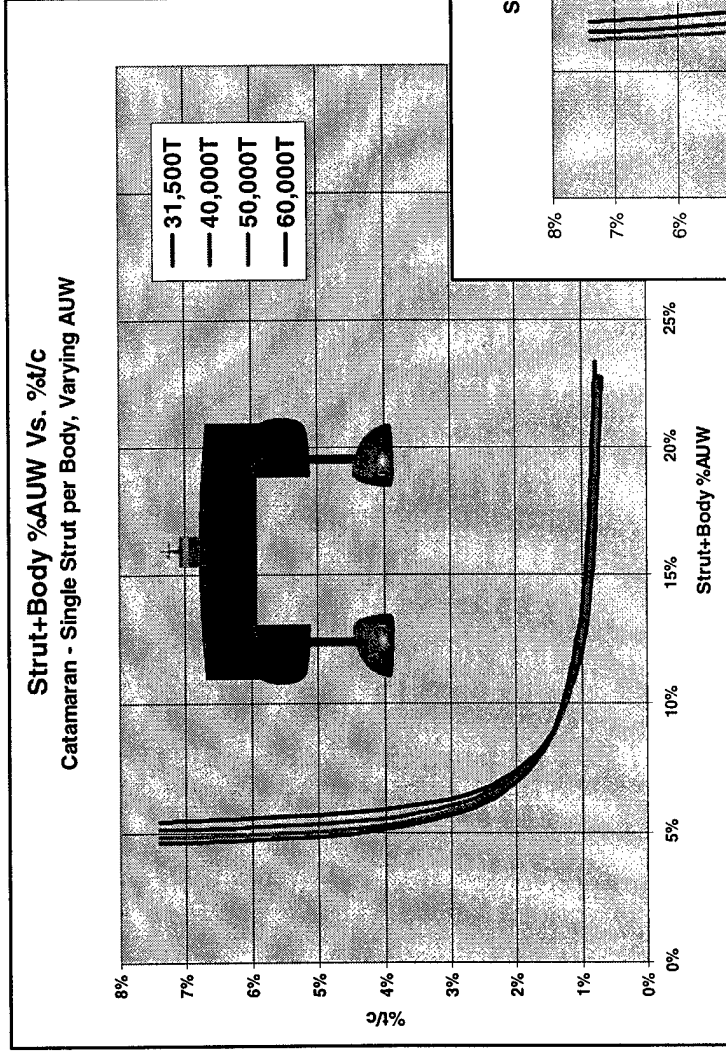


Thrust Required – 31.5KT SWATCH

31.5KT Ship Total Drag vs Available Thrust
P29TA12 Bodies, 1.5% t/c Struts

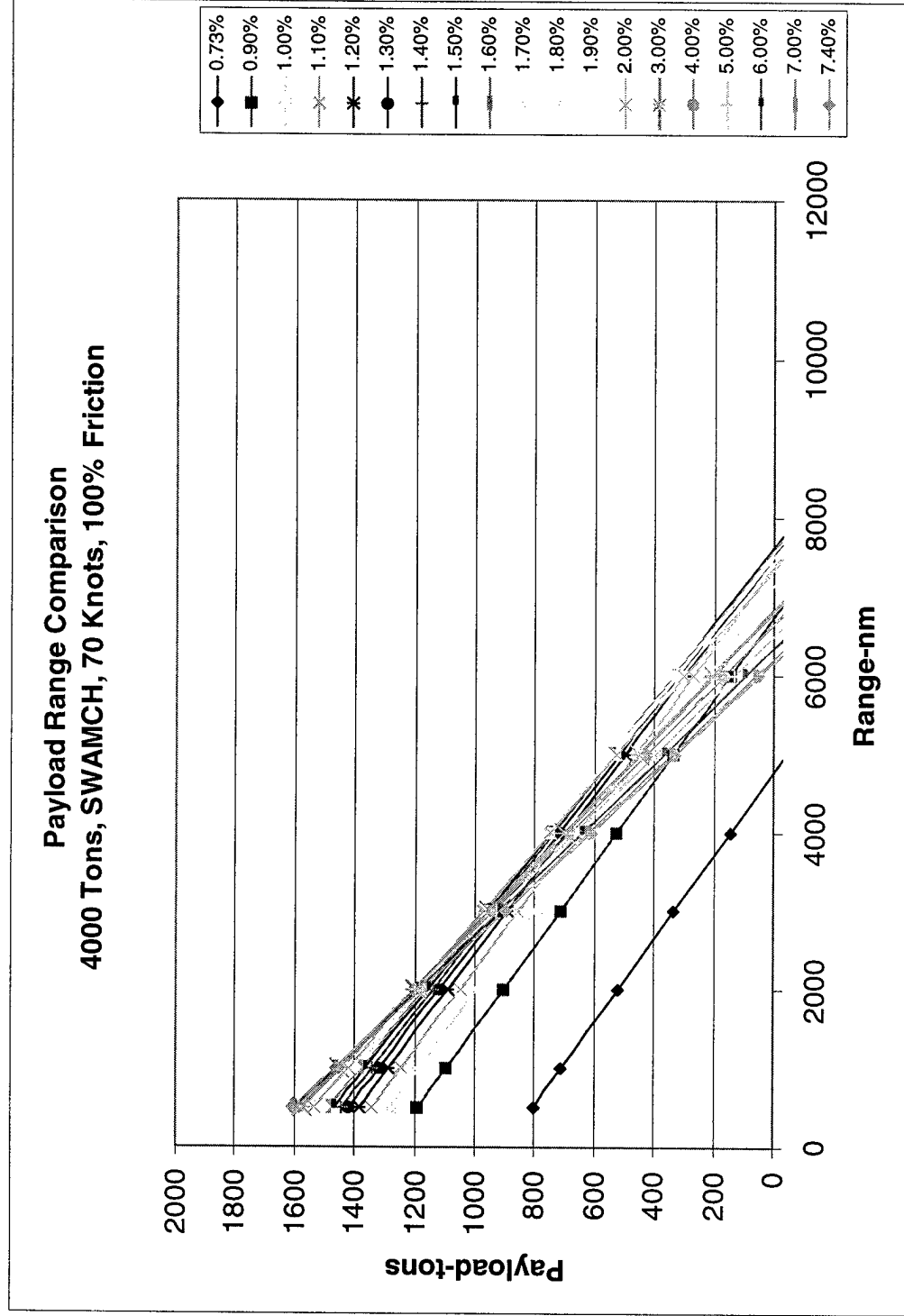


Structural Efficiency – Varied Designs



**Roll Control for the Single Hull
SWA Design Approach Imposes
Significant Impact on Sustention
System AUW Fraction ~5%**

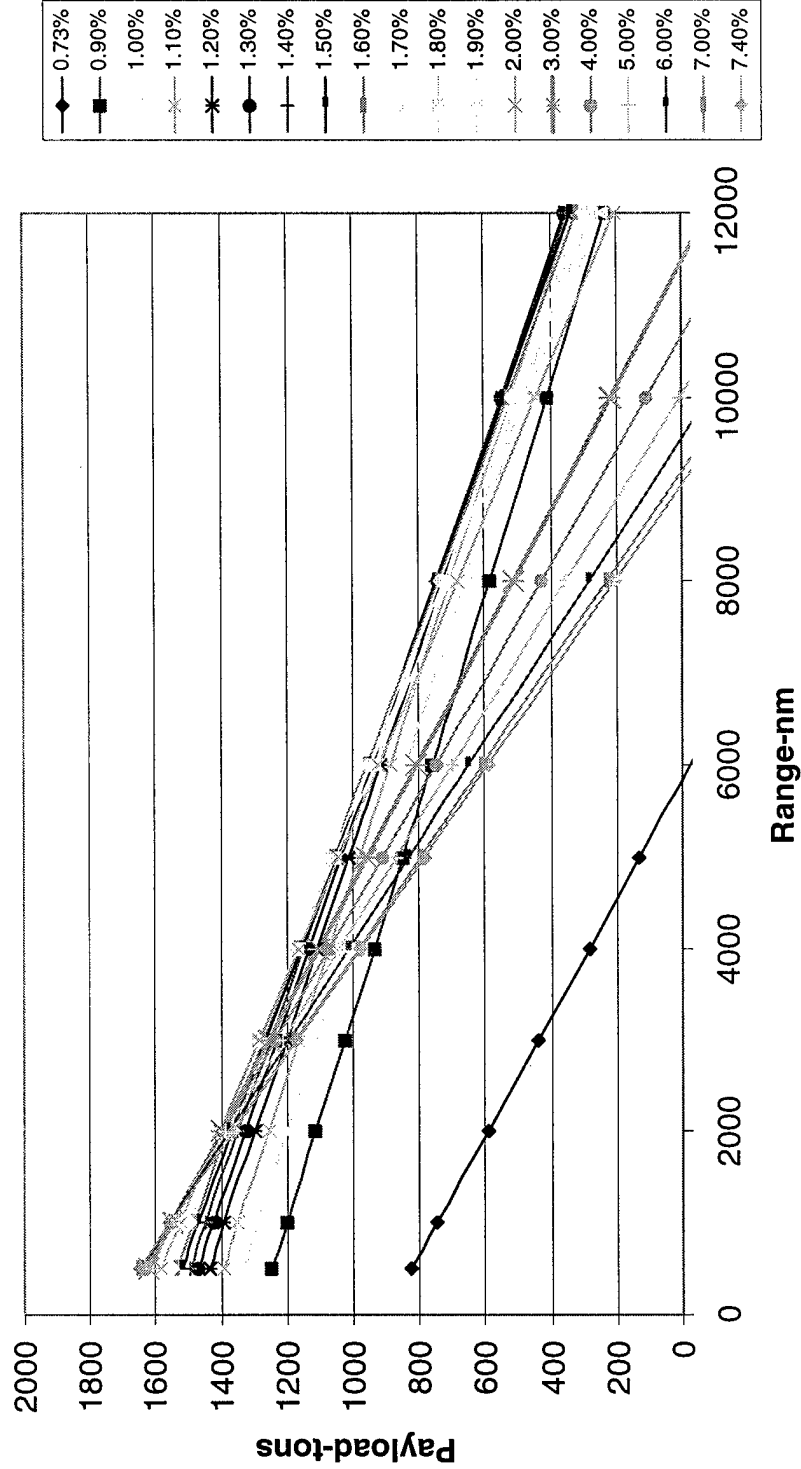
Strut Thickness - Payload Range Impact, 4KT



The %AUW of the sustention system was used to find to the Optimum Strut Thickness at a selected range and drag reduction level

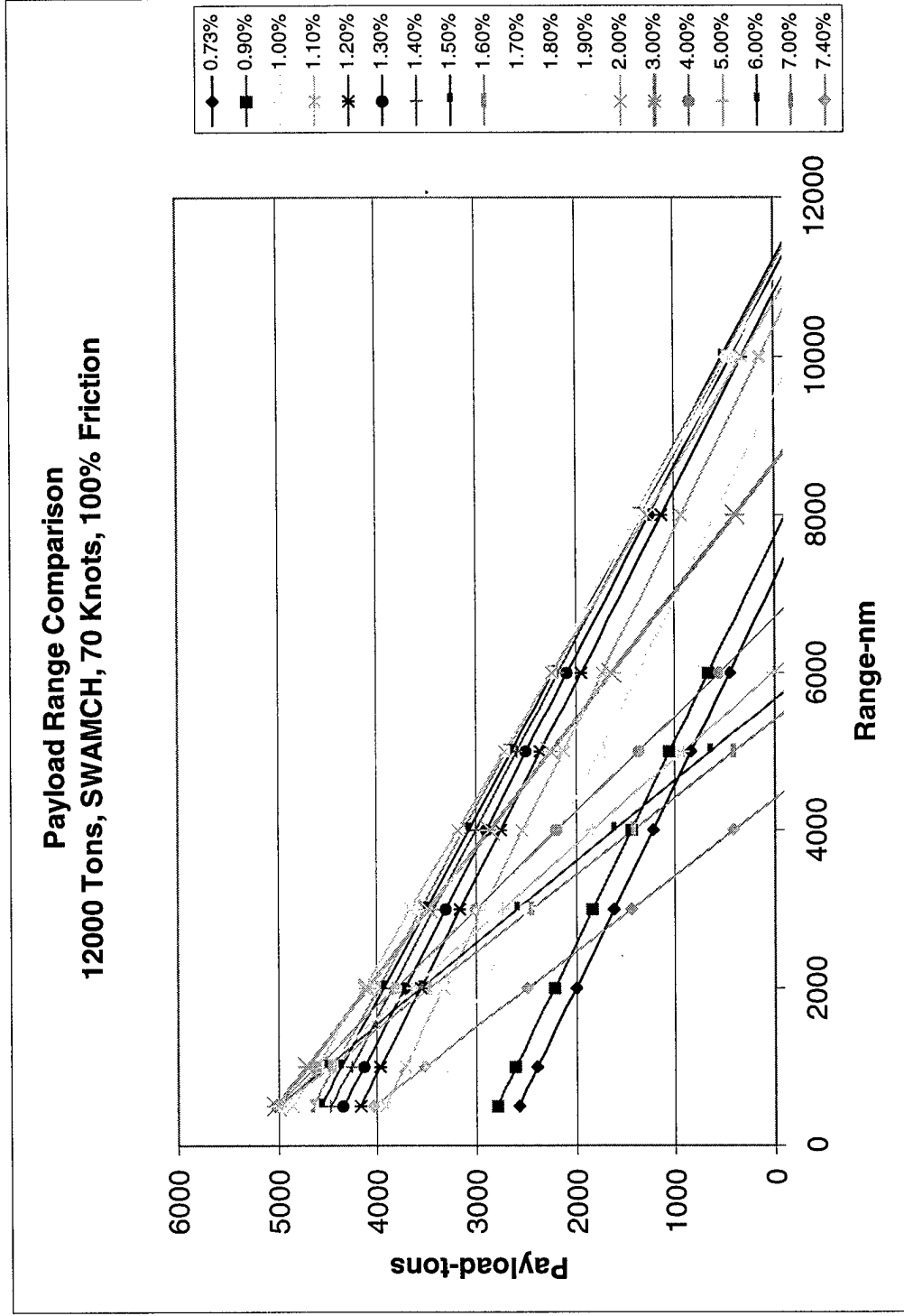
Strut Thickness - Payload Range Impact, 4KT

Payload Range Comparison
4000 Tons, SWAMCH, 70 Knots, 25% Friction



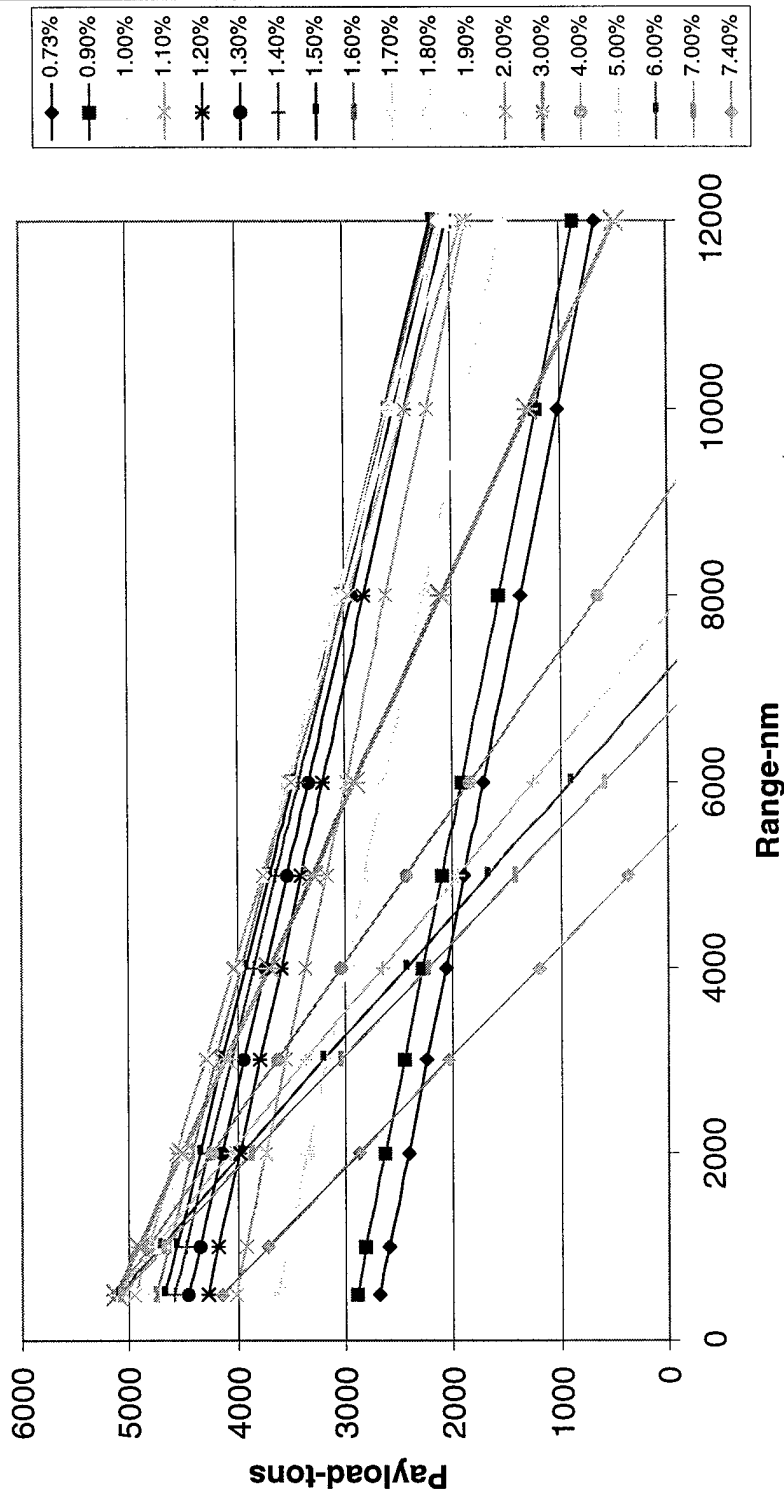
In most cases at 6000 nm the optimal strut thickness was in the range of 1.4% to 1.8% t/c.

Strut Thickness - Payload Range Impact, 12KT



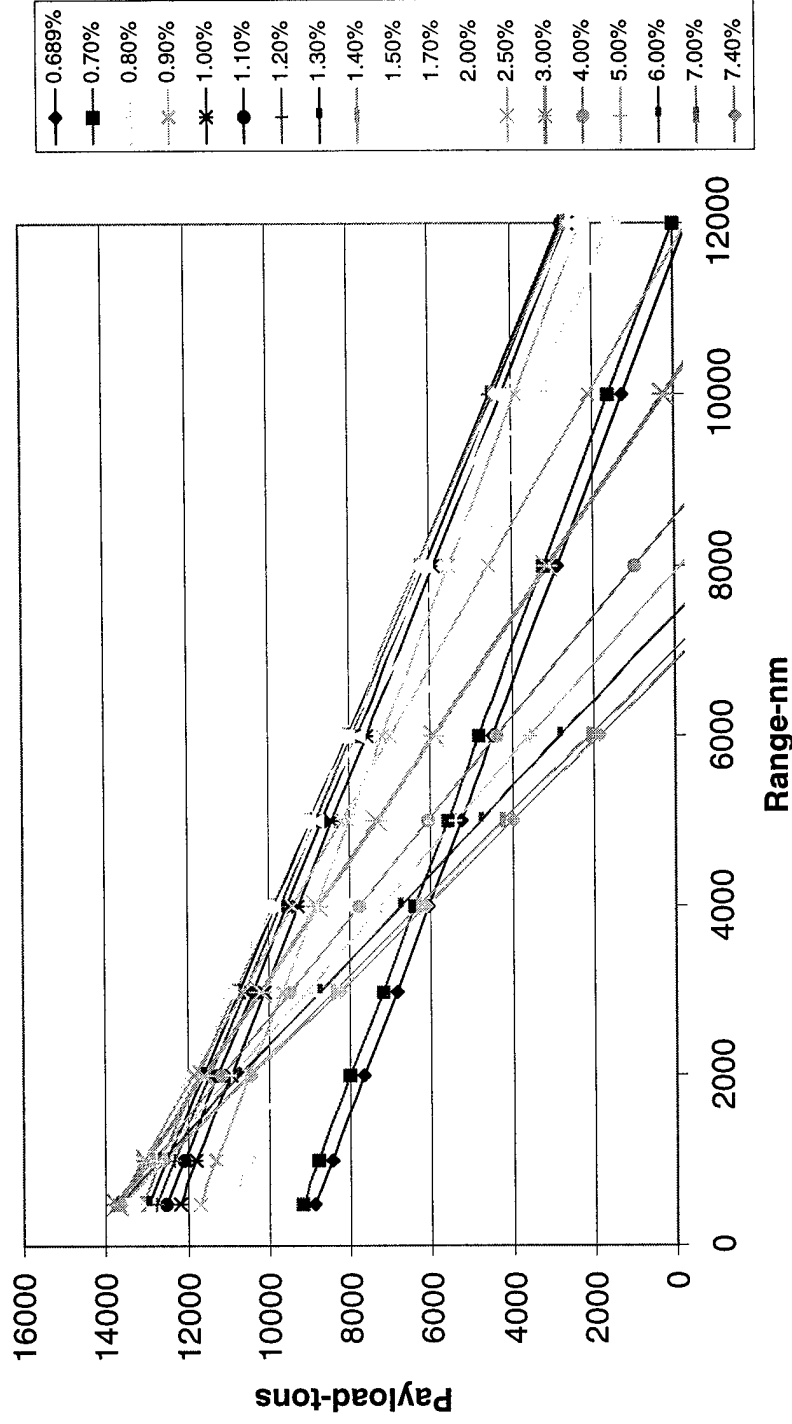
Strut Thickness - Payload Range Impact, 12KT

Payload Range Comparison
12000 Tons, SWAMCH, 70 Knots, 25% Friction



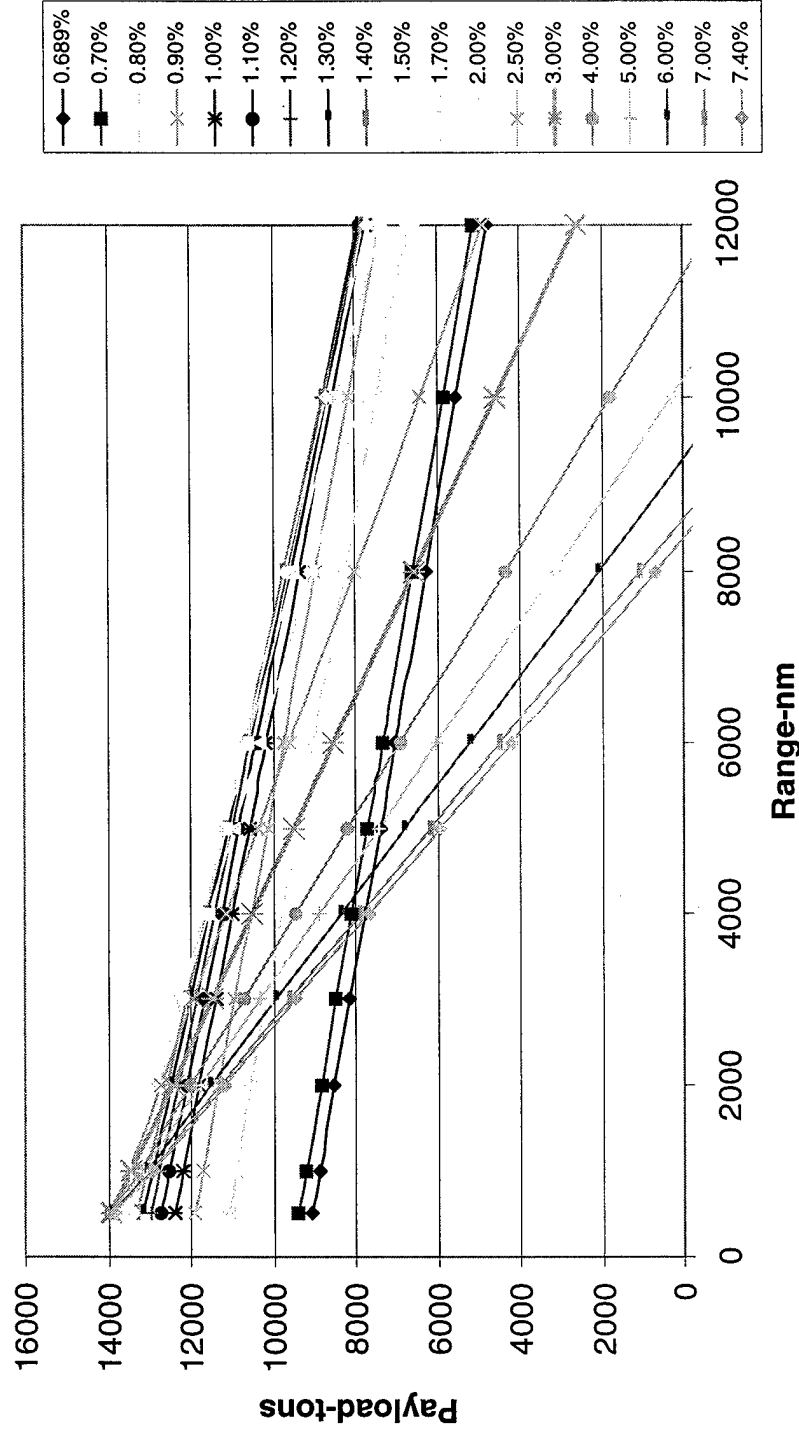
Strut Thickness - Payload Range Impact, 31.5KT

Payload Range Comparison with Strut Thickness
31500 Tons, SWATCH, 70 Knots, 100% Friction



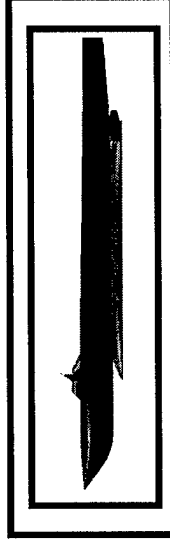
Strut Thickness - Payload Range Impact, 31.5KT

Payload Range Comparison with Strut Thickness
31500 Tons, SWATCH, 70 Knots, 25% Friction



Comparison of the Mission Sized Struts

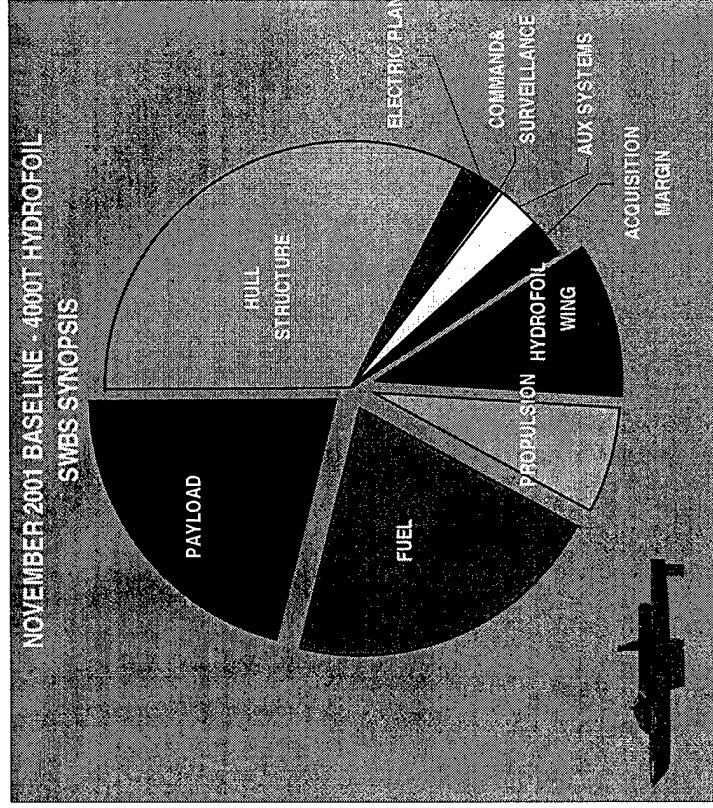
Ship Type	Ship Displ.	Design Speed	Selected Range	VDR K2	Strut t/c for Best P-R	Strut/Body % AUW
Hydrofoil	4KT	70	6000	100%	7.4%	10.0
SWAMCH	4KT	70	6000	100%	1.6%	17.6
SWAMCH	4KT	70	6000	25%	1.5%	19.9
SWAMCH	12KT	70	6000	100%	1.8%	15.0
SWAMCH	12KT	70	6000	25%	1.7%	16.1
SWATCH	31.5KT	70	6000	100%	1.5%	8.7
SWATCH	31.5KT	70	6000	25%	1.4%	9.1



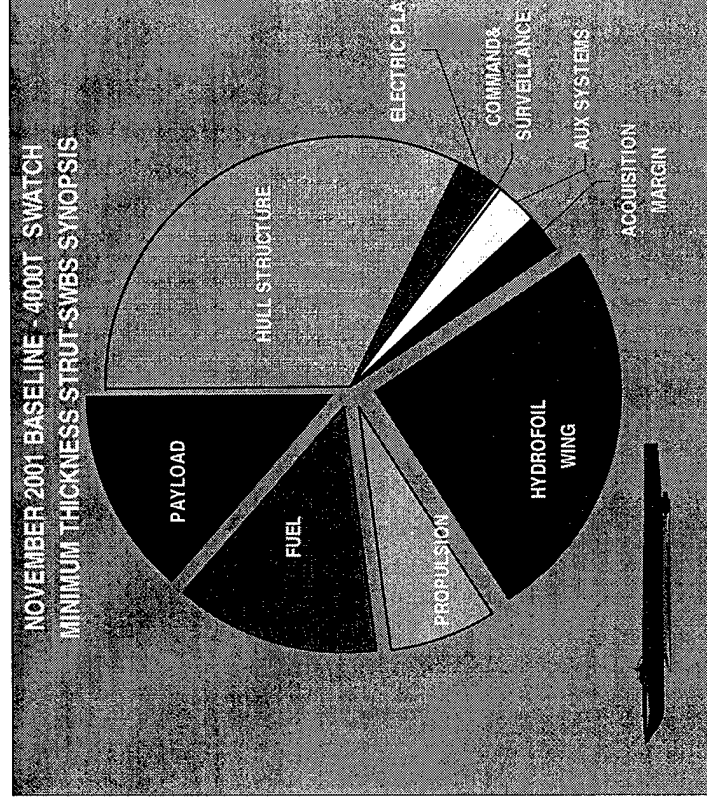
The sizing study showed that the optimum strut size for the 6000 nm mission varied slightly as the amount of viscous drag reduction was varied. Furthermore, the SWATCH (catamaran) had an additional weight advantage with the roll control system removed.

SWBS Comparison - Summary

4000T Hydrofoil





4000T SWAMCH Minimum Thickness Strut



The fraction of the All Up Weight (AUW) is higher for the SWA at this point without re-weighing the hull structure to account for any differences in structural layout.....



SWBS Comparison – Top Level Breakout

SWBS CATEGORY		
	MIN WEIGHT HYDROFOIL	MIN THICK SWAMCH
HULL STRUCTURE	1,297.39	1,297.39
ELECTRIC PLANT	115.26	115.26
COMMAND & SURVEILLANCE	12.86	12.86
AUXILIARY SYSTEMS	104.00	104.00
ACQUISITION MARGINS	108	108
SUSTENTION	400	992.00
PROPULSION PLANT	279.00	279.00
FUEL	842	546
PAYLOAD	842	546
AUW - TOTAL	4,000.50	4,000.50
LIGHTSHIP	2,316.50	2,908.50
		2,240.50

However, if the Minimum Weight Strut Support System is used the

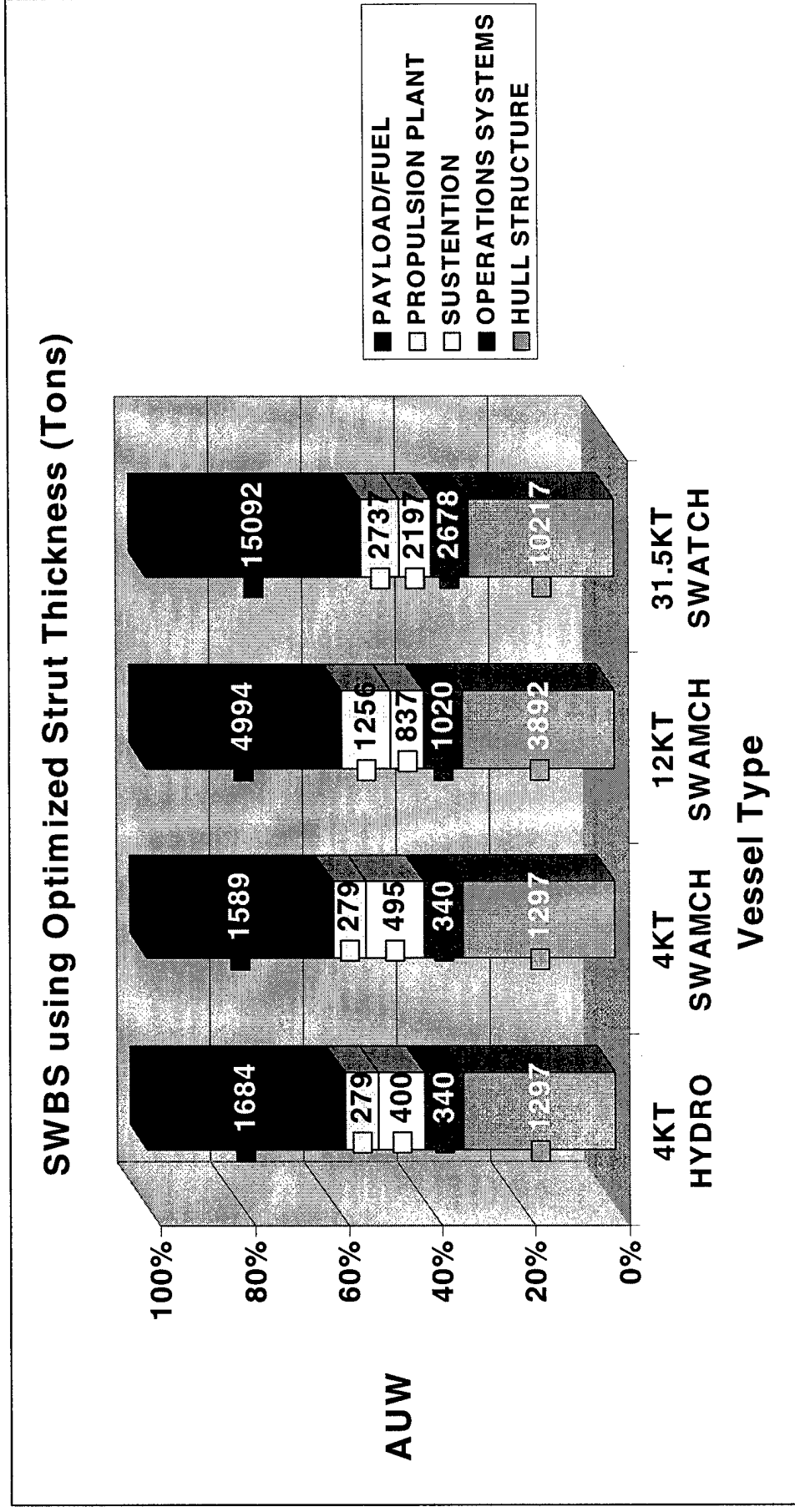
AUW changes considerably. There is a clear need to re-constrain the problem and re-run the optimization process for the strut design based on minimum integrated impact.

4KT SWBS Comparison – Revised Assessment

		
HULL STRUCTURE	MIN WEIGHT HYDRO	MIN THICK SWAMCH
OPERATIONS SYSTEMS	1297 340	1297 340
SUSTENTION	400	992
PROPULSION PLANT	279	279
PAYLOAD/FUEL	1684	1092
LIGHTSHIP	2317	2909
		1.6% t/c Strut SWAMCH
		1297 340 495
		279 1744 1589
		2256 2412

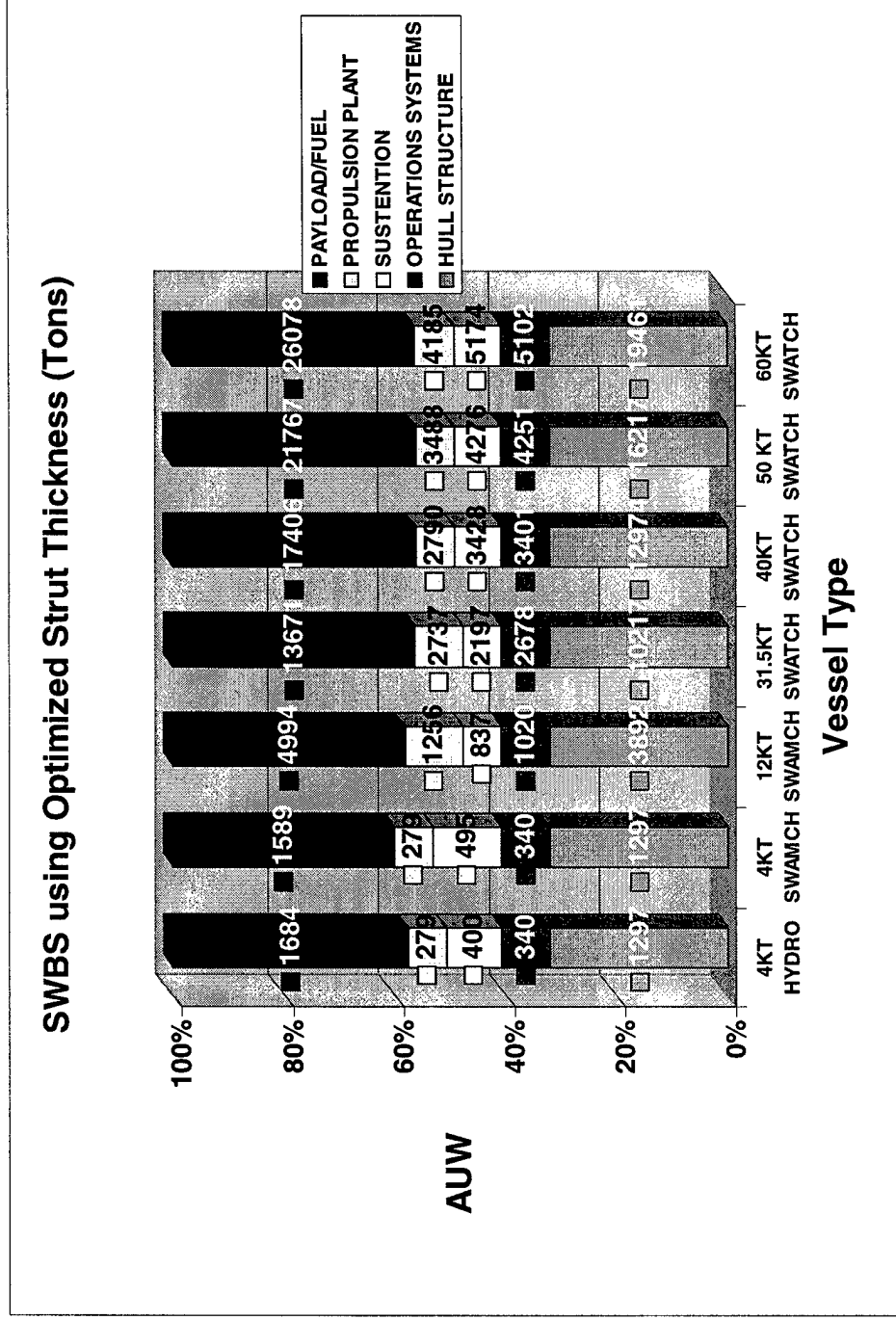
In the last quarter it was suggested that a optimal strut may depend on payload range and speed. The sizing study showed that the optimum strut size for the 4000 ton SWAMH was a 1.6% t/c support system for a full drag condition at 6000nm.

SWBS Comparison – CSC-based Assessment



CSC-based SWBS values were used and linearly scaled for the above water structure. Payload/Fuel and the Sustention mass properties were a fallout of the design synthesis process

SWBS Comparison – CSC-based Assessment



CSC-based SWBS values were used and linearly scaled for the above water structure. Payload/Fuel and the Sustention mass properties were a fallout of the design synthesis process

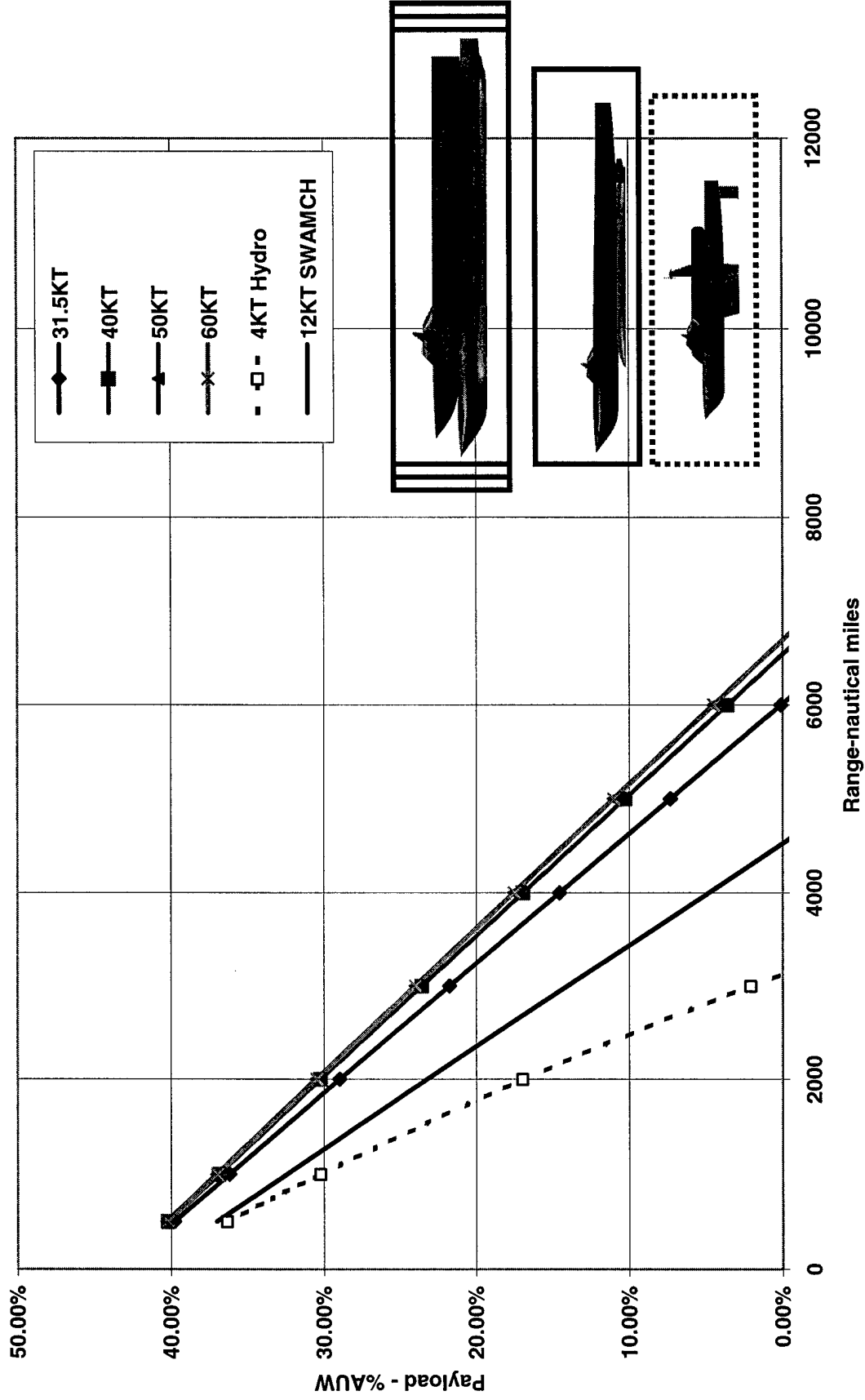
Design Comparison –Assessment in Tons

	4KT HYDRO	4KT SWAMCH	12KT SWAMCH	31.5KT SWATCH	40KT SWATCH	50 KT SWATCH	60KT SWATCH
HULL STRUCTURE	1297	1297	3892	10217	12974	16217	19461
OPERATIONS SYSTEMS	340	340	1020	2678	3401	4251	5102
SUSTENTION	400	495	837	2197	3428	4276	5174
PROPULSION PLANT	279	279	1256	2737	2790	3488	4185
PAYLOAD/FUEL	1684	1589	4994	13671	17406	21767	26078

CSC--based SWBS values were used and linearly scaled for the above water structure. Payload/Fuel and the Sustention mass properties were a fallout of the design synthesis process

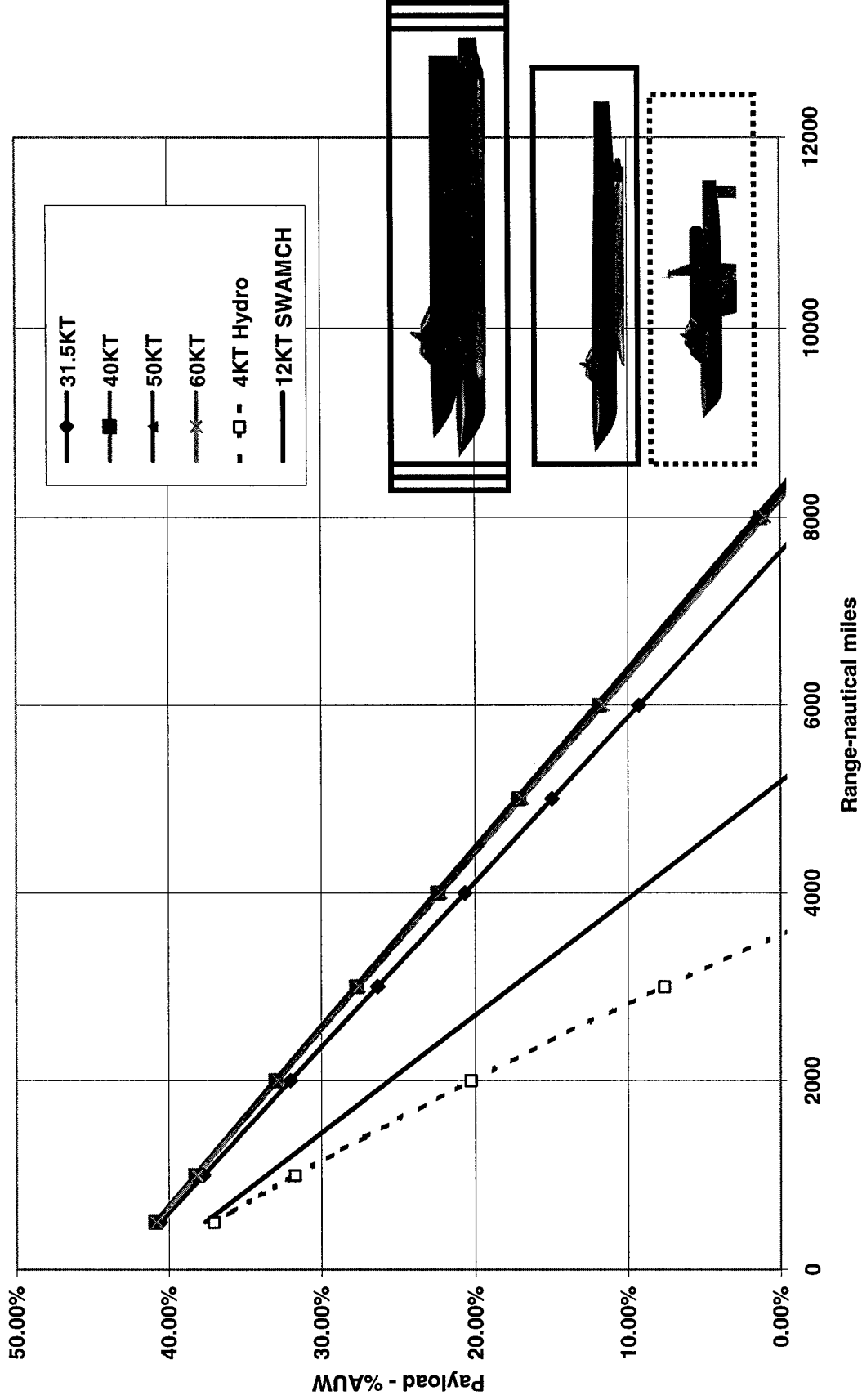
SWAxCH vs. Hydrofoil Sizing Comparisons

Payload vs. Range for SWATCH Designs - 100%K2 (Full Viscous Drag)
 P29TA12 Cavity Bodies, 1.5% t/c Struts, w/ Interference Effects, 1.4 JVR Pumps



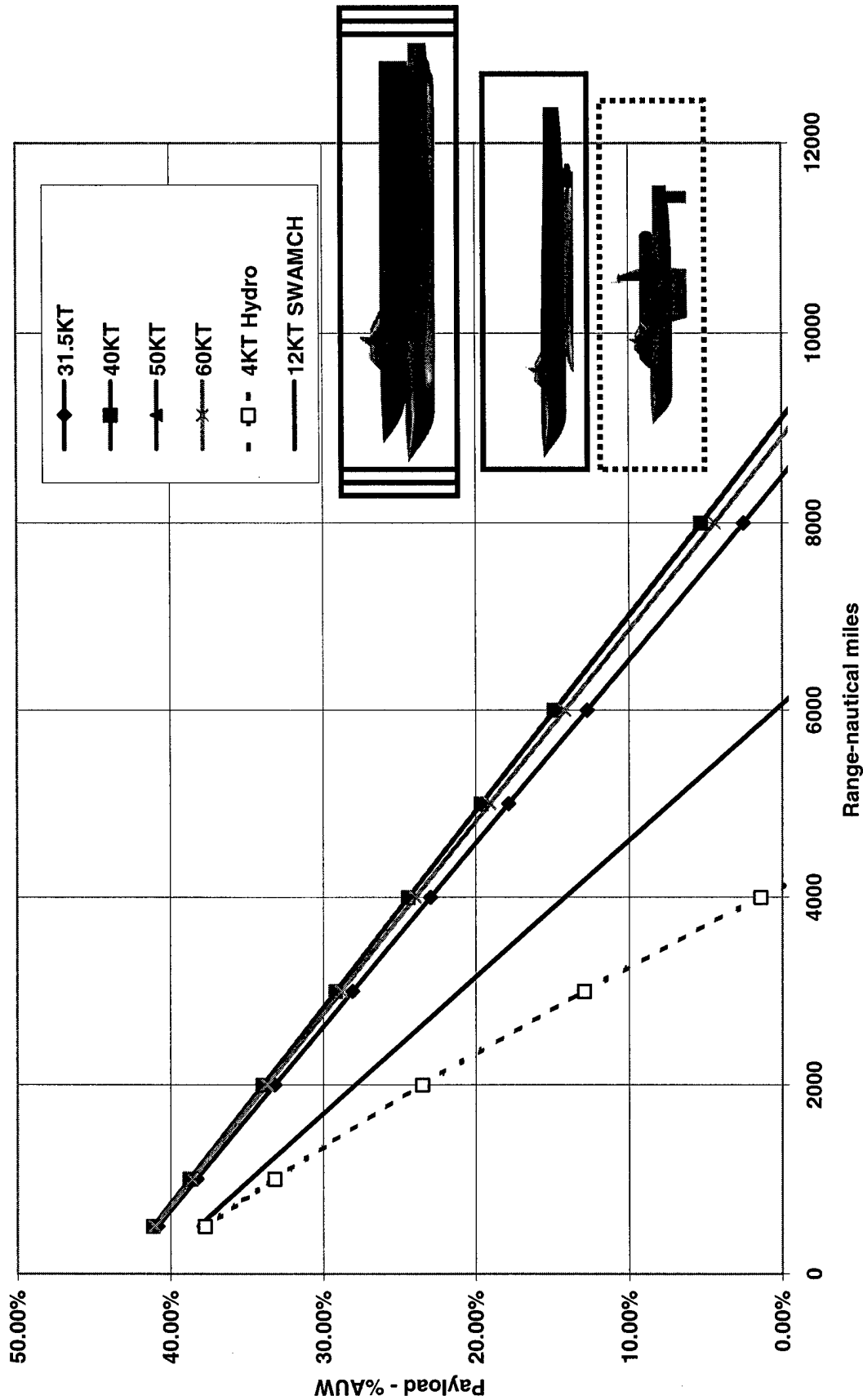
SWAxCH vs. Hydrofoil Sizing Comparisons

Payload vs. Range for SWATCH Designs - 75%K2 (75% Viscous Drag)
 P29TA12 Cavity Bodies, 1.5% t/c Struts, w/ Interference Effects, 1.4 JVR Pumps



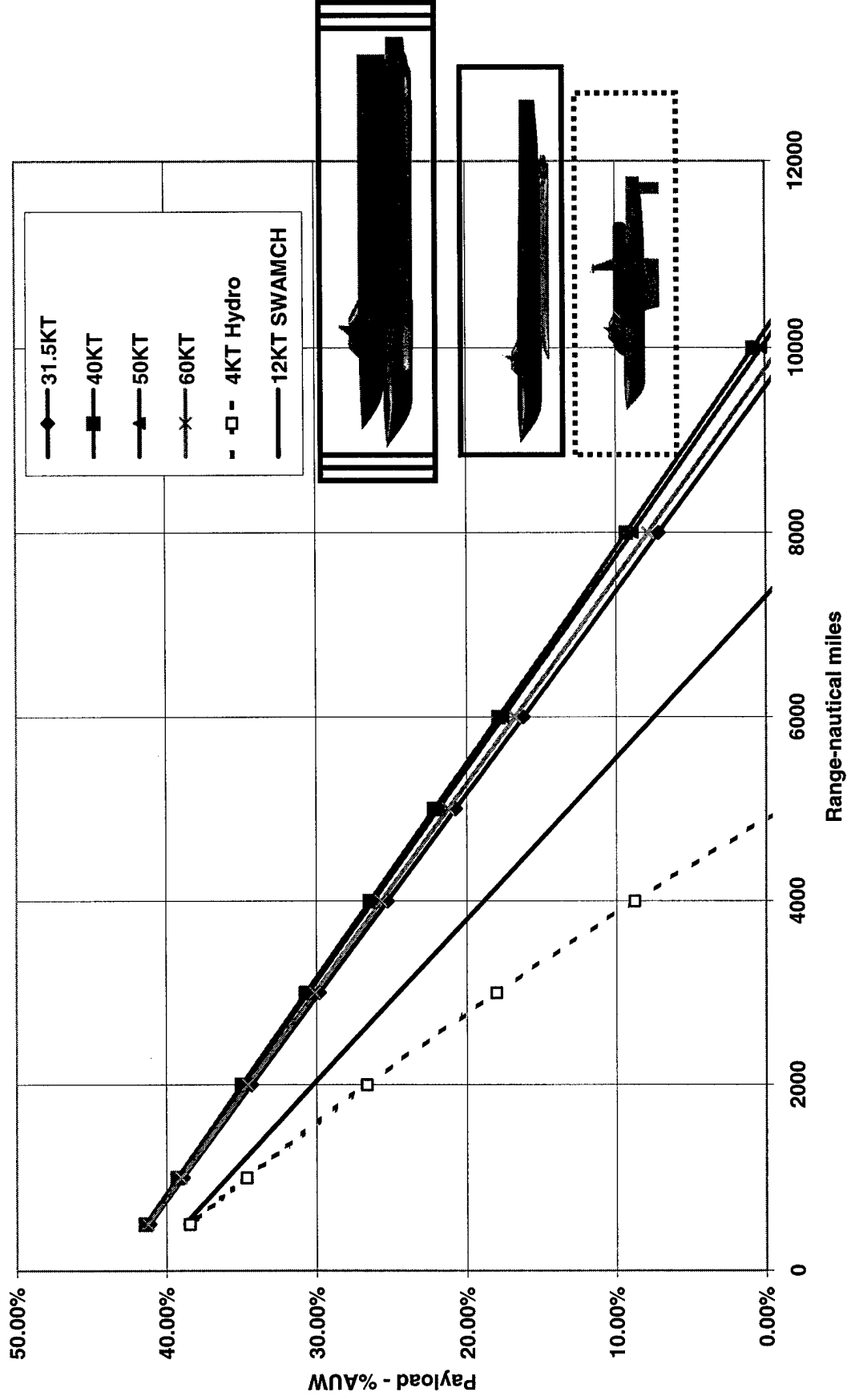
SWAxCH vs. Hydrofoil Sizing Comparisons

Payload vs. Range for SWATCH Designs - 50%K2 (50%Viscous Drag)
 P29TA12 Cavity Bodies, 1.5% t/c Struts, w/ Interference Effects, 1.4 JVR Pumps



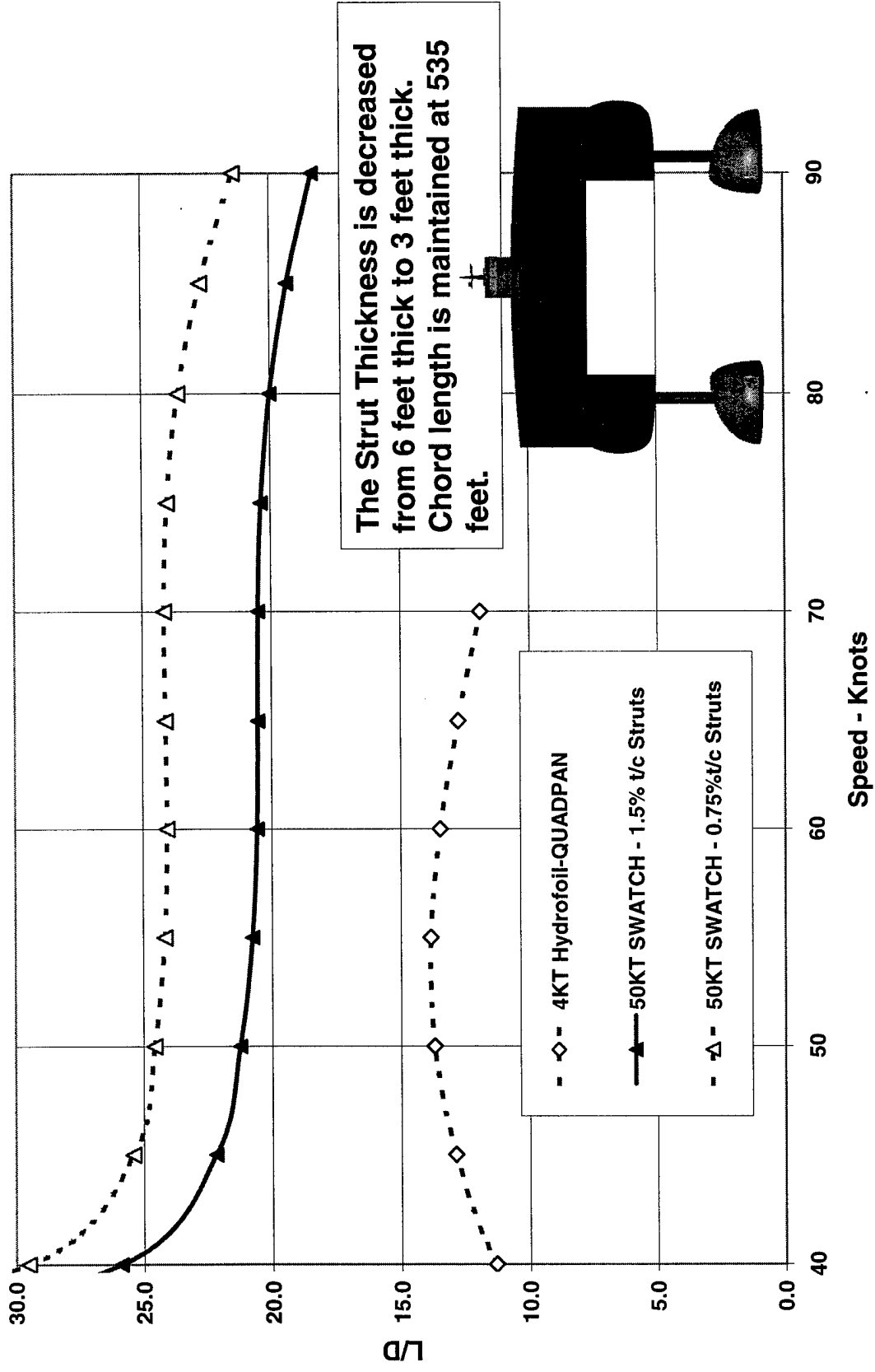
SWAxCH vs. Hydrofoil Sizing Comparisons

Payload vs. Range for SWATCH Designs - 25%K2 (25%Viscous Drag)
 P29TA12 Cavity Bodies, 1.5% t/c Struts, w/ Interference Effects, 1.4 JVR Pumps



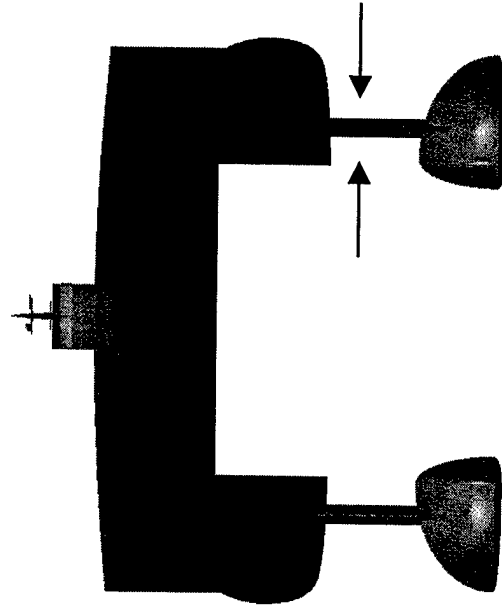
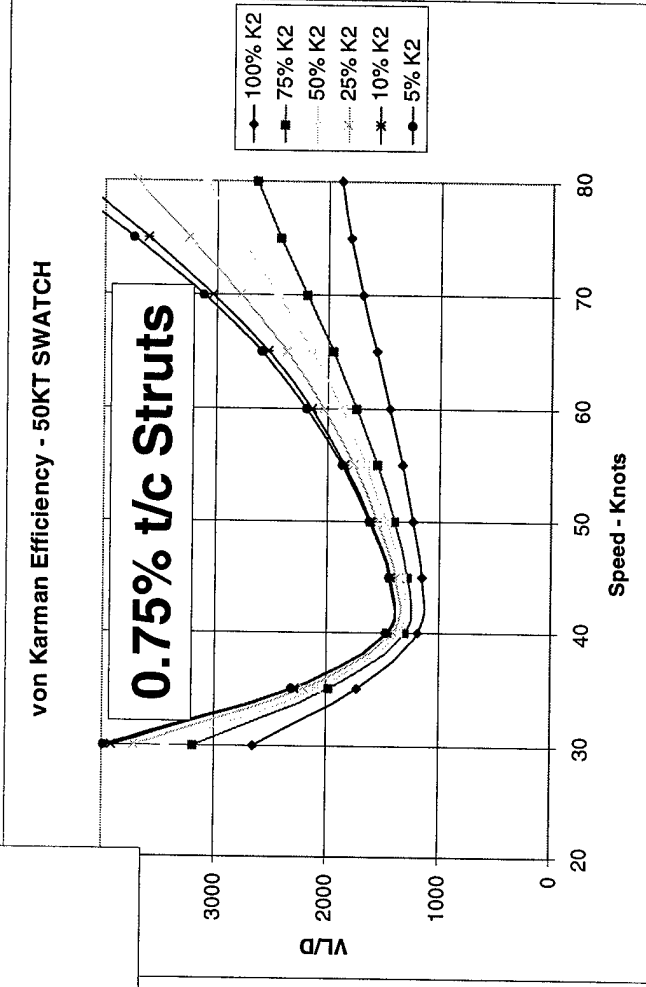
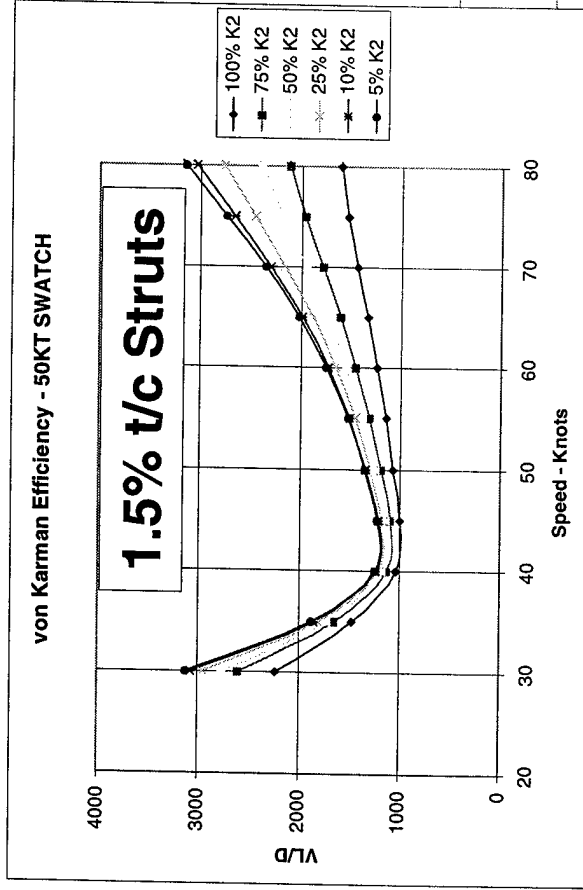
50KT SWATCH Strut Sizing Comparisons

Ship Lift-to-Drag Ratio
Full Skin Friction, Varied Struts, P29TA12 Bodies

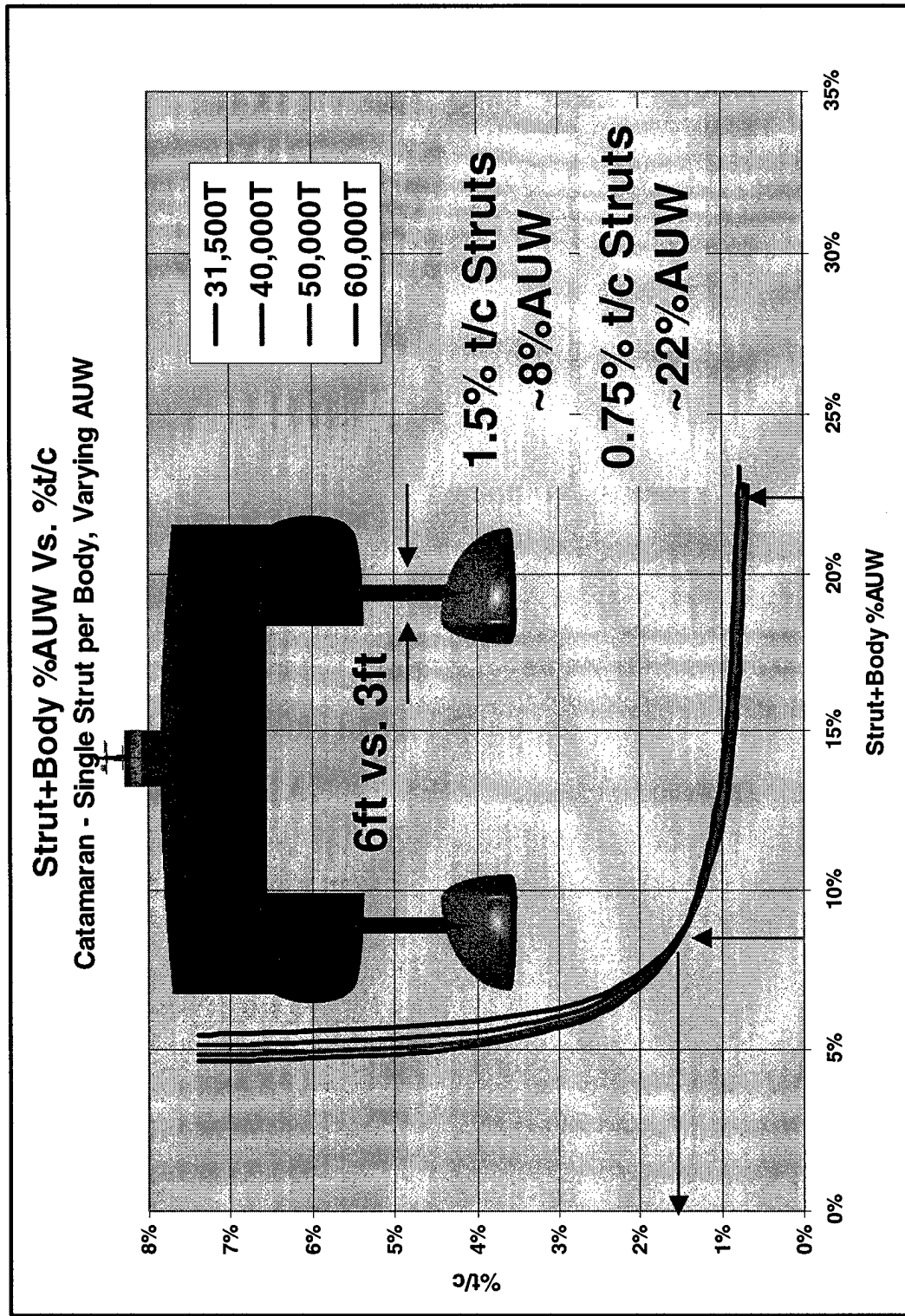


50KT SWATCH Strut Sizing Comparisons

As the Strut Thickness is decreased from 6 feet thick to 3 feet thick the von Karman Efficiency increases accordingly.

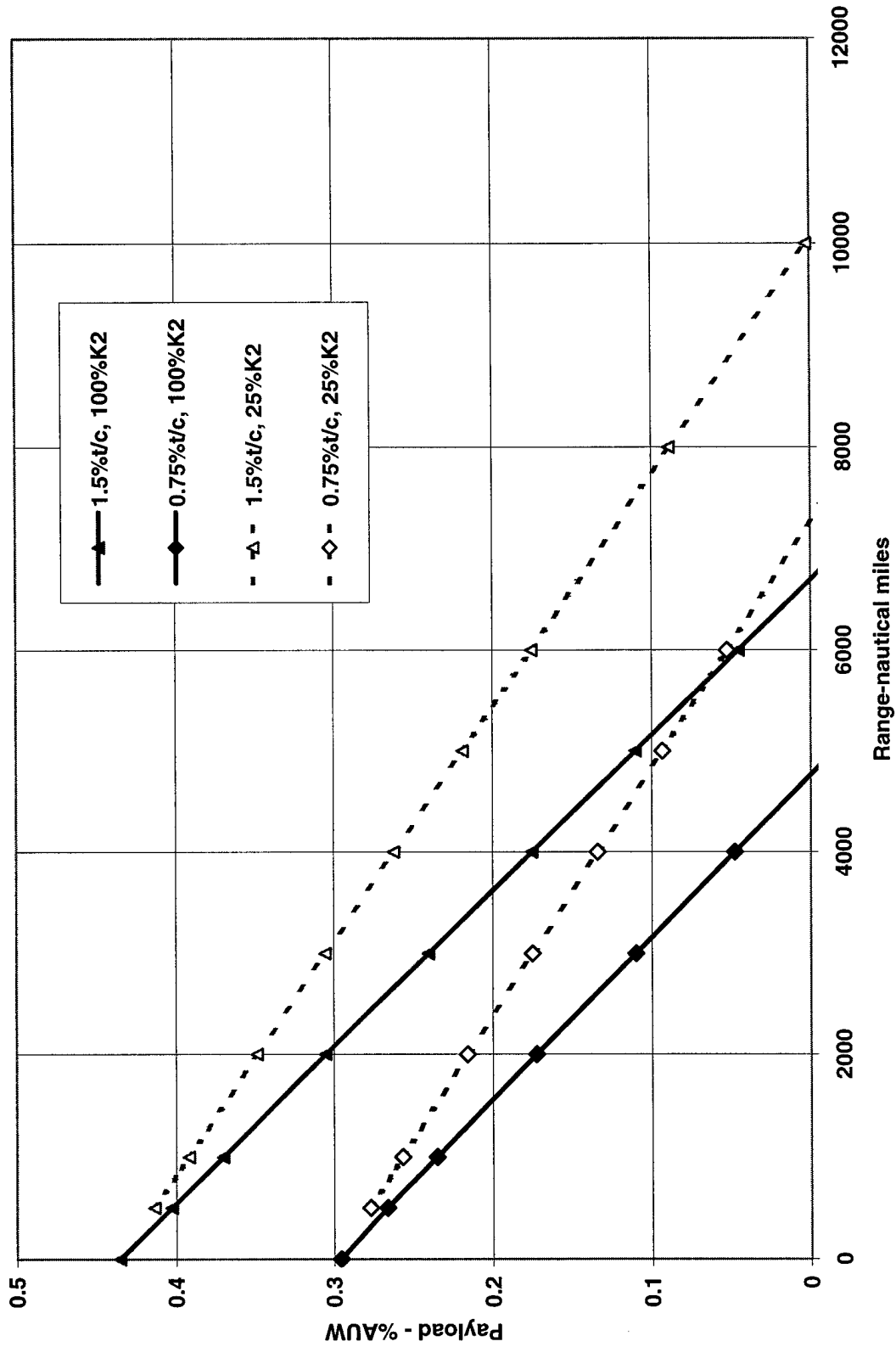


50KT SWATC^H Strut Sizing Comparisons



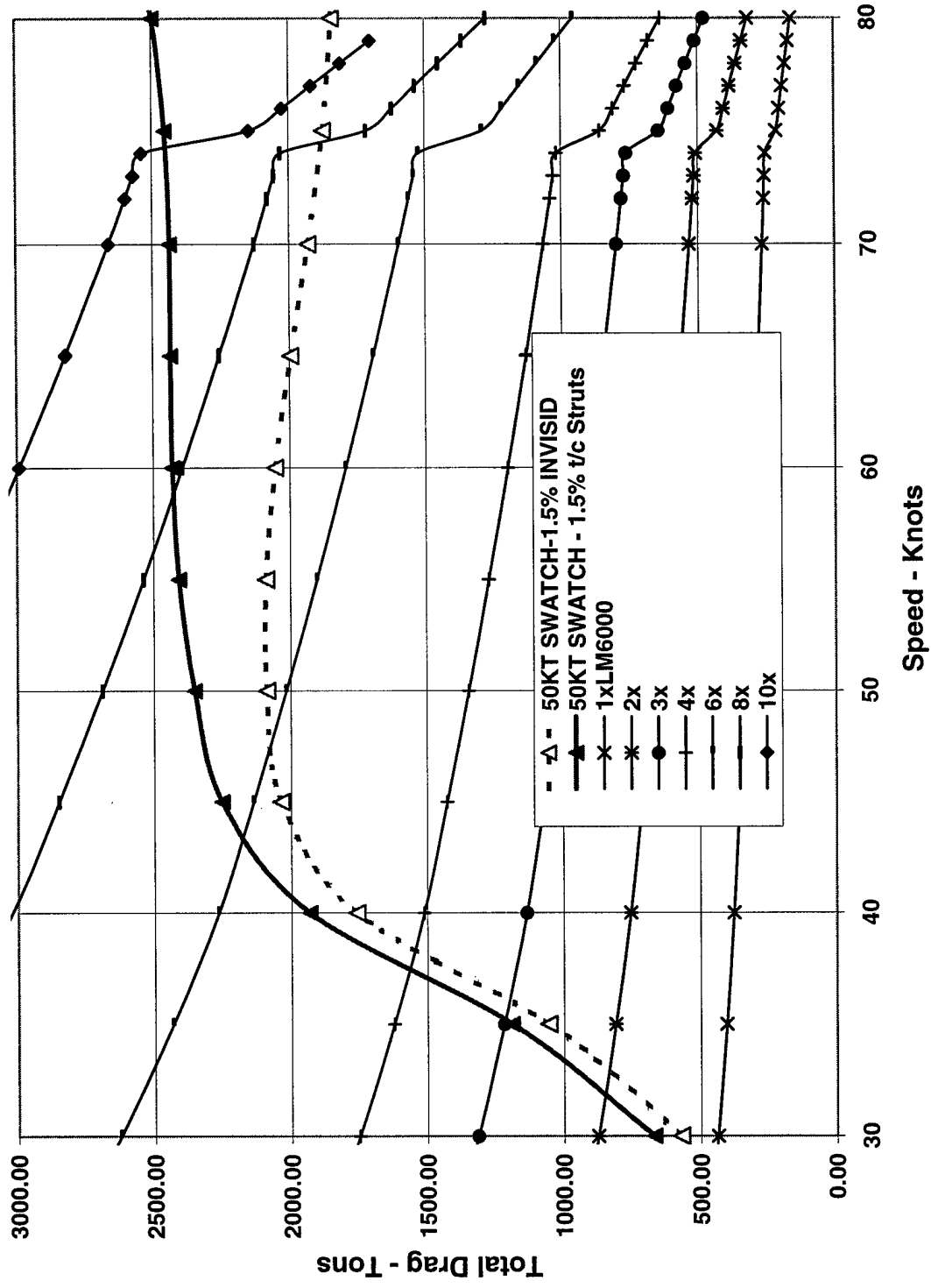
50KT SWATCH Strut Sizing Comparisons

Payload vs. Range for 50KT SWATCH Designs
P29TA12 Cavity Bodies, 1.5% and 0.75% t/c Struts, w/ Interference Effects, 1.4 JVR Pumps



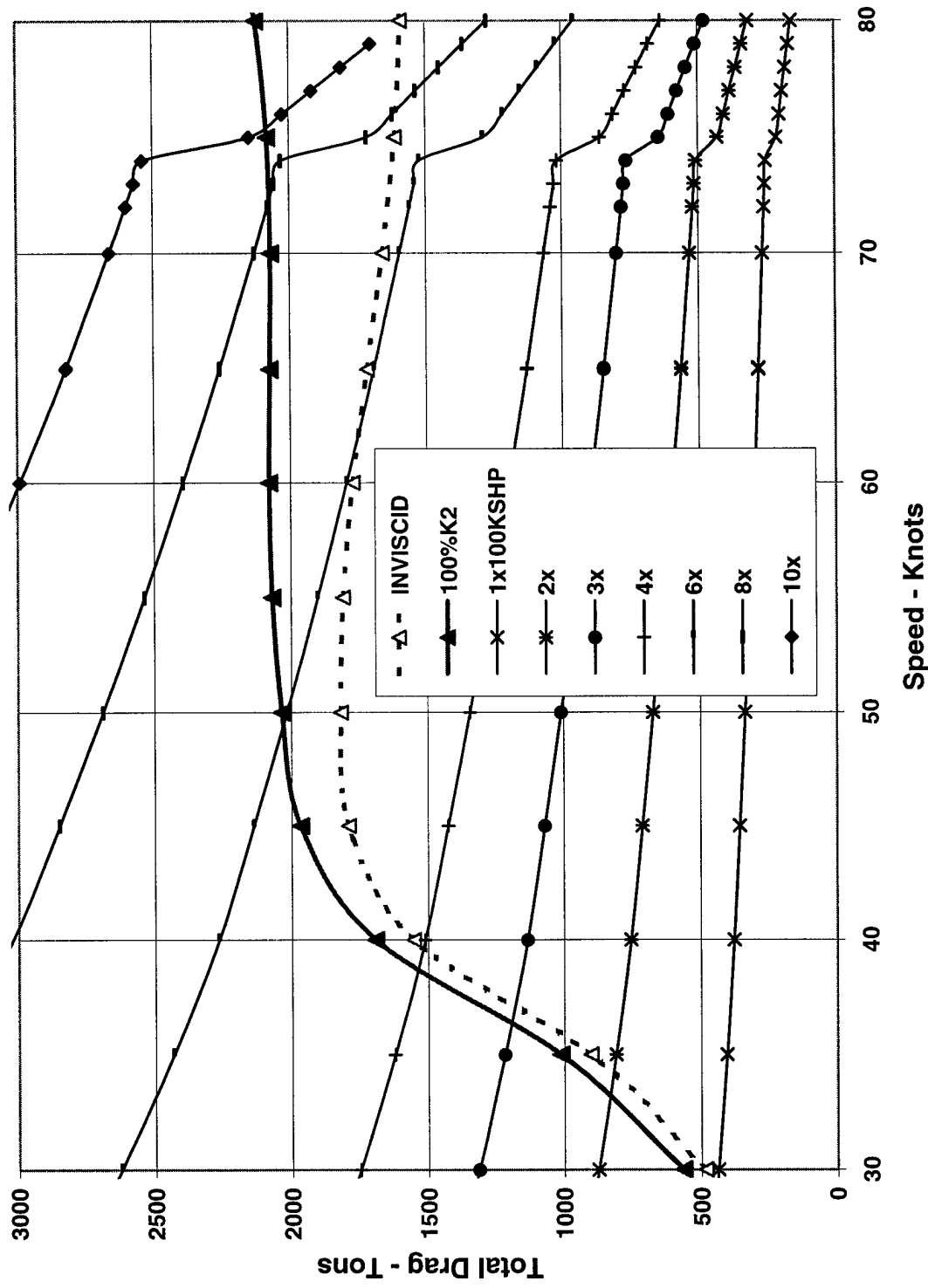
Thrust Required – 50KT SWATCH 1.5% Struts

50KT Ship Total Drag vs Available Thrust
P29TA12 Bodies, 1.5% t/c Struts



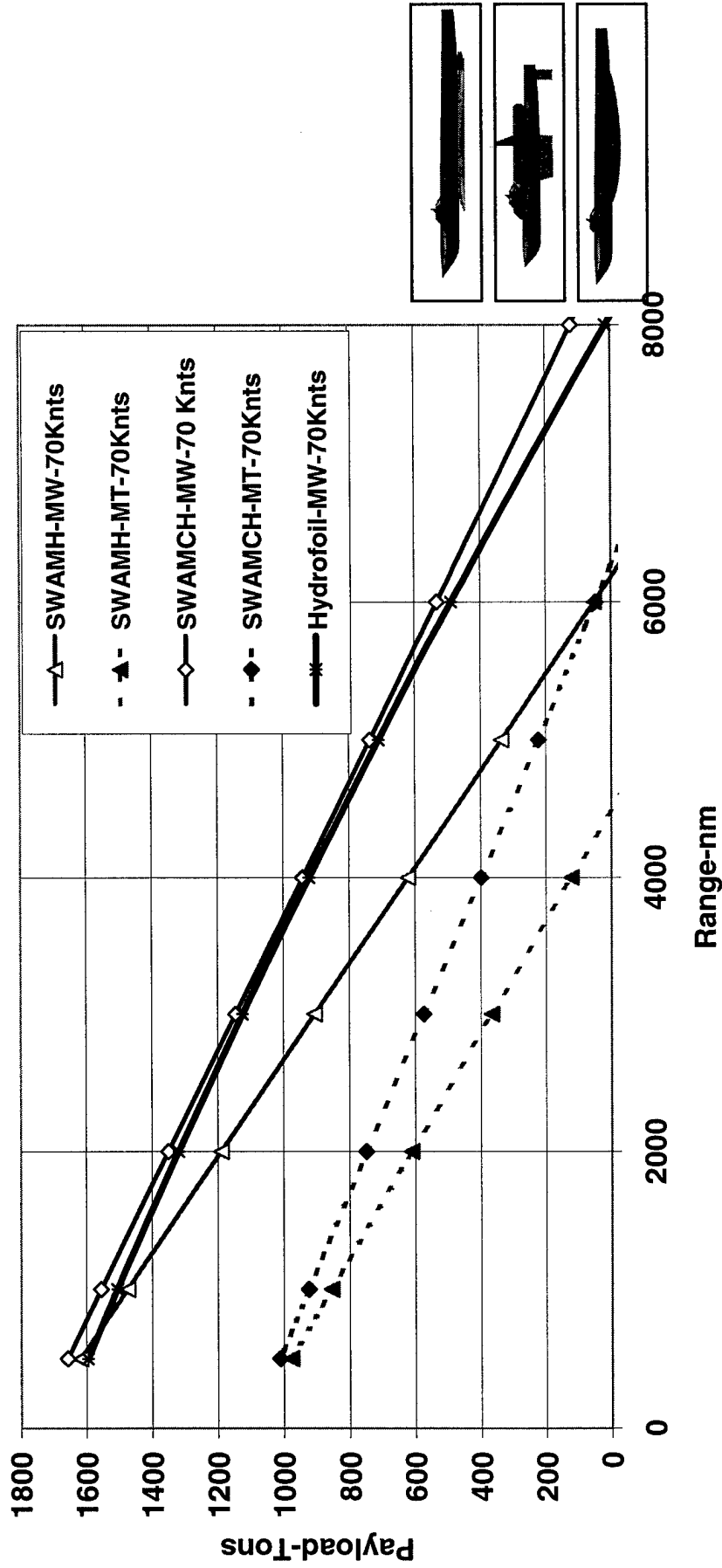
Thrust Required – 50KT SWATCH 1.5%Struts

50KT Ship Total Drag vs Available Thrust
P29TA12 Bodies, 0.75% t/c Struts



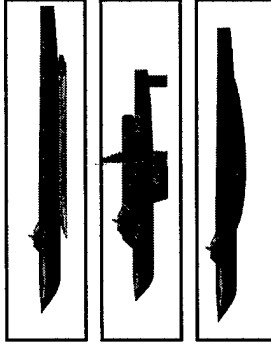
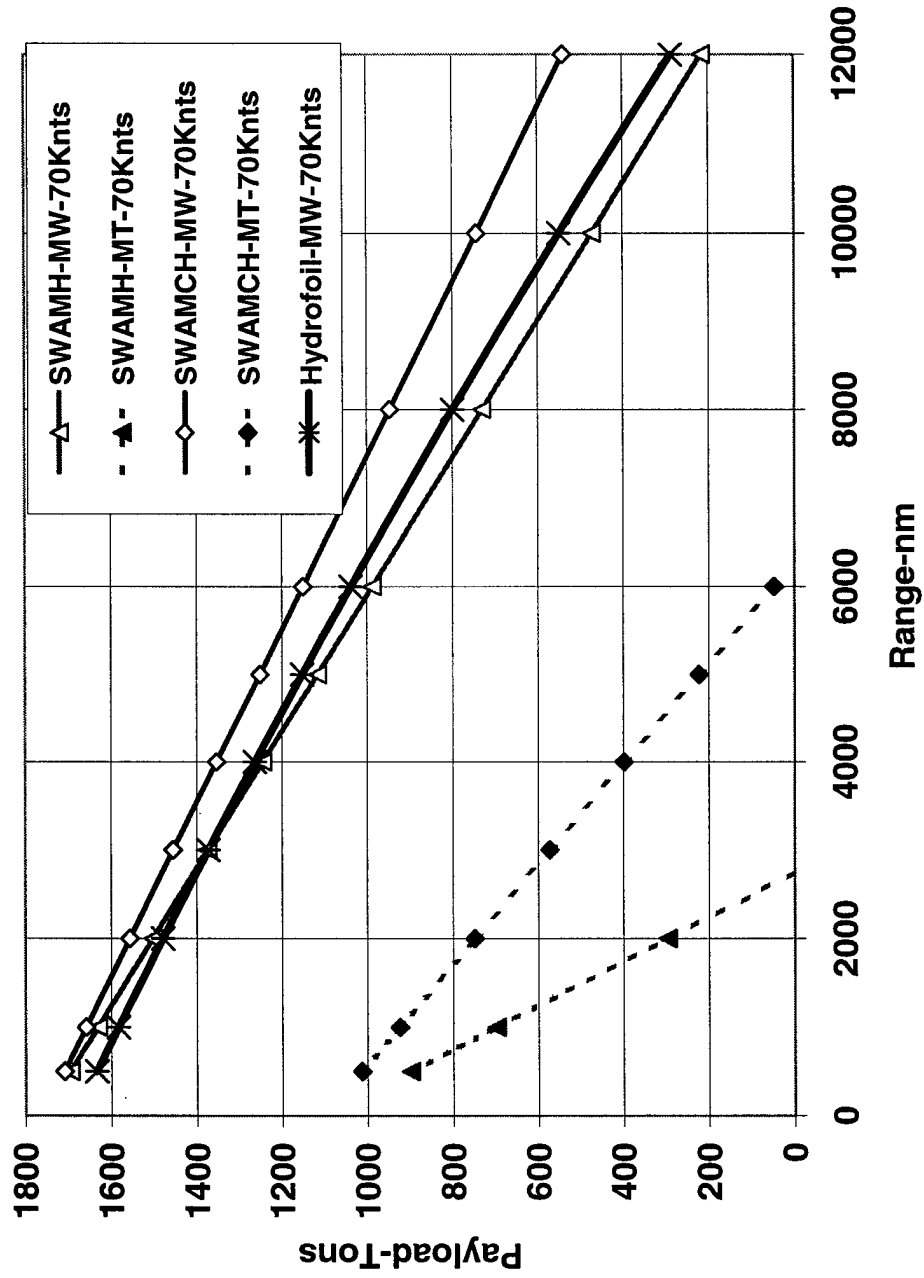
Payload Range at Full Drag - 4KT Summary

Payload-Range Comparison
 4000Tons, Full Drag, 70 Knots Cruise Speed

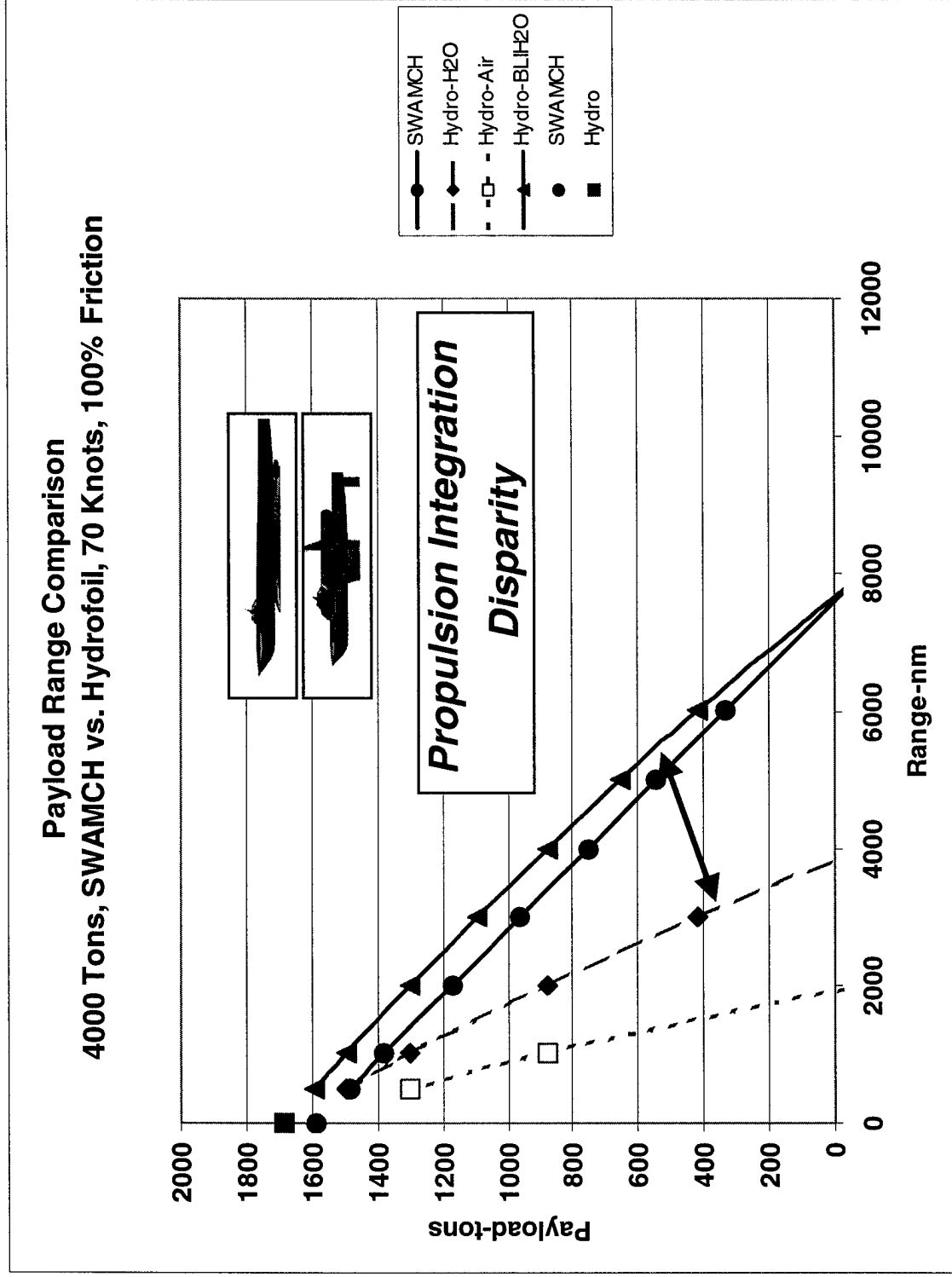


Payload Range at 25%K2 – 4KT Summary

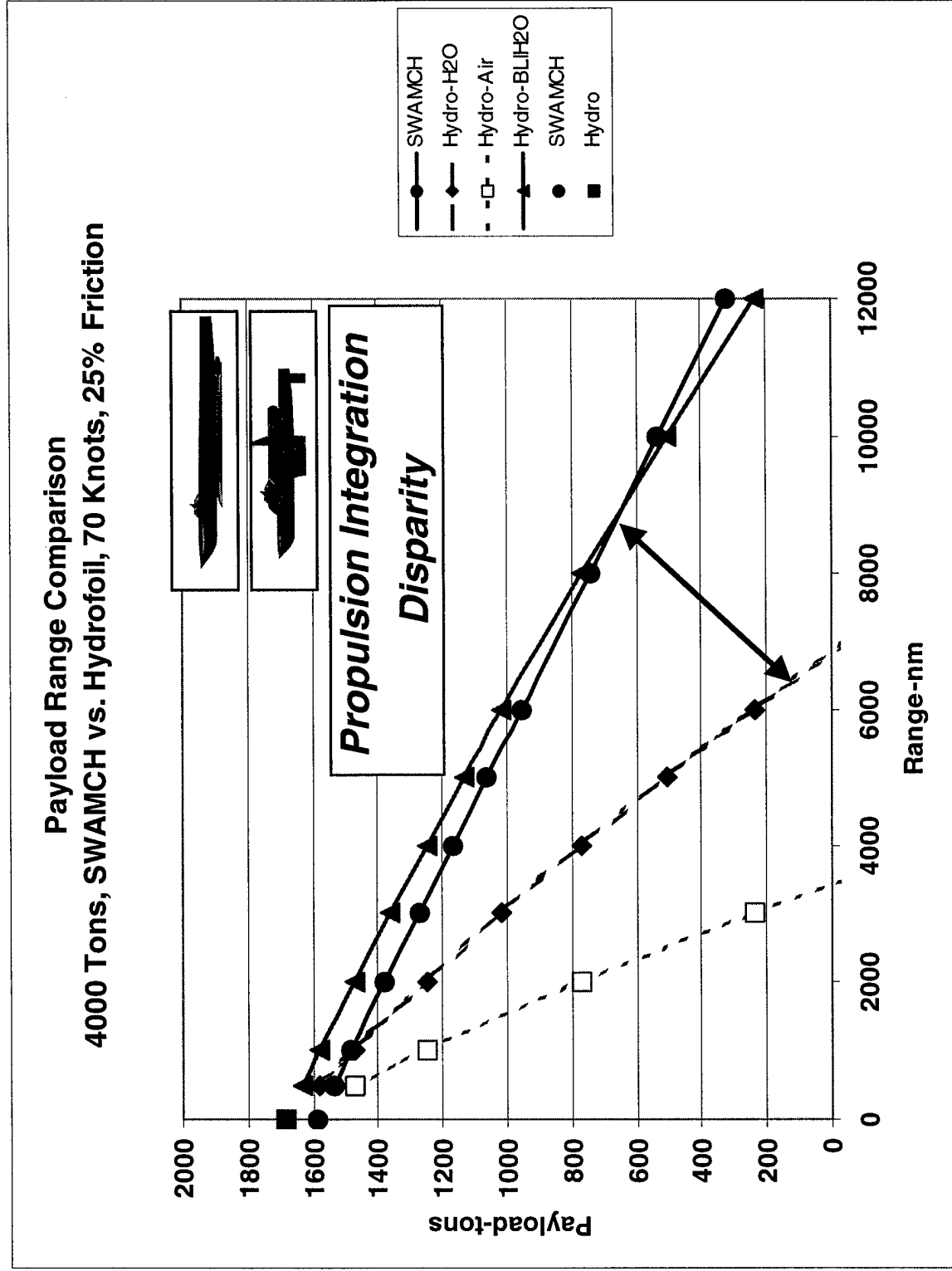
Payload-Range Comparison
 4000Tons, 75% Drag Reduction, 70 Knots Cruise Speed



Payload Range at Full Drag – Propulsion Comparison



Payload Range at 25%K2 – Propulsion Comparison



Hull Configuration Progress Briefing

Andrew R. Kondracki, P.E.

**CSC Advanced Marine
Arlington, VA**

Notional Design Requirements

Phase I Concept

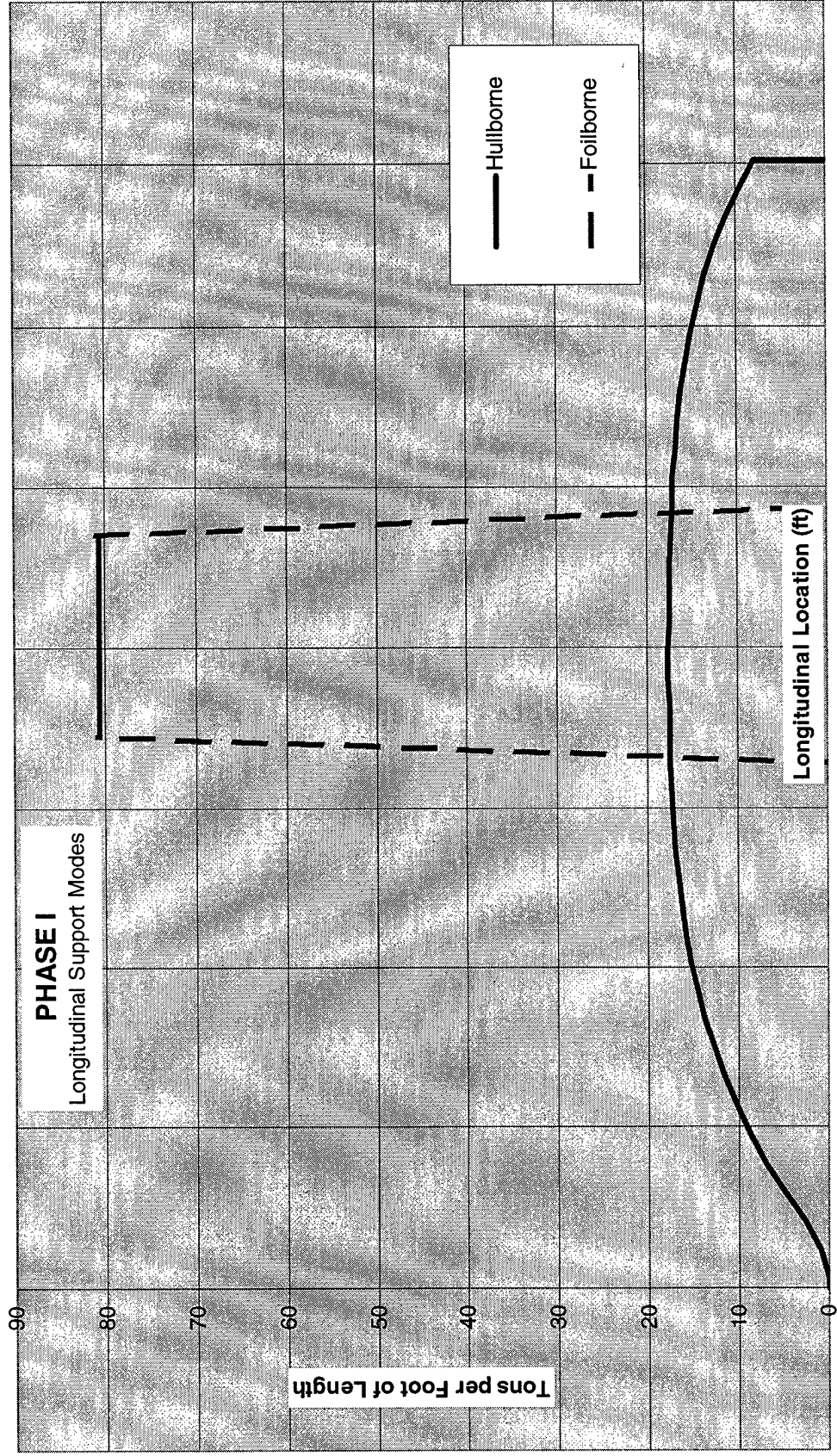
- All-up-weight approximately 5,000 T
- Fixed-weight-fraction $\leq 50\%$ of all-up-weight
- Fuel weight $\approx 1,200\text{T}$ s (for 6,000 nm range)
- Deck capacity to carry 2,200T of rolling stock (only 1,650T actually carried with endurance fuel load)
- Capability to carry battle-ready tanks and army rolling stock of all types in varying proportions
- Habitability and safety systems consistent with a minimum crew size
- Cargo handling equipment and ventilation systems consistent with the vehicles to be carried
- Retractable foils to minimize hull-borne navigational draft
- Suez-max beam (213 feet - nominal beam is 200 feet)
- Navigational draft ≤ 23 feet

Hull Configuration Trade-off Phase I Concept

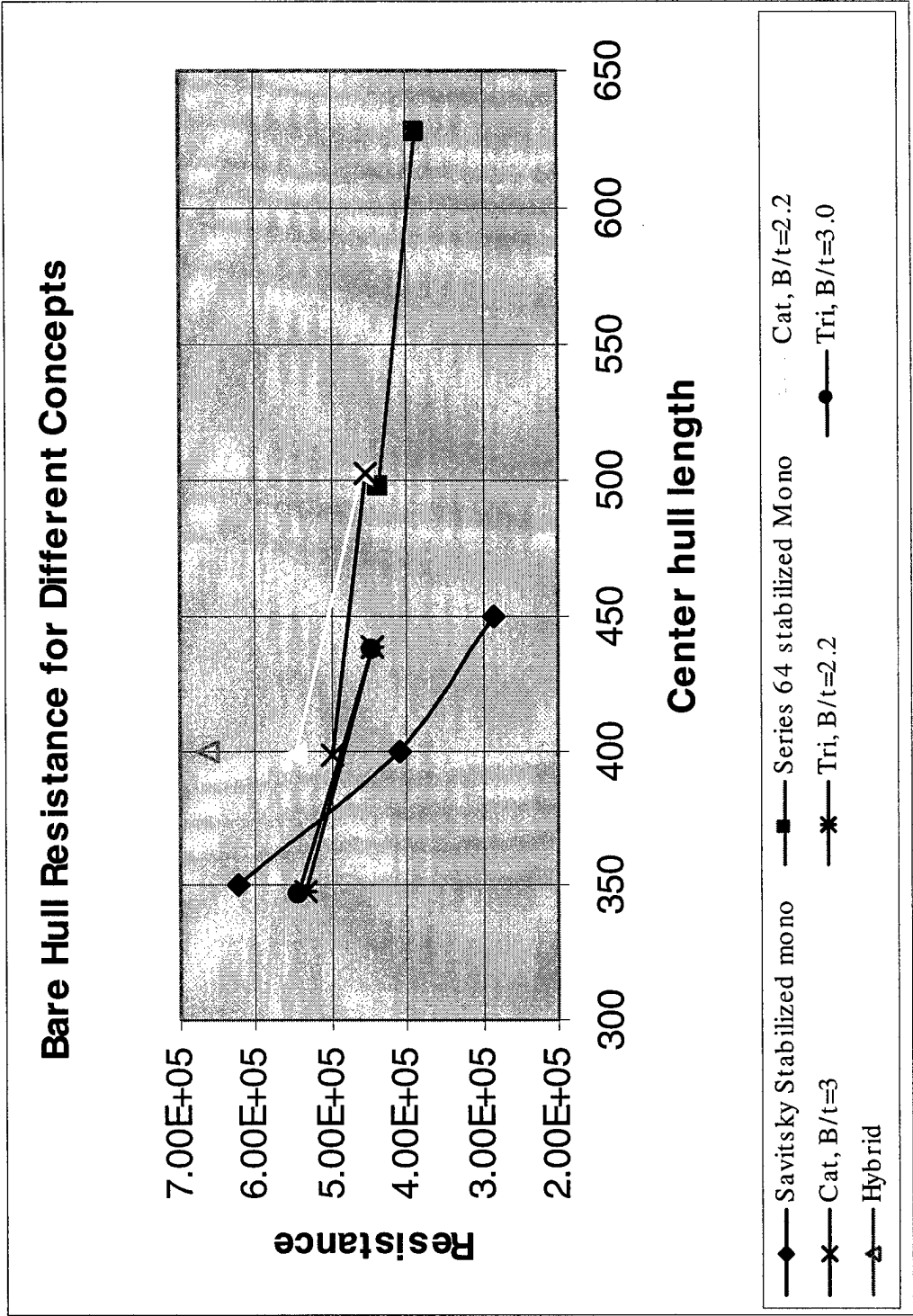
- **Optimum resistance vs. light weight**
 - Optimum resistance
 - » long slender trimaran with small side hulls
 - Minimum structural weight
 - » displacement distributed in same manner as foil support (short length, full beam)

Design Problem

Two Modes of Support



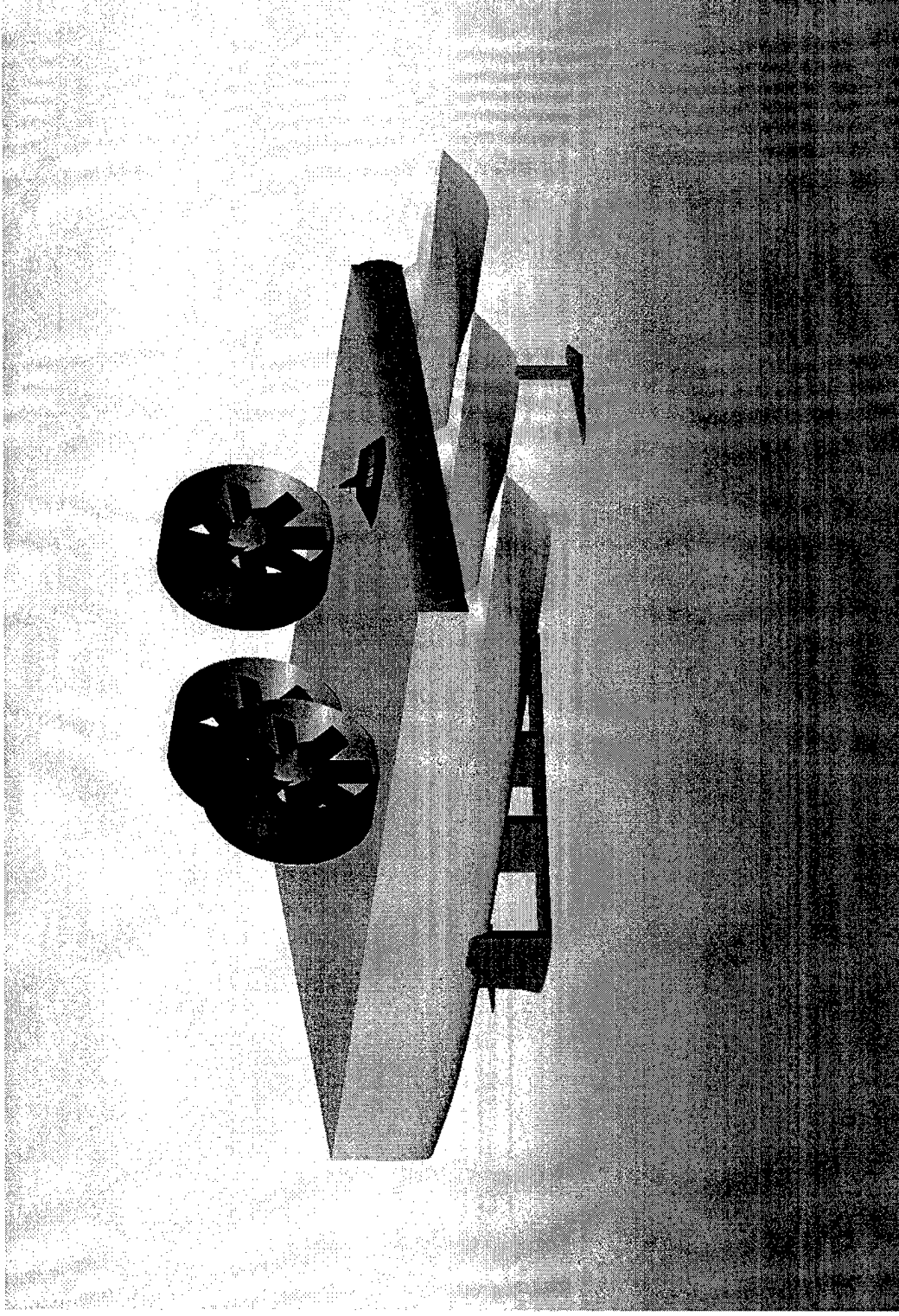
Hull Form Trade-off Results



Hull Form Selection Phase I Concept

- **3 Identical Hulls**
 - Provide three primary longitudinal members
 - Limit length to slightly more than that required for deck space
 - Reduce unsupported transverse span relative to catamaran
- **Deep slender hulls**
 - reduced wavemaking resistance
 - less waterplane area - reduced slamming loads in a seaway
 - Increased depth of longitudinal girder

Notional Configuration Phase I Concept



Estimated Vessel Weight Phase I Concept

SWBS GROUP	SWBS DESCRIPTION	WEIGHT (T)
1	HULL STRUCTURE	2,814
2	PROPULSION PLANT	463
3	ELECTRIC PLANT	114
4	COMMAND & SURVEILLANCE	11
5	AUXILIARY SYSTEMS	810
6	OUTFIT & FURNISHING	150
7	ARMAMENT	0
FULL LOAD CONDITION		6,862

Hull Structure

- **Significant SWBS 100 Weight Elements**
 - Shell Plating (615T)
 - Inner Bottom (1070T)
 - Stanchions (57T)
 - Transverse bulkheads (37T)
 - Cargo deck (663T)
 - Weather deck (254T)
 - Foundations (118T)

Propulsion Systems

- **Significant SWBS 200 Weight Elements**
 - Turbine / ducted propulsors (390T) *
 - » 3 LM6000 - 64-ft diameter axial propulsors
 - Lube oil systems (59T)
 - Fuel transfer and service systems (14T)

Electric Power Systems

- **Significant SWBS 300 Weight Elements**
 - Power distribution cabling (57T)
 - Ships service power generation (42T)
 - Power conversion equipment (12T)

Command & Control Systems

- **Total SWBS 400 Weight Group is 11T**

Auxiliary Systems

- **Significant SWBS 500 Weight Elements**
 - Struts and foil systems (~500T)
 - » conservative estimate coordinated with Lockheed Martin
 - Cargo ramps and systems (85T)
 - Cargo space A/C system (82T) (*eliminated in phase II*)
 - Cargo space ventilation system (74T)
 - Firemain system (43T)
 - Mooring and towing systems (16T)
 - Habitability spaces HVAC (10T)

Cargo Handling Systems

- **One ramp on each side (port / starboard)**
 - Ramp length is suitable for most pier heights
 - 2 ramps facilitate loading/unloading without having extensive backing or turning of vehicles in tight spaces
 - A possible trade-off is the weight of the ramp versus that of a suitable ballast system. Controlling the vessel draft may permit use of a shorter/lighter ramp.

Outfit & Furnishings

- **Significant SWBS 600 Weight Elements**
 - Hull Insulation (63T) (*reduced in Phase II*)
 - Painting (44T)
 - Cathodic Protection (20T)
 - Habitability Spaces (17T)
 - » Total Crew of 19 people (6 man shifts)
 - 9 Officers (3 per shift)
 - 3 CPOs (1 per shift)
 - 7 Enlisted (2 per shift plus a utility man)
 - Deck Fittings (6T)

Results of Phase I Concept

- The fixed weight of 4,362T only permits a useful payload of 638T for a 5,000T ship.
- The endurance fuel load is 1,200T
- \therefore the design cannot go 6,000 nm even with no cargo onboard.
- The fixed weight fraction commensurate with the full load condition is ~64%.

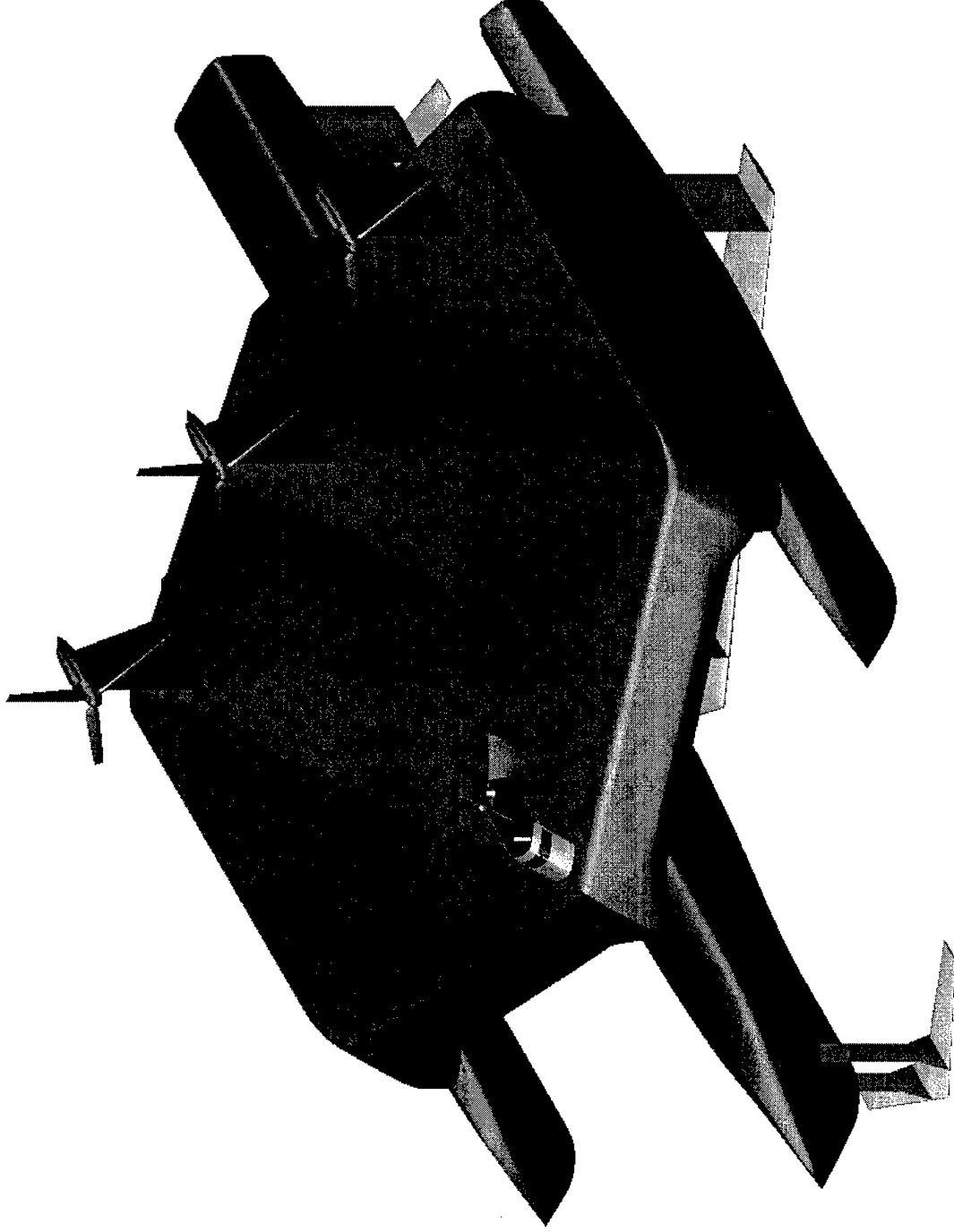
Issues Identified by the Phase I Concept Design

- The material selected for Phase I (HY-100) was too heavy
- Need to add a maneuvering propulsor for docking and undocking
- Massive structure required for foil and propulsor support
- Deck plating thickness driven by wheel loads and slam loads on (cargo/wet decks)
- Cargo A/C is not required
- Hull insulation can be reduced or eliminated
- Should have a reasonable acquisition margin in the weight estimate

Phase II Concept Design

- **Exclusive use of Marine Grade Aluminum (estimated weight savings of ~30% of SWBS Group 1)**
- **Reduced Deck area by 24,000 sq.ft. (weight savings in SWBS Group 1)**
- **Unsymmetric hulls**
 - Center : 365-ft length, 26.5-ft beam
 - Outriggers : 180-ft length, 13.5-ft beam
- **Add retracting azimuthing propulsor(s) sized for docking / undocking**
- **Use an acquisition weight margin of 7.5% of the lightship weight**

Notional Configuration for Phase II Concept Design



Estimated Vessel Weight Phase II Concept

SWBS GROUP	SWBS DESCRIPTION	WEIGHT (T)
1	HULL STRUCTURE	1,600
2	PROPULSION PLANT	463
3	ELECTRIC PLANT	114
4	COMMAND & SURVEILLANCE	11
5	AUXILIARY SYSTEMS	728
6	OUTFIT & FURNISHING	75
7	ARMAMENT	0
<hr/>		
	LIGHTSHIP	2,991
	ACQ. MARGIN	224
	FUEL	1,000
	FUEL OR CARGO	1,000
<hr/>		
	FULL LOAD CONDITION	5,215

Phase II Concept Results

- **The fixed weight ratio has been improved to ~57% of the total ship weight**
- **The Phase II concept design appears to be a reasonable baseline for parametric studies**

Plan for Continued Work

- **Develop hull weight sensitivity equations to feed Lockheed design optimization tools**

Hull Configuration Progress Briefing

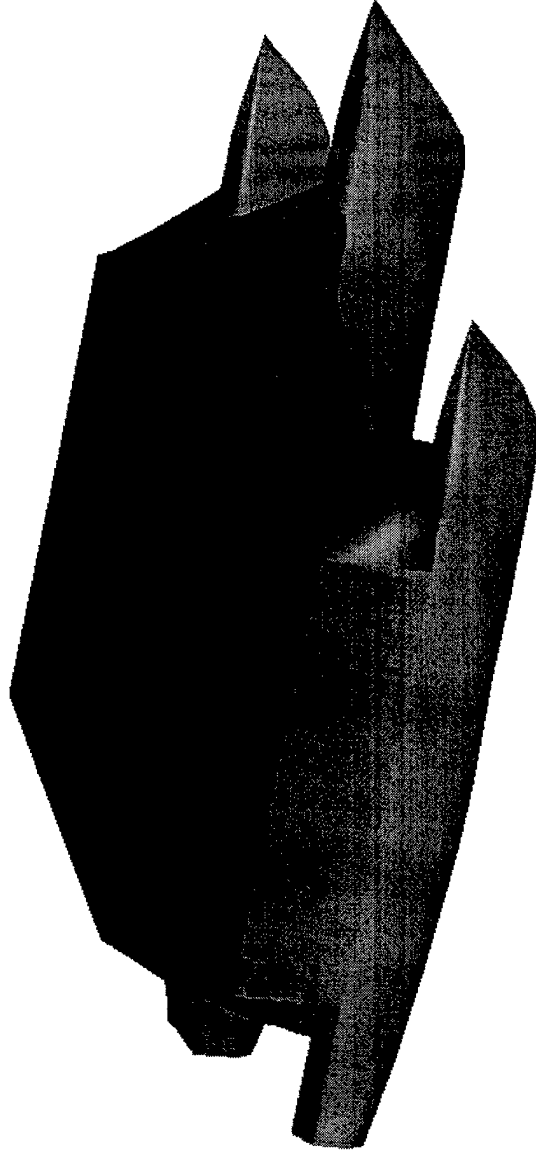
J. Otto Scherer

**CSC Advanced Marine
Arlington, VA**

Activities for this Cycle

- **Develop hull form, weight estimate, and resistance estimate for a 4k ton vessel**
 - Explore novel ways to reduce or eliminate decking since its not driven by primary hull stresses
- **Examine ability to beach / extract from beach to eliminate in-stream cargo ops**
- **Summarize why sweep is useful in the hydrofoil design**

Phase III Hull Concept



Phase III Design Particulars

- **Length overall = 250 feet**
- **Beam overall = 213 feet**
- **Static Draft at Full Load = 17.0 feet**
 - (foils retracted)
- **Static Draft at Full Load = 47.0 feet**
 - (foils deployed)
- **All aluminum hull**
- **Structures to DNV high speed rules**

Weight Changes Phase II to III

- **Reexamined all weight elements**
- **Big changes**
 - Added anchor, chain, and windlass and foil retraction system weights
 - Reduced outfit and furnishings (1 ramp v. 2) and auxiliary systems
 - Added approximations for centers of gravity
- **Examined ways to eliminate/reduce cargo decking**
 - All ideas required addition of special fittings and handling equipment and would seriously reduce cargo ops throughput

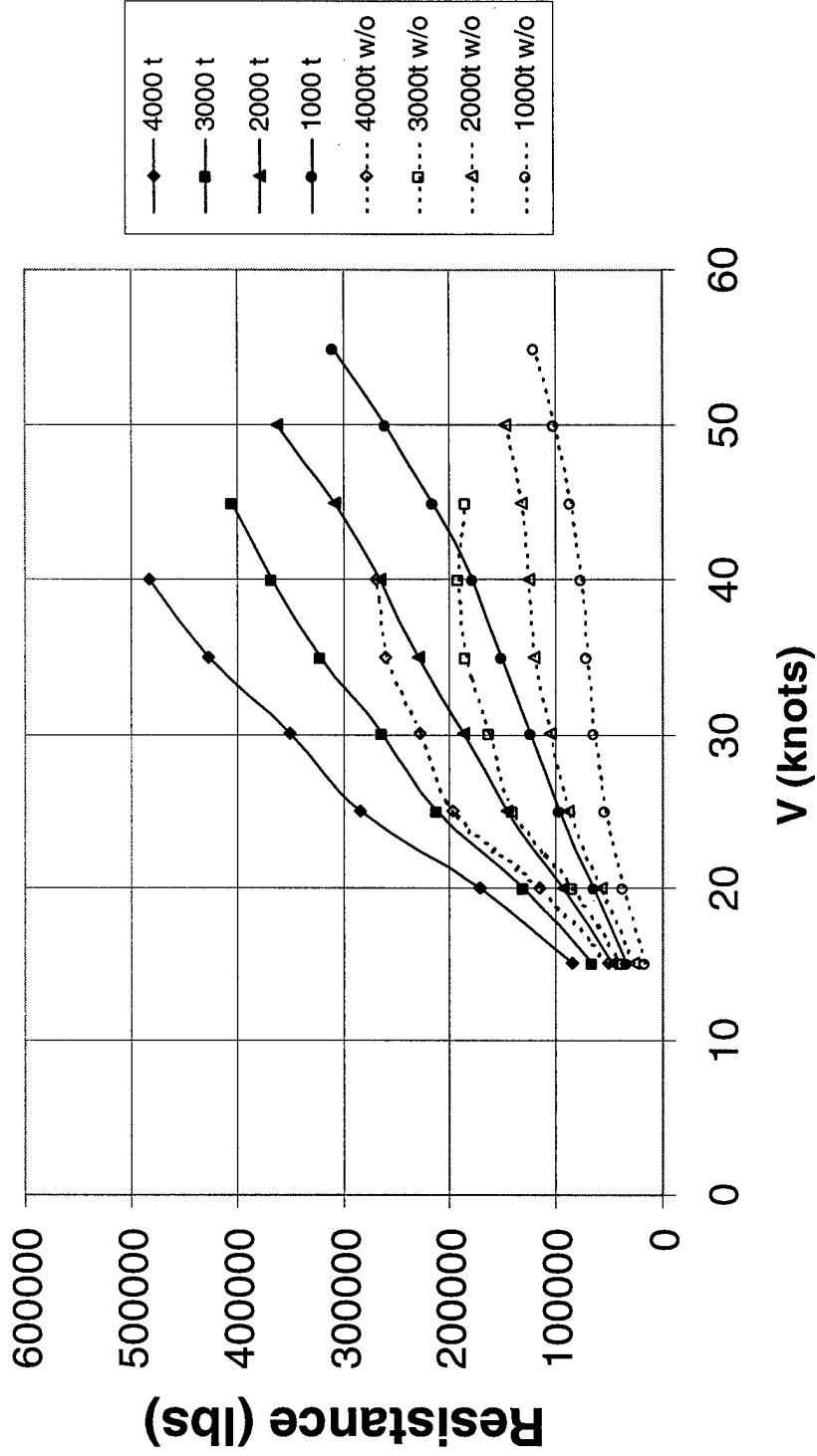
Phase III Weights

SWBS GROUP	SWBS DESCRIPTION	WEIGHT (S-Tons)	VCG FT-ABL	VMOM (FT-Tons)	LCG FT-Aft FP	LMOM (FT-Tons)
210T FOR 3xLM6000x64-ft PROP						
1	HULL STRUCTURE	1,297.39	22.7			
2	PROPULSION PLANT	283.50	69.7			
3	ELECTRIC PLANT	115.26	33.01	3,805	91.36	10,530
4	COMMAND AND SURVEILLANCE	12.86	44.00	566	83.11	1,068
5	AUXILIARY SYSTEMS	370.00	-5.91	-2,186	204.99	75,847
6	OUTFIT AND FURNISHING	17.61	24.76			
7	ARMAMENT	0.00				
275T "NET" WEIGHT FOR FOIL						
1-7	LIGHTSHIP	2,096.61	24.76	51,921	146.77	307,720
M	ACQUISITION MARGINS (7.5% of Lightship)	157.25	24.76	3,894	146.77	23,079
1-7 w/M	LIGHTSHIP w/MARGINS	2,253.86	24.76	55,815	146.77	330,799
F	LOADS	1,013.01	8.14	8,250	140.04	141,864
F	LOADS CARGO	1,000.00	41.00	41,000	155.00	155,000
FL	FULL LOAD CONDITION	4,266.87	24.62	105,065	147.10	627,663

Fixed Weight is 53% of Full Load Weight, 56% of 4000T

Phase III Hull Resistance

Lockheed Hydrofoil Hull Resistance (with and without skin friction)



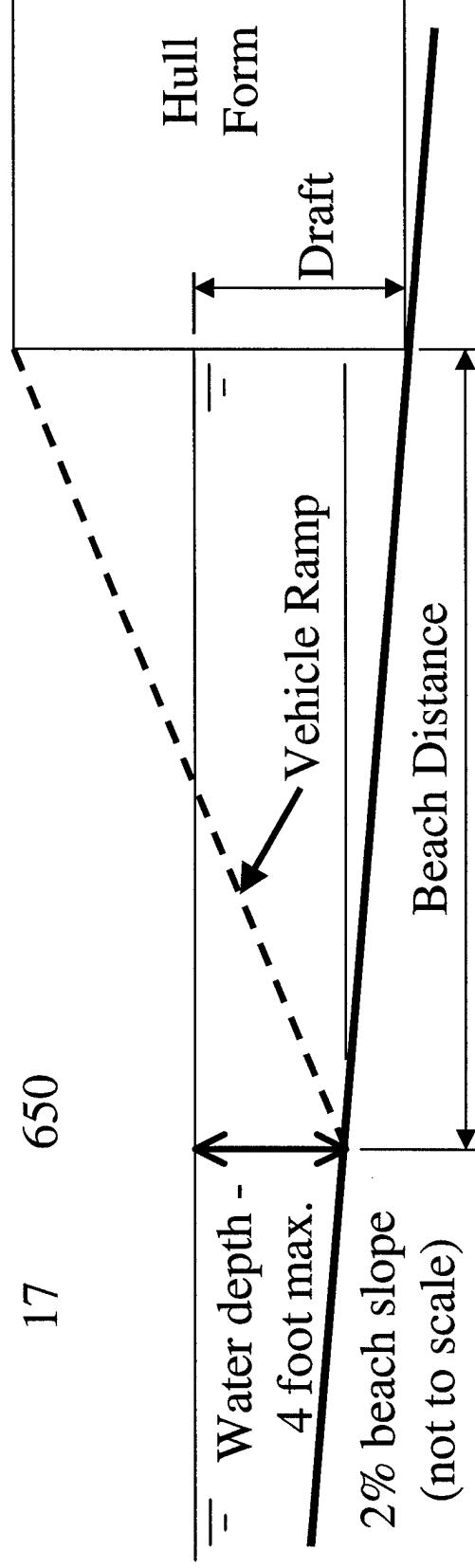
Beaching Problem

$$\text{Beach Distance} = (\text{Draft} - 4) / .02$$

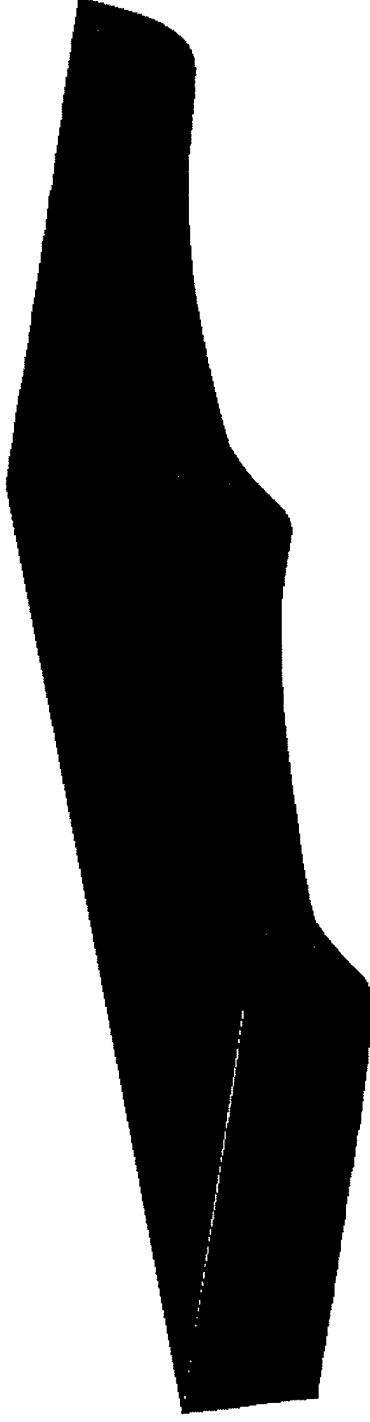
- Vessel must have:
- Significant ballast capability
 - Rugged hull structure
 - Damage tolerance
 - Mooring gear - anchor(s)
 - Extraction gear - anchor(s)

Draft Beach Distance

(ft)	(ft)
4	0
6	100
8	200
10	300
12	400
17	650



Beaching Concept Design



Major Issues

- Seakeeping / Slamming during takeoff, landing, and on foil
- Resistance during takeoff and landing

Why Sweep?

O. Scherer Apr. 27, 2000 1:30:50 PM

4% and 6% (t_{mean}/c) Symmetric Sections 35.264 deg sweep, $\text{COS}^2(\text{sweep})=0.667$

